BURGETT

September 1981
Final Report

DOT HS-806-244

U.S. Department
of Transportation
**National Highway
Traffic Safety
Administration**

Collision Avoidance System Cost-Benefit Analysis

Volume III—Appendices F-M

A. V. Khadilkar
D. Redmond
V. K. Ausherman

Kinetic Research
A Division of Minicars, Inc.
55 Depot Road
Goleta, California 93117

Contract No. DTNH 22-80-C-07530
Contract Amount $151,948

Technical Report Documentation Page

1. Report No.	2. Government Accession No.	3. Recipient's Catalog No.
DOT-HS-806 244		

4. Title and Subtitle	5. Report Date
Collision Avoidance System Cost-Benefit Analysis - Final Report, Volume III, Appendices F - M	30 September 1981
	6. Performing Organization Code
7. Author's) A.V. Khadilkar, D. Redmond, V.K. Ausherman	8. Performing Organization Report No. KR-TR-108
9. Performing Organization Name and Address Kinetic Research A Division of Minicars, Inc. 55 Depot Road Goleta, California 93117	10. Work Unit No. (TRAIS)
	11. Contract or Grant No. DTNH22-80-C-07530
12. Sponsoring Agency Name and Address U.S. Department of Transportation National Highway Traffic Safety Administration 400 Seventh Street, S.W. Washington, DC 20590	13. Type of Report and Period Covered Final Report Oct 1980 to Sep 1981
	14. Sponsoring Agency Code
15. Supplementary Notes	
16. Abstract	

ABSTRACT

Collision-avoidance systems under development in the U.S.A., Japan and Germany were evaluated. The performance evaluation showed that the signal processing and the control law of a system were the key parameters that decided the system's capability, in terms of target discrimination, and the ability to avoid false alarms and missed the targets. The benefits evaluation of selected radar systems was conducted using the Kinetic Research Accident Environment Simulation and Projection (KRAESP) Model and an accident data base which was adjusted to be nationally representative. The results indicated that radar braking systems were most effective in the rear impact mode as well as substantial benefits in frontal, vehicle-to-vehicle, and fixed-object impacts. The effectiveness of the radar systems in the side impact mode was very limited. Non-motorist impacts may be avoided by radar braking systems; however, the ability of the radar to detect pedestrians, bicyclists, and motorcyclists needs further study.

17. Key Words	18. Distribution Statement
Automotive Radar, Collision Avoidance Systems, Brakes, Anti-skid Brakes, Cost-Benefit Analysis, Accident Data, KRAESP, North Carolina 1979 Accident Data	Document is available to the U.S. public through the National Technical Information Service, Springfield, Virginia 22161

19. Security Classif. (of this report)	20. Security Classif. (of this page)	21. No. of Pages	22. Price
Unclassified	Unclassified	459	

Form DOT F 1700.7 (8-72)

METRIC CONVERSION FACTORS

Approximate Conversions to Metric Measures

Symbol	When You Know	Multiply by	To Find	Symbol
	LENGTH			
in	inches	*2.5	centimeters	cm
ft	feet	30	centimeters	cm
yd	yards	0.9	meters	m
mi	miles	1.6	kilometers	km
	AREA			
in^2	square inches	6.5	square centimeters	cm^2
ft^2	square feet	0.09	square meters	m^2
yd^2	square yards	0.8	square meters	m^2
mi^2	square miles	2.6	square kilometers	km^2
	acres	0.4	hectares	ha
	MASS (weight)			
oz	ounces	28	grams	g
lb	pounds	0.45	kilograms	kg
	short tons (2000 lb)	0.9	tonnes	t
	VOLUME			
tsp	teaspoons	5	milliliters	ml
Tbsp	tablespoons	15	milliliters	ml
fl oz	fluid ounces	30	milliliters	ml
c	cups	0.24	liters	l
pt	pints	0.47	liters	l
qt	quarts	0.95	liters	l
gal	gallons	3.8	liters	l
ft^3	cubic feet	0.03	cubic meters	m^3
yd^3	cubic yards	0.76	cubic meters	m^3
	TEMPERATURE (exact)			
°F	Fahrenheit temperature	5/9 (after subtracting 32)	Celsius temperature	°C

*1 in = 2.54 (exactly). For other exact conversions and more detailed tables, see NBS Misc. Publ. 286, Units of Weights and Measures, Price $2.25, SD Catalog No. C13.10:286.

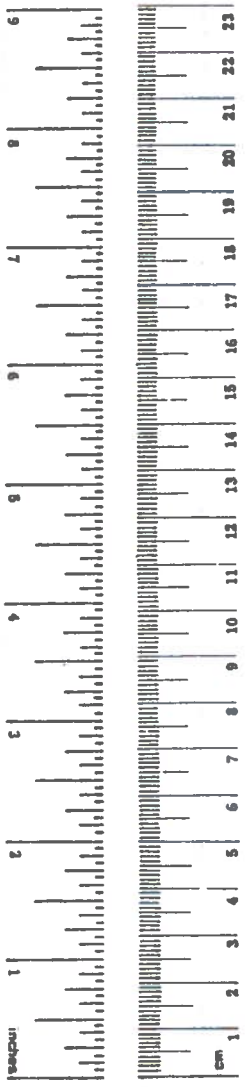

Approximate Conversions from Metric Measures

Symbol	When You Know	Multiply by	To Find	Symbol
	LENGTH			
mm	millimeters	0.04	inches	in
cm	centimeters	0.4	inches	in
m	meters	3.3	feet	ft
m	meters	1.1	yards	yd
km	kilometers	0.6	miles	mi
	AREA			
cm^2	square centimeters	0.16	square inches	in^2
m^2	square meters	1.2	square yards	yd^2
km^2	square kilometers	0.4	square miles	mi^2
ha	hectares (10,000 m^2)	2.5	acres	
	MASS (weight)			
g	grams	0.035	ounces	oz
kg	kilograms	2.2	pounds	lb
t	tonnes (1000 kg)	1.1	short tons	
	VOLUME			
ml	milliliters	0.03	fluid ounces	fl oz
l	liters	2.1	pints	pt
l	liters	1.06	quarts	qt
l	liters	0.26	gallons	gal
m^3	cubic meters	35	cubic feet	ft^3
m^3	cubic meters	1.3	cubic yards	yd^3
	TEMPERATURE (exact)			
°C	Celsius temperature	9/5 (then add 32)	Fahrenheit temperature	°F

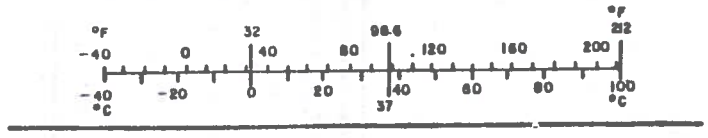

ACKNOWLEDGEMENT

The authors of this report gratefully acknowledge the guidance and support provided by the NHTSA Contract Technical Manager for this work, Dr. Y.K. Wu.

The significant conributions by Drs. L. Carpenter and D. Grimes are also appreciated.

APPENDIX F

PROPAGATION SYSTEMS IN AUTOMOTIVE RADAR

The Pennsylvania State University

The Graduate School

Department of Engineering

Propagation Systems in Automotive Radar

A Thesis in

Electrical Engineering

by

Henri Pruvot

Submitted in Partial Fulfillment
of the Requirements
for the Degree of

Master of Science

August 1981

ABSTRACT

This study is an analytical approach to some of the propagation problems encountered in the field of automotive collisions avoidance radars. Models are developed, with the aid of computer programs, to predict the radiation patterns of the most recently developed systems. These predictions provide the basis of a technical evaluation of current systems. The influence of various multipath effects is also studied in order to check the validity of some usual assumptions. The effect of atmospheric perturbations on collision avoidance radar systems is evaluated.

TABLE OF CONTENTS

LIST OF TABLES

LIST OF FIGURES

LIST OF CHARTS

ACKNOWLEDGEMENTS

The author wishes to express his gratitude to Dr. Lynn A. Carpenter and to Dr. Dale M. Grimes for their advice and guidance during the course of this work.

He wishes to extend his appreciation to Dr. Anthony J. Ferraro for sitting in his committee.

Also he would like to thank Jean-Marc Laugénie for his constant cooperation and patience.

CHAPTER I

INTRODUCTION

1.1 GENERAL STATEMENT OF THE PROBLEM

Automotive radars have been developed in order to help avoid collisions or, at least, to reduce the damage resulting from these collisions. Many studies (NHTSA-Bendix, 1973 and 1976; RCA, 1980; Bundesminister fur Forschung und Technologie, 1978 and 1979) have been done to investigate this area since the beginning of the 1970's. The major impetus initially came from the United States, Department of Transportation. Now, several automotive companies and automotive suppliers are also working towards completion of an efficient, reliable, automatic or semi-automatic, radar braking system. More comparative evaluation of those devices is needed before decisions on production and marketing can be made.

1.2 DESCRIPTION OF SYSTEMS

Many papers have been written about Automotive Radars. Grimes and Jones (1974) have drawn up a good overview of the potential applications of on-board radars. The interested reader can also refer to the NHTSA-Bendix technical report (Phase II, 1976), which presents both experimental investigations and theoretical analysis. More specific information will be found in papers issued by companies currently in the process of developing collision avoidance systems: Nissan-Mitsubishi (Fujikawa et al., 1979); C.A. Research (1981); VDO (Hahn, 1980).

1.2.1 Block Diagram

Figure 1.2.1 shows a simplified block diagram of a typical braking system. It is deliberately general in form and must be adapted to each system considered. Characteristics of currently available devices are shown in Table 1. Diagram units are described below.

1.2.2 Antenna

Several types of antenna can be used in Automotive Radars. The most widespread is the horn- or waveguide-fed parabolic reflector with circular rim shape. Other rim shapes are possible, though uncommon. Parabolas offer the advantage of high directivity and low cost. Horns are sometimes used. Horns are probably the simplest and least

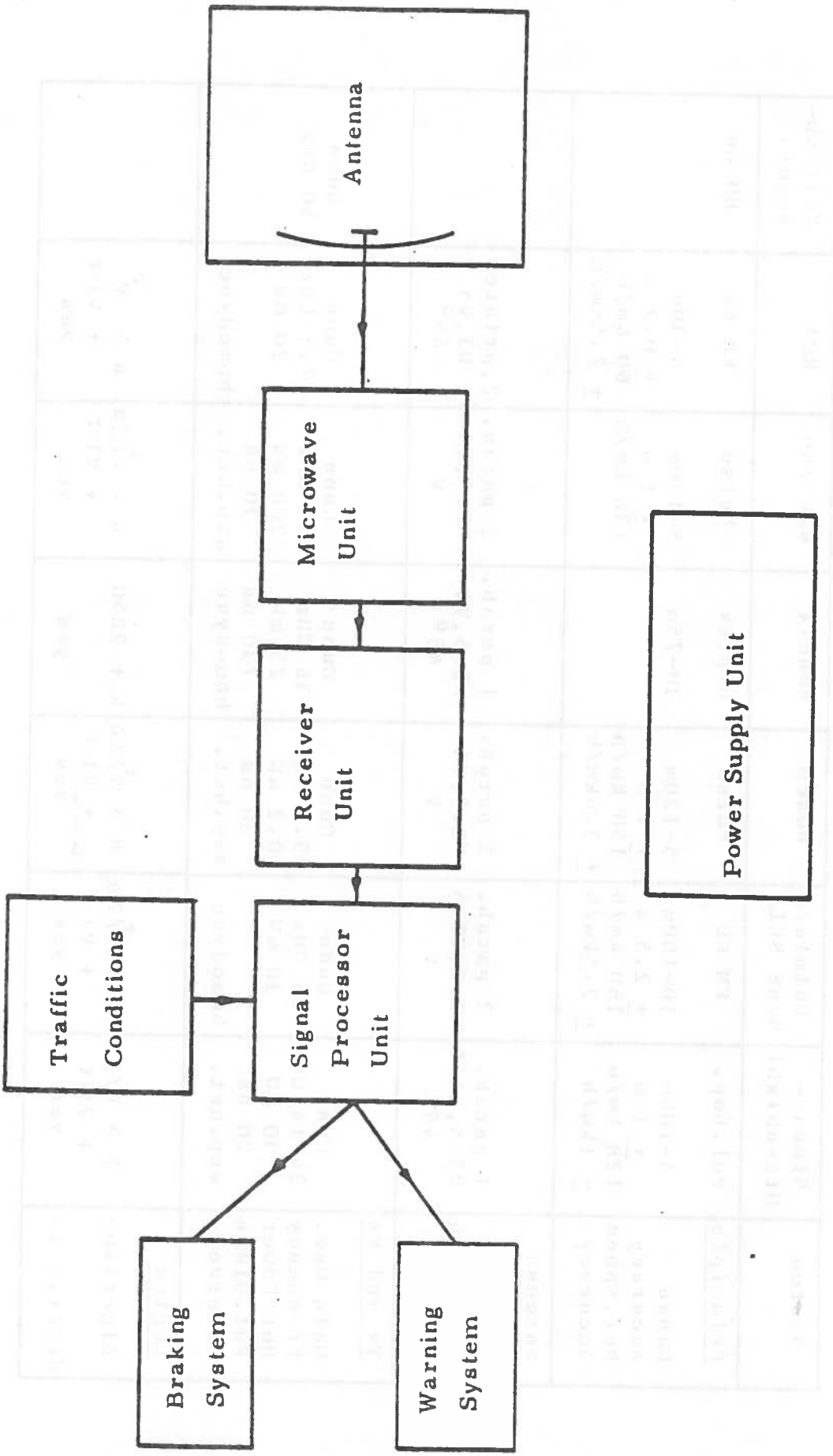

Figure 1.2.1 : System block diagram.

Table 1: Systems characteristics.

System	Nissan-Mitsubishi	Daimler-Benz SEL	Bosch	Bendix	BMW-VDO	RCA	Fujitsu-Toyota
Principle	Pul.Dop.	FM CW	Pulse	Diplex	Pulse	FM CW	FM CW
Range Accuracy Rel.Speed Accuracy	5-100m ± 1 m 128 km/h ± 1km/h	10-100m ± 2.5 m 160 km/h ± 2.5km/h	5-120m ± 1 m 150 km/h ± 3.6km/h	30-75m	5-120m ± 1 m 130 km/h	6-30m ± 0.2 m 60 km/h ± 2.5km/h	
Antenna							
# & Type Beamwidth Polar.	1 parab. H3.5,V4.5 45°	2 parab. H2.5,V3.5 V	2 parab. H2.5,V4 V	1 parab. H2.5,V4 45°	2 parab. H2.5,V4 V	2,printed H3,V5 45°	
Tx and Rx							
Main Osc. Frequency Out Power Pul.Width Receiver	Gunn 24.14 GHz 30 mW 20 ns sup.het.	Gunn 35 GHz 30 mW homodyne	Gunn 35.6 GHz 0.2 mW 30 ns sup.het.	Gunn 36 GHz 25 mW 730 ns homodyne	Gunn 35 GHz 200 mW 30 ns sup.het.	Gunn 17.5 GHz 20 mW homodyne	Gunn 50 GHz
Logics							
Algorithm Steer.w.a.	$R > V^2/2a + V1 \cdot \tau$ yes	$R > V^2/2a + V1 \cdot \tau$ yes	$R > V^2/2a + V1 \cdot \tau$ yes	$R + 2\dot{R} > 0$ yes	$R > V^2/2a + V1 \cdot \tau$ yes	$R > V^2 + V1 \cdot \tau$ yes	

expensive antenna, but the trade-off is a lower directivity and a higher side-lobe level. Arrays, dipoles and printed devices (RCA, 1980) have also been considered.

Automotive Radar antennas can be either monostatic or bistatic. A monostatic system uses the same antenna for transmission and reception. When separate antennas are used, the system is bistatic. Bistatic radars are more expensive, but more suited to overcome weather effect limitations in some cases. Though several bistatic radars have been built, the trend is now towards the monostatic configuration. Modulation, as it will be seen further, plays a critical role in that choice.

The chosen polarization is also a function of modulation. Linear polarization is generally preferable to circular polarization because it is easier to achieve. Most antennas are linearly polarized at 45^{o}, in order to avoid the blinding effects of other vehicles. Circularly polarized antennas also reduce blinding and weather clutter, the price to pay being a decrease in the power returned from the targets of interest.

1.2.3 Microwave Unit

The microwave unit generates the electromagnetic energy that is sent to the antenna; its structure depends on the type of modulation involved. As shown on Table 1, the operating frequencies of the Automotive Radars are between

10 and 40 GHz (X, Ku, K and Ka band). However, recent studies (Jones and Grimes, 1979) lead us to think that higher frequencies (around 60 to 90 GHz) will be of interest in the future. Frequency choice is critical. First, it determines the physical size and the cost of the system. Atmospheric effects severely limit the operation at higher frequencies. Finally, frequency allocation considerations must be taken into account. This is the reason that the 60 GHz Oxygen absorption peak, which is seldom used in terrestrial applications, may be chosen for Automotive Radar. This would also reduce radiation hazards.

Almost all systems consist of a Gunn diode as a main oscillator. The resulting continuous wave is then modulated. Various modulations are possible : pulse, pulse Doppler, FM-CW (with triangular, sawtooth or sinusoidal modulation), and DIPLEX (double-frequency). Extraction of the necessary information about the target is performed differently for each principle. In the pulse mode, the continuous wave is modulated by rectangular pulses, whereas more complicated shapes are involved in continuous waves devices. The FM-CW mode requires less peak power, due to the duty cycle equal to unity, but presents more danger of radiation exposure.

1.2.4 Receiver Unit

The returned signal provides information about target range and target relative velocity.

1) For a pulse-modulated radar, range is determined by measuring the time taken by the pulse to travel and return. Pulse repetition frequency must be chosen so that the maximum unambiguous range is sufficiently large (≃ 100 m). The velocity is determined either by measuring range variation with time or measuring the Doppler frequency. Pulse Doppler radars have the ability, as opposed to ordinary pulse radars, to discern moving targets even in the presence of fixed targets producing an echo several orders of magnitude greater.

2) In FM-CW modulation, except for sinusoidal modulation, the relative velocity is obtained from the Doppler frequency. Frequency modulation allows the range to be measured. However, as a beat frequency measurement is performed by counting, a fixed error is introduced. The relative velocity determination is more precise with FM-CW than with pulse radars.

3) Square wave FM-CW systems use, for modulation, two slightly different frequencies. Range is extracted in this case by measuring the relative phase of the two Dopplers. The fixed error is eliminated but radial motion is needed to obtain range information from the Doppler signals. This configuration is therefore less suited for cruise-control applications.

4) Sinusoidal FM-CW radars do not require radial motion to extract the range, but are more complicated to build. Pulse-modulated radars are often considered as better suited to long-range measurements, whereas the various FM-CW and DIPLEX systems are short-range radars.

1.2.5 Signal Processor Unit

With the advent of microcomputers, radar signal processing has been noticeably improved. These improvements have been particularly important for the development of Automotive Radar braking systems. The typical auto environment is very complex. In addition to the targets of interest, which are those for which braking or warning must be activated, other non-hazardous targets may produce enough return to generate a "false-alarm." It is clear that the best system will be the one which achieves the best compromise between actual detection of hazardous targets and the false-alarm rate.

The purpose of the signal processing unit is then to determine, from the extracted information, whether or not the alarm will be activated. Basically, signal processing is achieved in three steps: target acquisition, target detection, algorithm analysis. Signal processing units are classified into three groups, depending on the level of sophistication.

1) The first group consists of the simplest models. The target acquisition is achieved as soon as the returned signal exceeds a given threshold. The detection is automatically ensured. If the algorithm analysis produces a positive result (hazardous target), activation occurs.

2) However, for the first class of processors, a malfunction may result from the detection of a peak of noise. Processors of the second class overcome this problem. A target is detected only if, after acquisition, signal threshold is exceeded during more than a given interval of time or, alternately, more than a given interval of distance. Acquisition and detection are now two separate steps.

Various algorithms have been developed for the processors of the first two groups. All must include traffic conditions: dry or icy, smooth or rough road surfaces lead to a different maximum admissible deceleration. In addition to this, the carrier vehicle velocity and the steering wheel angle must also be taken into account. In particular, the adjunction of a steering wheel angle coefficient substantially reduces the number of false-alarms occurring on curves.

3) Systems of the third generation are still in the process of being developed. C.A. Research Corporation is working on a device which involves a more sophisticated algorithm. Activation is enabled only when the vehicle is

found to be on a collision course, a technique similar to that used by some missile guidance systems. This technique requires subdivision of the vehicle environment in elementary cells, so that a course can be determined and identified.

1.3 ANTENNA MODELING

Antenna modeling is the basis of this theoretical analysis of Automotive Radars. Radiation patterns determine the vehicle environment as it is seen by the radar. These patterns must therefore be known with a high degree of accuracy. For instance, the amount of power returned from a stop sign or a guardrail, a non-hazardous target, is directly influenced by the side-lobe level. Simple analytical models turn out to be a very inappropriate representation. This is the main reason that antenna modeling must be developed.

Beyond a confirmation of experimental results, theoretical antenna modeling, associated with target detection simulation, allows target detection to be evaluated for unusual occurrences. Hence, further improvements may be suggested and tested.

As shown in Table 1, parabolic reflectors are the most commonly encountered type of Automotive Radar antennas. They have therefore been chosen to be modeled in this study. Calculations involved in antenna modeling could not have

been successfully achieved without the aid of computer programs. These codes are described in CHAPTER III.

It must be noted that Automotive Radar antennas are operating in very particular conditions. Ground reflections, for instance, completely alter the initial antenna pattern. Therefore the modeling of the antennas would not be thorough if such propagation effects were not studied.

1.4 SYSTEMS EVALUATED

Among the various systems listed in Table 1, three will be evaluated in the context of this study.

1.4.1 Bendix System

This radar is a DIPLEX monostatic device, using a waveguide-fed parabolic antenna ($\theta v = 4^{o}$, $\theta h = 2.5^{o}$). The antenna is polarized at 45^{o}. The operating frequency is 36 GHz $\pm$ 410 kHz. The transmitted peak power is 25 mW. The receiver is a superheterodyne type. Detection is enabled if the returned signal exceeds the threshold on a given distance: 0, 11.5, and 23 feet have been tested. The processing includes steering wheel angle information and uses the following algorithm:

$$R + 2\dot{R} < 0$$

Where R is the range to the target and $\dot{R}$ is the range rate.

Dr. Grimes and Dr. Carpenter have had the opportunity to drive for several months an experimental vehicle equipped with the Bendix system. Noteworthy information has been found in the technical report issued by Bendix Research Laboratories (Bendix-NHTSA report, Phase II, 1976).

1.4.2 Nissan-Mitsubishi System

The Nissan-Mitsubishi system is a pulse-gated radar, monostatic, operating at 24.15 GHz. The horizontal and vertical antenna beamwidths are equal to 4^{o}. The antenna is a horn-fed parabolic reflector, polarized at 45^{o}. The pulse width is 20 ns and peak power 20 mW. The receiver is a superheterodyne type. The 20 ms pulses are generated by rectangular modulation of the Gunn oscillator continuous wave: the remaining CW waves are shifted 160 MHz from the original frequency and transmitted to the mixer as local oscillator signals. This produces, after mixing, intermediate frequency pulses of 160 MHz. Range information is obtained from the delay time of echo pulses, and the relative velocity is extracted from the Doppler frequency by sensing the polarity change of IF-pulses.

The processing includes a range gate controlled in accordance with the vehicle velocity and steering wheel angle. In the chosen algorithm, the safe distance is defined by:

$$R > \frac{V1^2}{a} + V1 \cdot \tau + K$$

Where :
- τ Driver's reaction time
- V1 vehicle speed
- K constant

Further information can be found in a paper issued by Nissan Motors Corporation in collaboration with Mitsubishi (Fujikawa et al., 1979). Dr. Grimes has personally visited the Japanese facilities and has been allowed to test a vehicle equipped with the Nissan-Mitsubishi system.

1.4.3 Daimler-Benz-SEL System

The Daimler-Benz-SEL radar system has been developed in Germany. Two vertically polarized antennas are used in this bistatic device. Dr. Carpenter, who went to Germany and tested a Daimler-Benz-SEL equipped vehicle, reported that a very similar monostatic radar had been developed by Bosch to replace the bistatic one: VDO, SEL and Bosch all use the same antenna by agreement. The horizontal and vertical beamwidths are 2.5° and 4° respectively. The operating frequency is 35 GHz. The chosen modulation is FM-CW and the receiver is a superheterodyne type.

The processing includes information about road conditions, steering wheel angle, and carrier vehicle velocity. The algorithm law is the following:

$$R > \frac{V1^2}{a} - \frac{V2^2}{a} + V1 \cdot \tau + K$$

Where : V2 target velocity

Target detection occurs only if the threshold is exceeded for more than 0.2 s. The false-alarm rate is reduced by eliminating targets for which relative velocity remains constant with time, such as guardrails. For more information, refer to the trip report written by Dr. Carpenter (private information, 1981) and to the documentation published by the German companies (Hahn, 1980; Düll, 1978).

1.5 PURPOSE OF THIS WORK

1.5.1 Analytical Evaluation of Available Systems

The purpose of this study is to provide the necessary information for an analytical evaluation of the three systems described in the previous section of this chapter. The results have enabled Jean-Marc Laugénie to develop an efficient simulation process to test the abilities of the devices described above. This work deals more specifically with propagation systems in Automotive Radars.

The emphasis has been put on antenna modeling considerations. Various models are derived and discussed. Hence, comparison with experimental measurements is made. These models allow the test of most of the possible configurations and offer, therefore, the opportunity to evaluate Automotive Radars other than these considered. Further improvements can also be taken into account, due to the versatility of the computer codes.

Influence of the multipath effects is also considered, so that those can be included in the general simulation program of J. M. Laugénie. In addition to this, various atmospheric perturbations like rain, fog, or snow, are modeled, and performance reduction for each radar is estimated.

1.5.2 Feed and Antenna

As it has been mentioned above, antenna modeling is deliberately restricted to horn-fed parabolic reflectors. This is the typical configuration encountered in almost all radars, and in particular in the three systems evaluated. As reflector antennas are considered, the modeling is broken into two parts.

1) Feed Modeling: The horn feed is modeled first. A computer program has been written in the course of this study to perform the somewhat tedious calculations involved. This code enables the radiation patterns of any horn,

pyramidal or not, to be calculated, and offers various possible outputs. In particular, the program creates, if desired, input files to the General Reflector Code which models a parabola. This results in saving considerable time during the interface between feed and reflector.

2) Parabolic Reflector and Antenna Pattern: Once feed patterns are computed, it is possible to model the antenna resulting from the association horn-parabola. Another code, GENREF, written by S. H. Lee and R. C. Rudduck, is used for that purpose. This program is versatile enough to accept practically any input feed pattern for parabolic reflectors with various rim shapes. Both programs are described in further details in CHAPTER III. In CHAPTER IV, the results of the runs are discussed and compared with experimental data.

1.5.3 Propagation Effects

As a necessary complement to antenna modeling, other propagation effects are studied and included in the evaluation.

1) Multipath Effects: Multipath propagation is characteristic of the complexity of the vehicle environment. Many multipath reflections can be considered. However, only a few ones can be modeled. Ground reflection has been emphasized because it is a permanent effect and, therefore, it alters permanently antenna patterns. Complete calculations

are developed for various types of road surfaces, smooth and rough, dry and wet. Conclusions are drawn and the validity of some commonly made assumptions is discussed. A similar analysis is used for other reflections due to the presence of reflecting surfaces on the shoulder of the road. The particular case of guardrails is also treated; backscattering from guardrails has been studied by J. M. Laugénie.

2) Atmospheric Particles: Atmospheric particles are found to be a serious problem at K-band, where Automotive Radars operate. Basically, limitations originate from two phenomena: attenuation and backscattering. Models coming from previous meteorological radar analysis are considered, simplified and applied to the present problem. Hence, with the aid of the derived models, the behavior of the three systems in the presence of weather clutter is estimated.

Gunn & East's compilation paper (1954), and the NHTSA-Bendix report have provided noteworthy information on this subject.

CHAPTER II

ANTENNA MODELING

The antennas modeled in this section are horn-fed parabolic dishes. This type of antenna is the most frequently used in Automotive Radars. Narrow beamwidths, high gain and reasonable cost motivate that choice. The modeling is achieved in two steps: modeling of the feed and modeling of the combination of the feed and the reflector. In this chapter, the method is described to determine the radiation patterns of such an antenna. This method also enables the influence of possible changes in geometry, frequency, or other parameters on antenna characteristics to be evaluated.

2.1 MODELING OF THE FEED

Parabolic reflectors are commonly fed by a waveguide, a flanged waveguide or a horn antenna. Horns are generally more suitable than waveguides because they have higher directivity, narrower beamwidth and, above all, because they achieve a much better matching between excitation source and

free space. A compromise must be found between matching, gain, and the physical limitations of the system, such as aperture blockage.

2.1.1 Feed Patterns Computations

Consider Figure 2.1.1. The horn geometry is characterized by the length of the flare L, and by the aperture dimensions a and b. The problem is to determine, for a given illumination of the horn, the fields radiated from the aperture in a point of observation P defined by its spherical coordinates (R,θ,ϕ). Calculations are based on the principles of diffraction theory. Each point M of the surface is assumed to radiate spherical waves and the total field radiated by the aperture is the sum of those contributions. Some additional assumptions are also made.

The horn is assumed to be long enough that its dimensions are large compared to the wavelength. Therefore, contribution to radiation from the walls can be neglected.

A(x,y), the illumination function, is preserved from the cross-section of the feeding waveguide to the plane of aperture. In other words, if a TE_{01} mode is excited in the waveguide, it will be preserved in the horn as well. However, equiphase surfaces are no longer planes. A common assumption is to approximate these surfaces by spheres. Because of the sphericity of wavefronts, a phase factor $\Delta\Phi$ is introduced. Then, the radiated field is determined

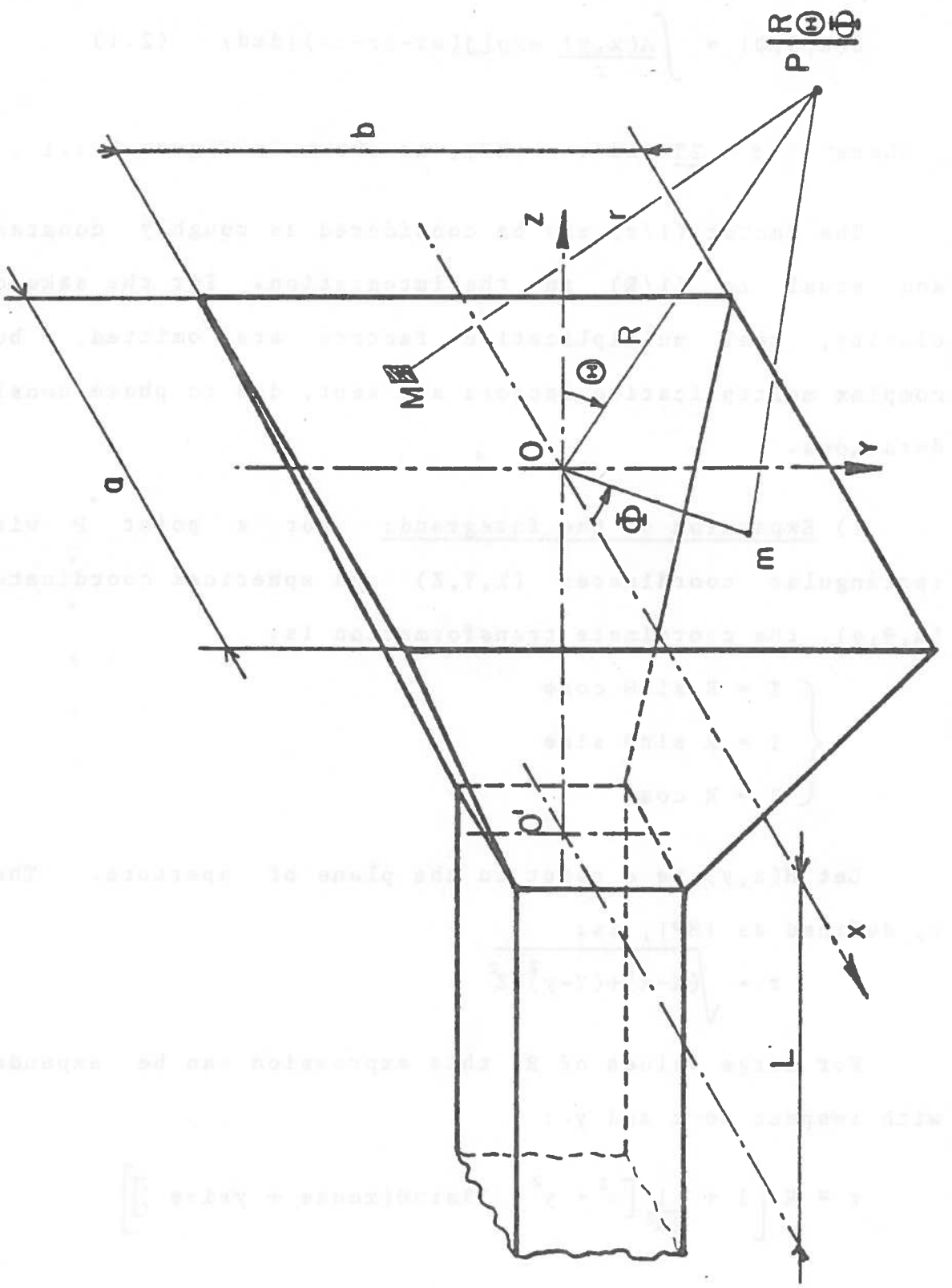

Figure 2.1.1: Horn geometry.

from:

$$E(R,\theta,\Phi) = \int \frac{A(x,y)}{r} \exp[j(wt-\beta r-\Delta\Phi)]dxdy \quad (2.1)$$

Where : $\beta = \frac{2\Pi}{\lambda}$ and $r = |MP|$, as shown in Figure 2.1.1..

The factor (1/r) may be considered as roughly constant and equal to (1/R) in the integration. For the sake of clarity, real multiplicative factors are omitted, but complex multiplicative factors are kept, due to phase considerations.

1) Expansion of the integrand: For a point P with rectangular coordinates (X,Y,Z) and spherical coordinates (R,θ,ϕ), the coordinate transformation is:

$$\begin{cases} X = R \sin\theta \cos\phi \\ Y = R \sin\theta \sin\phi \\ Z = R \cos\theta \end{cases}$$

Let M(x,y) be a point in the plane of aperture. Then r, defined as |MP|, is:

$$r = \sqrt{(X-x)^2+(Y-y)^2+Z^2}$$

For large values of R, this expression can be expanded with respect to x and y :

$$r \simeq R\left[1 + \frac{1}{2R^2}\left[x^2 + y^2 - 2R\sin\theta(x\cos\phi + y\sin\phi)\right]\right]$$

The phase error $\Delta\Phi$ introduced by the spherical wavefront corresponds to the path difference d=|MoM| shown in Figure 2.1.2 . Using straightforward trigonometry, d can be expressed as:

$$d = L\left[\sqrt{1 + \frac{(x^2+y^2)}{L^2}} - 1\right]$$

Which is expanded as:

$$d = \frac{(x^2+y^2)}{2L}$$

The integral expression for electric field becomes:

$$E = \int A(x,y) \cdot \exp\left[j\beta \left(\sin\theta(x\cos\phi + y\sin\phi) - \frac{(x^2+y^2)}{2}\left(\frac{R+L}{R\cdot L}\right)\right)\right] dxdy \quad (2.2)$$

2) <u>Choice of an illumination function:</u> A(x,y) is the last term of the integral in Equation (2.2) which must be evaluated before the integration can be performed. As shown in Figure 2.1.3, various illumination functions may be chosen. Three cases are treated here: a) constant illumination, b) cosine illumination or TE_{01} mode, and c) tapered illumination. Usually, horns are fed by a waveguide propagating the dominant mode TE_{01} (cosine mode). Tapered modes involve more complex calculations. It will be seen later how the choice of an illumination function influences the pattern shape.

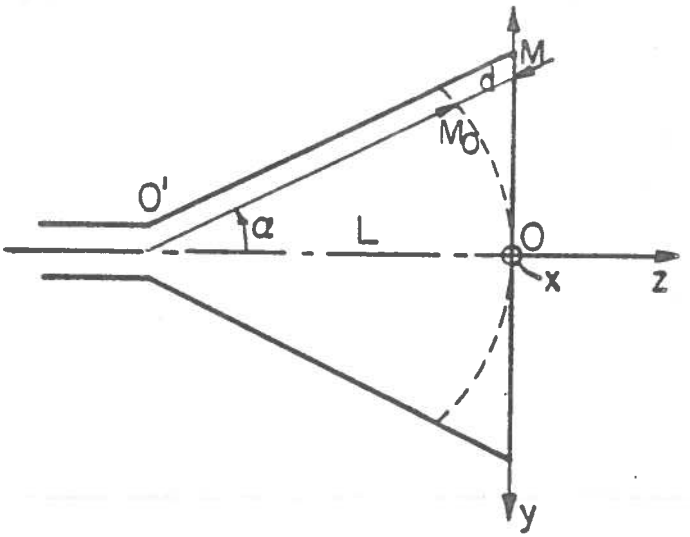

Figure 2.1.2: Phase error.

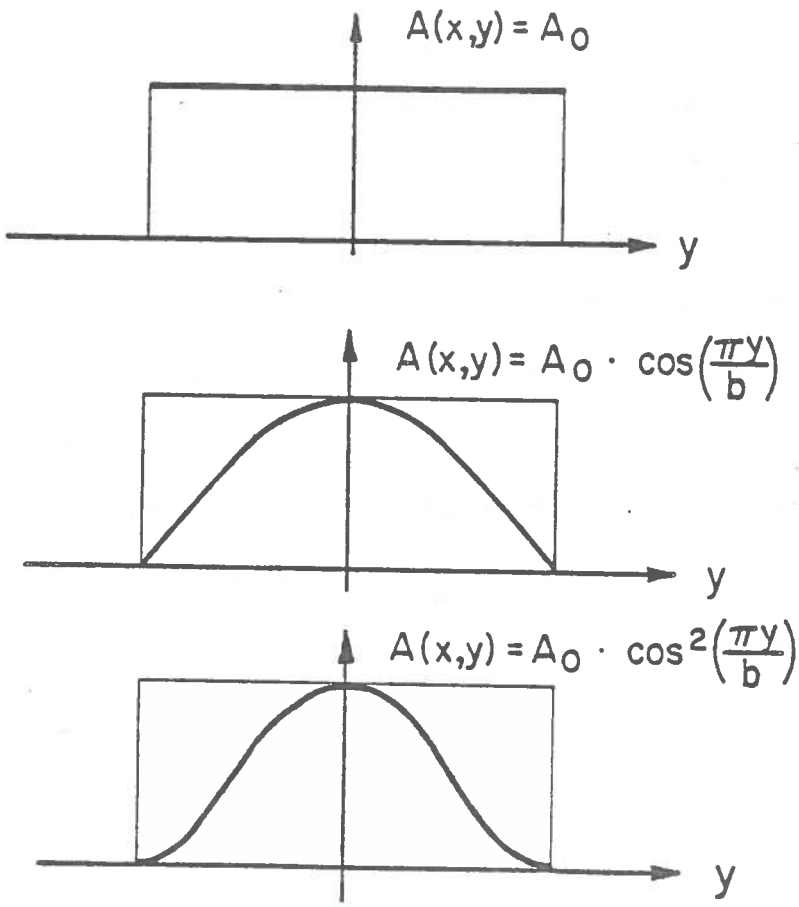

Figure 2.1.3: Illumination functions.

3) Case of a Constant Illumination: Calculations are similar for the three types of illumination chosen. For the sake of clarity, only the main results of these tedious integrations are presented below. The interested reader will refer to APPENDIX A for the details of the calculations.

For a constant illumination, A(x,y) is equal to a constant Ao. Since the integration domain is a rectangle, the integration variables can be separated, and the integral can be written as a product of two integrals on x and y :

$$E(R,\theta,\phi) = Ix \cdot Iy$$

Ix and Iy are similar. Computation of Ix and Iy involves Fresnel's integrals. Reducing the expression into a canonical form, the final result is :

$$E(R,\theta,\phi) = \alpha \cdot Jx \cdot Jy \qquad (2.3)$$

Where : $\alpha = \exp[j\frac{\pi X}{\lambda} \cdot \sin^2\theta]$

$$X = \frac{R \cdot L}{(R+L)} \text{ and } Y = \sqrt{\frac{\lambda X}{2}}$$

$$\begin{cases} A = \sin\theta \cdot \cos\phi \text{ and } B = \sin\theta \cdot \sin\phi \\ Jx = \Delta C(w\pm) - j\,\Delta S(w\pm) = \Delta F(w\pm) \\ Jy = \Delta C(u\pm) - j\,\Delta S(u\pm) = \Delta F(u\pm) \end{cases}$$

These reduced notations are explained in further detail in APPENDIX A. "F" refers to the Fresnel integral in its canonical form:

$$F(x) = \int_0^X \exp[-\frac{j\pi v^2}{2}] \cdot dv = C(x) - jS(x)$$

The integral boundaries of Jx and Jy are w+ and w-, u+ and u-, where :

$$\begin{cases} w\pm = [A \cdot X \pm \frac{a}{2}]/Y \\ \\ u\pm = [B \cdot X \pm \frac{b}{2}]/Y \end{cases}$$

4) Case of a Cosine Illumination: For this mode the illumination is :

$$A(x,y) = Ao \cdot \cos(\pi y/b)$$

The E-field will be written in a form similar to that found in the first case :

$$E(R,\theta,\phi) = \alpha \cdot Jx \cdot Jy \qquad (2.4)$$

With :

$$\begin{cases} Jx \text{ unchanged} \\ Jy = \gamma \cdot J(y,+) + \gamma^* J(y,-) \\ J(y,+) = \Delta F(u\pm) \text{ and } J(y,-) = \Delta F(v\pm) \end{cases}$$

And :

$$\alpha = \exp[\frac{j\pi X}{\lambda} \cdot (\sin^2\theta + \frac{\lambda^2}{4b^2}]$$

$Y = \exp[j \cdot \frac{X \pi B}{b}]$ and Y^{*} = complex conjugate of Y

$$\begin{cases} w_{\pm} = [A\,X \pm \frac{a}{2}]/Y \;, \quad u_{\pm} = \left[(B + \frac{\lambda}{2b}) \cdot X \pm \frac{b}{2}\right]/Y \quad , \text{ and} \\ v_{\pm} = \left[(B - \frac{\lambda}{2b}) \cdot X \pm \frac{b}{2}\right]/Y \end{cases}$$

In order to perform the integration, Jy is broken into two sub-integrals J(y,+) and J(y,-) which are introduced by the expansion of the cosine in its exponential form.

5) Case of a Tapered Illumination: The simplest tapered mode is a cosine squared illumination :

$$A(x,y) = Ao.\cos^{2}(\Pi y/b)$$

Calculations for this mode are much longer but quite similar :

Jx is the same as before.

Because of the linearization and the expansion of the cosine squared term, Jy must be broken into three sub-integrals. The final expression for the field in the tapered mode is then :

$$E(R,\theta,\phi) = \alpha \cdot Jx \cdot \left[J(y,+) + (1/2) \cdot \delta \cdot \left(\gamma \cdot J(y,-,+) + \gamma^{*} \cdot J(y,-,-) \right) \right] \qquad (2.5)$$

In which :
$$\begin{cases} J(y,+) = \Delta F(t\pm) \\ J(y,-,+) = \Delta F(u\pm) \\ J(y,-,-) = \Delta F(v\pm) \end{cases}$$

$$\begin{cases} \alpha = \exp\left[j\Pi X \cdot \dfrac{\sin^2\theta}{\lambda} \right] \\ \delta = \exp\left[j \dfrac{\Pi \lambda X}{b^2} \right] \end{cases}$$

$$\begin{cases} \gamma = \exp\left[2j\Pi \dfrac{X \cdot B}{b} \right] \end{cases}$$

With the corresponding integral boundaries :

$$\begin{cases} w\pm = [AX + a/2]/Y \; ; \quad t\pm = [BX \pm b/2]/Y \end{cases}$$

$$\begin{cases} u\pm = \left[(B + \lambda/a)X \pm b/2 \right]/Y \\ v\pm = \left[(B - \lambda/a)X \pm b/2 \right]/Y \end{cases}$$

2.1.2 Discussion of the Results

1) Preliminary remarks : It is noted that this calculation could have been performed using Maxwell's equations. Starting from Huygens' principle is implicitly equivalent to assuming E- and H-plane separation; this corresponds to the separation of the variables x and y. Consequently, the integral can be separated into a product of two sub-integrals.

The expression of the field is given in normalized values. However, as multiplicative complex factors have not been skipped in the calculations, it is possible to compute the phase of the integral which is the sum of the respective phase of each term of the product.

The coefficient $\exp[-j\beta R]/R$ does not appear in the expression of the field because, for a given pattern, it is kept constant as ϕ varies.

2) Validity of the assumptions: As mentioned above, horn dimensions must be large enough compared to.wavelength, so that radiation from the walls can be neglected. In addition to this, when the horn is sufficiently long, the aperture field would not be changed significantly if the horn extended to infinity. Edge effects are also negligible.

It is very important that only the dominant mode propagates in the horn. This is achieved by feeding the horn by an appropriate waveguide, that is to say a waveguide which allows propagation of the only chosen mode. However, higher order modes are generated by the abrupt termination of the horn.

The preservation of the mode in the horn is a complex problem. In order for the assumptions to hold, it is necessary that horn geometry be as symmetrical as possible. Otherwise, the wavefront is distorted from its assumed

shape.

3) Gain Calculations : The field can be related to the antenna directive gain by (Weeks,1963):

$$Gd = \sqrt{\frac{\epsilon_0}{\mu_0}} \frac{|E|^2 2\pi r^2}{Prad} \qquad (2.6)$$

Where Prad is the average radiated power per unit area. Prad must be computed for each type of illumination from:

$$Prad = (1/2)\,Re\left[\int_0^a\int_0^b \frac{Eo^2 \cdot A(x,y)}{\sqrt{\frac{\mu_o}{\epsilon_o}}}\,dxdy\right] \qquad (2.7)$$

The results for different cases are :

(I) Constant illumination : $Prad = \frac{Eo^2 \cdot ab}{\sqrt{\mu_o/\epsilon_o}} \cdot \frac{1}{2}$

(II) Cosine illumination : $Prad = \frac{Eo^2 \cdot ab}{\sqrt{\mu_o/\epsilon_o}} \cdot \frac{1}{4}$

(III) Tapered mode : $Prad = \frac{Eo^2 \cdot ab}{\sqrt{\mu_o/\epsilon_o}} \cdot \frac{3}{32}$

It is therefore possible, for illuminations other than TE_{01} mode, to generalize the expression of the gain, as given by Thourel (1960) for the case of a cosine:

$$G(R,\theta,\phi) = (\pi/32)\cdot[(\lambda/b)Ge]\cdot[(\lambda/a)Gh] \qquad (2.8)$$

Where : $Ge = \frac{64bL\cdot|Jx|^2}{a\pi\lambda}$ (E-plane gain)

And : $Gh = \frac{4\pi aL\cdot|Jy|^2}{b\lambda}$ (H-plane gain)

Defining for that purpose a coefficient (coeff), respectively equal to 1, (1/2), and (3/16) for each mode, and combining these expressions yields the final result :

$$G(R,\theta,\phi) = \frac{8\pi}{ab} L^2 \left| \frac{Jx\ Jy}{coeff} \right|^2 \qquad (2.9)$$

According to Thourel (1960), the values computed may differ from the measured ones by more than 10% in some cases. However, a much better precision is obtained for normalized values (see CHAPTER IV).

3) Optimization of horns: Two definitions are given for optimal horns. The first defines the optimal geometry as being the one for which $\Delta\Phi$, the maximum phase error, is equal to $\pi/2$. The second definition, which appears to have more physical meaning is: " the optimal geometry is that which maximizes the directivity (Collin and Zucker, 1969)." As a matter of fact, both definitions are nearly equivalent. This can be shown with the aid of the Cornu's spiral, which is plotted in Figure A.1 of APPENDIX A. Figure A.2 shows the magnitude of the integral versus the argument.

The Cornu's spiral is a representation of the Fresnel's integrals in the complex plane. This curve shows that if a or b is increased, the argument of Jx or Jy is increased and therefore the magnitude of the field increases first, then decreases and oscillates around a limit value. It seems intuitive that there must exist a geometry for which the gain is maximum, even when the integral boundaries are more

complex than in the simple case. Actually, this discussion of the Cornu's spiral properties is valid only in the case of a constant illumination, but the other cases are similar. Coming back to the optimization of the horn, the spiral shows that F(x), the Fresnel's integral, is maximum for x = 1.225 (Jordan and Balmain, 1968). Silver (1965) implicitly approximates this value by 1: taking this argument equal to 1 implies that, to a first approximation, aperture dimensions are such that $\Delta\Phi \simeq \pi/2$. In that case it is seen that both definitions are equivalent.

For the case of a pyramidal horn, there is an ambiguity in the definition of the maximum phase error. Rather than a maximum geometrical phase error, corresponding to the value computed in the diagonal planes, it is preferable to define a maximum phase error in each plane:

$$\begin{cases} \text{E-plane:} & \Delta\Phi \max = \dfrac{2\pi}{\lambda}\dfrac{a^2}{8L} \\ \text{H-plane:} & \Delta\Phi \max = \dfrac{2\pi}{\lambda}\dfrac{b^2}{8L} \end{cases}$$

Alternately, an optimum flare angle is defined by:

$$\theta o \max = 2 \operatorname{Arccos}\left[\frac{L}{L+do}\right] \qquad (2.10)$$

Where do is the path difference corresponding to the maximum phase error.

2.2 MODELING OF PARABOLIC REFLECTOR ANTENNAS

2.2.1 Principle of the Calculation

The problem of the parabolic reflector antenna is to determine, knowing the radiation patterns of a given feed, the final patterns resulting from the association of the feed and the reflector. In the case of Automotive Radar antennas, the feed is generally a horn or a waveguide. The previous section of this chapter enables the radiated fields of a horn to be determined. This section describes how the connection is done between feed and reflector.

Figure 2.2.1 shows a typical geometry for a horn-fed parabola. The feed is located at the focus of the paraboloid of equation:

$$r^2 = 4fz$$

Where (r,z) are the cylindrical coordinates and f is the focal distance.

The main property of the parabola is that if a point source is located at the focus f, any ray from the focus is reflected in a direction parallel to the axis. The pencil beam created that way is a plane wave. In any plane intersecting the beam, all points have the same phase, for the path length from the focus to the plane is a constant: this is also a way to define a parabola or a paraboloid.

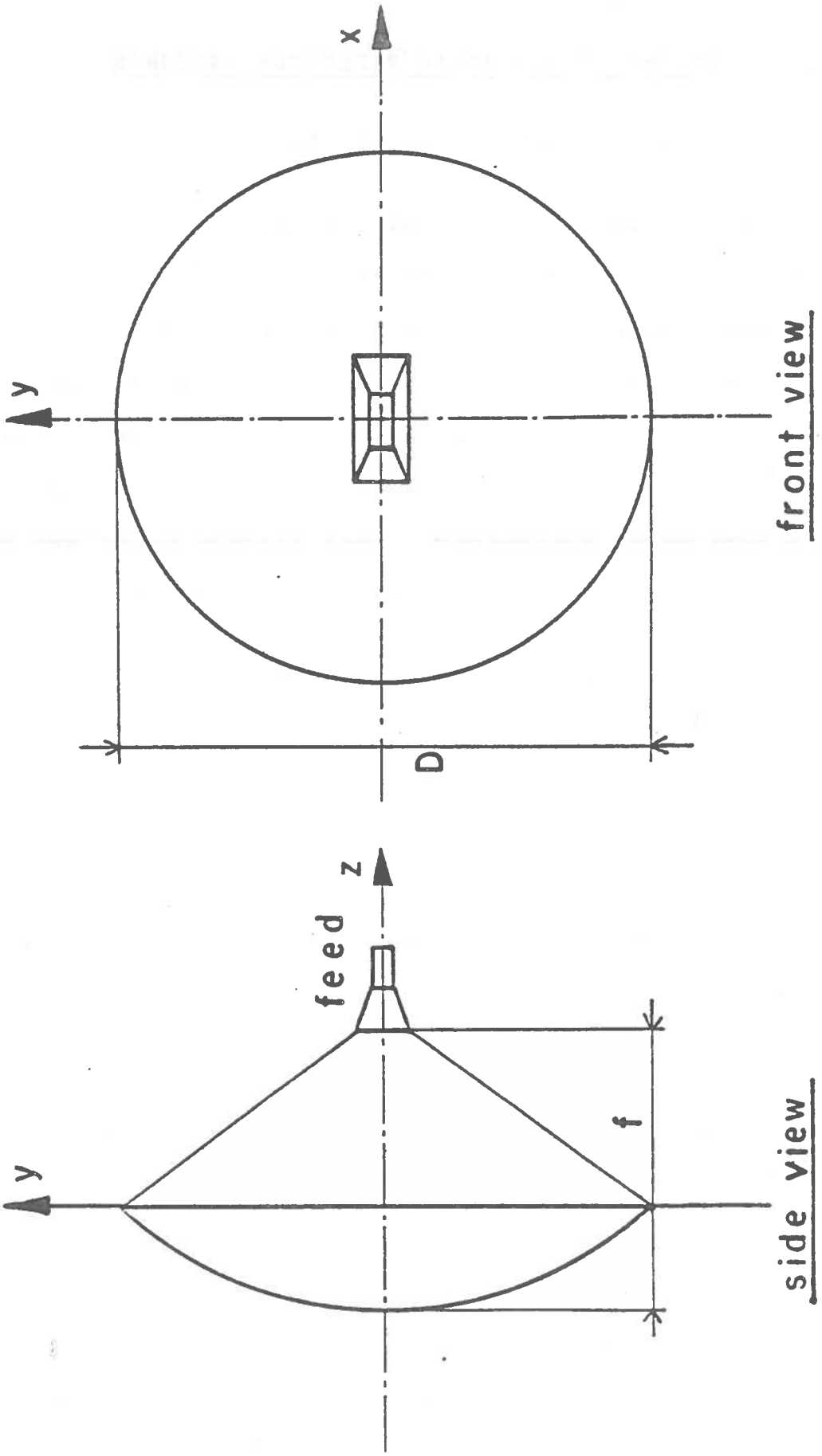

Figure 2.2.1: Reflector geometry.

However, a real plane wave is created only if the source is isotropic. For an anisotropic source, a different azimuth angle corresponds to a different field intensity.

These considerations are drawn from elementary Geometrical Optics. As a matter of fact, precise determination of the patterns is a very complex problem, and the calculations involved are far beyond the scope of this study. To solve the problem, a computer program, NECREF, is used. This code has been written by R. C. Rudduck and S. H. Lee (1979), from Ohio State University, under the sponsorship of the Navy: the original purpose of the code was to provide the necessary information to model parabolic reflectors, such as those used by the Navy. It is found that the problem of Automotive Radar antennas is very similar to that of a radar antenna in a complex ship environment. Both systems operate at Gigahertz frequencies, above a reflecting plane, at low grazing angles, and in a similar environment. The code and the computations it performs are described in further detail in the following chapter. NECREF is based on two techniques: Aperture Integration (AI), and Geometrical Theory of Diffraction (GTD). The interested reader may refer to the work of Keller (1962) for a general formulation of GTD, and to "Reflector Antenna Analysis and Design", from P. J. Wood (1980), for solutions to some of the canonical problems encountered in diffraction calculations.

Though the mathematics involved in GTD deal with modern complex analysis, the basic idea of the theory is simple. Keller's GTD is an improvement of ray theory, taking into account both diffracted rays and polarization. It is the logical link between Geometrical Optics (GO), and Physical Optics (PO). GO can be seen as the high frequency limit case, whereas PO is based on wave theory and Huygens' principle. The application of Green's vector identities to Maxwell's equations leads to the general set of equations known as K.H.S. equations (Kirchhoff-Huygens-Silver). The computation of the field requires asymptotic expansions of these equations. Recent improvements have been done to extend the theory to the regions of the space where GTD turns out to be invalid, shadow zones in particular.

2.2.2 Modeling of the Antenna

NECREF is a very versatile code. It provides an accurate representation of antenna patterns, for various possible geometries. Application of the code to the systems evaluated is done in CHAPTER IV. It will be seen that discrepancies with measured values occur, despite the efficiency of the program. These discrepancies result in part from some limitations of the code itself, such as the impossibility of evaluating aperture blockage limitations. The accuracy of the results is not discussed in this section. NECREF provides the connection between feed and reflector. Predetermined or measured feed patterns are

input to the program. A deck of command cards helps specify the geometry, the parameters of the problem and the desired output. In order to save time during the runs, an interface has been created between the feed modeling program and NECREF. Therefore, a substantial number of mistakes have been avoided. Moreover, additional runs do not require important modifications of the input deck. The emphasis has been put on the reduction of the amount of data input to the program or stored during the runs of the program.

CHAPTER III

PROGRAM DESCRIPTIONS

Antenna modeling has been achieved with the aid of the two computer codes described in this chapter: HORN and NECREF. These programs are written in VAX-11 FORTRAN. HORN deals with the modeling of pyramidal horns and has been developed in the course of this study. NECREF is the work of R. C. Rudduck and S. H. Lee (1979), from Ohio State University; it enables the radiation patterns of parabolic reflectors to be determined.

3.1 HORN

Given a horn geometry and the operating conditions, the basic problem is to determine the resulting spatial field distribution. It was necessary to develop a FORTRAN program to achieve the tedious integrations involved in patterns computations. In particular, Fresnel's integrals evaluation requires either asymtotic expansions, or Riemann or Simpson integrations.

Another purpose of HORN is to create a simple interface between feed modeling and reflector modeling. The program, in addition to patterns determinations, generates properly formatted files which are input to NECREF.

Flow charts are shown in Charts 1 and 2. The program itself is listed in APPENDIX B.

3.1.1 Input to the Code

There are 5 parameters input to the program HORN that are described as follows:

1) Horn Geometry: L, a, b, as defined on Figure 2.1.1 from CHAPTER II. All dimensions are input in units of cm.

2) Wavelength: From the value of λ, the frequency is computed and printed on the terminal; this allows one to check if no mistake has been committed in the conversion.

3) Pattern Parameters: these are the distance of observation R, in cm, ϕ which defines the plane of observation, in degrees, and N, number of pattern points for which field calculation is requested. At that stage, the program computes the maximal phase error and compares it to $\pi/2$: the maximal geometrical phase error has been chosen for simplicity. If $\Delta\Phi$ max is greater than $\pi/2$, a message is printed.

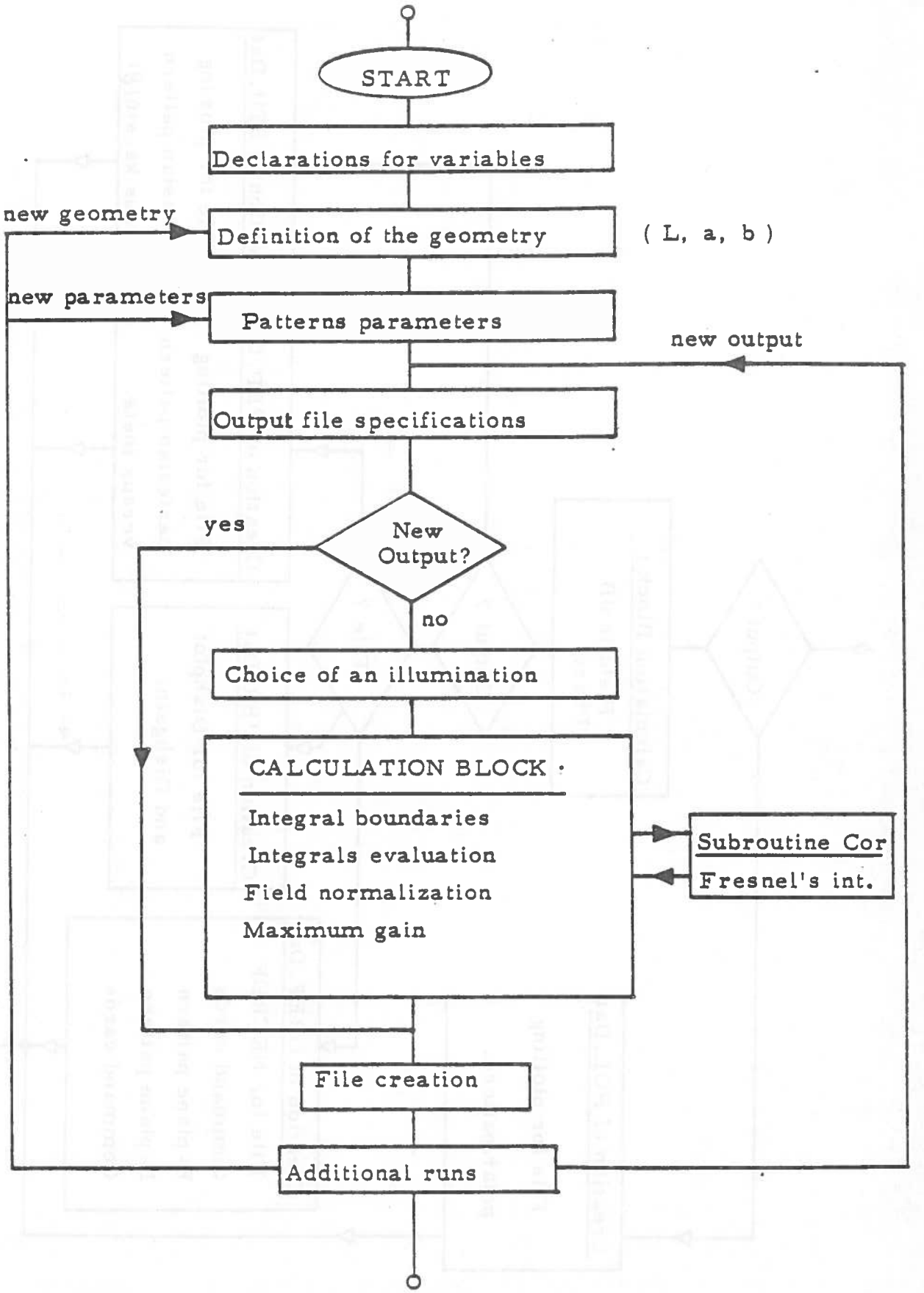

Chart 1: HORN. Flow chart diagram.

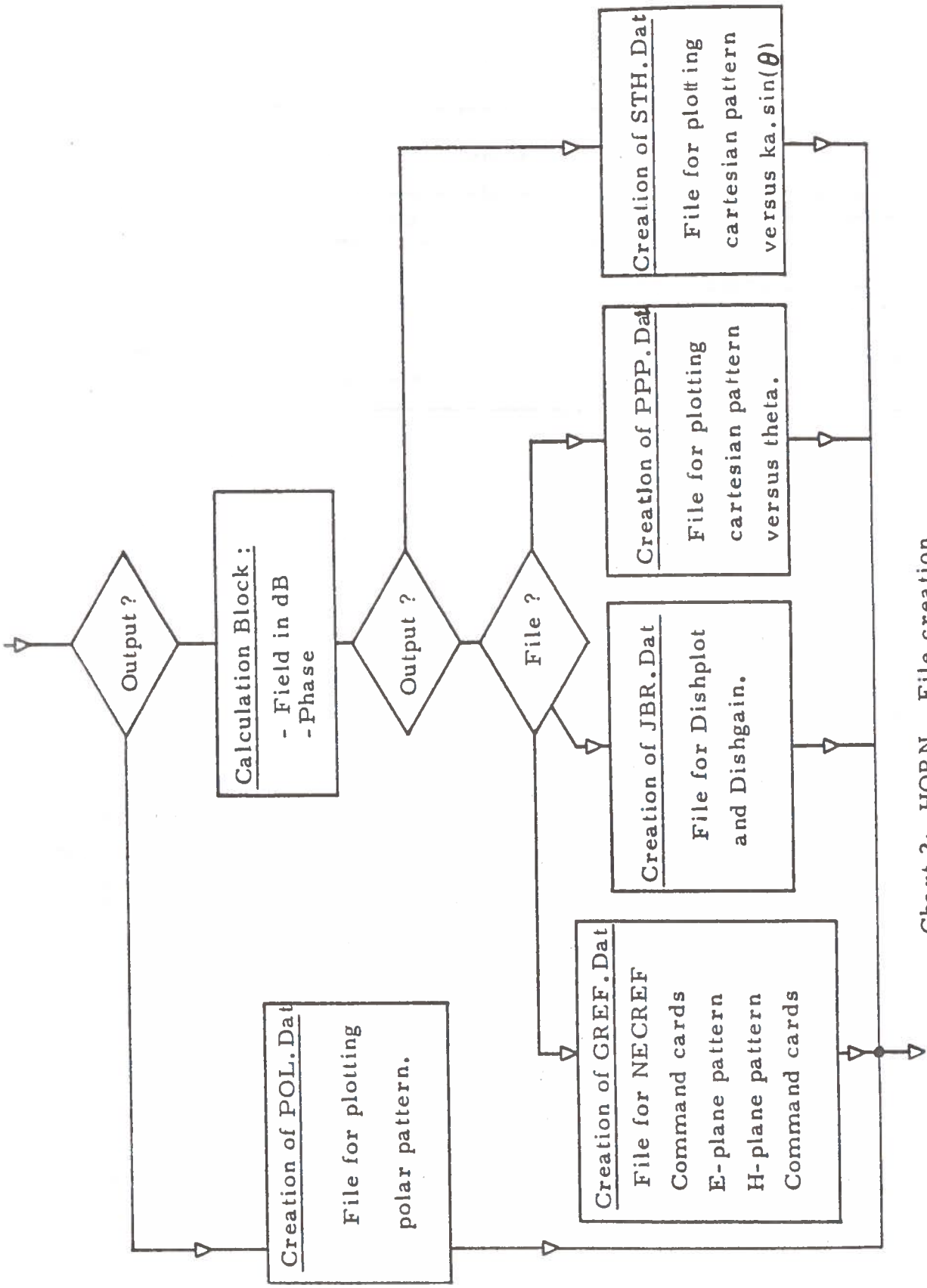

Chart 2: HORN. File creation.

4) Output Files: The nature of the output file is specified. It is possible to choose various types of pattern representations: polar pattern, cartesian representation versus θ, or versus $k \cdot a \cdot \sin\theta$, with $k = (2\pi/\lambda)$. The user must also specify whether or not he intends to create an input file for NECREF. Another code, DISHPLOT, had been considered at the beginning of the study. Though it was decided later to use only NECREF, there still remains the DISHPLOT option in the program.

5) Illumination Function: The choice of an illumination function is the last input to the code. Three functions are allowed : constant, cosine or cosine squared illumination.

3.1.2 Integrals Evaluation

Integrals evaluation is achieved in two steps for each value of θ considered in the DO LOOP.

1) Integral Boundaries: Integrals boundaries are determined first, according to the type of illumination selected. Instead of rewriting the integral expression of the complex field, it is much more suitable to find a more general modular expression, and to replace each module by its corresponding value, determined for the type of illumination. The complex coefficients computed in the previous chapter (α, δ, γ) and the boundaries are therefore illumination dependent.

2) Fresnel's Integrals: Complex integrals evaluation requires an estimation of Fresnel's integrals, discussed in CHAPTER II and APPENDIX A. A subroutine COR is used for that purpose. Real and imaginary parts of F(x) are computed by the program COR, with:

$$\mathrm{Re}[\ F(x)\ ] = \int_0^X \cos\frac{\pi u^2}{2}\cdot du = C(x) \qquad (3.1)$$

$$\mathrm{Im}[\ F(x)\ ] = \int_0^X \sin\frac{\pi u^2}{2}\cdot du = -\ S(x) \qquad (3.2)$$

These expressions are the canonical forms of Fresnel's integrals. Two methods of evaluation are possible. The first method is an asymptotic expansion of the integrals for small and large values of the argument x. But this implies storage of a large number of coefficients, if high accuracy is desired. The second opportunity is to use a simple Riemann integration method. The only restriction is that the increment must be carefully chosen to achieve the required precision. COR is based on this method. The increment has been set to 1/500th of the value of the argument x: Cornu's spiral plotted in APPENDIX A shows that this value produces good results.

3.1.3 Horn Directivity

Determination of the directivity of the horn follows from the evaluation of the integrals. The directivity is defined as the gain in the principal direction. Its value in dB is :

$$GdB\ max = 10 \cdot \log\left[\frac{8\pi L^2}{ab \cdot coeff}\right] + 20 \cdot \log\left[\max|Jx \cdot Jy|^2\right] \quad (3.3)$$

The value of GdB max is stored and printed in the end after file creation. Coeff is a coefficient, defined in the former chapter, which takes into account the change of illumination function A(x,y), in the evaluation of the average power radiated from the aperture. Jx and Jy are integrals defined in chapter II.

3.1.4 File Creation

As mentioned above, file creation depends on the further intentions of the user.

When only feed pattern determination is desired, a sequential file is written, without character data, in order to enable the drawing of a computer plot. According to the type of output selected at the beginning of the run, different files are created. A single file is opened and named after the choice of output. Polar patterns are computed in normalized values (max=1), whereas cartesian patterns are in normalized dB values (max=0).

If, instead of plotting feed patterns, the user wants to input the computed values to NECREF, a file GREF.DAT is then created. GREF.DAT is much more complicated to write. It must be formatted to the exact specifications of NECREF. The deck of input command cards required is described in the next section of this chapter. A compromise must be found

between accuracy of the modeling and CPU time spent. Therefore, it has been decided to input only two feed patterns (E- and H- planes), each one being computed for 14 points. A first deck of command cards is written before the E-plane pattern is determined. Then, the program returns to the beginning of the DO LOOP, increments the value of ϕ by 90°, and computes the H-plane pattern. Finally, the remaining command cards are written and the file is closed.

3.1.5 Additional Runs

A test is included into the end of the program, in order to enable the user to perform additional runs. According to the desired changes (geometry, parameters, type of output...), various GO statements are issued, thus minimizing the amount of additional computations. In particular, when another type of output is wanted, this procedure saves a lot of CPU time.

A series of tests is added to make possible the interconnection of the various options, in particular to ease the creation of GREF.DAT.

3.2 NECREF

3.2.1 General Description of the Code

NECREF has been developed under the sponsorship of the Navy in order to simulate reflector antennas at UHF and above frequencies, such as those operating in a complex ship environment. Practically any feed pattern may be input to the code. Another feature of the code is that various rim shapes can be considered: circular, elliptic, or rectangular with chopped corners, as usual Navy reflectors. However, the modeling is restricted to the only class of parabolic antennas. In addition to this, the feed must have a constant phase pattern. In this study, NECREF has been used only to determine radiation patterns of Automotive Radar antennas. But the code offers the opportunity to solve many other problems like near-field calculations, coupling of small antennas, and radiation hazard evaluation.

A flow diagram of the main program is listed in Charts 3 to 7. As mentioned in CHAPTER II, the basic techniques used are the Geometrical Theory of Diffraction, GTD, and Aperture Integration, AI. AI allows determination of the main beam and the first side-lobes, whereas GTD is used for computation of the wide-angle side-lobes and the back-lobes. Feed patterns may be input either from measured data, or under the form of analytical functions. In the case of a discrete input, in other words when measured values are input, linear interpolation between the values of

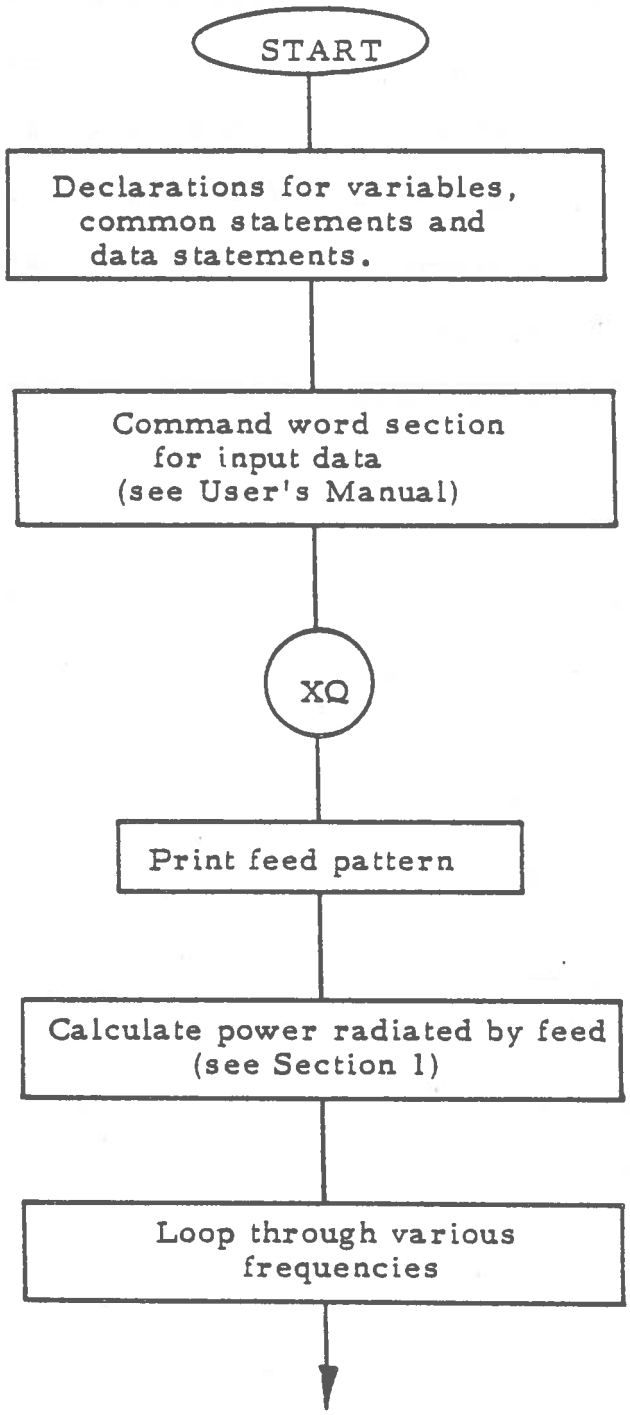

Chart 3: NECREF. Flow chart diagram (main).

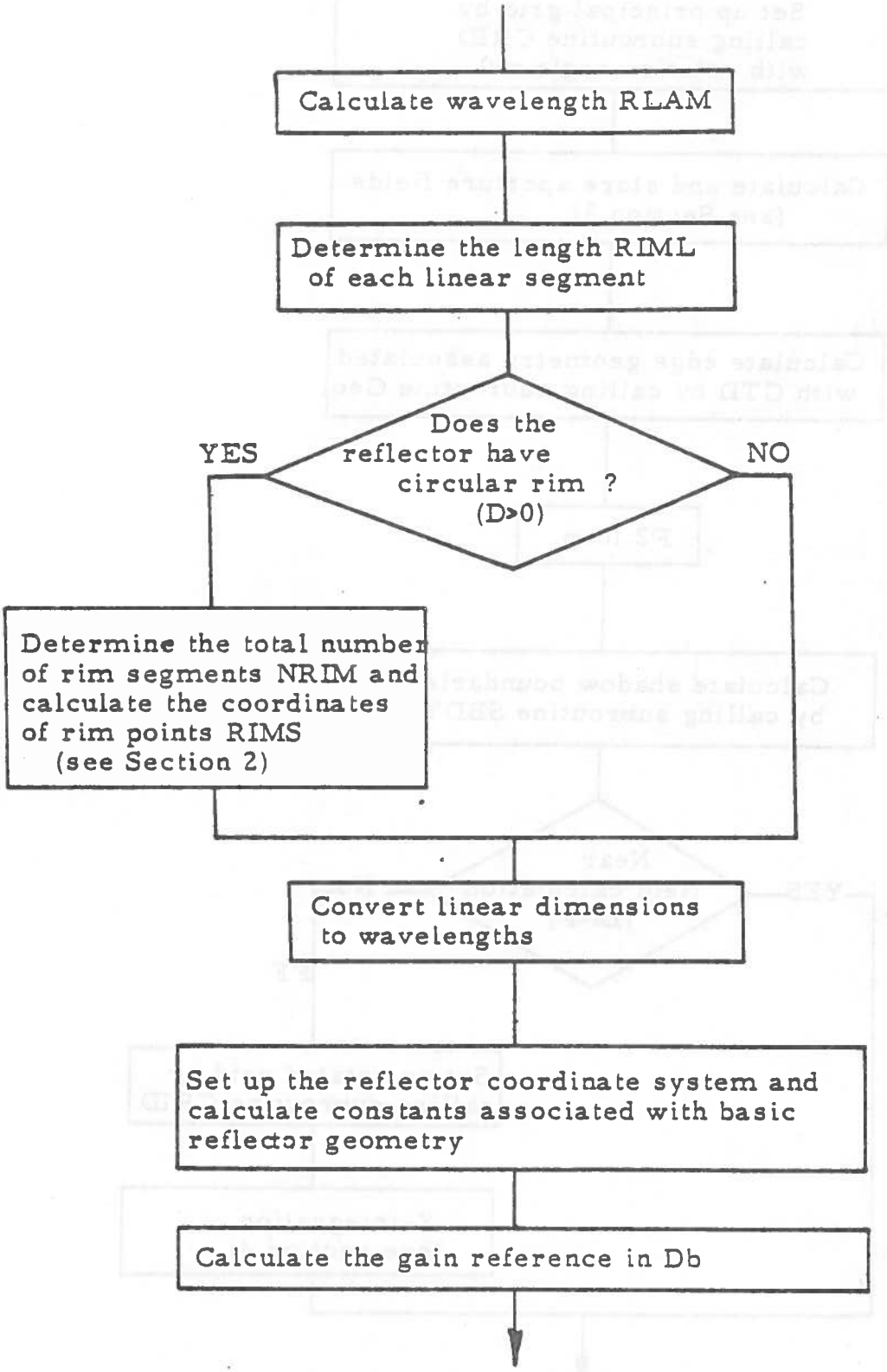

Chart 4: NECREF. Flow chart diagram (main).

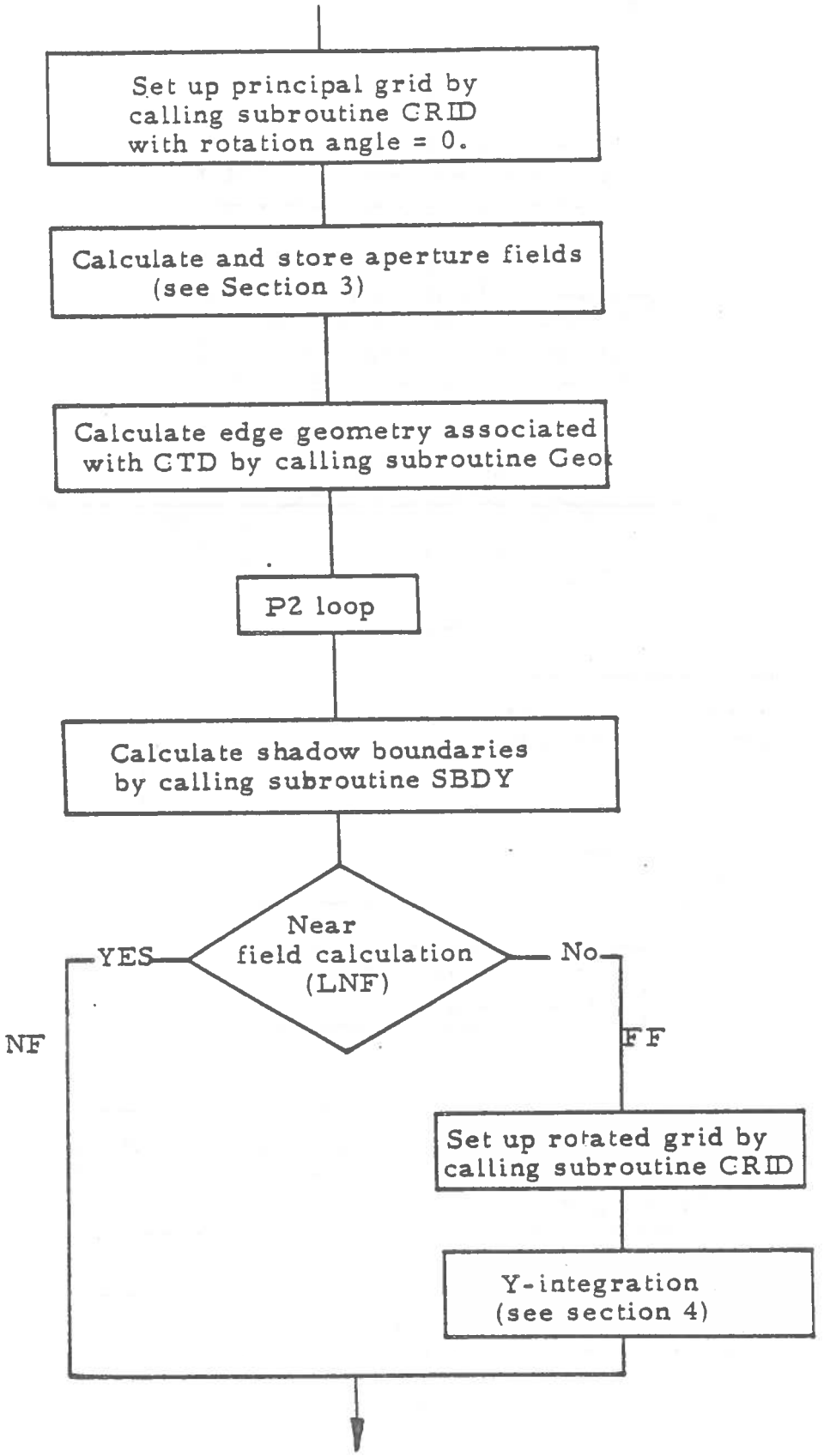

Chart 5: NECREF. Flow chart diagram (main).

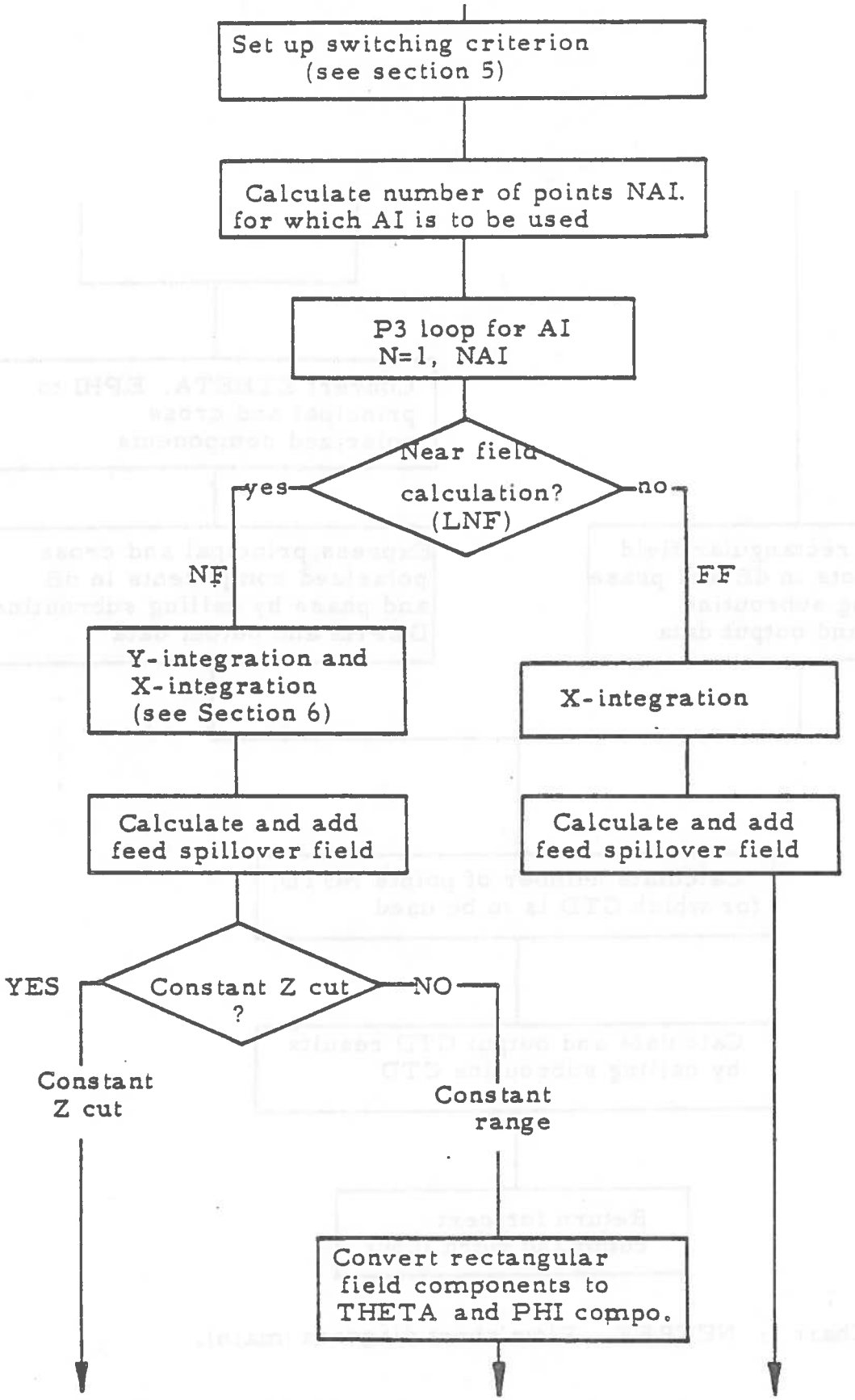

Chart 6: NECREF. Flow chart diagram (main).

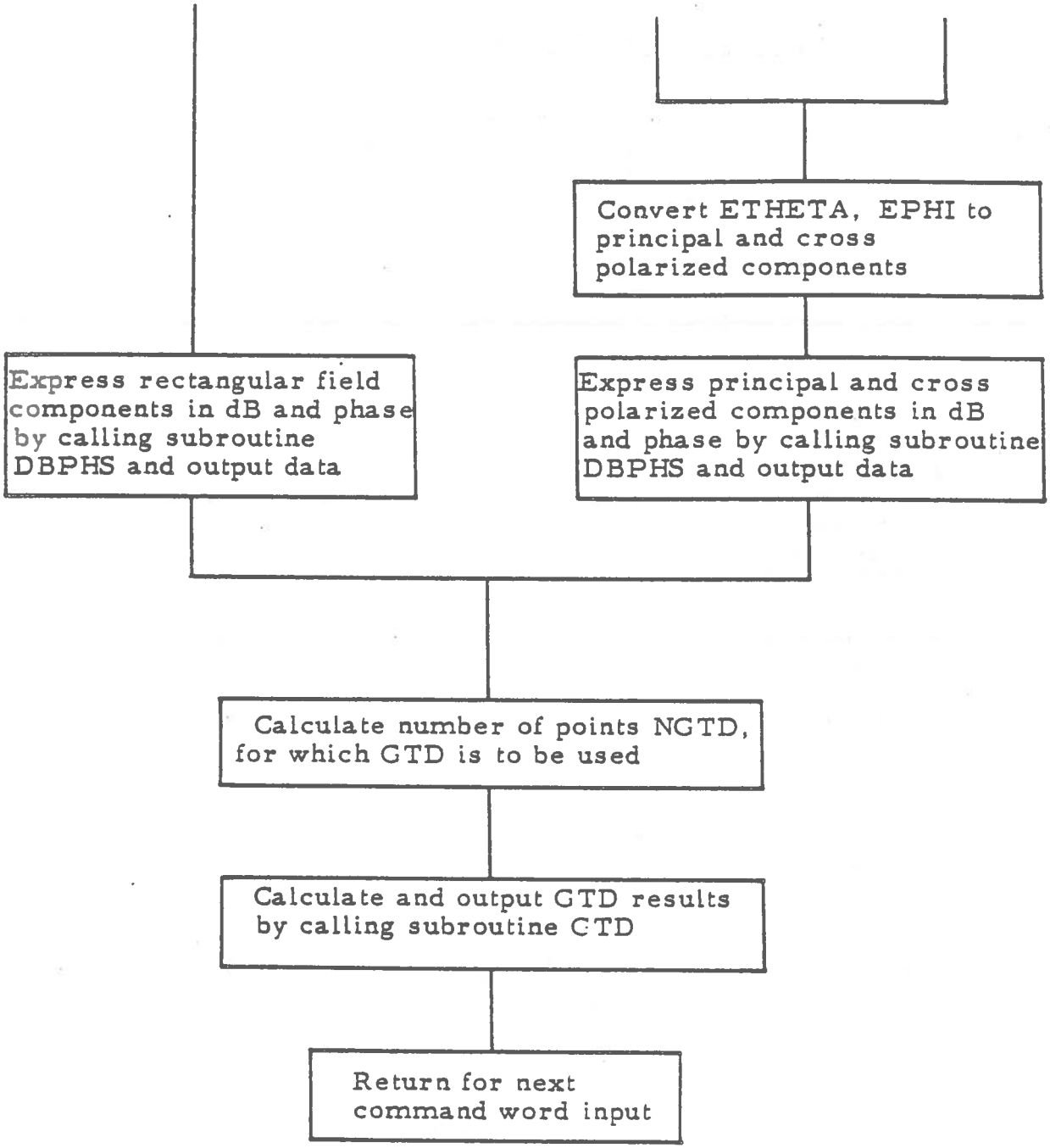

Chart 7: NECREF. Flow chart diagram (main).

the feed pattern avoids storage of large amounts of data. The interested reader can refer to the manuals (User's and Code Manuals) written by R. C. Rudduck and S. H. Lee (1979).

A principal grid is defined for use in the aperture integration. The field is computed for points on this grid and extrapolated for points off the grid. A piecewise linear representation of the aperture distribution minimizes the amount of numerical integration required. GTD analysis for parabolic surfaces is similar to that of diffraction by a flat plate, except the fact that the curvature of the reflector must be taken into account. The GTD approach is summarized in the Code Manual issued by Ohio State University (1979).

3.2.2 Switching Criterion

A switching criterion is needed to decide whether AI or GTD is used. Chart 8 shows the block diagram for switching criteria. Basically, in the far field, GTD is used for angles wider than an angle θx depending on the aperture width in the specific pattern cut. Otherwise, AI is used. In the near field, the angle criterion still applies but, in addition to this, a range criterion is introduced. For ranges smaller than a range threshold Zx, only GTD calculations are performed, whereas for Z greater than Zx, this is decided in accordance with the angle criterion.

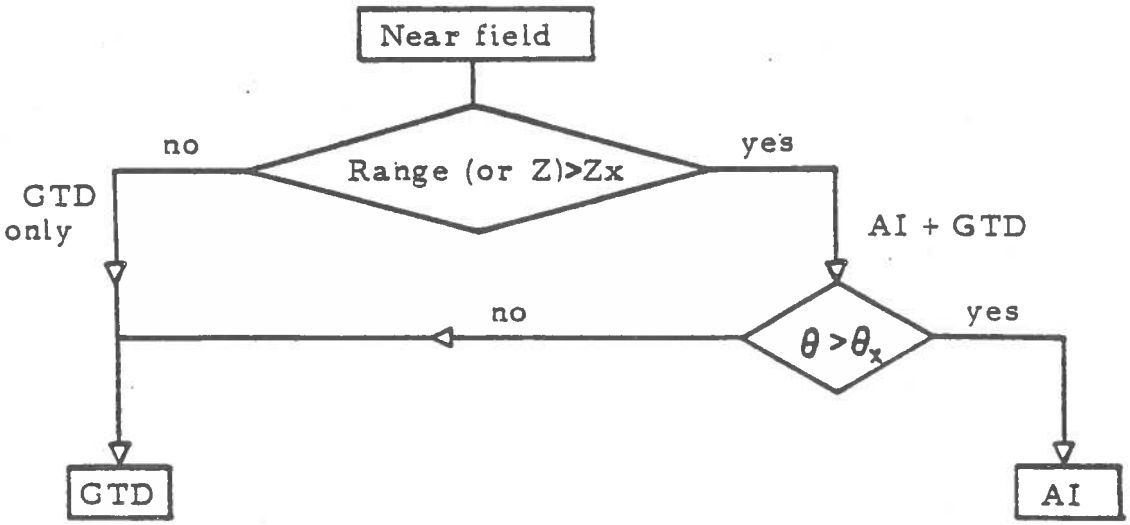

Chart 8. NECREF. Switching criterion.

3.2.3 Command Word Section

The command word section is the most important and every user of the code should be familiar with it before running the program. Several examples discussed in the User's Manual are helpful to the beginner.

Data is input to the code under the form of command cards. This procedure allows additional runs to be made without significant changes. A similar presentation had already been adopted in the former NEC program, the revised version of AMP, Antenna Modeling Program . NECREF is now a part of the NEC (Numerical Electromagnetics Code) package. A block diagram for input cards is shown on Charts 10 and 11.

The NECREF command cards are used to perform the functions as described here:

1) Command NX: It consists of default data which can be used for initial testing of the program. In normal utilization, this command is skipped.

2) Command DG: DG allows specification of the shape and the dimensions of the parabolic reflector: F, focal distance, and D, reflector diameter, define the geometry of a circular paraboloid. For complex rim shapes, a set of points is input which defines the actual rim geometry. Dimensions can be input in units of meters, feet, or inches. The rectangular grid dimensions are also specified for aper-

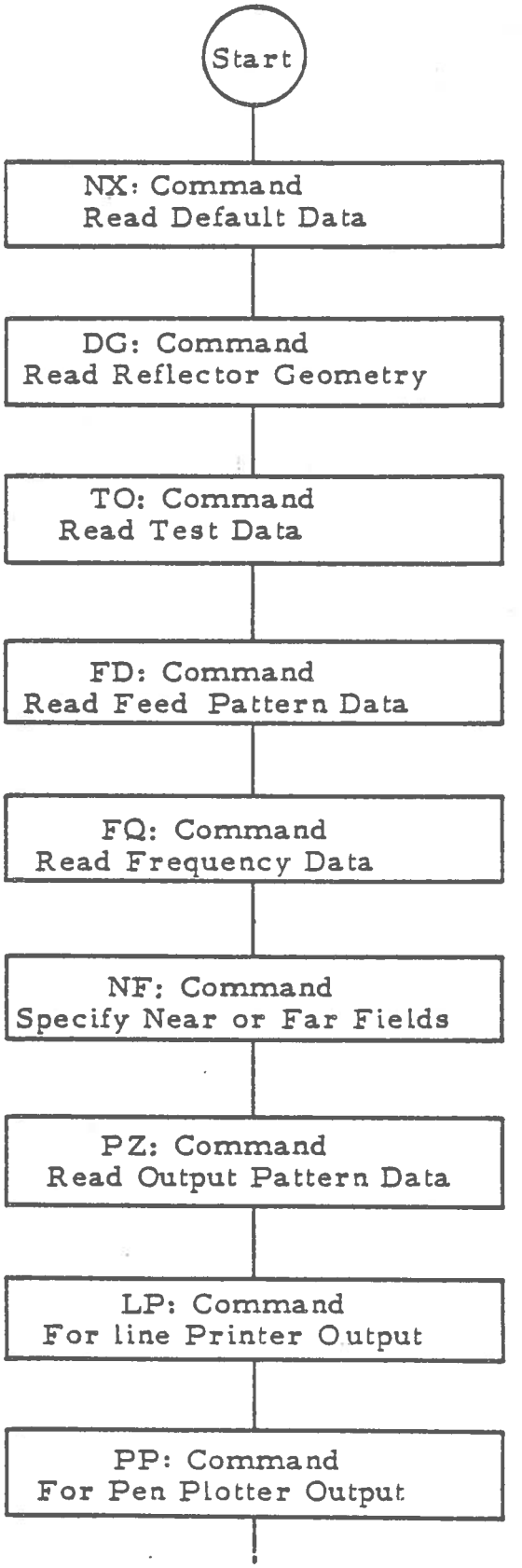

Chart 9: NECREF. Command word section.

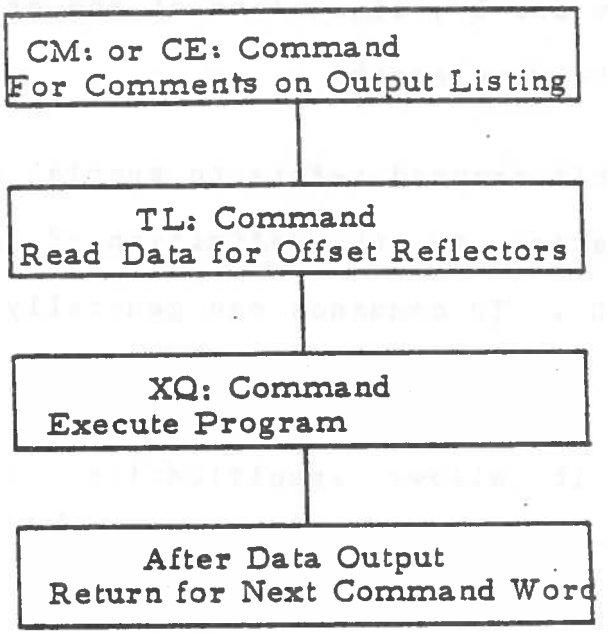

Chart 10; NECREF. Command word section.

ture integration. Dx and Dy, dimensions of the grid, must be large compared to the wavelength.

3) Command TO: This command refers to special uses as debugging or modification in the definition of switching criteria for AI and GTD . TO commands can generally be left out of the code.

4) Command FD: It allows specification of feed patterns. The specifications are the nature of the pattern, piecewise or analytical function, polarization, type of normalization, dB or linear, symetry of the pattern, angle of polarization, number of input patterns, and number of points per pattern. In this study, two feed patterns are used as input to the code, in dB normalized, with x-and y-axis symetry. $\phi=0^{o}$ corresponds to the E-plane and $\phi=90^{o}$ to the H-plane. No more than 15 points can be input.

5) Command FQ: This is to specify the frequency chosen. More than one can be considered.

6) Command NF: For far field calculations, this command is left out of the code. It determine whether near or far field calculations are to be done.

7) Command PZ: This is an important command. It enables the user to choose the data output from the code. It includes the number of pattern cuts, less than 10, the values of ϕ for which the field is computed, and the initial, final, and incremental values of θ.

8) Command XQ: XQ executes the computer code.

Other commands are available (LP, PP, CM), but are not used in the modeling and therefore are not described here.

These descriptions and the examples discussed in CHAPTER IV should provide the necessary information to run the programs HORN and NECREF. The interested reader can also refer to the examples discussed in NECREF User's Manual (1979).

CHAPTER IV

RESULTS FROM THE MODELS

This chapter mainly consists of results obtained from the antenna modeling programs discussed in the previous chapters and is divided into five sections. The first two sections illustrate the use of HORN. The three following sections give the results of the modeling of the three systems chosen.

4.1 MODELING OF A HORN

The first case corresponds to a pyramidal horn defined by its length L = 30 cm, its aperture dimensions a and b, respectively equal to 10 and 15 cm, and its operating frequency f = 22.4 GHz (λ = 1.3559 cm). The chosen mode is a cosine illumination. The modeled antenna is the antenna without reflector used by the Bendix Research Laboratories for experiments about Automotive Radars. Antenna measurements can be found in the NHTSA-Bendix report (1976).

In Table 2, the input file corresponding to this example is shown: a cartesian pattern is requested first, for $\phi=0^{o}$, then the test "OUTPUT" enables a polar pattern to be computed. The same procedure is used for the H-plane patterns.

Figures 4.1.1 and 4.1.2 show the polar patterns for the E- and H-planes. The E-plane beamwidth is slightly narrower than that of the H-plane, but the side-lobe level is much lower for $\phi=90^{o}$ than for $\phi=0^{o}$. The cartesian patterns, shown in Figures 4.1.3 and 4.1.4, enable one to evaluate the E- and H-plane beamwidths, and to compare the respective side-lobe levels. The experimental values are also plotted on the same graphs so that the accuracy of the model can be estimated. The E-plane beamwidth is 10^{o}. The curves exhibit good agreement with measurements, especially for the main beam and the first side-lobes. Therefore, the modeling of horn antennas produces satisfying results. In Figure 4.1.5, the H-plane pattern is shown for a tapered mode. As a matter of fact, the effect of the illumination can be seen on this series of three cartesian patterns: as the separation of the E- and H-planes has been implicitly assumed in the calculation, figures 4.1.3, 4.1.4 and 4.1.5 can also be considered to be the H-plane patterns drawn for a constant, cosine, and cosine squared illumination. The influence of the illumination function is obvious on the graphs. The higher the order of the mode is, the smoother the curve is, that is to say the wider the beamwidth is and the lower the

Table 2 :HORN. Input file.

```
30. 10. 15.
1.3559
3000. 0. 130
C
PPP
E
OUT
POL
PAR
1.3559
30090. 90. 130
C
PPP
E
OUT
POL
END
```

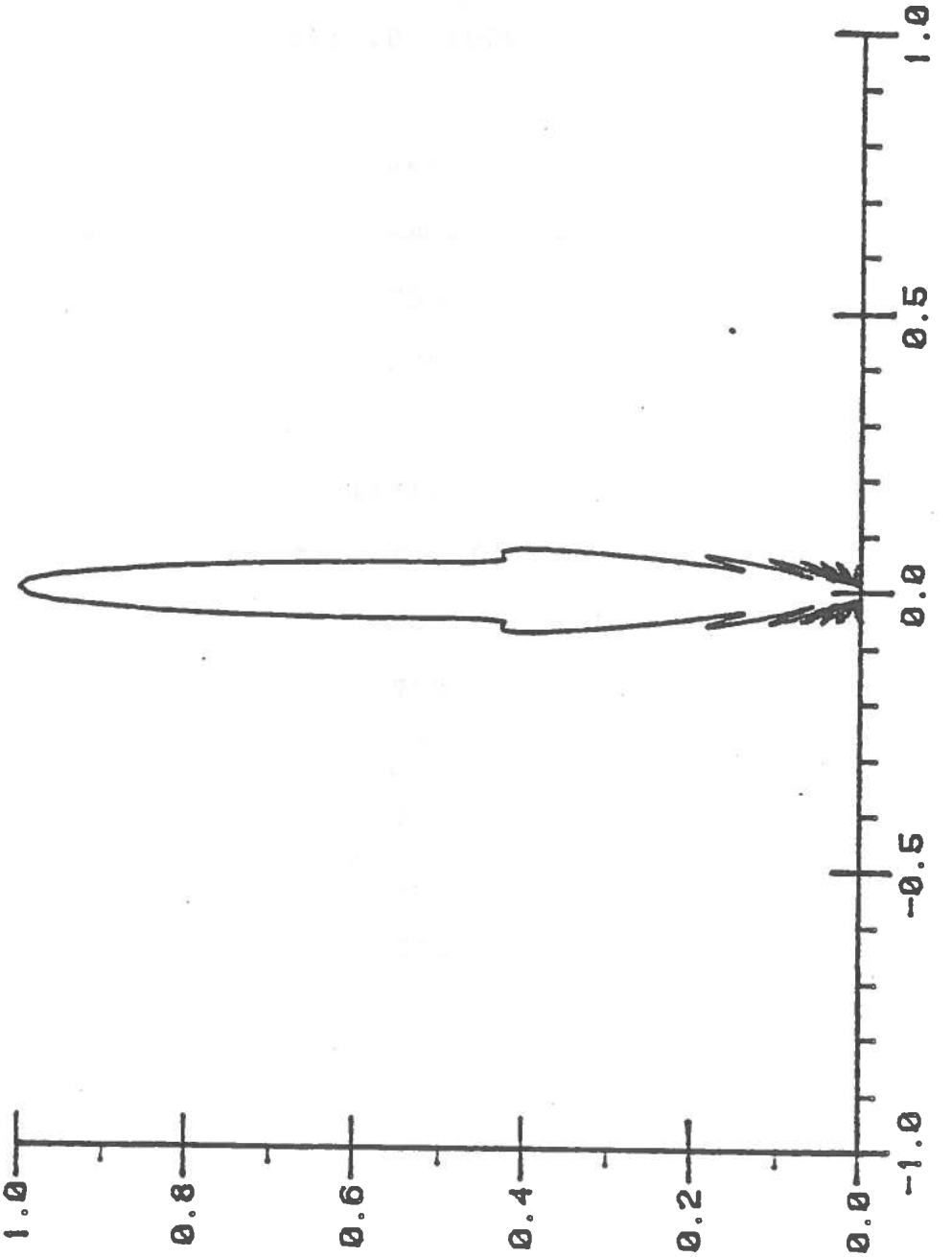

Figure 4.1.1: Standard 10^{o} horn, E-plane polar pattern.

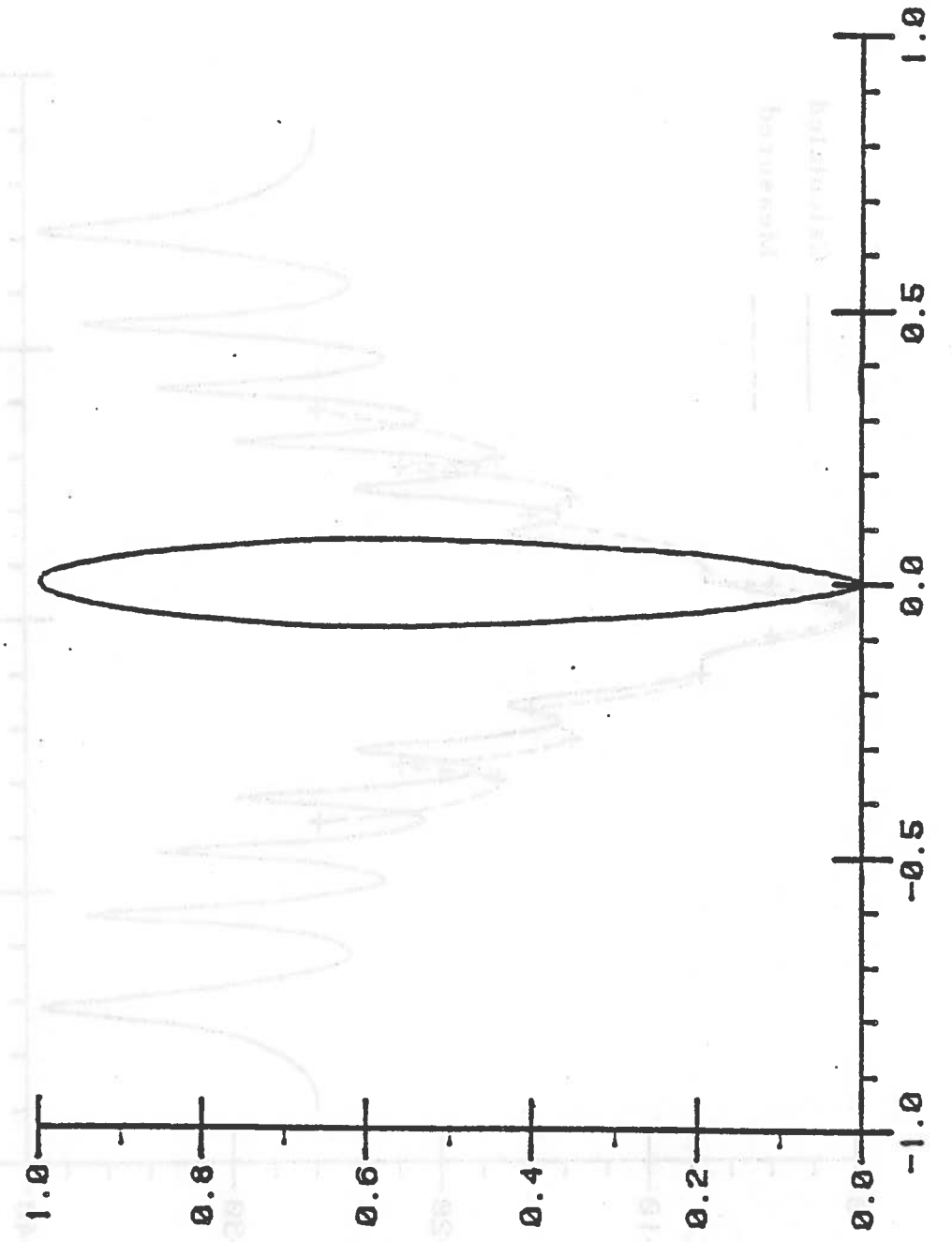

Figure 4.1.2: standard 10^{o} horn, H-plane polar pattern.

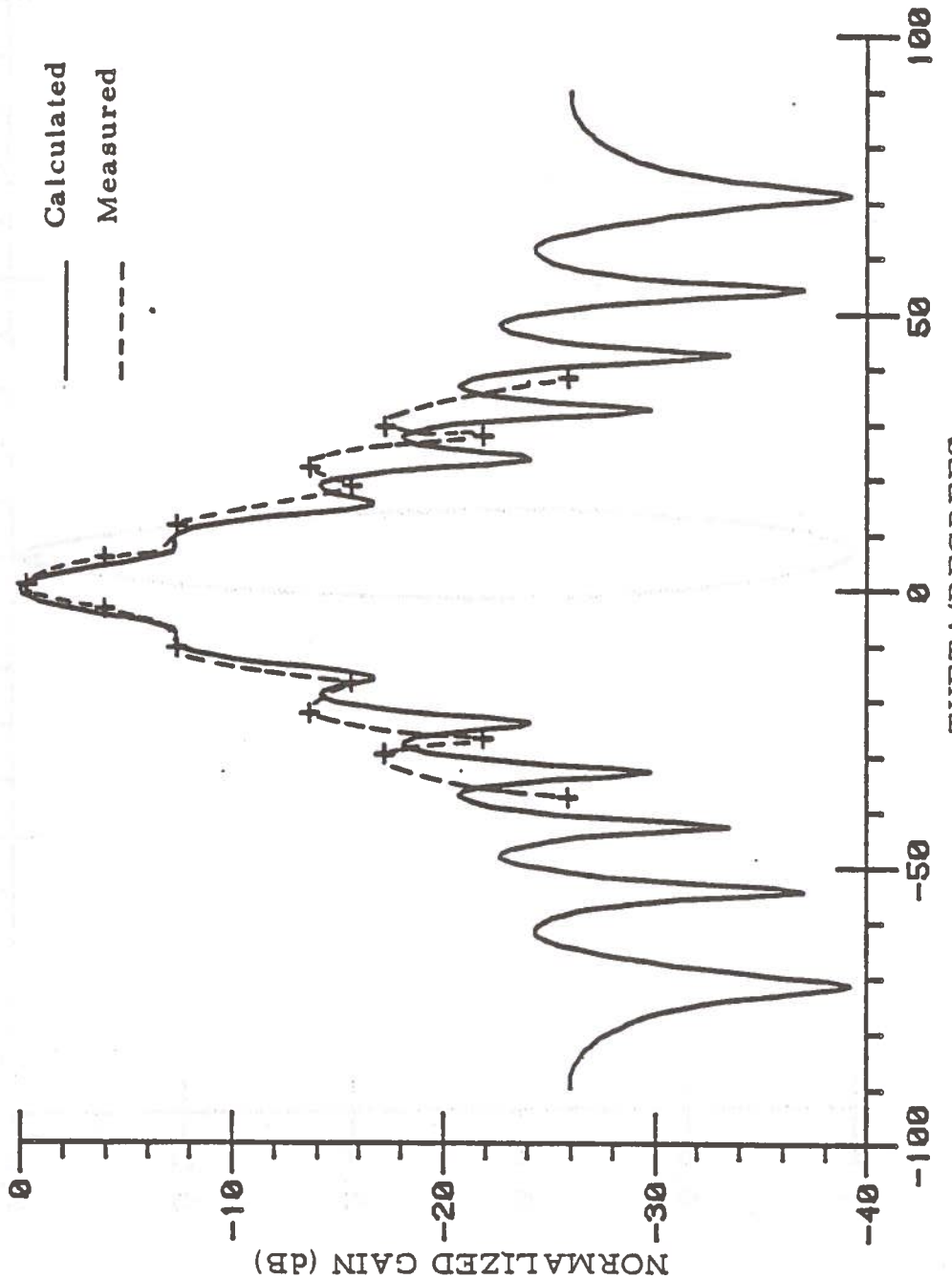

Figure 4.1.3: Standard 10^{o} horn, E-plane pattern.

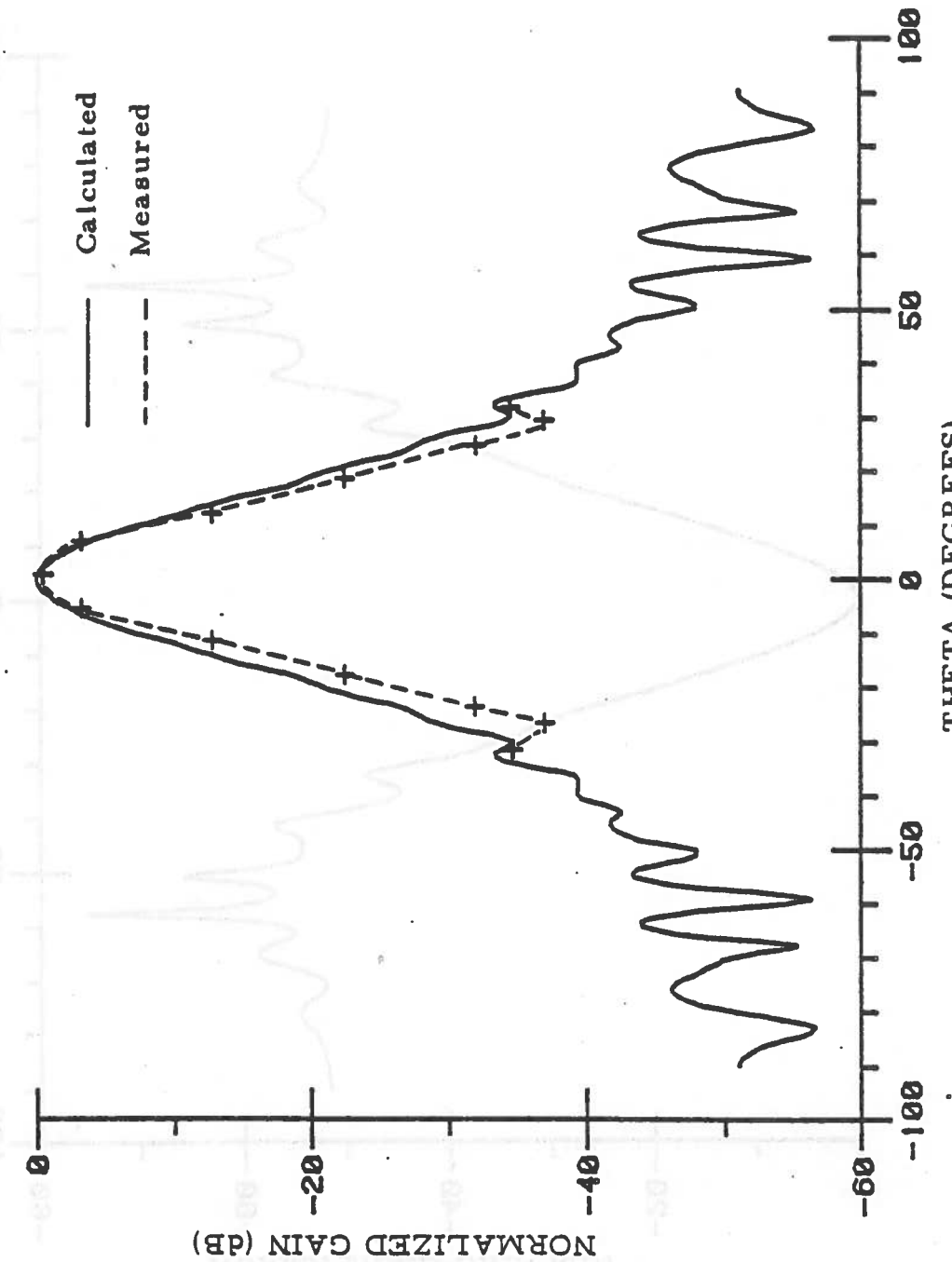

Figure 4.1.4: Standard 10^{o} horn, H-plane pattern.

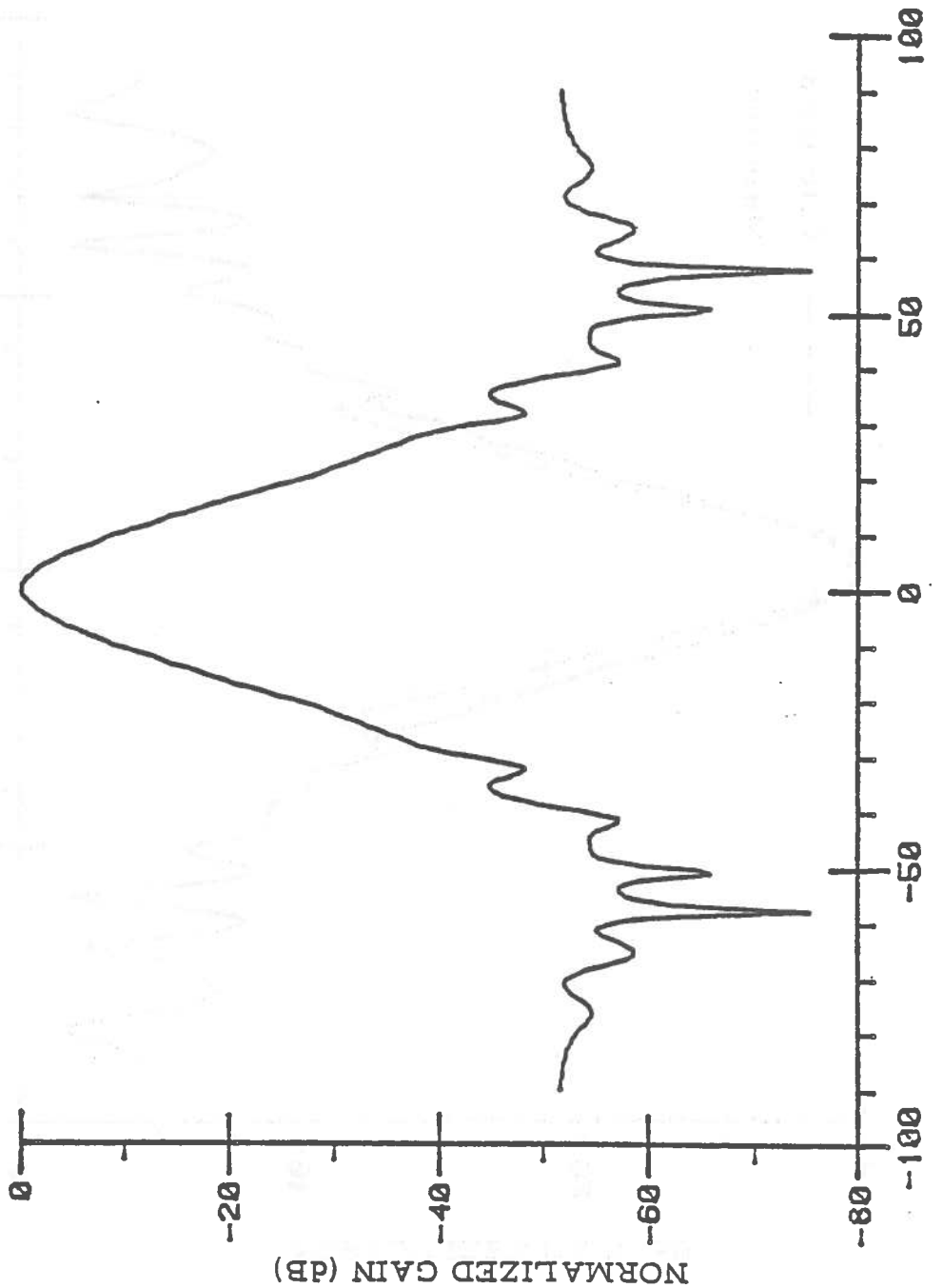

Figure 4.1.5: standard 10^{o} horn, H-plane (tapered illumination).

level of the sidelobes. It is a well-known rule in antenna engineering that, for any aperture antenna, the higher directivity is achieved by constant illumination (Freedman, 1951). It must be noted that the variations of the maximum gain do not appear on these normalized curves. In addition to this, the reader will notice that the polar patterns are not shown in their usual form. Though the curves are actually polar plots, there still remain horizontal and vertical axes. This is because the pen plotter used is unable to produce classical polar plots. A geometrical conversion has been used in the program HORN, in order to overcome the problem. When vertical and horizontal scales are different, the angles measured on the curves are not exactly the actual pattern angles. If Ux and Uy are x and y axis units, the actual angle θr is given as a function of the measured angle θm by:

$$\theta r = \text{Arctan}[\ \tan\theta m . \tan\theta o\ ]$$

Where: $\theta o = Ux/Uy$.

Figures 4.1.6 and 4.1.7 show the patterns versus ka sinθ.

4.2 OPTIMIZATION OF THE MODEL

The performances of a pyramidal horn can be optimized by an appropriate choice of the geometry. In the literature (Fradin, 1961), it is possible to find optimization curves

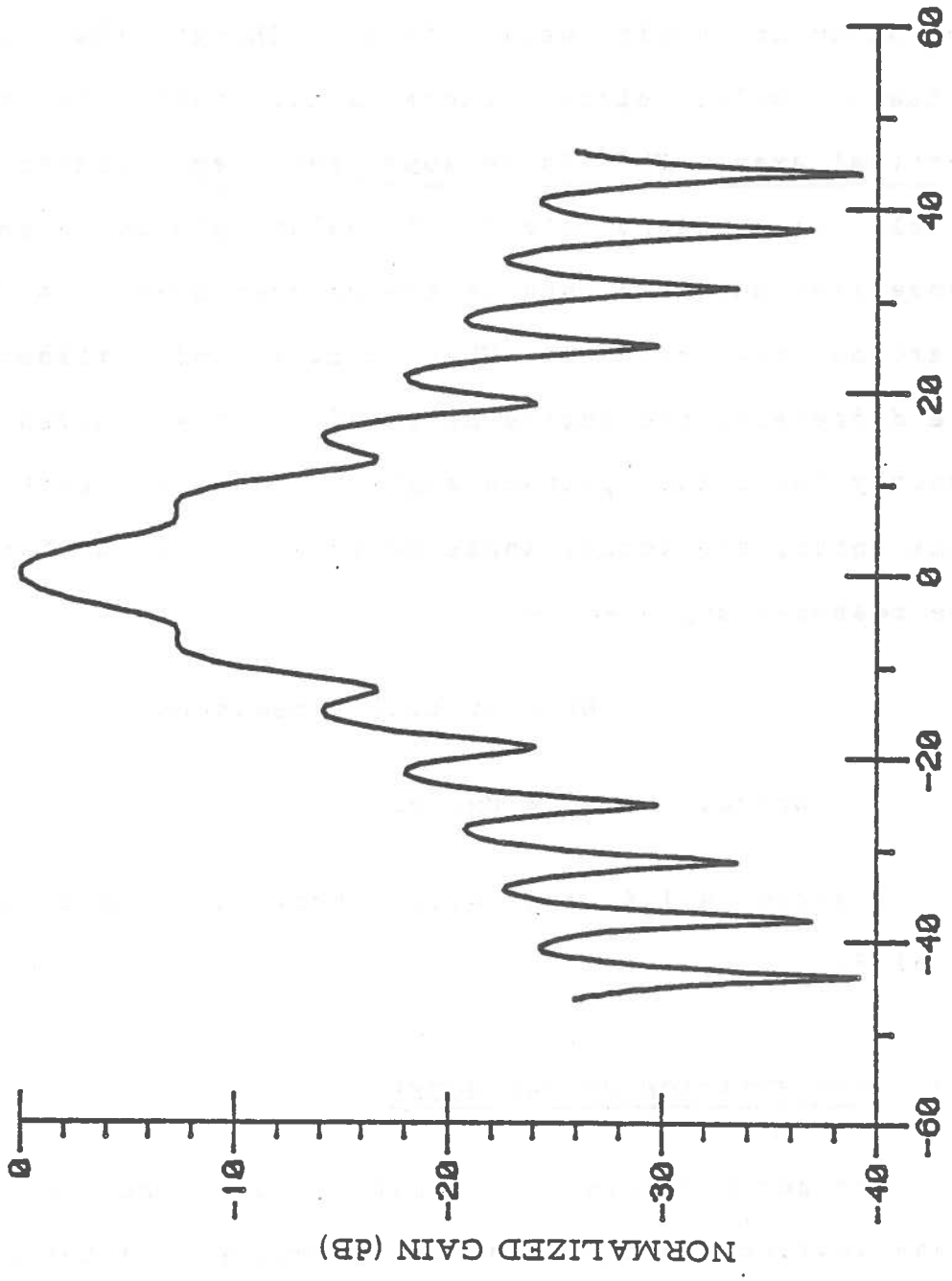

Figure 4.1.6: Standard 10^{o} horn, E-plane pattern vs. kasin(theta).

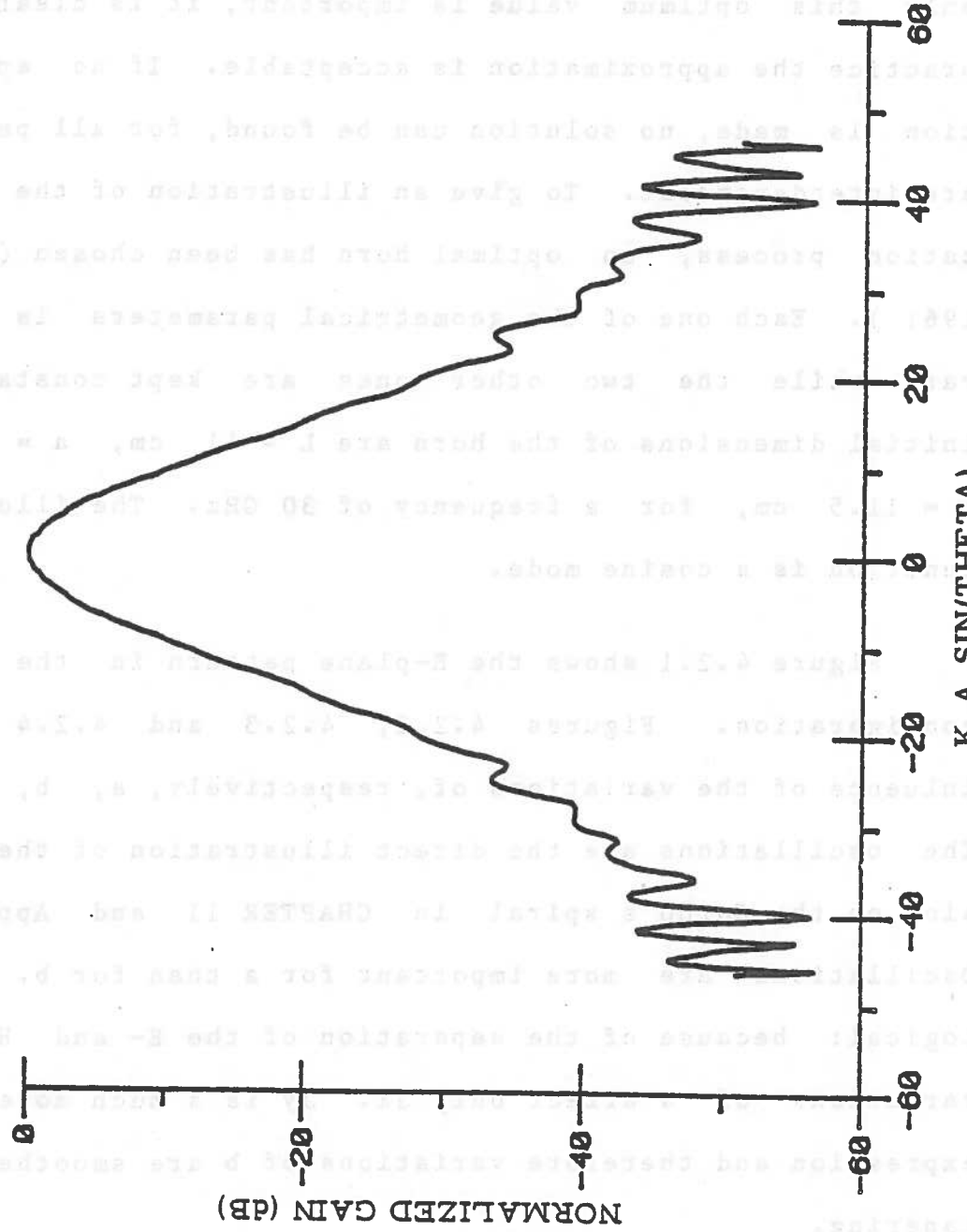

Figure 4.1.7: Standard 10^{o} horn, H-plane pattern vs. kasin(theta).

giving, for a chosen gain, the values of the horn dimensions. However, those graphs are derived from the approximation of the directivity by a (logx)/x function (Jasik, 1961). The curves drawn in this section show that this is a rough approximation as soon as the parameter considered is much different from its optimal value. Since only this optimum value is important, it is clear that in practice the approximation is acceptable. If no approximation is made, no solution can be found, for all parameters are interdependent. To give an illustration of the optimization process, an optimal horn has been chosen (Fradin, 1961). Each one of the geometrical parameters is set to vary while the two other ones are kept constant. The initial dimensions of the horn are L = 41 cm, a = 9.4 cm, b = 11.5 cm, for a frequency of 30 GHz. The illumination function is a cosine mode.

Figure 4.2.1 shows the E-plane pattern in the optimal configuration. Figures 4.2.2, 4.2.3 and 4.2.4 show the inluence of the variations of, respectively, a, b, and L. The oscillations are the direct illustration of the discussion on the Cornu's spiral in CHAPTER II and Appendix A. Oscillations are more important for a than for b. This is logical: because of the separation of the E- and H-planes, variations of a affect only Jx. Jy is a much more complex expression and therefore variations of b are smoothed by the tapering.

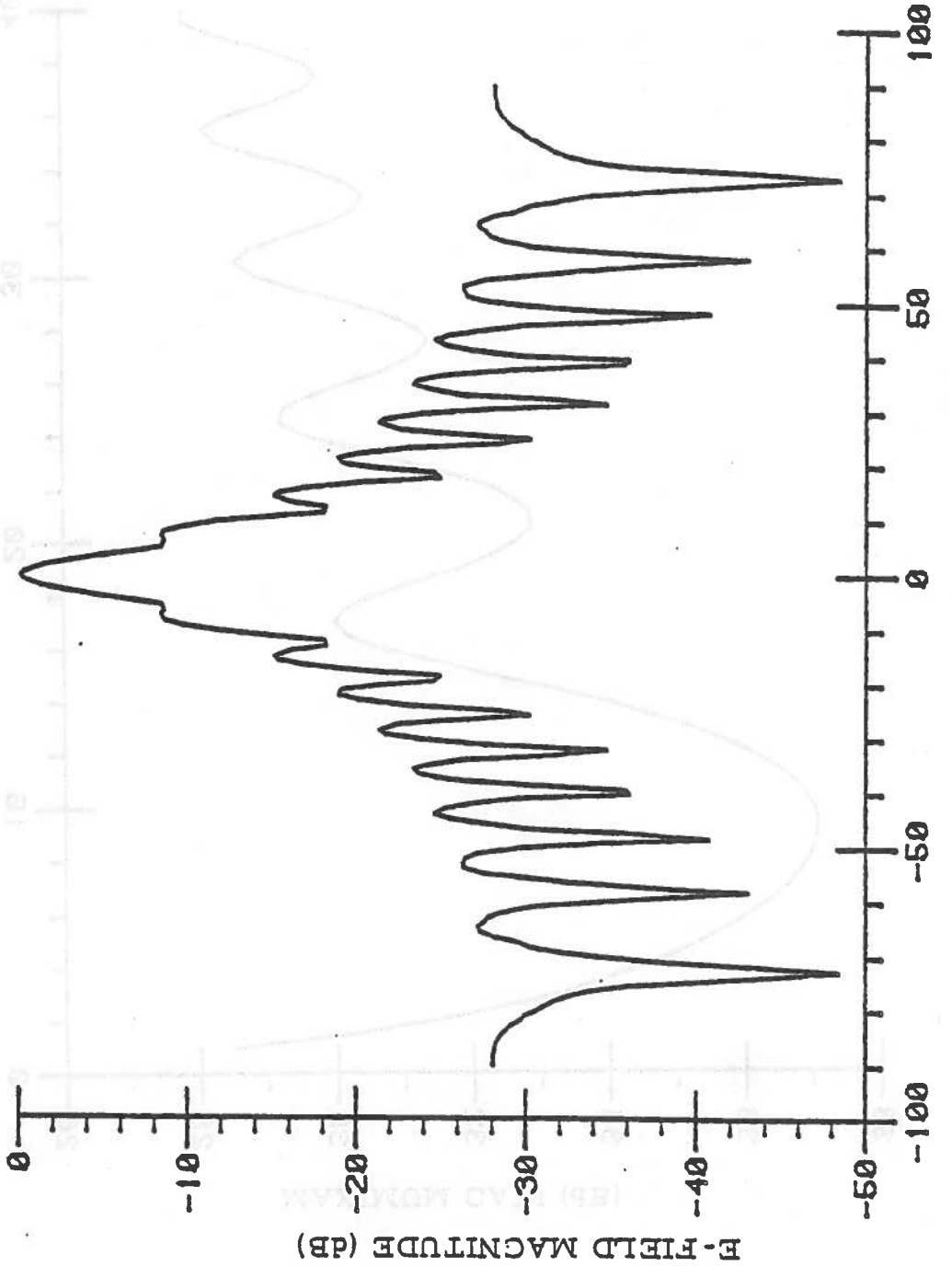

Figure 4.2.1: E-plane pattern for optimal horn.

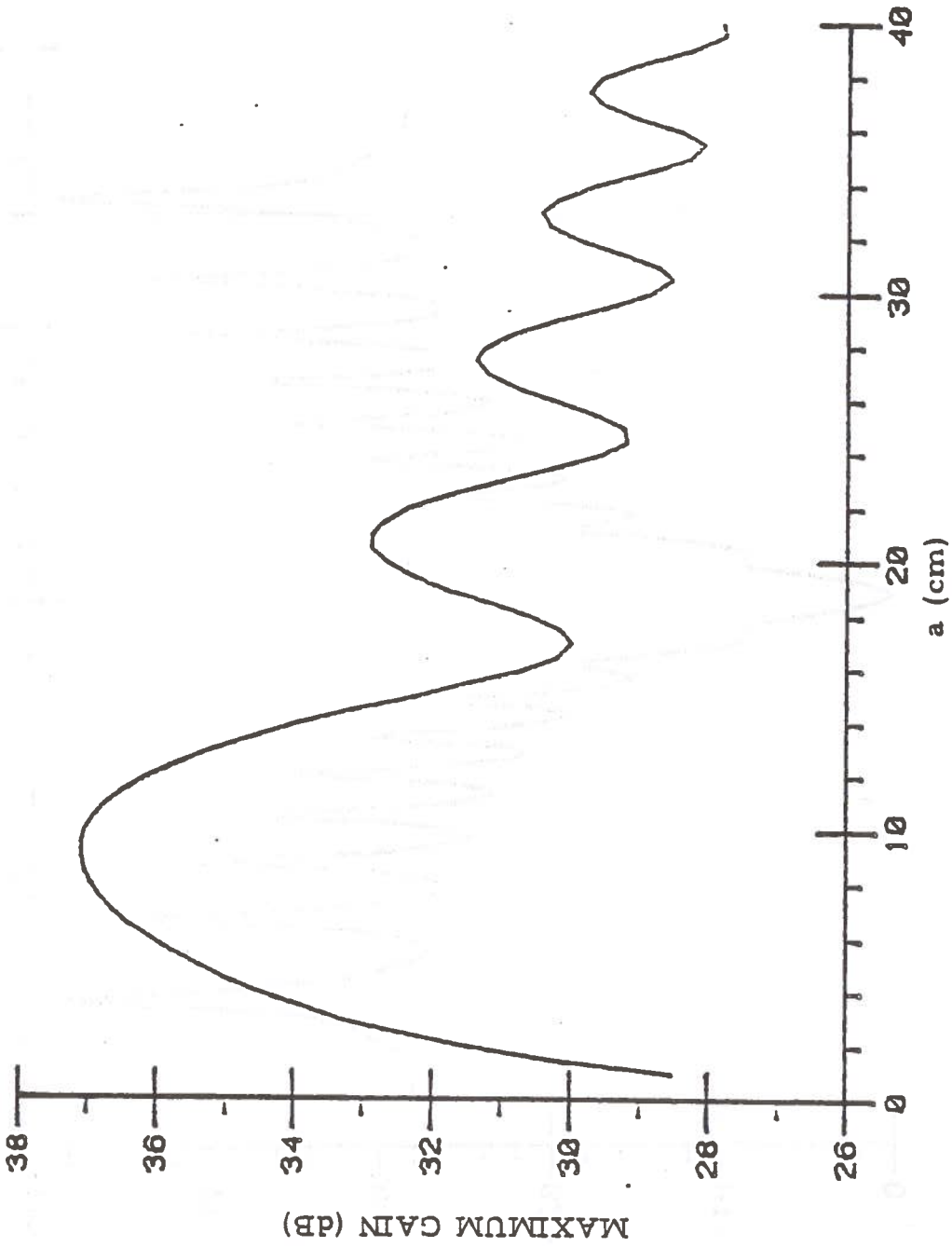

Figure 4.2.2: Optimization —Gain variations vs.a.

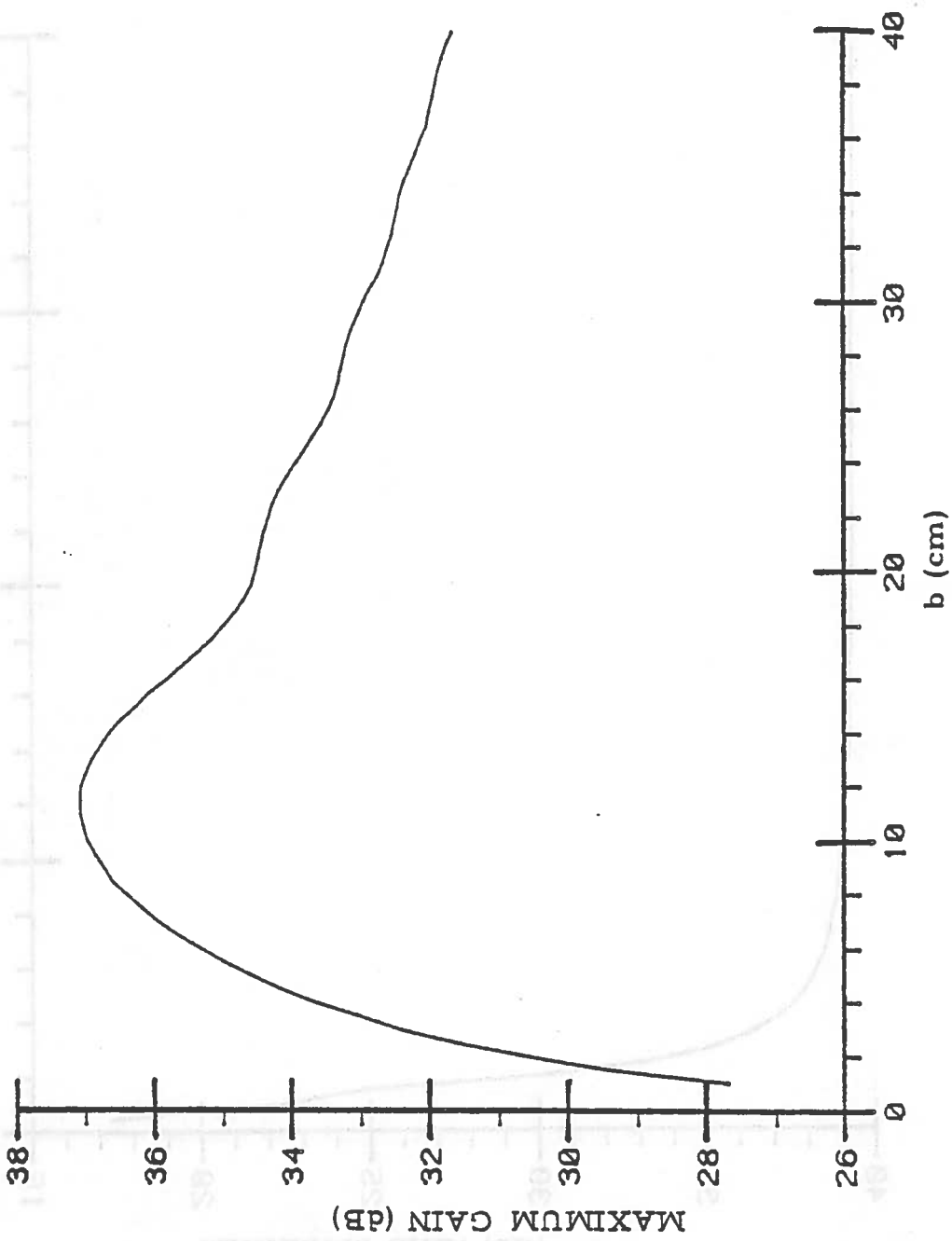

Figure 4.2.3: Optimization. Gain variations vs. b.

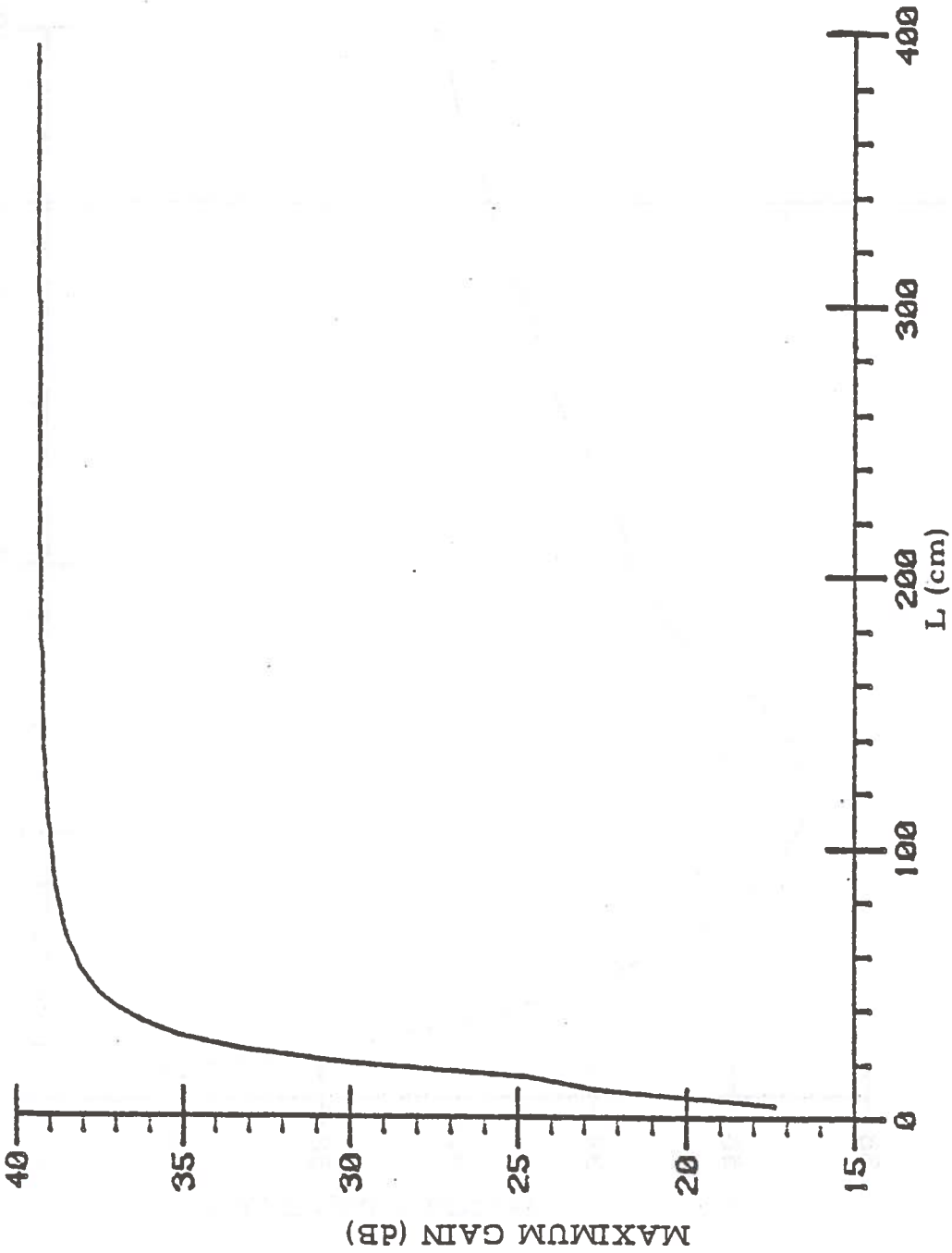

Figure 4.2.4: Optimization. Gain variations vs.L.

4.3 MODELING OF THE BENDIX SYSTEM

The geometry of the Bendix system is defined by:

Feed: a = 0.356 cm ; b = 0.711 cm ; L = 15 cm.

Reflector: Diameter D = 6 inches (15.24 cm).

Focal distance f = 2 inches (5.08 cm).

A ratio of (1/3) for F/D is chosen, as it is often the case with parabolic reflectors. The operating frequency is 36 GHz. For this system, two patterns are computed by the code, for the E- and H-plane. Table 3 is the input to the code for this system. Figures 4.3.1 and 4.3.2 show the antenna patterns for θ varying from 0° to 180°. Although values of θ above 90° are not used in the simulation program, they are displayed in order to estimate the level of the back-lobes. This level is far from being negligible. A discontinuity can be observed around $\theta=90^{\circ}$, which corresponds to the region where GTD is invalid. The relative importance of this discontinuity depends on the chosen model and the frequency.

On figures 4.3.3 and 4.3.4, θ varies from 0° to 90°. Figures 4.3.5 to 4.3.8 show the corresponding feed patterns.

Table 3 : Bendix. Input file.

```
DG:
          1    5.079E-02    3.811E-03    3.811E-03    0.1524

FD:
   T F T     1 90.00
    2   0.00 90.00
 14
  0.0000000E+00  0.0000000E+00
   6.923077      -4.0809169E-02
   13.84615      -0.1679123
   20.76923      -0.3338855
   27.69231      -0.5722063
   34.61538      -0.8610556
   41.53846       -1.179152
   48.46154       -1.512532
   55.38462       -1.842586
   62.30769       -2.145915
   69.23077       -2.411405
   76.15385       -2.629654
   83.07692       -2.737695
   90.00000       -2.775419
  0.0000000E+00  0.0000000E+00
   6.923077      -9.8693326E-02
   13.84615      -0.3420681
   20.76923      -0.7668406
   27.69231       -1.303917
   34.61538       -1.957970
   41.53846       -2.691628
   48.46154       -3.471839
   55.38462       -4.259258
   62.30769       -4.971049
   69.23077       -5.575528
   76.15385       -6.071818
   83.07692       -6.383281
   90.00000       -6.496091

PZ:
            2
  0.0000000E+00    90.00000
  0.0000000E+00    180.0000          1.000000

FQ:
   1    36.001

XQ:
```

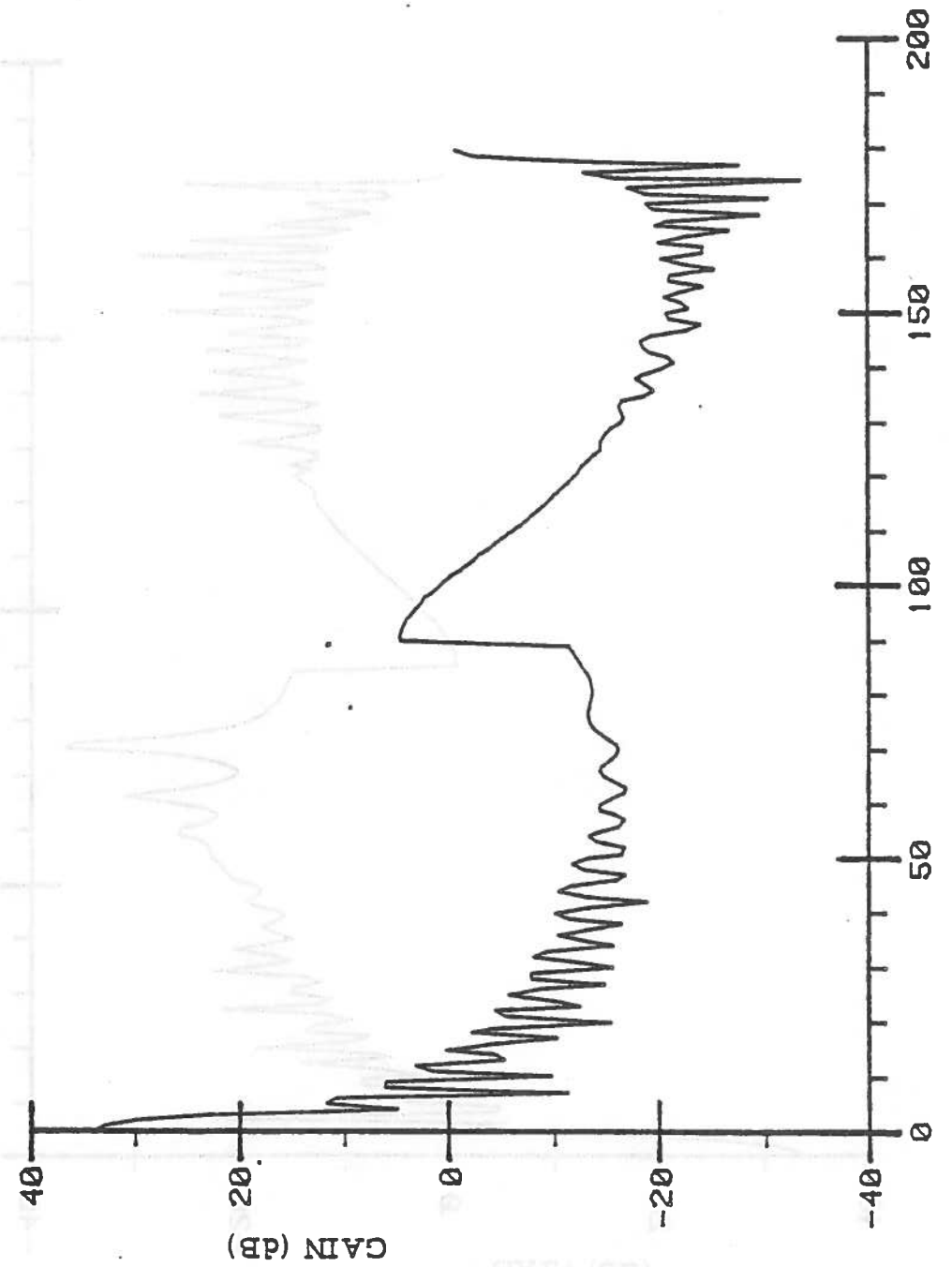

Figure 4.3.1: Bendix system, E-plane pattern.

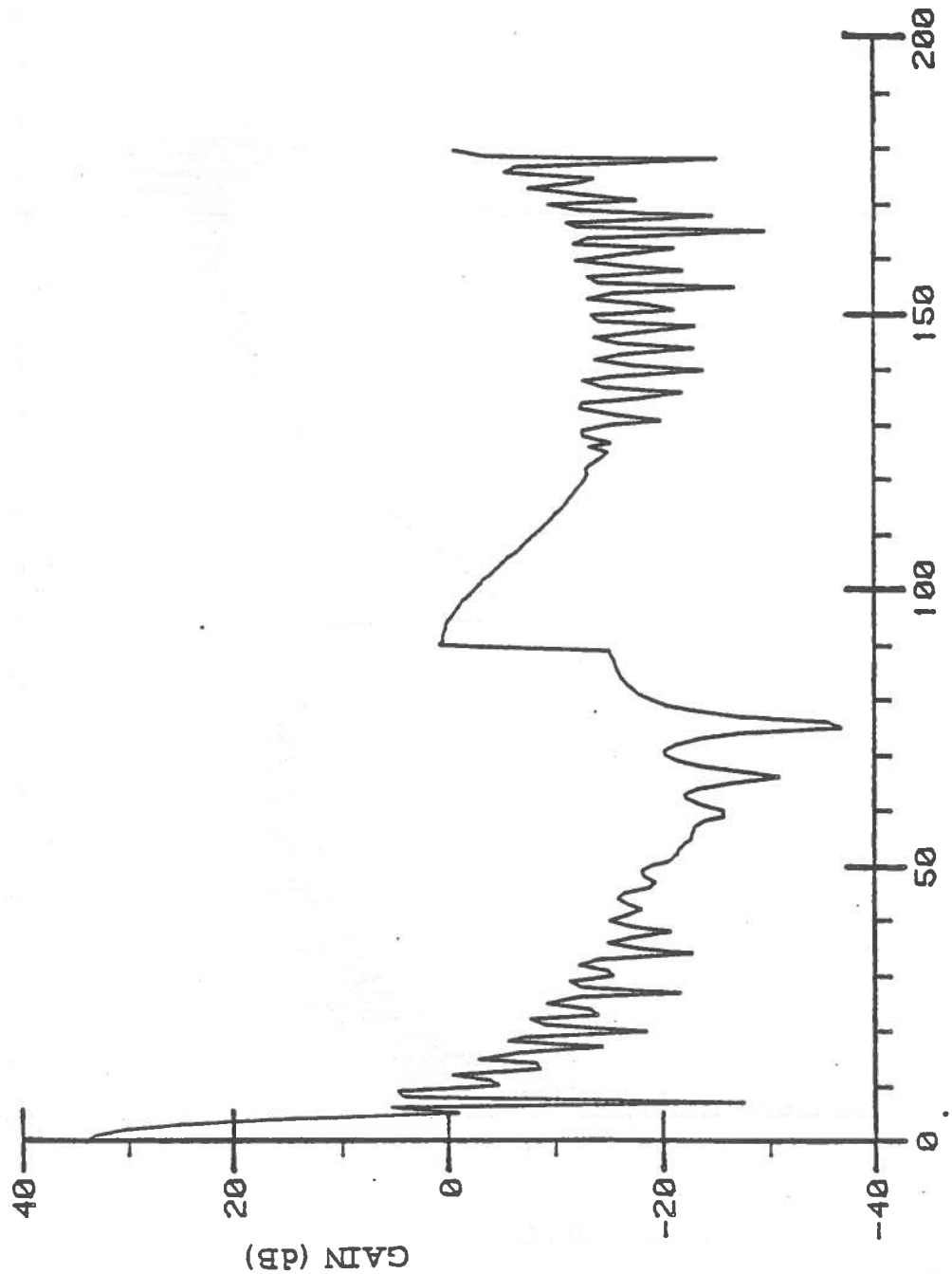

Figure 4.3.2; Bendix system, H-plane pattern.

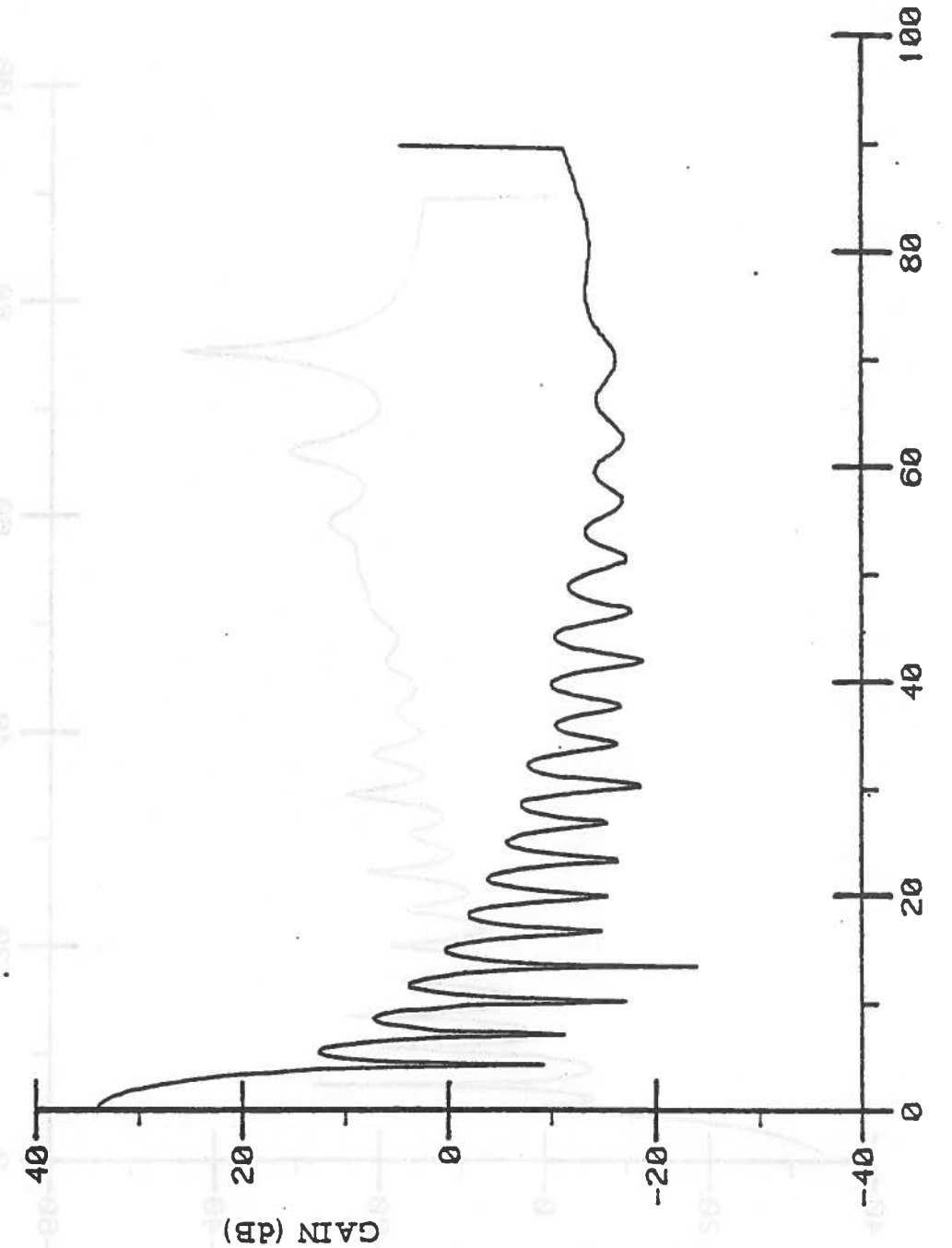

Figure 4.3.3; Bendix system, E-plane pattern.

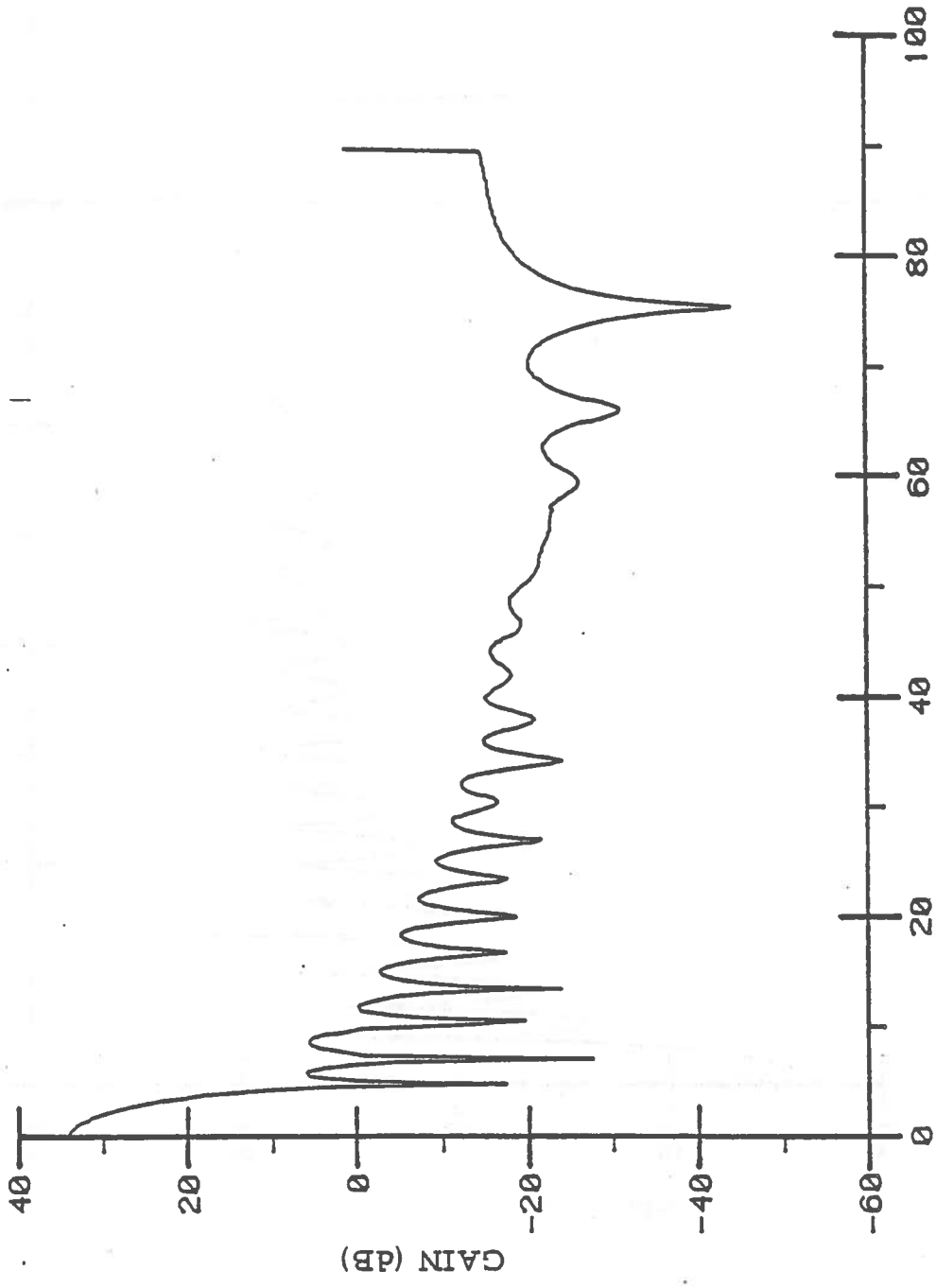

Figure 4.3.4: Bendix system, H-plane pattern.

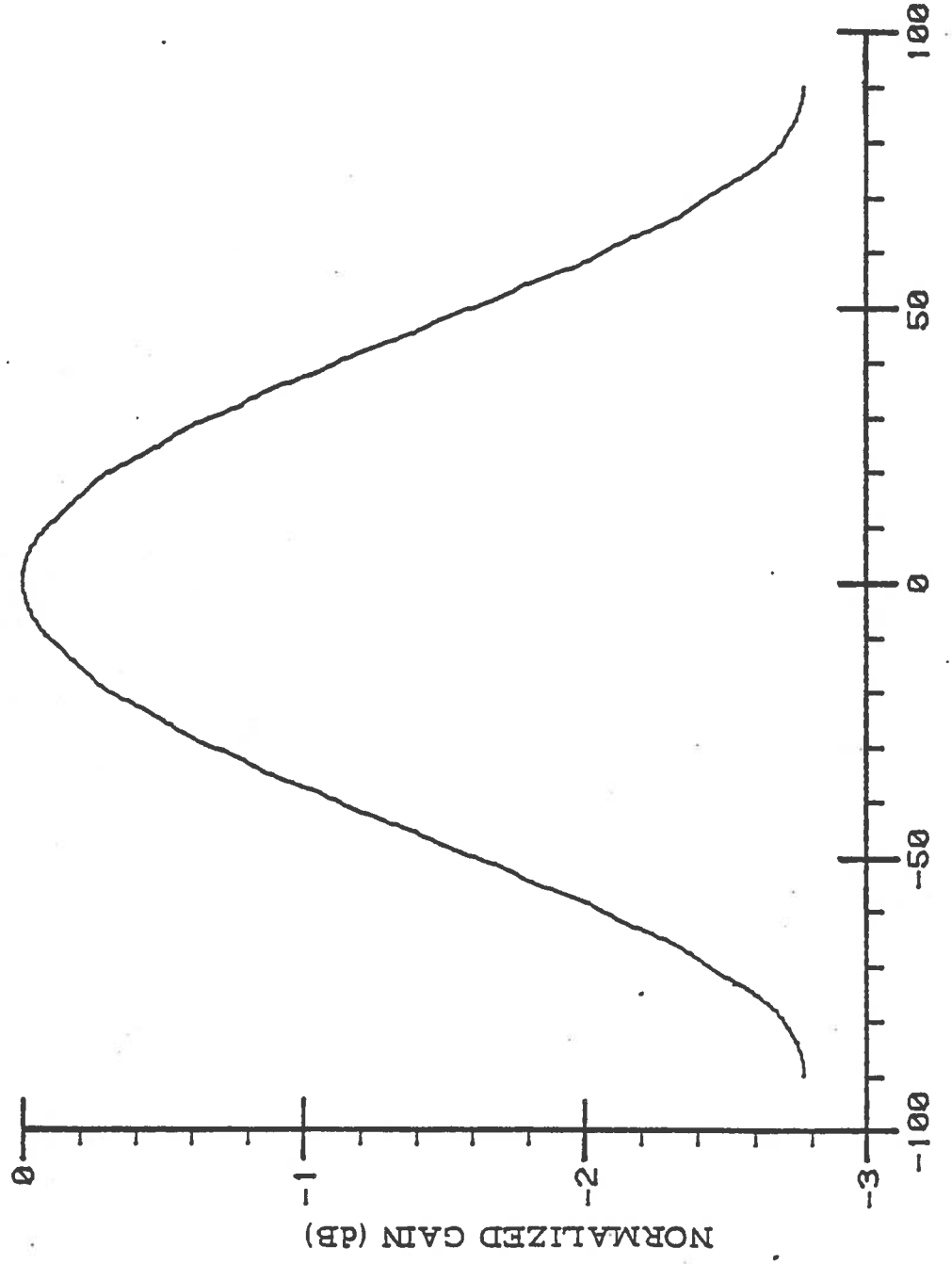

Figure 4.3.5: Bendix system, E-plane pattern (feed).

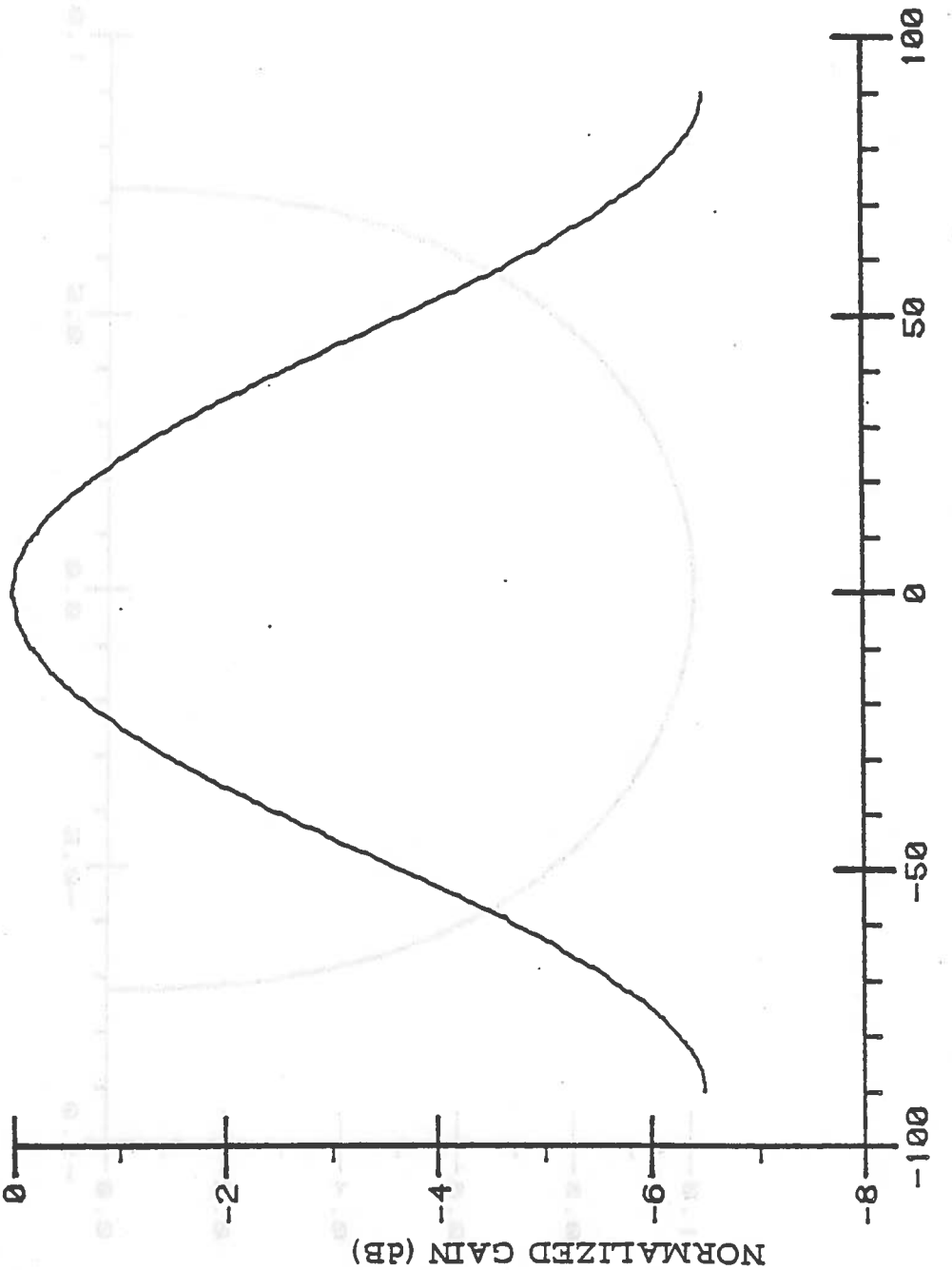

Figure 4.3.6: Bendix system, H-plane pattern (feed).

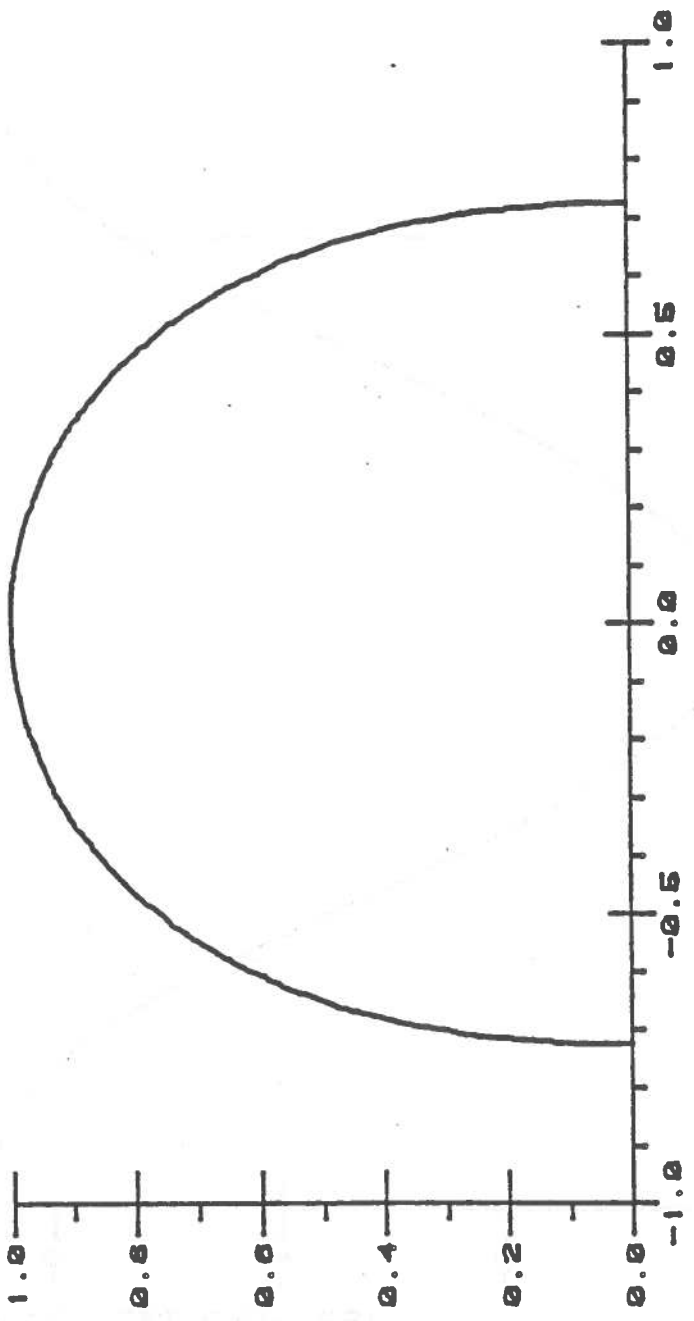

Figure 4.3.7: Bendix system. E-plane polar pattern (feed).

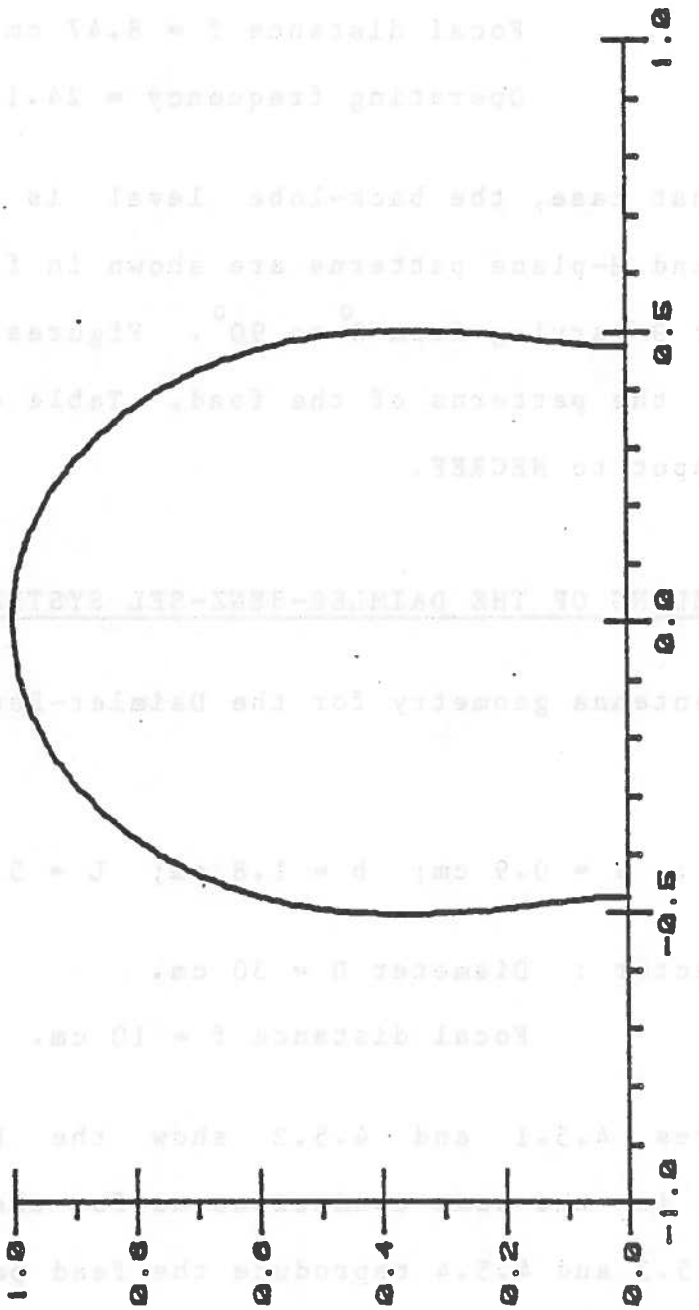

Figure 4.3.8: Bendix system, H-plane polar pattern (feed).

4.4 MODELING OF THE NISSAN-MITSUBISHI SYSTEM

The geometry of the Nissan-Mitsubishi antenna is :

Feed: a = 0.9 cm; b = 1.8 cm; L = 5 cm.

Reflector : Diameter D = 10 inches (25.4 cm).
Focal distance f = 8.47 cm.
Operating frequency = 24.15 GHz.

In that case, the back-lobe level is not displayed. Only E- and H-plane patterns are shown in figures 4.4.1 and 4.4.2, for θ varying from 0° to 90°. Figures 4.4.3 and 4.4.4 represent the patterns of the feed. Table 4 is the corresponding input to NECREF.

4.5 MODELING OF THE DAIMLER-BENZ-SEL SYSTEM

The antenna geometry for the Daimler-Benz-SEL system is:

Feed : a = 0.9 cm; b = 1.8 cm; L = 5 cm.

Reflector : Diameter D = 30 cm.
Focal distance f = 10 cm.

Figures 4.5.1 and 4.5.2 show the E- and H-plane patterns, in the same conditions as for the previous case. Figures 4.5.3 and 4.5.4 reproduce the feed patterns for the same planes. Table 5 is the deck of commands for this run.

Table 4 : Nissan-Mitsubishi. Input file.

```
DG:
         1  8.473E-02  6.354E-03  6.354E-03  0.254
FD:
  T F T     1 90.00
    2  0.00 90.00
 14
 0.0000000E+00  0.0000000E+00
  -6.923077      -0.1097480
   13.84615      -0.4375387
   20.76923      -0.9772772
   27.69231       -1.709743
   34.61538       -2.596676
   41.53846       -3.604702
   48.46154       -4.721616
   55.38462       -5.898077
   62.30769       -7.028883
   69.23077       -8.024692
   76.15385       -8.822020
   83.07692       -9.347139
   90.00000       -9.531416
 0.0000000E+00  0.0000000E+00
   6.923077      -0.2475312
   13.84615      -0.9767448
   20.76923       -2.178584
   27.69231       -3.866853
   34.61538       -5.982517
   41.53846       -8.484134
   48.46154       -11.41702
   55.38462       -14.59409
   62.30769       -17.83376
   69.23077       -20.94716
   76.15385       -23.39436
   83.07692       -24.75644
   90.00000       -25.15260
PZ:
           2
 0.0000000E+00    90.00000
 0.0000000E+00    90.0000         0.250000
FQ:
   1   24.151
XQ:
```

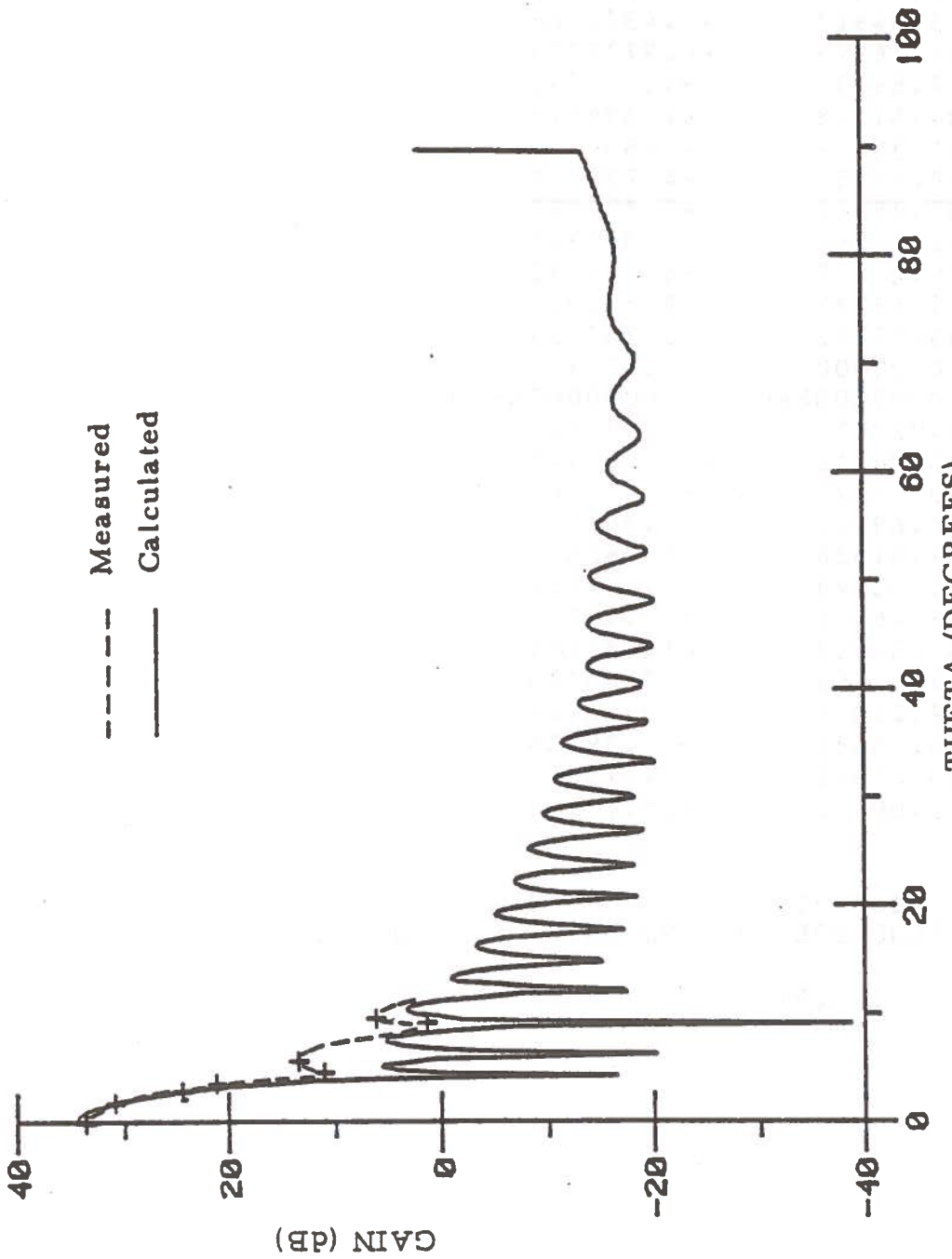

Figure 4.4.1: Nissan system, E-plane pattern.

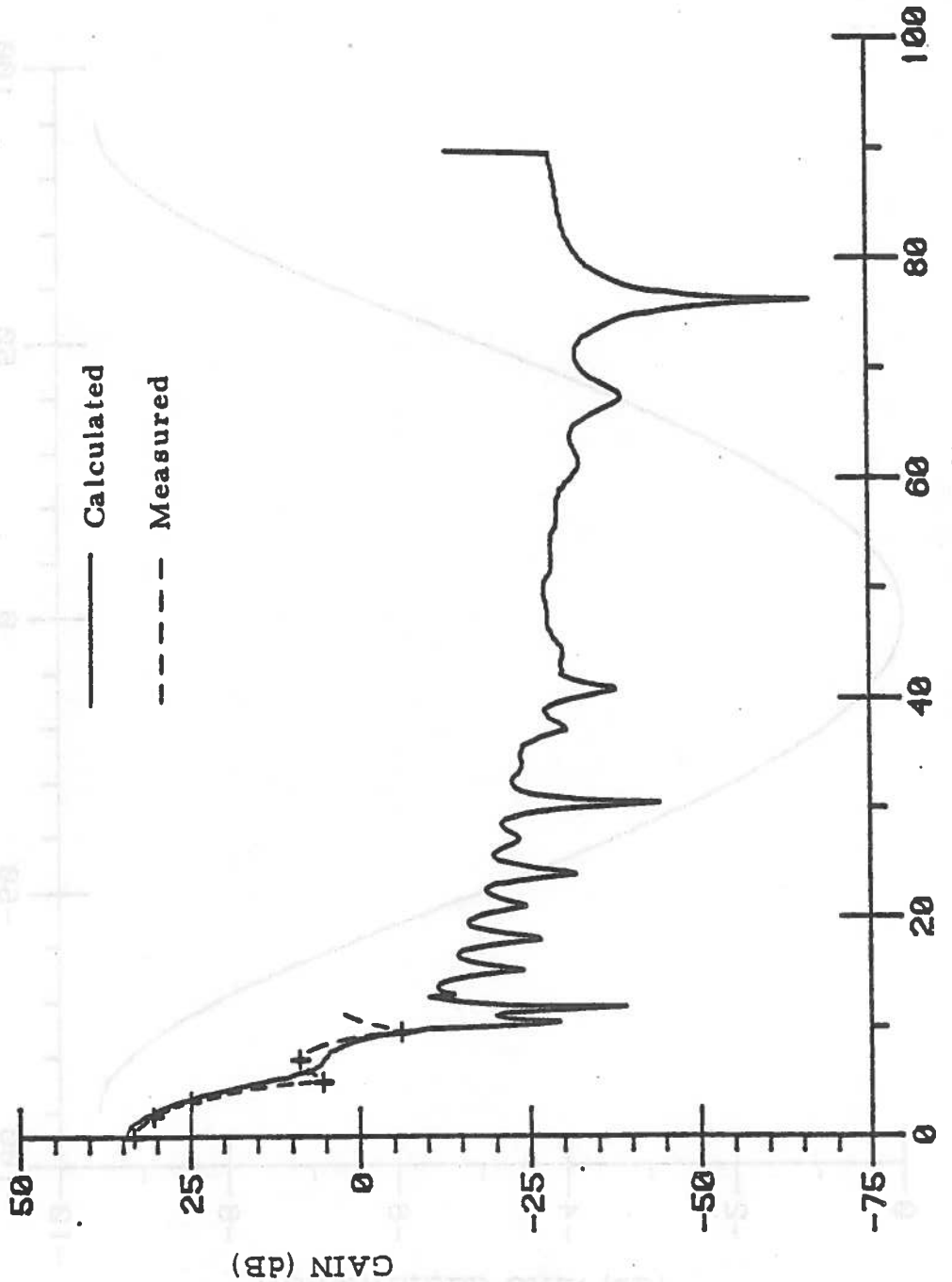

Figure 4.4.2: Nissan system, H-plane pattern.

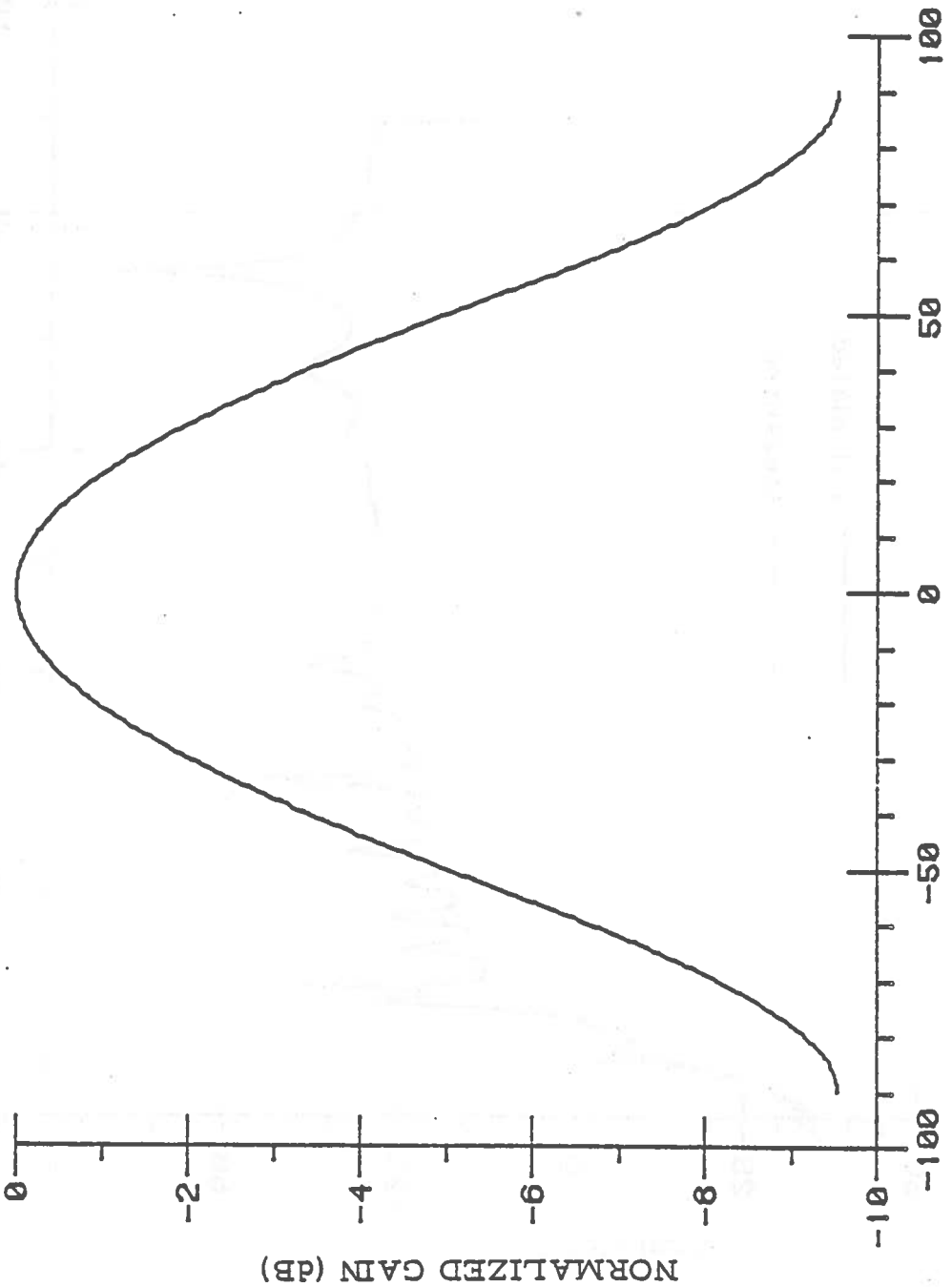

Figure 4.4.3: Nissan system, E-plane feed pattern.

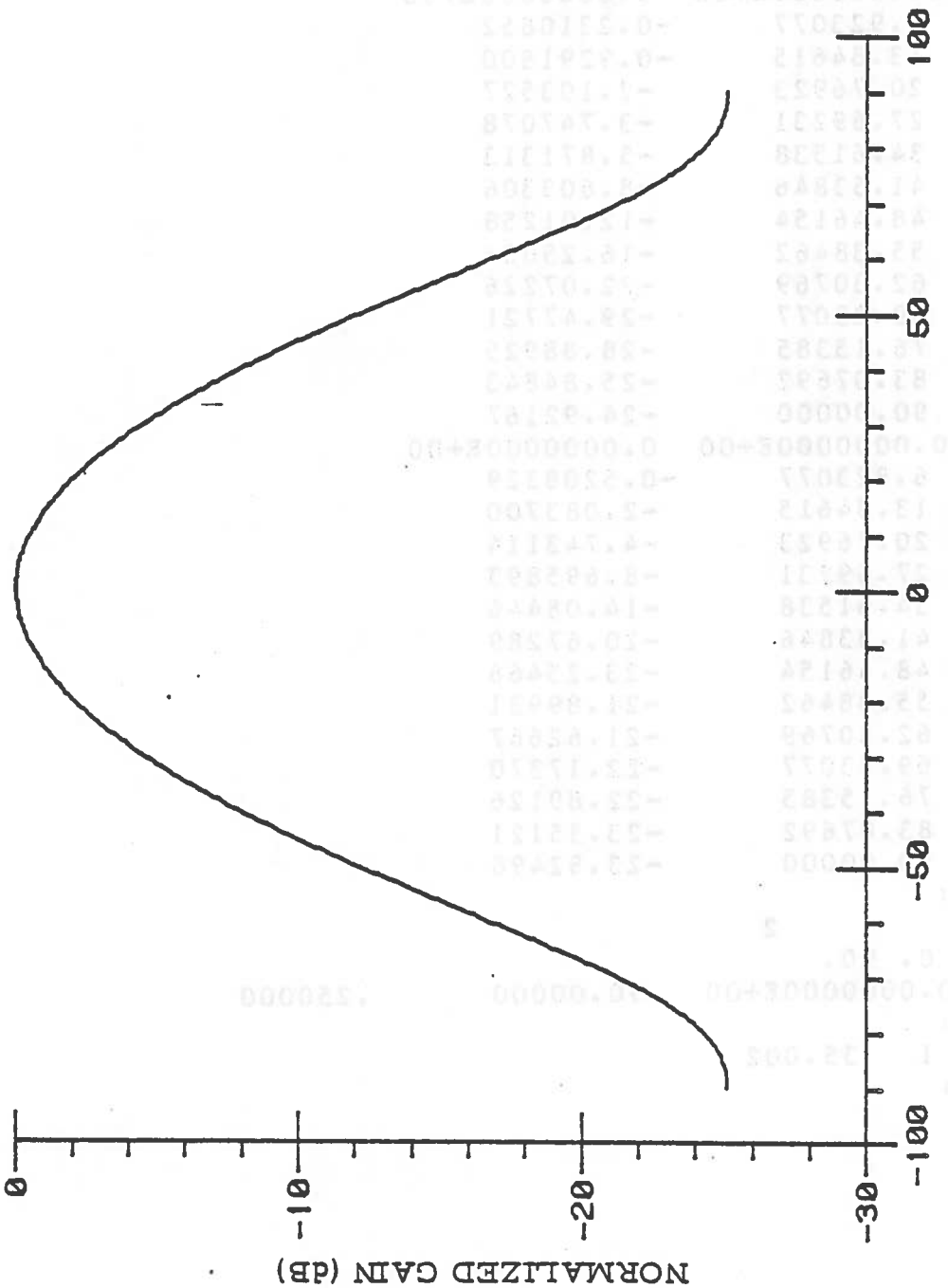

Figure 4.4.4: Nissan system, H-plane feed pattern.

Table 5 : Daimler-Benz-SEL. Input file.

```
DG:
           1 .1    6.29554E-03  6.29554E-03 .3
FD:
  T F T    1 90.00
   2  0.00 90.00
 14
  0.0000000E+00  0.0000000E+00
   6.923077      -0.2310852
   13.84615      -0.9291800
   20.76923       -2.103527
   27.69231       -3.747078
   34.61538       -5.871313
   41.53846       -8.603306
   48.46154       -12.01258
   55.38462       -16.25036
   62.30769       -22.07226
   69.23077       -29.47721
   76.15385       -28.88925
   83.07692       -25.84843
   90.00000       -24.92167
  0.0000000E+00  0.0000000E+00
   6.923077      -0.5208329
   13.84615       -2.083700
   20.76923       -4.743114
   27.69231       -8.695893
   34.61538       -14.08446
   41.53846       -20.67289
   48.46154       -23.25466
   55.38462       -21.89931
   62.30769       -21.62667
   69.23077       -22.17370
   76.15385       -22.89126
   83.07692       -23.55121
   90.00000       -23.82498
PZ:
          2
   0. 90.
  0.0000000E+00   90.00000       .250000
FQ:
   1   35.002
XQ:
```

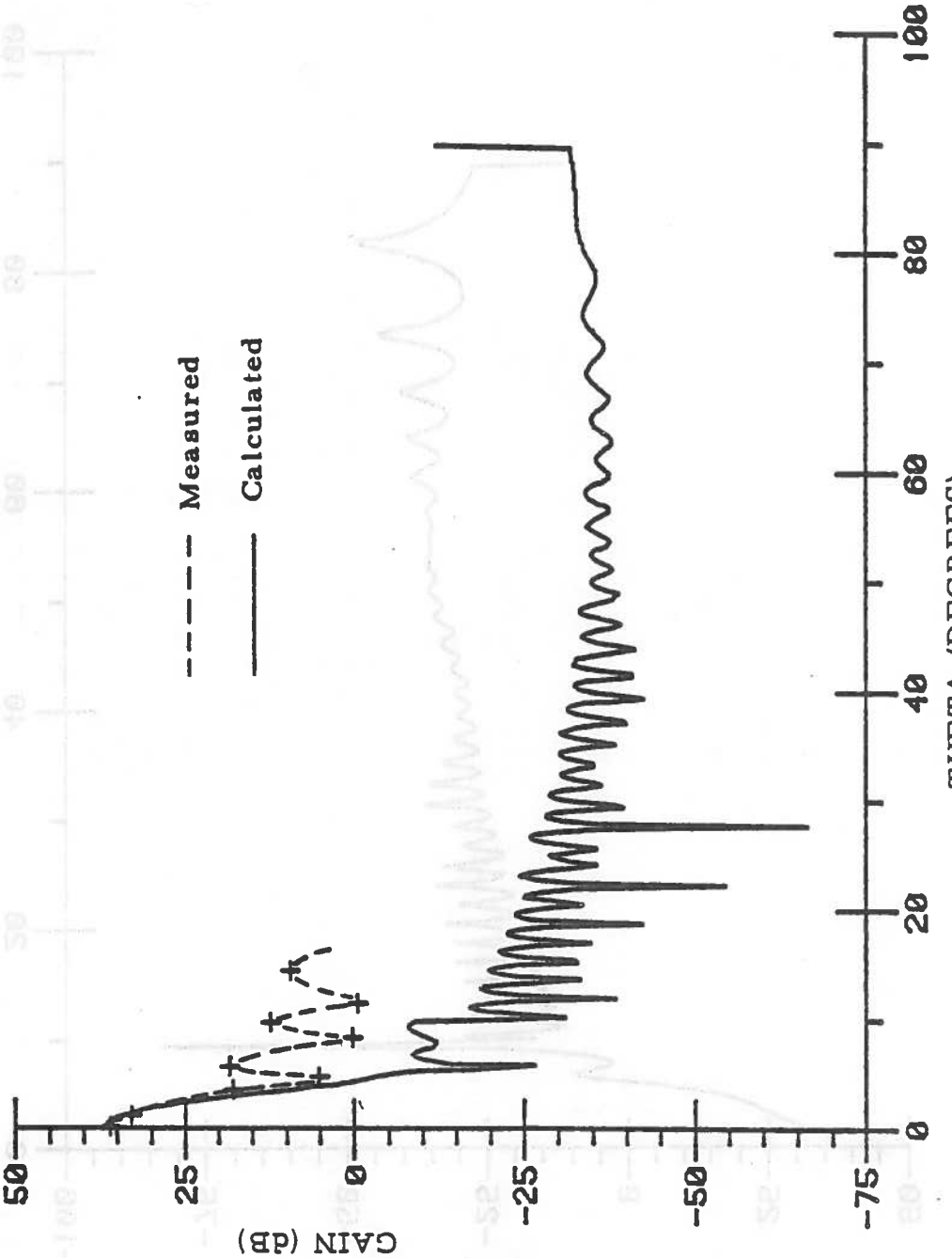

Figure 4.5.1: Benz-Sel system, E-plane pattern.

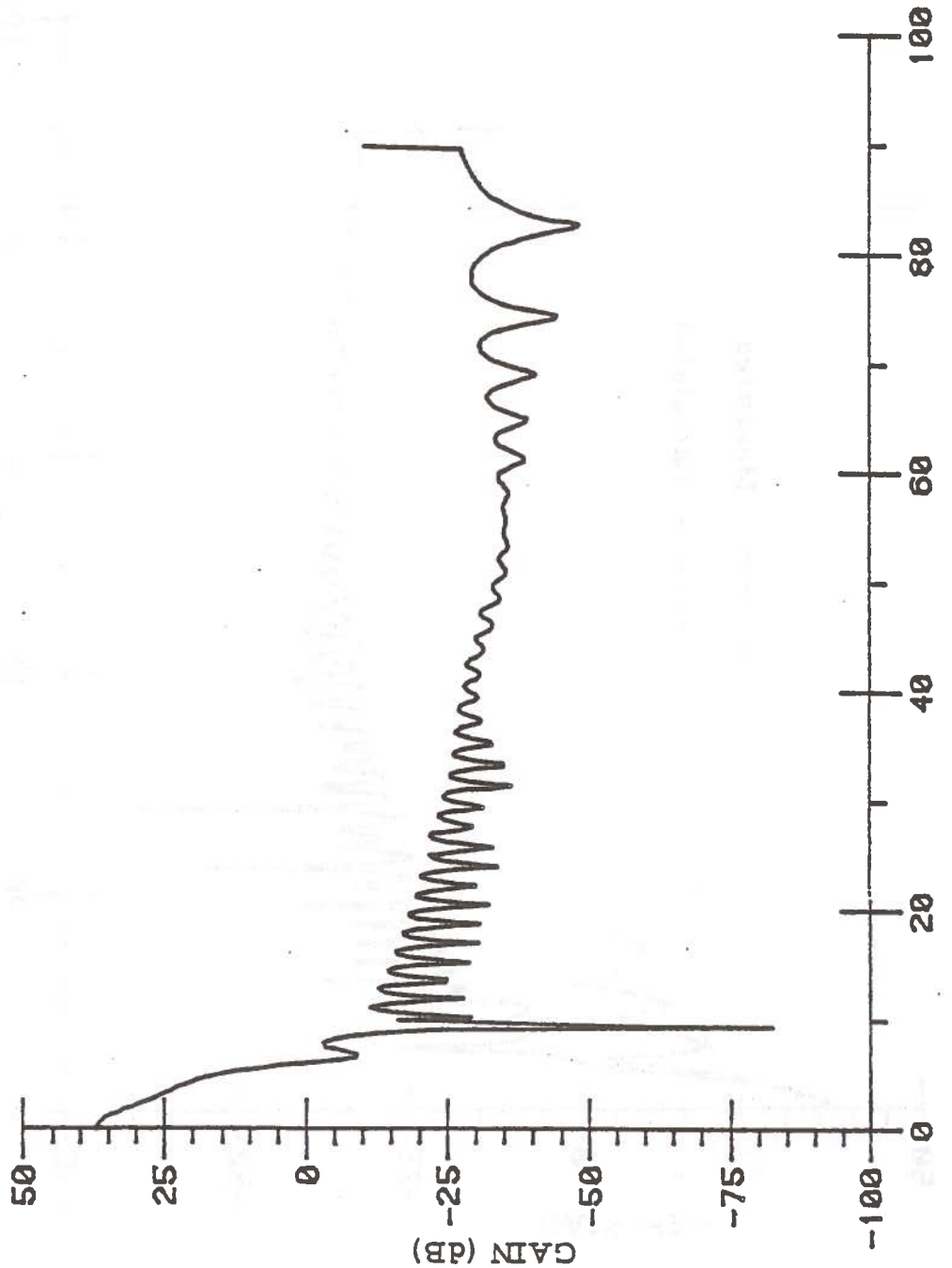

Figure 4.5.2: Benz-Sel system, H-plane pattern.

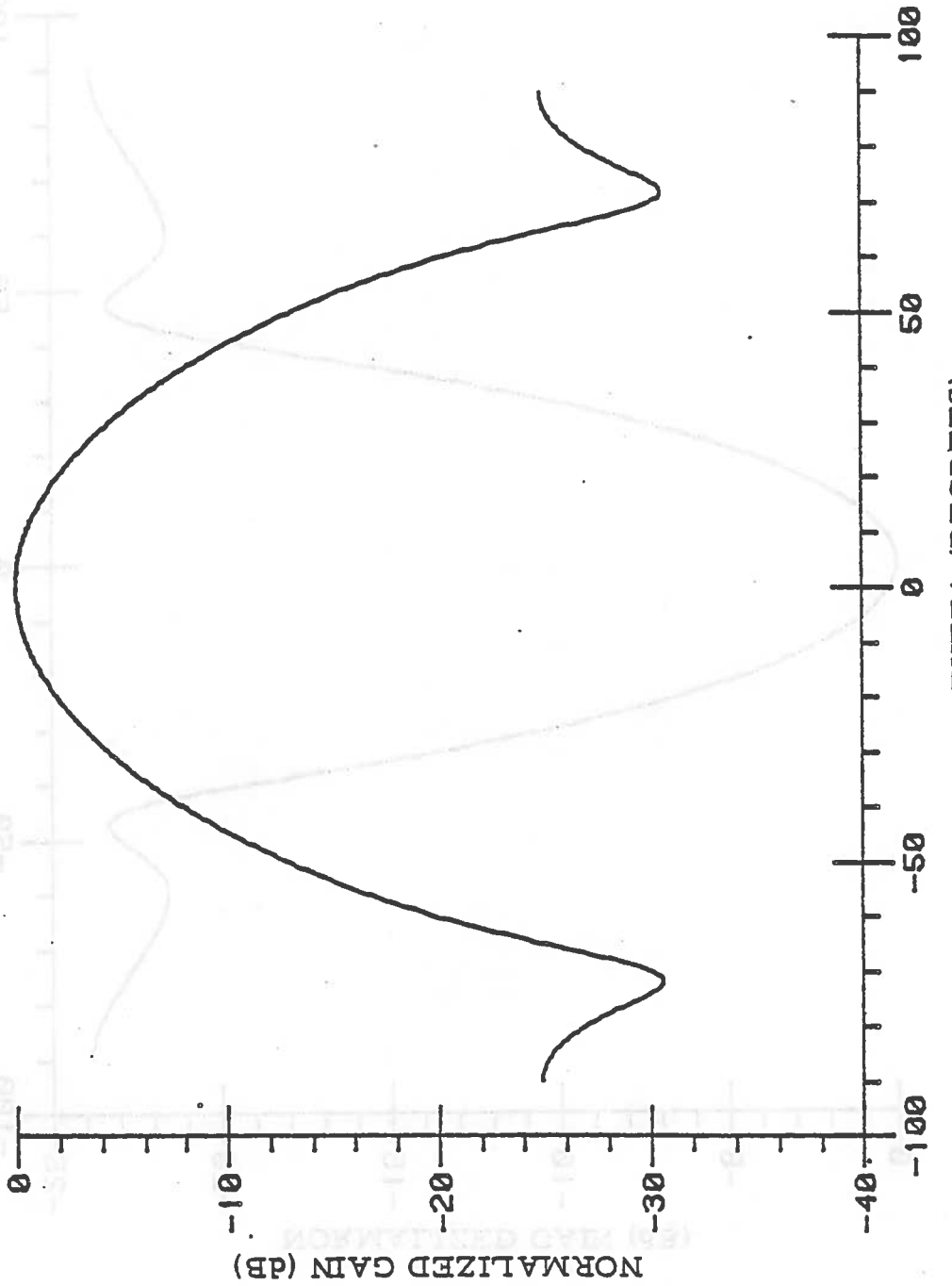

Figure 4.5.3: Benz-Sel system, E-plane feed pattern.

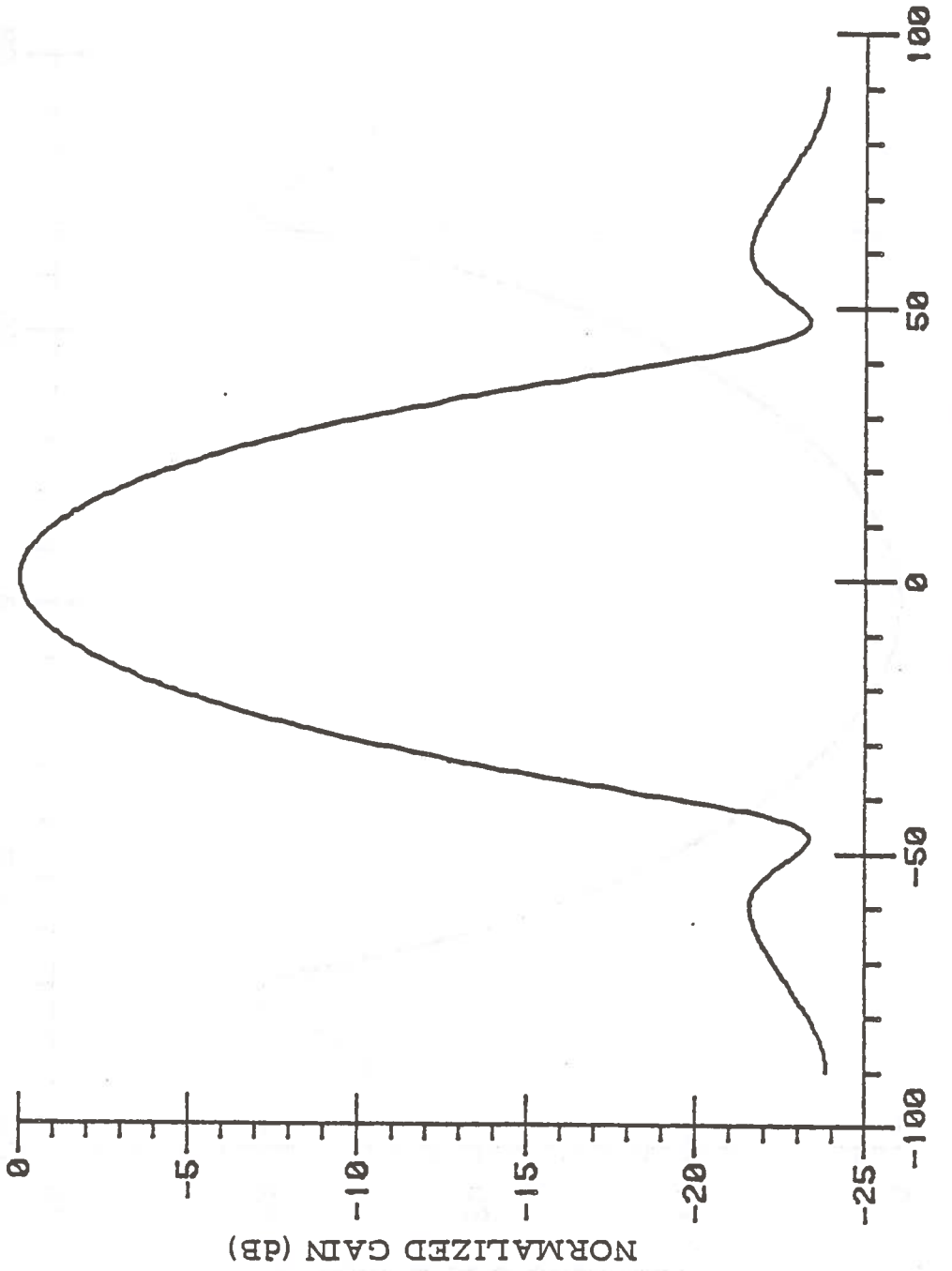

Figure 4.5.4: Benz-Sel system, H-plane feed pattern.

4.6 CONCLUSIONS

The various patterns corresponding to the systems evaluated are very similar in their characteristics. However, the gain of the German system is a little bit higher than that of the two other systems: 37 dB, compared to 34.4 dB for the Nissan-Mitsubishi, and 34 dB for the Bendix. Of course, this higher gain also means a higher side-lobe level. A thorough comparison with experimental patterns could not be made for each radar because of the time involved and the difficulty getting information from the companies. The measured values are plotted on some of the graphs. The predicted patterns exhibit good agreement with measurements for the main beam. However, for greater values of θ, a noticeable discrepancy is observed. The main source of discrepancy is the effect of feed aperture blockage. NECREF, in its present version, does not take the phenomenon into account. It should be noted that aperture blockage limitations are increased at higher frequencies. This comes from the fact that, when the wavelength goes to zero, diffraction phenomena are reduced and the rays tend to propagate according to the laws of Geometrical Optics.

Another source of discrepancy also originates from the code, which assumes that phase feed patterns are constant. This is far from being true in most cases. It is generally impossible to feed the dish with an optimal horn. Therefore, except for low azimuthal angles, phase variations are

strong. The coherence of the reflected beam is then reduced and so is the directivity.

Although several improvements are possible, the results produced by this modeling are satisfactory. In particular, the modeling of the feed exhibits remarkably good agreement with experimental data. As to the modeling of the reflector, it provides satisfactory results in the range from maximum gain to -20 dB. In Automotive Radars applications, this is precisely the range of importance. On the other hand, the reader will note that parabolic reflectors are particularly difficult to model. The code used, NECREF, was developed in the very recent years (1979). It provides more accurate results than the already existing programs. It is therefore a unique feature of this study to use the latest available computer code.

CHAPTER V

MULTIPATH PROPAGATION

This chapter deals with the effects of multipath reflections on Automotive Radar waves propagation. Typical vehicle environment is characterized by its high degree of complexity. In particular, the presence of many reflecting surfaces introduces multipath effects. The main reflecting surface is the roadway, because it is the one which reflects the largest amount of power towards the target, and also because the effect is permanent. Therefore, emphasis has been put on ground reflections in the following pages. Other possible sources of multipath propagation are also considered and their relative importance is evaluated.

5.1 GROUND REFLECTIONS

5.1.1 Statement of the Problem

The various possible paths for reflected rays are shown in Figure 5.1.1 . In Figures 5.1.2 and 5.1.3 the geometry of the problem is illustrated. The range of frequencies to be considered allows the principles of Geometrical Optics to be used. Therefore, to a first approximation, the problem of a radar antenna above the ground can be considered by using the image of the antenna with respect to the ground plane. Since ground reflection is far from being perfect, it is necessary to compute reflection coefficients to determine the amount of power reflected and the phase shift introduced by the reflection.

In addition to this phase shift, the effect of the path difference between direct and reflected ray must be taken into account. From Figure 5.1.2, it is possible to approximate the path difference by :

$$d = (R2 - R1) = 2h \sin\phi \qquad (5.1)$$

Then :

$$\Delta\Phi = \frac{2\pi d}{\lambda} = 4\pi \frac{Hh}{\lambda R} \qquad (5.2)$$

As a matter of fact, a more general statement of this problem must include target cross-section. The power returned from the target is what is important. The expression of the ratio of incident to reflected power is not shown here, but it can be found in the work of

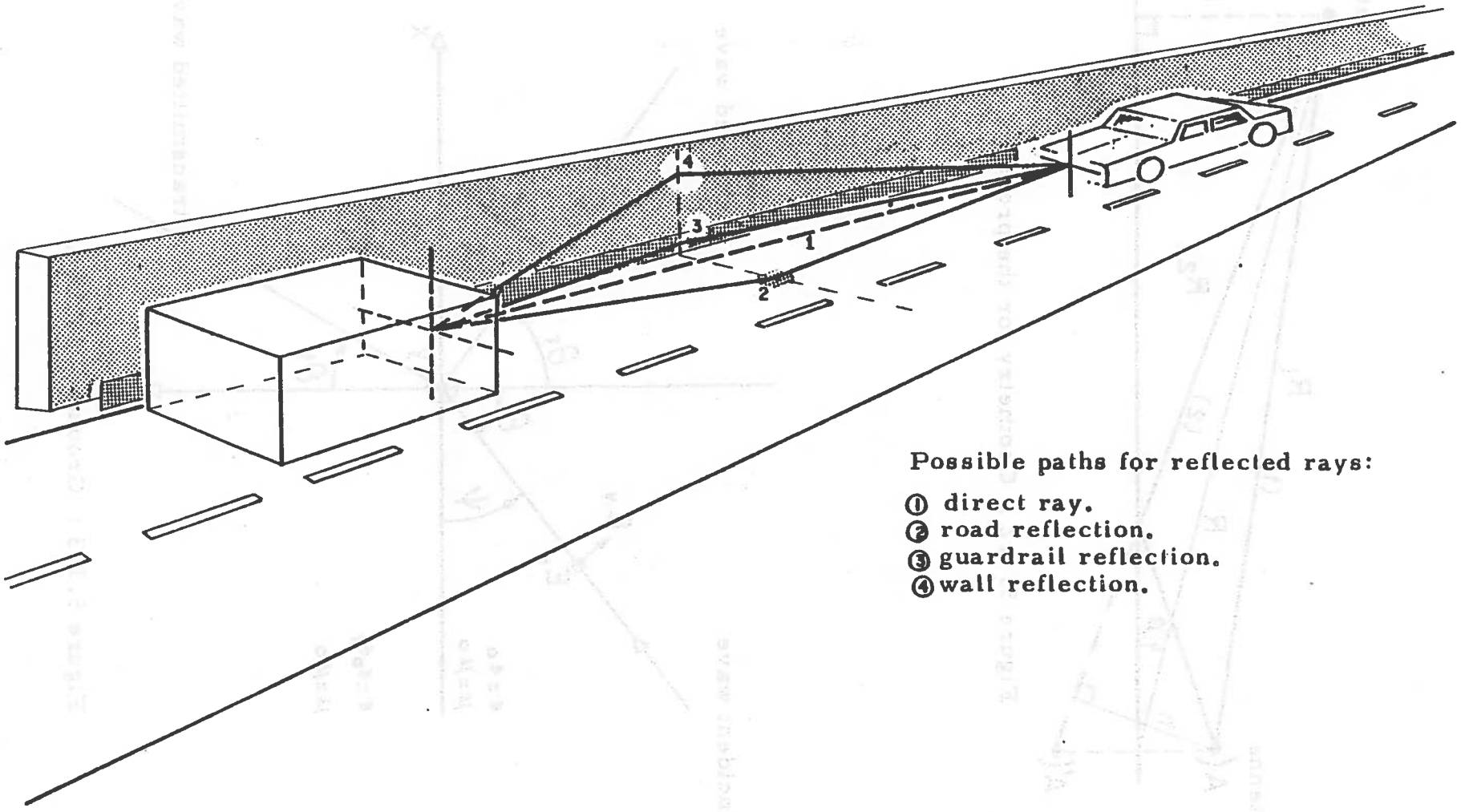

Figure 5.1.1: Various possible paths for reflected rays.

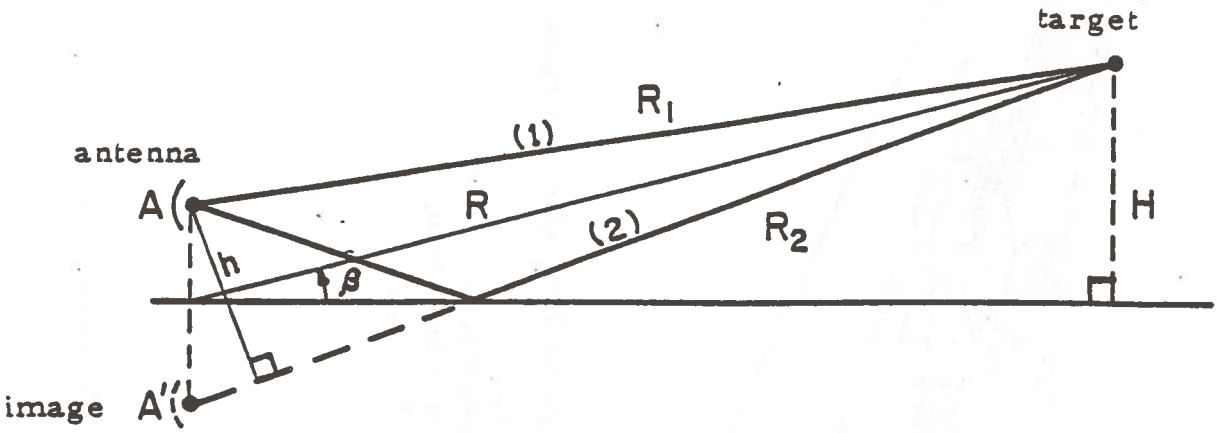

Figure 5.1.2 : Geometry for the problem.

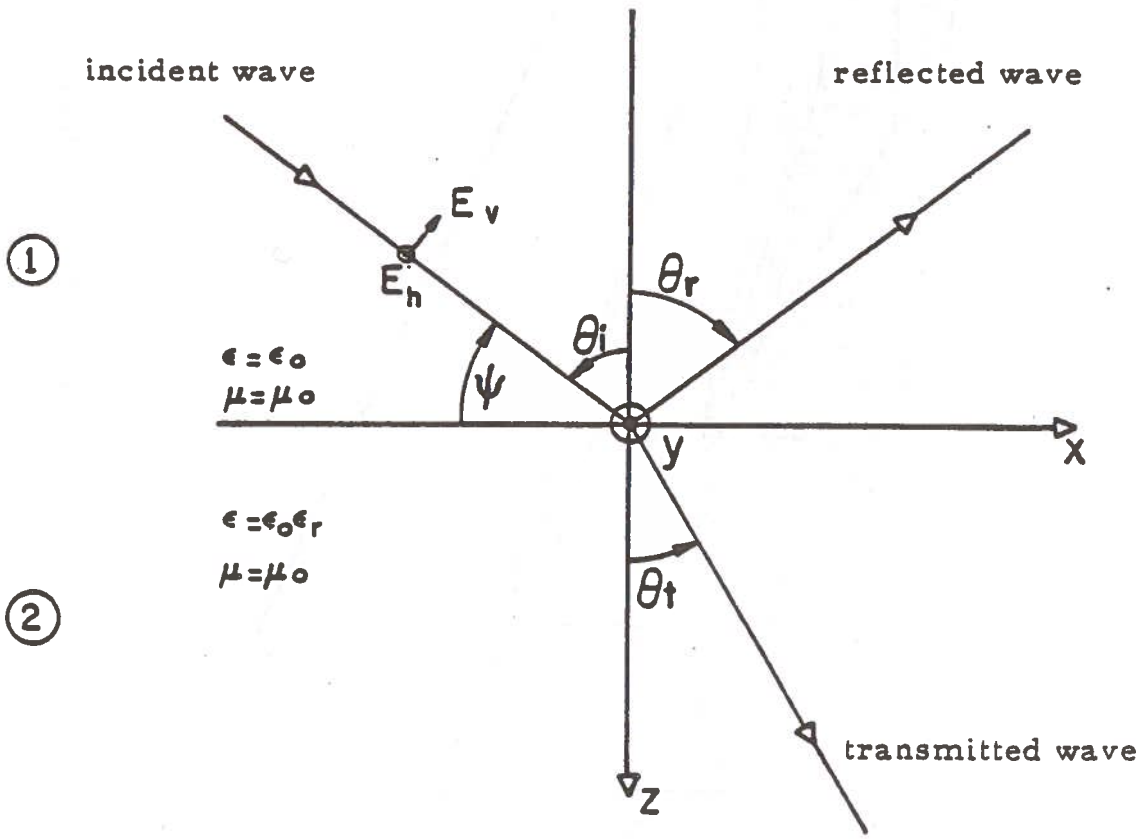

Figure 5.1.3 : Ground reflection.

J. M. Laugénie (1981). It takes into account the variations of the directive gain, the path difference between rays and the monostatic and bistatic cross-sections of the target. Basically, the relationship is an extension of the classical radar equation to all the possible paths between antenna and target.

It might be thought useless to introduce the variations of the gain and the cross-section because only small grazing angles are involved in this particular case. However, a quick look at the curves which give antenna patterns shows that, with such a narrow beamwidth, gain variations are far from being negligible, especially around the axis of the antenna.

5.1.2 Computation of Ground Reflection Coefficients

1) Case of a Perfectly Smooth Ground: Reflection coefficients for a smooth ground are well-known. The main results are reviewed here. Consider Figure 5.1.3 : the wave incident on the ground plane is split into two components (vertical and horizontal). The vertical component is in the plane of incidence, whereas the horizontal component is in the plane of the ground. Consequently, two different reflection coefficients are derived : one for the vertical component, and one for the horizontal component. Let Rv and Rh be these coefficients. If Ev and Eh are the vertical and horizontal components of the E-field, then the reflected

field is written as :

$$Er = Rv \cdot Ev + Rh \cdot Eh \qquad (5.3)$$

Note that Rv and Rh are complex quantities.

Calling η_1 and η_2 the intrinsic wave impedances of media 1 and 2, using the identity

$$E\ trans = E\ refl + E\ inc \qquad (5.4)$$

By equating the wave impedances, Z = E/H, at the boundary, it can be shown:

$$R_v = \frac{[\eta_2 \cdot \cos\theta t - \eta_1 \cdot \cos\theta i]}{[\eta_2 \cdot \cos\theta t + \eta_1 \cdot \cos\theta i]} \qquad (5.5)$$

Where θi and θt are the angles of incidence and transmission.

Recall that for free space, η is equal to $\sqrt{\mu/\epsilon}$. For a lossy medium, the expression becomes :

$$\eta = \sqrt{jw\mu/(\sigma + jw\epsilon)} \qquad (5.6)$$

Where σ is the conductivity, ϵ the permittivity, and w the pulsation of the wave.

For horizontal polarization, the coefficient becomes :

$$R_h = \frac{[\eta_2 \cdot \sec\theta t - \eta_1 \cdot \sec\theta 1]}{[\eta_2 \cdot \sec\theta t + \eta_1 \cdot \sec\theta i]} \qquad (5.7)$$

Introducing Ψ, grazing angle, and v_1 and v_2, phase velocities in medium 1 and 2, Snell's law is written :

$$v_2 \cdot \sin\theta i = v_1 \cdot \sin\theta t \qquad (5.8)$$

Where :

$$\begin{cases} v_1 = c \text{ (velocity of light)} \\ v_2 = w/\beta 2 \end{cases}$$

$$\begin{cases} \sin\Psi = \cos\theta i \\ \cos\theta t = [1 - (v_2/v_1)^2 \cdot \cos\Psi]^{1/2} \end{cases}$$

Where β_2 is the phase-shift factor for medium 2, defined as the imaginary part of γ, Helmholtz propagation constant :

$$\gamma = \sqrt{jw\mu \cdot (\sigma + jw\epsilon)} \qquad (5.9)$$

After calculation of β as a function of σ, ϵ, w, and μ, it can be shown:

$$\beta = w \sqrt{\frac{\mu\epsilon}{2}} \cdot \sqrt{\sqrt{\left(1 + \frac{\sigma^2}{w^2\epsilon^2}\right)} + 1} \qquad (5.10)$$

Then, the ratio (v_2/v_1) is computed, and the final expressions for the reflection coefficients of a smooth ground are found to be :

$$R_v = \left[\frac{\left(\sin\Psi - (1/\epsilon r \cdot A)^{1/2} \cdot [1 - 2 \cdot \cos^2\Psi/(\epsilon r \cdot B)]^{1/2}\right)}{\left(\sin\Psi + (1/\epsilon r\ A)^{1/2} \cdot [1 - 2 \cdot \cos^2\Psi/(\epsilon r \cdot B)]^{1/2}\right)}\right] \qquad (5.11)$$

$$R_h = \left[\frac{\left((1/\epsilon r \cdot A)^{-1/2} \cdot \sin\Psi \cdot [1 - 2 \cdot \cos^2\Psi/(\epsilon r \cdot B)]^{1/2} - 1\right)}{\left((1/\epsilon r \cdot A)^{-1/2} \sin\Psi \cdot [1 - 2 \cdot \cos^2\Psi/(\epsilon r \cdot B)]^{1/2} + 1\right)}\right] \qquad (5.12)$$

Where :

$$\begin{cases} A = [1 - jx] \\ B = [1 + \sqrt{1 + x^2}] \\ \text{and } x = (\sigma/w\varepsilon) \end{cases}$$

2) Case of a rough ground: Road surfaces may be approximated by smooth surfaces with a small error. However, it will be seen that in the range of frequency considered, this approximation holds only because the grazing angles of interest are very small, such as a few degrees. The theory of reflection on rough surfaces is complex and involves sophisticated mathematics which are not reproduced here. "Scattering and Reflection from Rough Surfaces", by Beckmann and Spizichino (1963), is a basic text on surface scattering phenomenon. Peake and Taylor (1959) have collected a large amount of experimental measurements. The most difficult part of the problem is generally finding an accurate enough model which describes the surface. In the case of a roadway, this is not difficult. The distribution function of the heigths above the average level can be taken as a Gaussian function.

If σh is the rms surface height variation above the average level, the following criterion, called Rayleigh criterion, enables the surface to be classified as "rough" or "smooth" :

$\sigma h < \lambda/(8 \cdot \sin\Psi)$ <=> " the surface is smooth "

Figure 5.1.4 helps one to understand the physical meaning of the Rayleigh criterion. For a surface with only two possible heights, the phase shift corresponding to the path difference of rays 1 and 2 shown in Figure 5.1.4 is :

$$\Delta\phi = \frac{4\pi h}{\lambda} \cdot \sin\Psi$$

For $\Delta\phi=\pi$, 1 and 2 are in phase opposition and the surface scatters. For $\Delta\phi=0$, the surface is smooth. The Rayleigh criterion corresponds to $\Delta\phi=(\pi/2)$, which is half-way between the two extremes.

Although, for a scattering surface, all the points of the surface contribute to reflection, it is found that the main contribution comes from a zone called the first Fresnel zone. In this region, the maximum path difference between two points is always less than $(\pi/2)$. Other Fresnel zones are defined by incrementing the maximum value of the path difference by $\lambda/2$. Each Fresnel zone is an ellipse, or more exactly an ellipsoid which produces an ellipse by intersection with the ground plane. To find an order of magnitude of the size of the region, the expressions given by Beckmann can be approximated, with the notations of Figure 5.1.5 for which $h1=h2=h$, by:

$$\begin{cases} \text{Semi-major axis} : & x1 = R/[2\sqrt{1 + (4h^2/r\lambda)}] \quad (5.13) \\ \text{Semi-minor axis} : & y1 = \sqrt{\lambda R/2} \quad (5.14) \end{cases}$$

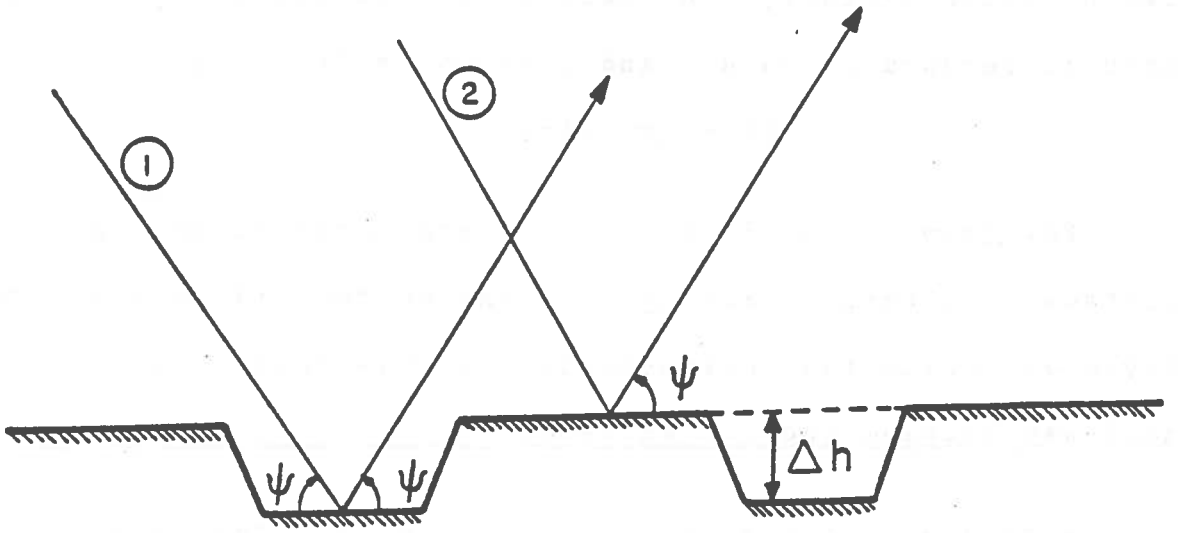

Figure 5.1.4: Rayleigh criterion.

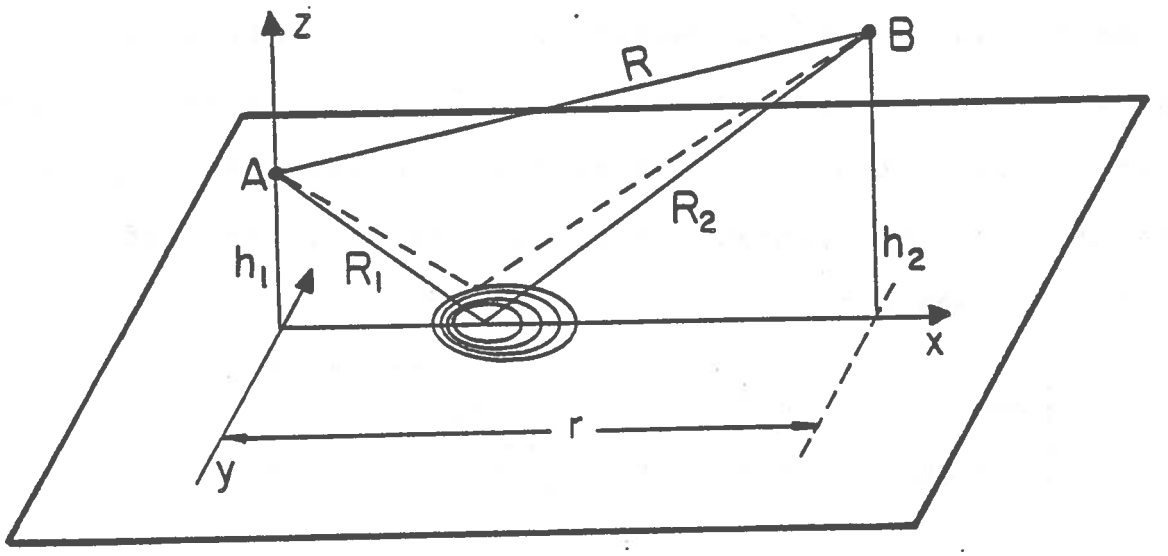

Figure 5.1.5: Fresnel's zones.

For instance, choosing R=50 m, h=0.50 m, λ=1 cm (30 GHz), x1 and y1 are :

x1 = 14.50 m; y1 = 0.35 m.

This proves that the first Fresnel zone is very long and narrow (Barton, 1974), and that the reflection phenomenon is not local.

Now, the problem is to relate reflection coefficients of a rough surface to those of a smooth surface. Assuming the gaussian model to represent road heights variations, the distribution is thoroughly defined by the data of σh, mean square value of the height variation. From Beckmann and Spizichino, the new reflection coefficients are equal to :

$$R = Ro.Rs \qquad (5.15)$$

Where Ro is the coefficient for a smooth ground, vertical or horizontal, and Rs is a term taking into account the roughness of the ground. Rs is related to the grazing angle Ψ and to σh by :

$$Rs^2 = \exp[-(4\pi\sigma h.\sin\Psi/\lambda)^2] \qquad (5.16)$$

It is clear that the critical part is to determine the value of σh. From Peake and Taylor, typical values are :

Asphalt driveway : σh = 1.6 10 cm.

Asphalt parking lot : σh = 1.9 10 cm.

Rough asphalt road : σh = 2.7 10 cm.

5.1.3 Results from the Models

1) Dry Smooth Road: Figures 5.1.6 to 5.1.9 show a first example for which ϵr is taken equal to 2, σ to 0.0005 and σh to 0. It represents the case of a perfect smooth dry road. The decrease of the coefficient is steeper for Rv than for Rh. Therefore, multipath effect is more important for horizontally polarized waves. But the figure also shows that, even if Rv is 0 at about 38°, pseudo-Brewster angle, there is no substantial decrease for an angle less than 5°. It is therefore possible to consider that, for Automotive Radar applications, Rh and Rv have a magnitude of 1. As the phase of the coefficient is equal to π, then :

$$Rv = Rh = -1 \qquad (5.17)$$

A reflection coefficient equal to -1 has for immediate consequence that, if the path difference between direct and reflected ray is a multiple of $\lambda/2$, the two rays will add destructively. This is particularly true in the vicinity of the ground plane. Therefore, a target lying in that plane will receive much less power, due to the destructive interference of the rays. But targets of interest in Automotive Radar are large enough that this aspect of multipath reflection is not a serious limitation.

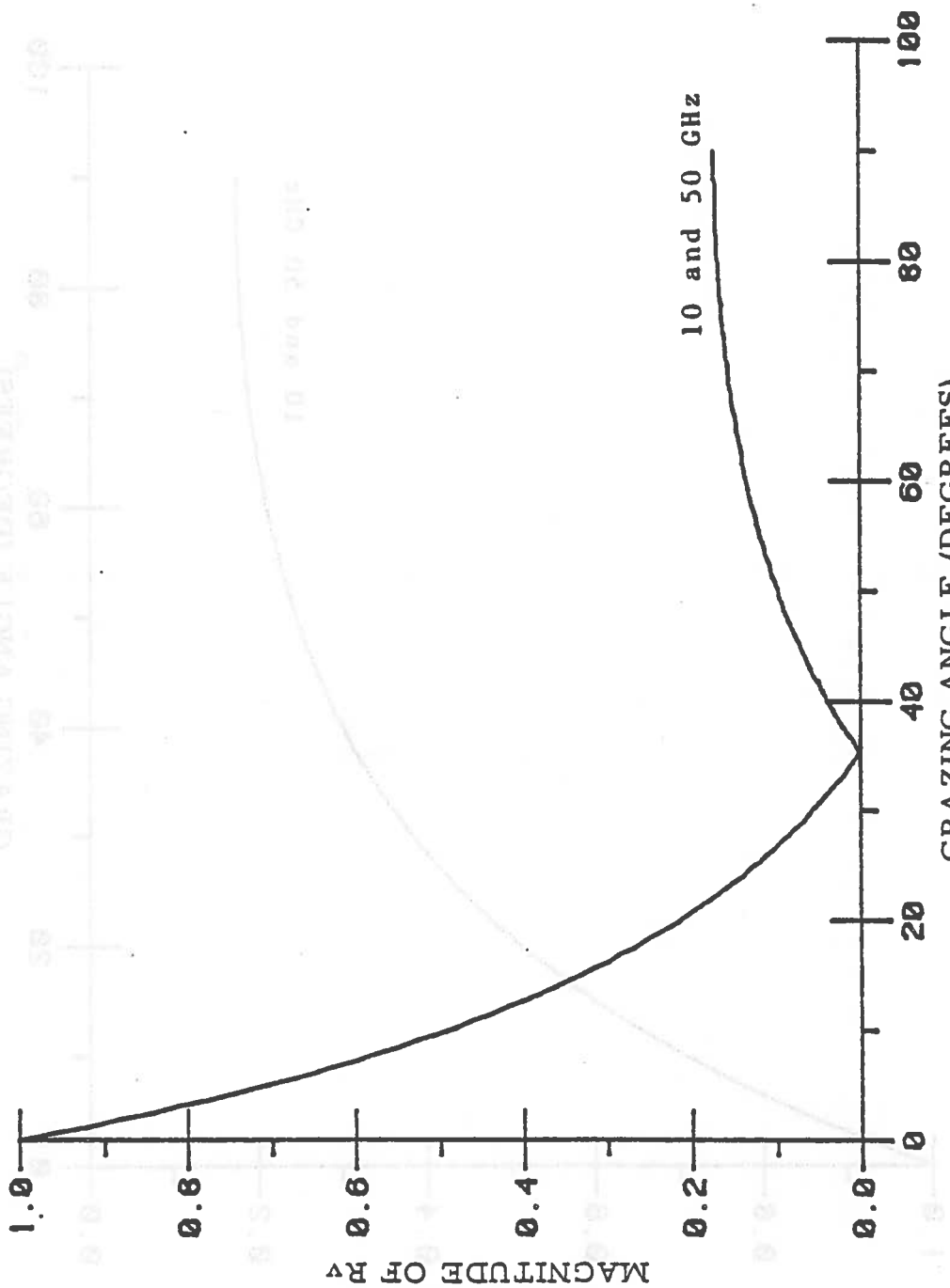

Figure 5.1.6: Vertical reflection coefficient variations vs. grazing angle for 10 and 50 GHz (case of a dry smooth road).

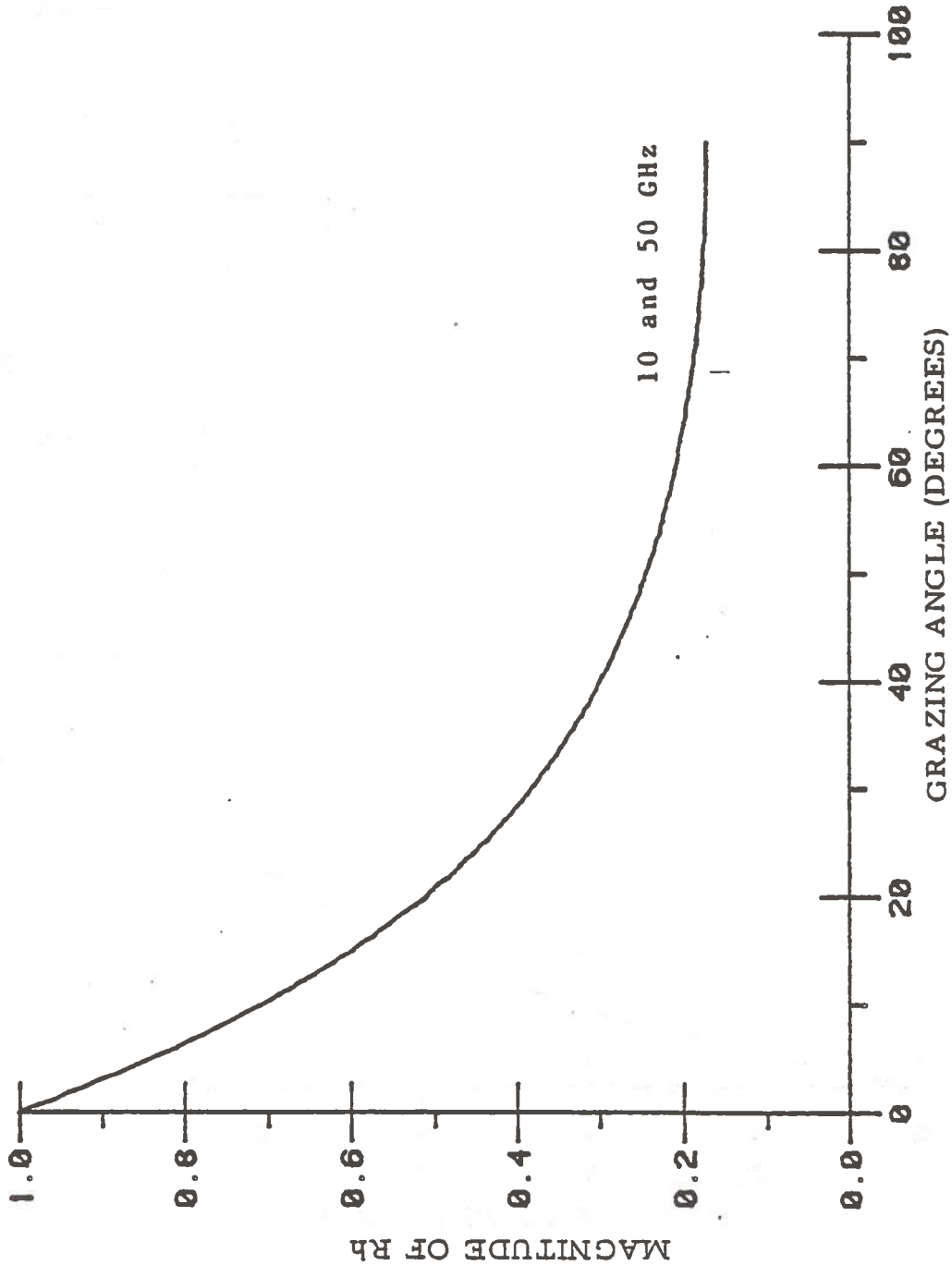

Figure 5.1.7: Horizontal reflection coefficient variations vs. grazing angle for 10 and 50 GHz (case of a dry smooth road).

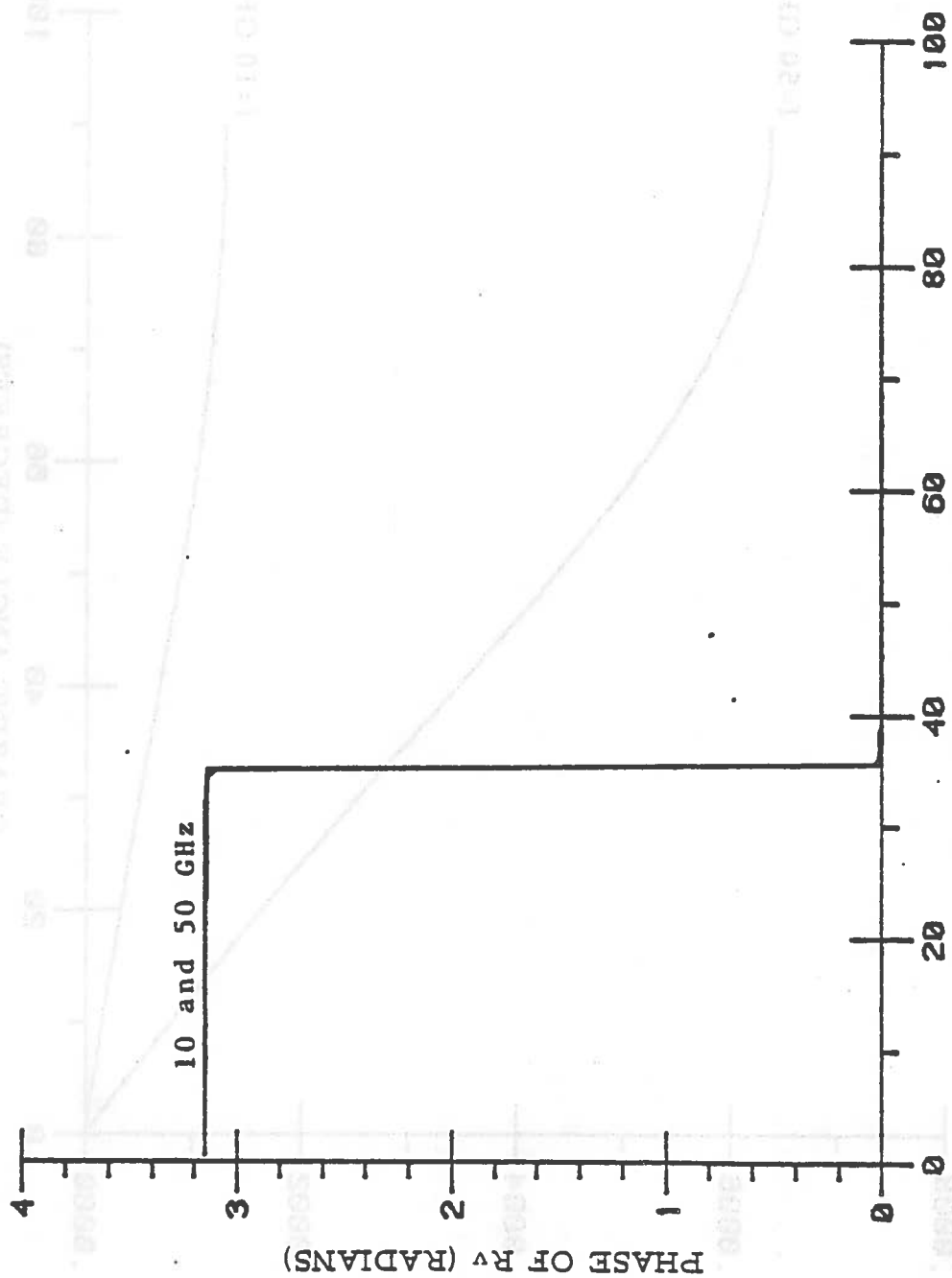

Figure 5.1.8: Phase variations of Rv vs.grazing angle for various frequencies (case of a dry smooth road).

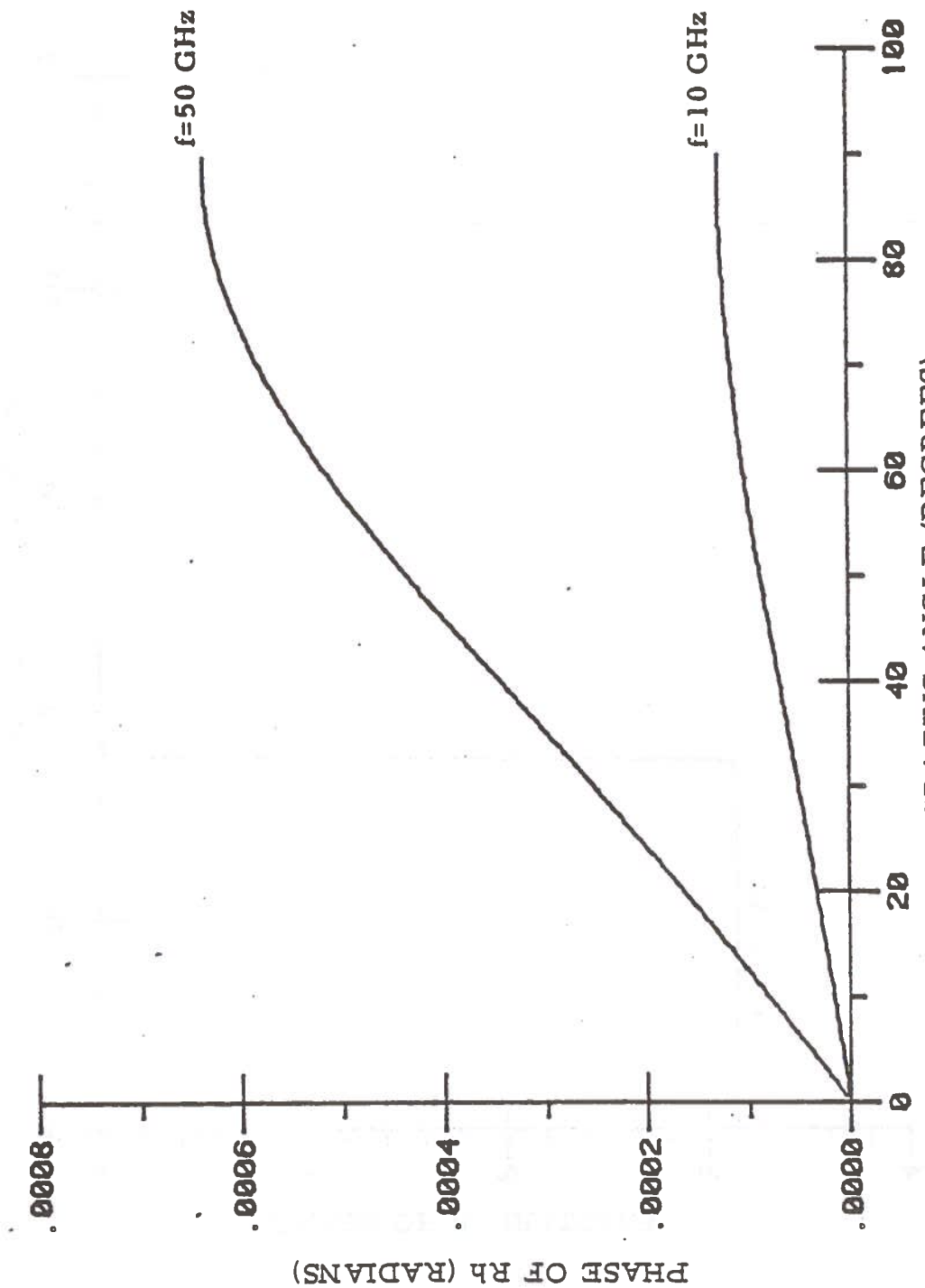

Figure 5.1.9: Phase variations of Rh vs. grazing angle for various frequencies (case of a smooth dry road).

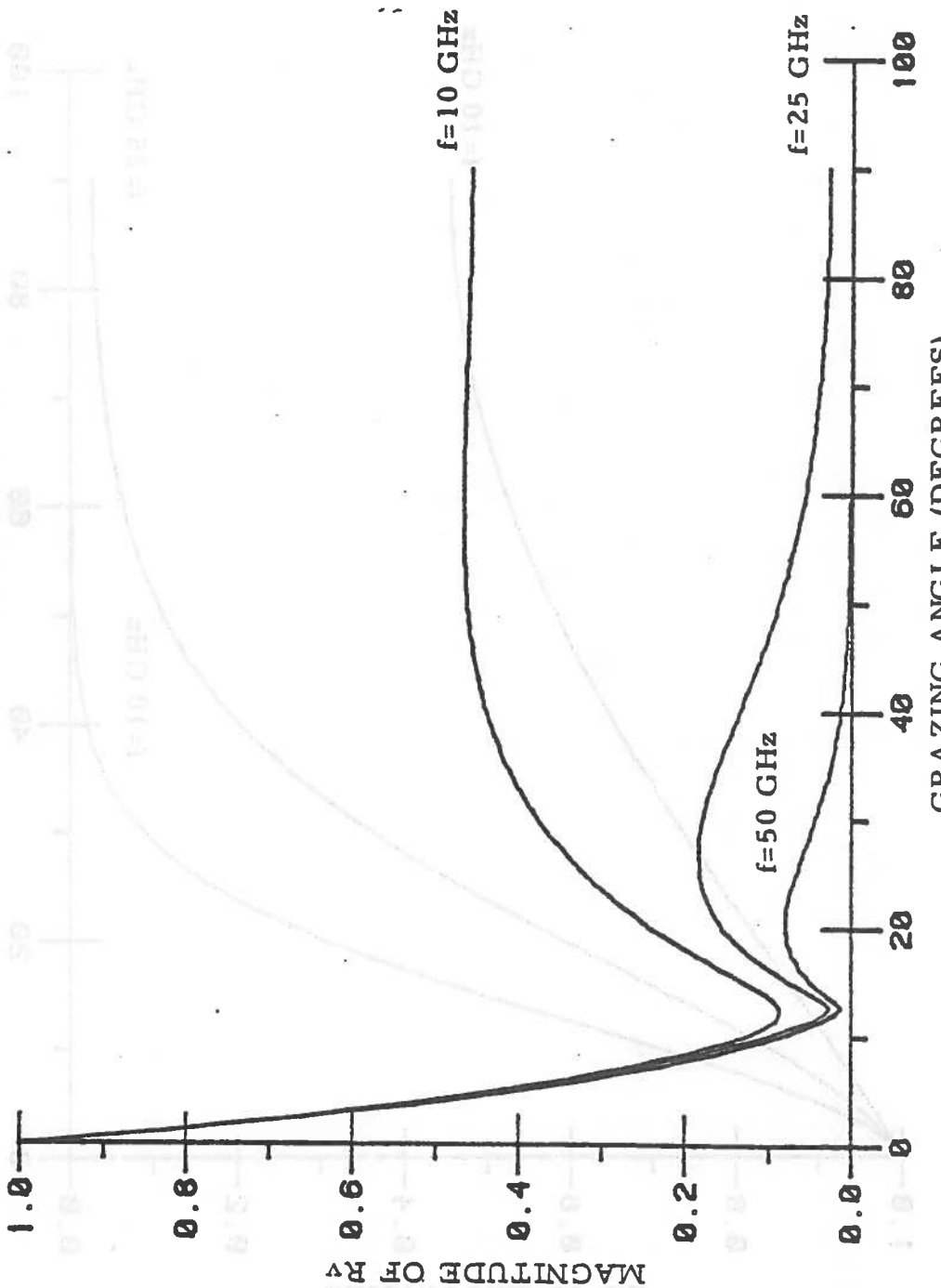

Figure 5.1.10: Vertical reflection coefficient variations vs. grazing angle for various frequencies (case of a wet rough road).

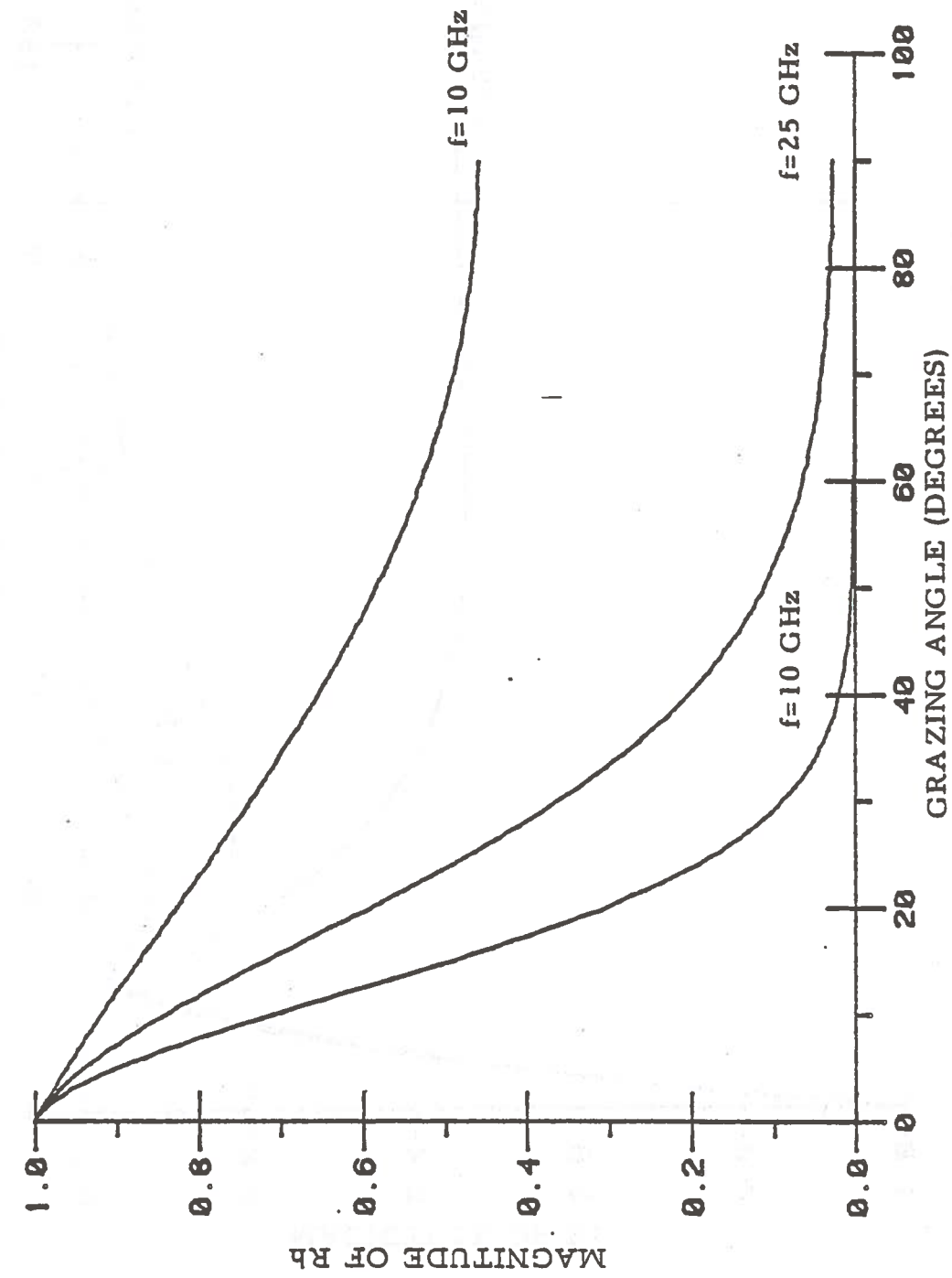

Figure 5.1.11: Horizontal reflection coefficient variations vs. grazing angle for various frequencies (case of a wet rough road).

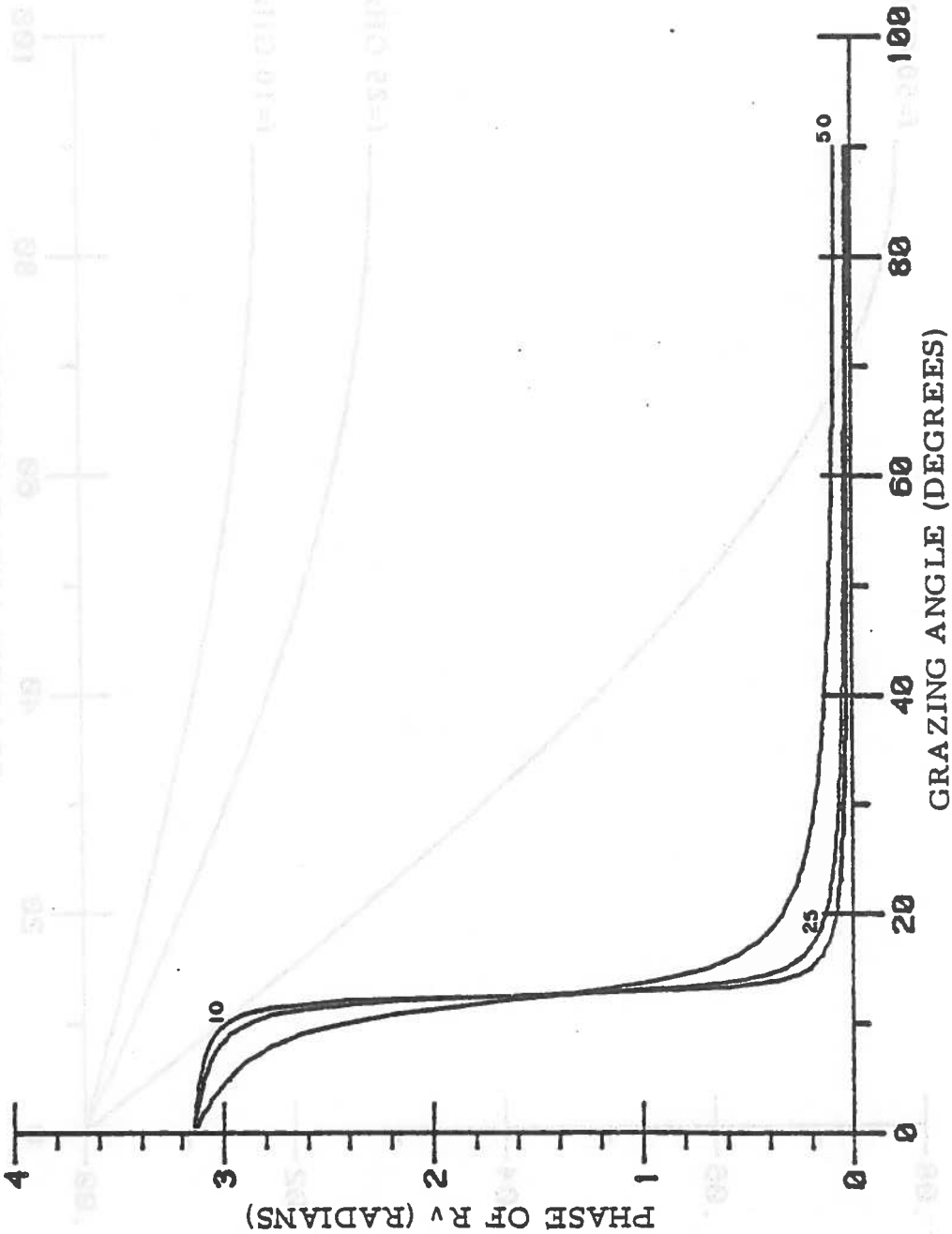

Figure 5.1.12: Phase variations of Rv vs. grazing angle for various frequencies (case of a wet rough road).

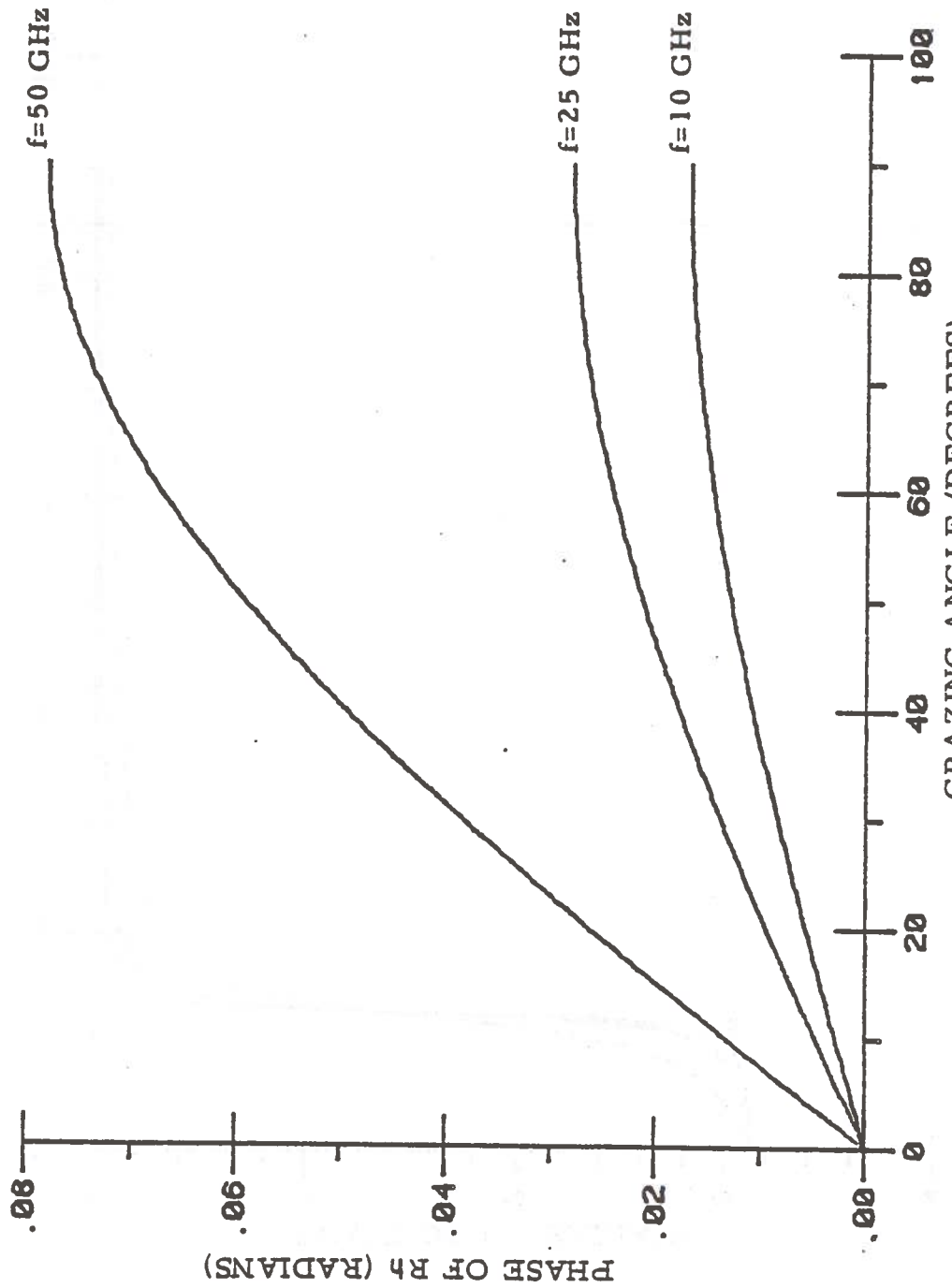

Figure 5.1.13: Phase variations of Rh vs. grazing angle for various frequencies (case of a wet rough road).

2) Wet Rough Road: Figures 5.1.10 to 5.1.13 show the other extreme situation of a very rough road, such as grooved pavement, wet, for which σ=4, σh=0.2 cm, and ϵr=20. For that example, it is seen that the decrease is much steeper when Ψ increases. At an angle of 5^{o}, Rv is only a half of its value. Frequency plays an important part only for high grazing angles. The phase reversal around the pseudo-Brewster angle is smoothed for the rough model case.

In the first case, the presence of the ground produced an alteration of the antenna pattern. The negative addition of the rays in the plane of reflection was equivalent to splitting the beam into two beams, symmetrical with respect to the ground. In the case of a rough wet ground, the effect is smoothed as can be seen on the curves.

5.2 OTHER MULTIPATH REFLECTIONS

The problem of ground reflection is not easy to analyze from a theoretical point of view. However, other multipath reflections occurring in Automotive Radar are even more complex. Semi-permanent effects can be analyzed in a similar way to permanent effects.

For instance, when there are buildings along the road, such as a wall, it is possible to apply the analysis developed for ground reflection, with the only difference being that vertical and horizontal components of the wave must be reversed. But it must be noted that the grazing angles of

interest in that type of reflection are much larger than for ground reflection. Then, it is reasonable to consider this phenomenon to be negligible.

Another important parasitic reflection occurs on guard-rails. This is a typical semi-permanent effect. Guard-rails, which are also potential false-targets, contribute to the reflection of radar waves. The reflection can be considered as perfect (Rv = Rh = +1). A path difference can be introduced between the direct and reflected rays, as it has been done for the ground :

$$\Delta\phi = (2\pi/\lambda) \cdot 4h1 \cdot h2/R$$

Where R is the distance to the target and h1 and h2 are the distances to the guardrails. Substituting these quantities by numerical values, it appears that the phase shift varies so quickly that it can be considered to be randomly distributed as a function of the distance to the rail. Therefore, the only influence of the reflection is to introduce signal fluctuations.

CHAPTER VI

ATMOSPHERIC PERTURBATIONS AND PROPAGATION

Attenuation and back-scattering resulting from atmospheric perturbations may strongly degrade performances of Automotive Radars. At microwave frequencies, the presence of hydrometeors can totally obscure a target of interest, in particular targets with small radar cross-section, such as a bike or a pedestrian. This chapter compares, with the aid of the models derived for rain, fog, and snow, the behavior of the various types of radar in the presence of meteorological perturbations.

6.1 SCATTERING AND ATTENUATION FROM SPHERICAL PARTICULES

6.1.1 Statement of the Problem

To a first approximation, rain, fog, and snow particles can be considered as spherical. Backscattering and attenuation from particles of that kind are well-known and have been studied by Mie (1908). Mie's theory has been restated by later researchers (Kerr, 1965). The basic problem is

to determine the two quantities σ and Q, defined as back-scattering and attenuation cross-sections.

If Pt is the power transmitted by the receiver, if Pr is the average power returned from a particle of cross-section σ, then, in the far field region (Fraunhofer region):

$$Pr = \frac{Pt \cdot G^2 \lambda^2 \sigma}{(4\pi)^3 \cdot R^4} \qquad (6.1)$$

Where G is the gain of the antenna and R the range to the target.

In practice, one is interested in the average effects from the whole ensemble of particles. It is the reason that the quantity $\eta = \sum_i \sigma$, total cross-section per unit volume, is introduced. η is also called reflectivity.

For the particular case of a pulse radar, Skolnik (1959) gives a similar expression :

$$Pr = (Pt \cdot Ae \cdot L \cdot \sum_i \sigma)/32R^2 \qquad (6.2)$$

Where Ae is the effective antenna aperture and L is the pulse length ($L=c\tau$, τ duration of the pulse).

An average value of Q is also used to describe attenuation by an ensemble of particles. Then, the attenuation corresponding to a distance L is $\exp[-\sum_i Q \cdot L]$. $\sum_i Q$ is the sum of the cross-sections of attenuation over the unit volume. In practical units, attenuation is given by :

$$A\ (dB/km) = 0.4343 \cdot \sum_i Q \qquad (6.3)$$

Starting from the Mie's expression for σ and Q, for a single particle, assuming that the entire scatterer is illuminated, after expansion with respect to $\alpha=(\pi D/\lambda)$ and $m = [n-jk]$, complex refractive index, it is found :

for $\alpha << 1$ (Rayleigh region)

$$\begin{cases} \sigma = (\lambda^2/2\pi)\cdot 2\alpha^6\cdot\left|(m-1)/(m+1)\right|^2 = \pi^5\cdot\left|K\right|^2\cdot(D^6/\lambda) & (6.4) \\ Q = (\lambda^2/2\pi)\cdot 2\alpha^6\cdot Im[-(m-1)/(m+1)] = \pi^2\cdot D^3\cdot[Im(-K)/\lambda] & (6.5) \end{cases}$$

With : $K = \left[(m-1)/(m+1)\right]$;

K is characteristic of the medium considered. Knowing σ and Q for a single particle, expressions for $\sum_i \sigma$ and $\sum_i Q$ can be derived.

6.1.2 Attenuation

For Q, this is usually done by intoducing M, liquid water content, in g/cm . M is related to $\sum_i D^3$ by :

$$(M/\rho) = (\pi/6)\sum_i D^3 \quad (6.6); \quad (\text{ for water } \rho = 1)$$

From this, A is written :

$$A\ (dB/km) = 0.4343\cdot(6\pi/\lambda)\cdot(M/\rho)\cdot Im(-K) \quad (6.7)$$

The validity of the expression will be discussed later. Note that A is a one-way attenuation.

The problem is to evaluate the integral $\int_0^{\infty} x^6 \cdot \exp(-x) \cdot dx$. A possible integration is given in the Bendix-NHTSA technical report (1976). However, it appears that the truncation of the integral is not necessary, even if raindrop size distribution does not extend to infinity. Recall that the integral of a product of an exponential and a polynomial is a function of the same kind, and recall that the integrals boundaries are 0 and $+\infty$: then the value of the integral is equal to the opposite of the constant term of the polynomial resulting from the integration.

This remark helps to save a lot of time because only this constant term Ao is computed now, by substitution, in the set of seven equations giving the coefficients of the integral polynomial.

Ao is found to be equal to 6! (or 720)

The final expression for the reflectivity is :

$$\eta = No \cdot \pi^5 \cdot |K|^2 \cdot 6! / (\lambda^4 \Delta^7) \quad (m^2/m^3) \qquad (6.11)$$

A similar, though more complex expression, is given in the Bendix report. Comparison with experimental measurements shows that the above formula produces satisfying results.

6.2 EFFECTS OF RAIN, FOG AND SNOW

First of all, recall that atmospheric gases also produce an attenuation. From Figure 6.2.1, it is seen that this attenuation is negligible, except around 60 GHz, which

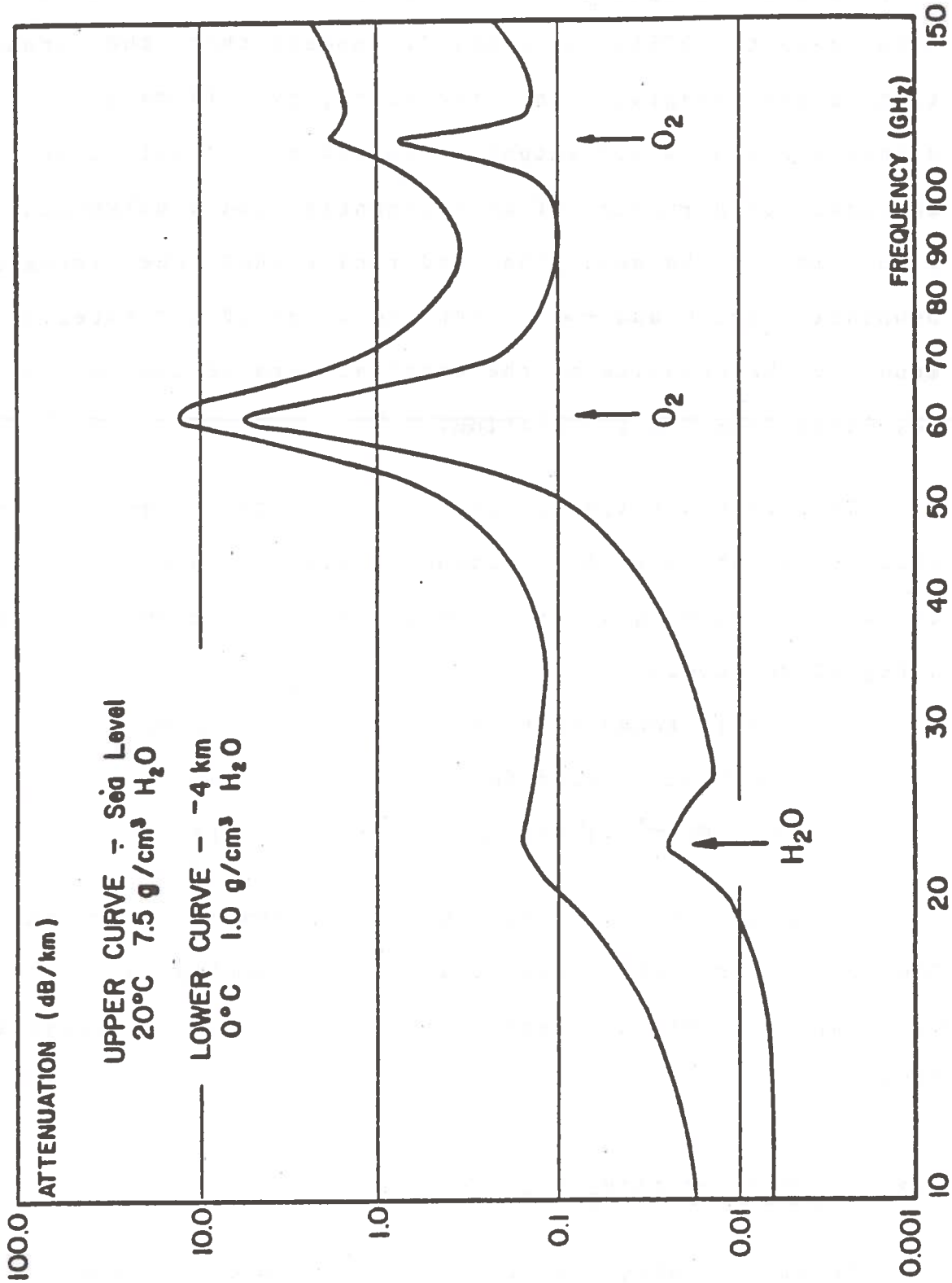

Figure 6.2.1: Atmospheric gases. Attenuation spectrum.

corresponds to a peak of absorption for Oxygen. Some thought has been given to an operating frequency of 60 GHz, in order to minimize radiation hazards caused by the presence of many radars on a roadway. The calculations made for backscattering effects do not take into account attenuation. When both effects are comparable, it is impossible to use simple approximations.

6.2.1 Case of Fog

Because fog is the most straightforward case, it will be discussed first. In order for the approximations to hold, the coefficient α must be much less than unity. The Rayleigh formulas can be used for fog even at 60 GHz. Fog droplets are about 1/100 the size of raindrops. As η varies as $\sum_i D_i^6$, it is reduced to a negligible value. Attenuation depends on M, water content, and Im(-K), which is related to the dielectric constant of water. Figure 6.2.2 shows the variations of Im(-K) as a function of frequency (from data collected by Gunn & East, 1954), at various temperatures. On a log scale, the values turn out to be located approximately on straight lines for each temperature. Therefore, Im(-K) can be written in the form :

$$\mathrm{Im}(-K) = b(T)\cdot\lambda^{-a(T)} \qquad (6.12)$$

Where: λ in cm and T in degrees Celsius.

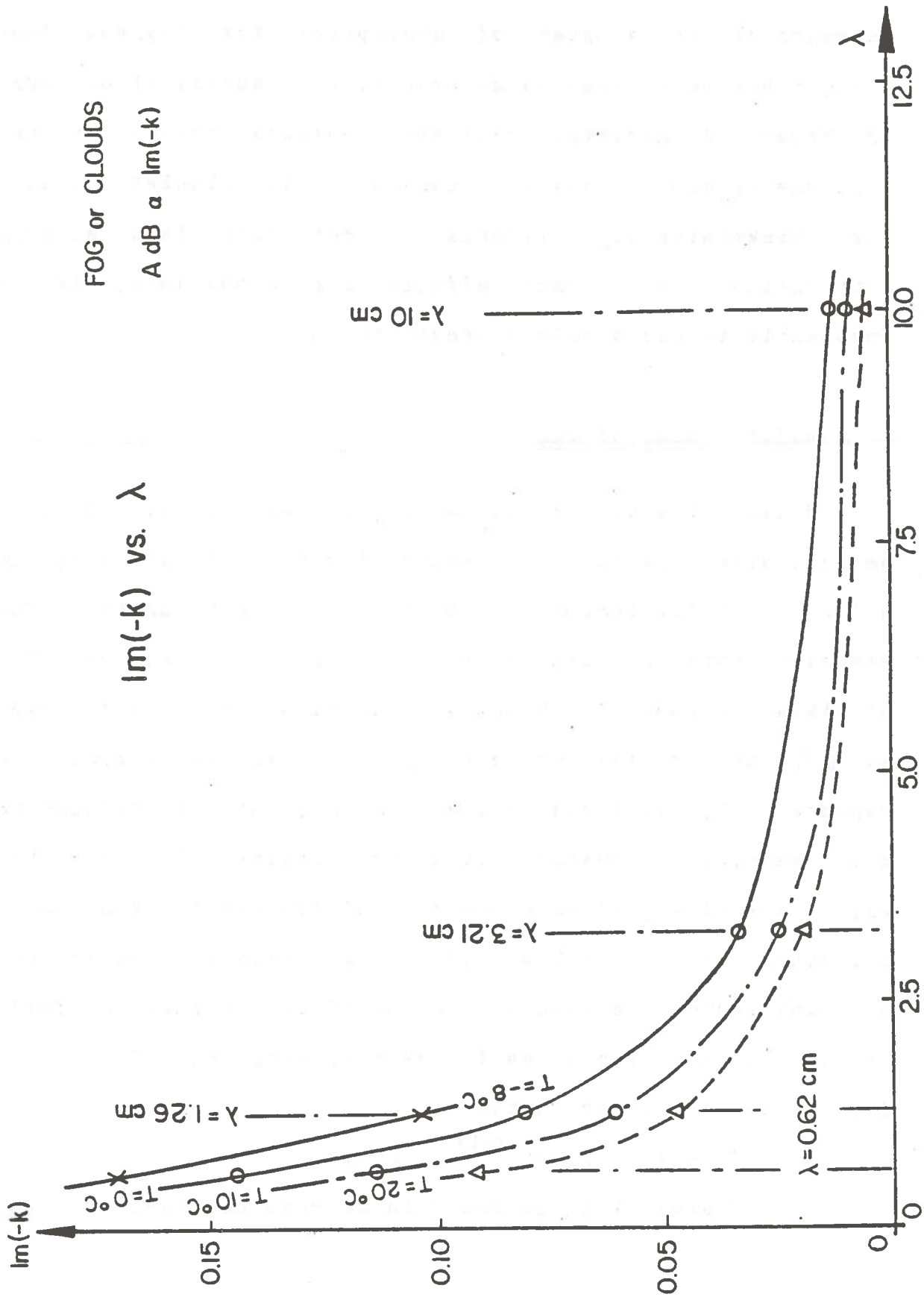

Figure 6.2.2: Variations of Im(-K) versus frequency for water.

The following values have been computed in the course of this study :

T	-8	0	10	20
a(T)	0.726	0.886	0.927	0.959
b(T)	0.121	0.0915	0.0746	0.0575

Between those temperatures, a(T) and b(T) can be interpolated with an error less than a few percent. On the other hand, a very important parameter for fog is the optical visibility d, which can be related to the water content M by :

$$\begin{cases} M = 1.660 \cdot d^{-1.43}, & (6.13) \text{ if d in feet.} \\ M = 0.3036 \cdot d^{-1.43}, & \text{if d in meters.} \quad (6.14) \end{cases}$$

Finally, attenuation can be written in the form :

$$\begin{cases} A\ (dB/km) = [\ 2.4854 b(T)\ ] \cdot d^{-1.43} \cdot \chi^{[1+a(T)]} & (6.15) \\ \text{or :} \quad A\ (dB/km) = [\ 2.4584 b(T)\ ] \cdot d^{-1.43} \cdot (F/30)^{[1+a(T)]} & (6.16) \end{cases}$$

The second expression is convenient for it deals with reduced frequency in GHz. Figures 6.2.3 and 6.2.4 show the variations of A for two extremes cases.

6.2.2 Case of Rain

Rain is the most important source of attenuation and backscattering. It is also the most complex case, for Automotive Radar frequencies are precisely in the zone where the Rayleigh criterion begins to be a matter of discussion.

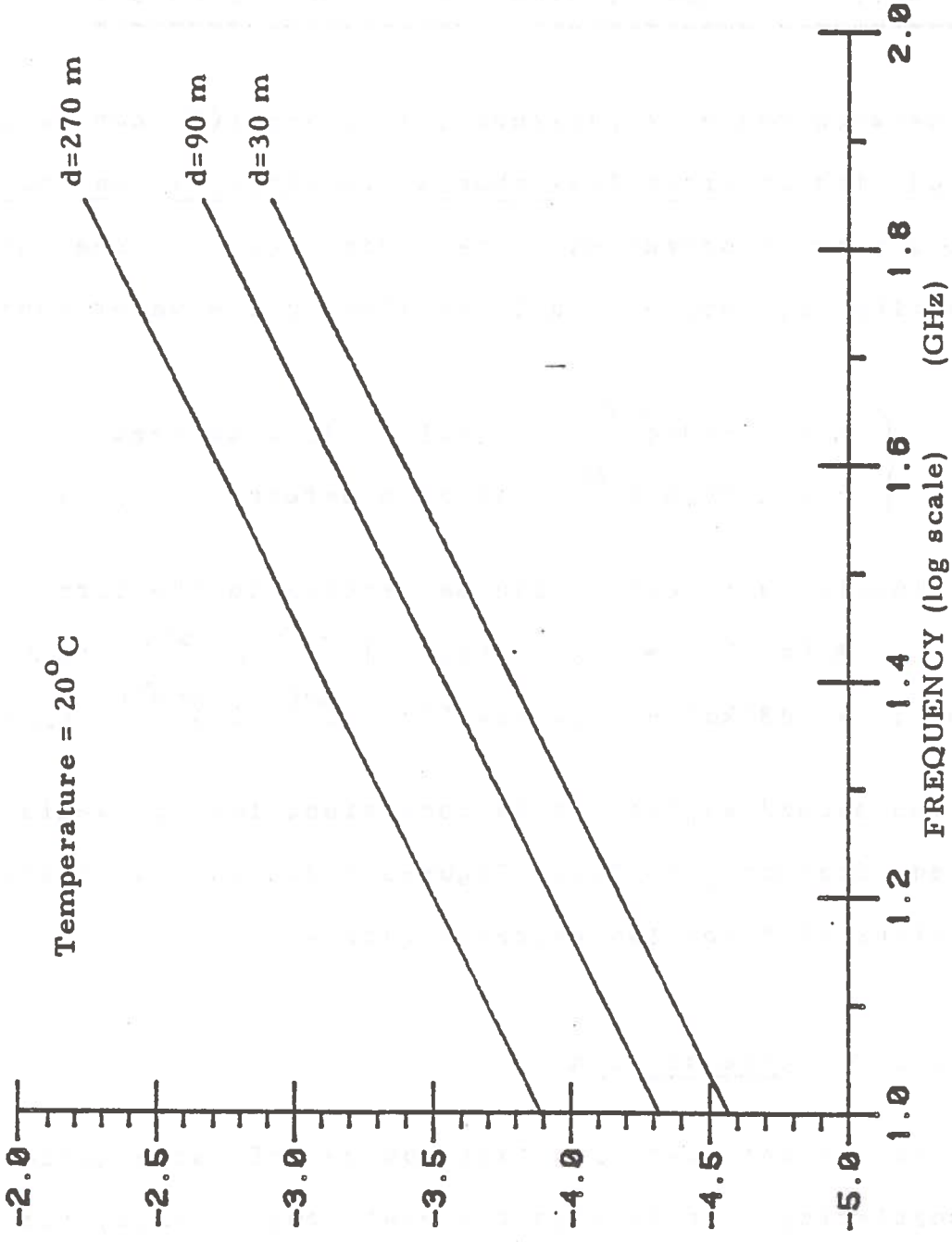

Figure 6.2.3: One-way attenuation in fog vs. frequency for various optical visibilities d.

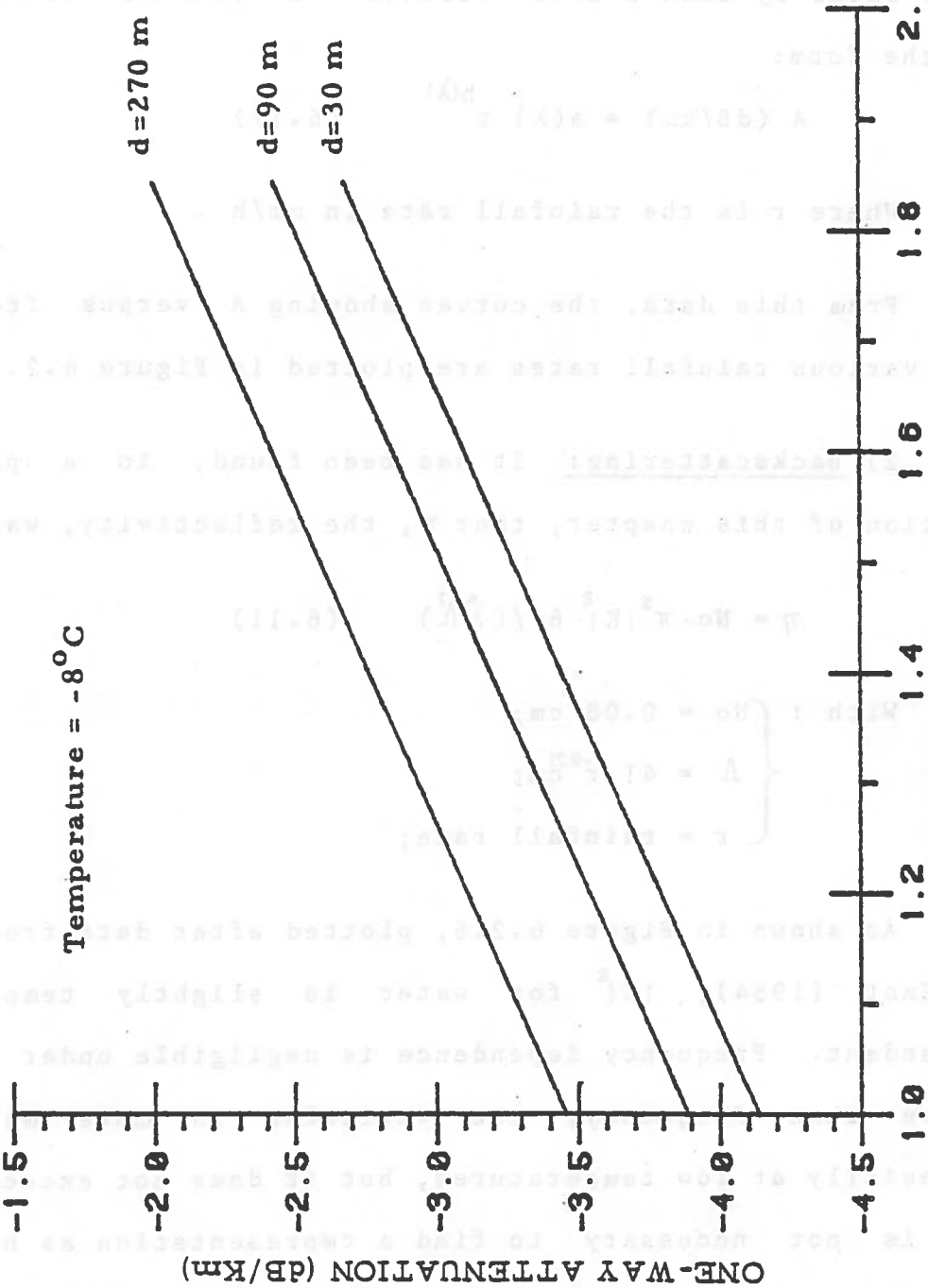

Figure 6.2.4: One-way attenuation in fog vs. frequency for various optical visibilities d.

1) Attenuation: As the Rayleigh criterion is not satisfied for wavelengths around 1 cm, the cross-section of attenuation obtained by Rayleigh approximations differs noticeably from the exact Mie cross-section. It is then preferable to refer to empirical relationships, such as those derived from measurements by Haddock (1948), reproduced by Gunn & East (1954). A (dB/km) is written in the form:

$$A\ (dB/km) = a(\lambda) \cdot r^{b(\lambda)} \qquad (6.17)$$

Where r is the rainfall rate in mm/h .

From this data, the curves showing A versus frequency for various rainfall rates are plotted in Figure 6.2.5 .

2) Backscattering: It has been found, in a previous section of this chapter, that η, the reflectivity, was :

$$\eta = No \cdot \pi^5 |K|^2 \cdot 6! / (\lambda^4 \Lambda^7) \qquad (6.11)$$

With : $\begin{cases} No = 0.08 \text{ cm}; \\ \Lambda = 41 \cdot r^{-0.21} \text{cm}; \\ r = \text{rainfall rate}; \end{cases}$

As shown in Figure 6.2.6, plotted after data from Gunn & East (1954), $|K|^2$ for water is slightly temperature dependent. Frequency dependence is negligible under 10 GHz. Above that frequency, the variation is more important, especially at low temperatures, but it does not exceed 15%. It is not necessary to find a representation as has been

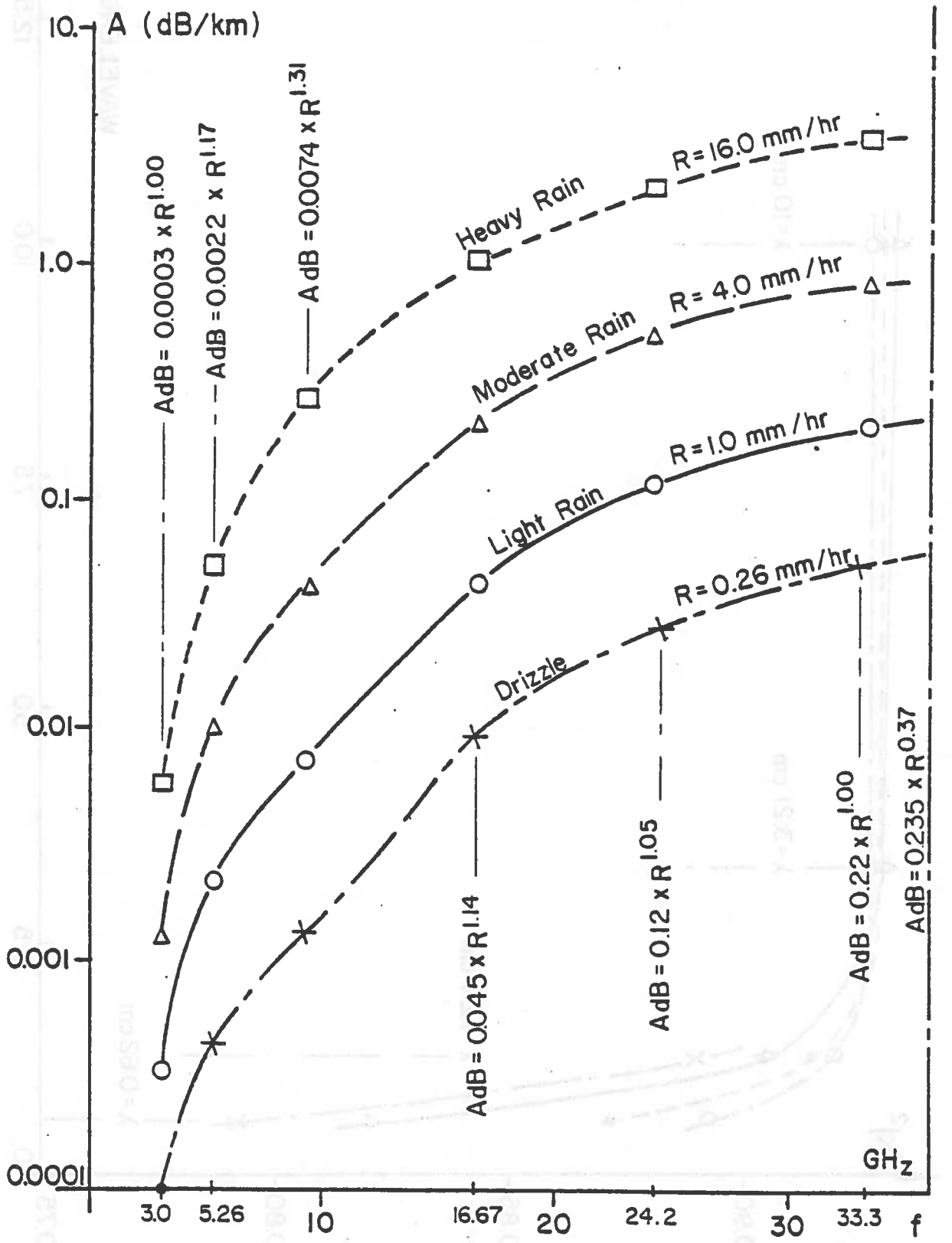

Figure 6.2.5: One-way attenuation in rain versus frequency for various rainfall rates.

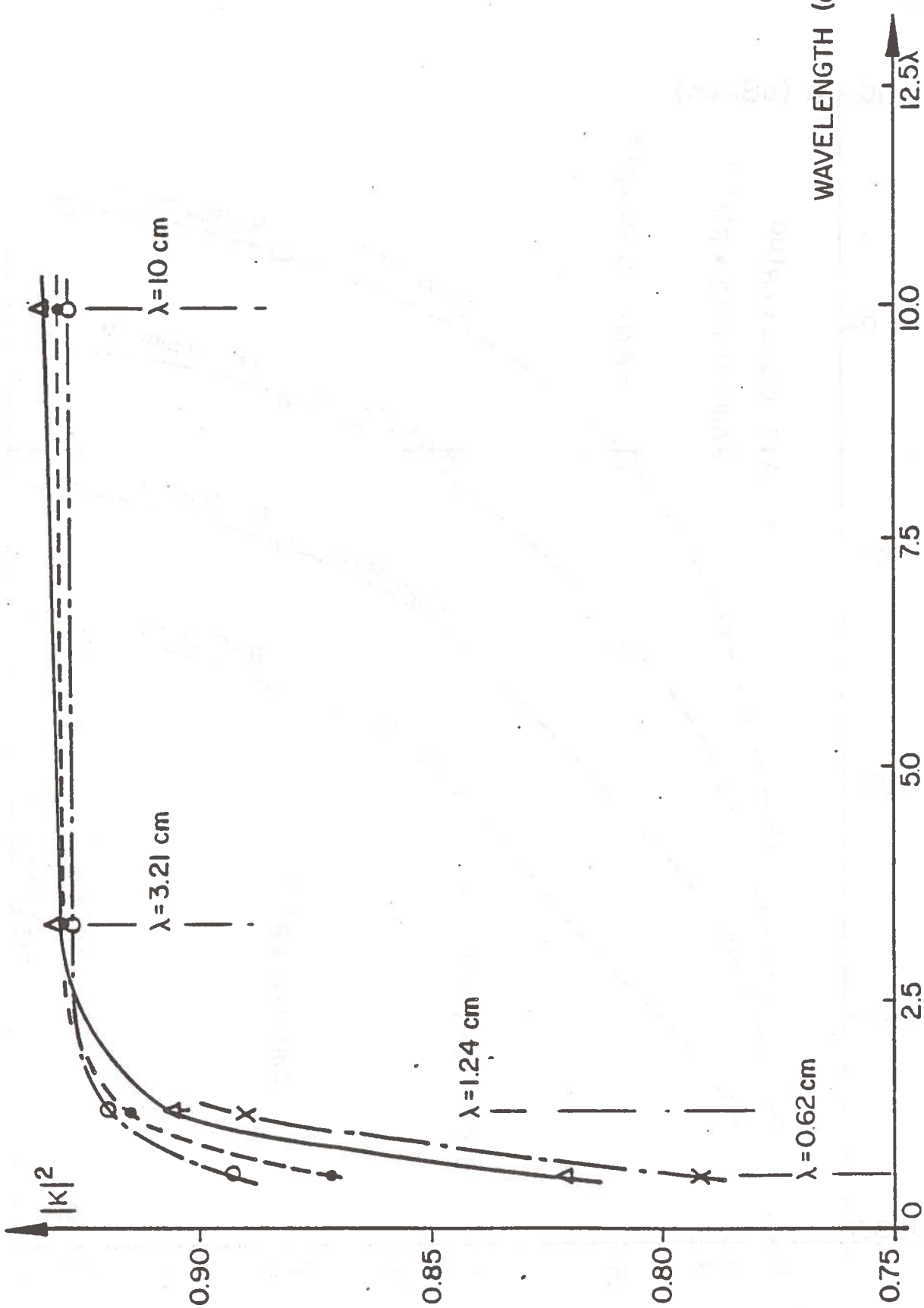

Figure 6.2.6: Variations of $|K|^2$ versus frequency for water.

done for Im(-K).

Figure 6.2.7 is a comparison of theoretical and experimental values. The reader will notice the accuracy of the model at lower frequency, whereas at higher frequencies and higher rainfall rates a discrepancy appears.

6.2.3 Case of Snow

For snow, $|K|^2$ and Im(-K) are related to the dielectric properties of ice. From the data in Gunn & East (1954), it turns out that Im(-K) and $|K|^2$ for ice are about a fifth of the values for water. Taking into account the fact that snowfall rates are much smaller than rainfall rates, snow will be of little importance in the perturbation of radar waves propagation.

6.3 WEATHER CLUTTER AND RADAR PERFORMANCES

From the previous calculations, it appears that backscattering by rain is the main effect which contributes to radar performance degradation. Rain clutter can produce a sufficient amount of power, called clutter power, to obscure targets with small cross-sections. As a matter of fact, the problem is different for FM-CW radars and pulse modulated radars.

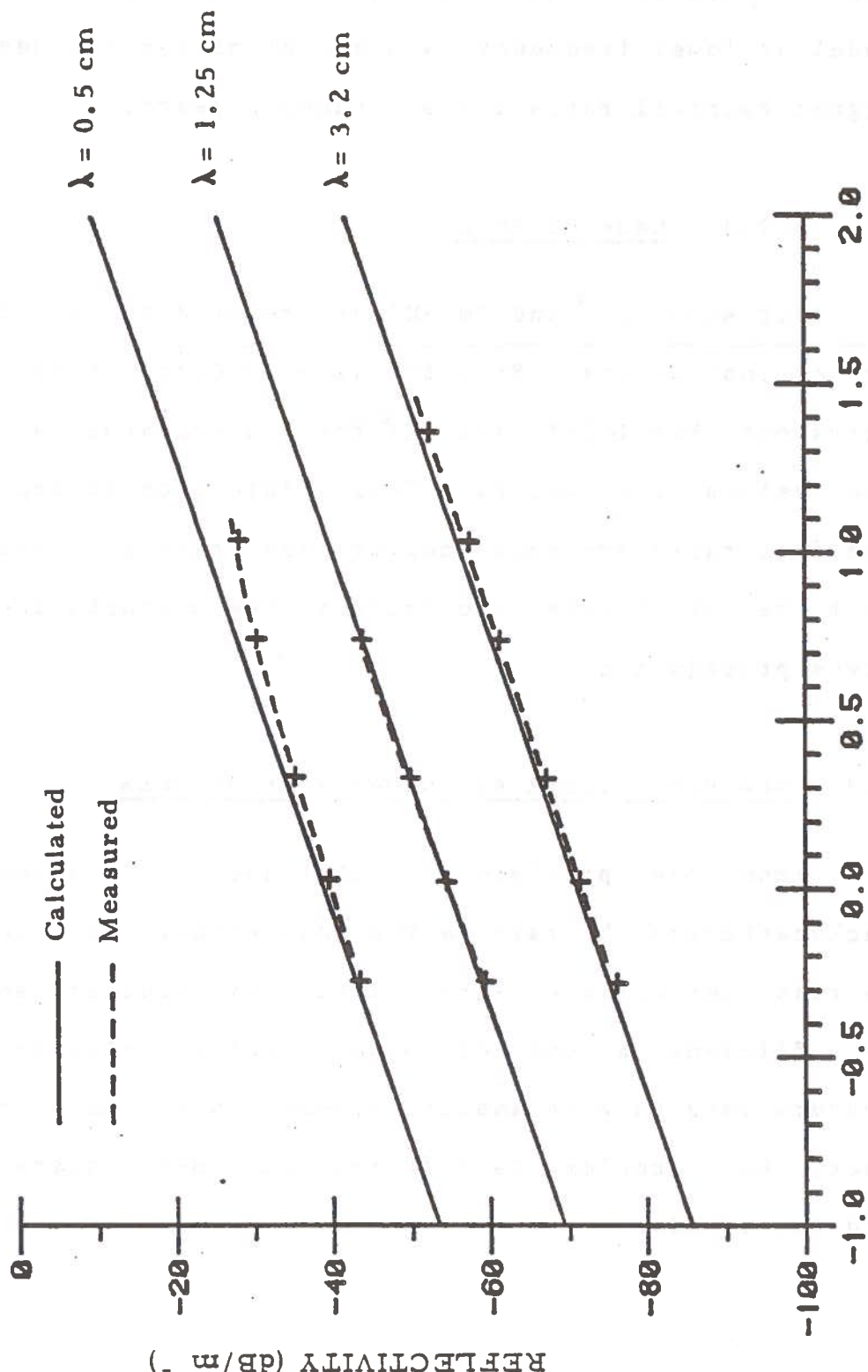

Figure 6.2.7: Reflectivity vs. rainfall rate for various wavelengths.

6.3.1 Continuous Wave Systems

For these devices, the ratio which is characteristic of clutter is that of Pr, rain clutter power, to P, signal returned from a target of cross-section σ. For a range R and a reflectivity η:

$$(Pr/P) = [2 \cdot \eta \cdot R^3/\sigma]; \qquad \text{(from Grimes, 1974)} \qquad (6.18)$$

In Figure 6.2.7 the limit range can be determined where the ratio is equal to unity, given the rainfall rate and the frequency. Beyond that range, the target cannot be detected.

There are several ways to increase the capability of detection of an FM-CW radar in the presence of weather clutter.

1) First, radar design parameters must be carefully chosen. In particular, the clutter signal depends on the horizontal and vertical beamwidths, with a narrower beam preferable. More precisely, as frequency is increased, beamwidth must be decreased to keep the clutter level constant.

2) Bistatic antennas have been suggested with the trade-off in higher cost and a reduced efficiency for targets lying in the near field. However, radar performances can be noticeably improved.

3) For a monostatic system, circularly polarized antennas can be used. The principle of operation is as follows: radar return from flat plates or from spherical particles is also a circularly polarized wave, but with a reversed polarization. In other words, a right-hand polarized wave is returned as a left-hand polarized wave. As the emitting antenna only detects waves with the same polarization as the emitted signal, return from the raindrops is strongly reduced (more than 20 dB), whereas signal returned from target is decreased by about 3 dB (Grimes and Jones, 1974). This is valid because targets of interest in Automotive Radars are generally complex. In other words, they present the opportunity to reflect the incident wave an odd number of times. If the number of reflections is odd, then original polarization is restored and the signal is detected.

6.3.2 Pulse Modulated Radars

Pulse modulated radars can easily get rid of clutter power. The averaged clutter power for a radar of that type is :

$$Pr = Pt\ Ae\ L\ \eta / 32R^2 \qquad (6.2)$$

Where L pulse length and Ae effective antenna aperture.

FM-CW radars receive power from the whole ensemble of particles; the main part comes from those lying in the main beam. Pulse radars only receive clutter power from a "resolution cell" of volume Vm defined by :

$$Vm = (\pi/4) \cdot R^2 \cdot \theta a \cdot \theta b \cdot (L/2) \qquad (6.19)$$

Where θa and θb are the horizontal and vertical beam-widths.

When a velocity dependent gate is included in the receiver, the amount of clutter received is even smaller and radar performances are improved.

CHAPTER VII

CONCLUSIONS

7.1 MODELING OF THE FEED

7.1.1 Accuracy of the Model

Feed patterns calculations are based on the principles of diffraction theory. The simple model derived exhibits good agreement with experimental measurements, as can be seen in the first example described in CHAPTER III. However, the value of the maximum gain, which does not appear on normalized graphs, differs, sometimes noticeably, from the measured values (but generally less than 15%). The model is more accurate for determination of normalized patterns, but less suited when the actual value of the gain is to be computed. This limitation mainly affects the modeling of horn antennas without reflectors. If the horn is coupled to a reflector, parabolic in the present case, only normalized patterns should be used as input to the code GENREF. Discrepancies due to normalized feed pattern deter-

minations are less than a few percent.

7.1.2 Validity of the Assumptions

The validity of the assumptions made in CHAPTER II depends on the chosen geometry.

1) Wavefront Distortion: The model is less accurate for horns with both small flare angle and aperture dimensions a and b differing by more than two orders of magnitude. If the values of A and B are too different, there is an important wavefront distortion from the assumed spherical shape. Therefore, phase error in the plane of the aperture is no longer quadratic.

2) Wavelength and Dimensions: Horn dimensions must be large enough compared to the wavelength. Otherwise, contribution to radiation from the walls cannot be neglected.

7.1.3 Optimization and Phase Error

Optimization of the horn is a delicate problem. A compromise must be found between optimum geometry and the physical limitations of the system, such as aperture blockage. Deviation from optimum geometry leads in particular to strong variations of the phase of the E-field. This is especially true at higher frequencies. As GENREF assumes a constant phase error for input feed patterns, discrepancies may result and final patterns may be altered.

7.1.4 Waveguide Feeds

Waveguide feeds can be seen as the limit case of horns with infinite flare length (or zero flare angle). This is equivalent to neglecting quadratic terms in the integrals. Waveguide feeds have a lower directivity and are poorly matched. This is the reason that horn feeds are usually prefered to waveguides.

7.2 MODELING OF PARABOLIC REFLECTORS

7.2.1 Discussion of the Results

The comparison in CHAPTER III of experimental and calculated patterns leads to the following conclusions:

1) The modeling of the main beam is accurate, especially in the range from maximum gain to - 20 dB.

2) The modeling of the first side-lobes is much less accurate. Depending on the curve considered, the discrepancy is about 10 to 15 dB (i.e. the values measured for the side-lobes are 10 to 15 dB above the predicted values). Comparison was only possible for the low-angle side-lobes.

Several explanations can be found to this failure of the model for wide angles.

7.2.2 Aperture Blockage

It must be noted that GENREF, in its current form, does not take into account aperture blockage effects. The presence of the feed in the main beam tends to decrease the value of the maximum gain, and to increase side-lobe level. In practice, the decrease of directivity turns out to be much lower than the increase of side-lobe level. Some examples discussed in GENREF User's manual (1979) prove that this discrepancy was predictable. More generally speaking, aperture blockage is more important at higher frequencies. In that range of wavelengths, wave propagation tends to follow the laws of Geometrical Optics, rather than those of Diffraction Theory. Therefore, perturbations due to the presence of the feed are increased. Note that if offset reflectors were considered, they could be easily modeled with the aid of GENREF.

7.2.3 Phase Distribution

Another limitation to this version of GENREF is the fact that the feed must have a constant phase pattern. As it has been seen above, this is seldom true in practice. Optimal horns, in addition to maximizing gain, have also the remarkable property of minimizing the phase variations.

Horns with wide flare angles tend to deviate from optimal geometry and, in some cases, the phase varies so rapidly that it can be considered to be randomly distributed with respect to the pattern angle. However, the variations are smoother around the axis ($\theta = 0^{o}$) than at wider angles. The result is that contributions to the radiation pattern will still add constructively in the main beam, but will tend to add destructively in the side-lobes. Hence, the side-lobes are smoothed.

7.3 AUTOMOTIVE RADARS AND MULTIPATH PROPAGATION

7.3.1 Ground Reflections

Various models have been derived in CHAPTER IV to describe the effects of multipath reflections on the propagation. The curves plotted have shown that :

1) For low grazing angles, both vertical and horizontal reflection coefficients Rv and Rh are decreasing with increasing angle.

2) The decrease is much steeper for Rv than for Rh.

3) There is an angle for which Rv is zero (smooth model) or nearly zero (rough model). Beyond this pseudo-Brewster angle, Rv increases again towards an asymptotic value.

4) For a dry smooth road, Rh is decreased by 50% around an angle of 10°. For a wet rough road, the half point angle is only 5°. Usual road surface parameters can be considered to be between these two extremes. Except maybe for the second case, the phase of Rv can be taken as a constant: $+\pi$ before Brewster angle, 0 beyond.

Considering the geometry of the system, it is obvious that grazing angles of interest in Automotive Radars are generally lower than 5°, 2° being a typical value. For such an angle, the curves from CHAPTER IV show that |Rh| and |Rv| are nearly equal to unity. As the phase is equal to π, it is reasonable to assume :

$$Rh = Rv = -1$$

These are the assumptions usually made in low angle radar systems, especially in naval applications. The only exception is the case of very rough road surfaces, such as grooved pavements.

When reflection coefficients are taken equal to unity, a phase shift of $+\pi$ radians is introduced by the reflection. In other words, the signal returned from targets lying in the vicinity of the ground plane is strongly reduced by the destructive addition of direct and reflected rays. For example, a fallen tree or a rock probably will not be detected by the radar. The main effect of roughness or water is to smooth pattern alterations.

7.3.2 Other Multipath Reflections

It has also been seen in CHAPTER IV that the models derived for ground reflections can be applied to other multipath occurrences, typically reflections from buildings on the side of the road. From the previous analysis, it is clear that, due to the larger grazing angles, Rh and Rv are much smaller than unity. Therefore, that type of multipath is negligible.

The last case is that of guardrails. A simple way to evaluate perturbations caused by the presence of guardrails is to take the model of a flat metallic plate. Then Rv and Rh are equal to +1. In that case, as targets of interest lie far enough from the plane of reflection, that is to say the vertical plane in which the guardrail is located, pattern alteration is minimized. However, considering the expression giving the phase shift between the direct and the reflected ray, the phase shift due to the path difference, it turns out that this shift behaves as if it were randomly distributed for the different possible geometries of the system car-guardrail. Fluctuations of the distance car-guardrail produce strong variations of the phase shift. Phase-shift fluctuations produce in turn fluctuations in the signal from a target. If the processing of the system does not include the necessary protections against this phenomenon, as range delay, malfunctions may result. However, the effects of the variations are smoothed for complex

targets, such as automobiles.

It must be noted that guardrails also produce a partial screening of the side of the road. This cannot be seen as a limitation for Automotive Radars, because it helps reduce the number of false alarms.

7.4 WEATHER EFFECTS

From the analysis of atmospheric perturbations on the propagaton of radar waves, the following conclusions are made.

7.4.1 Attenuation

The attenuation phenomenon is generally negligible in Automotive Radars. The atmospheric attenuation is very low and rain attenuation becomes perceptible only at higher frequencies (around 50 GHz) and higher rainfall rates (around 40 mm/h). For range lower than 130 m, it is reasonable to disregard attenuation.

7.4.2 Backscattering

Backscattering effects can be, in some cases, a serious limitation to radar performances. At that stage, the modulation plays a critical role.

Pulse modulated radars, and in particular pulse gated radars, are nearly immune to rain clutter. The clutter power received originates from a small cell surrounding the vehicle. The narrower the beamwidth, the smaller the cell and therefore the less clutter signal returned.

Monostatic FM-CW radars using linear polarization are much more sensitive to weather effects because they receive a continuous flow of radiation from meteorological particles. A consequence is that targets with a small cross-section, such as a bike or a pedestrian may not be detected in a heavy rain.

A bistatic configuration helps reduce the amount of clutter received, in particular near-field clutter.

Choosing a circular polarization is an efficient way to work out the problem, but the trade-off is a small decrease of the signal returned from targets of interest. It also helps the blinding problem.

7.5 SYSTEMS EVALUATION

In light of the previous comments, a comparison can be made between the three Automotive Radars evaluated. An overall evaluation of the systems will be found in Laugénie's thesis, in which a method of simulation for analysis of Automotive Radars is developed. It includes the results of the present study and also target cross-section

modeling and signal processing considerations. This enables the performances of each device to be estimated.

7.5.1 Antenna Modeling And Propagation

The antenna characteristics of the three systems are very similar, except for the fact that the Daimler-Benz-SEL system, in its original configuration, is bistatic. More precisely, the Japanese radar beamwidth is slightly smaller than that of the two other ones. The effect of such a small variation can only be evaluated during the simulation process. However, it must also be noted that the Nissan-Mitsubishi antenna has a very low side-lobe level.

All antennas are linearly polarized. Nissan-Mitsubishi and Bendix have chosen 45^{o} polarization, whereas the German bistatic system uses vertical polarization. The latter is therefore more sensitive to a possible blinding from other vehicles.

7.5.2 Modulation and Frequency

Daimler-Benz-SEL and Bendix radars operate at approximately the same frequency (around 35 Ghz). The Nissan-Mitsubishi system uses 24.15 Ghz.

The chosen modulations are the following :

1) Nissan-Mitsubishi : pulse-gated

2) Bendix : Diplex

3) Daimler-Benz-SEL: FM-CW

From this data and from the previous analysis it appears that the Nissan-Mitsubishi system is the most efficient in the presence of atmospheric perturbations, because of the pulse modulation and the gating of the receiver. The German system is less immune to rain, in particular in its monostatic configuration. The Bendix DIPLEX system is similar to the Daimler-Benz-SEL, since it is also a continuous wave device. The monostatic configuration is again a limitation in bad weather, but it would be unwise to claim that FM-CW radars should be rejected because of their sensitivity to rain clutter. Other considerations which are not discussed in this study have to be taken into account, such as the precision of the measurements. The interested reader will refer to Laugénie's work (1981), which is the logical continuation of this study.

APPENDIX A

FRESNEL'S INTEGRALS

The reader can find in this appendix further details about the calculations of the field radiated by a pyramidal horn. The horn geometry is defined in CHAPTER II. Here, only the case of the dominant mode is treated. The correspondant illumination is a cosine function $A(x,y) = Ao \cos(\pi y/b)$. As it has been seen in this chapter, the E-field can be written, in its integral form, as a product of two sub-integrals Ix and Iy. In other words, the integration variables x and y are separated. Ix and Iy are :

$$\begin{cases} Ix = \int_{a/2}^{a/2} \exp\left[j\beta\left(x \cdot \sin\theta \cos\phi - x^2 \cdot (R + L)/2RL\right)\right] \cdot dx \\ Iy = \int_{-b/2}^{b/2} \exp\left[j\beta\left(y \cdot \sin\theta \cos\phi - y^2 \cdot (R + L)/2RL\right)\right] \cos(\pi y/b) \cdot dy \end{cases}$$

Expanding the cosine in its exponential form, Iy is broken into two similar integrals I(y,+) and I(y,-), with :

$$Iy = \left[I(y,+) + I(y,-)\right] /2$$

With :

$$\begin{cases} I(y,+) = \int_{-b/2}^{b/2} \exp\left[j(2\pi/\lambda)\left(-y^2(R+L)/2RL + y\sin\theta\sin\phi\right) + j\pi y/b\right] \cdot dy \\ I(y,-) = \int_{-b/2}^{b/2} \exp\left[j(2\pi/\lambda)\left(-y^2(R+L)/2RL + y\sin\theta\sin\phi\right) - j\pi y/b\right] \cdot dy \end{cases}$$

1) Calculation of Ix :

Let X be the reduced variable RL/(R+L). Then, the argument of the exponential is :

$$\text{Arg} = j\,\beta\cdot[x\cdot\sin\theta\cdot\cos\phi - (x^2/2X)]$$

This argument Arg can be written in the form of a perfect square. A phase factor is then introduced. Let now w be the reduced variable defined by :

$$(\pi/2)\cdot w^2 = (\pi/\lambda X)\cdot[x - X\cdot\sin\theta\cdot\cos\phi]^2$$

or :

$$w = \pm\sqrt{(2/\lambda X)}\cdot[X\cdot\sin\theta\cdot\cos\phi - x]$$

Calling Y the quantity $\sqrt{(\lambda X/2)}$, and A the quantity $\sin\theta\cdot\cos\phi$, the integral Ix becomes :

$$Ix = \exp[j\pi A^2 X/\lambda]\cdot\int_{w_-}^{w_+}\exp[-j\pi w^2/2]\cdot dw$$

With :

$$w_{\pm} = [A\,X + (a/2)]/Y$$

From this expression, Ix is now equal to :

$$Ix = \alpha x\cdot Jx$$

With : $\alpha x = \exp[j\pi A^2 X/\lambda]$

Jx is a well-known integral in diffraction calculations. It is called Fresnel's integral. The standard form of F(x), Fresnel's integral, is the following :

$$F(x) = \int_0^X \exp[-j\pi u^2/2]\cdot du$$

Then, Jx is nothing but :

$$Jx(w\pm) = F(w+) - F(w) = \Delta F(w\pm)$$

A representation of F(x) in the complex plane produces the so-called Cornu's spiral, shown in figure A.1 . The imaginary and real part of the integral are usually named C(x) and S(x). As a matter of fact, the imaginary part is -S(x). C(x) and S(x) are two other integrals also called Fresnel's integrals :

$$\begin{cases} C(x) = \int_0^x \cos(\pi u^2/2)\, du \\ S(x) = \int_0^x \sin(\pi u^2/2)\, du \end{cases}$$

Therefore, C(x) and S(x) correspond to the x and y axis of the graph on figure A.1 . Figure A.2 shows the variations of the magnitude of F(x) versus x. It is seen that |F(x)| is a monotonous increasing function till the integral reaches a maximum value at x = 1.223. Then, the magnitude of F(x) oscillates around an asymtotic value, which is defined by the coordinates (0.5, 0.5). It is obvious that the curve is symmetrical with respect to the origin.

Finally, F(x) is equal to :

$$Ix = \alpha x \cdot \Delta F(w\pm)$$

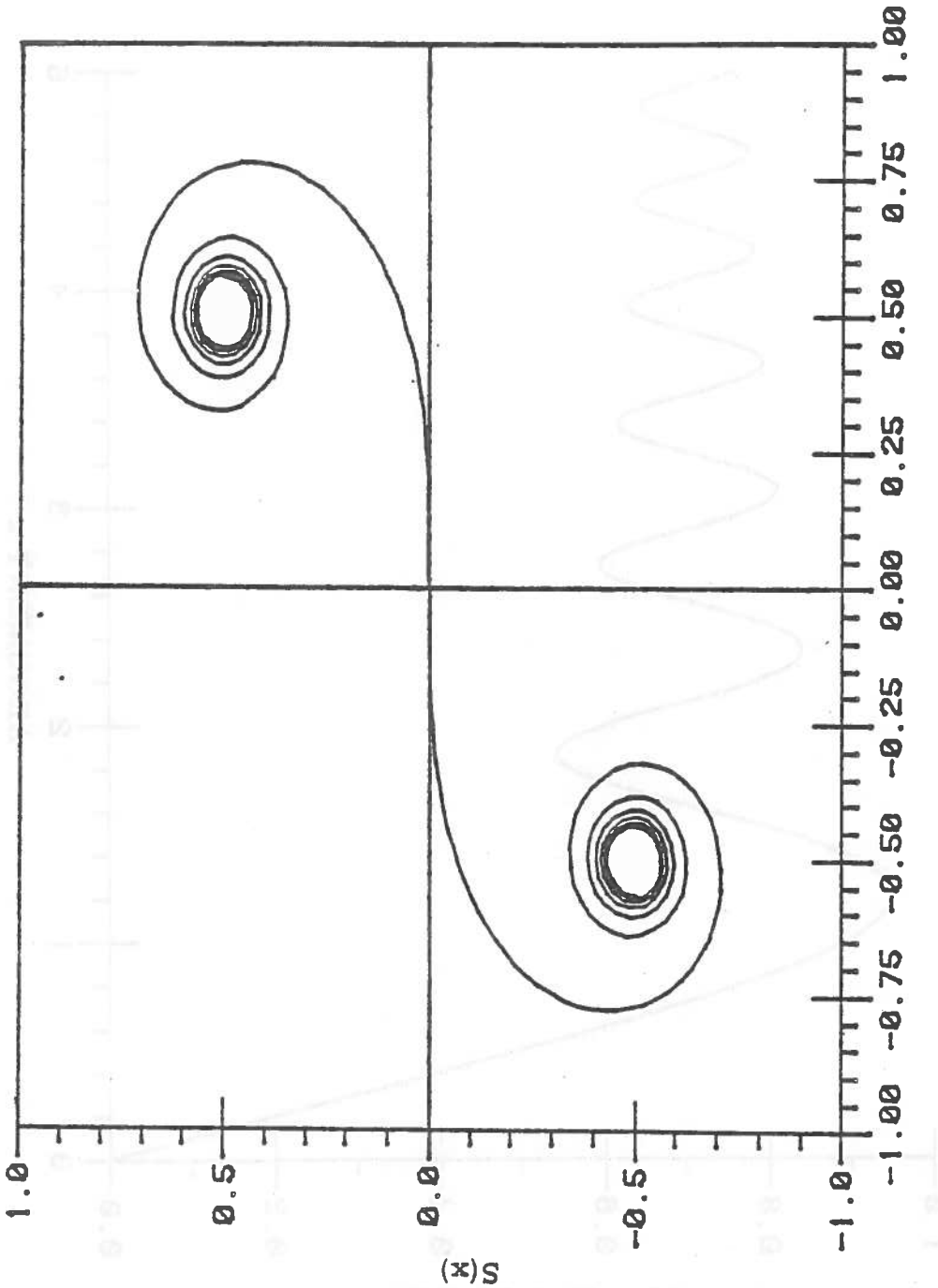

Figure A.1: Cornu's spiral.

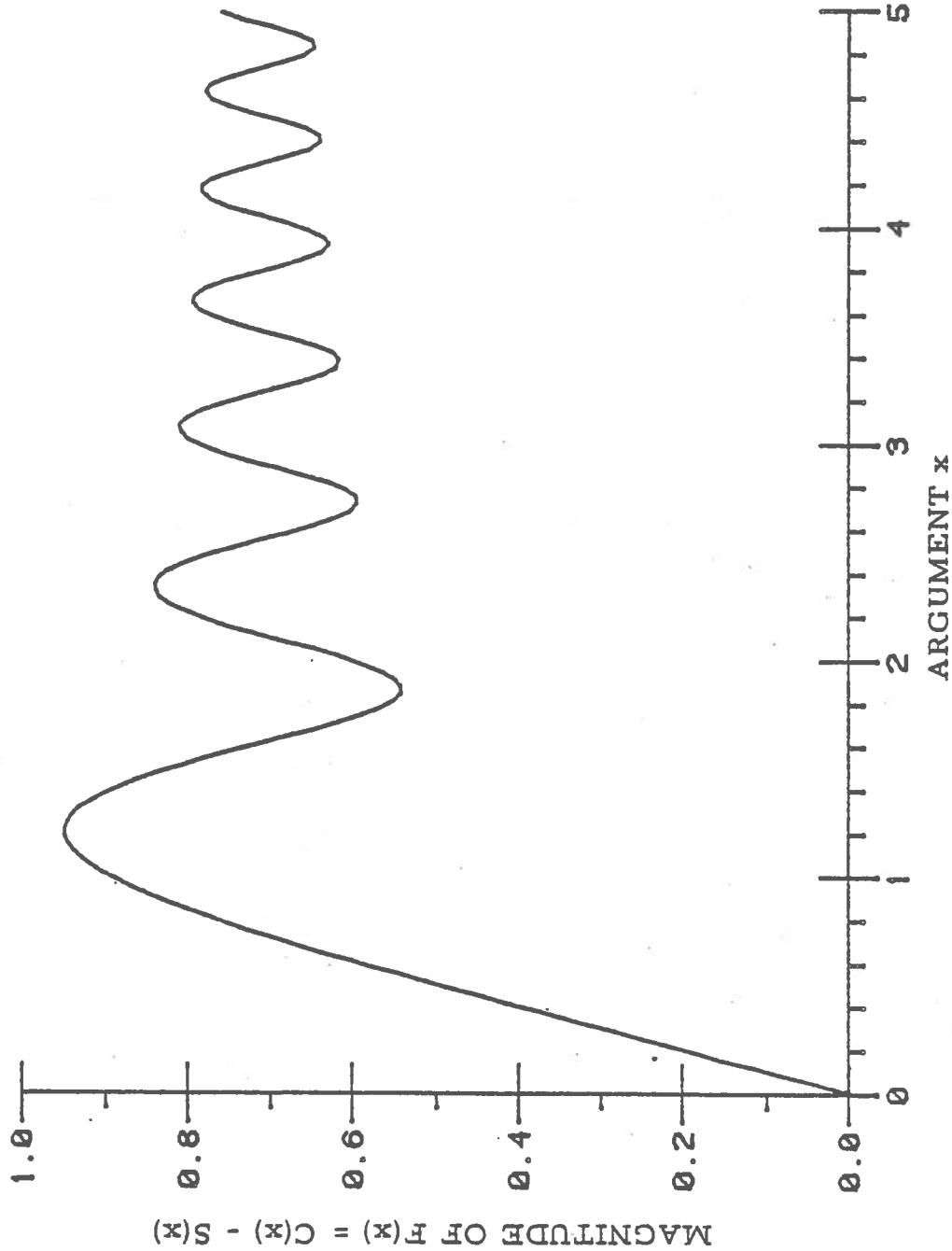

Figure A.2: Magnitude of Fresnel's integral.

2) Calculation of Iy :

Recall that Iy is the sum of I(y,+) and I(y,-), integrals which are also Fresnel's. Therefore, they will be reduced on a similar way. Introducing now the corresponding reduced variables :

$$B = \sin\theta \cdot \sin\phi$$

$$\begin{cases} u\pm = \left[[B + (\lambda/2b)] \cdot X \pm (b/2) \right] / Y \\ v\pm = \left[[B - (\lambda/2b)] \cdot X \pm (b/2) \right] / Y \end{cases}$$

From this :

$$\begin{cases} I(y,+) = \alpha(y,+) \cdot \Delta F(u\pm) = \alpha(y,+) \cdot J(y,+) \\ I(y,-) = \alpha(y,-) \cdot \Delta F(v\pm) = \alpha(y,-) \cdot J(y,-) \end{cases}$$

With :

$$\begin{cases} \alpha(y,+) = \exp\left[j(\pi X/\lambda) \cdot [B + (\lambda/2b)]^2 \right] \\ \alpha(y,-) = \exp\left[j(\pi X/\lambda) \cdot [B - (\lambda/2b)]^2 \right] \end{cases}$$

After expansion of the squared terms and factorization, the complex coefficients (y,+) and (y,-) are written as :

$$\begin{cases} \alpha(y,+) = \alpha y \cdot \gamma \\ \alpha(y,-) = \alpha y \cdot \gamma^* \end{cases} \quad (\gamma^* \text{ denotes the complex conjugate of } \gamma)$$

αy is a factor similar to αx derived in the previous paragraph.

$$\alpha y = \exp[j\pi BX/b]$$

Finally, the common complex factor in front of the initial integral I is reduced to :

$$\alpha = \alpha_x \cdot \alpha_y = \exp\left[j(\pi X/\lambda) \cdot (\sin^2\theta + \lambda^2/4b^2) \right]$$

The final expressions are :

$$E(R,\theta,\phi) = \alpha \cdot Jx \cdot \left[\gamma \cdot J(y,+) + \gamma^* J(y,-) \right]$$

With :

$$\begin{cases} Jx = \Delta F(w\pm) \\ J(y,+) = \Delta F(u\pm) \\ J(y,-) = \Delta F(v\pm) \end{cases}$$

$$\begin{cases} \alpha = \exp\left[j(\pi X/\lambda) \cdot (\sin^2\theta + \lambda^2/4) \right] \\ \gamma = \exp[j(\pi XB/b)] \end{cases}$$

$$\begin{cases} X = RL/(R + L) \\ Y = \sqrt{(\lambda X/2)} \end{cases}$$

$$\begin{cases} A = \sin\theta \cdot \cos\phi \\ B = \sin\theta \cdot \sin\phi \end{cases}$$

$$\begin{cases} w\pm = [A \cdot X \pm a/2]/Y \\ u\pm = \left[(B + \lambda/2b) \cdot X \pm b/2 \right]/Y \\ v\pm = \left[(B - \lambda/2b) \cdot X + b/2 \right]/Y \end{cases}$$

APPENDIX B

PROGRAM HORN

```
C-------------------------------------------------------
      IMPLICIT COMPLEX(Z),REAL(L-Y)
      DIMENSION THETA(0:400),XO(0:400),YO(0:400),ZI(0:400),
     1STH(0:400),EP(0:400),CMD(0:400)
      CHARACTER      ANSWER*1
      CHARACTER      ILLU*1
      CHARACTER      CHOICE*3
      CHARACTER     FILE*10
      CHARACTER*3  DG/'DG:'/,TO/'TO:'/,FD/'FD:'/,PZ/'PZ:'/
      CHARACTER*3  FQ/'FQ:'/,XQ/'XQ:'/,PP/'PP:'/,LP/'LP:'/
      CHARACTER*1  F/'F'/,T/'T'/
      PARAMETER      PI=3.1415927
C-------------------------------------------------------
111     TYPE 10
10      FORMAT('$ENTER  GEOMETRY:L,A1,B1 (A1<B1) (cm.): ')
       ACCEPT*,L,A1,B1
      WRITE(6,15) L,A1,B1
15      FORMAT(//T15'  GEOMETRY : '//T15'  LENGTH = ',F6.2,
     1' (cm) '/T15' A1 . B1 = ',F6.3,'(cm)*
     2',F6.3,' (cm) '///)
112     TYPE 20
C-------------------------------------------------------
20      FORMAT('$ENTER LAMDA (cm): ')
       ACCEPT*,LAM
       FREQ=(3.E8/LAM)/1.0E7
      WRITE(6,25) FREQ
25      FORMAT(///T15'  FREQUENCY= ',F6.3,' GHZ '//// )
       DELTAMAX=(((A1/2.)**2.)+((B1/2.)**2.))*PI/(LAM*L)
      WRITE(6,26) DELTAMAX
26      FORMAT(///T15'  DELTAMAX (max ph. er.) =
     1',F6.3,' (rad) '//)
      IF(DELTAMAX.GT.(PI/4.))THEN
       TYPE *,'Non-optimal horn. '
      ENDIF
      TYPE 30
C-------------------------------------------------------
30      FORMAT('$ENTER DISTANCE,PHI(DEGREES),VALUE OF IN: ')
       ACCEPT*,R,PHI,IN
       INN=(2*IN-1)
      WRITE(6,35) R, PHI,INN
35      FORMAT(//T15' R = ',F10.3,' (cm) '//T15' PHI = ',F6.3,
     1//T15' NUMBER OF POINTS = ',I3,/// )
11       PHI=PHI*PI/180.
      TYPE 40
C-------------------------------------------------------
40      FORMAT('$ POLAR PATTERN (P),CARTESIAN E=F(THETA),
     1 (C) , OR E=F(SIN(THETA)*2.*PI/LAMDA) (S)  ?  ')
       ACCEPT 50,ANSWER
50      FORMAT(A)
      IF (ANSWER.EQ.'P') THEN
       FILE='POL'
```

```
      ELSE IF (ANSWER.EQ.'S') THEN
       FILE='STH'
      ENDIF
      IF (ANSWER.EQ.'C') THEN
      TYPE 900
C-----------------------------------------------------------
900     FORMAT('$ FILE FOR DISHPLOT-GAIN (JBR),
     1, FOR GENREF (GREF) OR FOR PLOTTER (PPP)  ?  ')
       ACCEPT 901,FILE
901     FORMAT(A10)
      ENDIF
C-----------------------------------------------------------
      OPEN(UNIT=30,FILE=FILE,STATUS='NEW')
C-----------------------------------------------------------
      IF (CHOICE.EQ.'OUT') GO TO 1
C-----------------------------------------------------------
C          CALCULATION OF ZI:
C     ZI=Jx*[Jy,1+.5*DEL*(GAM*Jy,2,1+GAMBAR*Jy,2,2)]
C    WITH :     Jx= (DELTA C(W2,W1) - DELTA S(W2,W1))
C           Jy,1= (DELTA C(T2,T1) - DELTA S(T2,T1))
C            Jy,2,1=(DELTA C(U2,U1) - DELTA S(U2,U1))
C            Jy,2,2=(DELTA C(V2,V1) - DELTA S(V2,V1))
C     WHERE C AND S ARE REAL AND IMAGINARY PART OF
C     FRESNEL INTEGRAL , AND DELTA C(X2,X1)=C(X2)-C(X1)  .
C     DEL , GAM COMPLEX COEFFICIENTS DEFINED FURTHER .
C-----------------------------------------------------------
C     CHOICE OF ILLUMINATION FUNCTION
C-----------------------------------------------------------
      TYPE 60
60     FORMAT('$ : 1)CONSTANT ILLUMINATION(I), 2)TE01 MODE
     1(E) , 3) TAPERED ILLUMINATION (T) ? ')
      ACCEPT 70,ILLU
70     FORMAT(A)
C-----------------------------------------------------------
      IF(ILLU.EQ.'I')  THEN
      TYPE *,'         CONSTANT ILLUMINATION  '
      ELSE IF(ILLU.EQ.'E')  THEN
      TYPE *,'              TE01 MODE  '
      ELSE
      TYPE* ,'          TAPERED ILLUMINATION  '
      ENDIF
C-----------------------------------------------------------
C                  DO LOOP ON THETA
C-----------------------------------------------------------
23     DO 1 I=1,IN
       THETA(I)=(PI/2.)*(I-1)/(IN-1)
       A=SIN(THETA(I))*COS(PHI)
       B=SIN(THETA(I))*SIN(PHI)
       X=R*L/(R+L)
       Y=SQRT(LAM*X/2.)
C-----------------------------------------------------------
C        CALCULATION OF INTEGRAL BOUNDARIES:
C        (U1,U2), (V1,V2), (W1,W2), (T1,T2)
C-----------------------------------------------------------
```

```
      W1=(A*X-A1/2.)/Y
      W2=(A*X+A1/2.)/Y
     CALL COR(W1,C1,S1)
     CALL COR(W2,C2,S2)
      DELCW=C2-C1
      DELSW=S2-S1
     ZW=CMPLX(DELCW,-DELSW)
C-------------------------------------------------------
C         CONSTANT ILLUMINATION
C-------------------------------------------------------
     IF(ILLU.EQ.'I')  THEN
      U1=0
      U2=0
      V1=0
      V2=0
      T1=(B*X-B1/2.)/Y
      T2=(B*X+B1/2.)/Y
      ALPHA=0.
      ETA=0.
      COEFF=1.
C-------------------------------------------------------
C         TE01 MODE
C-------------------------------------------------------
     ELSE IF(ILLU.EQ.'E')  THEN
      U1=((B+LAM/(2.*B1))*X-B1/2.)/Y
      U2=((B+LAM/(2.*B1))*X+B1/2.)/Y
      V1=((B-LAM/(2.*B1))*X-B1/2.)/Y
      V2=((B-LAM/(2.*B1))*X+B1/2.)/Y
      T1=0.
      T2=0.
      ALPHA=PI*B*X/B1
      ETA=0.
      COEFF=.5
C-------------------------------------------------------
C         TAPERED ILLUMINATION
C-------------------------------------------------------
     ELSE
      U1=((B+LAM/B1)*X-B1/2.)/Y
      U2=((B+LAM/B1)*X+B1/2.)/Y
      V1=((B-LAM/B1)*X-B1/2.)/Y
        V2=((B-LAM/B1)*X+B1/2.)/Y
      T1=(B*X-B1/2.)/Y
      T2=(B*X+B1/2.)/Y
      ALPHA=(2.*PI*B*X)/B1
      ETA=(PI*X*LAM)/(B1**2.)
      COEFF=3./16.
     ENDIF
C-------------------------------------------------------
C         CALCULATION OF THE VARIOUS INTEGRALS
C-------------------------------------------------------
     CALL COR(U1,C1,S1)
     CALL COR(U2,C2,S2)
       DELCU=C2-C1
       DELSU=S2-S1
```

```
      CALL COR(V1,C1,S1)
      CALL COR(V2,C2,S2)
        DELCV=C2-C1
        DELSV=S2-S1
      CALL COR(T1,C1,S1)
      CALL COR(T2,C2,S2)
        DELCT=C2-C1
        DELST=S2-S1
        ZU=CMPLX(DELCU,-DELSU)
        ZV=CMPLX(DELCV,-DELSV)
        ZT=CMPLX(DELCT,-DELST)
        COSX=COS(ALPHA)
        SINX=SIN(ALPHA)
        COSY=COS(ETA)
        SINY=SIN(ETA)
        ZA1=CMPLX(COSX,SINX)
        ZA2=CMPLX(COSX,-SINX)
        ZE=CMPLX(COSY,SINY)
        ZI(I)=ZW*(ZT+.5*ZE*(ZU*ZA1+ZV*ZA2))
1     CONTINUE
       ZIMAX=ZI(1)
      GDB=10.*ALOG10(8.*(X**2.)*PI/(A1*B1*COEFF))
      GDBM=GDB+20.*ALOG10(CABS(ZIMAX))
C-------------------------------------------------------
C          POLAR REPRESENTATION
C-------------------------------------------------------
      IF (ANSWER.EQ.'P') THEN
      TYPE*,'POLAR REPRESENTATION '
      DO I=1,IN
       CM=CABS(ZI(I)/ZIMAX)
       XO(I)=CM*SIN(THETA(I))
       YO(I)=CM*COS(THETA(I))
      END DO
      ONE=1.
      AZERO=0.
       WRITE (30,*) (-ONE,AZERO)
      DO I=1,(IN-1)
       WRITE (30,*)(-XO(IN-I+1),YO(IN-I+1))
      END DO
      DO I=1,IN
       WRITE (30,*)(XO(I),YO(I))
      END DO
       WRITE (30,*) ONE,AZERO
      CLOSE(UNIT=30)
      GO TO 75
      ENDIF
C-------------------------------------------------------
C          CARTESIAN REPRESENTATIONS
C-------------------------------------------------------
      DO I=1,IN
       ZI(I)=ZI(I)/ZIMAX
       CMD(I)=20.*ALOG10(CABS(ZI(I)))
       RZ=REAL(ZI(I))
       AI=AIMAG(ZI(I))
```

```
      TG=AI/RZ
      STHI=SIN(THETA(I))
      EPP=(PI*X)*((STHI)**2.)/LAM
     EP(I)=ATAN((TG-TAN(EPP))/(1+TAN(EPP)*TG))
      STH(I)=2.*PI*STHI*A1/LAM
      THETA(I)=THETA(I)*180./PI
     END DO
C-------------------------------------------------------
C         1)  VERSUS THETA
C-------------------------------------------------------
     IF (ANSWER.EQ.'C') THEN
      TYPE*,' CARTESIAN PATTERN VERSUS THETA '
     IF (FILE.EQ.'PPP') THEN
     DO I=1,(IN-1)
      WRITE(30,*) (-THETA(IN-I+1)),CMD(IN-I+1),EP(IN-I+1)
     END DO
     DO I=1,IN
      WRITE(30,*) THETA(I),CMD(I),EP(I)
      THETA(I)=THETA(I)*PI/180.
     END DO
      CLOSE(UNIT=30)
      ENDIF
C-------------------------------------------------------
C                    CREATION OF JBR.DAT
C-------------------------------------------------------
      IF (FILE.EQ.'JBR') THEN
      READ(2,*),DIAM,DU,UMAX,IRIN,IRFIN,IRINC,FDD
      WRITE (30,*) DIAM,FREQ
      WRITE(30,*) DU,UMAX
      WRITE(30,*) IRIN,IRFIN,IRINC
      WRITE(30,*) F
      WRITE(30,*) FDD
     DO I=1,IN
      WRITE(30,*) (THETA(I),CMD(I),EP(1))
     END DO
      FFF=999
      WRITE (30,*) FFF,FFF,FFF
      CLOSE(UNIT=2)
      CLOSE(UNIT=30)
     ENDIF
C-------------------------------------------------------
C                    CREATION OF GREF.DAT
C-------------------------------------------------------
     IF (FILE.EQ.'GREF') THEN
      IF (PHI.EQ.0) THEN
      IP1=1
      TYPE *,'          FOCAL DISTANCE = ?  :  '
      ACCEPT *,FOC
      P2=FOC
      TYPE *,'          DIAMETER OF THE DISH = ?  '
      ACCEPT *,DIAM
      P3=DIAM/40.
      P4=P3
      P5=DIAM
```

```
      WRITE (30,734) DG
      WRITE (30,*) IP1,P2,P3,P4,P5
      WRITE(30,734) TO
      WRITE (30,750), ( F,F,F,F,F      )
750     FORMAT(X,A,X,A,X,A,X,A,X,A,X)
      WRITE (30,751) T,T
751     FORMAT(X,A,X,A,X)
      WRITE (30,752) T,T,T
752     FORMAT(X,A,X,A,X,A,X)
      P9=0
      WRITE(30,*) P9,P9
      WRITE (30,734) FD
734     FORMAT(A3)
      IP6=IP1
      P7=90.
      WRITE (30,801) ( T,F,T,IP6,P7 )
801     FORMAT(2X,A,X,A,X,A,X,I4,F6.2)
      IP8=2
      P9=0.
      P10=P7
      WRITE (30,802) IP8,P9,P10
802       FORMAT(I4,2F6.2)
      WRITE (30,603) (IN)
603     FORMAT(I3)
    ENDIF
    DO I=1,IN
     WRITE (30,*)(THETA(I),CMD(I))
    END DO
      IF (PHI.EQ.0) THEN
     PHI=1.57078
     GO TO 23
      ENDIF
     WRITE (30,734) PZ
     TYPE*,' ENTER INUM( PAT),PHO,PH1,PH2(PHI) ,
    1THO,TH1,TH2(THE)
    ACCEPT *,INUM,PHO,PH1,PH2,THO,TH1,TH2
     WRITE (30,604) INUM
604    FORMAT(I)
     IF (INUM.EQ.1)THEN
     WRITE (30,*) PHO
     ELSE IF (INUM.EQ.2) THEN
     WRITE (30,*) PHO,PH1
     ELSE
     WRITE (30,*) PHO,PH1,PH2
     ENDIF
     WRITE (30,*) THO,TH1,TH2
     WRITE (30,734) FQ
     WRITE (30,800) IP6,FREQ
800     FORMAT(I4,2X,F7.3)
     WRITE(30,734) XQ
    CLOSE(UNIT=30)
    ENDIF
    ENDIF
```

```
C-------------------------------------------------------
C         2)  VERSUS K*A1*SIN(THETA)
C-------------------------------------------------------
     IF (ANSWER.EQ.'S') THEN
      TYPE*,' CARTESIAN PATTERN VS. K*A1*SIN(THETA) '
     DO I=1,(IN-1)
      WRITE(30,*)(-STH(IN-I+1)),CMD(IN-I+1)
     END DO
     DO I=1,IN
      WRITE(30,*) STH(I),CMD(I)
      THETA(I)=THETA(I)*PI/180.
     END DO
     ENDIF
     WRITE(6,74) GDBM
74     FORMAT(///T15' Maximum Gain in dB = ',F8.3///)
C-------------------------------------------------------
C         OTHER RUNS IF DESIRED
C-------------------------------------------------------
75     TYPE 80
80     FORMAT('$ ANOTHER RUN WITH A NEW GEOMETRY (NGE),
     1NEW PARAMETERS (PAR) , OTHER OUTPUT (OUT) ? ')
       ACCEPT 90,CHOICE
90     FORMAT(A3)
     IF(CHOICE.EQ.'NGE')THEN
C              -----
     TYPE *,'       NEW GEOMETRY  '
     GO TO 111
     ENDIF
     IF(CHOICE.EQ.'PAR')THEN
C              -----
     TYPE *,'       NEW PARAMETERS  '
     GO TO 112
     ENDIF
     IF(CHOICE.EQ.'OUT')THEN
C              -----
     TYPE *,'      OTHER OUTPUT  '
     GO TO 11
     ENDIF
     END
C-------------------------------------------------------
     SUBROUTINE COR(X,C,S)
C-------------------------------------------------------
     PARAMETER     PI=3.1415927
     C=0.
     S=0.
     DO 1 I=1,500
      C=C+(.002*X)*COS((PI/2.)*((FLOAT(I-1)*X/499.)**2.))
      S=S+(.002*X)*SIN((PI/2.)*((FLOAT(I-1)*X/499.)**2.))
 1   CONTINUE
     RETURN
     END
```

REFERENCES

Barton, D. K., Low Angle Radar Tracking, Proc. IEEE 62, No 6, June 1974, pp. 687-704.

Beckmann, P. and A. Spizichino, The Scattering of EM Waves from Rough Surfaces, New York Pergamon, 1963.

Bullington, K., Reflection Coefficients of Irregular Terrain, Proc. IRE, vol. 43, pp1258-1262, Aug. 1954.

Der Bundesminister fur Forschung und Technologie, Entwicklungslinien in Kraftfahrzeugtechnik und Strassenverkehr, Forschungsbilanz, Verlag TUV Rheinland Gmbh, 1978.

Der Bundesminister fur Forschung und Technologie, Entwicklungslinien in Kraftfahrzeugtechnik und Strassenverkehr, Forschungsbilanz, Verlag TUV Rheinland Gmbh, 1979.

C.A. Research Corporation, Development project, Private Communication, 1981.

Collin, R. E. and F. J. Zucker, Antenna Theory, Mc Graw-Hill New York, 1969.

Dull, E. H. and H. J. Peters, Collision Avoidance System for Automobiles, Bosch Research Laboratories, March 1978.

Fradin, A. Z., Microwaves Antennas, New York Pergamon, 1961.

Freedman, J., Resolution in Radar Systems, Proc. IRE 39, No7, July 1951, pp.813-818.

Fujikawa, T. et al., A Study of the Automatic Braking System, Central Engineering Laboratories, Nissan Motor Corporation, June 1979.

Grimes, D. M. and T. O. Jones, Automotive Radar : A Brief Review, Proc. IEEE, 1974.

Gunn, K. L. S. and T. W. R. East, The Microwave properties of Precipitation Particles, Mc. Gill University Montreal, July 1954.

Haddock, F. T., Scattering and Attenuation of Microwave Radiation through Rain, Naval Research Laboratories, Washington 1948.

Hahn, L., Further Development of Autarkic Headway Warning Radar Systems, VDO Adolf Schindling AG, Jan. 1980.

Jasik, H., Antenna Engineering Handbook, Mc Graw-Hill New York, 1961.

Jones, T. O. and D. M. Grimes, Some Automotive Radar System Considerations, Microwave Journal, 1979.

Jordan, E. C. and K. G. Balmain, Electromagnetic Waves and Radiating Systems, Prentice-Hall, 1968.

Keller, J. B., Geometrical Theory of Diffraction, J. Opt. Soc. Am.,1962.

Kerr, D. E., Propagation of Short Radio Waves, New York Dover, 1965.

Kraus, J. D., Antennas, Mc Graw-Hill, 1950.

Laugénie, J-M., Simulation of Detection in Automotive Radar, Pennsylvania State University, MS Thesis, 1981.

Liao, S. Y., Microwave Devices and Circuits, Prentice-Hall, N.J. 1980.

Marshall, J. S. and W. Mck. Palmer, Distibution of Raindrops with Size, Journal of Meteorology, Aug. 1948, pp. 165-166.

Mie, G., Ann. Physik, 25, p. 377, 1908.

Nathanson, F. E., Radar Design Principles, Mc Graw-Hill, 1969.

NHTSA-Bendix Research Laboratories, Analysis of Problems on the Application of Radar Sensors to Automotive Collision Prevention, Report, Dec. 1973.

NHTSA-Bendix Research Laboratories, Collision Avoidance Radar Braking Systems Investigation - Phase II Study, Volume II, Technical Report, Sept. 1976.

Peake, W. H., Theory of Radar Return from Terrain, IRE Conv. Rec. ,Part I, pp. 27-41, 1959.

RCA Laboratories, Electronic Subsystems for the Research Safety Vehicle (Phase III), Final Report, March 1980.

Rudduck, R. C. and S. H. Lee, Numerical Electromagnetics Code (NEC) - Reflector Antenna Code, Part I : User's Manual, The Ohio State University, Sept. 1979.

Rudduck, R. C. and S. H. Lee, Numerical Electromagnetics Code (NEC) -Reflector Antenna Code, Part II : Code Manual, The Ohio State University, Sept. 1979.

Silver, S., Microwave Antenna Theory and Design, New York Dover, 1965, p. 586.

Skolnik, M. I., Introduction to Radar Systems, New York Mc Graw-Hill, 1962.

Skolnik, M. I., Weather Effects on Radar, Radar Handbook, New York Mc Graw-Hill, 1970, pp.24-30.

Taylor, R. C., Terrain Return Measurements at X, Ku and Ka band, IRE Conv. Rec., 1959, Part I, pp. 19-26.

Thourel, L., The Antenna, New York Wiley and Sons, 1960, pp. 245-249.

Weeks, W. L., Antenna Engineering, Mc Graw-Hill, 1968, pp. 30, 240-249.

Wood, P. J., Reflector Antenna Analysis and Design, Peregrinus, 1980.

APPENDIX G

SIMULATION OF TARGET DETECTION

IN

AUTOMOTIVE RADAR

The Pennsylvania State University

The Graduate School

Department of Engineering

Simulation of Target Detection in Automotive Radar

A Thesis in

Electrical Engineering

by

Jean-Marc Laugénie

Submitted in Partial Fulfillment
of the Requirements
for the Degree of

Master of Science

November 1981

We approve the thesis of Jean-Marc Laugénie.

Date of Signature:

8/21/81

Lynn A. Carpenter, Professor of Electrical Engineering, Thesis Advisor.

8/27/81

Dale M. Grimes, Head of the Department of Electrical Engineering. Professor of Electrical Engineeering.

8/18/81

Anthony J. Ferraro, Professor of Electrical Engineering.

ABSTRACT

This thesis summarizes the results obtained by computer simulation of various existing Automotive Radars.
A simple computer model has been developed that describes the variations in the radar cross-section of complex bodies, such as cars or road signs. This model simulates a complex target by combinations of rectangular flat plates. It is used to evaluate the probability of detection and the probability of false alarm for some systems currently being developed.

TABLE OF CONTENTS

Page

LIST OF TABLES

LIST OF FIGURES

The author wishes to express his gratitude to Dr. L. A. Carpenter for his advice and guidance during the course of this study. The author also wishes to express his appreciation to Dr. D. M. Grimes and Dr. A. J. Ferraro for their suggestions and support.

The author would also like to thank the staff of the Electrical Engineering Computer Center for their assistance in the computer programming, and Henri Pruvot for his patience and cooperation.

This work was supported by National Highway Traffic Safety Administration through a grant to Minicar, Inc. Galeta, California.

CHAPTER 1

INTRODUCTION

1.1 COLLISION AVOIDANCE SYSTEMS

Rear-end collisions are the most frequent type of highway accidents, so the design of an automatic system for collision prevention, or for traffic regulation, is of special interest. In selecting a basic system, one must keep in mind the following demands (VDO information, 1980):

1) Range: approximately 120 meters.

2) Resolution: must allow discrimination between targets in and adjacent to the driver's lane.

3) Operation: guaranteed under all environmental conditions: guardrails, bridges, road signs, and weather conditions: fog, rain, snow.

4) Functioning: must be self-contained.

Mostly because of criteria 1) and 3), the use of any acoustic or optical technique has been ruled out, and radar has been chosen as the only applicable solution.

The simulation of target detection in Automotive Radar is basically performed in three steps: modeling of the antenna, modeling of the targets, and study of the propagation effects, to link the two first parts together.

1.2 TYPES OF RADAR

Automotive Radar must be able to determine range and velocity rather accurately, and to function well in rain or snow. Basically, four systems can be used, as described below.

1.2.1 Pulse-Modulated Radar

Grimes and Jones (1974) have shown that ranging for nearby targets in pulsed systems demands that the transmitted power drop to a level much lower than the received power level well in advance of the signal returns if signals from the target are to be recognized as such. This requires the use of very short pulses, and therefore of a large receiver bandwidth, which lowers the signal-to-noise ratio.

Pulse-modulated radar determines range by measuring the time between the emitted and the received pulses. Velocity is determined by measuring the range rate; hence, it be-

comes very difficult to discern moving targets in the presence of stationary targets when the echo signals from both targets are of the same order of magnitude. In this study, stationary targets have a zero relative velocity (with respect to the automobile), while fixed targets, such as road signs, have a non-zero relative velocity and are considered by the radar as moving targets. Mutual blinding from similarly equipped vehicles can be minimized with pulsed radar, and can almost be completely suppressed by varying the pulse rate with velocity (CA Research, 1981).

1.2.2 Pulse Doppler Radar

The Doppler shift in frequency caused by a moving target is used to determine its velocity, thus allowing discrimination between moving and stationary targets, even when the echo signal from the latter is orders of magnitude greater (Skolnik, 1962).This may be of prime importance in the case of Automotive Radar.

1.2.3 FM-CW Radar

CW radars use the Doppler shift to measure the relative velocity; in FM-CW, range determination is performed by modulating the frequency and measuring the frequency difference between transmitted and received signals. Because CW radar emits continuously, the isolation between transmitter and receiver is of importance. The use of two separate

antennas can provide a high degree of isolation; if a single antenna is to be used, isolation can be performed with a hybrid junction, circulator, or with separate polarizations, the latter generally giving rather poor results.

1.2.4 Diplex Radar

In Diplex radar, the relative velocity is deduced from the Doppler shift of a first CW signal; a second CW signal, at a nearby frequency, gives a double measurement of this relative velocity, while the phase difference between the two Doppler frequencies provides the range information. Range information for stationary targets (resulting in no Doppler shift) can be determined either by measuring the phase difference between the two RF signals, or by simulating the Doppler frequency shift by translating the echo frequency.

1.3 RADIATING SYSTEMS

Pruvot (1981) developed an analytical model for parabolic dishes fed by a horn, which are commonly used in Automotive Radar. Given the geometry of the antenna, the dimensions of the horn, and the operating frequency, this model provides the information concerning the antenna gain in all directions. For false alarm considerations, a good Automotive Radar requires a very narrow beamwidth, of about 2° to 5°, to avoid detection of obstacles on the side of the

road or in the left lane. Therefore, one would be tempted to use a very simple model for the gain, such as a parabolic or exponential variation with the angle of observation; this approximation could be accurate for the main lobe, but would not account at all for the side lobes, which play a primary important role in the false alarm rate evaluation.

Consequently, this more elaborate model, based on the General Theory of Diffraction, is used to predict the antenna gain in any direction.

1.4 TARGET MODELING

It is assumed that in the usual driving environment, most of the targets encountered can be analytically modeled by rectangular flat plates, combined in an appropriate way. The radar cross-section of a rectangular flat plate with dimensions much greater than one wavelength can be approximated by an analytical formula, using the Standard Physical-Optics Method.

This first model is improved by adding the plate edge contributions, to introduce a polarization dependence in the cross-section of a flat plate. The next step is the combination, with an appropriate phase factor, of several flat plates, to represent a complex body. The final model gives a reliable representation of the very sharp variations of a complex body cross-section with the aspect angle.

1.5 PROPAGATION EFFECTS

To determine whether a target is to be detected or not, the ratio of the power returned from target to the power transmitted by radar must be computed. In order to get this information, it is necessary to make a link between the antenna and the target; this is done through propagation effect considerations. Because it is surrounded by all sorts of moving obstacles, creating a large amount of noise, Automotive Radar is in an extremely unfavorable environment. It must function accurately in the presence of a permanent close reflecting surface (the road), and must remain efficient in rain, fog, or snow.

These constraints will obviously produce different results from the results of radar operating in free space, and must be accounted for.

The effect of the road is represented by a reflection coefficient depending on the frequency and on the nature of the ground.

The weather effects (atmospheric absorption, rain clutter, fog attenuation) are studied by Pruvot (1981), so the results are shortly summarized here, and used in the rest of the study without further explanations.

1.6 DETECTION CONSIDERATIONS

The power returned to the radar, as computed by the combination of the three models presented above, gives an average value, for no statistical or randomized quantity appears in these models. Unfortunately, Automotive Radar deals with complex targets in a noisy environment, so radar cross-sections have a very randomized behavior, and in these conditions, detection can be expressed only in terms of probability. The analytical model gives an average cross-section, and the instantaneous cross-section fluctuates around this value, and cannot be uniquely determined. These fluctuations are due to an extreme sensitivity of complex body cross-sections to variations in aspect angle, and also to the surrounding of targets by other obstacles; this can be simulated by an addition of random noise. The statistical behavior in general is described by a probability density function, leading to the determination of a detection criterion.

1.7 EVALUATION OF SYSTEMS

1.7.1 Detection Criteria

Two basic criteria can be used to compare the different systems:

1) Distance at which brakes are activated as a function of automobile velocity.

2) Detection Capacity Rate (DCR), defined as:

$$DCR = \ln(Dt/Fa+1),$$

where Dt is the number of detected targets for some standard length of time depending on the driving conditions so that the number of potential targets were approximately 100, and Fa is the number of false alarms for the same period.

Each system is rated according to its efficiency in terms of braking distance, and studied in different driving conditions, such as rain or fog. Unfortunately, an evaluation of the "DCR" for each system was not possible, due to the statistical definition of this quantity; only experimental results can be given in terms of DCR.

1.7.2 Braking Algorithm

Each system has its own algorithm which is used to determine under what conditions the brakes must be activated. Basically, the brakes are activated after the following tests have been performed:

1) Acquisition of Target: signal returned to radar exceeds a certain threshold "Sth".

2) Detection of Target: threshold is exceeded during a sufficient period of time "Tdel".

3) Danger Criterion: an algorithm, depending on various parameters such as range, automobile velocity, relative velocity, deceleration, defines a safety condition; as soon as this condition is verified, the brakes must be applied.

4) Activation Time: a time delay occurs before application of the brakes, depending on the mode of activation (automatic or manual).

1.7.3 Levels of Signal Processing

Three levels of signal processing can be defined:

1) First Level: there is no difference between acquisition and detection of a target, because the radar time delay is zero. This gives rise to many false alarms, since any peak of noise exceeding the threshold is considered to be a valid signal, and starts the braking process.

2) Second Level: a time integration is performed during a certain period of time "Tdel"; it increases the signal-to-noise ratio, and recognizes a possible peak of noise exceeding the threshold during a short period of time. Two different approaches are possible: either a constant range delay, or a constant time delay. The latter is more efficient at low speeds than at high speeds, since the distance covered before detection increases with automobile

velocity.

Third Level: a time integration is included with an elaborate braking algorithm allowing predetermination of target trajectory. In this way, targets with collisionless trajectories are eliminated. This system requires very elaborate signal processing, performed by a microcomputer to calculate the trajectory of a target, and recognize the signature of some non-hazardous targets such as guardrails, road signs, and bridges.

These three levels correspond to an increasing efficiency in reducing the false alarm rate. Experimental data have led to the following estimate:

For every 100 km under normal driving conditions, level 1 would result in an average of 9 false alarms, level 2 in 4 false alarms, and level 1 in 1, or possibly 0 false alarms.

CHAPTER 2

ANTENNA MODELING

2.1 PRINCIPLE

Antennas are modeled using the General Theory of Diffraction by Pruvot (1981). The desired information is the antenna gain in any direction. Direction is represented by θ and ϕ, as shown on figure 2.1.1.

In most of the systems, the antenna is a parabolic reflector fed by a horn. Therefore, the antenna pattern is determined in two steps: first, the feed pattern is computed; secondly, this feed pattern is used to compute the final gain in any direction. This last step is performed using an existing, very powerful program called "GENREF". The results are stored into a file under the following form:

$\phi = 0°$:

$\theta = 0.0°$ G(1,1)

$\theta = 0.5°$ G(1,2)

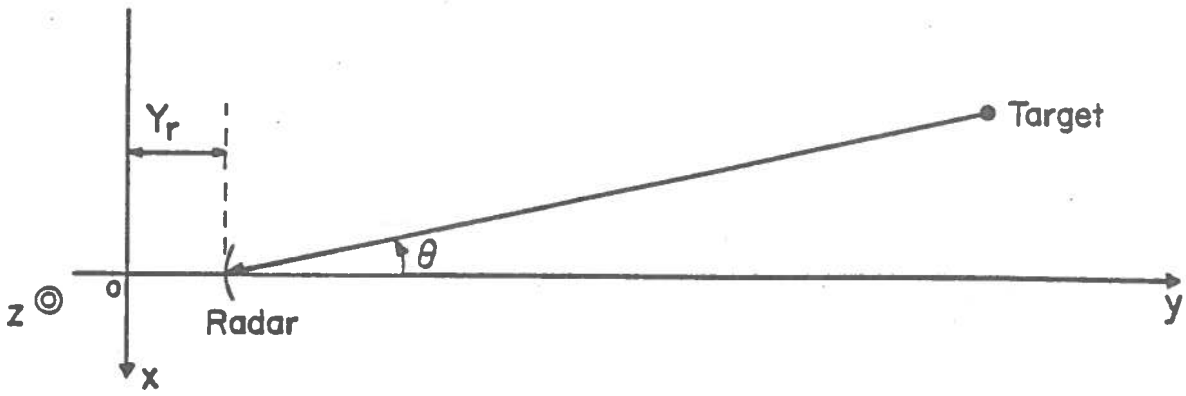

TOP VIEW

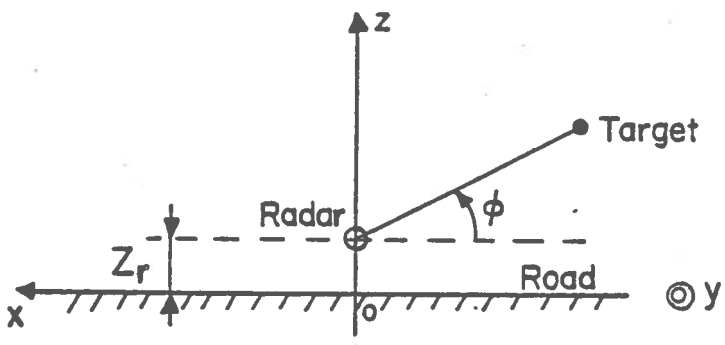

FRONT VIEW

Figure 2.1.1: Radar geometry.

.

.

.

$\theta = 40.0^\circ$ G(1,81)

$\phi = 90^\circ$:

$\theta = 0.0^\circ$ G(2,1)

$\theta = 0.5^\circ$ G(2,2)

.

.

.

$\theta = 40.0^\circ$ G(2,81)

For time and room efficiency reasons, gain is not stored for angles θ greater than 40°. Since antennas in Automotive Radar are quite directive, it can be assumed without too much of an error that the gain is constant between 40° and 90°. Reading of the gain is performed by a subroutine, as explained in greater details in CHAPTER 6.

2.2 RESULTS

2.2.1 Bendix

Figure 2.2.1 shows the gain of the Bendix system in the plane $\phi = 0^\circ$, and figure 2.2.2 in the plane $\phi = 90^\circ$. Bendix uses a 45° polarization, so the plane of observation is rotated 45° before data is read from the corresponding file.

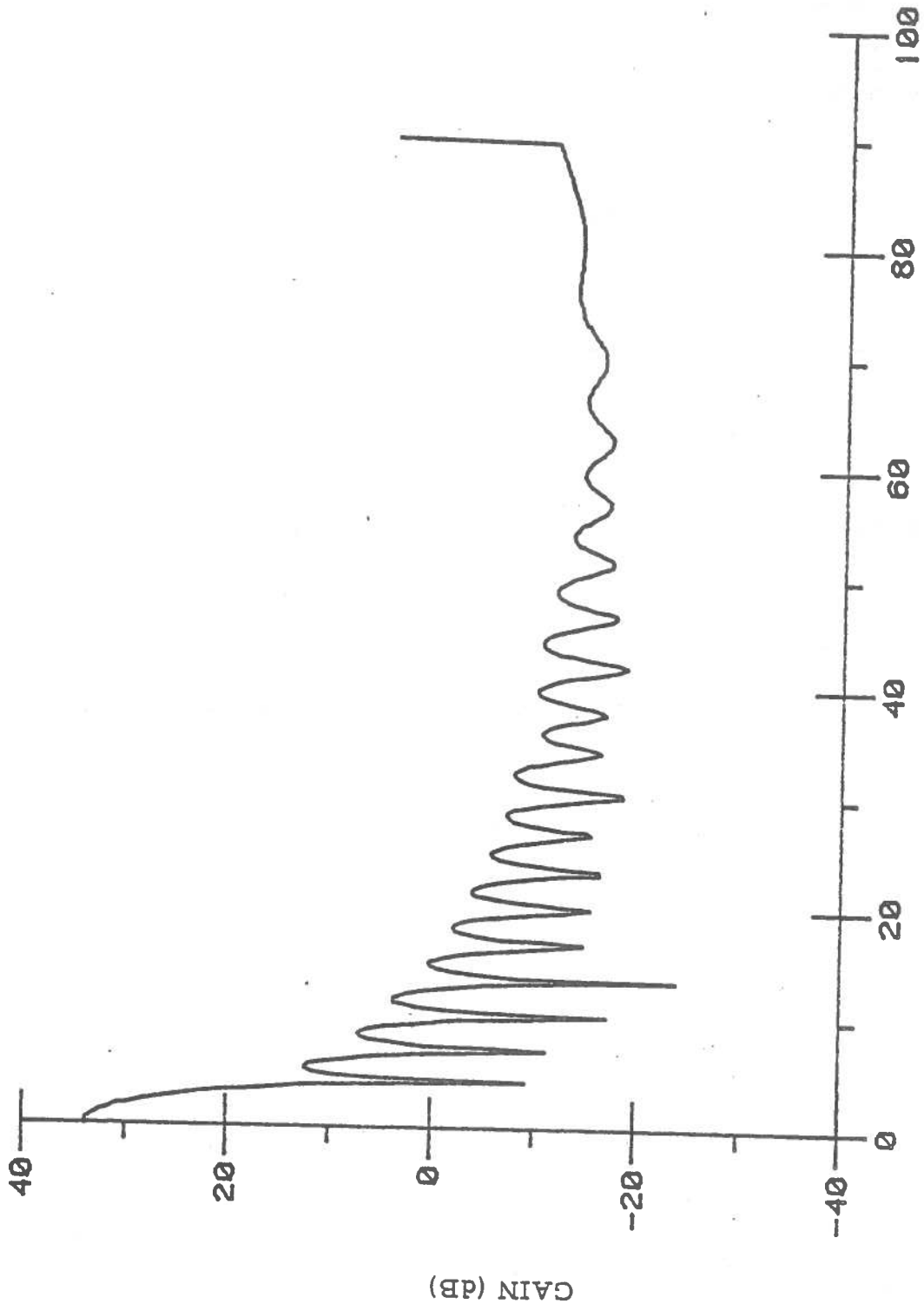

Figure 2.2.1: BENDIX System. Gain in the E-plane.

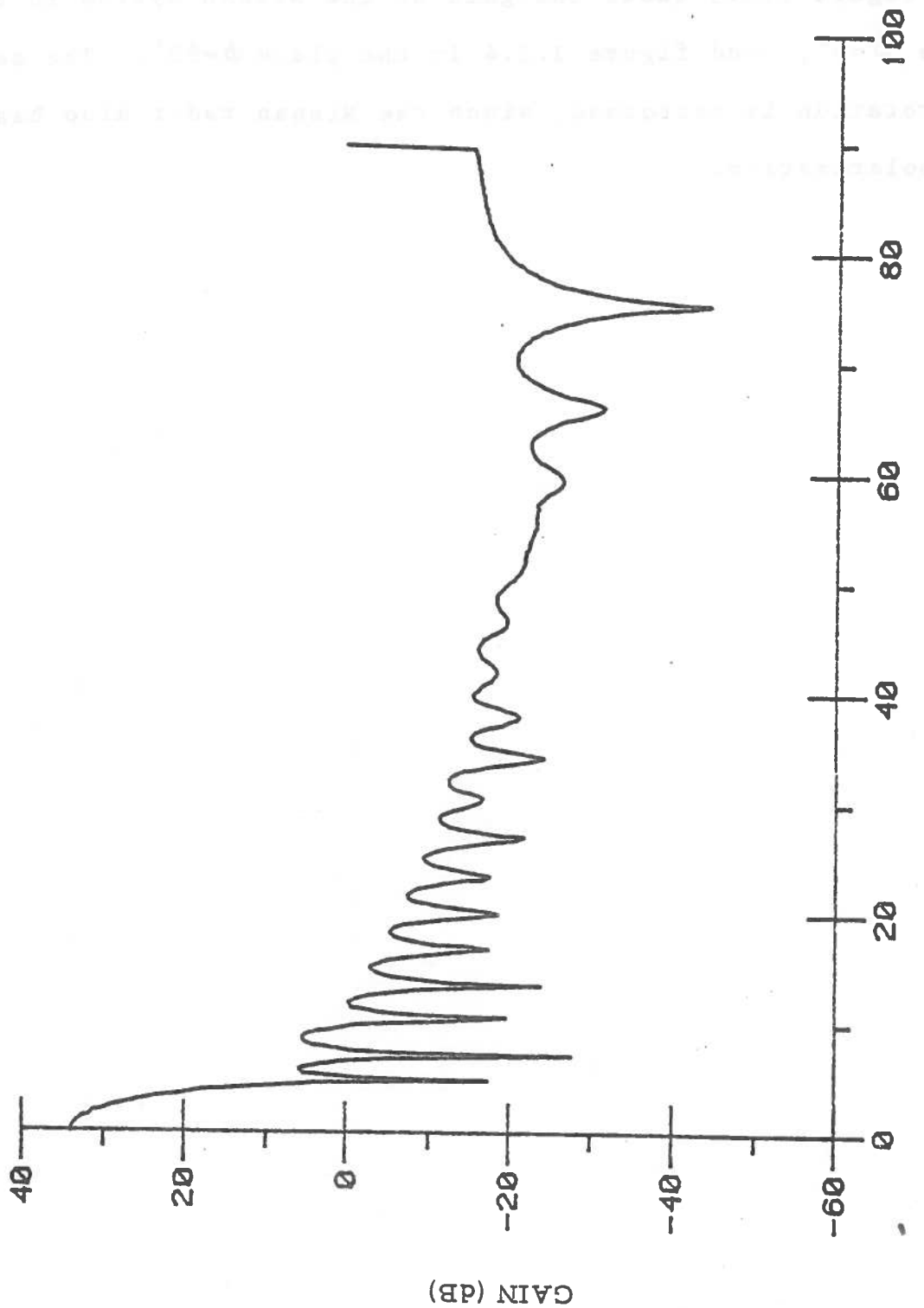

Figure 2.2.2: BENDIX System. Gain in the H-plane.

2.2.2 Nissan

Figure 2.2.3 shows the gain of the Nissan system in the plane $\phi=0^\circ$, and figure 2.2.4 in the plane $\phi=90^\circ$. The same 45°-rotation is performed, since the Nissan radar also has a 45° polarization.

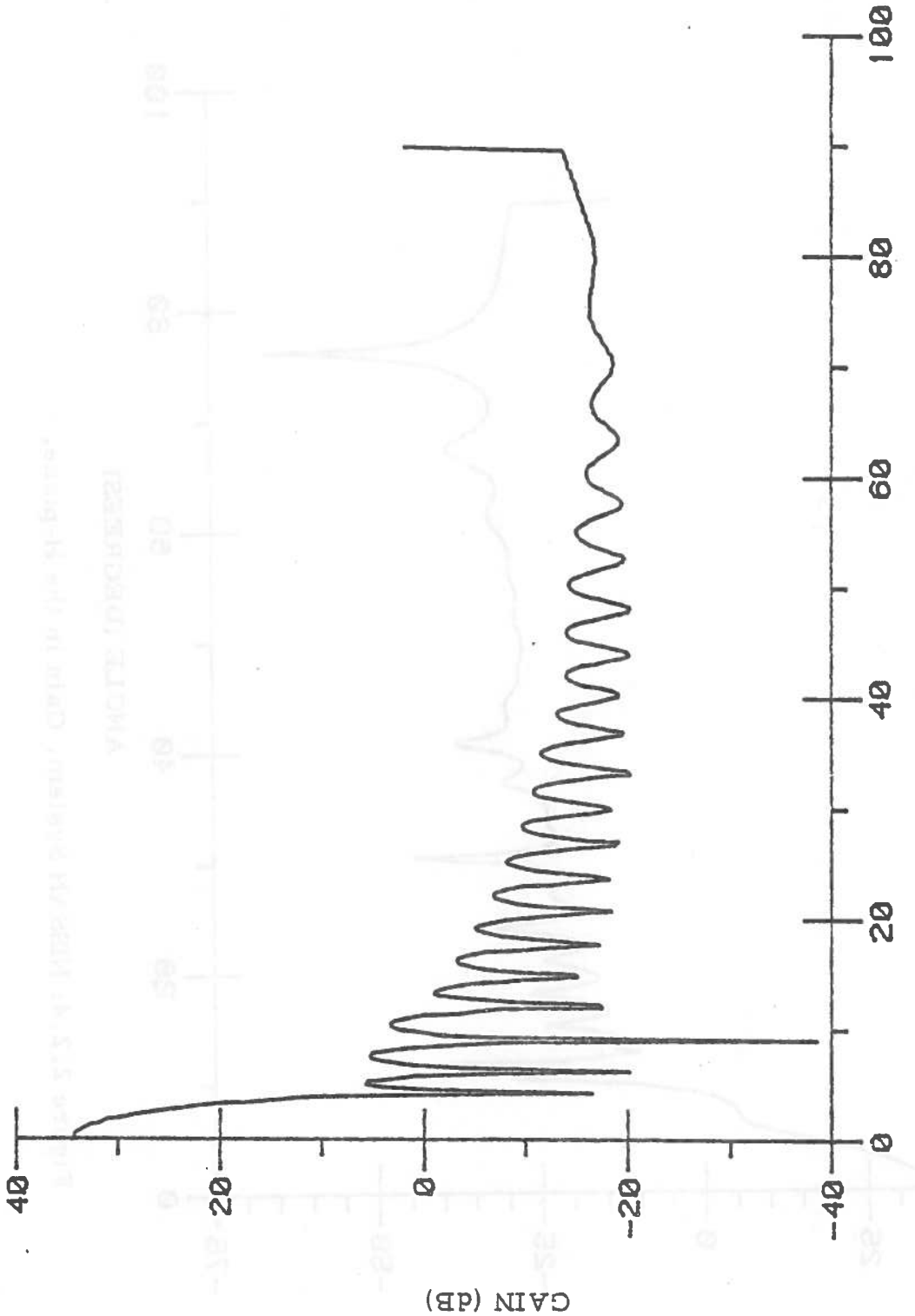

Figure 2.2.3: NISSAN System. Gain in the E-plane.

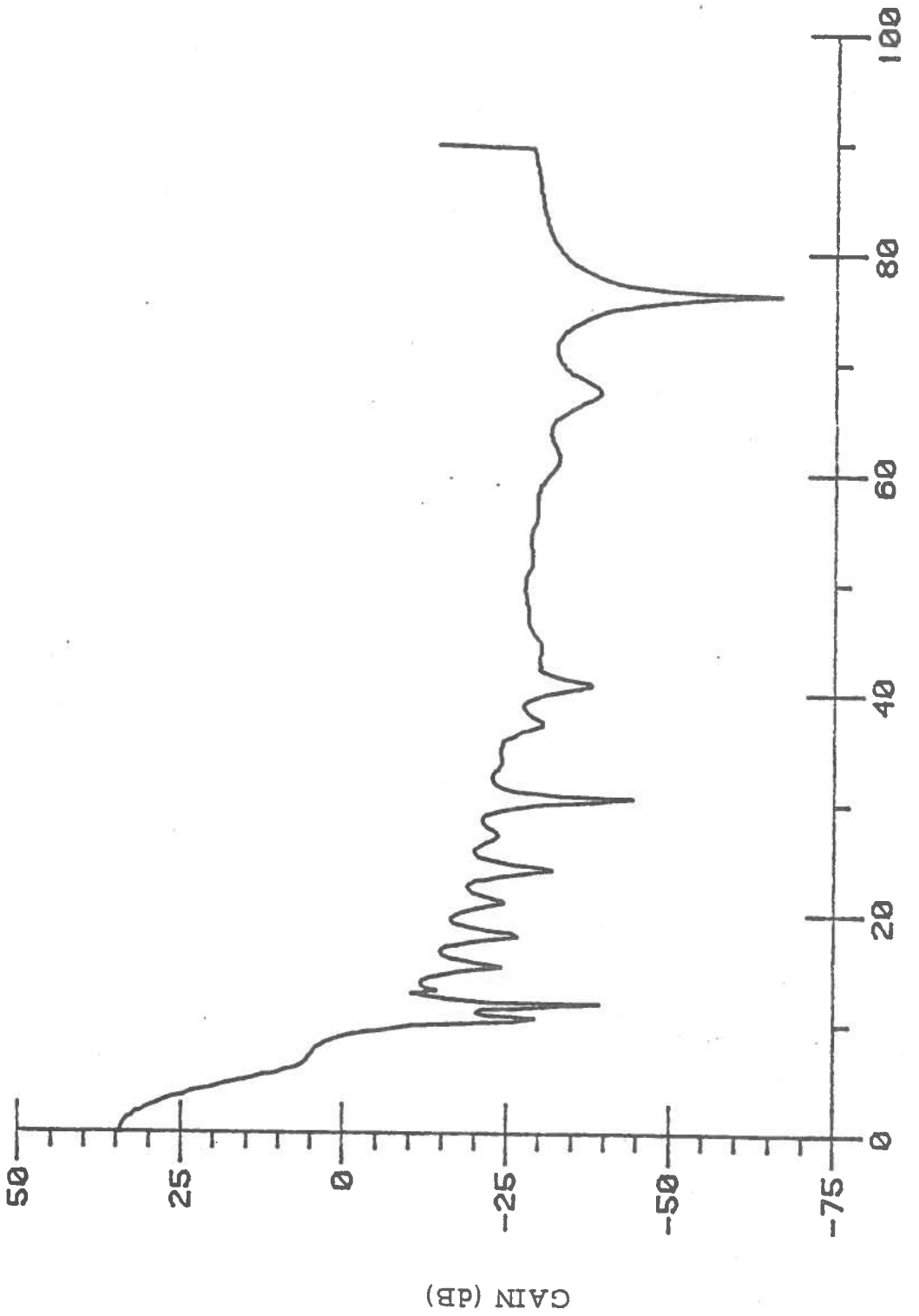

Figure 2.2.4: NISSAN System. Gain in the H-plane.

CHAPTER 3

TARGET MODELING

3.1 PRINCIPLE

As soon as the radar cross-section σ of a target is known, it becomes possible, given the coordinates of this target and the radar characteristics, to compute the returned-power to transmitted-power ratio (Skolnik, 1962):

$$Sr = \frac{St \cdot Gr \cdot Gt \cdot \sigma \cdot c}{(4\pi)^3 \cdot R^4 \cdot f^2} \qquad (3.1)$$

Where: - St = Signal transmitted by radar.

- Sr = Signal returned to radar.

- Gt = Gain of transmitting antenna in the direction of target.

- Gr = Gain of receiving antenna in the direction of target.

- R = distance radar-target (assuming Rt=Rr=R).

- f = frequency.

- c = speed of light ($c \simeq 3.10^8$ m/sec).

The purpose of this chapter is to present a model of complex targets with rectangular flat plates; returns from each flat plate are combined with a phase factor, to account for destructive and constructive interferences.

3.0.1 Cross-Section of a Flat Plate

Assuming that the transmitting and receiving antennas are the same (monostatic configuration), only the back-scattering cross-section needs to be computed.

Skolnik (1962) defines radar cross-section as:

$$\sigma = \lim_{R \to \infty} 4\pi R^2 \frac{|Es|^2}{|Ei|^2} \qquad (3.2)$$

Where R is the distance from the point of observation to the origin of a coordinate system centered near or in the scattering body, |Ei| is the magnitude of the incident electric field, and |Es| is the magnitude of the scattered electric field.

The standard Physical-Optics method (Crispin and Siegel, 1968) is applied; this approximation is valid in the far-field, defined as: D^2/λ, where D is the diameter of the antenna. Then, at a frequency of 36 GHz, with a 20 cm-diameter parabolic reflector, the far-field corresponds to about 4.8 meters. Also, the object must be entirely in the antenna beam. In the situations studied here, targets are at an initial distance of 100 meters, so they can be consi-

dered as point-targets without too much of an error. It yields, for the geometry defined in figure 3.1.1, and in the limits of wavelengths shorter than dimensions of the plate (see Appendix A):

$$\sigma = \frac{1}{\pi} [A \cdot B \cdot W]^2 \frac{[\sin(A \cdot U)]^2}{(A \cdot U)^2} \frac{[\sin(B \cdot V)]^2}{(B \cdot V)^2} \quad (3.3)$$

Where: - $A = 2\pi L/\lambda$

- $B = 2\pi l/\lambda$
- $U = \sin\theta \cdot \cos\phi$
- $V = \sin\theta \cdot \sin\phi$
- $W = \cos\theta$

Then, for speculiar reflection ($\theta=0$), the cross-section is maximum:

$$\sigma_{max} = 4\pi \frac{(l \cdot L)^2}{\lambda^2} \quad (3.4)$$

The restriction of short wavelengths is not a problem in the case of Automotive Radar, since the frequency is in the range 20-60 GHz, and the targets considered here are large enough to ensure the conditions: $l >> \lambda$ and $L >> \lambda$.

On the other hand, diffraction on the edges of each plate introduces a polarization-dependent term which does not appear in this first model (Ross, 1966), and this is not admissible. Therefore, the next step is to account for the perturbation introduced by the edges.

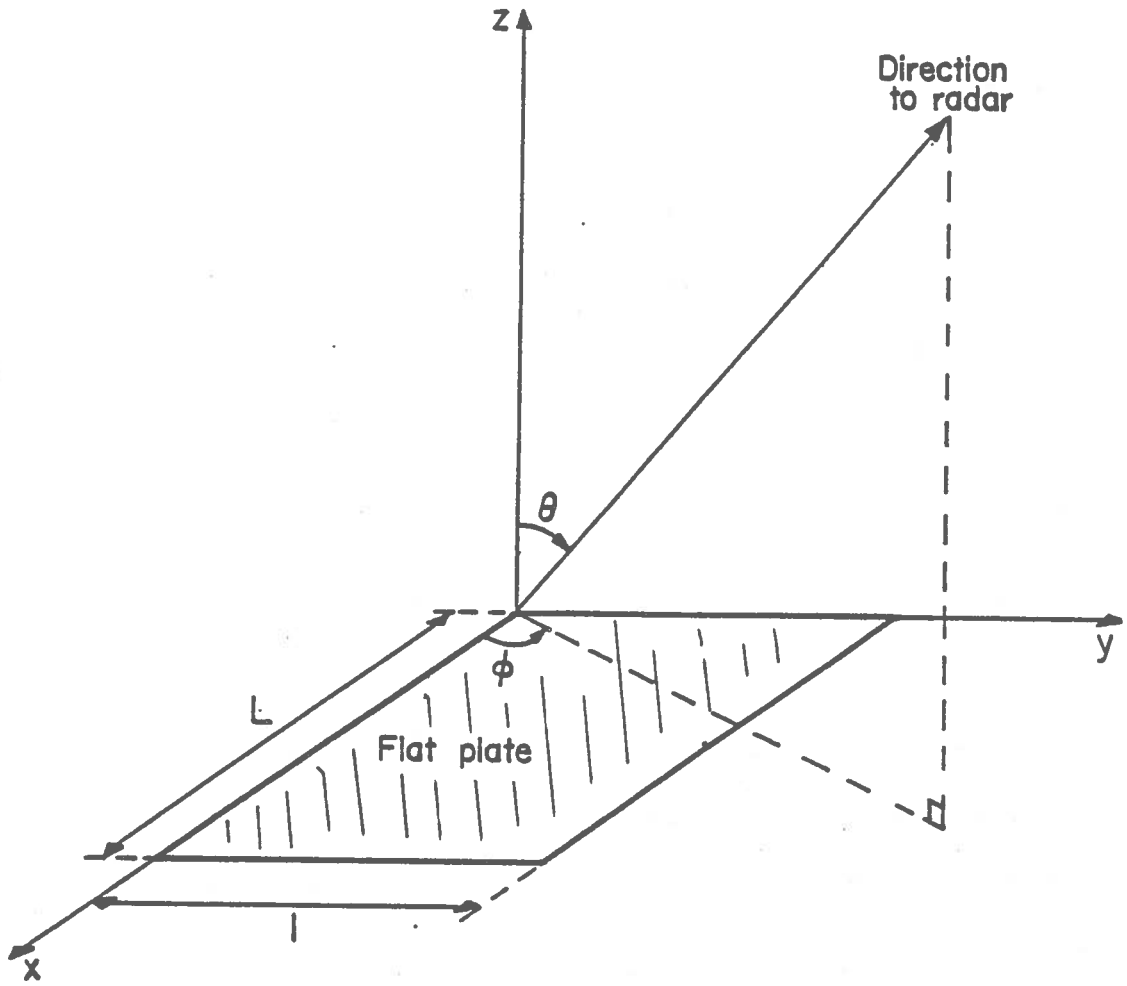

Figure 3.1.1: Flat plate geometry.

3.1.2 Cross-Section of Edges

Crispin and Siegel (1968) propose to represent the edges of a flat plate by wires. Chu's formula gives, for a perfectly conducting wire that is many wavelengths long but only a fraction of a wavelength thick:

$$\sigma = \frac{\pi L^2 \cdot \sin^2\theta \; [\sin(A\cdot\cos\theta)/(A\cdot\cos\theta)]^2 \cos^4\Phi}{(\pi/2)^2 + [\mathrm{Log}(\pi\cdot\gamma\cdot a\cdot\sin\theta/\lambda)]^2} \qquad (3.5)$$

Where: - L is the length of the wire.

- a is the radius of the wire.

- θ is the angle between the wire and the direction of incidence.

- Φ is the angle between the polarization direction and the plane formed by the wire and the direction of incidence.

- $\gamma \simeq 1.78...$

- $A = (2\pi L/\lambda)$

Good results are obtained, in the case of flat plates, by setting the radius of the wire "a" equal to $\lambda/85$.

3.1.3 Cross-Section of Complex Targets

Given a complex body composed of Np plates and Nw wires (representing the edges), the next step is to combine these Np+Nw cross-sections to get the entire body cross-section.

Because of destructive and constructive interferences between each component of a complex target, the simple addition of all the different cross-sections would give erroneous results. The relative phase angle of the returned signal must be taken into account for each element.

One method of combination (Crispin and Siegel, 1968) leads to the following expression:

$$\sigma = \left| \sum_k (\sigma k)^{1/2} \exp(j\Phi k) \right|^2 \qquad (3.6)$$

Where k is the cross-section of the k-th component and Φk is the relative phase angle associated with the k-th component:

$$\Phi k = \frac{2\pi}{\lambda} \cdot 2Dk \qquad (3.7)$$

Where Dk is the distance from the radar, or from any plane of reference, to the "point" at which the k-th component scatters. Twice the distance is used because the wave travels from radar to target, and then back to radar.

3.1.4 Ground Reflection

The problem of ground reflection will be studied in greater details in CHAPTER 4, but its interaction with the computation of cross-sections makes it necessary to present it here.

Consider a target at a distance R from radar, and at a height D above the road; radar is at a height d (figure 3.1.2).

The energy transmitted along R1 is scattered back along R1 to the radar by a scattering cross-section $\sigma 11$, and along R2 to the radar by a scattering cross-section $\sigma 12$. The energy transmitted along R2 is scattered back following the same process, so the radar now deals with 4 cross-sections: $\sigma 11$, $\sigma 22$, $\sigma 12$, $\sigma 21$.

Because of reciprocity, $\sigma 12 = \sigma 21$, but 3 different cross-sections still remain. $\sigma 11$ and $\sigma 22$ are backscattering cross-sections, but $\sigma 12$ is a bistatic cross-section, because the energy is transmitted in one direction and scattered back in another direction. The model presented above deals only with backscattering cross-sections, so the easiest way to solve the problem of ground reflection is to relate $\sigma 12$ to some backscattering cross-sections, which are possible to compute.

The Bistatic Cross-Section Theorem states that in the limit of vanishing wavelength, the bistatic cross-section for transmitter direction K and receiver direction N is equal to the monostatic cross-section for the transmitter-receiver direction K+N, with $K \neq N$, for bodies that are sufficiently smooth (Crispin and Siegel, 1968).

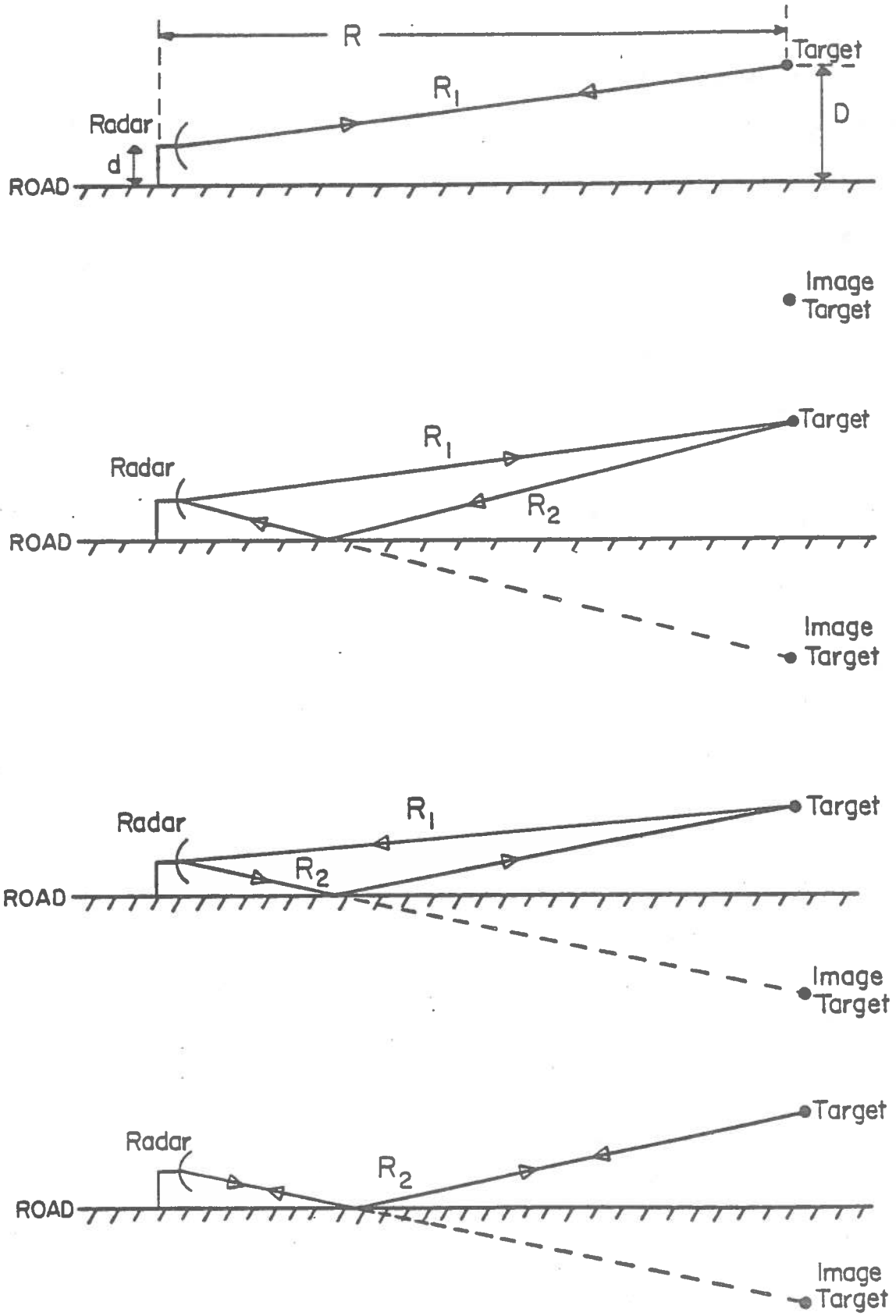

Figure 3.1.2: Direct and ground-reflected waves.

If the wavelength is small compared with the dimensions of the body, it gives the interesting result:

$$\sigma(\theta r,\theta t) = \sqrt{\sigma(\theta r)\cdot\sigma(\theta t)} \qquad (3.8)$$

Where: - θr is the angle to the receiver.

- θt is the angle to the transmitter.

- $\sigma(\theta r,\theta t)$ is the bistatic cross-section in the directions θr, θt.

- $\sigma(\theta r)$ is the monostatic cross-section in the direction θr.

- $\sigma(\theta t)$ is the monostatic cross-section in the direction θt.

The combination of the 3 cross-sections $\sigma 11$, $\sigma 22$, and $\sigma 12$ is performed using a modified version of equation 3.6, which takes into account the absorption and the phase shift of the ground-reflected wave. Assuming the absorption and phase shift due to the ground are represented by a complex coefficient $r=q\ \exp(j\Psi)$ (r will be studied in more details in CHAPTER 4), then the total cross-section becomes:

$$\sigma = \left| \sqrt{\sigma 11}\exp(j\Phi 1) + 2r\sqrt{\sigma 12}\exp j(\Phi 1+\Phi 2)/2 + r^2\sqrt{\sigma 22}\exp(j\Phi 2) \right|^2 \qquad (3.9)$$

3.2 FINAL COMPUTATION

Equation 3.9 can be easily transformed, and generalized to the case of a complex body composed of Np plates and Nw wires:

$$\sigma = \left| \sum_{k=1}^{N} \{ \sigma^{1/4}11(k) \exp(j\Phi 1(k)/2) + r\sigma^{1/4}22(k) \exp(j\Phi 2(k)/2) \} \right|^4 \qquad (3.10)$$

Where N=Np+Nw, and where the bistatic cross-section has been supressed, by use of equation 3.8.

Given the radar frequency, and the position of radar and target, the backscattering cross-section of the target can be computed. A block diagram of the computer program is included (figure 3.2.1). This program will be used as a subroutine in the final program computing the relative power returned to the radar, and the probability of detection of the target.

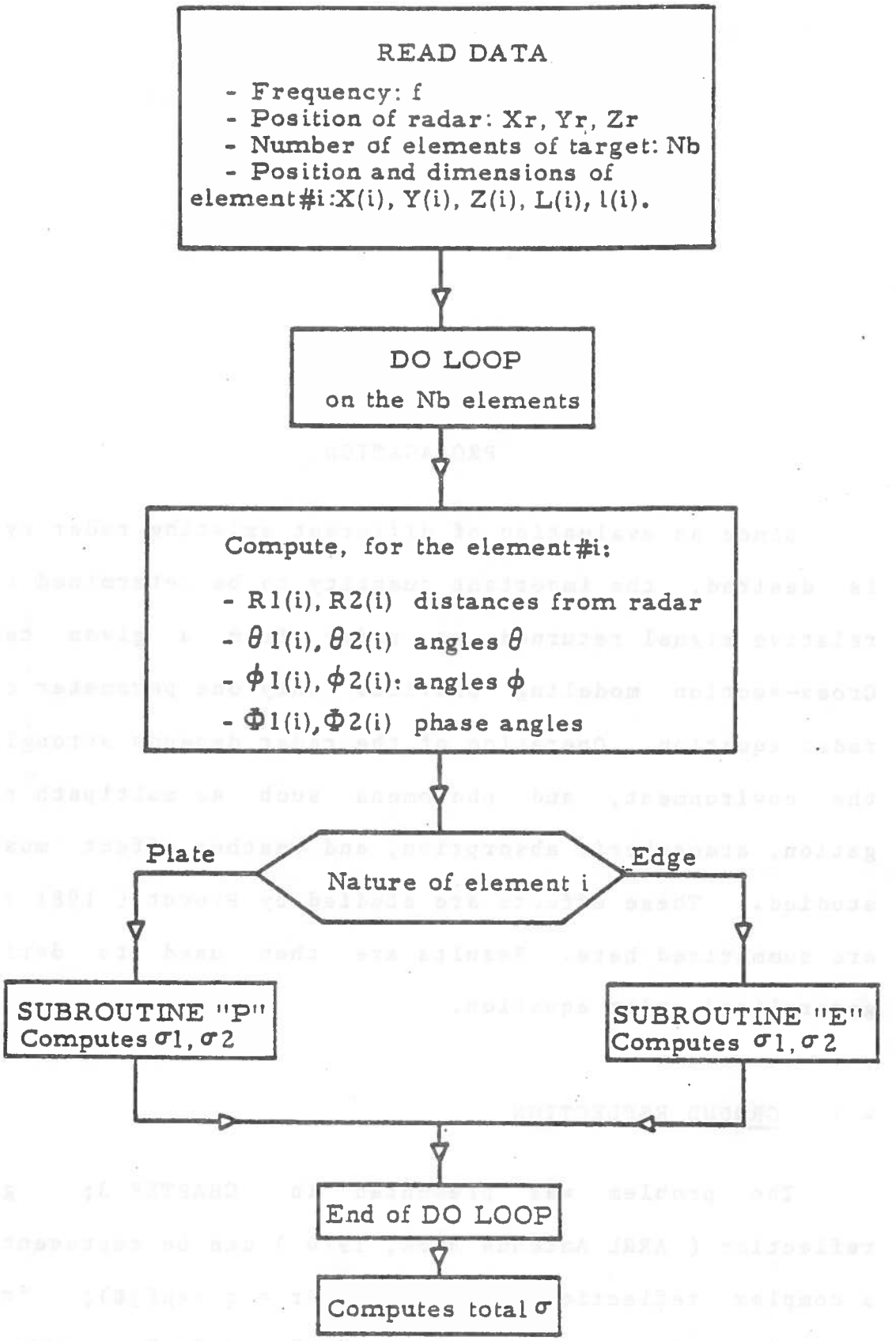

Figure 3.2.1: Cross-section computation.

CHAPTER 4

PROPAGATION

Since an evaluation of different existing radar systems is desired, the important quantity to be determined is the relative signal returned to radar from a given target. Cross-section modeling provides only one parameter of the radar equation. Operation of the radar depends strongly on the environment, and phenomena such as multipath propagation, atmospheric absorption, and weather effect must be studied. These effects are studied by Pruvot (1981), and are summarized here. Results are then used to derive a generalized radar equation.

4.1 GROUND REFLECTION

The problem was presented in CHAPTER 3; ground reflection (ARRL Antenna Book, 1974) can be represented by a complex reflection coefficient $r = q \exp(j\Psi)$; "r" is actually split into two terms: "rv" and "rh", respectively for the vertical and the horizontal components. This

reflection coefficient depends on frequency, angle of incidence, and nature of the reflecting surface (smooth or rough ground).

4.1.1 Perfectly Smooth Surface

"rv" and "rh" are computed as follow (Liao, 1980):

$$rh = \frac{\eta 2 \cdot \sec\theta t - \eta 1 \cdot \sec\theta i}{\eta 2 \cdot \sec\theta t + \eta 1 \cdot \sec\theta i}$$

$$rv = \frac{\eta 2 \cdot \cos\theta t - \eta 1 \cdot \cos\theta i}{\eta 2 \cdot \cos\theta t + \eta 1 \cdot \cos\theta i}$$

where: - $\eta 1 = \sqrt{(\mu o / \epsilon o)}$

- $\eta 2 = 1/\sqrt{\epsilon r}$
- θt=angle of transmitted wave.
- θi=angle of incident wave.

4.1.2 Rough Surface

The rough ground reflection coefficient "r" can be deduced from the smooth ground reflection coefficient "ro" (computed above) by the formula:

$$r = ro \cdot rs \qquad (4.3)$$

Where "rs" is a correcting factor accounting for the ground roughness, and related to β (grazing angle) and h (r.m.s. surface height variation above average level) by:

$$rs^2 = \exp -\frac{(4\pi h \cdot \sin\beta)^2}{\lambda^2} \qquad (4.4)$$

Typical values for "h" are:

Asphalt driveway: h = 0.040 cm

Asphalt parking lot: h = 0.044 cm

Rough asphalt road: h = 0.052 cm

4.1.3 Conclusion

It can be shown (Pruvot, 1981) that, in the case of a rough road, "r" does not significantly vary from 0° to 5°. Automotive Radar deals with grazing angles of typically 0° to 5°, therefore, only smooth surfaces are considered here (figures 4.1.1 and 4.1.2), and results concerning these surfaces (equations 4.1 and 4.2) are used in a subroutine to compute the reflection coefficient. This subroutine computes "r" as a function of polarization angle, angle of incidence, and frequency.

4.2 ATMOSPHERIC ATTENUATION

Except around 60 GHz (Oxygen absorption), the atmospheric attenuation is negligible (see figure 4.2.1). At 60 GHz, the absorption loss is 15 dB per kilometer; maximum range in Automotive Radar is about 100 meters, corresponding to a total attenuation of 2x1.5 = 3 dB, which is a still acceptable figure in radar system.

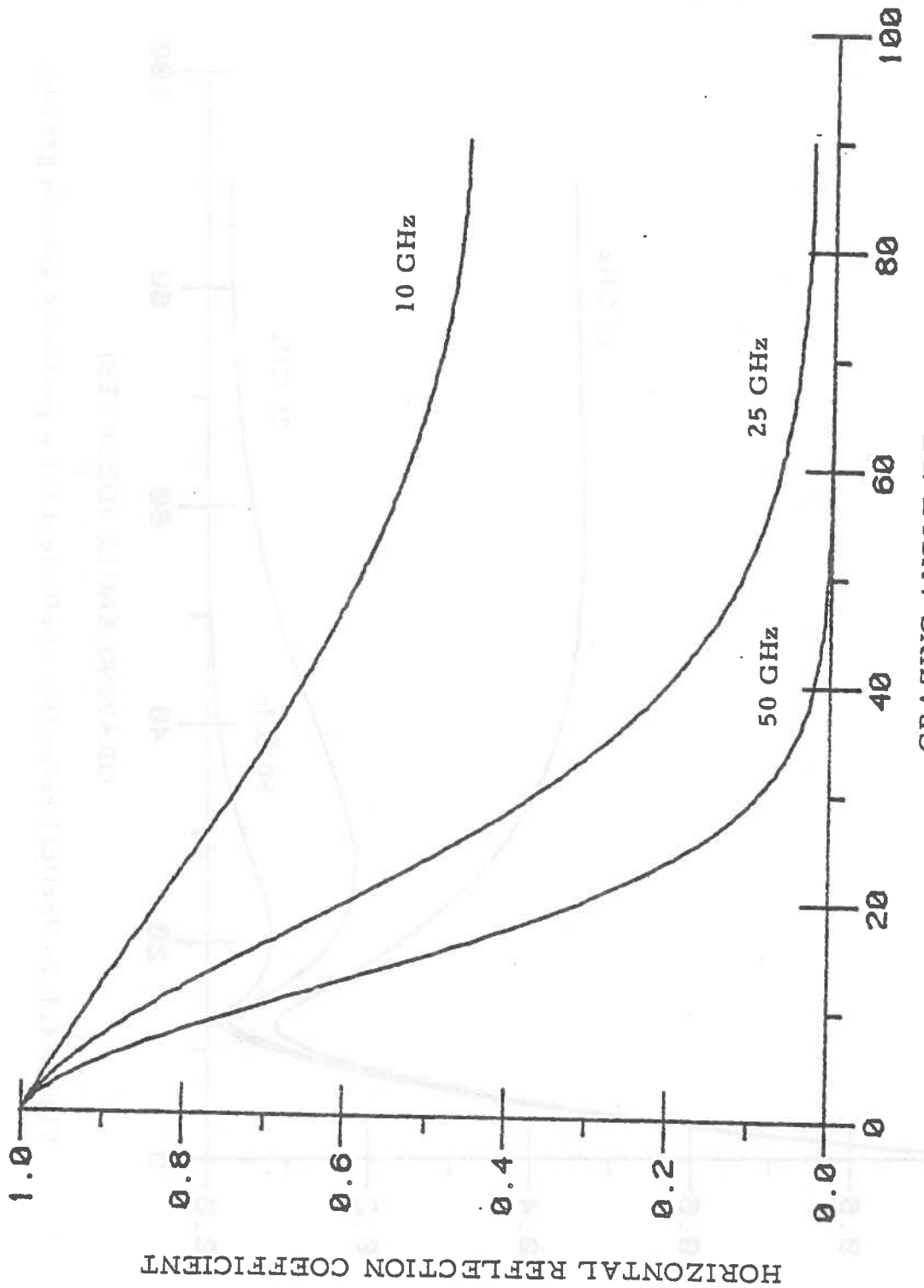

Figure 4.1.1: Horizontal reflection coefficient for a perfectly smooth ground.

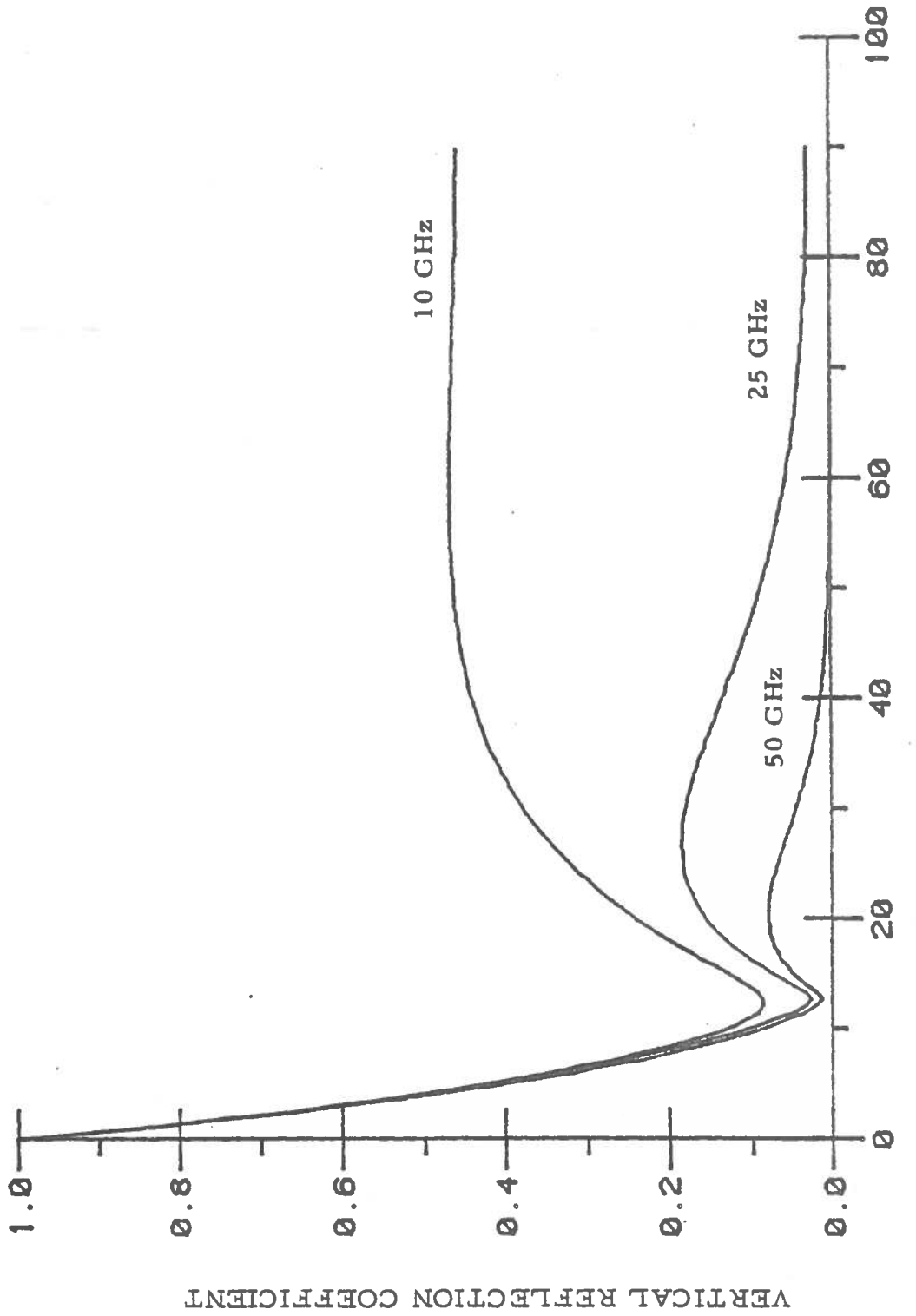

Figure 4.1.2: Vertical reflection coefficient for a perfectly smooth ground.

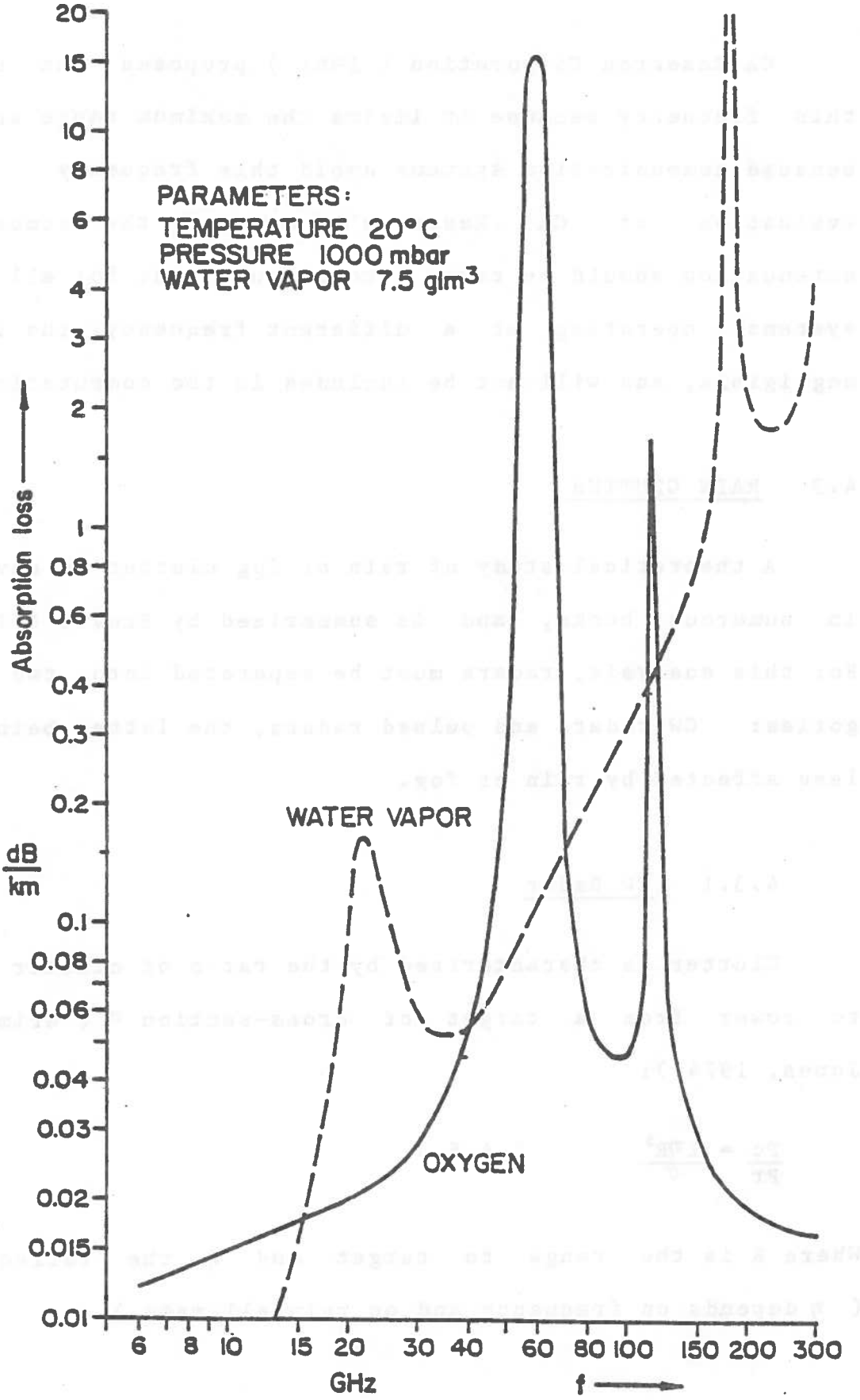

Figure 4.2.1: Atmospheric absorption.

CA Research Corporation (1981) proposes the use of this frequency because it limits the maximum range and also because communication systems avoid this frequency. In an evaluation of CA Research's system, the atmospheric attenuation should be taken into account, but for all other systems, operating at a different frequency, the loss is negligible, and will not be included in the computation.

4.3 RAIN CLUTTER

A theoretical study of rain or fog clutter is developed in numerous books, and is summarized by Pruvot (1981). For this analysis, radars must be separated into two categories: CW radars and pulsed radars, the latter being much less affected by rain or fog.

4.3.1 CW Radar

Clutter is characterized by the ratio of clutter power to power from a target of cross-section σ (Grimes and Jones, 1974):

$$\frac{Pc}{Pr} = \frac{2\eta R^3}{\sigma} \qquad (4.5)$$

Where R is the range to target and η the reflectivity (η depends on frequency and on rainfall rate).

4.3.2 Pulsed Radar

The time-averaged return from rain clutter is:

$$\frac{Pc}{Pr} = \frac{Ae \cdot L \cdot \eta}{32R^2} \qquad (4.6)$$

Where Ae is the effective antenna aperture, and L is the pulse duration.

4.3.3 Model

If the rain clutter effect is to be included in the general computation, it must be represented by the same model for CW and for pulsed radars; a simple way to accomplish this is to account for this effect in terms of noise added to the returned signal. From NHTSA's Report (1976), and from Raff (1977), the following expressions can be derived:

- For CW Radars:

$$Nrel = \frac{\lambda \cdot \eta}{16} \left[1 + Ln\left(\frac{4}{\pi B}\right)\right] \qquad (4.7)$$

Where: Nrel is the relative noise

λ is the wavelength

η is the reflectivity

B is the beamwidth

- For Pulsed Radars

$$Nrel = \frac{(\lambda^2 \cdot G^2)}{(4\pi)^3} \frac{(\pi \cdot B^2)}{4} \frac{(\eta \cdot c \cdot t)}{Rt^2} \qquad (4.8)$$

Where: G is the antenna gain

t is the pulse width

c is the speed of light

Rt is the range to target

From either theory or from experimental measurements, η can be determined for any frequency and rainfall rate. Therefore, it is possible, for any configuration, to compute the relative clutter noise, and to add it to the relative signal. Noise added by rain clutter is in general negligible for pulsed radars, but for CW radars, it can result in false alarms or in masking of small targets.

It was observed that when operating CW radar during heavy rainfall, false alarms often occurred: clutter noise computed with equation 4.7 was added to the relative signal in the simulation. However, no masking effect was observed, for two reasons: first, the two models (target and clutter noise) give good relative results, but do not fit well together; as discussed in CHAPTER 3, cross-section fluctuations are well-represented by the simulation, in terms of relative variations. Secondly, adding the two signals together (rain clutter and return from target) does not account for constructive and destructive interferences; hence, target masking by rain clutter cannot be observed in this simulation (relative phase of return from target and of noise should be determined, and then the two signals should be combined together).

Nevertheless, from simple considerations and from experience, it can be qualitatively stated that:

Rain clutter is generally a problem for CW radars, but it can be minimized by the use of circular polarization, and bistatic antennas.

For pulsed radars, the use of very short pulses ensures very good operation in almost any kind of weather.

4.4 GENERALIZED RADAR EQUATION

The simple model presented in CHAPTER 3 gave the total cross-section of a given target, with ground reflected waves. The next problem is to make a link with the antenna characteristics and with the propagating medium properties, to derive a generalized radar equation giving the relative power.

Differentiation between direct and ground-reflected waves yields the following expression:

$$Srel = \frac{\lambda^2}{(4\pi)^3} \left| A \cdot \exp(2j\Phi 1) + r \cdot B \cdot \exp j(\Phi 1 + \Phi 2) + r^2 \cdot C \cdot \exp(2j\Phi 2) \right|^2 \qquad (4.9)$$

Where: $A = (G1 \cdot \sqrt{\sigma 11}) / R1^2$

$B = (\sqrt{G1 \cdot G2 \cdot \sigma 12}) / R1 \cdot R2$

$C = (G2 \cdot \sqrt{\sigma 22}) / R2^2$

Using equation 3.8, and generalizing equation 4.9 to the case of a complex target composed of N elements gives:

$$Srel = \frac{\lambda^2}{(4\pi)^3} \left| \sum_{k=1}^{N} \left[A1(k) \cdot \exp[j\Phi 1(k)] + r \cdot A2(k) \cdot \exp[j\Phi 2(k)] \right] \right|^4 \qquad (4.10)$$

Where:

$$A1(k) = \frac{[G1(k)]^{1/2} \cdot [\ 11(k)]^{1/4}}{R1(k)}$$

$$A2(k) = \frac{[G2(k)]^{1/2} \cdot [\ 22(k)]^{1/4}}{R2(k)}$$

Subscript 1 refers to the direct wave and subscript 2 refers to the ground-reflected wave; the index "k" represents the element # k of the complex target. The phase factors $\Phi 1$ and $\Phi 2$ are, respectively, equal to $(2\pi R1)/\lambda$ and $(2\pi R2)/\lambda$; it is important to differentiate between G1 (gain in the direction of the target) and G2 (gain in the direction of the "image-target"), for the gain varies quite quickly with the angle of observation, and a difference of 1° can make a difference of several dB in power.

It must be emphasized that the ground reflection coefficient "r" actually depends on the index k, for "r" depends on the angle of incidence of the wave, and therefore on the position of the target element which is considered. Consequently, "r" must be computed every time the contribution of another element is being considered, and also, of course, every time the target moves.

The attenuation due to atmospheric losses, which appeared to be negligible for the ranges considered, can easily be added to equation 4.10. It takes the form $\exp(-2 \cdot a \cdot R)$, where "a" is the one-way attenuation in neper per meter, and R is the range to target in meters.

CHAPTER 5

TARGET DETECTION

5.1 DEFINITION OF PARAMETERS

5.1.1 Range Cut-Off: "RCO"

In most of the systems, a Range Cut-Off "RCO" is defined, so that no target beyond this range can be detected by radar. It is the easiest way to reduce the number of false alarms, by suppressing the echos from large remote obstacles.

A velocity-dependent Range Cut-Off can easily be set for pulse radar, by varying the pulse modulation frequency with the carrier vehicle velocity. It is also an attractive way to account for the increase of safe stopping distance with increasing velocity.

Some systems provide a modified Range Cut-Off on curves: radar detection on curves is limited to a shorter distance, depending on the steering wheel angle. This should be effective in preventing detection of guardrails or trees on the roadside.

5.1.2 Detection Threshold: "Sth"

Basically, a target is detected when the signal returned to radar exceeds a certain threshold, which needs to be defined. This threshold can either be constant, or depend upon several parameters, such as carrier velocity, steering wheel angle, weather conditions (fog). A velocity-dependent threshold allows earlier detection of targets at high speeds, hence increasing collision avoidance efficiency. On the other hand, steering wheel angle dependence seems inappropriate: range detection must be shortened on curves, to avoid detection of sideroad obstacles, but capacity of detection must remain the same in the vicinity of the carrier vehicle.

5.1.3 Radar Delay: "Tdel" or "Rdel"

A radar delay is set to avoid detection of short peaks of noise. Once the detection threshold "Sth" defined above is exceeded, there is acquisition of the target; detection of the target occurs only if the returned signal remains above the threshold during a certain period of time "Tdel".

This period of time can be defined either as a constant or as the time necessary for the carrier vehicle to cover a fixed distance "Rdel". In the first case, the parameter is called Radar Time Delay, noted "Tdel", while in the second case it is called Radar Range Delay, and noted "Rdel".

A Radar Time Delay is in general more efficient at low speeds than at high speeds, because the distance covered between the processes "acquisition" and "detection" increases with velocity. Nevertheless, it still gives fairly good results up to 60 or 70 mph, lowers the false alarm rate, and is simple to generate.

5.1.4 Activation Time: "Tact"

It is a time delay corresponding to the method of activating brakes; if brakes are automatically applied, it can be quite short, and even negligible; if brakes are manually applied, as in the German system (the driver himself, warned by an alarm, activates the brakes), then this delay can be much longer, and an average value must be chosen as the mean driver reaction time.

5.1.5 Braking Deceleration: "Brd"

This depends mainly on the driving conditions: "Brd" can vary from 0.15g (g ≈ 9.81 m/sec) for an icy road, to 0.7g for a dry road. An anti-lock system can significantly improve the braking efficiency (+15%) on icy roads, but

not on dry roads. Nevertheless, an anti-lock system offers vehicle stability, which is a major accident prevention factor, and it is recommended by NHTSA that all test vehicles be equipped with four-wheel anti-lock.

5.1.6 Radar Control Law: "RCL"

Assuming a target has been acquired and detected, it must be determined whether the brakes are to be activated or not. An algorithm is used to compute the minimum safe distance and to decide if the target is hazardous. It can involve various parameters, in particular range and range rate (relative velocity), but also braking deceleration and carrier vehicle velocity.

As soon as the target has been detected, this Radar Control Law is checked, and an alarm is set (optionally brakes are applied) if the target is hazardous.

A more elaborate algorithm can be used, involving the target "past life", and predicting its trajectory. A microprocessor can memorize the location of a few targets at several instants, and determine whether any of these targets is on a collision trajectory; it could also possibly memorize the signature of certain well-known false targets, such as guardrails or bridges, and compare the signal to these signatures. Non-hazardous targets could be partly eliminated this way, so it would significantly reduce the number of false alarms.

5.2 RANDOM VARIATION OF CROSS-SECTIONS

5.2.1 Probability of Detection

The cross-section of a complex body, such as a car, fluctuates very quickly with time, so the target modeling, using flat plates (described in CHAPTER 3) actually gives an average value. These fluctuations are well-represented by a Rayleigh density function f (Skolnik, 1962).

$$f(\sigma) = \frac{1}{\sigma_{av}} \exp\left[-\frac{\sigma}{\sigma_{av}}\right] \qquad (5.1)$$

The relative power "Srel", computed by the program, is proportional to σ, therefore the probability density function for the returned signal "S" is also a Rayleigh function:

$$f(S) = \frac{1}{Sav} \exp\left[-\frac{S}{Sav}\right] \qquad (5.2)$$

Where "Sav" is the average relative signal computed by the program.

Then the probability of detecting the target at the instant t is:

$$p\{Srel > Sth\} = \int_{Sth}^{\infty} \frac{1}{Sav} \exp\left[-\frac{Srel}{Sav}\right] \cdot dSrel \qquad (5.3)$$

This gives the final result:

$$p\{Srel > Sth\} = \exp\left[\frac{-Sth}{Sav}\right] \qquad (5.4)$$

This shows that an important error would be made if it was assumed that the target is detected as soon as Sav=Sth (when Sav=Sth, the target has a probability of being detected p = 0.36).

5.2.2 Cumulative Probability of Detection

Given that a target at a range R has a probability of being detected p(R) as computed above, the problem now is to determine its probability of being detected at or before R; it will be noted "P", and called "Cumulative Probability of Detection".

In the program used for this simulation, the relative signal "S" is computed at discrete ranges "Rk", where "Rl" is the Range Cut-Off. Assuming the events are independent (Larsen and Shubert, 1979), the probability of not being detected at or before Rk is:

$$Q(Rk) = 1 - P(Rk) = \prod_{k}\left[1 - p(Rk)\right] \qquad (5.5)$$

This gives:

$$P(Rk) = 1 - \prod_{k}\left[1 - p(Rk)\right] \qquad (5.6)$$

Q(Rk) is related to Q(Rk-1) by the relation:

$$Q(Rk) = Q(Rk-1) \cdot \left[1 - p(Rk) \right] \qquad (5.7)$$

Hence, the final result is:

$$P(Rk) = P(Rk-1) + \left[1 - P(Rk-1) \right] \cdot p(Rk) \qquad (5.8)$$

This relationship will be used in the program to compute the cumulative probability of detection at range Rk. Then, it will be assumed that detection occurs at a range Rn where $P(Rn-1) < 0.99$ and $P(Rn) > 0.99$.

The assumption concerning the independence of the events is true if the difference (Rk - Rk-1) is greater than the average target correlation distance, which is very difficult to evaluate. However, computations are performed at every meter, which seems a reasonable correlation distance.

CHAPTER 6

PROGRAM DESCRIPTION

6.1 GENERAL INPUT

General information is entered directly into the program by the user. It consists of: Frequency, Velocity of Carrier Vehicle, Polarization (Horizontal, Vertical, or 45°), Reference Number of Target (each target characteristics are stored into a file), and Detection Process Characteristics (Range Cut-Off, Detection Threshold, Radar Delay, Activation Time).

6.2 ANTENNA GAIN

A first model was used, as described below:

- $G = G_{max} \left(1 - \frac{|\theta|^2}{3} \right)$ if $-3° < \theta < 3°$ (θ in degrees)

- $G = 0$ otherwise

This parabolic model gave fairly good results, but no side-lobes were included. A more complex model, summarized in CHAPTER 2, solved the problem. Gain is stored into a file, for $\phi = 0^\circ$ and $\phi = 90^\circ$, and for θ varying from 0° to 40°, every 0.5°. For angles θ greater than 40°, the gain is very small, so it will be supposed constant from 40° to 90°. Gain in a given direction (θ,ϕ) is approximated elliptically in ϕ, and linearly in θ:

Approximation in θ:

$$\Big[G(\theta) - G(\theta i-1)\Big]\cdot\Big[\theta i - \theta i-1\Big] = \Big[G(\theta i) - G(\theta i-1)\Big]\cdot\Big[\theta - \theta i-1\Big] \qquad (6.1)$$

Approximation in ϕ:

$$G^2(\phi)\cdot\left[\frac{\cos^2\phi}{G^2(0)} + \frac{\sin^2\phi}{G^2(90)}\right] = 1 \qquad (6.2)$$

This is computed in a separate subroutine.

6.3 TARGET DESCRIPTION

The characteristics of a target are stored into a file; necessary information is: location of target, velocity of target, and description of all its elements (plates and edges).

General information is displayed on the first line of the corresponding file, under the form:

JTRGT, JPLT, XTRGT, YTRGT, ZTRGT, VXTRGT, VYTRGT

Where:

- JTRGT is an integer in the range 1 to 60, representing the number of elements (plates and edges) of the target.

- JPLT is an integer in the range 1 to JTRGT, representing the number of plates composing the target (then (JTRGT-JPLT) is the number of edges).

- XTRGT, YTRGT, ZTRGT are the coordinates of the center of the target.

- VXTRGT, VYTRGT are the components of the velocity of the target on the x and y-axes of the same coordinate system. Vertical motion is not considered.

Each following line of the file represents the characteristics of each element (plate or edge) of the target. Therefore, there are JPLT lines for the plates, and (JTRGT-JPLT) lines for the edges; this makes a total of JTRGT lines. Each line is composed of 11 values:

GL,SL,XN,YN,ZN,XGL,YGL,ZGL,XC,YC,ZC

6.3.1 Plate Description

- "GL" is the length of the plate.

- "SL" is the width of the plate.

- "XN,YN,ZN" are the components of a vector N normal to the plate.

- "XGL,YGL,ZGL" are the components of a vector GL parallel to the long edge of the plate.

- "XC,YC,ZC" are the coordinates of the center of the

plate.

It must be emphasized that the vector N, normal to the plate, represents its orientation with respect to radar, so if N points toward radar, the plate is visible, otherwise it is not (see figure 6.3.1). This accounts for the shadowing effect.

6.3.2 Edge Description

- "GL" is the length of the edge.
- "SL" is a value defining the "angle of blindness" of the edge (explained below).
- "XN,YN,ZN" is a vector N defining the orientation of the edge (explained below).
- "XGL,YGL,ZGL" is a vector GL parallel to the edge.
- "XC,YC,ZC" are the coordinates of the middle of the edge.

Explanation: depending on the target orientation, an edge can be masked by a plate; to eliminate the masked edge contributions, the following method is used:

Let U be a vector representing the direction of the target (see figure 6.3.2). If the angle Ψ defined by the vectors N and U is greater than the angle "SN", then the edge is visible.

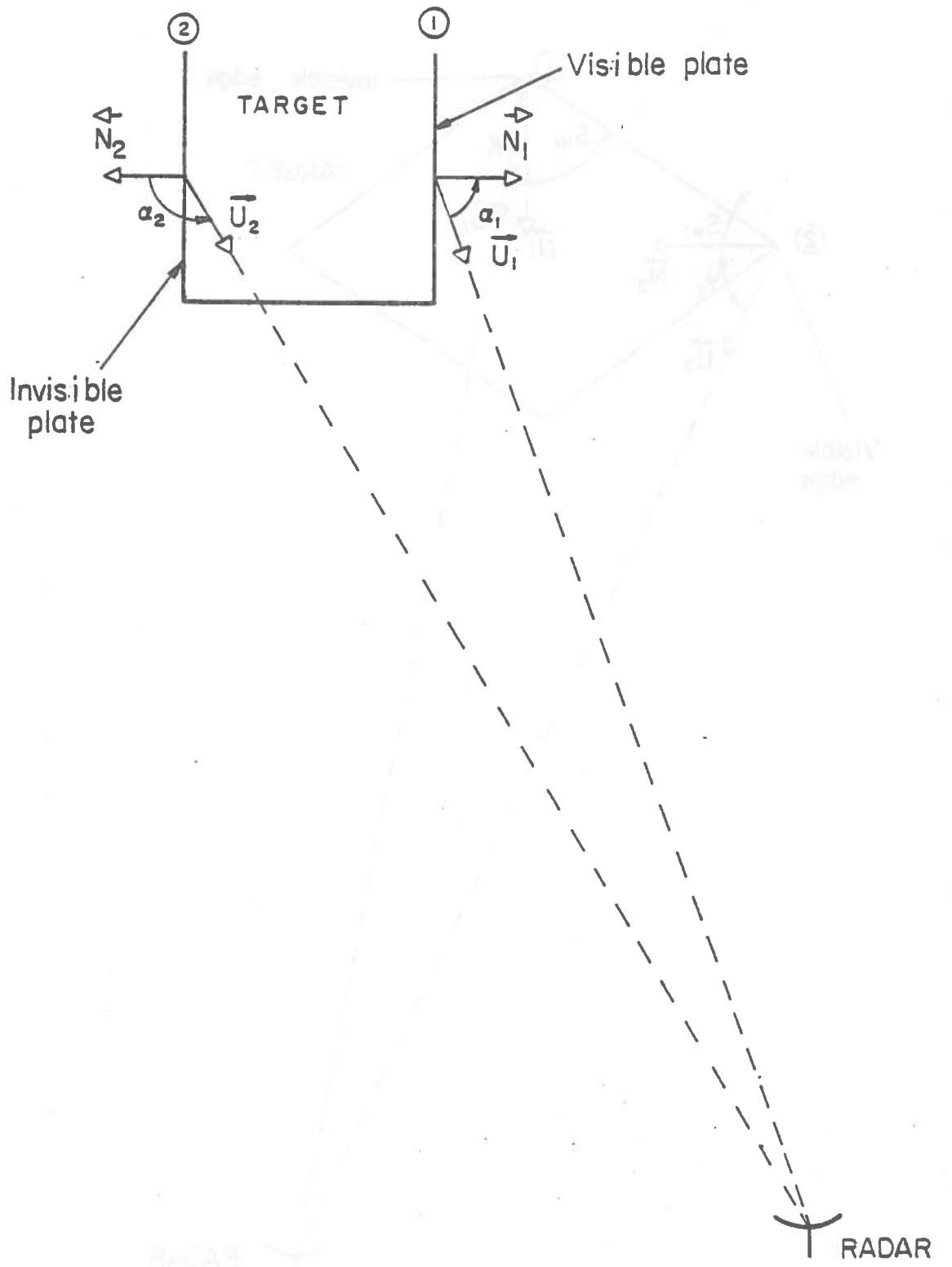

Figure 6.3.1: Geometry for the blinding of the plates.

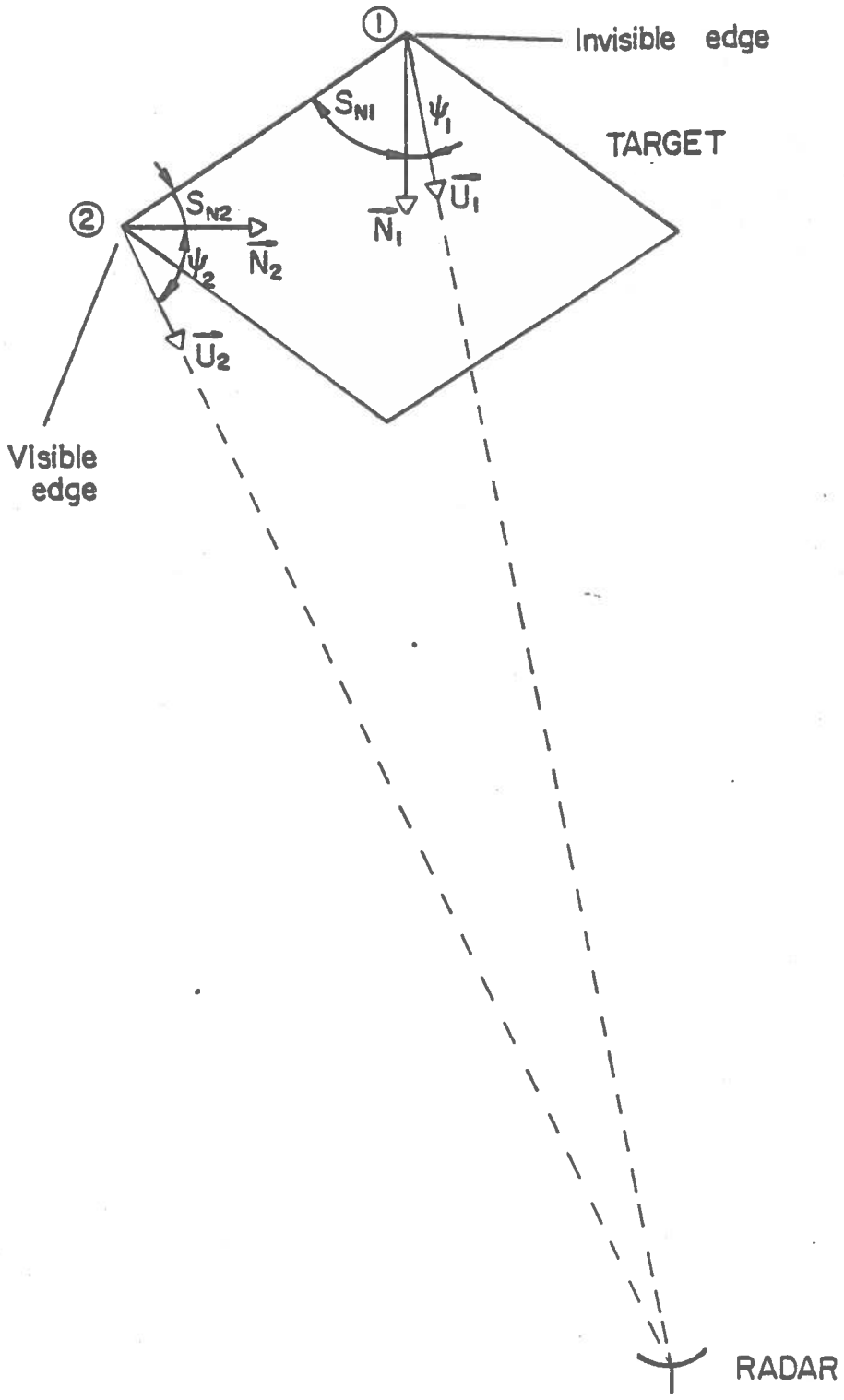

Figure 6.3.2: Geometry for the blinding of the edges.

6.4 COMPUTATION

6.4.1 Principle

Computation starts at time t=0; radar position is defined by: Xr=0, Yr=0, Zr=0.5 (in unit of meters); target position is as described in the corresponding file.

The desired output: distance radar-target "Dist", relative power "Srel", detection threshold "Sth", and cumulative probability of detection "P" are computed at discrete instants T0, T1, T2..., so that T0=0 and Ti+1 - Ti = ΔT. This interval of time ΔT is defined so that the carrier vehicle covers a distance of one meter between two consecutive calculations (i.e. $\Delta T = 1/Vcar$, which prohibits negative velocities). After each computation, target and radar are repositioned, according to their relative velocities, and a new computation is performed. This process ends either after 300 iterations have been performed, corresponding to 300 meters covered by the carrier vehicle, or after the target has moved behind the radar, thus becoming invisible.

6.4.2 Output

1) Distance to Target "Dist": given the coordinates of target and radar, "Dist" is easily computed:

$$Dist = \sqrt{(Xr-Xt)^2 + (Yr-Yt)^2 + (Zr-Zt)^2} \qquad (6.3)$$

2) Relative Signal "Srel": it is computed using the generalized radar equation described in CHAPTER 5; returns from each target element are combined with an appropriate phase factor, and ground reflection is accounted for.

3) Detection Threshold "Sth": its definition depends on the system considered; generally, it is a function of antenna gain in the main direction, carrier vehicle velocity, and possibly range to target and relative velocity (German system).

4) Cumulative Probability "P": as presented in CHAPTER 5, it is a function of relative signal "Srel" and threshold "Sth", but also of the entire target past life; therefore, it needs to be computed at every iteration, memorized, and used to compute the next cumulative probability of detection. If the index "i" represents iteration number, then the cumulative probability of detection at iteration # i can be written:

$$P = f\left\{ Srel(i), Sth(i), P(i-1) \right\} \qquad (6.4)$$

This is a very important concept, because it is the only realistic way to define any event, such as "detection", or "false alarm". A flow-chart of the main program is included (figure 6.4.1).

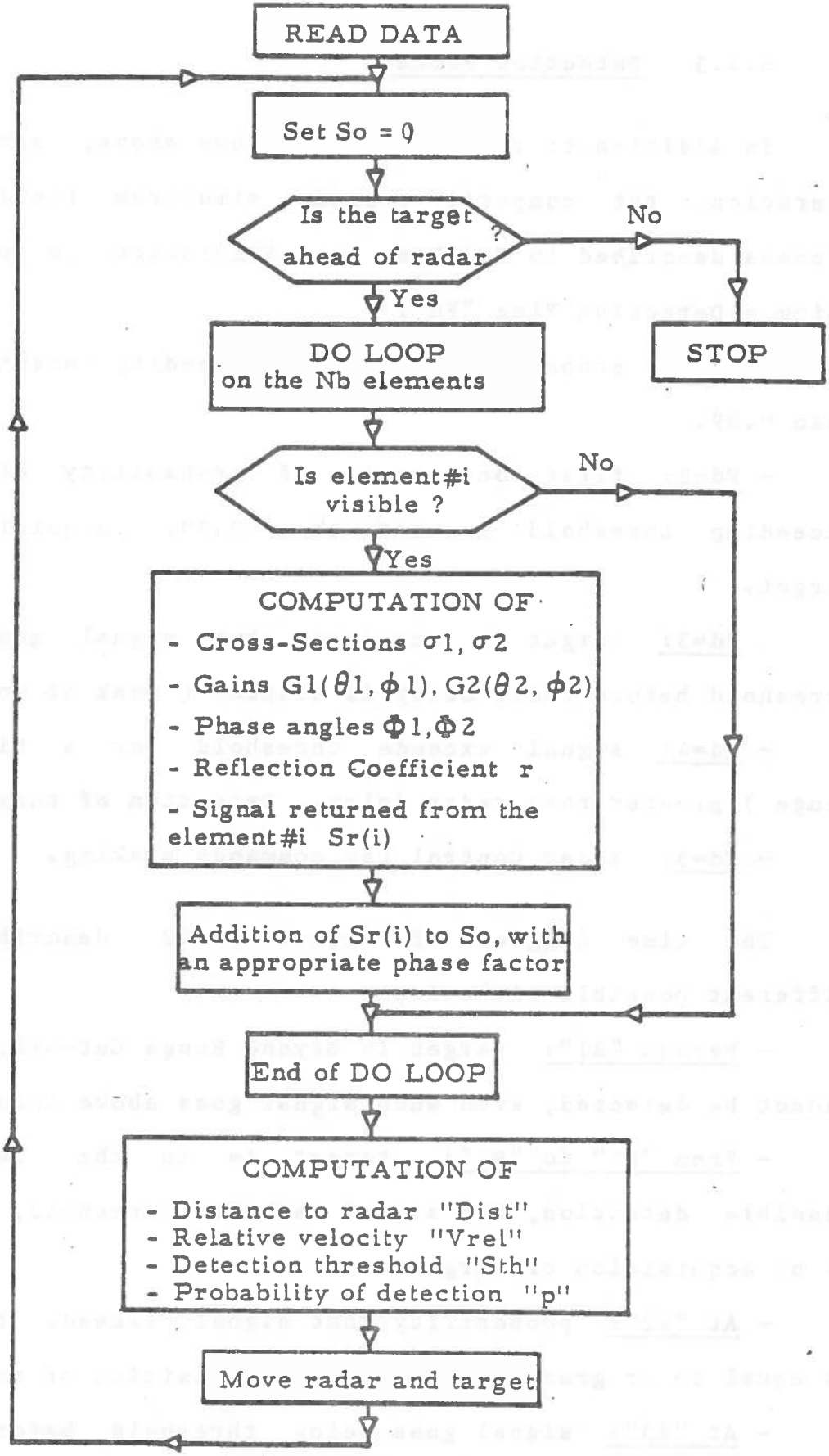

Figure 6.4.1: Flow-chart of the main program.

6.4.3 Detection Process

In addition to the output described above, after each iteration, the computer program simulates the detection process described in CHAPTER 5. Simulation is performed using a Detection Flag "Fd":

- Fd=1: probability of signal exceeding threshold less than 0.99.

- Fd=2: first occurrence of probability of signal exceeding threshold greater than 0.99. Acquisition of target.

- Fd=3: target is acquired, but signal goes below threshold before radar delay is elapsed (peak of noise).

- Fd=4: signal exceeds threshold for a time (or range) greater than radar delay. Detection of target.

- Fd=5: Radar Control Law commands braking.

The time diagram of figure 6.4.2 describes the different possible situations:

- Beyond "R1": target is beyond Range Cut-Off, so it cannot be detected, even when signal goes above threshold.

- From "R1" to "R2": target is in the range of possible detection, but signal is below threshold, so there is no acquisition of target.

- At "R2": probability that signal exceeds threshold is equal to or greater than 0.99. Acquisition of target.

- At "R3": signal goes below threshold before radar delay is elapsed, so target is not detected.

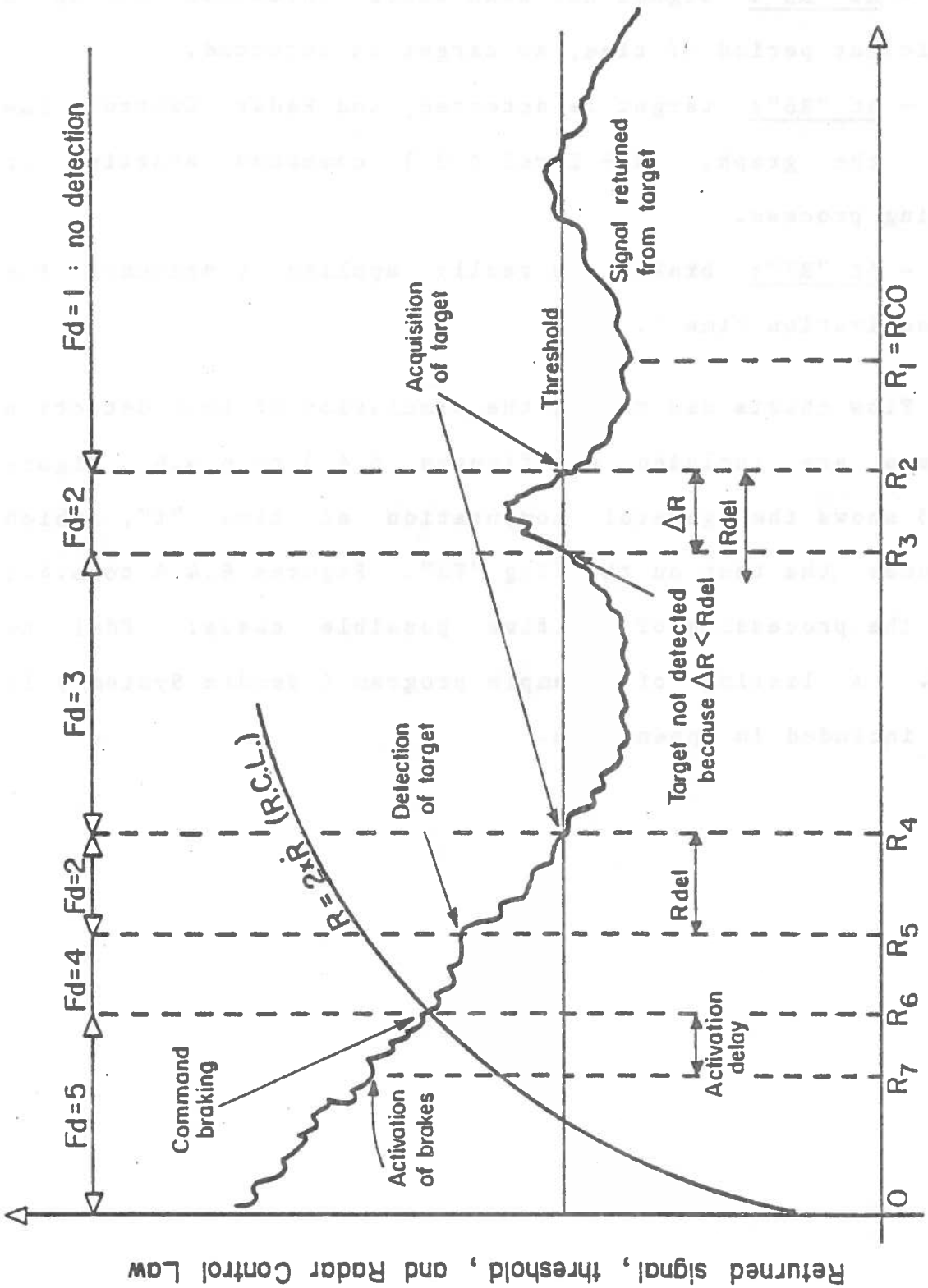

Figure 6.4.2: Sample time-diagram of the detection process.

- At "R4": same as at "R2": acquisition of target.

- At "R5": signal has been above threshold during a sufficient period of time, so target is detected.

- At "R6": target is detected, and Radar Control Law (on the graph: $R + 2Vrel < 0$) commands starting of braking process.

- At "R7": brakes are really applied (accounts for the activation time).

Flow charts describing the simulation of this detection process are included on figures 6.4.3 to 6.4.6. Figure 6.4.3 shows the general computation at time "t", which includes the test on the flag "Fd". Figures 6.4.4 to 6.4.6 show the processing of the five possible cases: Fd=1 to Fd=5. A listing of a sample program (Bendix System) is also included in Appendix B.

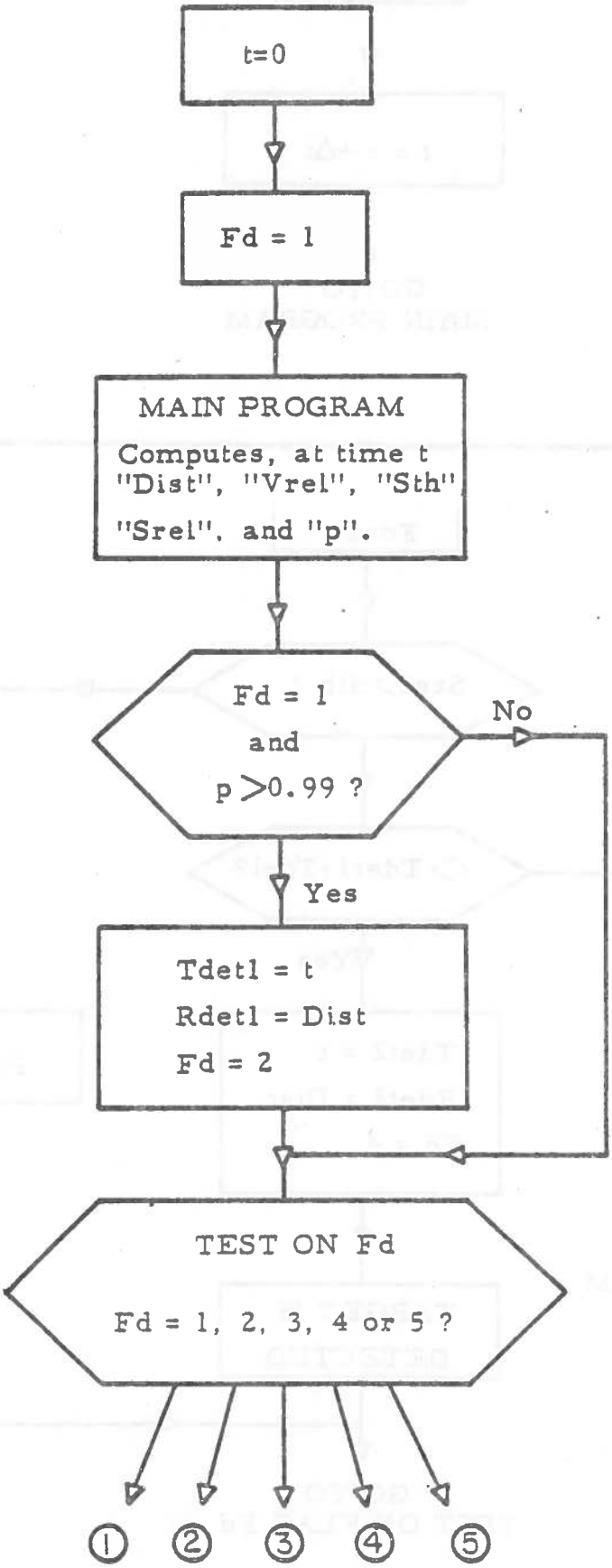

Figure 6.4.3: Detection flags.

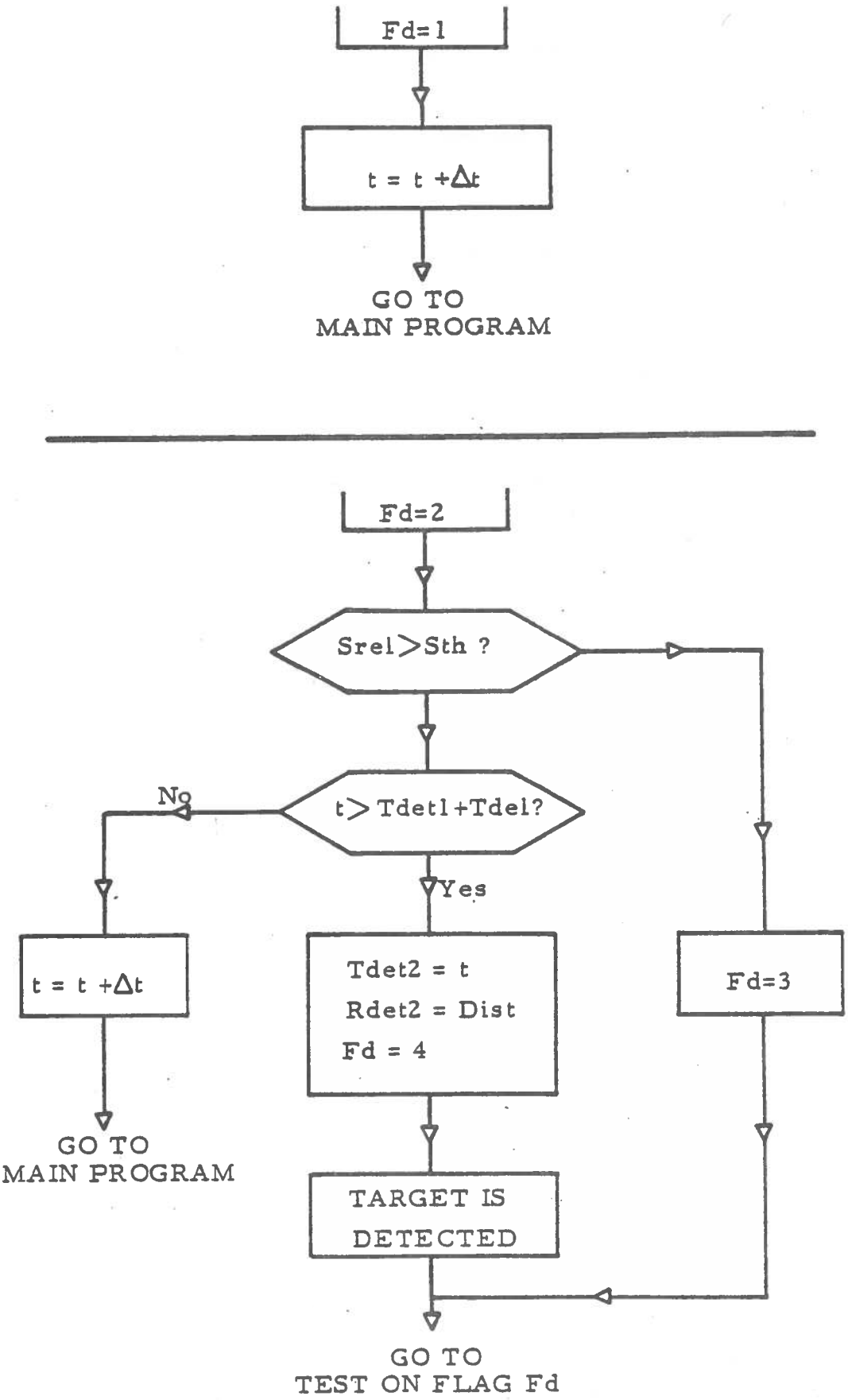

Figure 6.4.4: Detection flags 1 and 2.

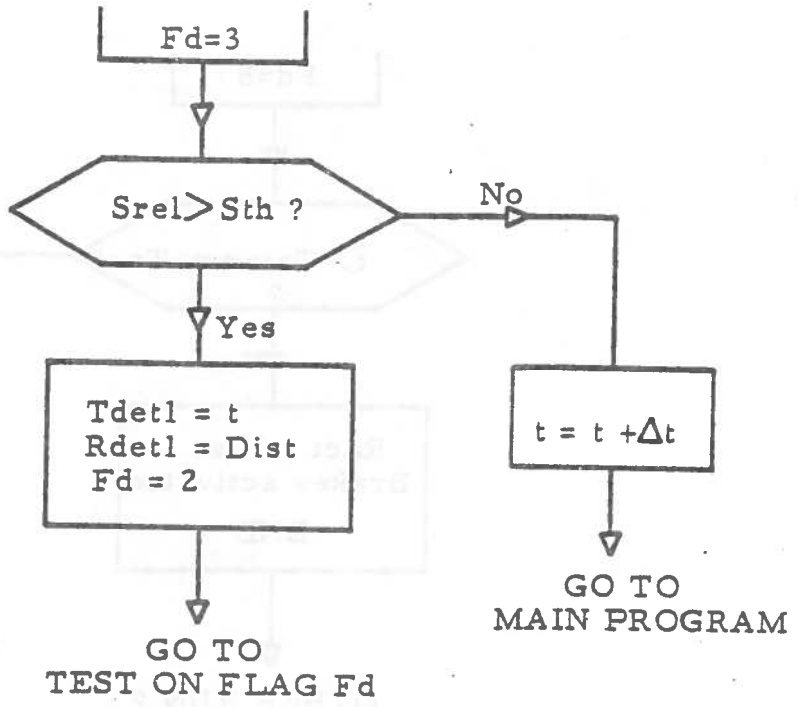

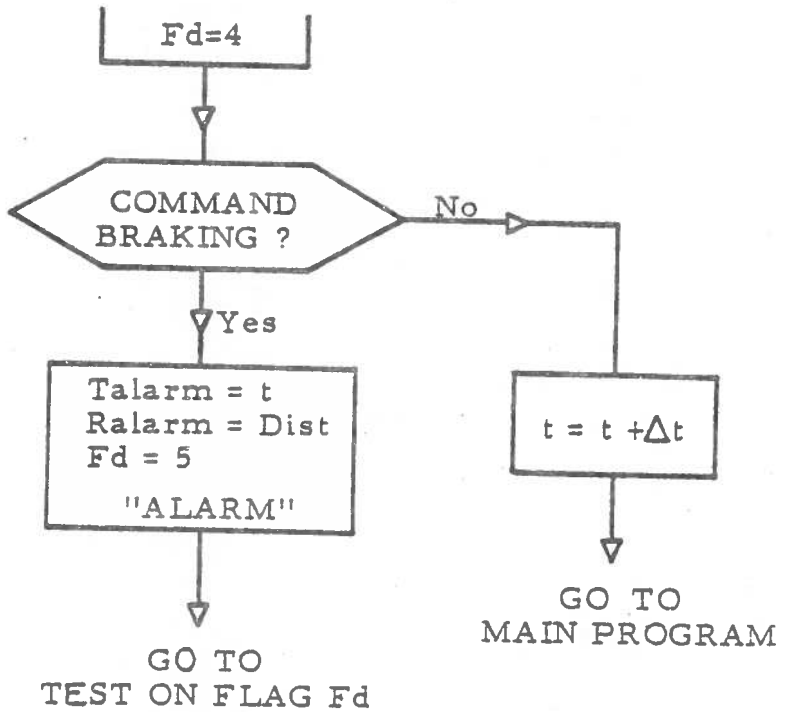

Figure 6.4.5: Detection flags 3 and 4.

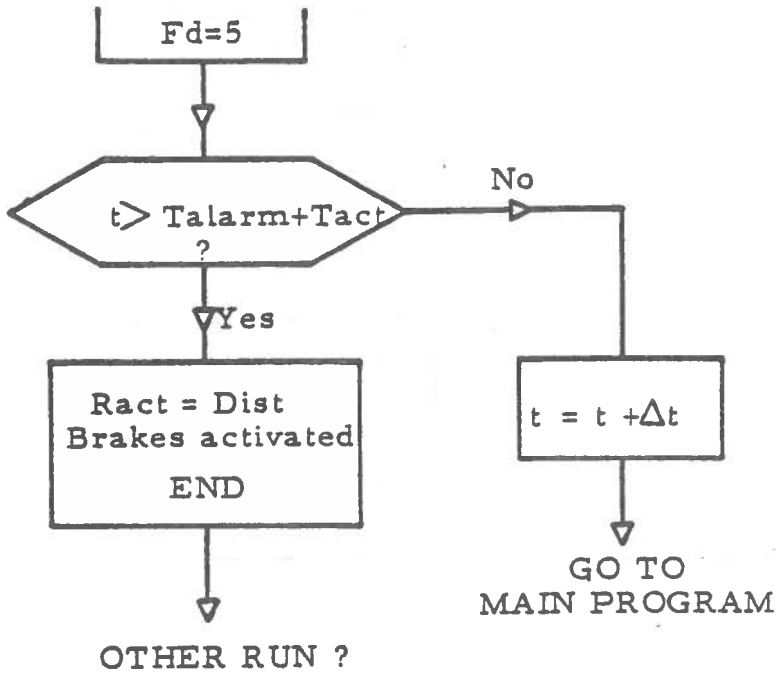

Figure 6.4.6: Detection flag 5.

CHAPTER 7

EVALUATION OF SYSTEMS

7.1 PRESENTATION

7.1.1 Test Conditions

The characteristics of seven existing systems are presented in table 1; because of the time involved and the difficulty getting information from the companies, only two of them are studied here. The evaluation consists of a simulation of radar response in the following situations:

- Situation # 1: sign on the side of the road (figure 7.1.2).

- Situation # 2: car in left lane, running at Vt=2 m/sec (figure 7.1.2).

- Situation # 3: car crossing ahead, running at Vt=3 m/sec (figure 7.1.3).

- Situation # 4: car crossing from left lane (figure 7.1.4).

- Situation # 5: car fixed ahead (figure 7.1.5).

Table 1: Systems characteristics.

System	Nissan-Mitsubishi	Daimler-Benz-SEL	Bosch	Bendix	BMW-VDO	RCA	Fujitsu-Toyota
Principle	Pul.Dop.	FM-CW	Pulse	Diplex	Pulse	FM-CW	FM-CW
Range	5-100m	10-100m	5-120m	30-75m	5-120m	6-30m	-
Accuracy	± 1 m	± 2.5 m	± 1 m		± 1 m	± 0.2 m	-
Rel.Speed	128 km/h	160 km/h	150 km/h		130 km/h	60 km/h	-
Accuracy	± 1km/h	± 2.5km/h	± 3.6km/h			± 2.5km/h	-
Antenna							
# & Type	1 parab.	2 parab.	2 parab.	1 parab.	2 parab.	2,printed	-
Beamwidth	H3.5,V4.5	H2.5,V3.5	H2.5,V4	H2.5,V4	H2.5,V4	H3,V5	-
Polar.	45°	V	V	45°	V	45°	-
Tx and Rx							
Main Osc.	Gunn	Gunn	Gunn	Gunn	Gunn	Gunn	Gunn
Frequency	24.14 GHz	35 GHz	35.6 GHz	36 GHz	35 GHz	17.5 GHz	50 GHz
Out Power	30 mW	30 mW	0.2 mW	25 mW	200 mW	20 mW	-
Pul.Width	20 ns	-	30 ns	730 ns	30 ns	-	-
Receiver	sup.het.	homodyne	sup.het.	homodyne	sup.het.	homodyne	-
Logics							
Algorithm	R > a·V/2 +b·V1	R > a·V/2 +b·V1	R > a·V/2 +b·V1	R + 2Ṙ>0	R > a·V/2 +b·V1	R > a·V +b·V1	-
Steer.w.a.	yes	yes	yes	yes	yes	yes	-

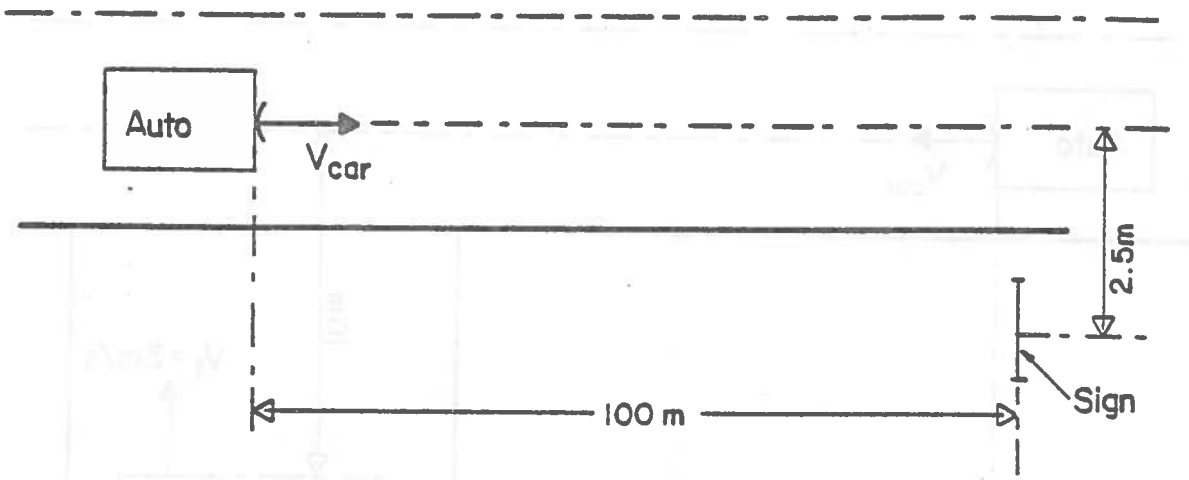

Figure 7.1.1 Geometry for a road sign.

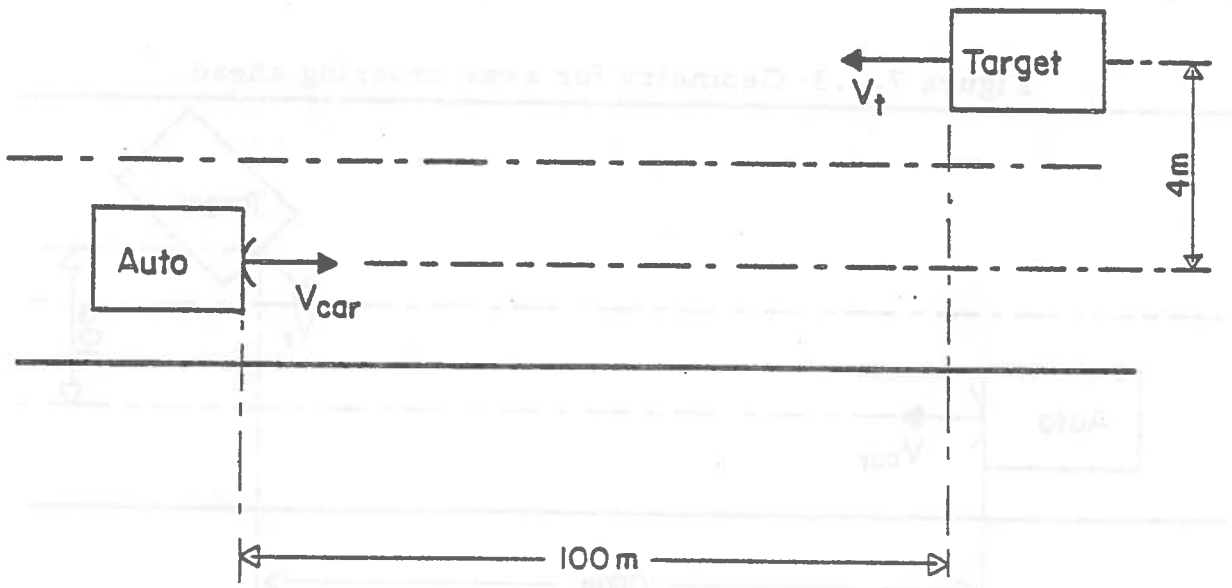

Figure 7.1.2· Geometry for a car in the left lane.

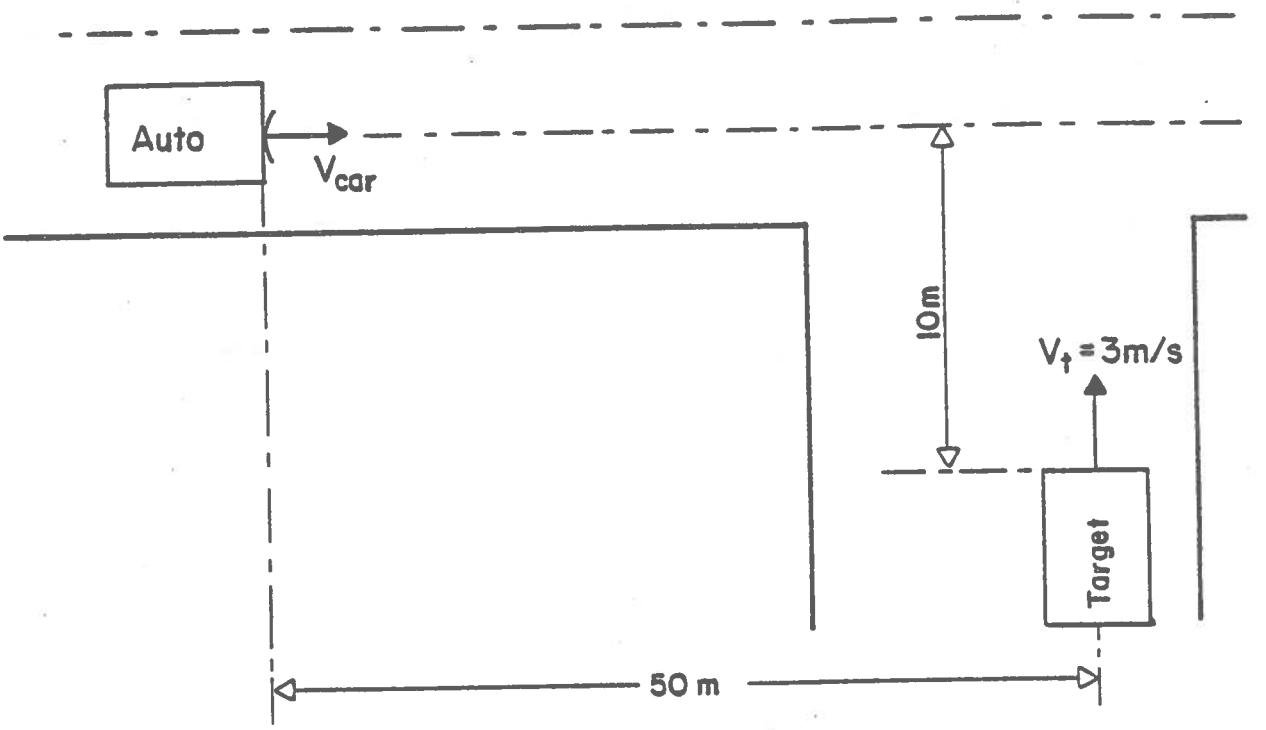

Figure 7.1.3: Geometry for a car crossing ahead.

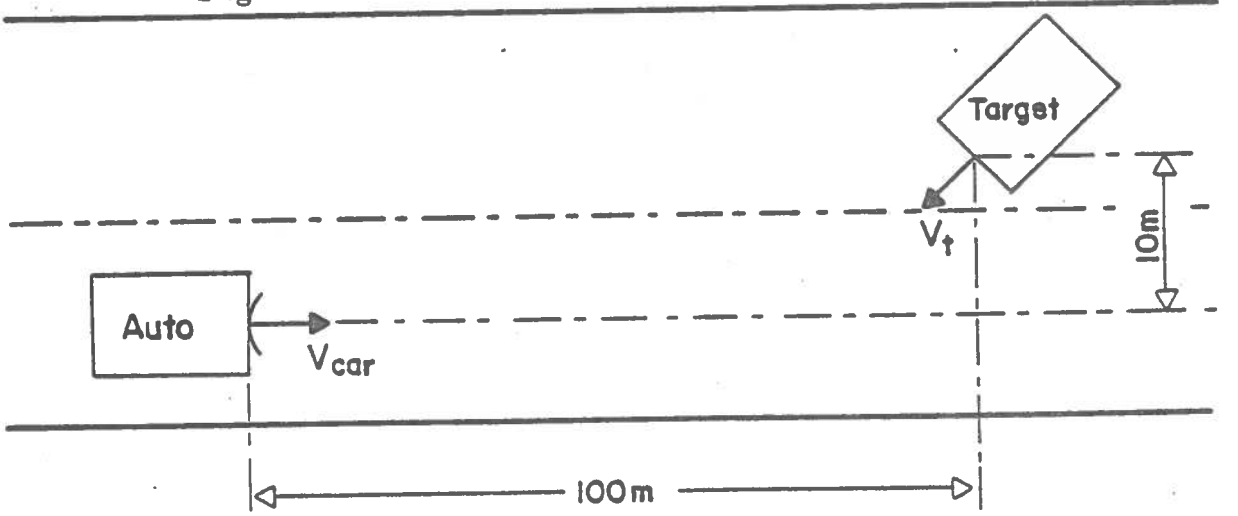

Figure 7.1.4: Geometry for a car crossing from the left lane.

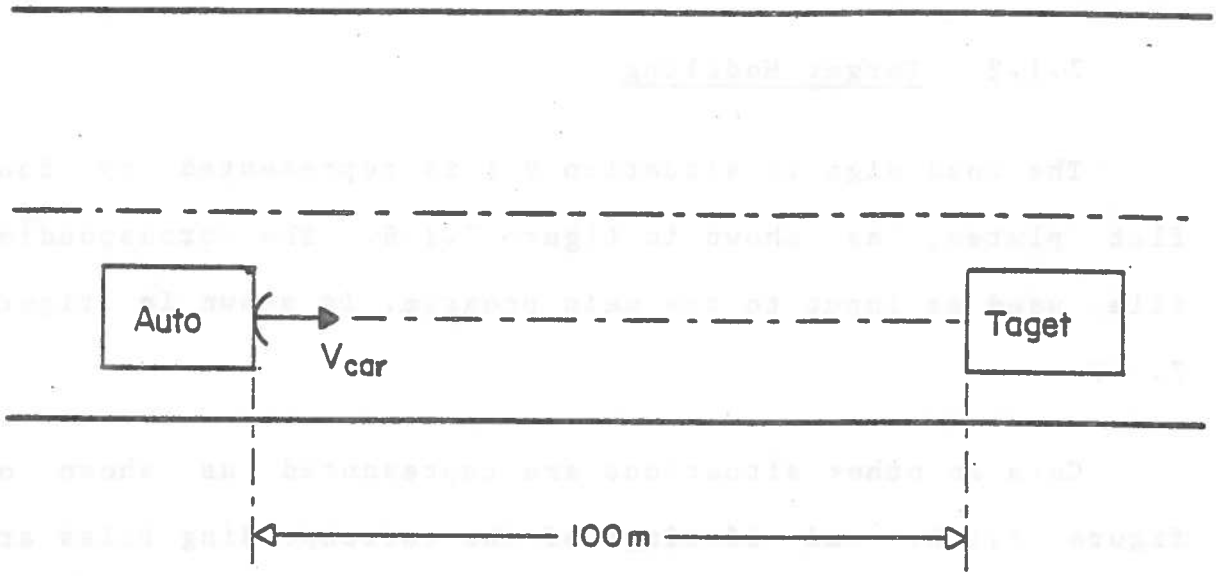

Figure 7.1.5: Geometry for a car fixed ahead.

These five situations are simulated, with more emphasis on situations # 3 and # 5.

7.1.2 Target Modeling

The road sign in situation # 1 is represented by four flat plates, as shown in figure 7.1.6. The corresponding file, used as input to the main program, is shown in figure 7.1.7.

Cars in other situations are represented as shown on figure 7.1.8, and listings of the corresponding files are shown in figures 7.1.9 to 7.1.12.

7.1.3 Presentation of Results

Results are presented under three forms for each situation:

1) Relative Signal, Detection Threshold, and Probability of Detection (all in dB) are plotted as a function of distance to target (in feet), on the same graph.

2) If Radar Control Law commands braking, the distance at which brakes are applied (in feet) is plotted as a function of carrier vehicle velocity (in feet/sec).

3) A summary table presents the distance at which every step is performed (in feet), for different carrier vehicle velocities (in feet/sec). For each velocity, it shows: distance at which target is detected, distance at which Radar Control Law commands braking, distance at which brakes

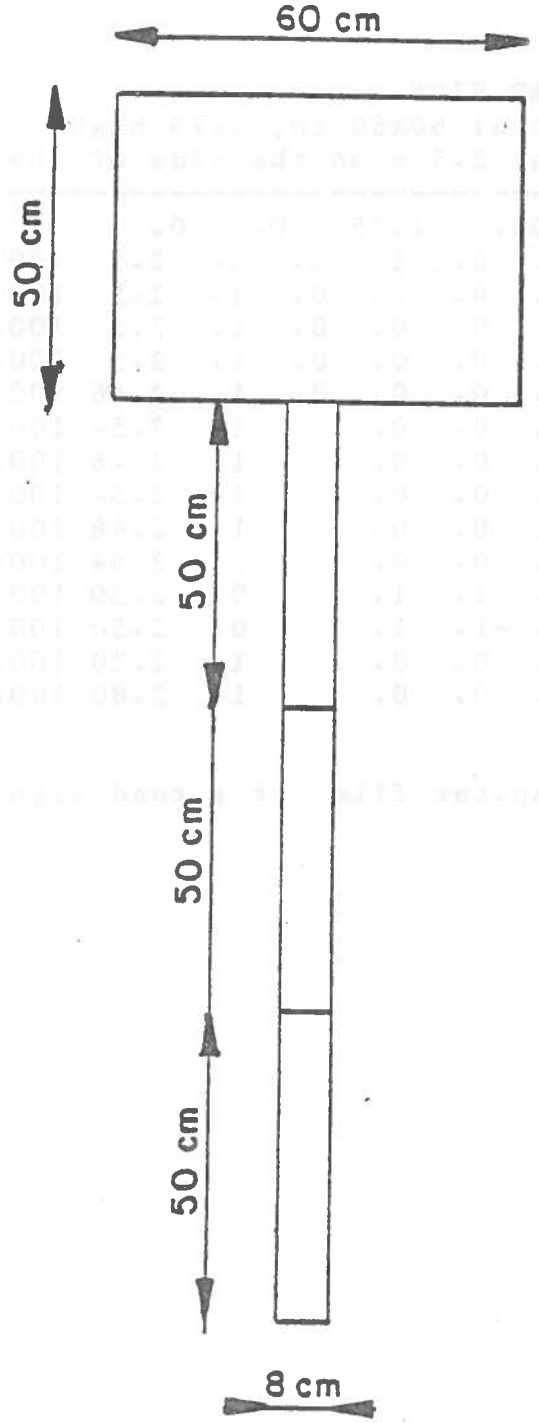

Figure 7.1.6: Flat plate model for a road sign.

```
C         SIGN ROAD SIGN
C         Dimensions: 60x50 cm, 1.75 high
C         Position: 2.5 m on the side of the car
A         ---------------------------------------
14    4    2.5    100.    1.75    0.    0.
0.6   0.5    0. -1.   0.   1.   0.   0.   2.5   100.   1.75
0.5   0.08   0. -1.   0.   0.   0.   1.   2.5   100.   0.25
0.5   0.08   0. -1.   0.   0.   0.   1.   2.5   100.   0.75
0.5   0.08   0. -1.   0.   0.   0.   1.   2.5   100.   1.25
0.5   0.     1.   0.   0.   0.   0.   1.   2.46  100.   0.25
0.5   0.    -1.   0.   0.   0.   0.   1.   2.54  100.   0.25
0.5   0.     1.   0.   0.   0.   0.   1.   2.46  100.   0.75
0.5   0.    -1.   0.   0.   0.   0.   1.   2.54  100.   0.75
0.5   0.     1.   0.   0.   0.   0.   1.   2.46  100.   1.25
0.5   0.    -1.   0.   0.   0.   0.   1.   2.54  100.   1.25
0.6   0.     0.   0.   1.   1.   0.   0.   2.50  100.   1.50
0.6   0.     0.   0.  -1.   1.   0.   0.   2.50  100.   2.00
0.5   0.     1.   0.   0.   0.   0.   1.   2.20  100.   1.75
0.5   0.    -1.   0.   0.   0.   0.   1.   2.80  100.   1.75
```

Figure 7.1.7: Computer file for a road sign.

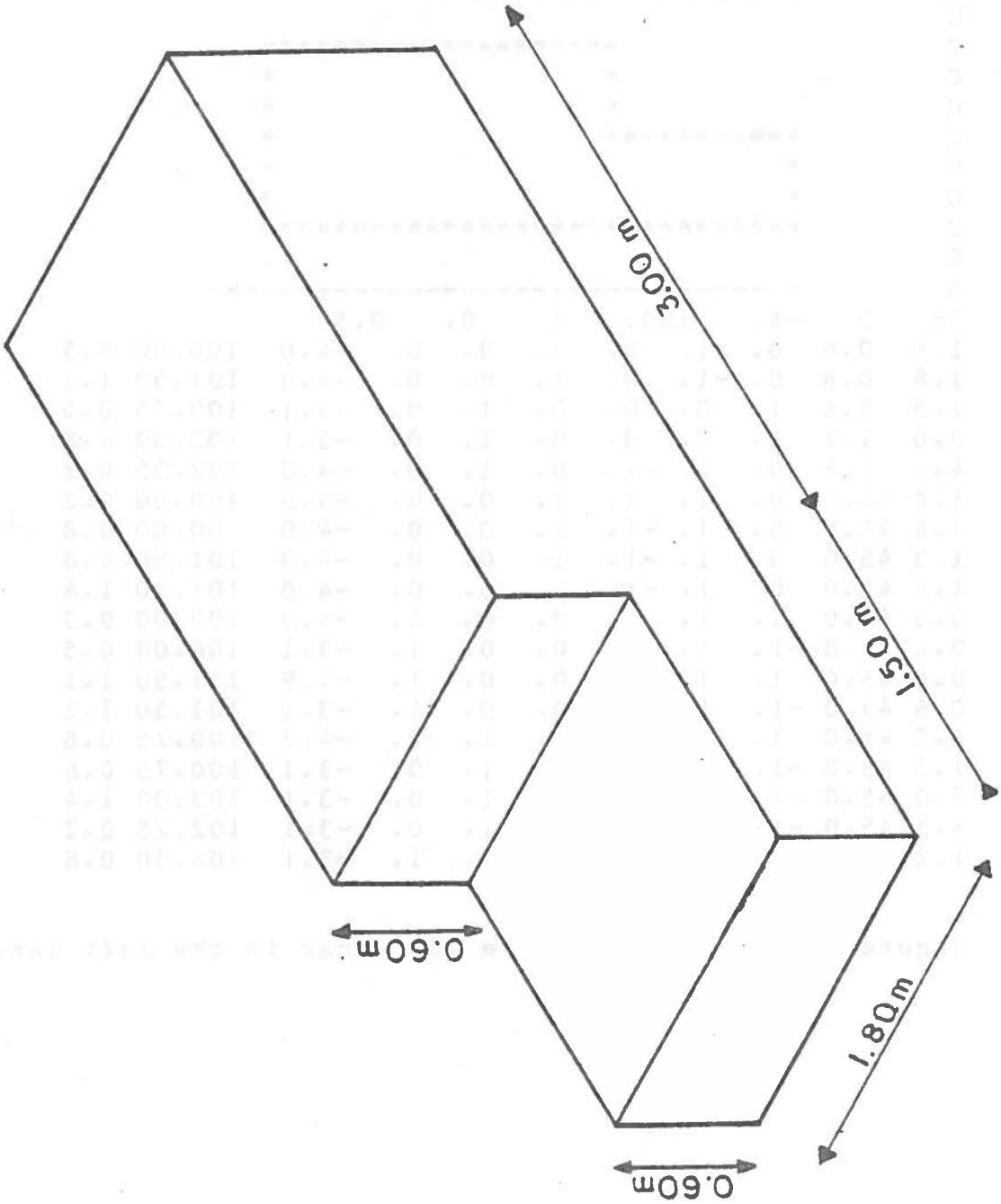

Figure 7.1.8: Flat plate model of a car.

```
C          CAR ON THE SIDE LANE
C
C                     **********************
C                     *                     *
C                     *                     *
C          ***********                      *
C          *                                *
C          *                                *
C          **********************************
C
A          ----------------------------------
18    5    -4.    100.    1.    0.    0.5
1.8   0.6   0. -1.   0.   1.   0.   0.   -4.0   100.00 0.5
1.8   0.6   0. -1.   0.   1.   0.   0.   -4.0   101.50 1.1
1.5   0.6   1.   0.   0.   0.   1.   0.   -3.1   100.75 0.5
3.0   1.2   1.   0.   0.   0.   1.   0.   -3.1   103.00 0.8
4.5   1.8   0.   0. -1.   0.   1.   0.   -4.0   102.25 0.2
1.8  45.0   0.   1.   1.   1.   0.   0.   -4.0   100.00 0.2
1.8  45.0   0.   1. -1.   1.   0.   0.   -4.0   100.00 0.8
1.8  45.0   0.   1. -1.   1.   0.   0.   -4.0   101.50 0.8
1.8  45.0   0.   1. -1.   1.   0.   0.   -4.0   101.50 1.4
0.6  45.0   1.   1.   0.   0.   0.   1.   -4.9   100.00 0.5
0.6  45.0  -1.   1.   0.   0.   0.   1.   -3.1   100.00 0.5
0.6  45.0   1.   1.   0.   0.   0.   1.   -4.9   101.50 1.1
0.6  45.0  -1.   1.   0.   0.   0.   1.   -3.1   101.50 1.1
1.5  45.0   1.   0. -1.   0.   1.   0.   -4.9   100.75 0.8
1.5  45.0  -1.   0. -1.   0.   1.   0.   -3.1   100.75 0.8
3.0  45.0  -1.   0. -1.   0.   1.   0.   -3.1   103.00 1.4
4.5  45.0  -1.   0.   1.   0.   1.   0.   -3.1   102.25 0.2
1.2  45.0  -1. -1.   0.   0.   0.   1.   -3.1   104.50 0.8
```

Figure 7.1.9: Computer file for a car in the left lane.

```
C          CAR CROSSING AHEAD
A          ------------------
21    6    10.    50.    1.    3.    0.
1.8   0.6  -1.    0.     0.    0.    1.    0.    10.00   50.00   0.5
1.8   0.6  -1.    0.     0.    0.    1.    0.    11.50   50.00   1.1
1.5   0.6   0.   -1.     0.    1.    0.    0.    10.75   49.20   0.5
3.0   0.6   0.   -1.     0.    1.    0.    0.    13.00   49.20   0.8
4.5   1.8   0.    0.    -1.    1.    0.    0.    12.25   50.00   0.2
1.8   1.2   1.    0.     0.    0.    1.    0.    14.50   50.00   0.8
1.8  45.0   1.    0.     1.    0.    1.    0.    10.00   50.00   0.2
1.8  45.0   1.    0.    -1.    0.    1.    0.    10.00   50.00   0.8
1.8  45.0   1.    0.    -1.    0.    1.    0.    11.50   50.00   0.8
1.8  45.0   1.    0.    -1.    0.    1.    0.    11.50   50.00   1.4
1.8  45.0  -1.    0.    -1.    0.    1.    0.    14.50   50.00   1.4
1.8  45.0  -1.    0.     1.    0.    1.    0.    14.50   50.00   0.2
0.6  45.0   1.   -1.     0.    0.    0.    1.    10.00   50.80   0.5
0.6  45.0   1.    1.     0.    0.    0.    1.    10.00   49.20   0.5
0.6  45.0   1.   -1.     0.    0.    0.    1.    11.50   50.80   1.1
0.6  45.0   1.    1.     0.    0.    0.    1.    11.50   49.20   1.1
1.2  45.0  -1.    1.     0.    0.    0.    1.    14.50   49.20   0.8
1.2  45.0  -1.   -1.     0.    0.    0.    1.    14.50   50.80   0.8
1.5  45.0   0.    1.    -1.    1.    0.    0.    10.75   49.20   0.8
3.0  45.0   0.    1.    -1.    1.    0.    0.    13.00   49.20   1.4
4.5  45.0   0.    1.     1.    1.    0.    0.    12.25   49.20   0.2
```

Figure 7.1.10: Computer file for a car crossing ahead.

```
C          CAR CROSSING FROM LEFT LANE
A          ---------------------------
17    5    -10.    100.    1.    -2.5   2.5
1.8   0.6    1.  -1.   0.   1.   1.   0.   -10.00   100.00   0.5
1.8   0.6    1.  -1.   0.   1.   1.   0.   -11.06   101.06   1.1
1.5   0.6   -1.  -1.   0.   1.  -1.   0.   -11.10    99.96   0.5
3.0   1.2   -1.  -1.   0.   1.  -1.   0.   -12.69   101.56   0.8
4.5   1.8    0.   0.  -1.   1.  -1.   0.   -11.59   101.59   0.2
1.8  45.0   -1.   1.   1.   1.   1.   0.   -10.00   100.00   0.2
1.8  45.0   -1.   1.  -1.   1.   1.   0.   -10.00   100.00   0.8
1.8  45.0   -1.   1.  -1.   1.   1.   0.   -11.06   101.06   0.8
1.8  45.0   -1.   1.  -1.   1.   1.   0.   -11.06   101.06   1.4
0.6  45.0    0.   1.   0.   0.   0.   1.   -10.57    99.43   0.5
0.6  45.0   -1.   0.   0.   0.   0.   1.    -9.43   100.57   0.5
0.6  45.0    0.   1.   0.   0.   0.   1.   -11.63   100.49   1.1
0.6  45.0   -1.   0.   0.   0.   0.   1.   -10.50   101.62   1.1
1.5  45.0    1.   1.  -1.   1.  -1.   0.   -11.10    99.96   0.8
3.0  45.0    1.   1.  -1.   1.  -1.   0.   -12.69   101.56   1.4
4.5  45.0    1.   1.   1.   1.  -1.   0.   -12.16   101.03   0.2
1.2  45.0    1.   0.   0.   0.   0.   1.   -13.75   102.62   0.8
```

Figure 7.1.11: Computer file for a car crossing from the left lane.

```
C                    CAR AHEAD
C
A          ------------------------------------
11   3   0.    99.    1.    0.    0.
1.8   0.6    0.   -1.    0.    1.    0.    0.    0.0   100.00   0.5
1.8   0.6    0.   -1.    0.    1.    0.    0.    0.0   101.50   1.1
4.5   1.8    0.    0.   -1.    0.    1.    0.   -4.0   102.25   0.2
1.8  45.0    0.    1.    1.    1.    0.    0.    0.0   100.00   0.2
1.8  45.0    0.    1.   -1.    1.    0.    0.    0.0   100.00   0.8
1.8  45.0    0.    1.   -1.    1.    0.    0.    0.0   101.50   0.8
1.8  45.0    0.    1.   -1.    1.    0.    0.    0.0   101.50   1.4
0.6  45.0    1.    1.    0.    0.    0.    1.   -0.9   100.00   0.5
0.6  45.0   -1.    1.    0.    0.    0.    1.    0.9   100.00   0.5
0.6  45.0    1.    1.    0.    0.    0.    1.   -0.9   101.50   1.1
0.6  45.0   -1.    1.    0.    0.    0.    1.    0.9   101.50   1.1
```

Figure 7.1.12: Computer file for a car fixed ahead.

are really applied (accounting for the Activation Time), and final velocity at target location.

Different messages can appear on a table, as explained below.

- "Probability of Detection Less Than 0.99": target is not even detected, because the probability of exceeding threshold is less than 0.99.

- "Target not Detected": target is acquired (i.e. threshold is exceeded), but not detected because the carrier vehicle arrives at target location before the time corresponding to Radar Delay has elapsed.

- "Target Seen as a Peak of Noise": target is acquired but not detected because signal goes below threshold before the time corresponding to Radar Delay is elapsed, and then remains below threshold.

- "No Alarm": target is detected, but Radar Control Law determines that target is not hazardous.

- "Brakes not Activated": target is detected, and Radar Control Law commands braking, but the carrier vehicle arrives at target location before brakes can be applied (due to Activation Time).

7.2 BENDIX SIMULATION

7.2.1 Radar System

The Bendix system is a CW Diplex radar operating at 36 GHz. The antenna is monostatic, with a 2.5° horizontal beamwidth and a 4° vertical beamwidth, polarized at 45° to avoid blinding from other vehicles.

7.2.2 Detection Parameters

1) Range Cut-Off: NHTSA's Report (1973) presents a 300-foot maximum range, which decreases with decreasing velocity. However, no further details were provided. The final report (1976) presents 36 systems, with three different ranges: 100, 200, and 300 feet. The solution of a velocity-dependent Range Cut-Off has disappeared, and this final report states that Range Cut-Offs of 200 and 300 feet result in high false alarm rates, and should not be investigated. A Range Cut-Off of 150 feet is recommended as a good compromise.

2) Detection Threshold: "Sth" is defined, in NHTSA's last report, as the power returned to the radar by a reference cross-section σ_{ref}=139.6 m^2, 300 feet away.

3) Radar Delay: "Rdel" is a constant Range Delay, with three possible values: 0, 11.5, or 23 feet. A Range Delay of 11.5 feet is recommended by NHTSA.

4) Activation Time: Bendix proposes two methods of activating the brakes: in the automatic mode, brakes are

applied rather quickly with a "Tact" of about 0.1 sec. In the manual (or semi-automatic) mode, the driver himself, warned by an alarm, activates the brakes, so "Tact" corresponds to the driver's mean reaction time, approximated to 0.9 sec.

5) Braking Deceleration: "Brd" can take two different values: standard, and anti-lock. For the standard system, coefficients of friction for the dry, wet, and icy surfaces are respectively 0.7, 0.4, and 0.15 g's. The anti-lock improvements are 0 on dry, +10% on wet, and +15% on icy. Wet road with standard configuration is studied here, so "Brd" is 0.4g.

6) Radar Control Law: it depends only on range and relative velocity, and is defined as:

$$R + 2Vrel < 0 \qquad (7.1)$$

Among the 36 initially proposed systems, six are studied here, with the addition of two systems with a constant Time Delay "Tdel" of 0.2 sec. This brings the final number to eight, as described in table 2 (each system has an Activation Time of 0.1 sec and a mean Braking Deceleration "Brd" of 0.4g).

Table 2: Bendix Systems.

System #	Range Cut-Off	Radar Delay
1	100 feet	Rdel=23.0 feet
2	100 feet	Rdel=11.5 feet
3	100 feet	Rdel= 0.0 feet
4	200 feet	Rdel=23.0 feet
5	200 feet	Rdel=11.5 feet
6	200 feet	Rdel= 0.0 feet
7	100 feet	Tdel= 0.2 sec
8	200 feet	Tdel= 0.2 sec

7.2.3 Results

1) Road Sign: figure 7.2.1 shows that, with a Range Cut-Off "RCO" of 300 feet, this road sign is detected; geometry is defined in figure 7.1.1. Provided the sign is normally oriented, perpendicular to the road axis, its radar cross-section decreases when the vehicle approaches; hence, the signal decreases with decreasing range. Therefore, only "RCO" of 100 and 200 feet are considered: it can be seen on the figure that the signal goes below threshold at about 200 feet, so if "RCO" is smaller than 200 feet, this target will not be detected, and there will be no false alarm. This corresponds to Bendix's conclusions, recommending the use of a Range Cut-Off of less than 200 feet.

2) Car in Left Lane: due to the distance D1 between the two cars (see figure 7.1.2), the target is outside the radar beamwidth most of the time, so the returned signal is quite low. Consequently, it should not be detected, and should not cause any problems. Figure 7.2.2 shows Power Returned, Threshold, and Probability of Detection with a Range Cut-Off of 300 feet.

3) Car Crossing Ahead: in this configuration, a 23-foot Radar Delay results in no braking: at low velocities, the target is too far away, and is not detected at all, and at higher velocities, threshold is exceeded during too short a period of time, and the target is seen as a peak of noise. The collision velocity, for the geometry defined in figure

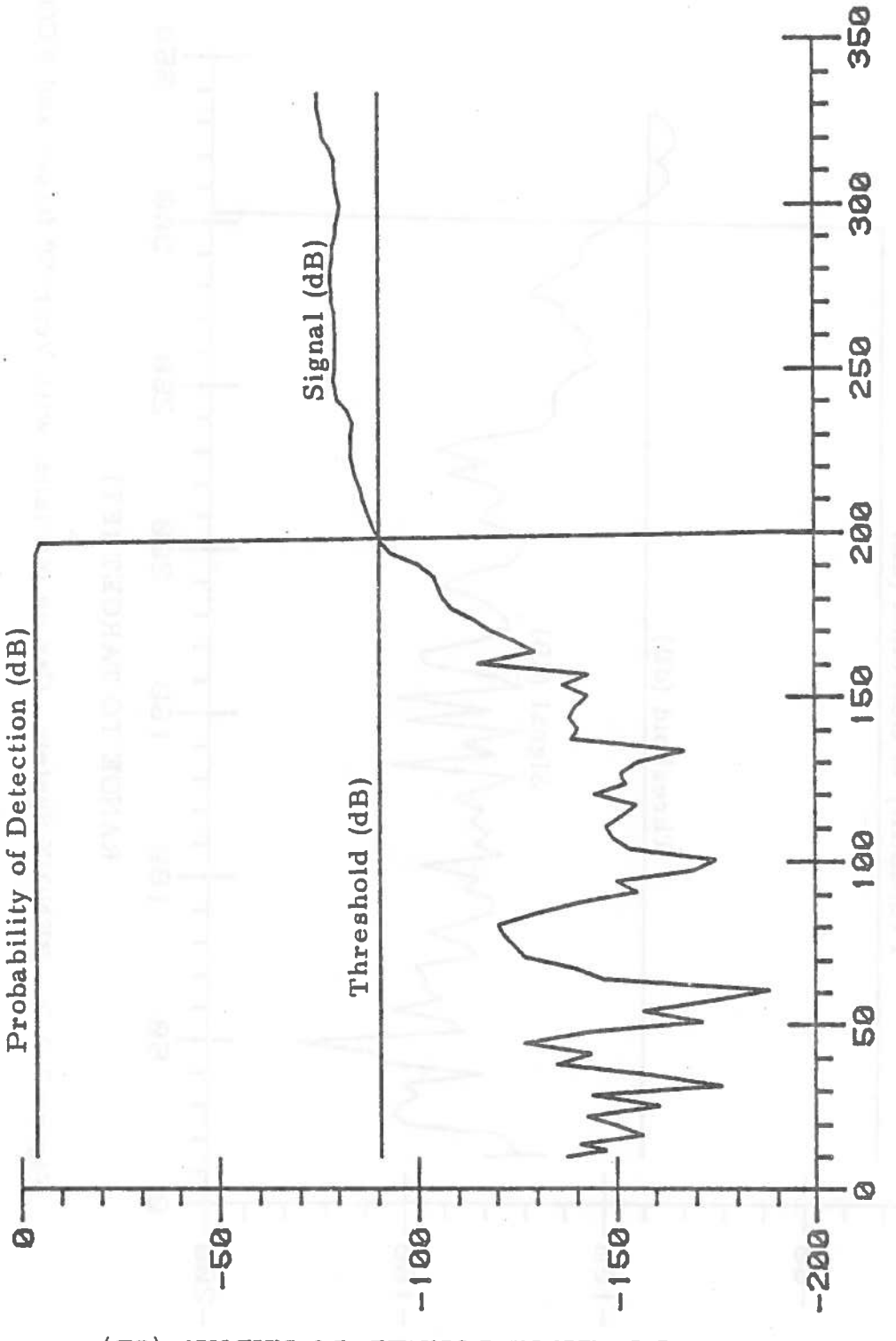

Figure 7.2.1: BENDIX System. Road Sign at Vcar=40 ft/sec, with RCO=200 ft

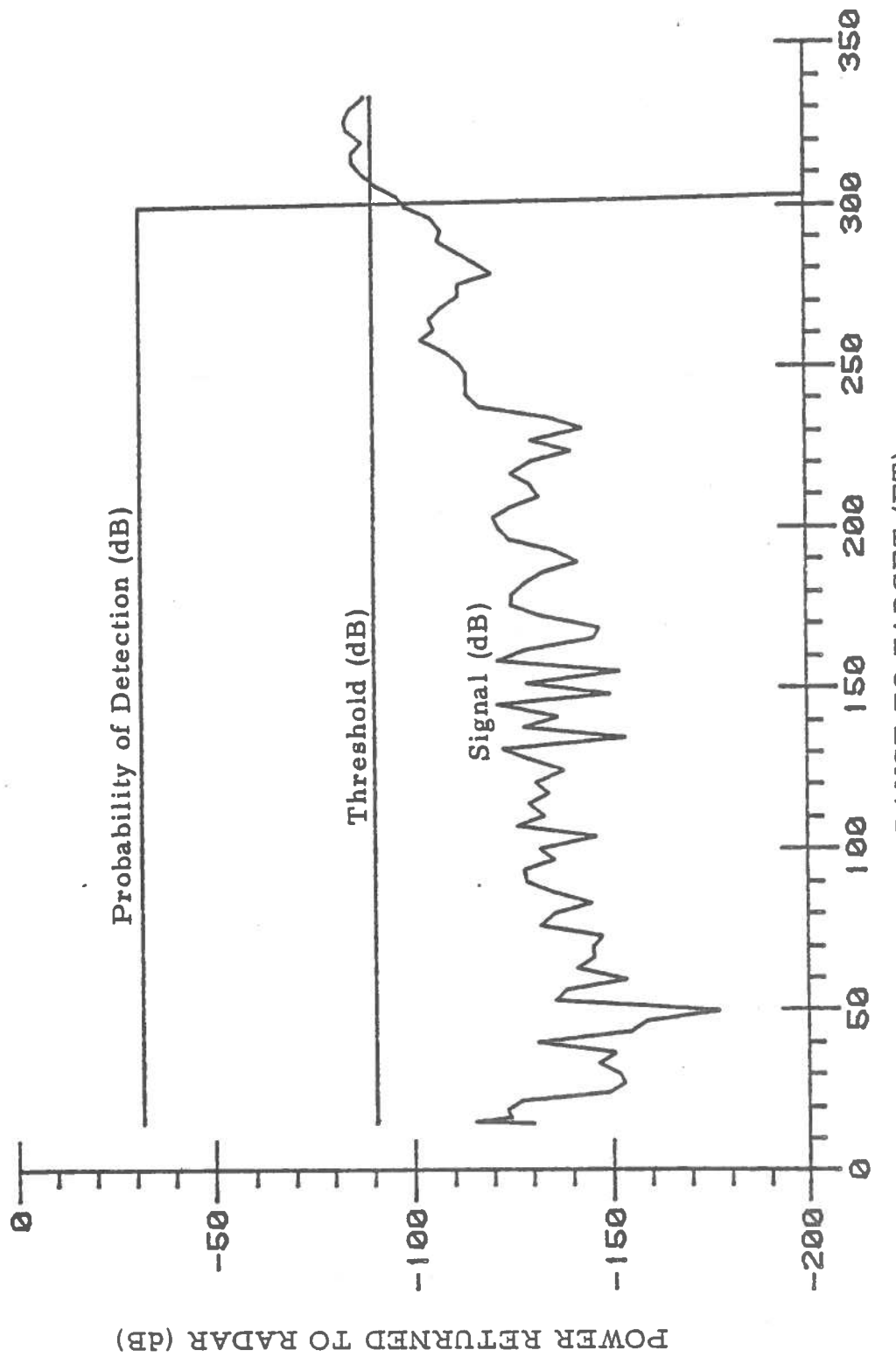

Figure 7.2.2: BENDIX System. Car on left lane, with Vcar=50 ft/sec and RCO=300 ft

7.1.3, is approximately 50 feet/sec, which means that, for higher velocities, the carrier vehicle passes the crossing before the target arrives there. In this case, there is neither danger nor detection, so velocities greater than 50 feet/sec will not be considered here.

Figures 7.2.3 to 7.2.9 show that, in the case of a car crossing an intersection in front of the carrier vehicle, Automotive Radar in its present form is inefficient: brakes are applied for velocities lower than the critical velocity, when there is no real danger of collision. On the contrary, brakes are not activated at the critical velocity because the target is detected too late, when it is directly in front of the vehicle. Therefore, even with a zero Radar Delay, a collision occurs before the brakes are applied. It is interesting to note that on the figures showing the distance at which brakes are applied as a function of velocity, this distance first increases, and then decreases very rapidly with increasing velocity. Tables 3 to 5 explain this phenomenon:

- For low velocities, the target is detected before Radar Control Law is satisfied. In this case, the alarm is set at the exact range R=2Vrel, since the system waits until this condition is met, and then either warns the driver, or activates the brakes. Thus, the range at which brakes are applied increases with increasing velocity, as in any efficient system.

- For high velocities, the Radar Control Law is already

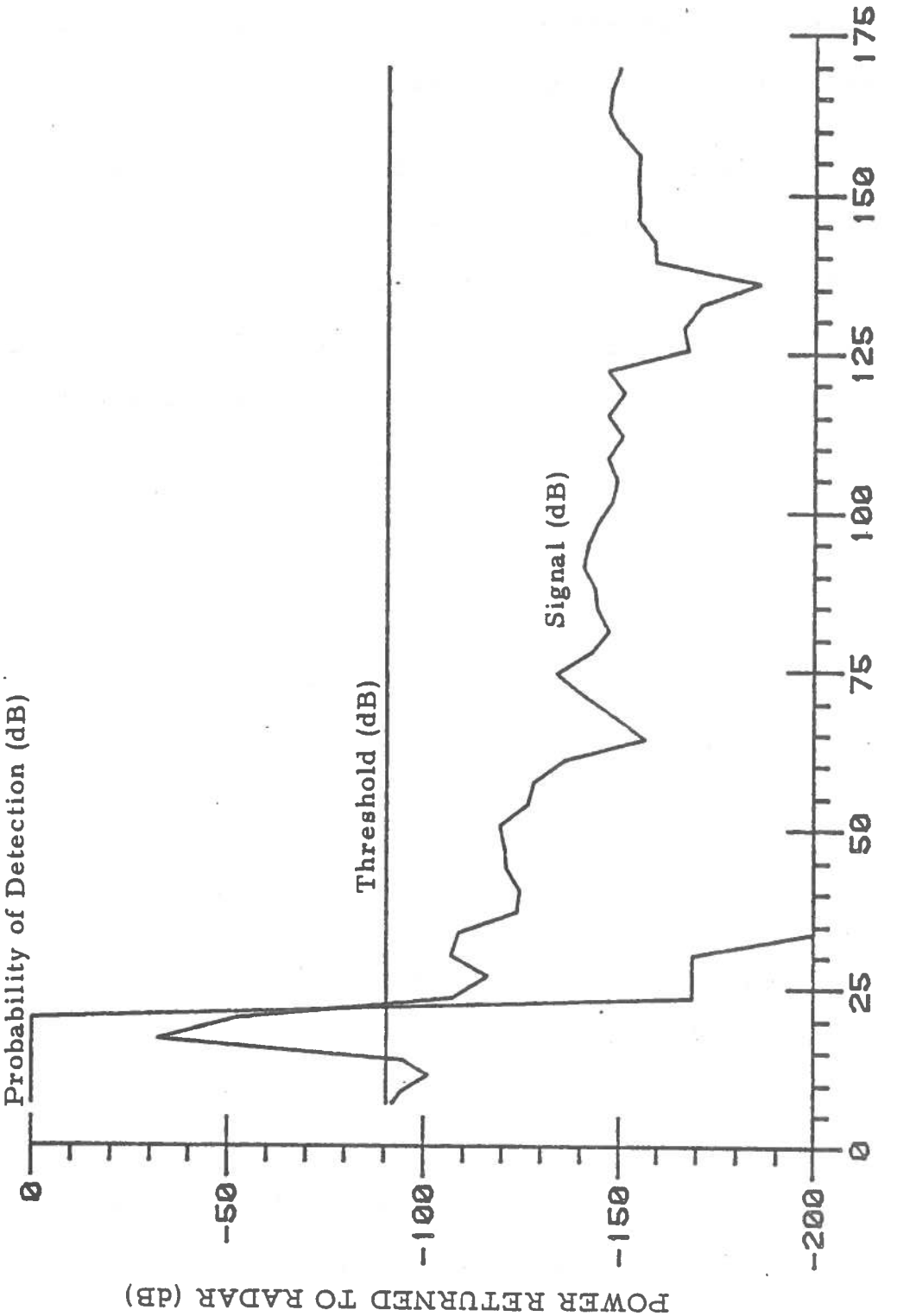

Figure 7.2.3: BENDIX System. Car crossing ahead, with Vcar=45 ft/sec and RCO=100 ft.

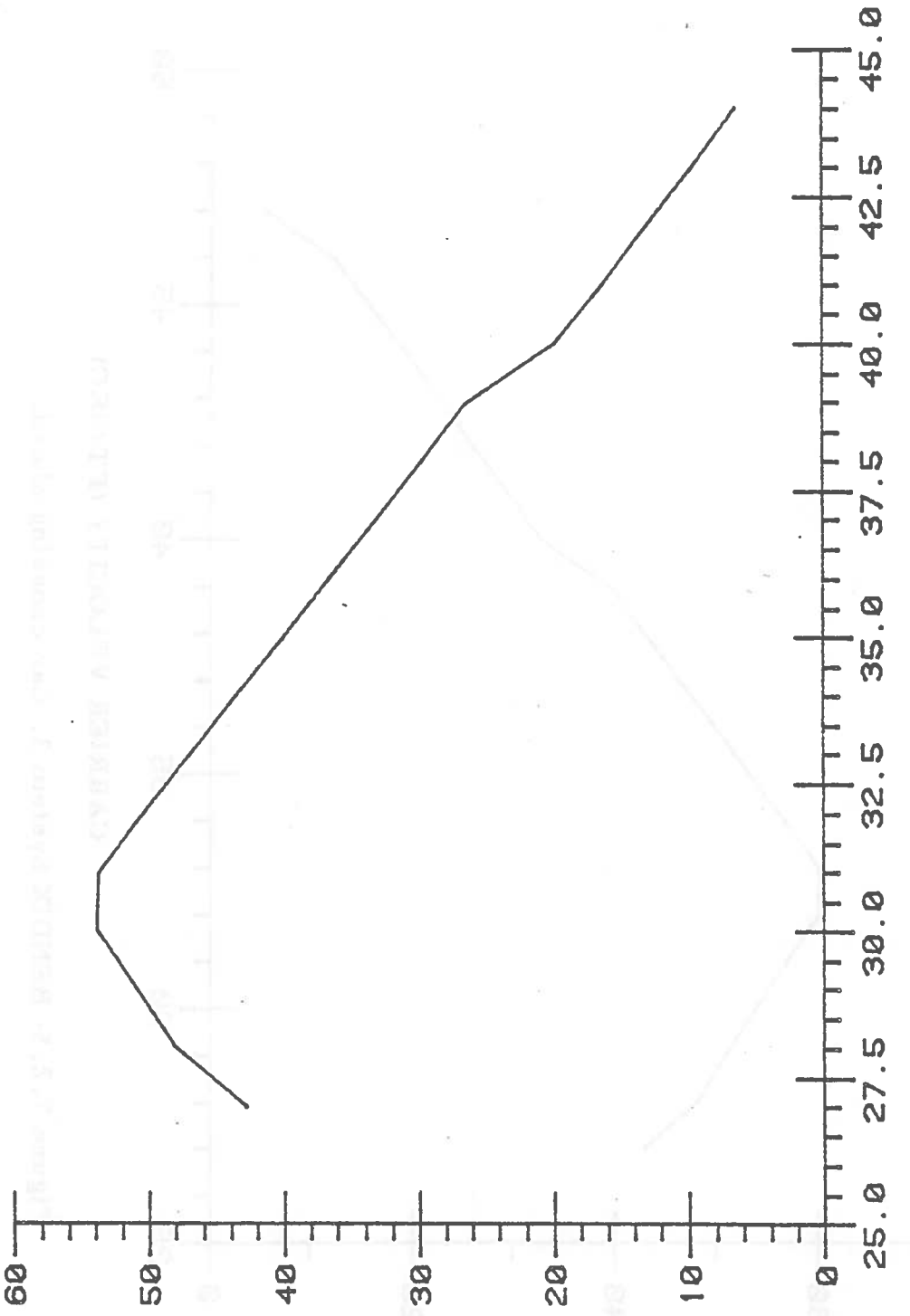

Figure 7.2.4: BENDIX System 2. Car crossing ahead.

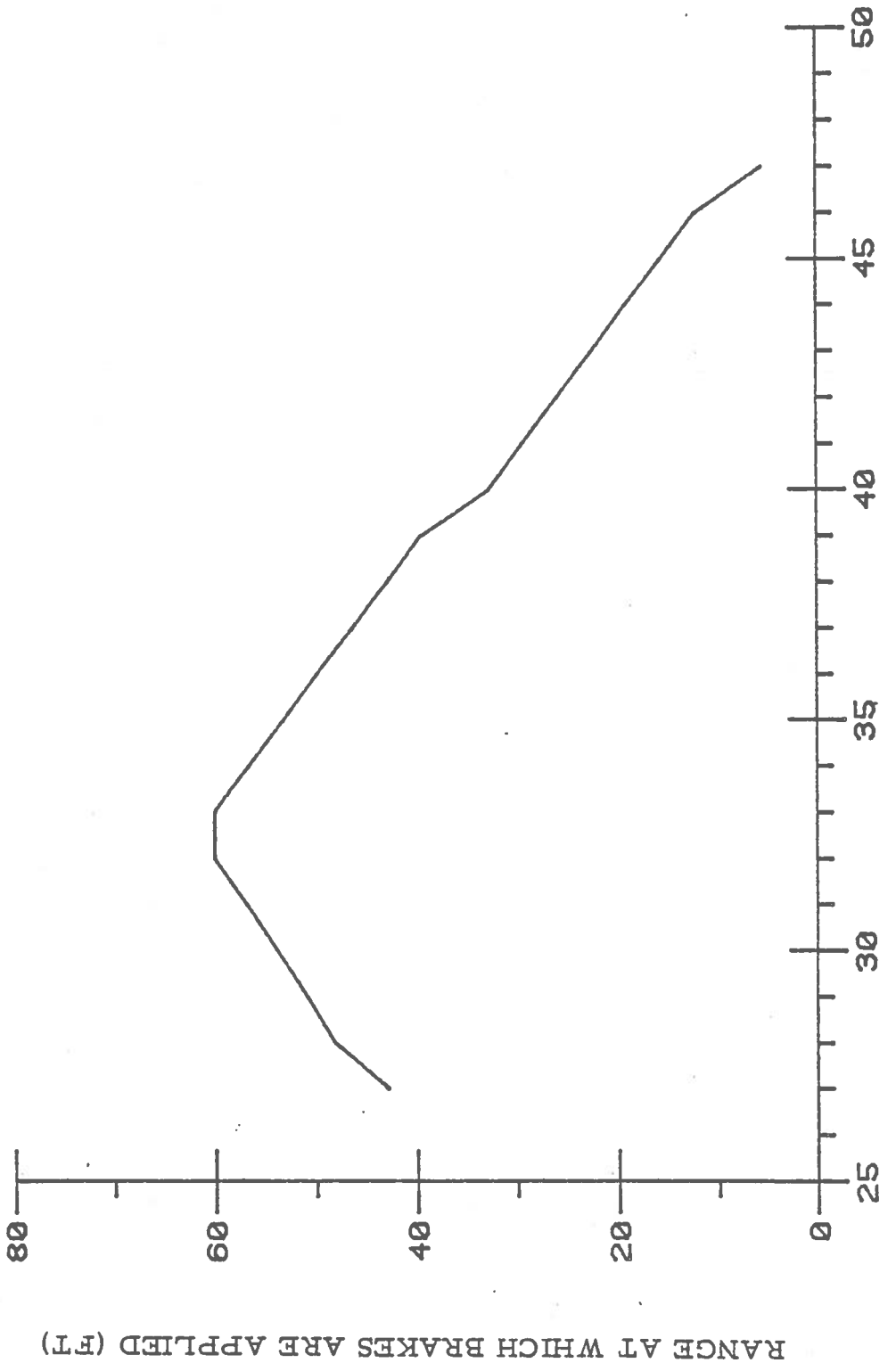

Figure 7.2.5: BENDIX System 3. Car crossing ahead.

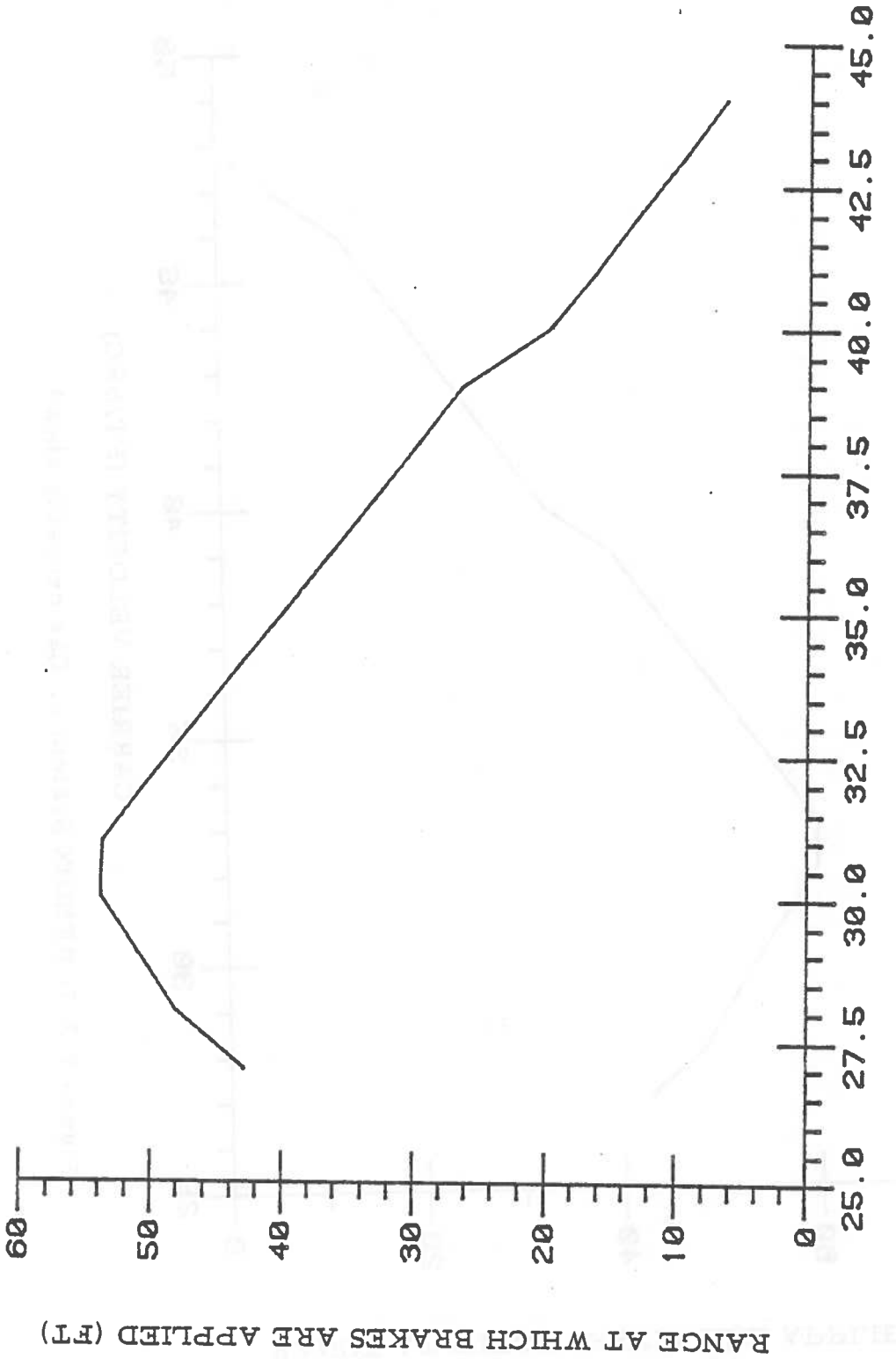

Figure 7.2.6: BENDIX System 5. Car crossing ahead.

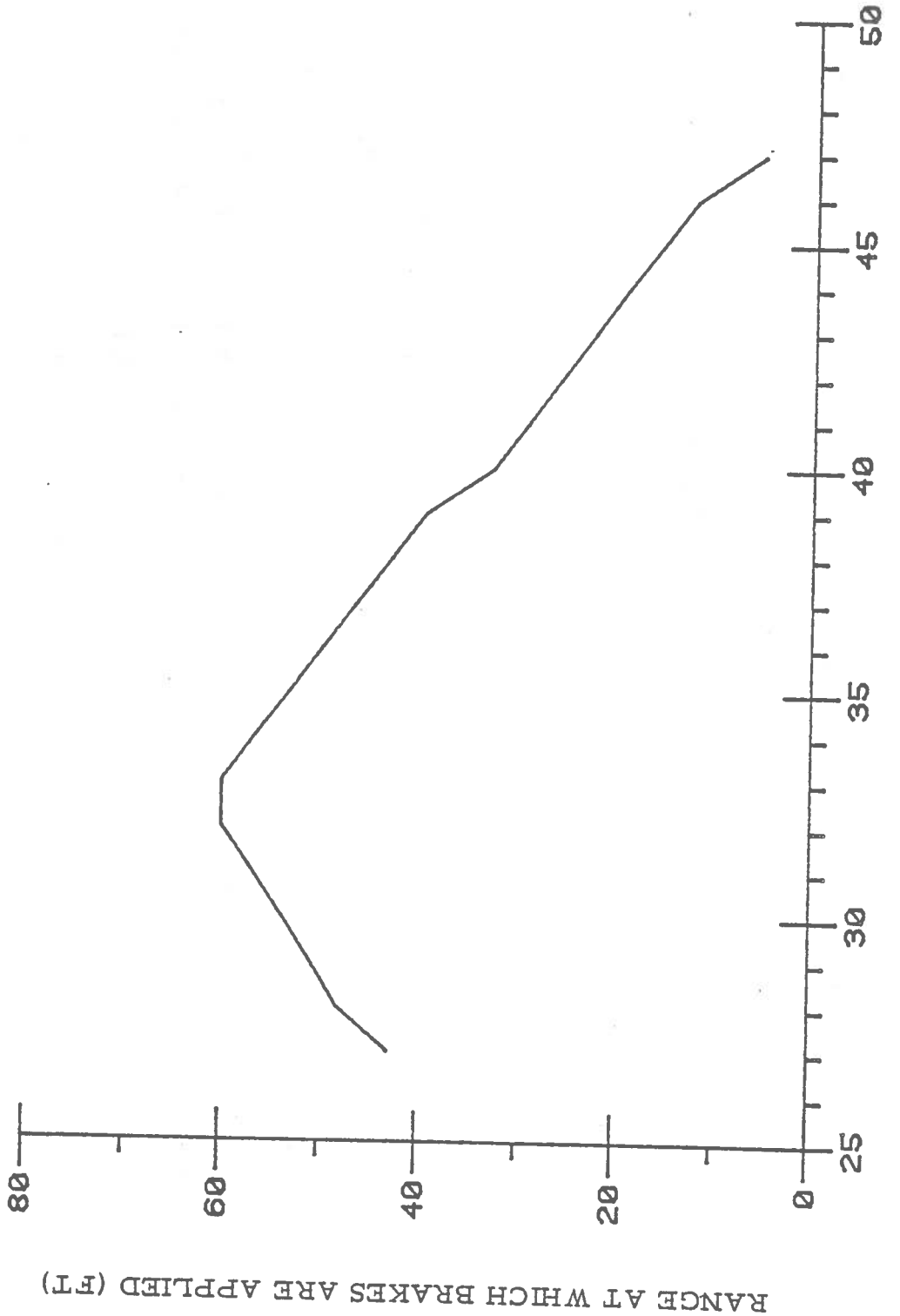

Figure 7.2.7: BENDIX System 6. Car crossing ahead.

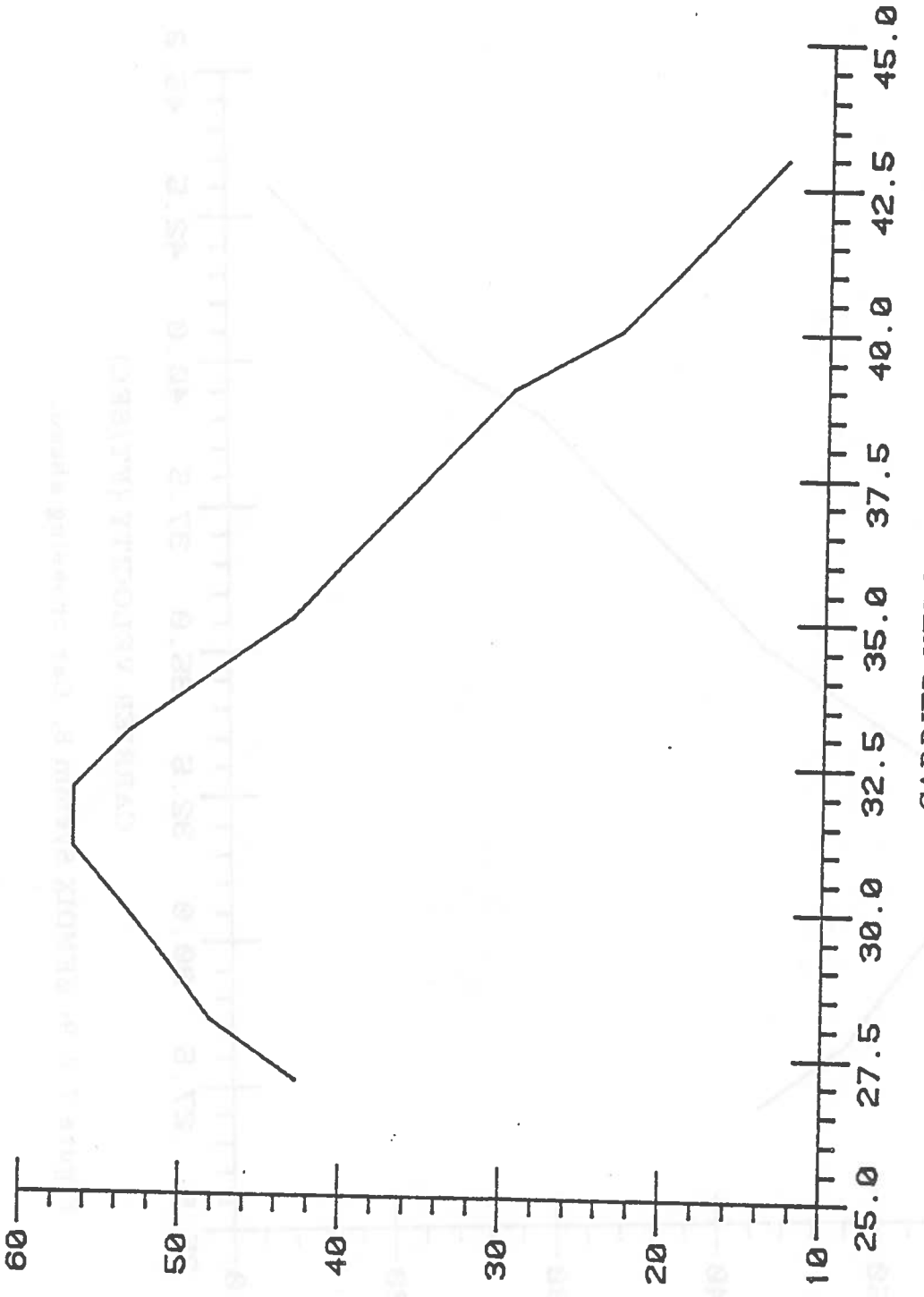

Figure 7.2.8: BENDIX System 7. Car crossing ahead.

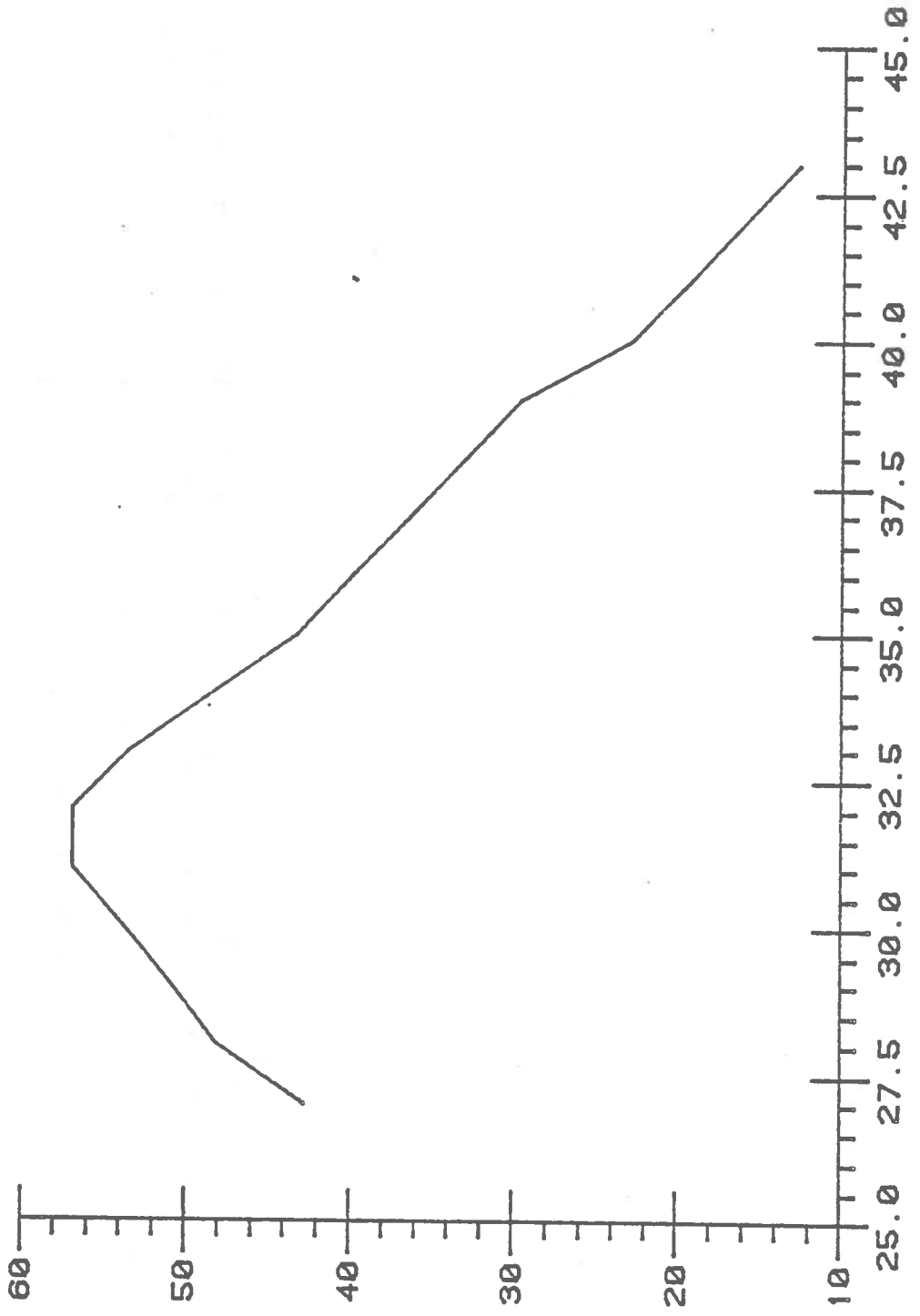

Figure 7.2.9: BENDIX System 8. Car crossing ahead.

Table 3: BENDIX System # 2. Car crossing ahead.

RANGE CUT-OFF: 100.00
ACTIVATION TIME: 0.10
BRAKING DECELERATION: 3.92
RADAR DELAY: 11.50

VELOCITY OF CAR	RANGE OF DETECTION	RANGE AT ALARM	RANGE FOR BRAKES	FINAL VELOCITY
20.00	TARGET SEEN AS A PEAK OF NOISE			
21.00	85.35	NO ALARM		
22.00	85.26	NO ALARM		
23.00	81.92	NO ALARM		
24.00	81.87	NO ALARM		
25.00	78.54	NO ALARM		
26.00	75.20	NO ALARM		
27.00	71.87	45.09	42.80	0.00
28.00	68.54	50.72	48.14	0.00
29.00	65.21	53.67	50.91	0.00
30.00	61.87	56.79	53.87	0.00
31.00	58.54	58.54	53.69	0.00
32.00	55.21	55.21	50.26	0.00
33.00	51.88	51.88	46.83	0.00
34.00	TARGET SEEN AS A PEAK OF NOISE			
35.00	45.21	45.21	39.95	13.41
36.00	41.88	41.88	36.53	18.45
37.00	38.55	38.55	33.11	22.43
38.00	35.22	35.22	29.69	25.83
39.00	31.90	31.90	26.27	28.88
40.00	25.30	25.30	19.67	32.94
41.00	21.98	21.98	16.29	35.42
42.00	TARGET SEEN AS A PEAK OF NOISE			
43.00	15.36	15.36	9.62	39.97
44.00	TARGET SEEN AS A PEAK OF NOISE			
45.00	TARGET NOT DETECTED			
46.00	TARGET NOT DETECTED			
47.00	TARGET NOT DETECTED			
48.00	TARGET NOT DETECTED			
49.00	TARGET NOT DETECTED			
50.00	PROBABILITY OF DETECTION LESS THAN .99			

Table 4: BENDIX System # 3. Car crossing ahead.

RANGE CUT-OFF: 200.00
ACTIVATION TIME: 0.10
BRAKING DECELERATION: 3.92
RADAR DELAY: 11.50

VELOCITY OF CAR	RANGE OF DETECTION	RANGE AT ALARM	RANGE FOR BRAKES	FINAL VELOCITY
20.00	91.93	NO ALARM		
21.00	88.60	NO ALARM		
22.00	85.26	NO ALARM		
23.00	81.92	NO ALARM		
24.00	81.87	NO ALARM		
25.00	78.54	NO ALARM		
26.00	75.20	NO ALARM		
27.00	71.87	45.09	42.80	0.00
28.00	68.54	50.72	48.14	0.00
29.00	65.21	53.67	50.91	0.00
30.00	61.87	56.79	53.87	0.00
31.00	58.54	58.54	53.69	0.00
32.00	55.21	55.21	50.26	0.00
33.00	51.88	51.88	46.83	0.00
34.00	48.55	48.55	43.38	4.60
35.00	45.21	45.21	39.95	13.41
36.00	41.88	41.88	36.53	18.45
37.00	38.55	38.55	33.11	22.43
38.00	35.22	35.22	29.69	25.83
39.00	31.90	31.90	26.27	28.88
40.00	25.30	25.30	19.67	32.94
41.00	21.98	21.98	16.29	35.42
42.00	TARGET SEEN AS A PEAK OF NOISE			
43.00	15.36	15.36	9.62	39.97
44.00	TARGET SEEN AS A PEAK OF NOISE			
45.00	TARGET NOT DETECTED			
46.00	TARGET NOT DETECTED			
47.00	TARGET NOT DETECTED			
48.00	TARGET NOT DETECTED			
49.00	TARGET NOT DETECTED			
50.00	PROBABILITY OF DETECTION LESS THAN .99			

Table 5: BENDIX System # 7. Car crossing ahead.

RANGE CUT-OFF: 100.00
ACTIVATION TIME: 0.10
BRAKING DECELERATION: 3.92
RADAR DELAY: 0.20

VELOCITY OF CAR	RANGE OF DETECTION	RANGE AT ALARM	RANGE FOR BRAKES	FINAL VELOCITY
20.00	92.74	NO ALARM		
21.00	92.49	NO ALARM		
22.00	92.28	NO ALARM		
23.00	88.75	NO ALARM		
24.00	88.55	NO ALARM		
25.00	85.02	NO ALARM		
26.00	81.48	NO ALARM		
27.00	77.95	45.09	42.80	0.00
28.00	74.42	50.72	48.14	0.00
29.00	70.89	53.67	50.91	0.00
30.00	67.35	56.79	53.87	0.00
31.00	63.82	60.03	56.96	0.00
32.00	60.29	60.29	56.83	0.00
33.00	56.76	56.76	53.40	0.00
34.00	TARGET SEEN AS A PEAK OF NOISE			
35.00	49.69	49.69	43.23	9.70
36.00	46.16	46.16	39.80	15.96
37.00	42.63	42.63	36.37	20.43
38.00	39.10	39.10	32.95	24.13
39.00	35.57	35.57	29.52	27.36
40.00	28.73	28.73	22.86	31.66
41.00	25.21	25.21	19.45	34.24
42.00	TARGET SEEN AS A PEAK OF NOISE			
43.00	18.18	18.18	12.67	38.95
44.00	TARGET SEEN AS A PEAK OF NOISE			
45.00	TARGET NOT DETECTED			
46.00	TARGET NOT DETECTED			
47.00	TARGET NOT DETECTED			
48.00	TARGET NOT DETECTED			
49.00	TARGET NOT DETECTED			
50.00	PROBABILITY OF DETECTION LESS THAN .99			

satisfied when the target is detected, meaning that it is already too late; hence, the alarm is set at the same time as the target is detected. When the carrier vehicle velocity increases, the detection range decreases, and consequently the range at which brakes are applied also decreases.

4) Car Crossing From Left Lane: figure 7.2.10 is drawn for RCO=100 feet and Vcar=45 feet/sec. Figure 7.2.11, drawn for RCO=100 feet and Vcar=57 feet/sec, illustrates an interesting point: signal exceeds threshold for ranges between 125 feet and 80 feet, then goes below threshold at 80 feet, and again exceeds threshold between 80 feet and 40 feet. Hence, with a Radar Delay of 23 feet, the target is acquired at 100 feet, but between 100 feet and 100-23=77 feet, the signal goes below threshold, cancelling the first acquisition of the target. Indeed, the target is not detected at 77 feet, but at 80-23=57 feet. This explains why the range at which brakes are applied is so short at the speed of 57 feet/sec, as it can be seen on figures 7.2.12 to 7.2.20. With a Radar Delay of 23 feet, the target is not detected at critical (collision) velocity.

5) Car Fixed Ahead: figure 7.2.20 shows radar return as a function of range; figures 7.2.21 to 7.2.28 and tables 6 to 13 show the results for the different Bendix systems. It can be seen on figure 7.2.20 that the signal is always above threshold (not represented here) Sth=-90 dB. There-

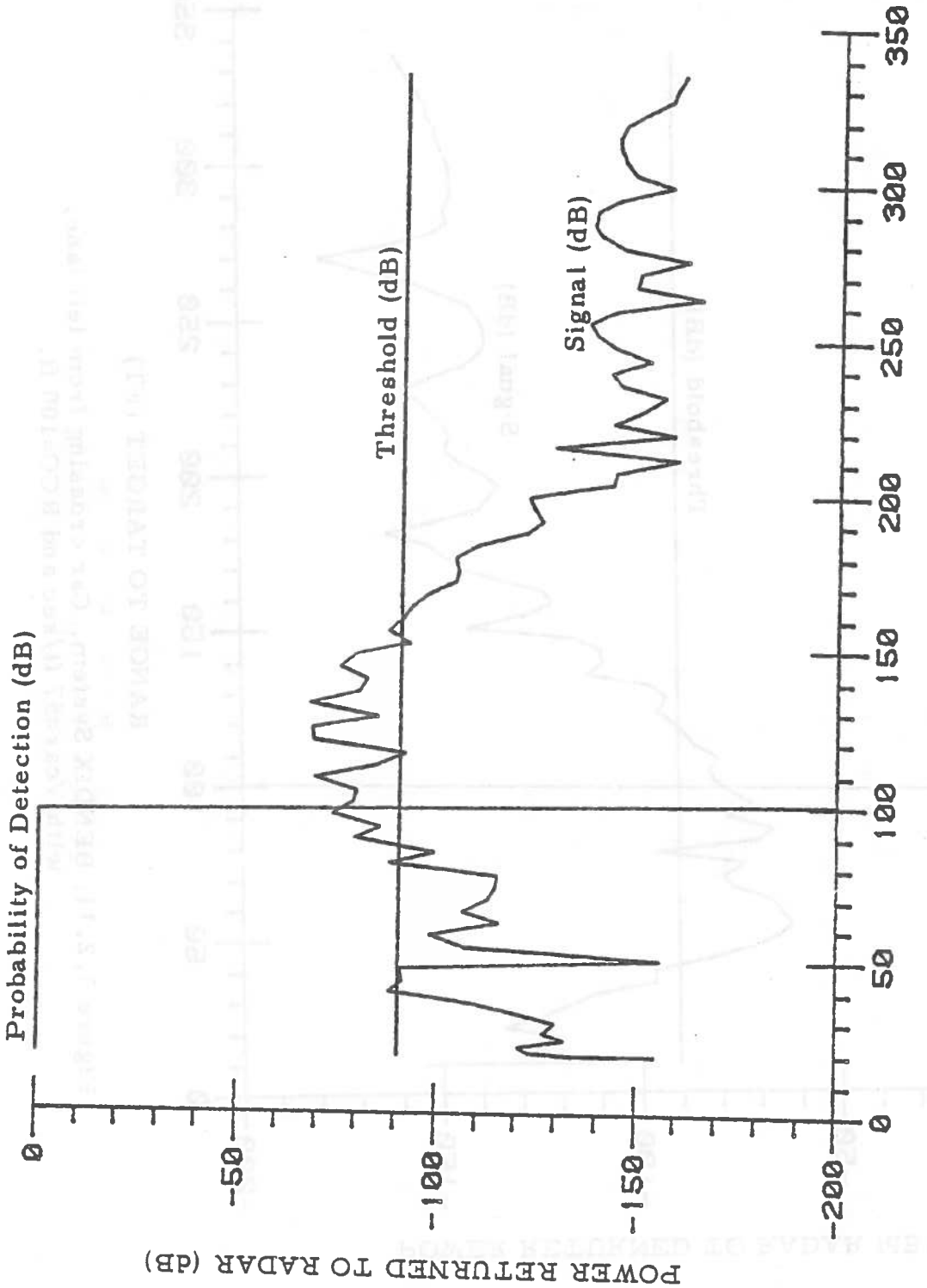

Figure 7.2.10: BENDIX System. Car crossing from left lane, with Vcar=45 ft/sec and RCO=100 ft.

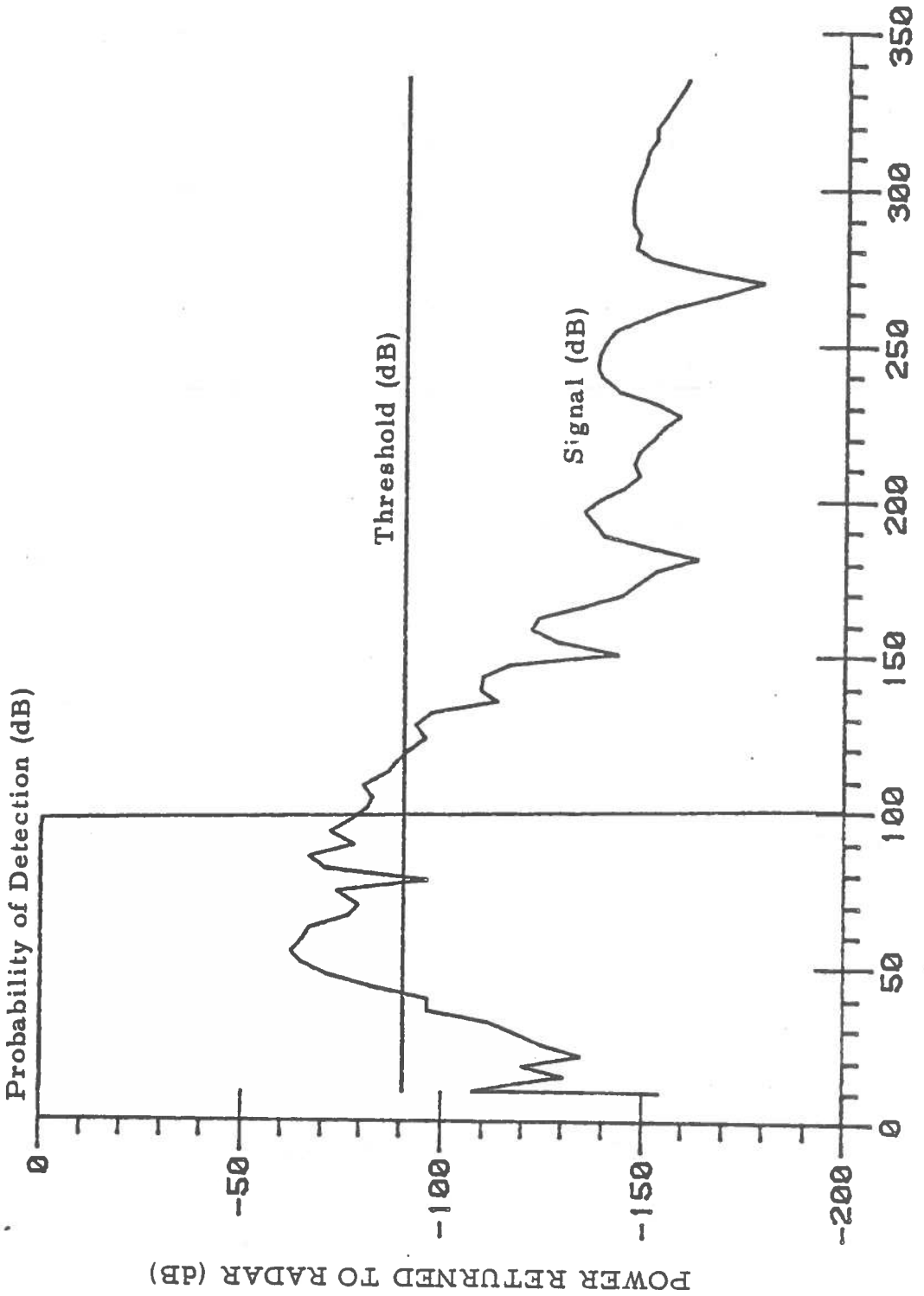

Figure 7.2.11: BENDIX System. Car crossing from left lane, with Vcar=57 ft/sec and RCO=100 ft.

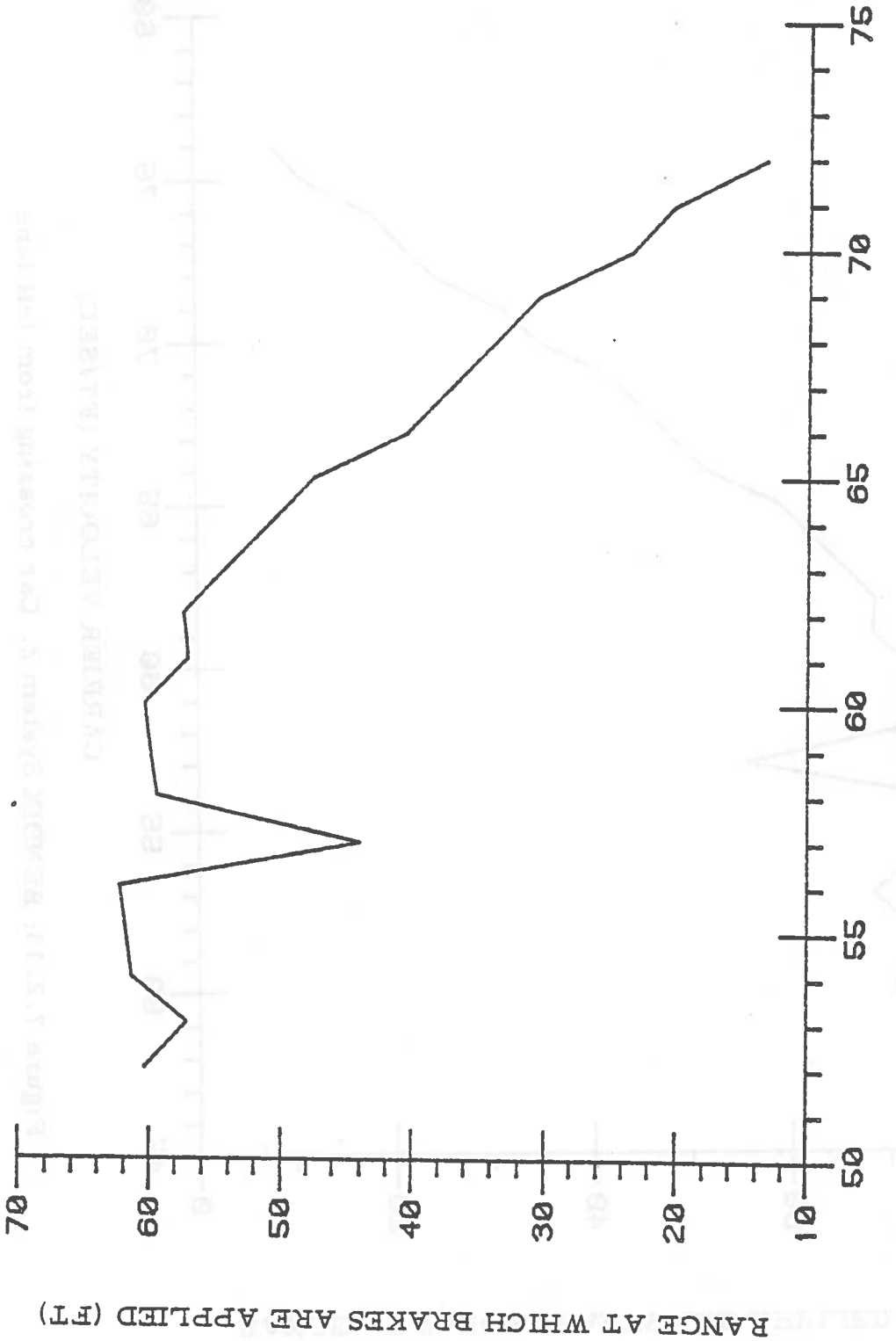

Figure 7.2.12: BENDIX System 1. Car crossing from left lane.

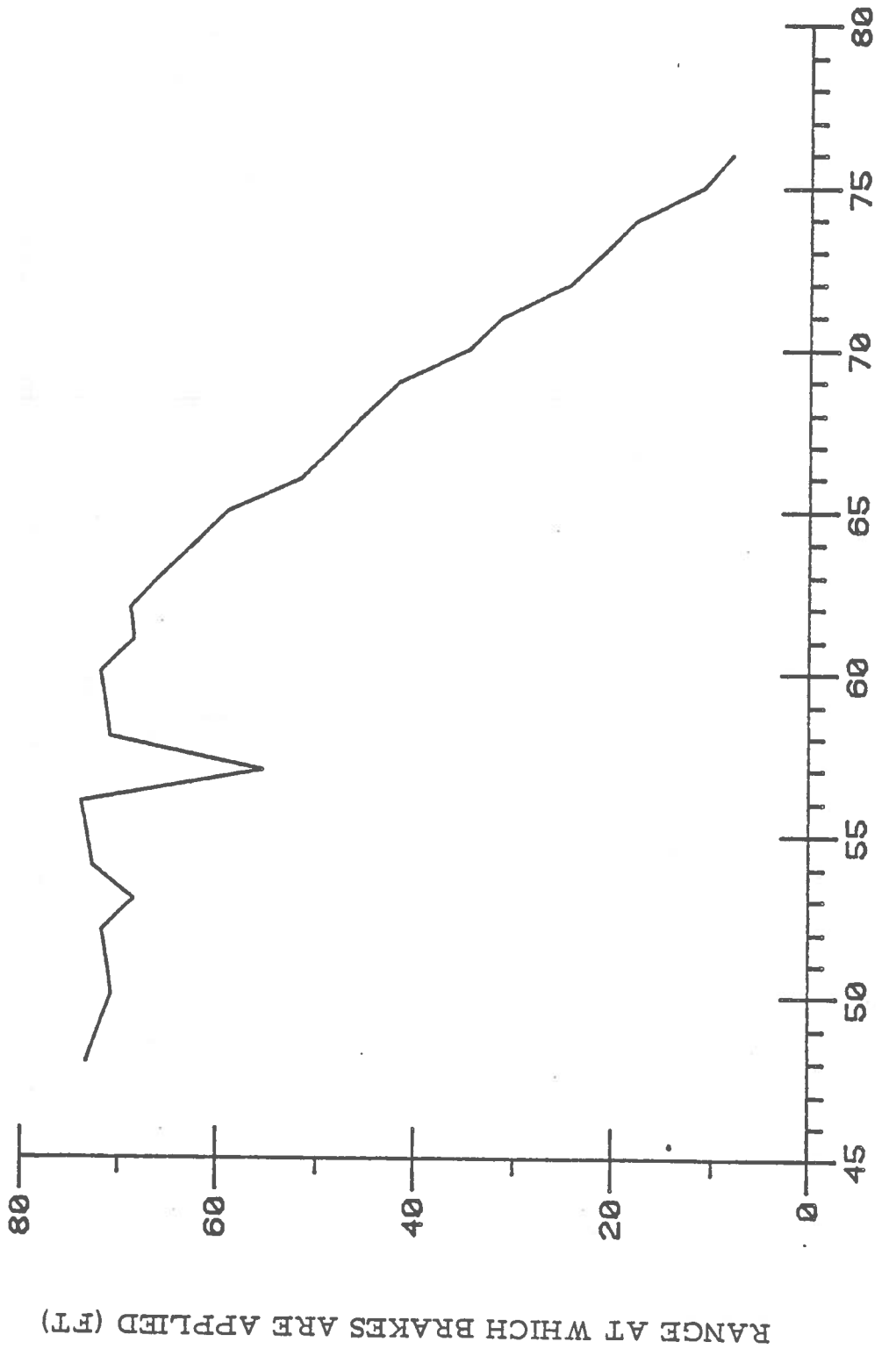

Figure 7.2.13: BENDIX System 2. Car crossing from left lane.

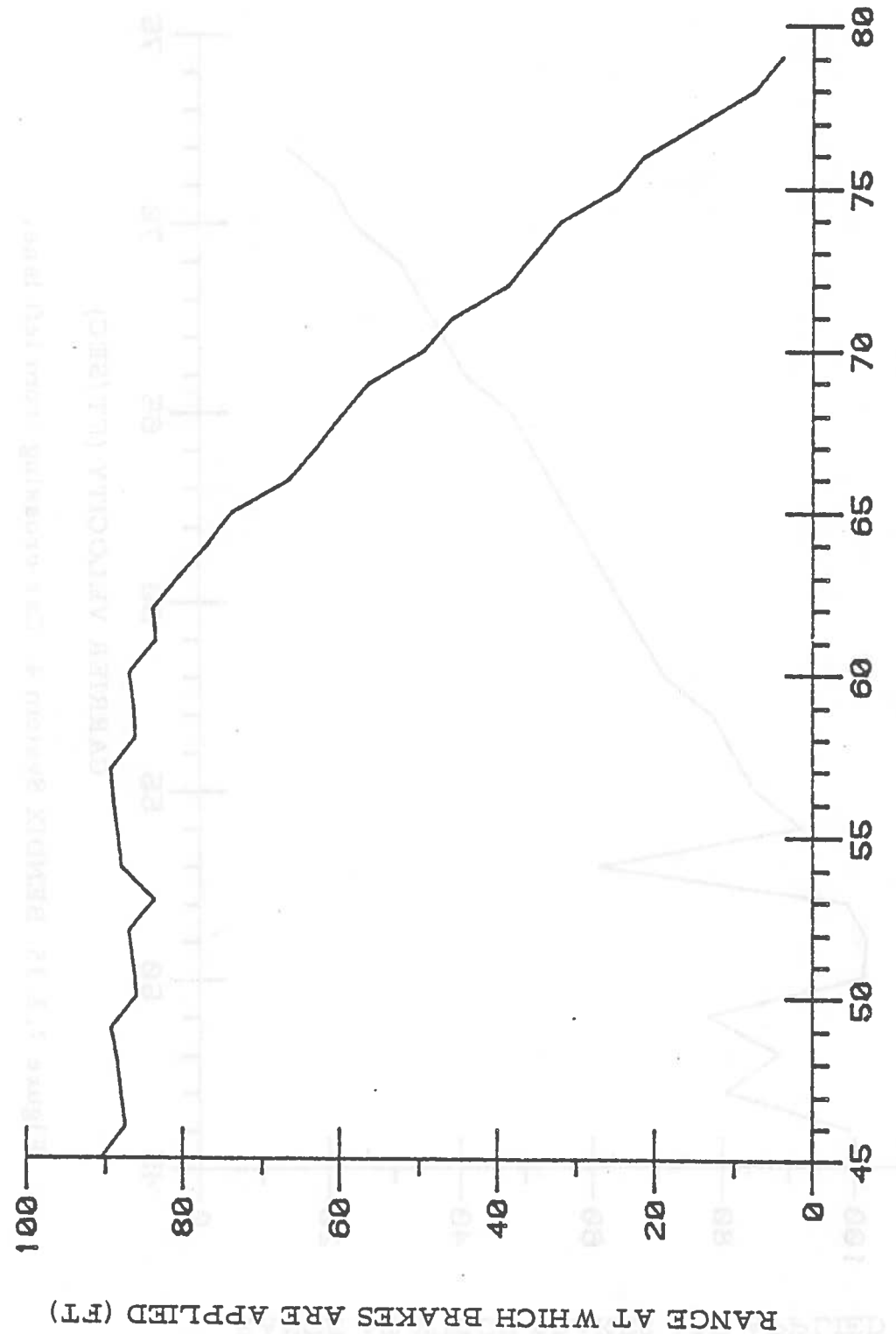

Figure 7.2.14: BENDIX System 3. Car crossing from left lane.

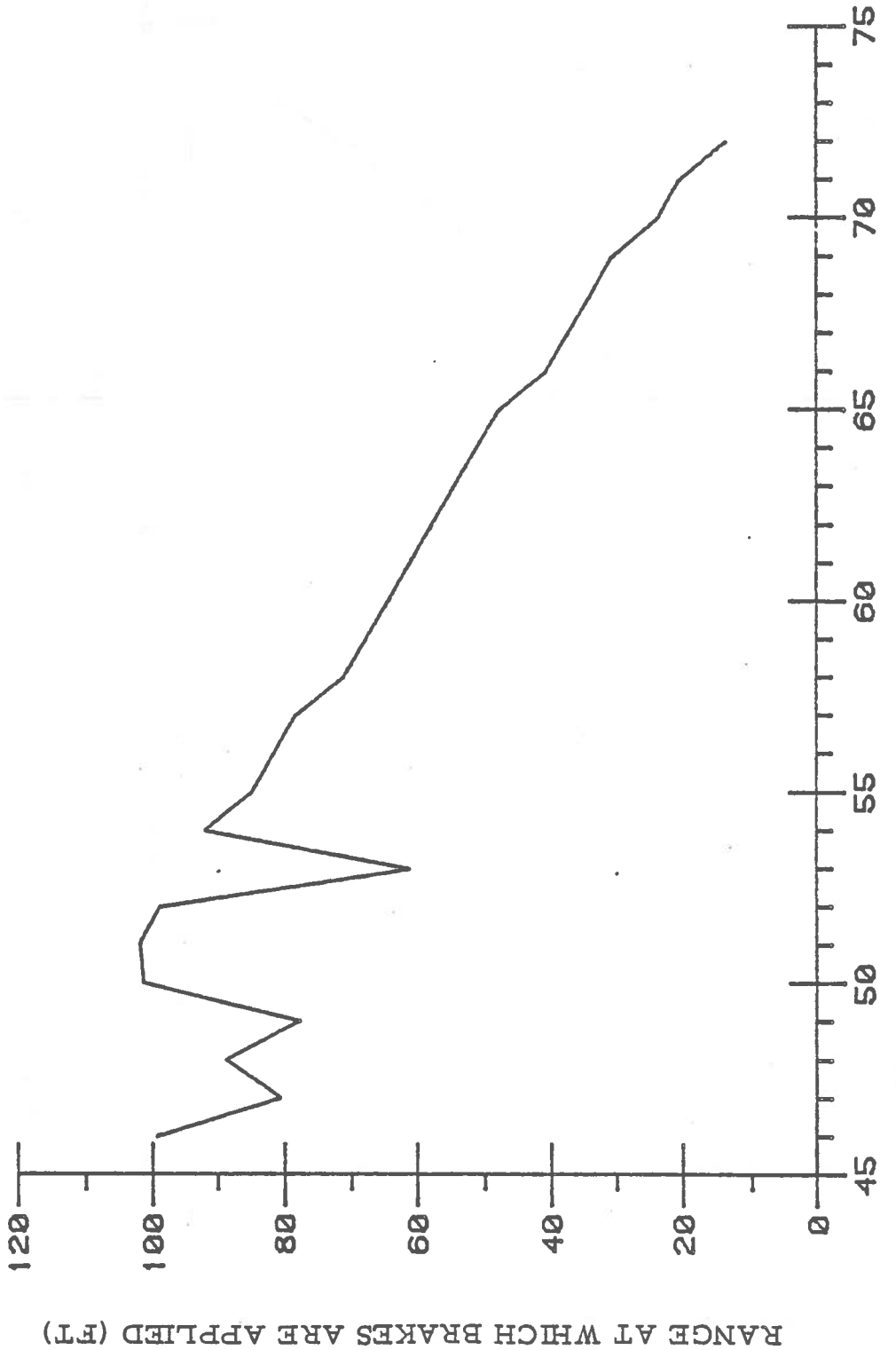

Figure 7.2.15. BENDIX System 4. Car crossing from left lane.

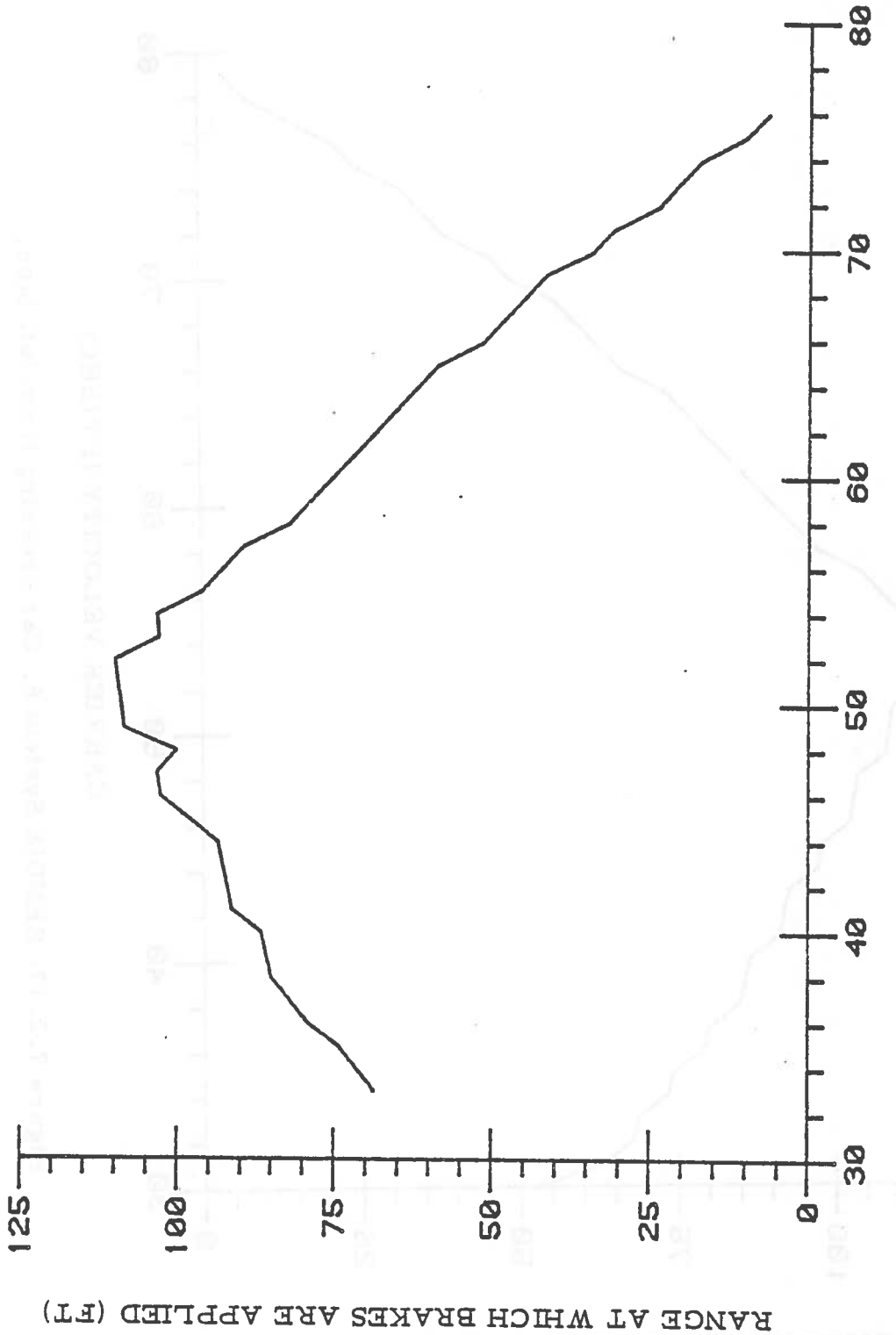

Figure 7.2.16: BENDIX System 5. Car crossing from left lane.

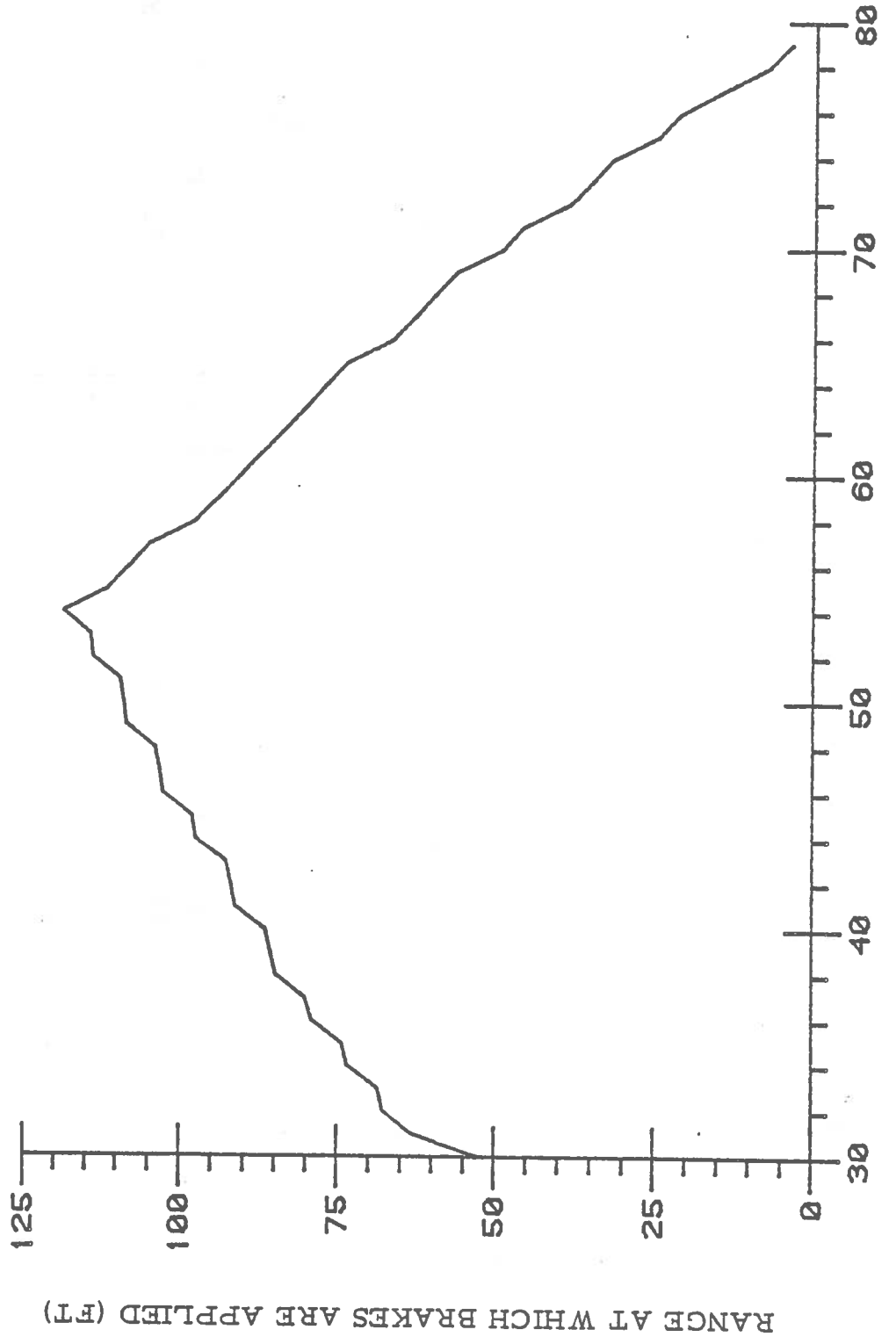

Figure 7.2.17. BENDIX System 6. Car crossing from left lane.

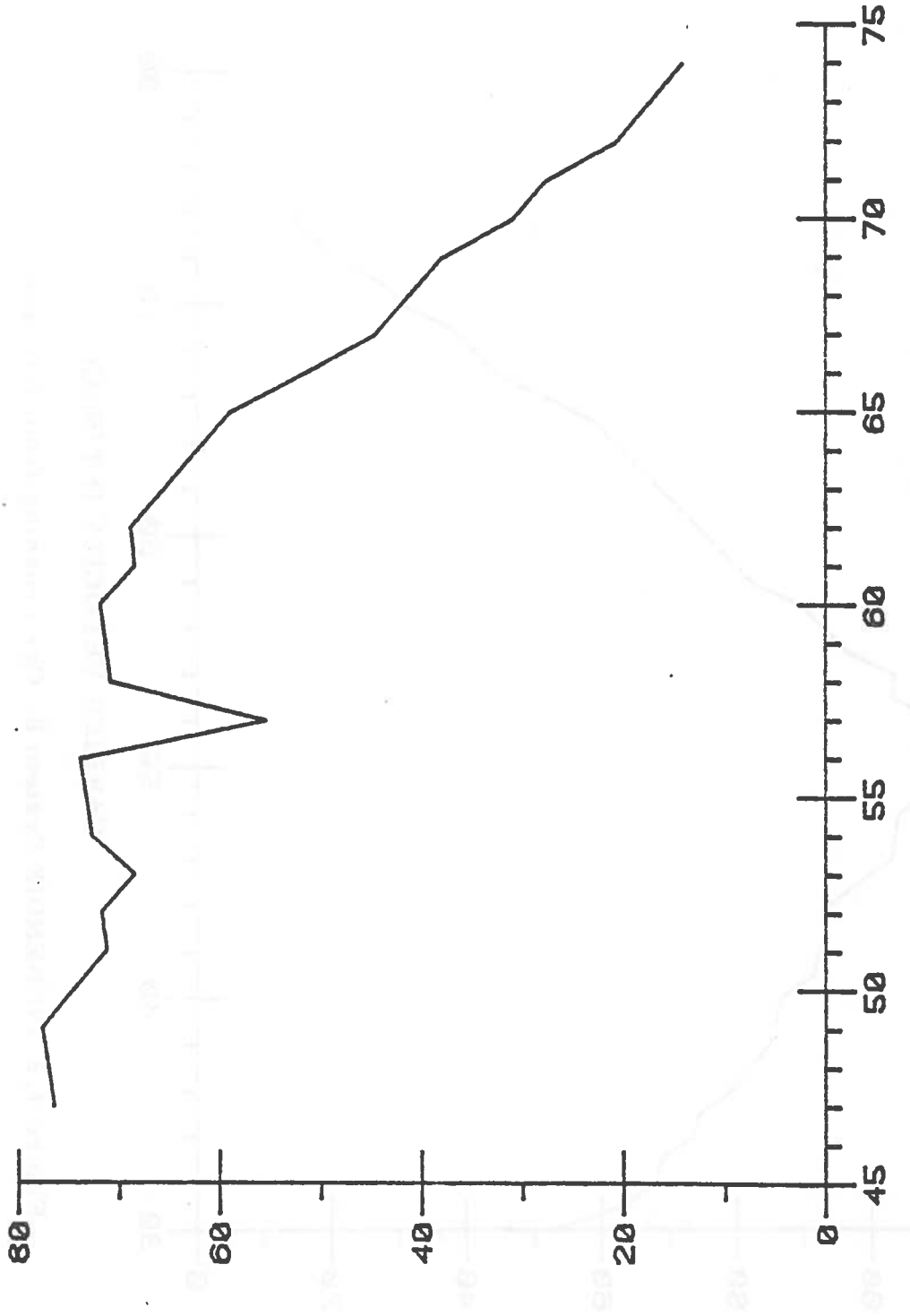

Figure 7.2.18: BENDIX System 7. Car crossing from left lane.

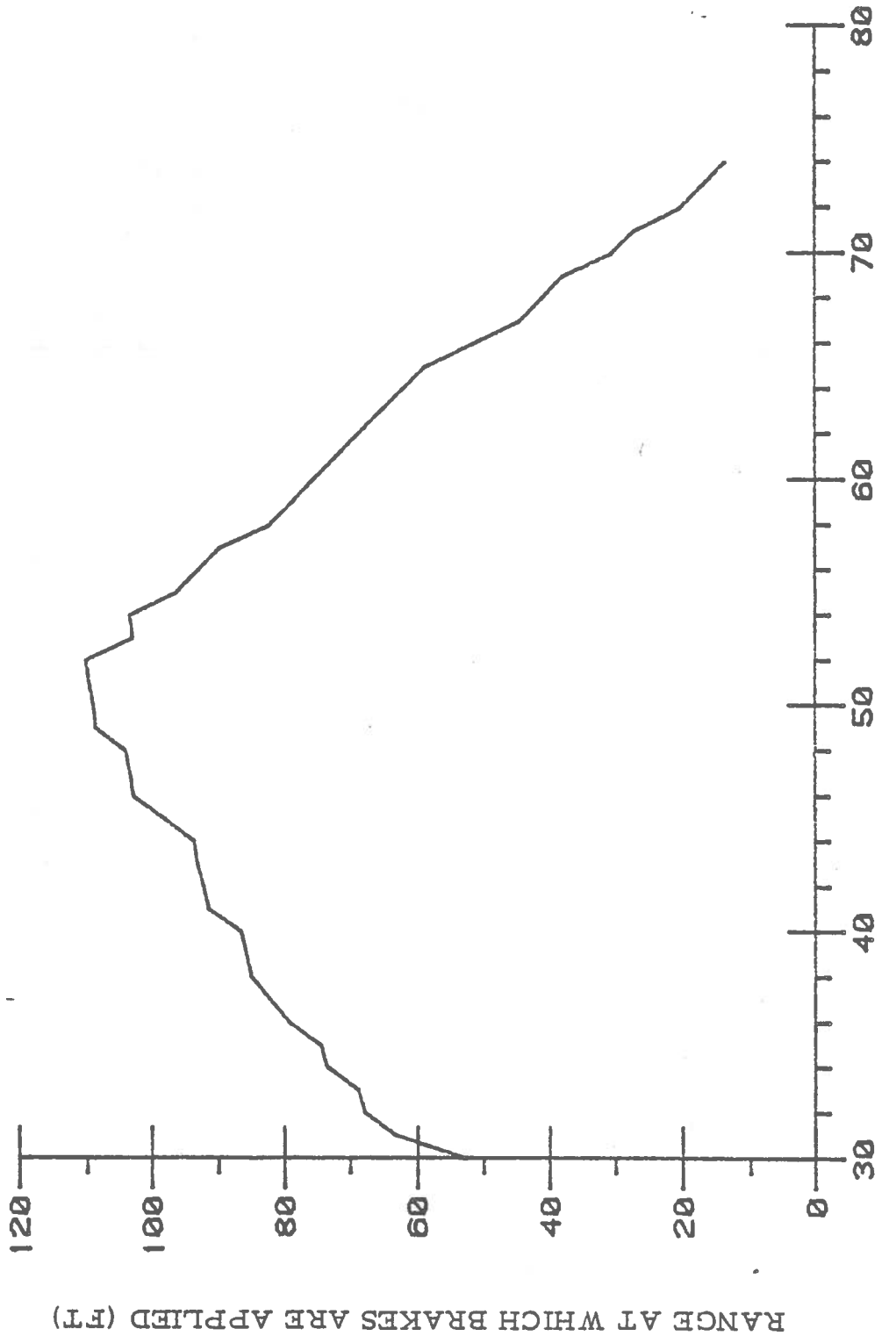

Figure 7.2.19: BENDIX System 8. Car crossing from left lane.

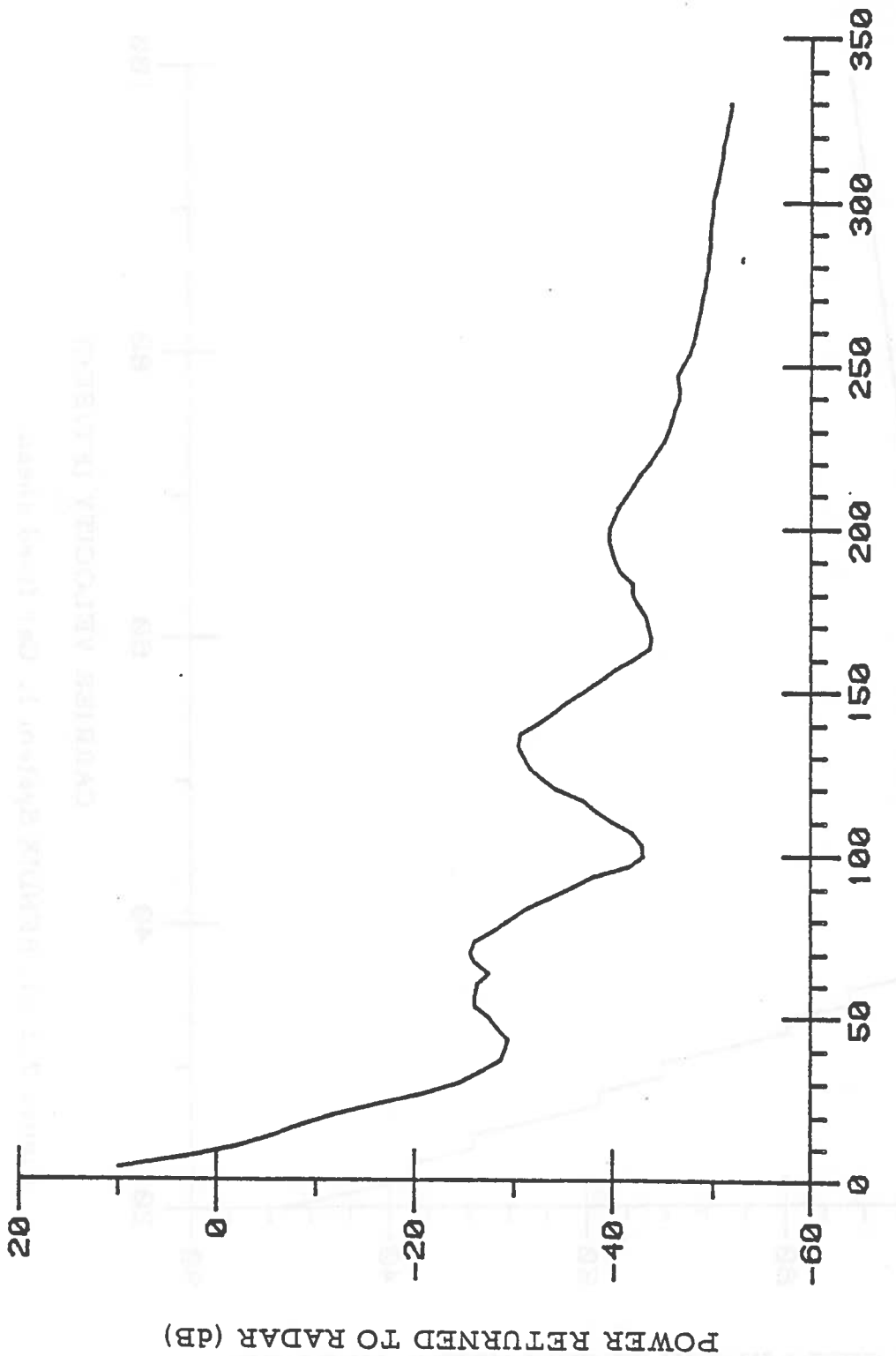

Figure 7.2.20: BENDIX System. Car fixed ahead, with Vcar=40 ft/sec, and RCO=200 ft.

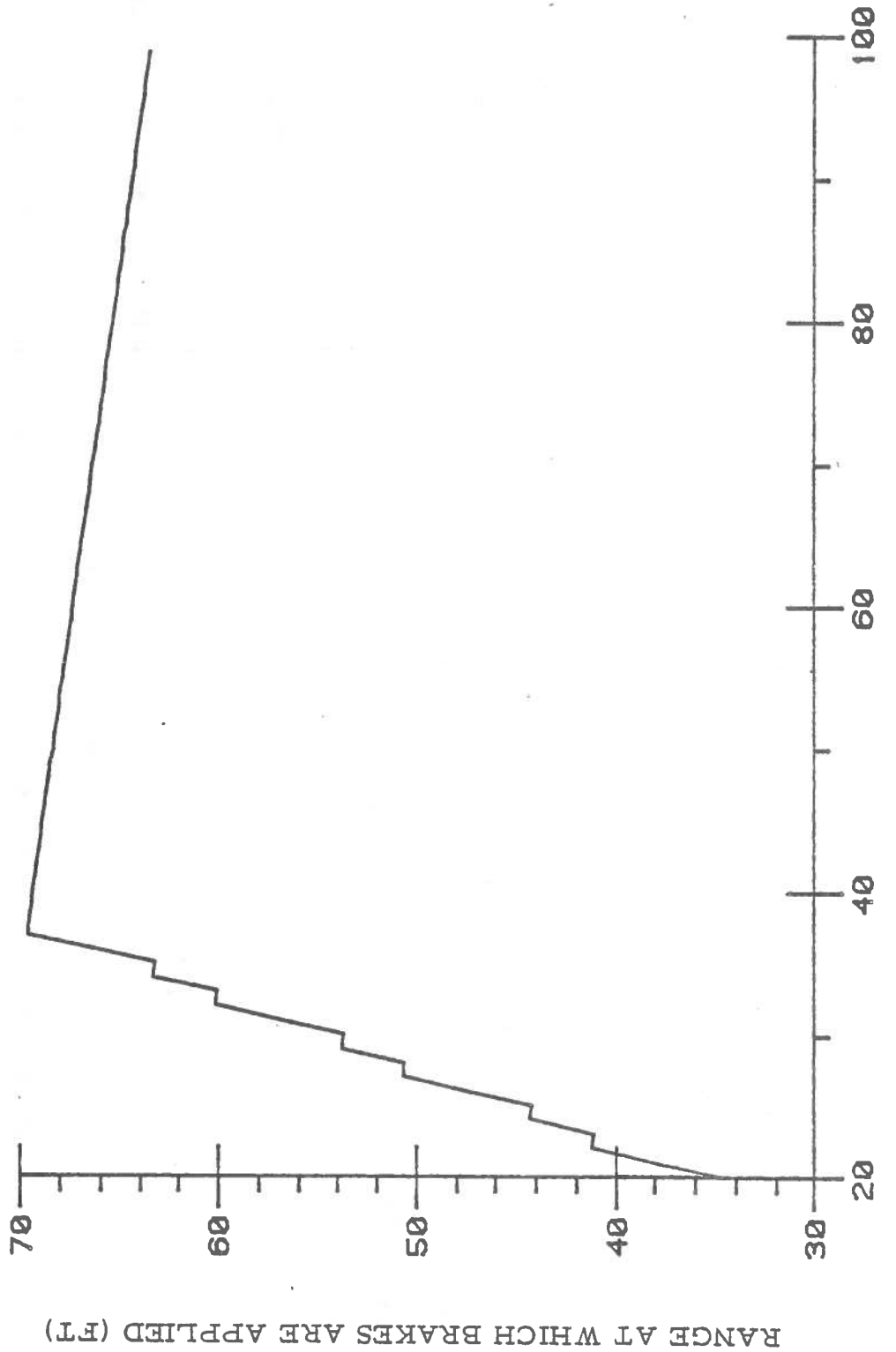

Figure 7.2.21: BENDIX System 1. Car fixed ahead.

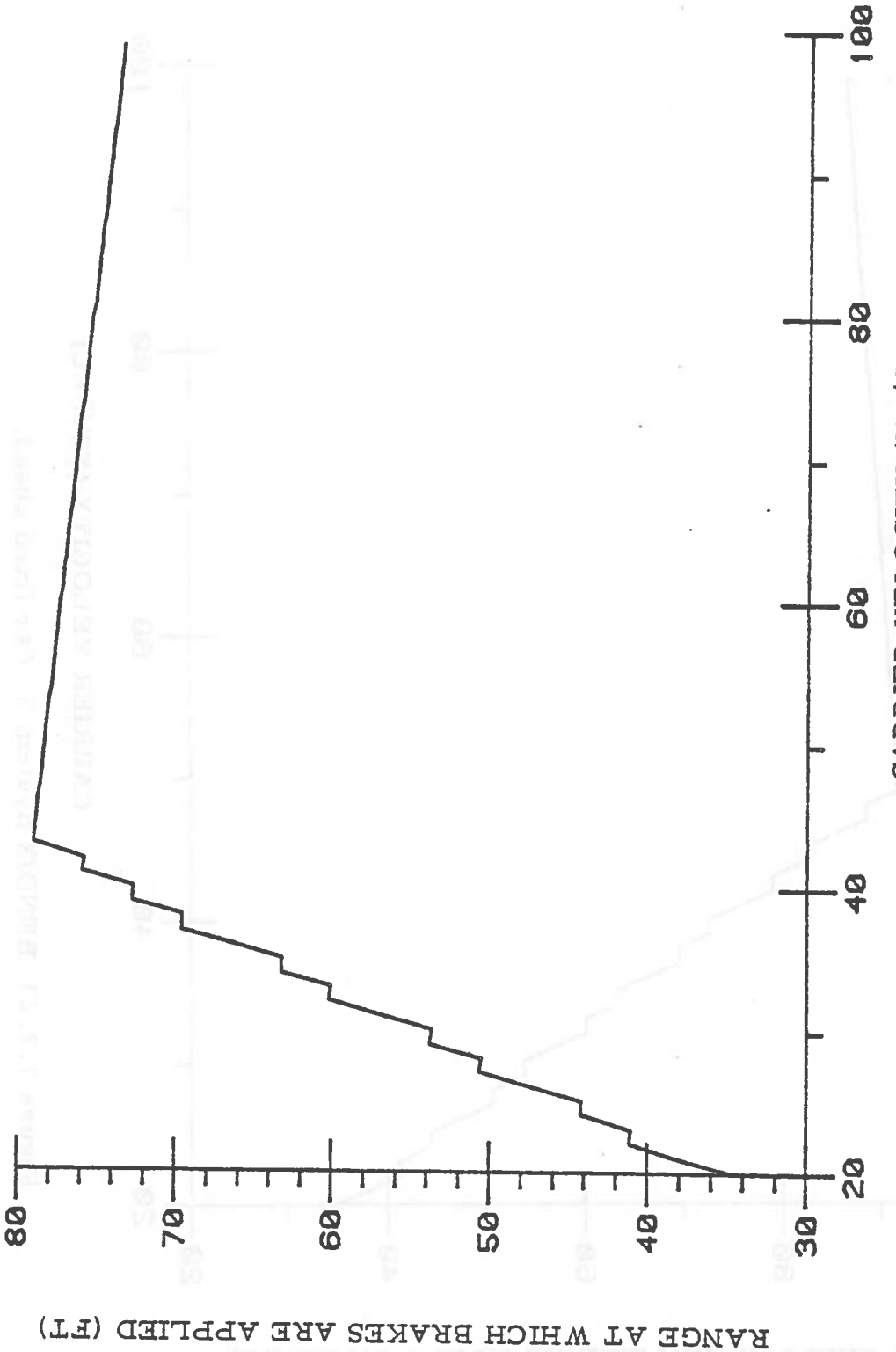

Figure 7.2.22: BENDIX System 2. Car fixed ahead.

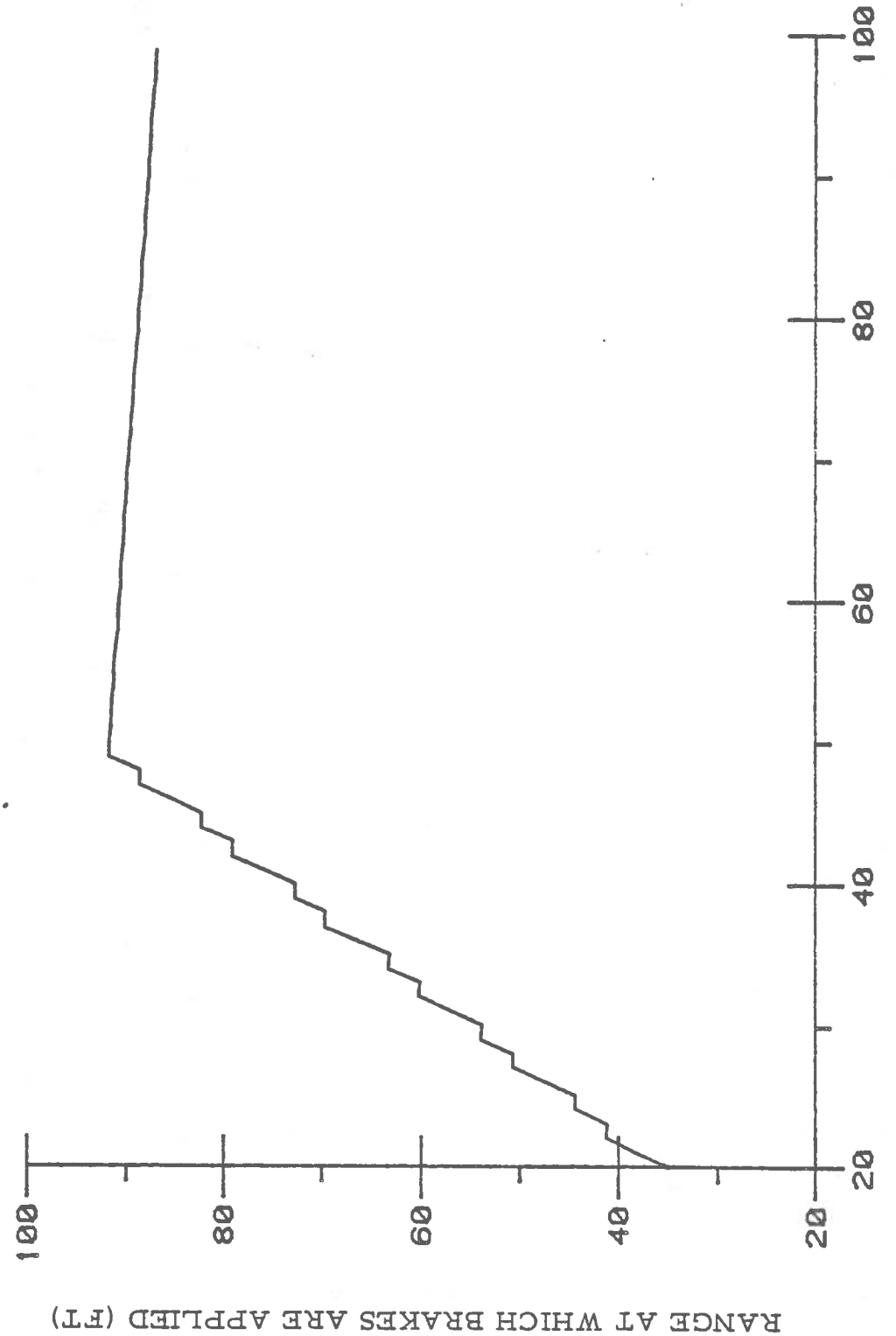

Figure 7.2.23: BENDIX System 3. Car fixed ahead.

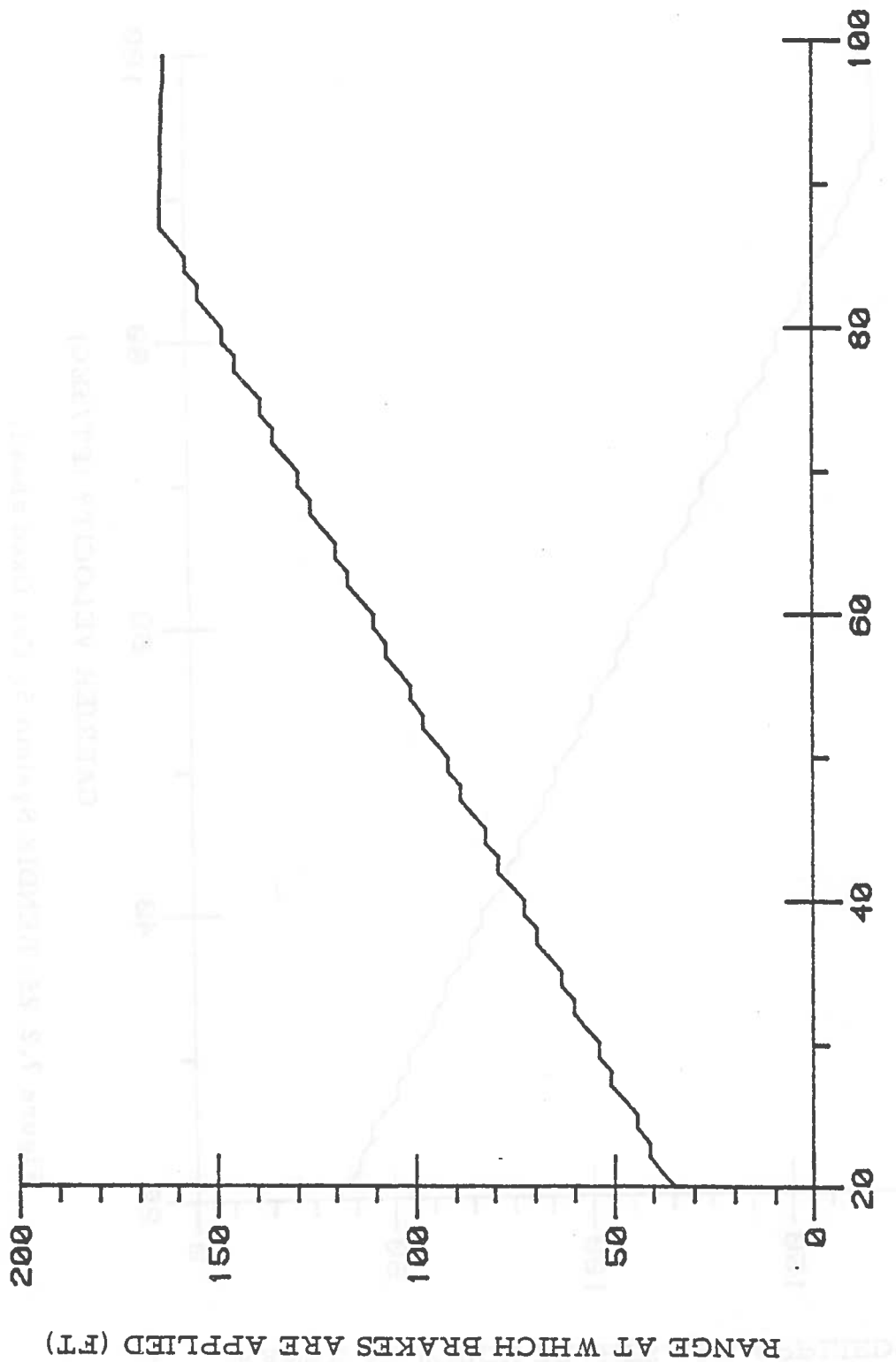

Figure 7.2.24: BENDIX System 4. Car fixed ahead.

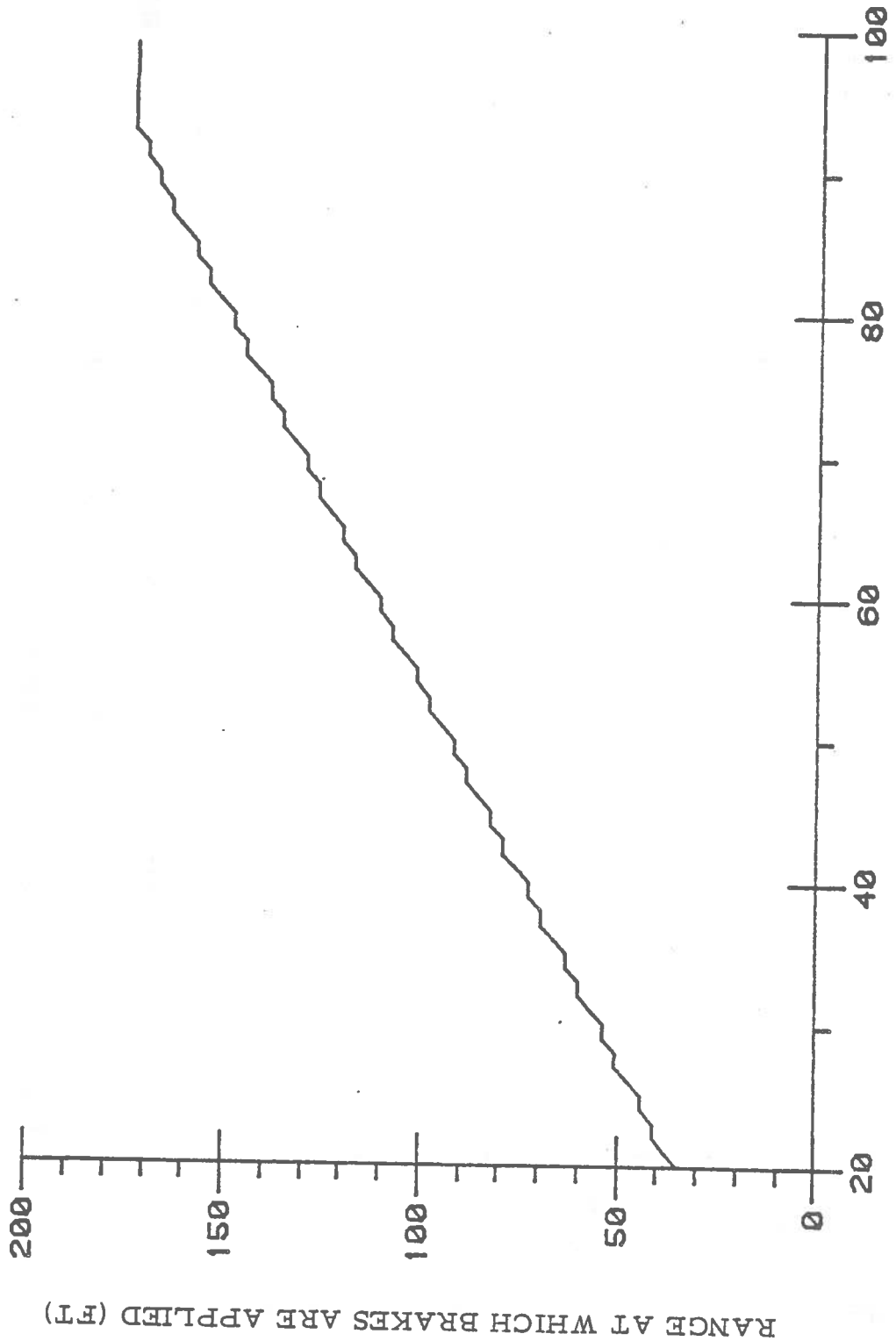

Figure 7.2.25: BENDIX System 5. Car fixed ahead.

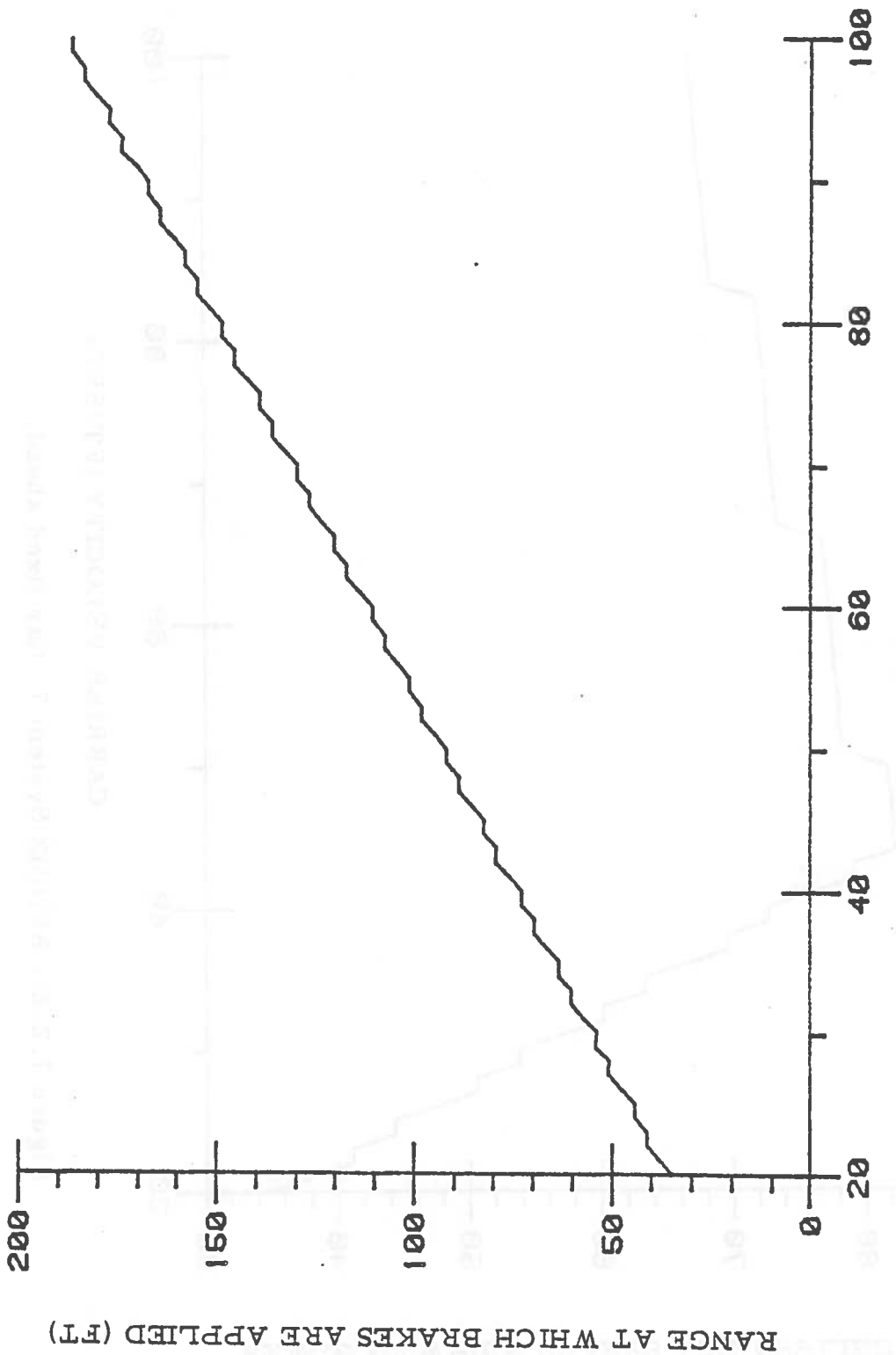

Figure 7.2.26: BENDIX System 6. Car fixed ahead.

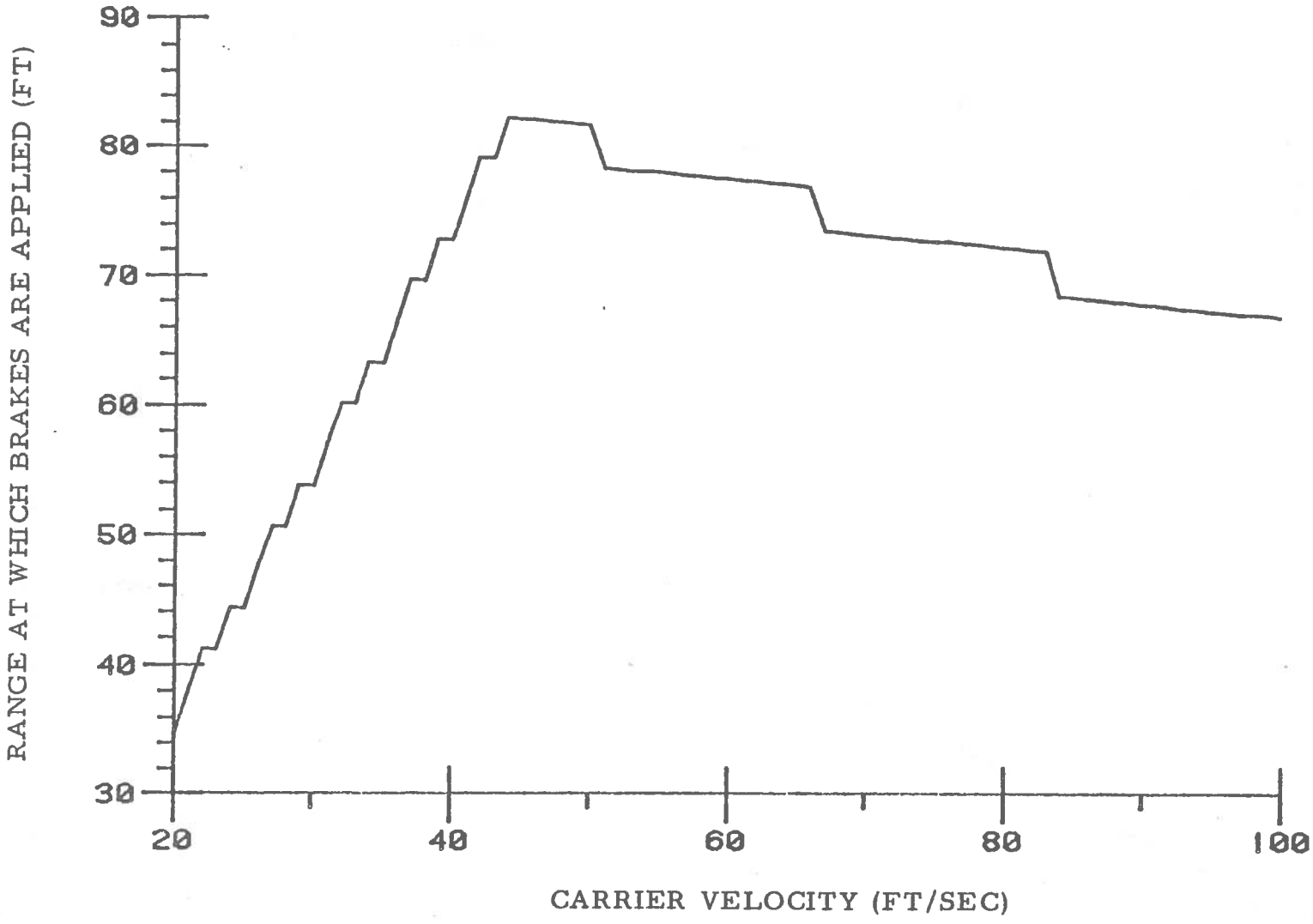

Figure 7.2.27: BENDIX System 7. Car fixed ahead.

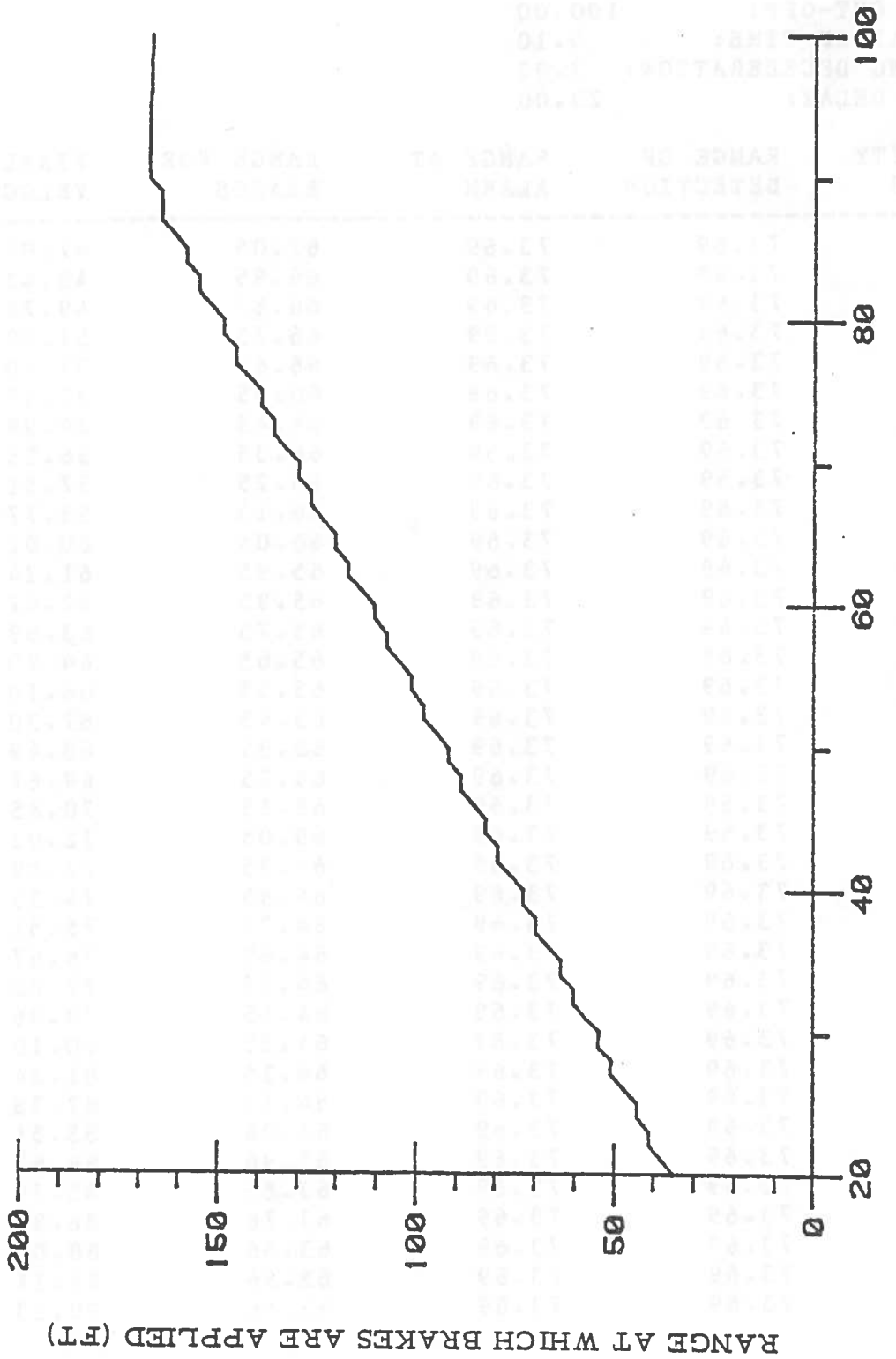

Figure 7.2.28: BENDIX System 8. Car fixed ahead.

Table 6: BENDIX System # 1. Car fixed ahead.

RANGE CUT-OFF: 100.00
ACTIVATION TIME: 0.10
BRAKING DECELERATION: 3.92
RADAR DELAY: 23.00

VELOCITY OF CAR	RANGE OF DETECTION	RANGE AT ALARM	RANGE FOR BRAKES	FINAL VELOCITY
63.00	73.69	73.69	67.05	47.06
64.00	73.69	73.69	66.95	48.42
65.00	73.69	73.69	66.85	49.76
66.00	73.69	73.69	66.75	51.09
67.00	73.69	73.69	66.65	52.40
68.00	73.69	73.69	66.55	53.69
69.00	73.69	73.69	66.45	54.98
70.00	73.69	73.69	66.35	56.25
71.00	73.69	73.69	66.25	57.51
72.00	73.69	73.69	66.15	58.77
73.00	73.69	73.69	66.05	60.01
74.00	73.69	73.69	65.95	61.24
75.00	73.69	73.69	65.85	62.47
76.00	73.69	73.69	65.75	63.69
77.00	73.69	73.69	65.65	64.90
78.00	73.69	73.69	65.55	66.10
79.00	73.69	73.69	65.45	67.30
80.00	73.69	73.69	65.35	68.49
81.00	73.69	73.69	65.25	69.67
82.00	73.69	73.69	65.15	70.85
83.00	73.69	73.69	65.05	72.02
84.00	73.69	73.69	64.95	73.19
85.00	73.69	73.69	64.85	74.35
86.00	73.69	73.69	64.75	75.51
87.00	73.69	73.69	64.65	76.67
88.00	73.69	73.69	64.55	77.82
89.00	73.69	73.69	64.45	78.96
90.00	73.69	73.69	64.35	80.10
91.00	73.69	73.69	64.25	81.24
92.00	73.69	73.69	64.15	82.38
93.00	73.69	73.69	64.06	83.51
94.00	73.69	73.69	63.96	84.63
95.00	73.69	73.69	63.86	85.76
96.00	73.69	73.69	63.76	86.88
97.00	73.69	73.69	63.66	88.00
98.00	73.69	73.69	63.56	89.11
99.00	73.69	73.69	63.46	90.23

Table 7: BENDIX System # 2. Car fixed ahead.

RANGE CUT-OFF: 100.00
ACTIVATION TIME: 0.10
BRAKING DECELERATION: 3.92
RADAR DELAY: 11.50

VELOCITY OF CAR	RANGE OF DETECTION	RANGE AT ALARM	RANGE FOR BRAKES	FINAL VELOCITY
63.00	85.18	85.18	77.05	44.20
64.00	85.18	85.18	76.95	45.64
65.00	85.18	85.18	76.85	47.06
66.00	85.18	85.18	76.75	48.46
67.00	85.18	85.18	76.65	49.84
68.00	85.18	85.18	76.55	51.20
69.00	85.18	85.18	76.45	52.55
70.00	85.18	85.18	76.35	53.88
71.00	85.18	85.18	76.25	55.19
72.00	85.18	85.18	76.15	56.50
73.00	85.18	85.18	76.05	57.79
74.00	85.18	85.18	75.95	59.07
75.00	85.18	85.18	75.85	60.34
76.00	85.18	85.18	75.75	61.60
77.00	85.18	85.18	75.65	62.85
78.00	85.18	85.18	75.55	64.09
79.00	85.18	85.18	75.45	65.32
80.00	85.18	85.18	75.35	66.55
81.00	85.18	85.18	75.25	67.77
82.00	85.18	85.18	75.15	68.98
83.00	85.18	85.18	75.05	70.18
84.00	85.18	85.18	74.95	71.38
85.00	85.18	85.18	74.85	72.57
86.00	85.18	85.18	74.75	73.76
87.00	85.18	85.18	74.65	74.94
88.00	85.18	85.18	74.55	76.12
89.00	85.18	85.18	74.45	77.29
90.00	85.18	85.18	74.35	78.45
91.00	85.18	85.18	74.25	79.62
92.00	85.18	85.18	74.15	80.77
93.00	85.18	85.18	74.05	81.93
94.00	85.18	85.18	73.95	83.07
95.00	85.18	85.18	73.85	84.22
96.00	85.18	85.18	73.75	85.36
97.00	85.18	85.18	73.65	86.50
98.00	85.18	85.18	73.55	87.63
99.00	85.18	85.18	73.45	88.77

Table 8: BENDIX System # 3. Car fixed ahead.

RANGE CUT-OFF: 100.00
ACTIVATION TIME: 0.10
BRAKING DECELERATION: 3.92
RADAR DELAY: 0.00

VELOCITY OF CAR	RANGE OF DETECTION	RANGE AT ALARM	RANGE FOR BRAKES	FINAL VELOCITY
63.00	96.68	96.68	90.38	40.06
64.00	96.68	96.68	90.28	41.64
65.00	96.68	96.68	90.18	43.20
66.00	96.68	96.68	90.08	44.72
67.00	96.68	96.68	89.98	46.21
68.00	96.68	96.68	89.88	47.67
69.00	96.68	96.68	89.78	49.12
70.00	96.68	96.68	89.68	50.54
71.00	96.68	96.68	89.58	51.94
72.00	96.68	96.68	89.48	53.32
73.00	96.68	96.68	89.38	54.69
74.00	96.68	96.68	89.28	56.04
75.00	96.68	96.68	89.18	57.38
76.00	96.68	96.68	89.08	58.70
77.00	96.68	96.68	88.98	60.01
78.00	96.68	96.68	88.88	61.31
79.00	96.68	96.68	88.78	62.60
80.00	96.68	96.68	88.68	63.88
81.00	96.68	96.68	88.58	65.14
82.00	96.68	96.68	88.48	66.40
83.00	96.68	96.68	88.38	67.65
84.00	96.68	96.68	88.28	68.90
85.00	96.68	96.68	88.18	70.13
86.00	96.68	96.68	88.08	71.36
87.00	96.68	96.68	87.98	72.58
88.00	96.68	96.68	87.88	73.79
89.00	96.68	96.68	87.78	75.00
90.00	96.68	96.68	87.68	76.20
91.00	96.68	96.68	87.58	77.39
92.00	96.68	96.68	87.48	78.58
93.00	96.68	96.68	87.38	79.77
94.00	96.68	96.68	87.28	80.95
95.00	96.68	96.68	87.18	82.12
96.00	96.68	96.68	87.08	83.29
97.00	96.68	96.68	86.98	84.46
98.00	96.68	96.68	86.88	85.62
99.00	96.68	96.68	86.78	86.78

Table 9: BENDIX System # 4. Car fixed ahead.

RANGE CUT-OFF: 200.00
ACTIVATION TIME: 0.10
BRAKING DECELERATION: 3.92
RADAR DELAY: 23.00

VELOCITY OF CAR	RANGE OF DETECTION	RANGE AT ALARM	RANGE FOR BRAKES	FINAL VELOCITY
63.00	173.67	123.34	117.05	30.12
64.00	173.67	126.68	120.28	30.81
65.00	173.67	126.68	120.18	32.88
66.00	173.67	130.01	123.41	33.58
67.00	173.67	133.34	126.64	34.29
68.00	173.67	133.34	126.54	36.24
69.00	173.67	136.68	129.78	36.96
70.00	173.67	136.68	129.68	38.83
71.00	173.67	140.01	132.91	39.55
72.00	173.67	143.34	136.14	40.28
73.00	173.67	143.34	136.04	42.07
74.00	173.67	146.68	139.28	42.81
75.00	173.67	146.68	139.18	44.54
76.00	173.67	150.01	142.41	45.28
77.00	173.67	153.34	145.64	46.03
78.00	173.67	153.34	145.54	47.71
79.00	173.67	156.68	148.78	48.47
80.00	173.67	156.68	148.68	50.11
81.00	173.67	160.01	151.91	50.86
82.00	173.67	163.34	155.14	51.63
83.00	173.67	163.34	155.04	53.23
84.00	173.67	166.67	158.28	54.00
85.00	173.67	166.67	158.18	55.56
86.00	173.67	170.01	161.41	56.33
87.00	173.67	173.67	164.64	57.11
88.00	173.67	173.67	164.54	58.65
89.00	173.67	173.67	164.44	60.16
90.00	173.67	173.67	164.34	61.65
91.00	173.67	173.67	164.24	63.12
92.00	173.67	173.67	164.14	64.58
93.00	173.67	173.67	164.04	66.01
94.00	173.67	173.67	163.94	67.43
95.00	173.67	173.67	163.84	68.84
96.00	173.67	173.67	163.74	70.23
97.00	173.67	173.67	163.64	71.61
98.00	173.67	173.67	163.54	72.98
99.00	173.67	173.67	163.44	74.33

Table 10: BENDIX System # 5. Car fixed ahead.

RANGE CUT-OFF: 200.00
ACTIVATION TIME: 0.10
BRAKING DECELERATION: 3.92
RADAR DELAY: 11.50

VELOCITY OF CAR	RANGE OF DETECTION	RANGE AT ALARM	RANGE FOR BRAKES	FINAL VELOCITY
63.00	185.17	123.34	117.05	30.12
64.00	185.17	126.68	120.28	30.81
65.00	185.17	126.68	120.18	32.88
66.00	185.17	130.01	123.41	33.58
67.00	185.17	133.34	126.64	34.29
68.00	185.17	133.34	126.54	36.24
69.00	185.17	136.68	129.78	36.96
70.00	185.17	136.68	129.68	38.83
71.00	185.17	140.01	132.91	39.55
72.00	185.17	143.34	136.14	40.28
73.00	185.17	143.34	136.04	42.07
74.00	185.17	146.68	139.28	42.81
75.00	185.17	146.68	139.18	44.54
76.00	185.17	150.01	142.41	45.28
77.00	185.17	153.34	145.64	46.03
78.00	185.17	153.34	145.54	47.71
79.00	185.17	156.68	148.78	48.47
80.00	185.17	156.68	148.68	50.11
81.00	185.17	160.01	151.91	50.86
82.00	185.17	163.34	155.14	51.63
83.00	185.17	163.34	155.04	53.23
84.00	185.17	166.67	158.28	54.00
85.00	185.17	166.67	158.18	55.56
86.00	185.17	170.01	161.41	56.33
87.00	185.17	173.34	164.64	57.11
88.00	185.17	173.34	164.54	58.65
89.00	185.17	176.67	167.77	59.43
90.00	185.17	176.67	167.67	60.94
91.00	185.17	180.01	170.91	61.73
92.00	185.17	180.01	170.81	63.21
93.00	185.17	185.17	174.04	64.00
94.00	185.17	185.17	173.94	65.47
95.00	185.17	185.17	173.84	66.91
96.00	185.17	185.17	173.74	68.34
97.00	185.17	185.17	173.64	69.76
98.00	185.17	185.17	173.54	71.16
99.00	185.17	185.17	173.44	72.55

Table 11: BENDIX System # 6. Car fixed ahead.

RANGE CUT-OFF: 200.00
ACTIVATION TIME: 0.10
BRAKING DECELERATION: 3.92
RADAR DELAY: 0.00

VELOCITY OF CAR	RANGE OF DETECTION	RANGE AT ALARM	RANGE FOR BRAKES	FINAL VELOCITY
20.00	196.67	36.70	34.71	0.00
21.00	196.67	40.03	37.94	0.00
22.00	196.67	43.37	41.17	0.00
23.00	196.67	43.37	41.07	0.00
24.00	196.67	46.70	44.30	0.00
25.00	196.67	46.70	44.20	0.00
26.00	196.67	50.03	47.43	0.00
27.00	196.67	53.36	50.66	0.00
28.00	196.67	53.36	50.56	0.00
29.00	196.67	56.69	53.79	0.00
30.00	196.67	56.69	53.69	0.00
31.00	196.67	60.02	56.92	0.00
32.00	196.67	63.36	60.16	0.00
33.00	196.67	63.36	60.06	0.00
34.00	196.67	66.69	63.29	0.00
35.00	196.67	66.69	63.19	0.00
36.00	196.67	70.02	66.42	0.00
37.00	196.67	73.35	69.65	0.00
38.00	196.67	73.35	69.55	0.00
39.00	196.67	76.68	72.79	0.00
40.00	196.67	76.68	72.69	0.00
41.00	196.67	80.02	75.92	0.00
42.00	196.67	83.35	79.15	0.00
43.00	196.67	83.35	79.05	0.00
44.00	196.67	86.68	82.28	0.00
45.00	196.67	86.68	82.18	0.00
46.00	196.67	90.02	85.42	0.00
47.00	196.67	93.35	88.65	0.00
48.00	196.67	93.35	88.55	0.00
49.00	196.67	96.68	91.78	0.00
50.00	196.67	96.68	91.68	10.08
51.00	196.67	100.01	94.91	10.86
52.00	196.67	103.35	98.15	11.68
53.00	196.67	103.35	98.05	15.62
54.00	196.67	106.68	101.28	16.33
55.00	196.67	106.68	101.18	19.45
56.00	196.67	110.01	104.41	20.11
57.00	196.67	113.35	107.65	20.81
58.00	196.67	113.35	107.55	23.46
59.00	196.67	116.68	110.78	24.15
60.00	196.67	116.68	110.68	26.54
61.00	196.67	120.01	113.91	27.22
62.00	196.67	123.34	117.15	27.92

Table 12: BENDIX System # 7. Car fixed ahead.

RANGE CUT-OFF:	100.00
ACTIVATION TIME:	0.10
BRAKING DECELERATION:	3.92
RADAR DELAY:	0.20

VELOCITY OF CAR	RANGE OF DETECTION	RANGE AT ALARM	RANGE FOR BRAKES	FINAL VELOCITY
63.00	84.08	84.08	77.05	44.20
64.00	83.88	83.88	76.95	45.64
65.00	83.68	83.68	76.85	47.06
66.00	83.48	83.48	76.75	48.46
67.00	83.28	83.28	73.32	50.70
68.00	83.08	83.08	73.22	52.04
69.00	82.88	82.88	73.12	53.37
70.00	82.68	82.68	73.02	54.68
71.00	82.48	82.48	72.92	55.98
72.00	82.28	82.28	72.82	57.26
73.00	82.08	82.08	72.72	58.54
74.00	81.88	81.88	72.62	59.80
75.00	81.68	81.68	72.52	61.06
76.00	81.48	81.48	72.42	62.30
77.00	81.28	81.28	72.32	63.54
78.00	81.08	81.08	72.22	64.77
79.00	80.88	80.88	72.12	65.99
80.00	80.68	80.68	72.02	67.20
81.00	80.48	80.48	71.92	68.41
82.00	80.28	80.28	71.82	69.61
83.00	80.08	80.08	71.72	70.80
84.00	79.88	79.88	68.29	72.59
85.00	79.68	79.68	68.19	73.76
86.00	79.48	79.48	68.09	74.93
87.00	79.28	79.28	67.99	76.09
88.00	79.08	79.08	67.89	77.25
89.00	78.88	78.88	67.79	78.41
90.00	78.68	78.68	67.69	79.56
91.00	78.48	78.48	67.59	80.70
92.00	78.28	78.28	67.49	81.84
93.00	78.08	78.08	67.39	82.98
94.00	77.88	77.88	67.29	84.12
95.00	77.68	77.68	67.19	85.25
96.00	77.48	77.48	67.09	86.38
97.00	77.28	77.28	66.99	87.50
98.00	77.08	77.08	66.89	88.62
99.00	76.88	76.88	66.79	89.74

Table 13: BENDIX System # 8. Car fixed ahead.

RANGE CUT-OFF: 200.00
ACTIVATION TIME: 0.10
BRAKING DECELERATION: 3.92
RADAR DELAY: 0.20

VELOCITY OF CAR	RANGE OF DETECTION	RANGE AT ALARM	RANGE FOR BRAKES	FINAL VELOCITY
63.00	184.07	123.34	117.05	30.12
64.00	183.87	126.68	120.28	30.81
65.00	183.67	126.68	120.18	32.88
66.00	183.47	130.01	123.41	33.58
67.00	183.27	133.34	126.64	34.29
68.00	183.07	133.34	126.54	36.24
69.00	182.87	136.68	129.78	36.96
70.00	182.67	136.68	129.68	38.83
71.00	182.47	140.01	132.91	39.55
72.00	182.27	143.34	136.14	40.28
73.00	182.07	143.34	136.04	42.07
74.00	181.87	146.68	139.28	42.81
75.00	181.67	146.68	139.18	44.54
76.00	181.47	150.01	142.41	45.28
77.00	181.27	153.34	145.64	46.03
78.00	181.07	153.34	145.54	47.71
79.00	180.87	156.68	148.78	48.47
80.00	180.67	156.68	148.68	50.11
81.00	180.47	160.01	151.91	50.86
82.00	180.27	163.34	155.14	51.63
83.00	180.07	163.34	155.04	53.23
84.00	179.87	166.67	158.28	54.00
85.00	179.67	166.67	158.18	55.56
86.00	179.47	170.01	161.41	56.33
87.00	179.27	173.34	164.64	57.11
88.00	179.07	173.34	164.54	58.65
89.00	178.87	173.34	164.44	60.16
90.00	178.67	178.67	167.67	60.94
91.00	178.47	178.47	167.57	62.43
92.00	178.27	178.27	167.47	63.90
93.00	178.07	178.07	167.37	65.35
94.00	177.87	177.87	167.27	66.78
95.00	177.67	177.67	167.17	68.20
96.00	177.47	177.47	167.07	69.61
97.00	177.27	177.27	166.98	71.00
98.00	177.07	177.07	166.87	72.38
99.00	176.87	176.87	166.78	73.74

fore, the Probability of Detection is greater than 0.99, and the target is detected as soon as Range Cut-Off is reached. At very short ranges, the far-field approximation used in the model is invalid, and the relative signal exceeds 0 dB, but signal magnitude is inconsequential at these distances.

7.3 NISSAN-MITSUBISHI SIMULATION

7.3.1 Radar System

The Nissan-Mitsubishi system is a pulse-Doppler radar operating at 24 GHz; its peak power is 20 mW, with a pulse width of 20 ns. The oscillator is a Gunn diode and the detection is superheterodyne. Its maximum range is 120 meters (400 feet).

7.3.2 Detection Parameters

1) Range Cut-Off: range of radar detection is limited on curves, to prevent detection of objects along the road-side. In Nissan's presentation paper, range limitation on straight roads is not mentioned, so "RCO" is supposed to be equal to the maximum range, fixed by the pulse repetition frequency, i.e. 120 meters, or 400 feet.

2) Detection Threshold: no information was available about the Detection Threshold. Therefore, a constant threshold is used, defined as in the Bendix system by the signal returned from a reference cross-section of 139.6 m^2, 300 feet away.

3) Radar Delay: no information was available about Radar Delay. A constant Time Delay "Tdel" of 0.2 sec is used, for it seems to be a reasonable value that should serve to lower the number of false alarms.

4) Activation Time: a driver's mean reaction time "Tact" of 1 sec is used, as suggested in Nissan's report.

5) Breaking Deceleration: typical value of 0.4g, corresponding to a wet road, without anti-lock system, is used by Nissan-Mitsubishi.

6) Radar Control Law: this point is well described in Nissan's presentation. Three different algorithms are used, depending on the circumstances:

- Both leading and following vehicles come to a stop at deceleration "Brd":

$$Rs = Vrel\left[\frac{2Vcar-Vrel}{2Brd}\right] + Vcar \cdot Tact + K \qquad (7.2)$$

Where: Rs = safe interval

Vrel = relative velocity

Vcar = carrier vehicle velocity

Brd = deceleration

Tact = activation time

K = remaining interval

- Leading vehicle comes to a sudden stop:

$$Rs = \frac{Vcar^2}{2Brd} + Vcar \cdot Tact + K \qquad (7.3)$$

- Leading vehicle does not change its velocity, and

following vehicle is approaching at a higher speed:

$$Rs = \frac{Vrel^2}{2Brd} + Vrel \cdot Tact + K \qquad (7.4)$$

A limit to collision avoidance is K=0. which will be assumed in the remainder of this study. This Radar Control Law is a better approximation of the required safe distance than the one proposed by Bendix, and should produce better results. Unfortunately, a rigourous evaluation of the Nissan-Mitsubishi system is not possible, due to a lack of information concerning other parameters, especially the Detection Threshold and the Range Cut-Off, which are of prime importance.

The range limitation in curves seems to be a good way to eliminate spurious echos; experimental studies have shown that the Nissan-Mitsubishi system is much more efficient than the Bendix system, especially in terms of false alarm rate (Dr. Grimes and Dr. Carpenter, private communication).

7.3.3 Results

1) Road Sign: figure 7.3.1 shows that, with a Range Cut-Off of 400 feet, this road sign is detected. The problem here is the same as with Bendix: Range Cut-Offs of more than 100 feet result in many false alarms. Figure 7.3.1 also shows that the Detection Threshold is not very different from Bendix's threshold, despite the use of a much

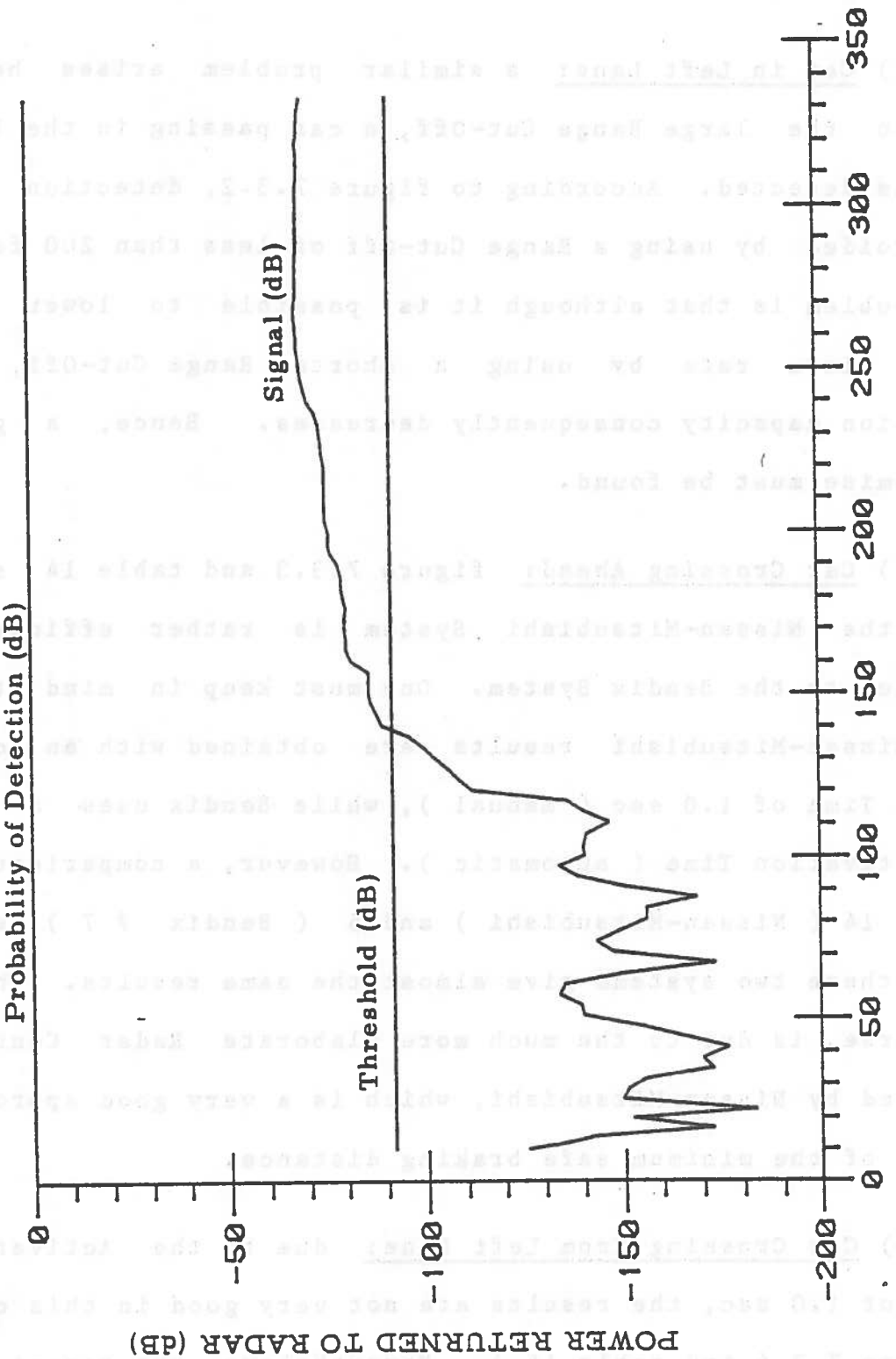

Figure 7.3.1: NISSAN System. Road Sign at Vcar=40 ft/sec

lower frequency. According to this figure, a Range Cut-Off of less than 140 feet must be used to prevent detection of this road sign.

2) Car in Left Lane: a similar problem arises here: due to the large Range Cut-Off, a car passing in the left lane is detected. According to figure 7.3.2, detection can be avoided by using a Range Cut-Off of less than 200 feet. The problem is that although it is possible to lower the false alarm rate by using a shorter Range Cut-Off, the detection capacity consequently decreases. Hence, a good compromise must be found.

3) Car Crossing Ahead: figure 7.3.3 and table 14 show that the Nissan-Mitsubishi System is rather efficient, compared to the Bendix System. One must keep in mind that the Nissan-Mitsubishi results are obtained with an Activation Time of 1.0 sec (manual), while Bendix uses a 0.1 sec Activation Time (automatic). However, a comparison of tables 14 (Nissan-Mitsubishi) and 5 (Bendix # 7) show that these two systems give almost the same results. This, of course, is due to the much more elaborate Radar Control Law used by Nissan-Mitsubishi, which is a very good approximation of the minimum safe braking distance.

4) Car Crossing From Left Lane: due to the Activation Time of 1.0 sec, the results are not very good in this case (figure 7.3.4 and table 15). Nevertheless, the target is detected, and it can be assumed that the use of an automatic

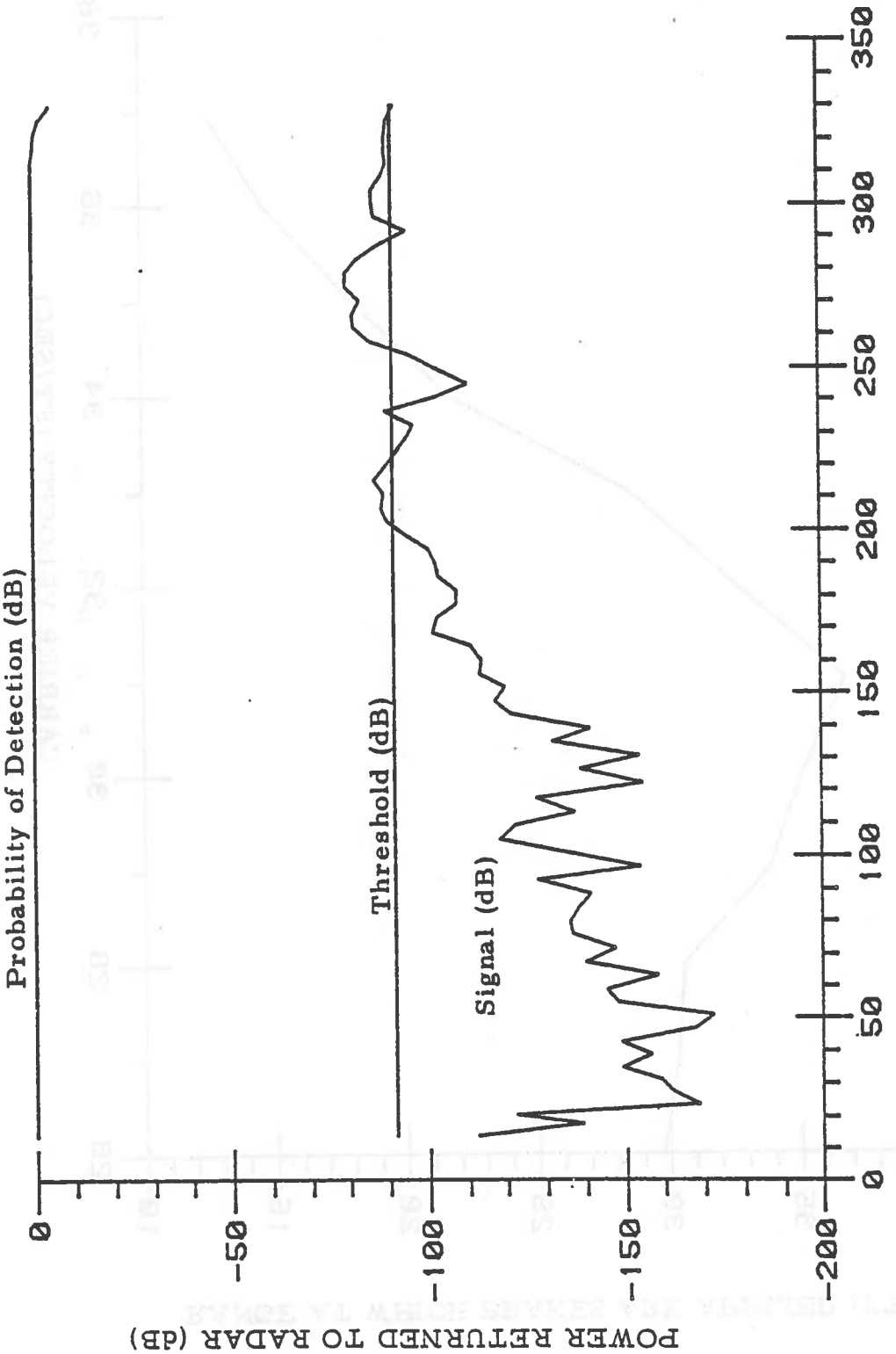

Figure 7.3.2: NISSAN System. Car in left lane, with Vcar=50 ft/sec.

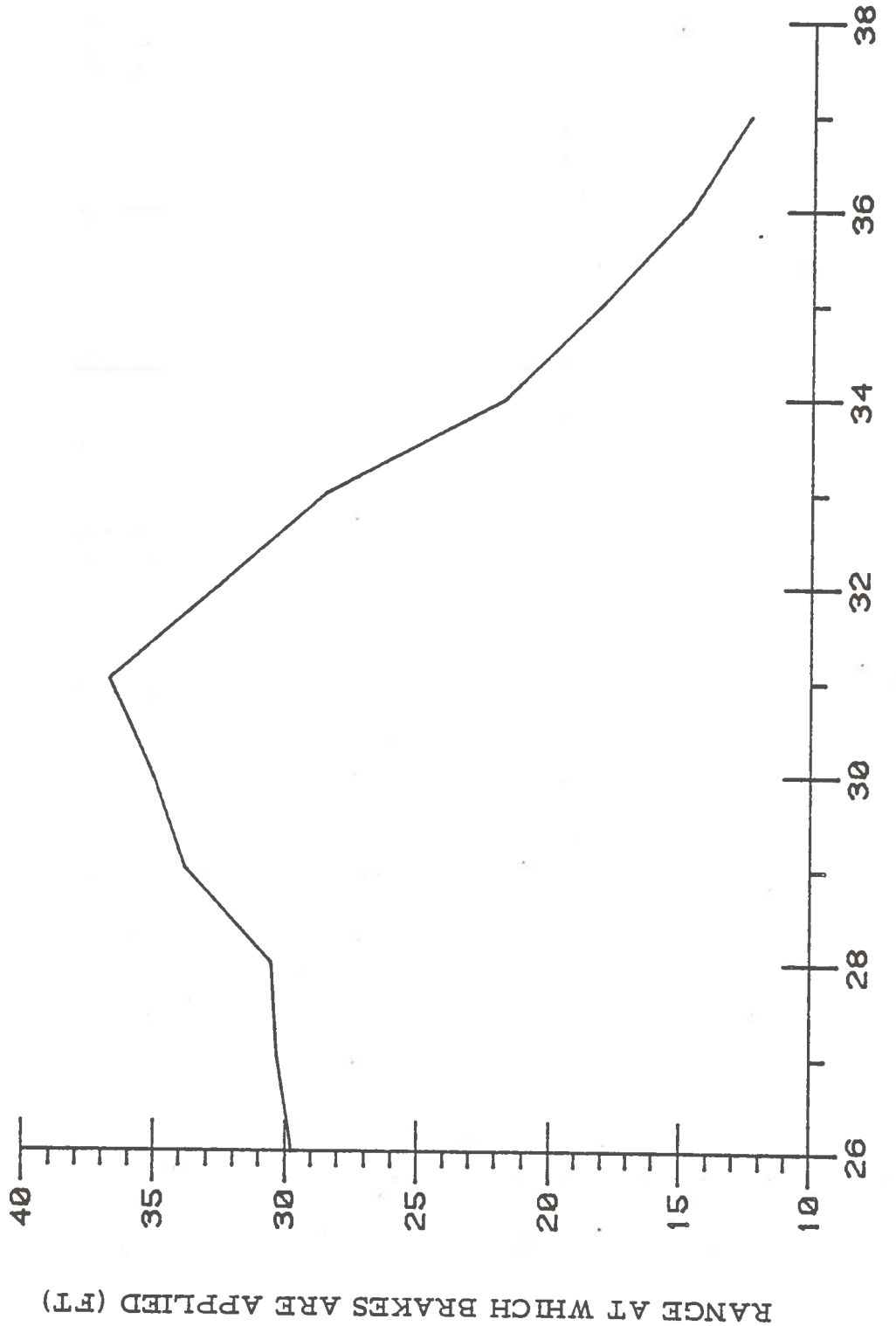

Figure 7.3.3: NISSAN System. Car crossing ahead.

Table 14: NISSAN System. Car crossing ahead.

RANGE CUT-OFF: 400.00
ACTIVATION TIME: 1.00
BRAKING DECELERATION: 3.92
RADAR DELAY: 0.20

VELOCITY OF CAR	RANGE OF DETECTION	RANGE AT ALARM	RANGE FOR BRAKES	FINAL VELOCITY
24.00	92.03	NO ALARM		
25.00	88.37	NO ALARM		
26.00	84.83	45.60	29.73	0.00
27.00	81.30	50.99	30.30	0.00
28.00	77.77	53.84	30.58	0.00
29.00	74.23	60.12	33.82	0.00
30.00	70.70	63.36	35.10	0.00
31.00	67.17	67.17	36.78	0.00
32.00	63.63	63.63	32.62	13.06
33.00	60.10	60.10	28.51	18.53
34.00	56.56	56.56	21.73	24.24
35.00	53.03	53.03	18.05	27.44
36.00	49.49	49.49	14.70	30.19
37.00	45.96	45.96	12.47	32.29
38.00	39.10	39.10	BRAKES NOT ACTIVATED	
39.00	35.88	35.88	BRAKES NOT ACTIVATED	
40.00	32.38	32.38	BRAKES NOT ACTIVATED	
41.00	28.90	28.90	BRAKES NOT ACTIVATED	
42.00	24.99	24.99	BRAKES NOT ACTIVATED	
43.00	21.47	21.47	BRAKES NOT ACTIVATED	
44.00	18.55	18.55	BRAKES NOT ACTIVATED	
45.00	TARGET SEEN AS A PEAK OF NOISE			
46.00	TARGET NOT DETECTED			
47.00	TARGET NOT DETECTED			
48.00	TARGET NOT DETECTED			
49.00	TARGET NOT DETECTED			

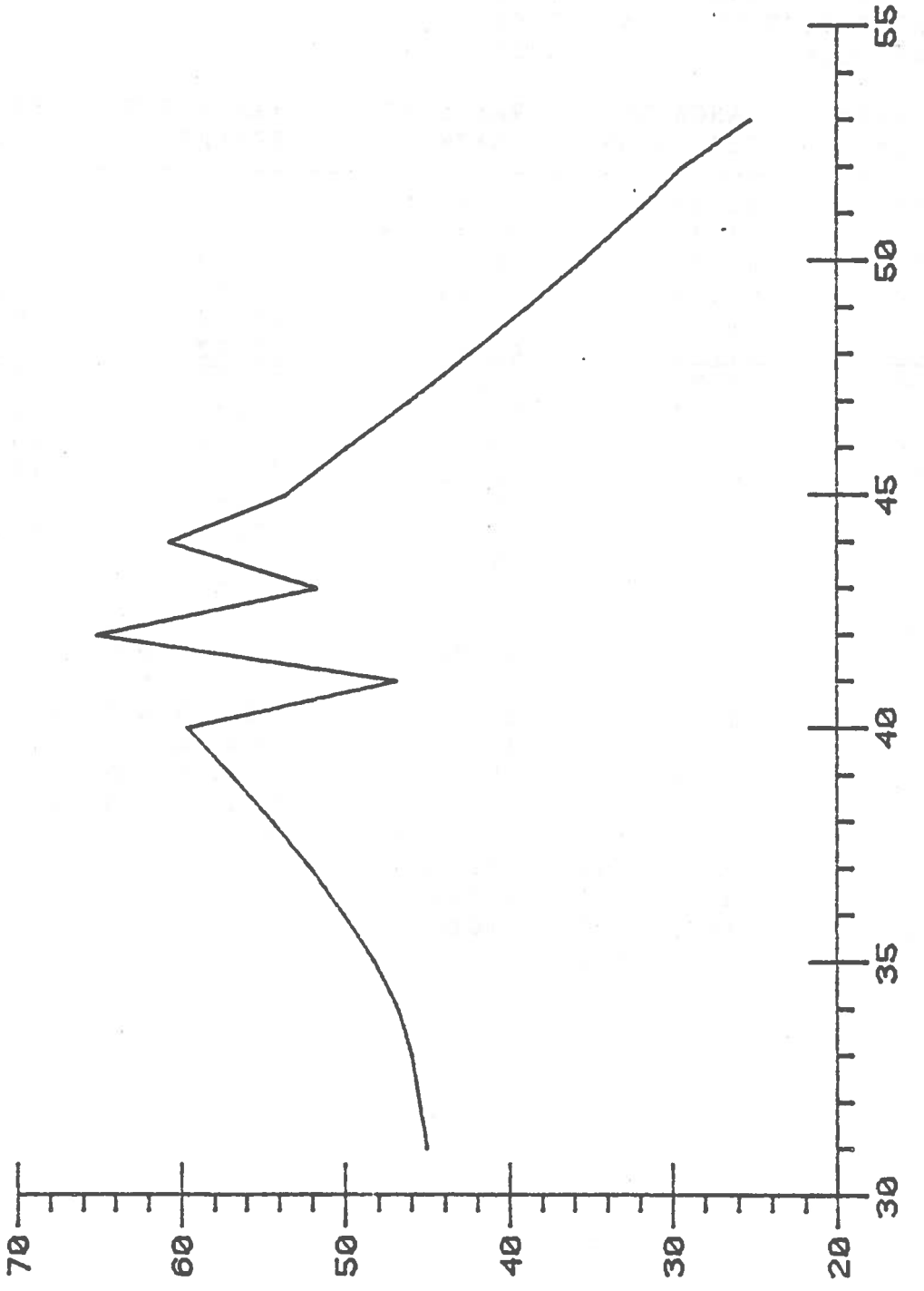

Figure 7.3.4: NISSAN System. Car crossing from left lane.

Table 15: NISSAN System. Car crossing from left lane.

RANGE CUT-OFF: 400.00
ACTIVATION TIME: 1.00
BRAKING DECELERATION: 3.92
RADAR DELAY: 0.20

VELOCITY OF CAR	RANGE OF DETECTION	RANGE AT ALARM	RANGE FOR BRAKES	FINAL VELOCITY
30.00	156.06	NO ALARM		
31.00	164.64	61.97	45.09	0.00
32.00	145.63	68.43	45.54	0.00
33.00	154.05	72.25	45.98	0.00
34.00	135.22	76.26	46.84	0.00
35.00	139.63	80.41	48.29	0.00
36.00	124.84	84.64	50.09	0.00
37.00	129.16	88.94	52.10	2.48
38.00	114.50	93.27	54.46	4.41
39.00	118.73	97.62	56.98	5.52
40.00	115.41	101.98	59.63	6.33
41.00	89.90	89.90	46.89	21.32
42.00	116.21	110.68	65.22	7.60
43.00	98.00	98.00	51.62	22.33
44.00	109.47	109.47	60.75	18.62
45.00	102.39	102.39	53.60	24.96
46.00	99.02	99.02	49.82	28.51
47.00	95.64	95.64	46.04	31.69
48.00	92.27	92.27	42.42	34.56
49.00	88.89	88.89	38.90	37.19
50.00	85.51	85.51	35.51	39.64
51.00	85.75	85.75	32.22	41.93
52.00	82.35	82.35	29.30	44.02
53.00	75.37	75.37	25.20	46.37
54.00	68.43	68.43	BRAKES NOT ACTIVATED	
55.00	61.57	61.57	BRAKES NOT ACTIVATED	
56.00	54.79	54.79	BRAKES NOT ACTIVATED	
57.00	48.12	48.12	BRAKES NOT ACTIVATED	
58.00	44.89	44.89	BRAKES NOT ACTIVATED	
59.00	38.48	38.48	BRAKES NOT ACTIVATED	
60.00	32.38	32.38	BRAKES NOT ACTIVATED	
61.00	24.37	24.37	BRAKES NOT ACTIVATED	
62.00	20.42	20.42	BRAKES NOT ACTIVATED	
63.00	18.47	NO ALARM		
64.00	TARGET NOT DETECTED			
65.00	TARGET NOT DETECTED			
66.00	PROBABILITY OF DETECTION LESS THAN .99			
67.00	TARGET NOT DETECTED			
68.00	PROBABILITY OF DETECTION LESS THAN .99			

braking system, with a very short Activation Time, would significantly improve the results.

5) Car Fixed Ahead: figure 7.3.5 and table 16 illustrate the definite advantage of Nissan-Mitsubishi's Radar Control Law. Even at a velocity of 78 feet/sec, the predicted collision velocity is quite low (3.8 feet/sec). It can be seen on figure 7.3.4 that the distance at which brakes are applied increases very rapidly with increasing carrier vehicle velocity, up to about 80 feet/sec. However, it must be remembered that these results are obtained with a Range Cut-Off of 400 feet, which gives rise to many false alarms. The use of a smaller Range Cut-Off would decrease the false alarm rate, but it would also decrease the detection capacity, since the detection of targets would occur later.

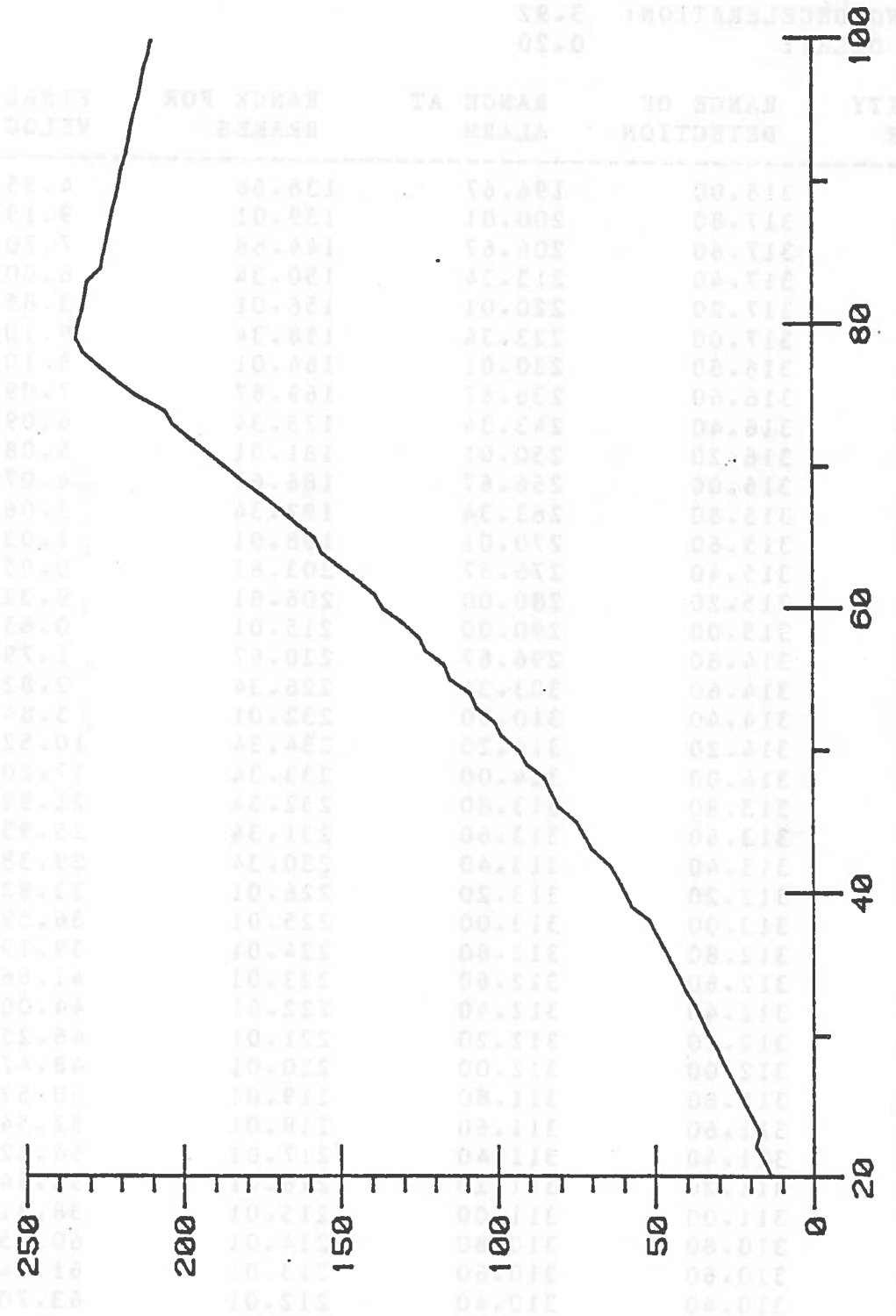

Figure 7.3.5: NISSAN System. Car fixed ahead.

Table 16: NISSAN System. Car fixed ahead.

RANGE CUT-OFF:	400.00
ACTIVATION TIME:	1.00
BRAKING DECELERATION:	3.92
RADAR DELAY:	0.20

VELOCITY OF CAR	RANGE OF DETECTION	RANGE AT ALARM	RANGE FOR BRAKES	FINAL VELOCITY
60.00	318.00	196.67	136.68	4.95
61.00	317.80	200.01	139.01	9.19
62.00	317.60	206.67	144.68	7.70
63.00	317.40	213.34	150.34	6.00
64.00	317.20	220.01	156.01	3.85
65.00	317.00	223.34	158.34	9.10
66.00	316.80	230.01	164.01	8.10
67.00	316.60	236.67	169.67	7.09
68.00	316.40	243.34	175.34	6.09
69.00	316.20	250.01	181.01	5.08
70.00	316.00	256.67	186.67	4.07
71.00	315.80	263.34	192.34	3.06
72.00	315.60	270.01	198.01	2.03
73.00	315.40	276.67	203.67	0.95
74.00	315.20	280.00	206.01	9.32
75.00	315.00	290.00	215.01	0.65
76.00	314.80	296.67	220.67	1.79
77.00	314.60	303.34	226.34	2.82
78.00	314.40	310.00	232.01	3.84
79.00	314.20	314.20	234.34	10.52
80.00	314.00	314.00	233.34	17.20
81.00	313.80	313.80	232.34	21.98
82.00	313.60	313.60	231.34	25.93
83.00	313.40	313.40	230.34	29.38
84.00	313.20	313.20	226.01	33.82
85.00	313.00	313.00	225.01	36.59
86.00	312.80	312.80	224.01	39.19
87.00	312.60	312.60	223.01	41.66
88.00	312.40	312.40	222.01	44.00
89.00	312.20	312.20	221.01	46.25
90.00	312.00	312.00	220.01	48.42
91.00	311.80	311.80	219.01	50.52
92.00	311.60	311.60	218.01	52.54
93.00	311.40	311.40	217.01	54.52
94.00	311.20	311.20	216.01	56.44
95.00	311.00	311.00	215.01	58.31
96.00	310.80	310.80	214.01	60.15
97.00	310.60	310.60	213.01	61.94
98.00	310.40	310.40	212.01	63.70

CHAPTER 8

CONCLUSION

8.1 GENERAL CONCLUSIONS ABOUT THE MODEL

The model developed in this study provides relative results, which need to be interpreted. Its accuracy depends mainly on the chosen representation of the targets: dividing a given target into a large number of flat plates does not necessarily increase the accuracy of the results, since the dimensions of each plate must remain large compared to one wavelength. Moreover, it can significantly increase the computation time. A compromise must be found, so that the shape of a target is well represented, with a minimum number of plates.

As previously stated, since no ideal flat plate can be found in the usual environment of a car, the magnitude of the returned signal cannot be accurately predicted. However, the relative variations are quite reliable and the shape of the relative power returned obtained here corres-

ponds fairly well to the experimental data recorded by NHTSA.

The evaluation of the Detection Capacity Rate "DCR" is possible with this model, given certain statistical data. The most common "potential false targets" must be determined and modeled; the average occurrence of these false targets must be known. Indeed, the present definition of "DCR" (CHAPTER 1) makes it very difficult to theoretically estimate: if the number of potential (true) targets is approximately 100, the number of false alarms can be evaluated only when the number of potential false targets is known, and this statistical quantity is difficult to predict theoretically.

This model succeeded in accurately predicting the performances of the Nissan system, experimentally tested to this point; it also simulated the lack of precision of the Bendix system Radar Control Law. It can be deduced from this study that the Nissan system probably uses a Range Cut-Off shorter than 400 feet: indeed, a very low false alarm rate was experimentally observed, while the computer simulation shows that a 400-foot Range Cut-Off will give rise to many false alarms.

The interested reader can refer to RCA Laboratories Report (1980) and to Bundesminister fur Forschung und Technologie Reports (1978 and 1979).

8.2 SUGGESTIONS FOR FUTURE WORK

This model can be improved in several ways:

- A more precise representation of targets could be used, with more plates, to increase the accuracy.

- A few common targets, such as fire hydrants, cannot be modeled, because a flat plate representation is not appropriate. Hence, the introduction of a cylindrical shape would improve the model.

- The addition of a roughness factor would provide a better representation of the surfaces encountered in the usual environment of a car. Then, one could possibly obtain some results in terms of absolute predicted signal, instead of relative predicted signal.

- Systems could be rated according to two parameters, instead of one (DCR): first, a Detection Capacity parameter, defined as the number of detected targets among a certain number of potential (true) targets. Secondly a False Alarm parameter could be introduced, defined as the number of detected targets among a certain number of potential false targets. These two independent parameters are more convenient, since they include no relationship between the number of potential true targets and the number of potential false targets. In addition, the two proposed independent parameters could be easily estimated with this model.

APPENDIX A

CROSS-SECTION COMPUTATION

The Standard Physical-Optics Method (Crispin and Siegel, 1968) gives:

$$\sigma = \frac{4\pi}{\lambda^2} \left| \int \frac{dA}{dx} \cdot \exp(2i \cdot k \cdot x) dx \right|^2 \qquad (A.1)$$

where: - $k = 2\pi/\lambda$

- x = direction of incidence.
- A = projected area in the direction x.

Let L and l be respectively the long and small edge of the plate. Let θ be the angle between the direction of incidence x and the axis perpendicular to the plate, and ϕ the angle between the long edge of the plate and the projection of x in the plan of the plate.

Then it can be shown that: $dA = \cos\theta \cdot dAo$ (equation A.2),with:

- $dAo = \dfrac{x \cdot dx}{\sin^2\theta \cdot \sin\phi \cdot \cos\phi}$

  for $0 < x < l \cdot \sin\theta \cdot \sin\phi$

$$- dAo = \frac{1 \cdot dx}{\sin\theta \cdot \sin\phi}$$

for $1 \cdot \sin\theta \cdot \sin\phi < x < L \cdot \sin\theta \cdot \cos\phi$

$$- dAo = \frac{L \cdot dx}{\sin\theta \cdot \sin\phi} + \frac{1 \cdot dx}{\sin\theta \cdot \cos\phi} - \frac{x \cdot dx}{\sin^2\theta \cdot \sin\phi \cdot \cos\phi}$$

for $L \cdot \sin\theta \cdot \cos\phi < x < L \cdot \sin\theta \cdot \cos\phi + 1 \cdot \sin\theta \cdot \sin\phi$

Let I be the integral: $\frac{dAo}{dx} \cdot \exp(2i \cdot k \cdot x) \cdot dx$.

Then I can be split into four terms: I1, I2, I3, I4, where:

$$- I1 = \frac{1}{\sin^2\theta \cdot \sin\phi \cdot \cos\phi} \int_0^{x1} x \cdot \exp(2i \cdot k \cdot x) \cdot dx$$

$$- I2 = \frac{1}{\sin\theta \cdot \cos\phi} \int_{x1}^{x2} \exp(2i \cdot k \cdot x) \cdot dx$$

$$- I3 = \left[\frac{L}{\sin\theta \cdot \sin\phi} + \frac{1}{\sin\theta \cdot \cos\phi} \right] \int_{x2}^{x3} \exp(2i \cdot k \cdot x) \cdot dx$$

$$- I4 = \frac{-1}{\sin^2\theta \cdot \sin\phi \cdot \cos\phi} \cdot \int_{x2}^{x3} x \cdot \exp(2i \cdot k \cdot x) \cdot dx$$

where: $- x1 = 1 \cdot \sin\theta \cdot \sin\phi$

$- x2 = L \cdot \sin\theta \cdot \cos\phi$

$- x3 = L \cdot \sin\theta \cdot \cos\phi + 1 \cdot \sin\theta \cdot \sin\phi$

The terms I2 and I3 are easily computed, while the terms I1 and I4 are integrated by parts. The final integral I is expressed as:

$$I = \frac{[\ \exp(2i \cdot k \cdot 1 \cdot \sin\theta \cdot \sin\phi) - 1\ ]\ [\ \exp(2i \cdot k \cdot L \cdot \sin\theta \cdot \cos\phi) - 1\ ]}{4 \cdot k^2 \cdot \sin^2\theta \cdot \sin\phi \cdot \cos\phi}$$

Multiply by cosθ to account for the projection of the area A (equation A.2), and square the magnitude gives the result:

$$\frac{\sin(k\cdot l\cdot\sin\theta\cdot\sin\phi)\cdot\sin(k\cdot L\cdot\sin\theta\cdot\cos\phi)\cdot\cos\theta}{(k\cdot\sin\theta\cdot\sin\phi)\ (k\cdot\sin\theta\cdot\cos\phi)} \qquad (A.3)$$

The final result is obtained from equation A.1, and can be written:

$$= \frac{4\cdot\pi\cdot l^2\cdot L^2}{\lambda^2}\ \frac{\sin^2(k\cdot l\cdot\sin\theta\cdot\sin\phi)}{(k\cdot l\cdot\sin\theta\cdot\sin\phi)^2}\ \frac{\sin^2(k\cdot L\cdot\sin\theta\cdot\cos\phi)}{(k\cdot L\cdot\sin\theta\cdot\cos\phi)^2}\cdot\cos^2\theta \qquad (A.4)$$

APPENDIX B

BENDIX SIMULATION PROGRAM

```
C
C     ------------------------------------------
C          PROGRAM SAM :
C          SIMULATION OF TARGET CROSS-SECTIONS
C     ------------------------------------------
          IMPLICIT REAL (L-O)
          COMPLEX E,GAM
          DIMENSION GL(60),SL(60),XN(60),YN(60),ZN(60)
         1          ,XGL(60),YGL(60),ZGL(60)
         2          ,XC(60),YC(60),ZC(60)
          COMMON G(2,81)
          CHARACTER *9 FIL1,FIL2*15,FILE*11,COM*1
          CHARACTER *2 NBR,ANS*1
          PARAMETER (PI=3.14159,CO=3.E08)
          FIL1='TARG.DAT;'
          XRDR=0.
          YRDR=0.
          ZRDR=.5
          DO 7 I=1,2
          DO 7 J=1,81
          READ(60,*)X,G(I,J)
          G(I,J)=10.**(G(I,J)/10.)
7         CONTINUE
C     ---------------------
C          ENTER FREQUENCY
C     ---------------------
          PRINT *, 'FREQUENCY IN GHZ'
          READ(5,200) FREQ
200       FORMAT(F6.2)
          FREQ=FREQ*1.E09
C     -------------------------
C          ENTER MODE OF OUTPUT
C     -------------------------
9         PRINT *, 'MODE OF OUTPUT:'
          READ(5,201)IMOD
201       FORMAT(I1)
          IF(IMOD.EQ.4) THEN
          IMOD=2
```

```
          IOUT=8
          ELSE IF(IMOD.EQ.5) THEN
          IMOD=3
          IOUT=8
          ELSE
          IOUT=6
          ENDIF
C
C     ------------------------
C         ENTER RANGE CUT-OFF
C     ------------------------
          PRINT *, 'RANGE CUT-OFF IN FT:'
          READ(5,200)RCOF
          RCO=RCOF*.3
          IF(IMOD.NE.1) THEN
C
C     ------------------------------------------
C         ENTER CHARACTERISTICS OF BRAKING SYSTEM
C     ------------------------------------------
          PRINT *, 'ACTIVATION TIME IN SEC:'
          READ(5,202)TACT
202       FORMAT(F4.2)
          PRINT *, 'BRAKING DECELERATION IN G-UNITS:'
          READ(5,200)AMUSG
          PRINT *, 'RADAR DELAY IN SEC:'
          READ(5,202)TDEL
          AMUSG=AMUSG*9.81
          ENDIF
C
C     ---------------------
C         FILE FOR INPUT
C     ---------------------
          PRINT *, 'INPUT FILE NUMBER'
          READ(5,101)NBR
101       FORMAT(A2)
C****READ DATA ON THE FILE 'TARG.DAT;NBR'****
          FILE=FIL1//NBR
          OPEN(1,FILE=FILE,STATUS='OLD')
10        READ(1,102)COM
102       FORMAT(A1)
          IF(COM.EQ.'C') GOTO 10
          READ(1,*) (JTRGT,JPLT,XTRGT,YTRGT,ZTRGT
         1           ,VXTRGT,VYTRGT)
          DO 21 J=1,JTRGT
          READ(1,*) (GL(J),SL(J),XN(J),YN(J),ZN(J),
         1           XGL(J),YGL(J),ZGL(J),
         2           XC(J),YC(J),ZC(J))
21        CONTINUE
          CLOSE(1)
11        IF(IMOD.NE.2) THEN
C
C     ---------------------
C         OUTPUT FILE NAME
C     ---------------------
          PRINT *, 'OUTPUT FILE NAME:'
          READ(5,103)FIL2
103       FORMAT(A15)
C****OPEN FILE FOR RESULTS STORAGE****
```

```
      OPEN(7,FILE=FIL2,STATUS='NEW')
      ENDIF
C
C     ENTER VELOCITY OF THE CAR
C     -------------------------
      PRINT *, 'VELOCITY OF THE CAR IN FT/SEC:'
      READ(5,200)VRDRF
      VRDR=VRDRF*.3
      TIME=1./VRDR
      IF(IMOD.EQ.3) THEN
C
C     ENTER MAXIMUM VELOCITY OF THE CAR
C     ---------------------------------
      PRINT *, 'MAXIMUM VELOCITY IN FT/SEC:'
      READ(5,200)VMAXF
      VMAX=VMAXF*.3
      ENDIF
      IF(IMOD.NE.1) THEN
      WRITE(IOUT,114)RCOF
114   FORMAT(' RANGE CUT-OFF:',T23,F6.2)
      WRITE(IOUT,115)TACT
115   FORMAT(' ACTIVATION TIME:',T23,F6.2)
      WRITE(IOUT,116)AMUSG
116   FORMAT(' BRAKING DECELERATION:',T23,F6.2)
      WRITE(IOUT,117)TDEL
117   FORMAT(' RADAR DELAY:',T23,F6.2)
      PRINT *
      WRITE(IOUT,111)
111   FORMAT(' VELOCITY',T17,'RANGE OF',T32,'RANGE AT',
     1       T47,'RANGE FOR',T62,'FINAL')
      WRITE(IOUT,112)
112   FORMAT(' OF CAR',T17,'DETECTION',T32,'ALARM',
     1       T47,'BRAKES',T62,'VELOCITY')
      WRITE(IOUT,113)
113   FORMAT(69('-'))
      ENDIF
C****COMPUTE THRESHOLD****
      SIGREF=139.6
      GOO=G(1,1)*G(2,1)*SQRT(2./(G(1,1)**2+G(2,1)**2))
      PTHR=10.*ALOG10(SIGREF*(CO*GOO/FREQ)**2)
      PTHR=PTHR-60.*ALOG10(4*PI)-40.*ALOG10(90.)
2     PROB=0.
      IFLG1=0
      IFLG2=1
      DO 29 ICOUNT=0,300
      E=(0.,0.)
      XTR=XTRGT-VXTRGT*TIME*FLOAT(ICOUNT)
      YTR=YTRGT-VYTRGT*TIME*FLOAT(ICOUNT)
C****COMPUTE DISTANCE AND RELATIVE VELOCITY****
      CALL VECT (XTR,YTR,ZTRGT,XRDR,YRDR,ZRDR
     1           ,XTP,YTP,ZTP)
      CALL NORM (XTP,YTP,ZTP,DIST,X,Y,Z,*100)
      VAV=-(XTP*VXTRGT+YTP*(VYTRGT+VRDR))/DIST
C*************************************************
```

```
        IF((YTR-YRDR).LT.0.2) GOTO 12
C****DO LOOP ON THE JTRGT ELEMENTS OF TARGET****
        DO 31 J=1,JTRGT
        XXC=XC(J)-VXTRGT*TIME*FLOAT(ICOUNT)
        YYC=YC(J)-VYTRGT*TIME*FLOAT(ICOUNT)
        IF((YYC-YRDR).LE.0.) GOTO 31
        CALL NORM (XGL(J),YGL(J),ZGL(J),MODGL,
     1             XGL1,YGL1,ZGL1,*100)
        CALL NORM (XN(J),YN(J),ZN(J),MODN,
     1             XN1,YN1,ZN1,*100)
        CALL PROD (XN(J),YN(J),ZN(J),XGL(J),
     1             YGL(J),ZGL(J),XSL,YSL,ZSL)
        CALL NORM (XSL,YSL,ZSL,MODSL,XSL1,YSL1,ZSL1,*100)
C****DO LOOP FOR GROUND REFLECTIONS****
        DO 1 IMG=1,2
        CALL VECT (XXC,YYC,ZC(J),XRDR,
     1             YRDR,ZRDR,XTP,YTP,ZTP)
        CALL NORM (XTP,YTP,ZTP,MODC,XC1,YC1,ZC1,*100)
        PHA=2.*PI*FREQ*MODC/CO
        IF(J.GT.JPLT) GOTO 5
C****CROSS-SECTION FOR FLAT PLATES****
        CALL DOT (XN1,YN1,ZN1,XC1,YC1,ZC1,COSC)
        CALL DOT (XSL1,YSL1,ZSL1,XC1,YC1,ZC1,COSB)
        CALL DOT (XGL1,YGL1,ZGL1,XC1,YC1,ZC1,COSA)
        CALL SIGM (FREQ,COSA,COSB,COSC,SL(J),
     1             GL(J),SIG)
        SIG=SIG/1000.
        GOTO 6
C****CROSS-SECTION FOR EDGES****
5       CALL DOT (XC1,YC1,ZC1,XN1,YN1,ZN1,COSP)
        COSM=COS(PI*SL(J)/180.)
        IF(COSP.GT.COSM) GOTO 31
        CALL DOT (XGL1,YGL1,ZGL1,XC1,YC1,ZC1,COSA)
        SINA=SQRT(ABS(1.-COSA*COSA))
        CALL PROD (XC1,YC1,ZC1,XGL1,YGL1,ZGL1,XTP,YTP,ZTP)
        CALL POLAR (3,XC1,YC1,ZC1,XE,YE,ZE)
        CALL DOT (XE,YE,ZE,XTP,YTP,ZTP,BETA)
        BETA=SQRT(ABS(1.-BETA*BETA))
        CALL SIGW (FREQ,SINA,COSA,BETA,GL(J),SIG)
C****COMPUTE GAIN IN (THETA,PHI) DIRECTION****
6       THETA=ACOS(-YC1)
        PHI=ACOS(XC1)
        CALL GAIN (THETA,PHI,GA)
        ZRDR=-ZRDR
C****COMPUTE THE GROUND REFLECTION COEFFICIENT****
        IF(IMG.EQ.1) THEN
        GAM=(1.,0.)
        ELSE
        CALL DOT (XC1,YC1,ZC1,0.,0.,-1.,PSI)
        PSI=ASIN(PSI)
        CALL GAMMA (3,FREQ,PSI,GAM)
        ENDIF
C****ADD THE FIELDS WITH A PHASE FACTOR****
        E=E+(GA**.5)*(SIG**.25)*GAM
```

```
     1      *CEXP(CMPLX(0.,PHA))/MODC
1         CONTINUE
C****END OF DO LOOP FOR GROUND REFLECTIONS****
31        CONTINUE
C****COMPUTE POWER FOR CW RADAR****
          RELPWR=((CABS(E)**4)/((4.*PI)**3))*
     1          ((CO/FREQ)**2)
          IF (RELPWR.LT.1.E-20) THEN
          PWRDB=-200.
          ELSE
          PWRDB=10.*ALOG10(RELPWR)
          ENDIF
C****COMPUTE PROBABILITY OF DETECTION****
          PR=(PTHR-PWRDB)/10.
          PR=10.**PR
          PR=EXP(-PR)
          PROB=PROB*(1.-PR)+PR
          PRT=-200.
          IF(PROB.GE.1.E-20) THEN
          PRT=10.*ALOG10(PROB)
          ENDIF
          IF(DIST.GT.RCO) THEN
          PROB=0.
          PR=0.
          PRT=-200.
          ENDIF
          IF(IMOD.EQ.1) THEN
          DISTF=DIST/.3
          WRITE(7,*)(DISTF,PWRDB,PRT,PTHR)
          GOTO 20
          ENDIF
          IF(PROB.GE..99.AND.IFLG2.EQ.1) THEN
          IFLG2=2
          RDET1=DIST
          RDET1F=DIST/.3
          TDET1=FLOAT(ICOUNT)*TIME
          ENDIF
17        GOTO(20,13,14,15,16)IFLG2
13        IF(PWRDB.GE.PTHR) THEN
          TMEAS=FLOAT(ICOUNT)*TIME
          IF(TMEAS.LT.TDET1+TDEL) GOTO 20
          DIST=DIST+VAV*(TMEAS-TDET1-TDEL)
          RDET2F=DIST/.3
          IFLG2=4
          GOTO 17
          ELSE
          IFLG2=3
          GOTO 17
          ENDIF
14        IF(PWRDB.LT.PTHR) GOTO 20
          IFLG2=2
          RDET1=DIST
          RDET1F=DIST/.3
          TDET1=FLOAT(ICOUNT)*TIME
```

```
          GOTO 17
15        IF(DIST.GT.2.*VAV) GOTO 20
          IFLG2=5
          RALA=DIST
          RALAF=DIST/.3
          TALAR=FLOAT(ICOUNT)*TIME
          GOTO 17
16        TMEAS=FLOAT(ICOUNT)*TIME
          IF(TMEAS.LT.TALAR+TACT) GOTO 20
          RBRA=DIST+VAV*(TMEAS-TALAR-TACT)
          RBRAF=RBRA/.3
          VFIN=VRDR**2-2.*AMUSG*RBRA
          VFIN=AMAX1(0.,VFIN)
          VFIN=SQRT(VFIN)
          VFINF=VFIN/.3
          IF(IMOD.EQ.2) GOTO 18
          WRITE(7,*)(VRDRF,RBRAF)
18        WRITE(IOUT,105)VRDRF,RDET2F,RALAF,RBRAF,VFINF
105       FORMAT(5(F6.2,TR9))
          GOTO 8
C****MOVE RADAR****
20        YRDR=YRDR+VRDR*TIME
29        CONTINUE
12        IF(IMOD.EQ.1) GOTO 4
          IF(IFLG2.EQ.1) THEN
          WRITE(IOUT,106)VRDRF
106       FORMAT(F6.2,TR9,' PROBABILITY OF DETECTION LESS THAN
.99')
          GOTO 8
          ENDIF
          IF(IFLG2.EQ.2) THEN
          WRITE(IOUT,107)VRDRF
107       FORMAT(F6.2,TR9,' TARGET NOT DETECTED')
          GOTO 8
          ENDIF
          IF(IFLG2.EQ.3) THEN
          WRITE(IOUT,108)VRDRF
108       FORMAT(F6.2,TR9,' TARGET SEEN AS A PEAK OF NOISE')
          GOTO 8
          ENDIF
          IF(IFLG2.EQ.4) THEN
          WRITE(IOUT,109)VRDRF,RDET2F
109       FORMAT(2(F6.2,TR9),' NO ALARM')
          GOTO 8
          ENDIF
          IF(IFLG2.EQ.5) THEN
          WRITE(IOUT,110)VRDRF,RDET2F,RALAF
110       FORMAT(3(F6.2,TR9),' BRAKES NOT ACTIVATED')
          ENDIF
8         IF(IMOD.EQ.2) GOTO 3
          VRDR=VRDR+.3
          TIME=1./VRDR
          VRDRF=VRDR/.3
          YRDR=0.
```

```
      PRINT *,VRDRF
      IF(VRDR.LT.VMAX) GOTO 2
4     CLOSE(7)
3     PRINT *
      PRINT *, 'OTHER RUN ?'
      READ(5,102)ANS
      IF(ANS.EQ.'Y') THEN
      YRDR=0.
      GOTO 11
      ELSE IF(ANS.EQ.'C') THEN
      YRDR=0.
      GOTO 9
      ENDIF
      STOP
100   PRINT *, 'MOD=0'
      STOP
      END
C
C
C     ------------------------------
C         SUBROUTINE : UNIT VECTOR
C     ------------------------------
      SUBROUTINE NORM (X1,Y1,Z1,AMOD,X2,Y2,Z2,*)
      AMOD=SQRT(X1**2+Y1**2+Z1**2)
      IF(AMOD.LT.1.E-10) RETURN 1
      X2=X1/AMOD
      Y2=Y1/AMOD
      Z2=Z1/AMOD
      RETURN
      END
C     ------------------------------
C         SUBROUTINE : SCALAR PRODUCT
C     ------------------------------
      SUBROUTINE DOT (X1,Y1,Z1,X2,Y2,Z2,A)
      A=X1*X2+Y1*Y2+Z1*Z2
      RETURN
      END
C     ------------------------------
C         SUBROUTINE : CROSS PRODUCT
C     ------------------------------
      SUBROUTINE PROD (X1,Y1,Z1,X2,Y2,Z2,X3,Y3,Z3)
      X3=Y1*Z2-Y2*Z1
      Y3=Z1*X2-Z2*X1
      Z3=X1*Y2-X2*Y1
      RETURN
      END
C     ------------------------------
C         SUBROUTINE : VECTOR JOINING 2 POINTS
C     ------------------------------
      SUBROUTINE VECT (X1,Y1,Z1,X2,Y2,Z2,X3,Y3,Z3)
      X3=X2-X1
      Y3=Y2-Y1
      Z3=Z2-Z1
      RETURN
      END
```

```
C
C     ------------------------------------------------
C           SUBROUTINE : FLAT PLATE CROSS-SECTION
C     ------------------------------------------------
      SUBROUTINE SIGM(F,A,B,C,S,G,SIG)
      PARAMETER (PI=3.14159,C0=3.E08)
      IF (C.LT.0.) GOTO 1
      C1=2*PI*G*F/C0
      C2=2*PI*S*F/C0
      B=ABS(B)
      A=ABS(A)
      SIG=C1*C2*G*S*C*C/PI
      H1=C1*A
      H2=C2*B
      IF (H1.LT.1.E-09) GOTO 2
      IF (H2.LT.1.E-09) GOTO 3
      SIG=SIG*((SIN(H1)/H1)*(SIN(H2)/H2))**2
      RETURN
1     SIG=0.
      RETURN
2     IF (H2.LT.1.E-09) RETURN
      SIG=SIG*(SIN(H2)/H2)**2
      RETURN
3     SIG=SIG*(SIN(H1)/H1)**2
      RETURN
      END
C
C     ------------------------------------
C           SUBROUTINE : READ THE GAIN
C     ------------------------------------
      SUBROUTINE GAIN(T,P,GA)
      COMMON G(2,81)
      PARAMETER (PI=3.14159)
      TH=ABS(T)
      TH=TH*180./PI
      IF(TH.LE.40.) THEN
      J=INT(2.*TH)+1
      ELSE
      J=81
      ENDIF
      TI=.5*FLOAT(INT(2.*TH))
      G1=G(1,J)+(TH-TI)*(G(1,J+1)-G(1,J))
      G2=G(2,J)+(TH-TI)*(G(2,J+1)-G(2,J))
      GA=(G2*G2-G1*G1)*(COS(P+PI/4.))**2+G1*G1
      GA=SQRT(GA)
      GA=G1*G2/GA
      RETURN
      END
C
C     ------------------------------------------------
C           COMPUTES THE WIRE (EDGE) CROSS-SECTION
C     ------------------------------------------------
      SUBROUTINE SIGW (F,S,C,B,AL,SIG)
      PARAMETER (PI=3.14159,C0=3.E08)
      IF(S.LT.1.E-10) GOTO 1
      C1=2*PI*AL*C*F/C0
      C1=ABS(C1)
```

```
      C2=ALOG(.0658*ABS(S))
      C2=C2*C2+(PI/2.)**2
      SIG=PI*AL*AL*S*S*(ABS(B)**4)/C2
      IF(C1.LT.1.E-10) RETURN
      SIG=SIG*((SIN(C1)/C1)**2)
      RETURN
1     SIG=.0
      RETURN
      END
C
C     ------------------------------
C         SUBROUTINE : POLARIZATION
C     ------------------------------
      SUBROUTINE POLAR (I,XC,YC,ZC,X,Y,Z)
      COT=ZC
      SIT=SQRT(XC*XC+YC*YC)
      COP=XC/SIT
      SIP=YC/SIT
      IF(I)1,2,3
1     X=-SIT*SIP
      Y=SIT*COP
      Z=.0
      RETURN
2     X=COT*COP
      Y=COT*SIP
      Z=-SIT
      RETURN
3     X=(COT*COP-SIT*SIP)/(2.**.5)
      Y=(SIT*COP+COT*SIP)/(2.**.5)
      Z=-SIT/(2.**.5)
      RETURN
      END
C
C     ----------------------------------------
C         SUBROUTINE REFLECTION COEFFICIENT
C     ----------------------------------------
      SUBROUTINE GAMMA(I,F,P,G)
      IMPLICIT COMPLEX (G)
      PARAMETER (EPSR=3.,SIG=2.E-05)
      X=(18.*SIG)/(EPSR*F)
      GE=CMPLX(1.,-X)
      GE=CSQRT(GE)
      A=1.+SQRT(1.+X**2)
      B=SQRT(1.-2.*(COS(P)**2)/(EPSR*A))
      GF=SQRT(EPSR)*GE
      GV=(SIN(P)-B/GF)/(SIN(P)+B/GF)
      GH=(SIN(P)-B*GF)/(SIN(P)+B*GF)
      IF(IPOLAR)1,2,3
1     G=GH
      RETURN
2     G=GV
      RETURN
3     G=(GH+GV)/2.
      RETURN
      END
```

REFERENCES

AARL Antenna Book, published by The American Radio Relay League, Inc, 1974.

Der Bundesminister fur Forschung und Technologie, Entwicklungslinien in Kraftfahrzeugtechnik und Strassenverkehr, Forschungsbilanz, Verlag TUV Rheinland Gmbh, 1978.

Der Bundesminister fur Forschung und Technologie, Entwicklungslinien in Kraftfahrzeugtechnik und Strassenverkehr, Forschungsbilanz, Verlag TUV Rheinland Gmbh, 1979.

CA Research Corporation, Development Project, 1981, private communication.

Crispin, J. W., K. M. Siegel, Methods of Radar Cross-Section Analysis, Academic Press, 1968.

Grimes, D. M., T. O. Jones, Automotive Radar, a Brief Review, Proceedings of the IEEE, 804-821, June 1974.

Larsen, H. J., B. O. Shubert, Probabilistic Models in Engineering Sciences, Vol I, 1979, John Wiley & Sons.

Liao, S. Y., Microwave Devices and Circuits, Prentice-Hall, Inc, NJ 1980.

NHTSA, Collision Avoidance Radar Braking Systems Investigations, Phase II Study, Volume II, Technical Report, Sept. 1976.

NHTSA, Analysis of Problems on the Application of Radar Sensors to Automotive Collision Prevention, Report, Dec. 1973.

NISSAN MOTOR CO., LTD, A Study of the Automatic Braking System, Seventh International Conference on Experimental Safety Vehicles, Paris, June 8, 1979.

Pruvot, H., Propagation Systems in Automotive Radar, PSU M.S. Thesis, 1981.

Raff, S. J., Microwave System Engineering Principles, Pergamon Press, 1977.

RCA Laboratories Final Report, Electronic Subsystems for the Research Safety Vehicles (Phase 3), National Technical Information Service, Springfield, VA, March 1980.

Ross, R. A., Radar Cross-Section of Rectangular Flat Plates as a Function of Aspect Angle, Transactions on Antennas and Propagation, Vol AP-14, No 3, 330-335, May 1966.

Skolnik, M. I., Introduction to Radar Systems, McGraw-Hill Book Company, Inc, 1962.

VDO Information, Further Development of Autarkic Headway Warning Radar Systems, VDO Adolph Schindling AG, Jan 1980.

APPENDIX H
DEPENDENCE OF PROPERTY DAMAGE AND PEDESTRIAN INJURY ON RELATIVE VELOCITY

The Kinetic Research Accident Environment Simulation and Projection (KRAESP) Model is being used in NHTSA Contract DTNH22-80-C-07530, "Collision Avoidance System Cost-Benefit Analysis," to predict the societal losses of accidents in which vehicles are equipped with radar-activated brakes. This program's methodology calculates the relative velocity (Vrel) of each one and two vehicle collision and creates new Vrel distributions based on models of radar braking systems. The KRAESP Model uses the distributions as inputs and projects the number of injuries and fatalities to vehicle occupants.

Unfortunately, in its present formulation the KRAESP Model does not project two other significant components of societal costs: property damage and injuries to non-occupants. Property damage includes the damage to vehicles and surrounding property, while non-occupants include pesdestrians and people riding bicycles, mopeds and motorcycles. To include these costs, the property damage and non-occupant injuries reported in 1979 North Carolina accident data were analyzed to assess their dependence on Vrel. (The rationale for the selection of North Carolina data is discussed in References 1 and 2.)

PROPERTY DAMAGE

The North Carolina data file of police-reported accidents is unique in that it provides a large collection (over 150,000 cases) of accident records which include impact velocities and property damage for each vehicle and damage to the surrounding property. These data were obtained from police estimates and will contain whatever biases are inherent in their estimating procedures. Nevertheless, no other comparably large accident files are currently available to us which include more accurate information of this nature.

A random sampling of approximately 10 percent of the North Carolina data (or, more precisely, every tenth case number) was analyzed using the MINITAB and Kinetic Research MDX statistics packages. All data were filtered to remove cases

with missing or inconsistent data (see Reference 3). Only automobiles and station wagons were considered as case vehicles*. Each case vehicle was assigned to one of eight collision modes:

(1) Fixed-Object Front. The vehicle's front struck a solid fixed object, such as a tree, median or bridge support. Less solid objects such as mailboxes or fences were not considered.

(2) Fixed-Object Side. Same as above, except that the vehicle's side struck the object. These are usually cases in which a vehicle also skidded out of control.

(3) Non-collision/Rollover. These are cases found in the North Carolina category "Non-Collision in Road – Overturn."

(4) Vehicle-to-Vehicle Front. The vehicle's front struck another vehicle.

(5) Vehicle-to-Vehicle Side. The vehicle's side was struck by another vehicle.

(6) Vehicle-to-Vehicle Rear. The vehicle's rear was struck by another vehicle.

(7) Pedestrian/Bicyclist/Motorcyclist. The vehicle struck a person who is not inside a vehicle.

(8) Vehicle-to-Vehicle Unknown. The vehicle impacted another vehicle in an unknown configuration.

These impact modes are coded 1 through 8 using the variable KSPTYP in the program MAIN and the subroutine MODE in the braking cost-benefit analysis. The first six correspond to the six impact modes used in the KRAESP Program. The North Carolina data include entries for the property damage to each vehicle, additional property damage (to surrounding property) and the total property damage (the sum of the three other entries). For single vehicle accidents (KSPTYP=1,2,3 and 7) property damage is simply assumed to be all damage in the accident. For

*In the cost-benefit study, damage to other vehicles was not considered, since we assume that they are not equipped with radar brakes.

two-vehicle accidents (KSPTYP=4,5,6 and 8) property damage is the damage to the case vehicle plus one-half of the additional property damage. Thus, the two vehicles share the cost of the additional damage. As mentioned previously, accidents involving three or more vehicles* were not considered. Vrel was calculated by using the equations and logic shown in Table 1.

The correlation between property damage and Vrel was studied in each mode. In addition to the the filtering described in Reference 3, the cases were weighted to adjust for the rural/urban bias in the North Carolina data. Larger weights were given to cases occuring on roads with low speed limits (see Table 2) so that the distribution of speed limits would match that observed in the 1980 National Accident Sampling System (NASS) file. Comparison of other North Carolina and NASS variables showed that other adjustments were unnecessary (Reference 4). Finally, to prevent the possibility of a few cases having an inordinately large effect on the regressions, cases in which the total damage was greater than $50,000 were not considered.

Figures 1 and 2 show the relationship between total property damage and relative velocity in fixed-object collisions. Asterisks represent the mean damage observed in each 10 mph Vrel cell, and the Cs represent the 95 percent confidence limits of the calculated means. The figures also show a straight line fit by simple linear regressions of the randomly selected 15,000 cases. The R-squared in each figure indicates the percentage of total variation in property damage that can be attributed to Vrel. The large amount of scatter in the data - correlations of only about 10 percent are being observed - can be partially explained by the influences of other potentially significant regressor variables such as vehicle age and class, which were not examined in this analysis.

One might expect the relationship between damage and Vrel to be concave downward, implying that damage rises quickly with increasing Vrel up to a point where the vehicle is totalled and then levels off. Both figures suggest that this may be occurring, but the best regression correlations were obtained using concave upward equations (Damage versus Vrel and Damage versus ln(Vrel)). This, along

*Approximately five percent of all accidents involved more than two vehicles.

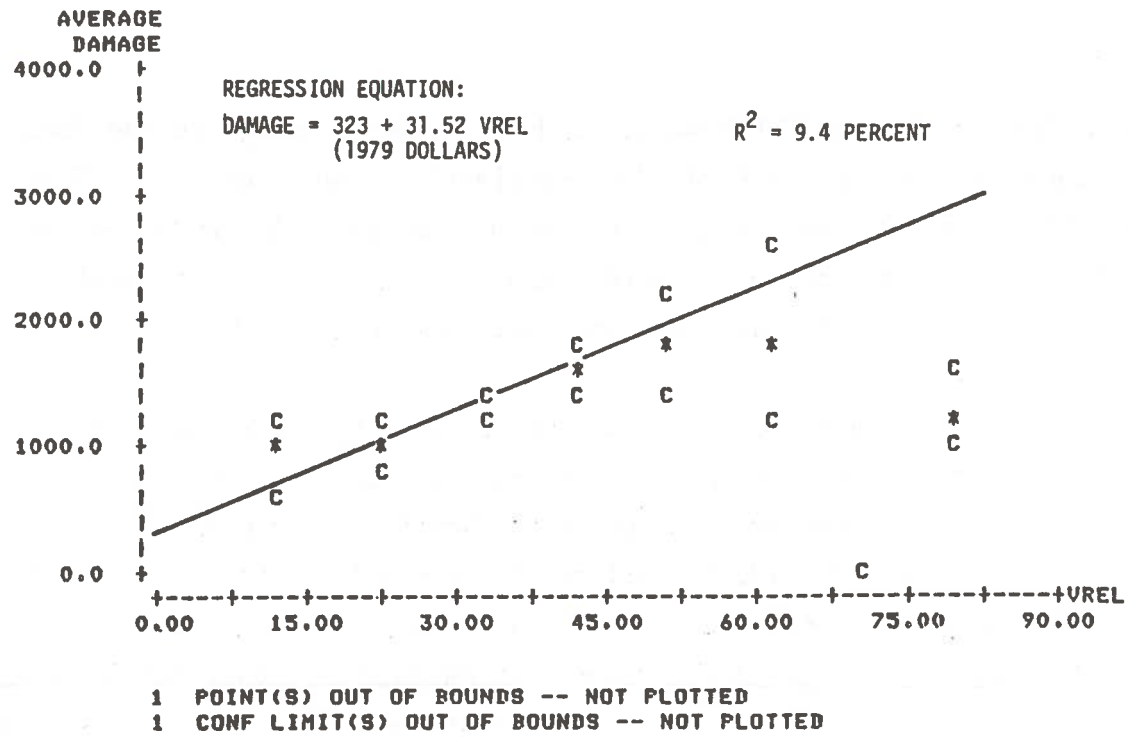

FIGURE 1. PROPERTY DAMAGE VERSUS RELATIVE VELOCITY
KSPTYP=1 (FIXED-OBJECT FRONT)

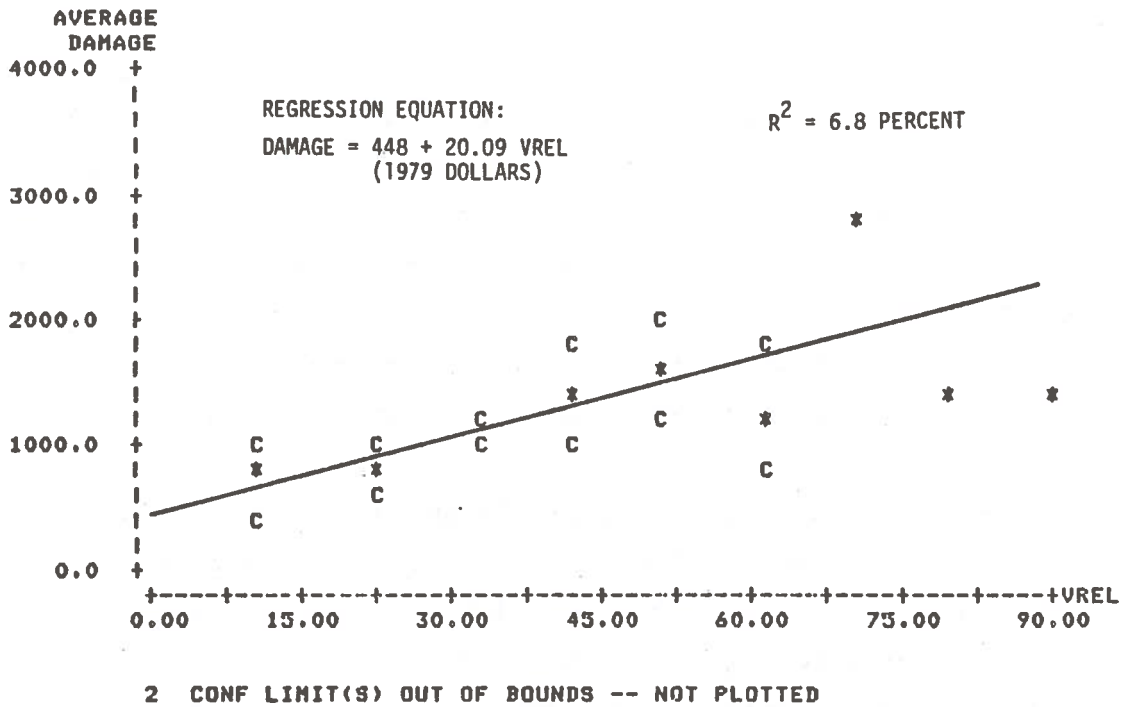

FIGURE 2. PROPERTY DAMAGE VERSUS RELATIVE VELOCITY
KSPTYP = 2 (FIXED-OBJECT SIDE)

TABLE 1. LOGIC AND EQUATIONS USED TO CALCULATE VREL

Case Vehicle Collision Mode	Other Vehicle Collision Mode			
	(4) Vehicle-to-Vehicle front	(5) Vehicle-to-Vehicle Side	(6) Vehicle-to Vehicle Rear	(8) Vehicle-to-Vehicle Unknown
(1) Fixed-Object Front	$Vrel = V_1$*			
(2) Fixed-Object Side	$Vrel = V_1$*			
(3) Non-Collision/Rollover	$Vrel = V_1$*			
(4) Vehicle-to-Vehicle Front	$Vrel = V_1 + V_2$	$Vrel = \sqrt{V_1^2 + V_2^2}$	$Vrel = V_1 - V_2$	$Vrel = \sqrt{V_1^2 + V_2^2}$
(5) Vehicle-to-Vehicle Side	$Vrel = \sqrt{V_1^2 + V_2^2}$	$Vrel = \sqrt{V_1^2 + V_2^2}$	$Vrel = \sqrt{V_1^2 + V_2^2}$	$Vrel = \sqrt{V_1^2 + V_2^2}$
(6) Vehicle-to-Vehicle Rear	$Vrel = V_2 - V_1$	$Vrel = \sqrt{V_1^2 + V_2^2}$	$Vrel = \sqrt{V_1^2 + V_2^2}$	$Vrel = \sqrt{V_1^2 + V_2^2}$
(7) Pedestrian/Bicyclist/Motorcyclist	$Vrel = V_1$*			
(8) Vehicle-to-Vehicle Unknown	$Vrel = \sqrt{V_1^2 + V_2^2}$	$Vrel = \sqrt{V_1^2 + V_2^2}$	$Vrel = \sqrt{V_1^2 + V_2^2}$	not considered

Vrel = Relative velocity
V_1 = Case vehicle impact speed
V_2 = Other vehicle impact speed

*Only one vehicle in these collisions.

TABLE 2. WEIGHTING OF 1979 NORTH CAROLINA DATA TO REMOVE RURAL/URBAN BIAS*

Speed Limit (mph)	N.C. Frequency (percent)	NASS Frequency (percent)	Weights Applied to N.C. Data
10 to 15	2.1	0.7	0.38
20 to 25	7.2	16.4	2.63
30 to 35	40.1	50.5	1.45
40 to 45	18.0	12.8	0.82
50 to 55	32.5	19.6	0.70

*Obtained from Reference 4.

with the fact that data above 50 mph was relatively scarce, led us to conclude that anything more sophisticated than a simple straight line regression was probably not warranted for the radar-braking study.

Figure 3 shows relatively poor correlation in the Non-collision/Rollover Mode. These accidents also exhibit the largest y-intercept of any mode. Of course, the regression equations are incorrect in predicting nonzero damage when Vrel=0, but the intercept does give some indication of the minimum damage that might be expected in reported accidents for each mode. And, not surprisingly, the equations indicate that the minimum damage in a rollover collision is considerably higher than that observed in other impact modes.

Figure 4 shows the same basic plot for all vehicle-to-vehicle modes. In these cases a linear model appears to give a good fit. Figures 5 through 8 then break down the vehicle-to-vehicle accidents into front, side, rear and unknown modes. The lowest y-intercept is observed for the Vehicle-to-Vehicle Front Mode; this may be due to the presence of no-damage front bumpers.

Finally, the total property damage in accidents involving automobiles and pedestrians, bicyclists and motorcyclists was studied. Because of the relative infrequency of such accidents, all appropriate cases (2,675 total) in the North Carolina file were used. As Figure 9 attests, there is a small increase in total damage with increasing Vrel. (Vrel in this case is simply equal to the striking vehicle impact speed.) Although the influence of Vrel only accounts for less than one percent of the variation in damage (R^2 - 0.45%), the relationship is statistically significant (the slope T-Ratio equals 3.50).

NONOCCUPANT INJURIES

The relationship of non-occupant injuries to striking vehicle impact velocity was also studied by using all 2,675 filtered and weighted cases in which KSPTYP=7. By making a single grouping of these accidents, we have assumed that pedestrians, bicyclists and motorcyclists all have identical injury probabilities. While there may be differences, all three are extremely

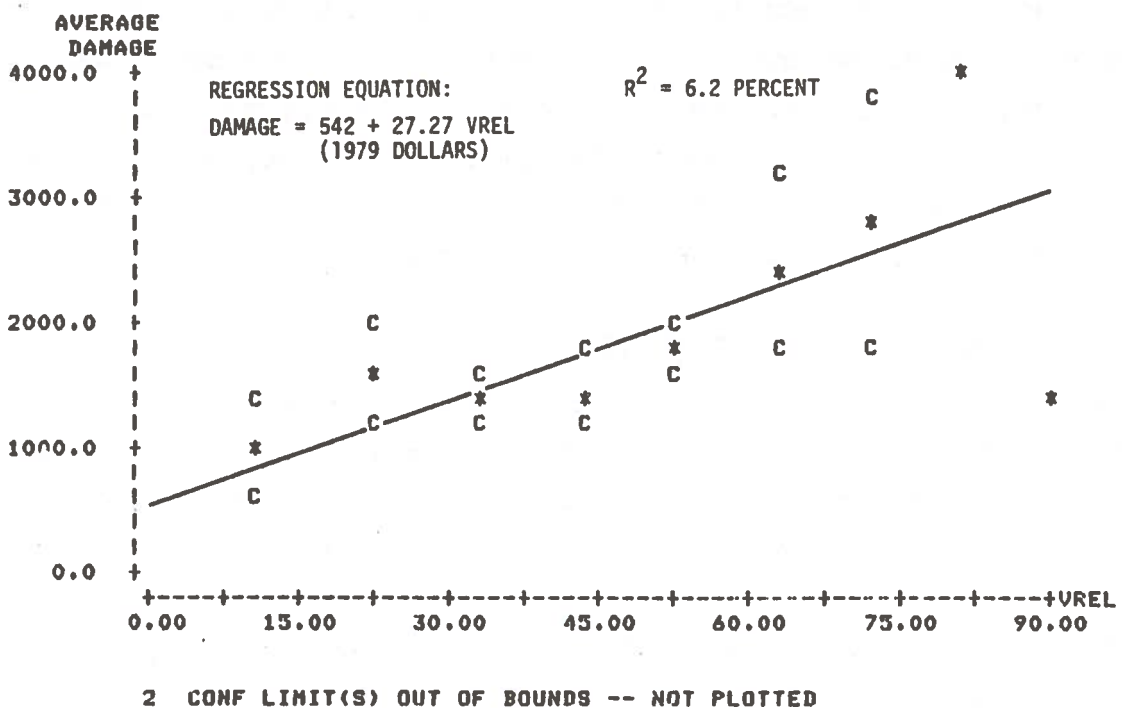

FIGURE 3. PROPERTY DAMAGE VERSUS RELATIVE VELOCITY
KSPTYP = 3 (ROLLOVER/NONCOLLISION)

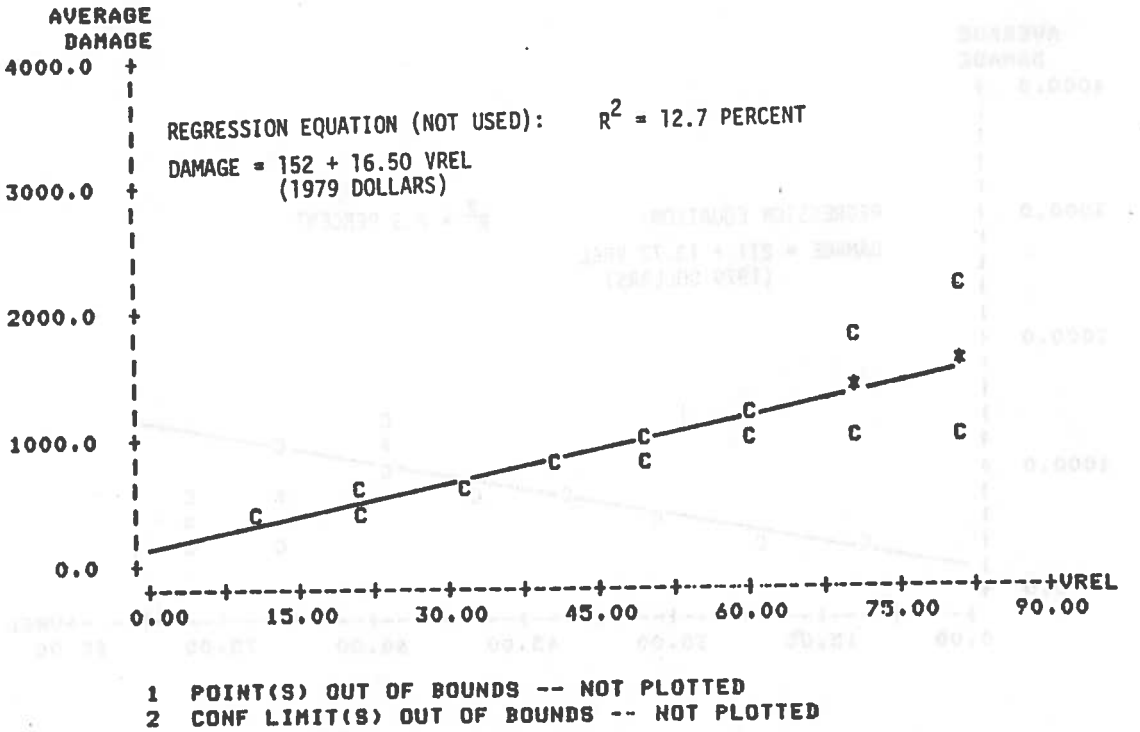

FIGURE 4. PROPERTY DAMAGE VERSUS RELATIVE VELOCITY
KSPTYP = 4-6, 8 (ALL VEHICLE-TO-VEHICLE)

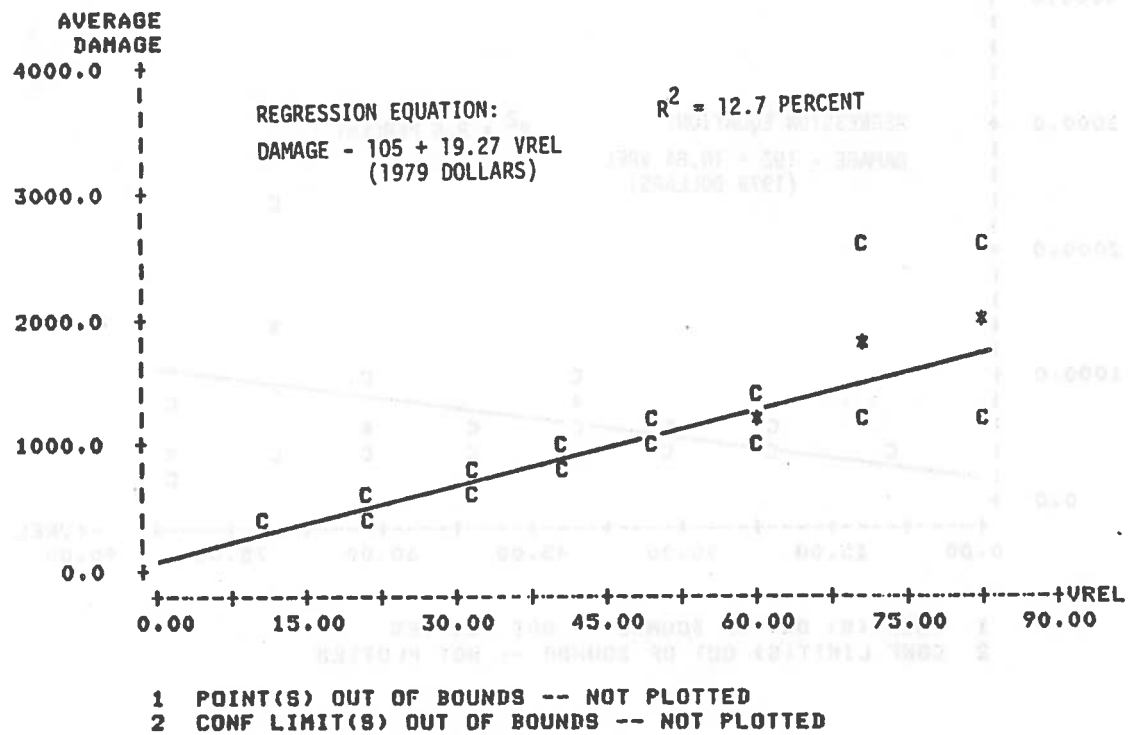

FIGURE 5. PROPERTY DAMAGE VERSUS RELATIVE VELOCITY
KSPTYP = 4 (VEHICLE-TO-VEHICLE FRONT)

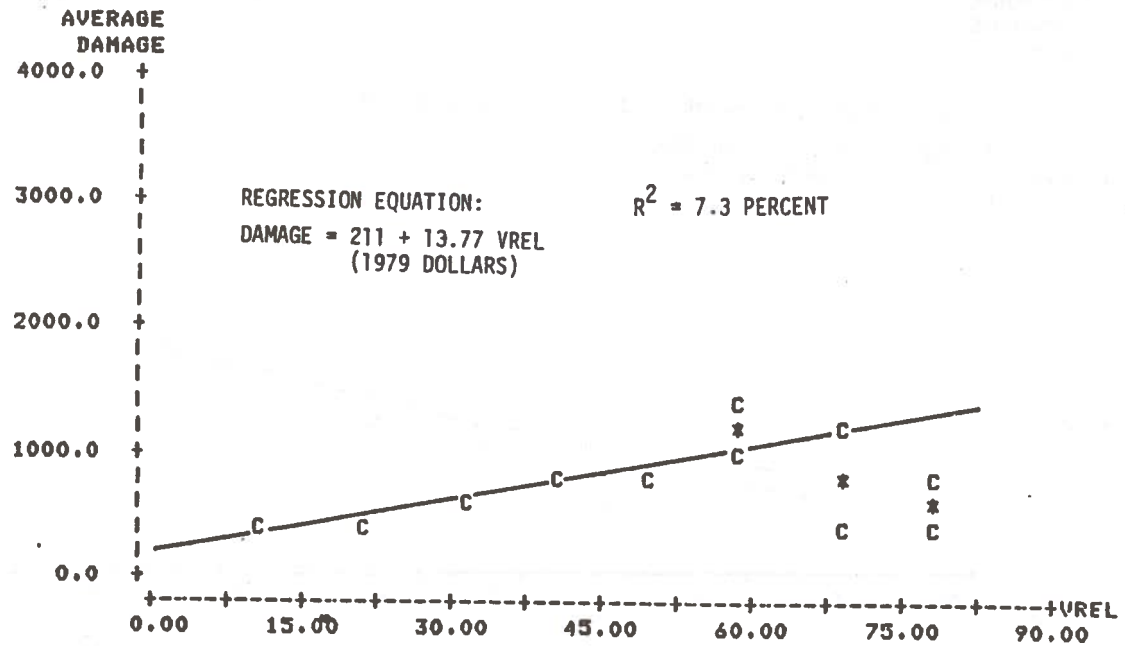

FIGURE 6. PROPERTY DAMAGE VERSUS RELATIVE VELOCITY
KSPTYP = 5 (VEHICLE-TO-VEHICLE SIDE)

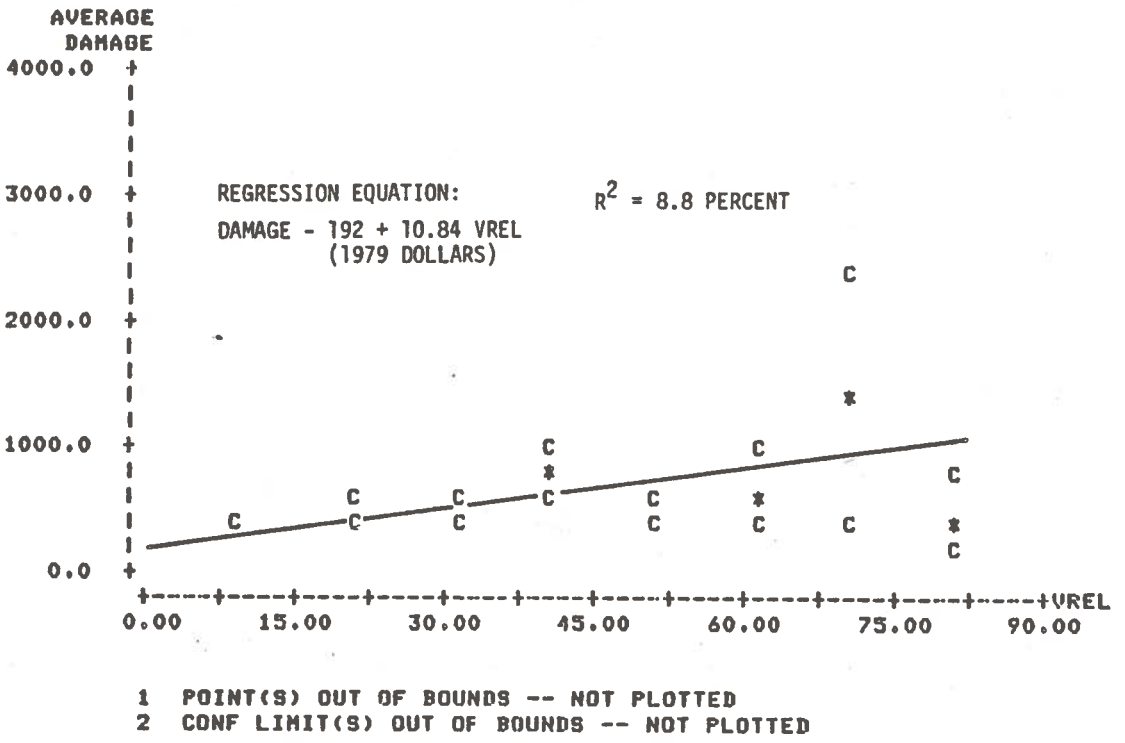

FIGURE 7. PROPERTY DAMAGE VERSUS RELATIVE VELOCITY
KSPTYP = 6 (VEHICLE-TO-VEHICLE REAR)

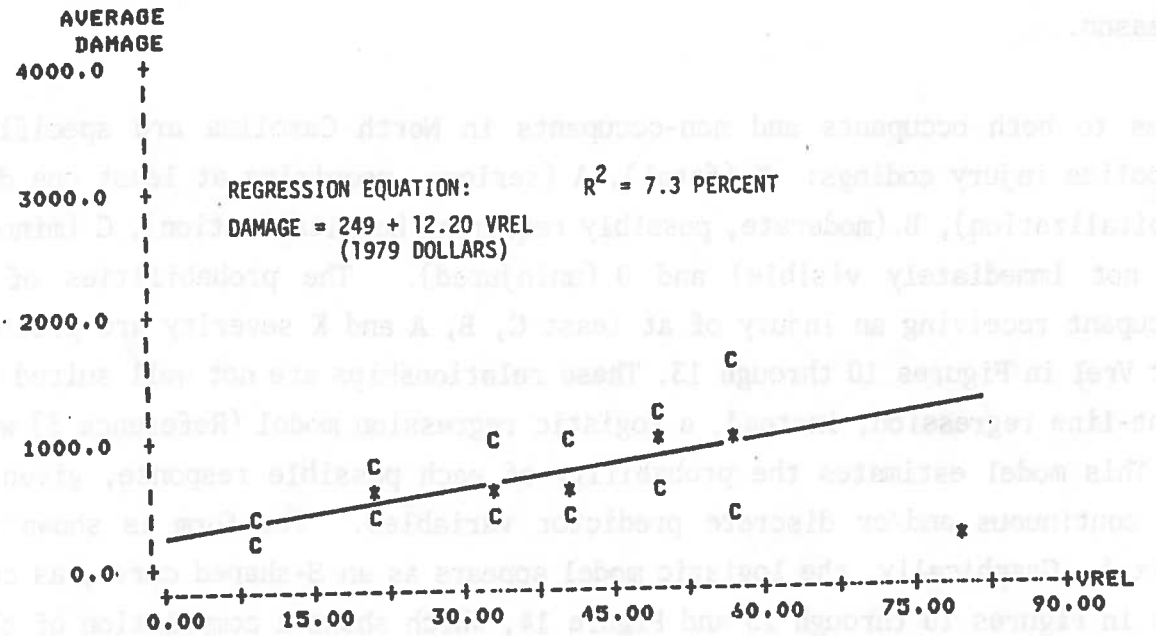

FIGURE 8. PROPERTY DAMAGE VERSUS RELATIVE VELOCITY
KSPTYP = 8 (VEHICLE-TO-VEHICLE, UNKNOWN CONFIGURATION*)

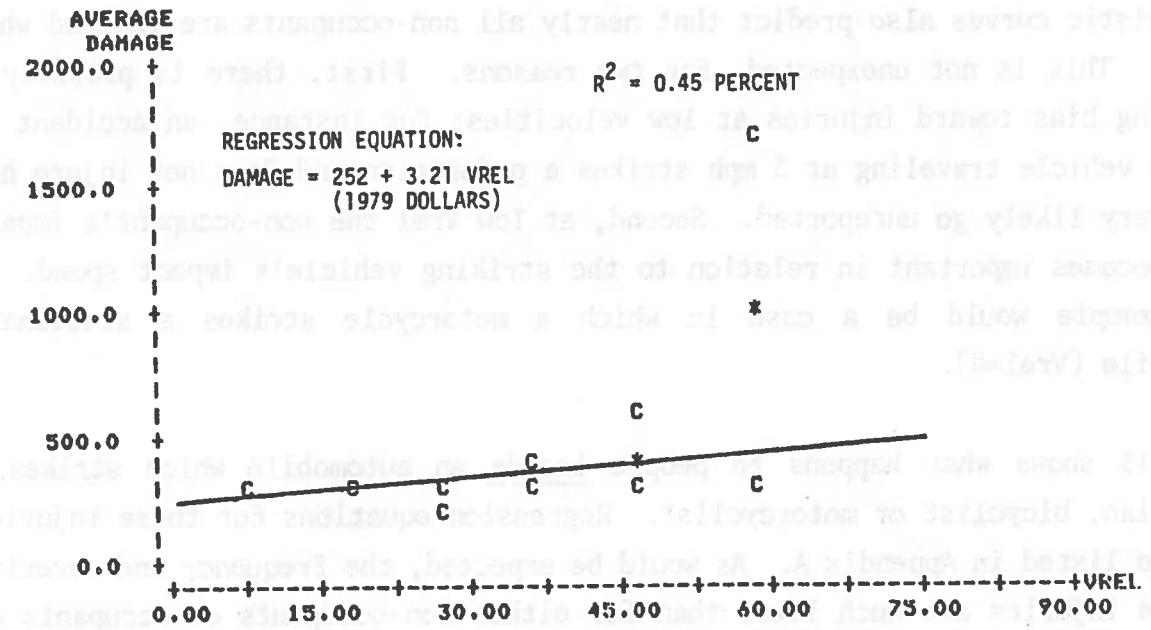

FIGURE 9. PROPERTY DAMAGE VERSUS RELATIVE VELOCITY
KSPTYP = 7 (VEHICLE STRIKING MOTORCYCLIST, BICYCLIST OR PEDESTRIAN)

*TYPCIALLY PARKED AUTOMOBILES

vulnerable in comparison to occupants, and were placed in a separate category for that reason.

Injuries to both occupants and non-occupants in North Carolina are specified using police injury codings: K (fatal), A (serious, requiring at least one day of hospitalization), B (moderate, possibly requiring hospitalization), C (minor, injury not immediately visible) and 0 (uninjured). The probabilities of a non-occupant receiving an injury of at least C, B, A and K severity are plotted against Vrel in Figures 10 through 13. These relationships are not well suited to straight-line regression; instead, a logistic regression model (Reference 5) was used. This model estimates the probability of each possible response, given a set of continuous and/or discrete predictor variables. Its form is shown in Appendix A. Graphically, the logistic model appears as an S-shaped curve, as can be seen in Figures 10 through 13 and Figure 14, which shows a compilation of the preceding curves. Because of limited high-speed data, these curves will not be particularly accurate beyond 50 or 60 mph, but we have drawn them out to 75 mph to help show the type of relationship which they predict.

The logistic curves also predict that nearly all non-occupants are injured when Vrel=0. This is not unexpected, for two reasons. First, there is probably a reporting bias toward injuries at low velocities; for instance, an accident in which a vehicle traveling at 3 mph strikes a pedestrian and does not injure him would very likely go unreported. Second, at low Vrel the non-occupant's impact speed becomes important in relation to the striking vehicle's impact speed. A good example would be a case in which a motorcycle strikes a stationary automobile (Vrel=0).

Figure 15 shows what happens to people inside an automobile which strikes a pedestrian, bicyclist or motorcyclist. Regression equations for these injuries are also listed in Appendix A. As would be expected, the frequency and severity of these injuries are much lower than for either non-occupants or occupants of vehicles which strike other vehicles or fixed objects. (For all KSPTYP=7 accidents, there were 3 fatalities to occupants versus 140 to non-occupants.) Consequently, the societal costs of these injuries are neglected in the radar-braking analysis.

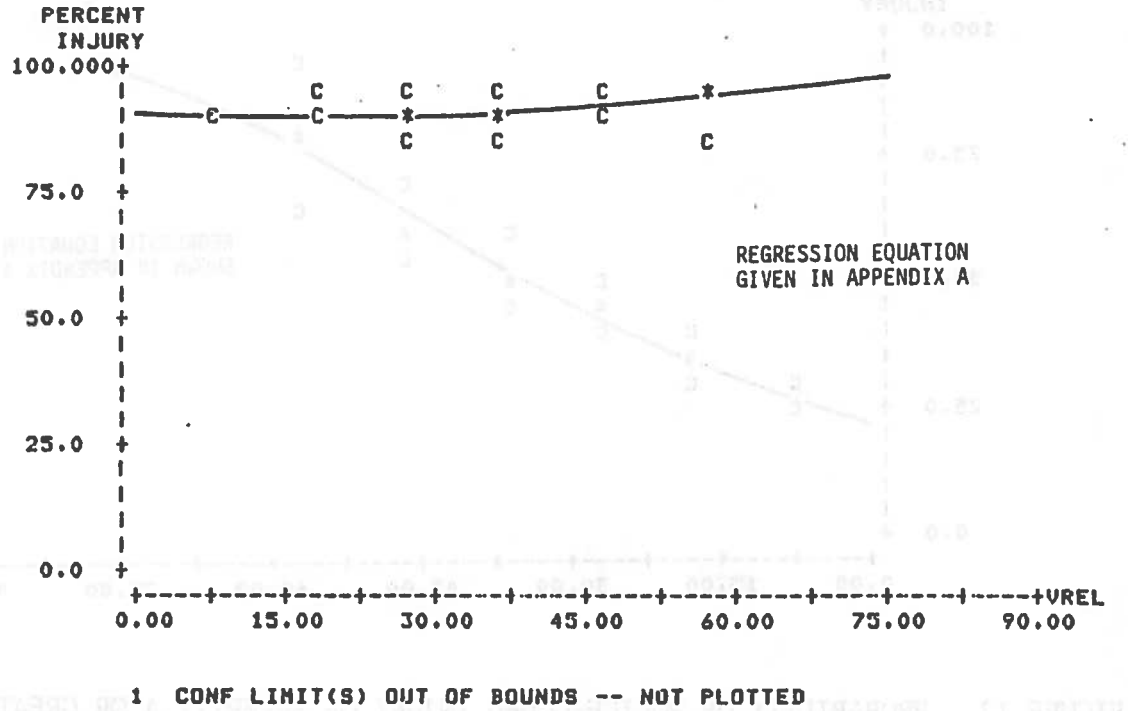

FIGURE 10. PROBABILITY OF INJURY (K, A, B OR C) VERSUS IMPACT VELOCITY FOR PEDESTRIANS, BICYCLISTS AND MOTORCYCLISTS STRUCK BY AUTOMBILES (KSPTYP=7)

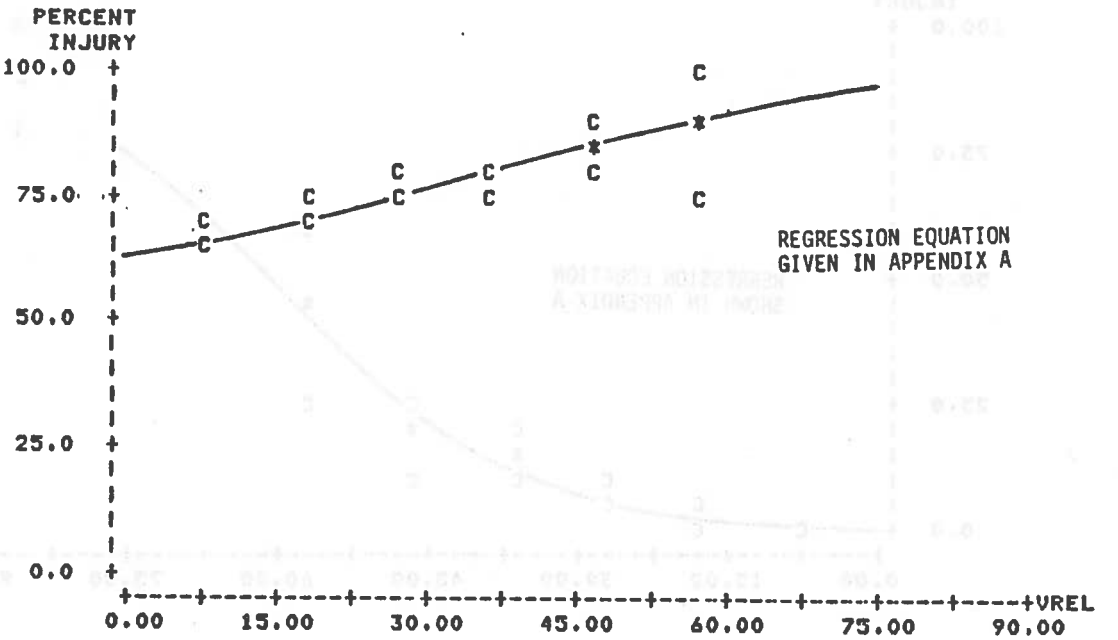

FIGURE 11. PROBABILITY OF POLICE-CODED INJURY OF SEVERITY B OR GREATER (K, A OR B) VERSUS IMPACT VELOCITY FOR PEDESTRIANS, BICYCLISTS AND MOTORCYCLES STRUCK BY AUTOMOBILES (KSPTYP = 7)

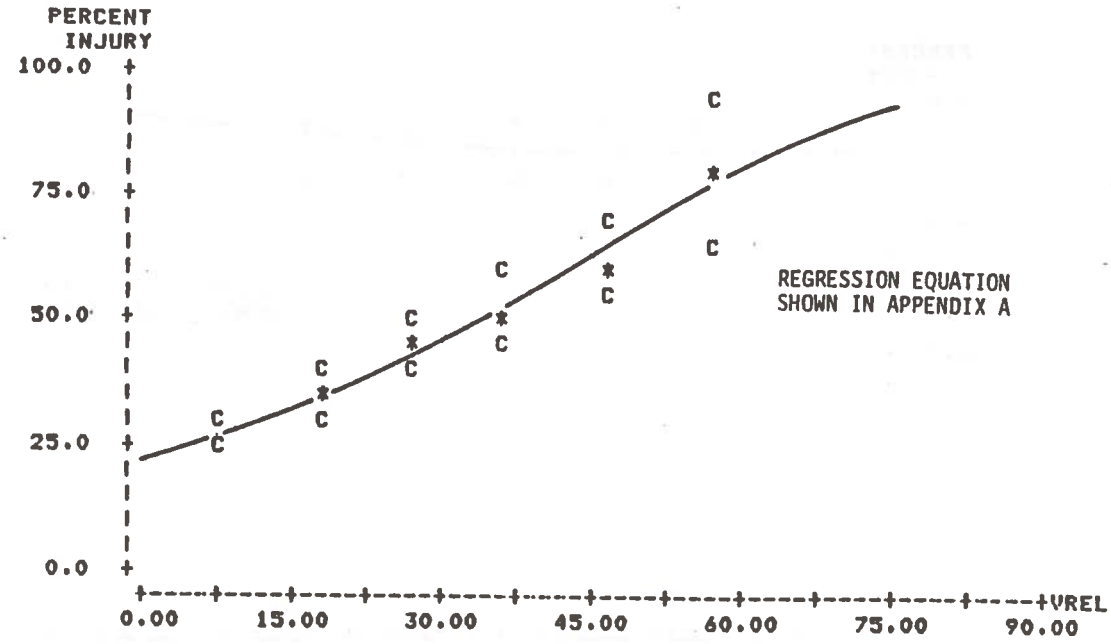

FIGURE 12. PROBABILITY OF POLICE-CODED INJURY OF SEVERITY A OR GREATER (K OR A) VERSUS IMPACT VELOCITY FOR PEDESTRIANS, BICYCLISTS AND MOTORCYCLISTS STRUCK BY AUTOMOBILES (KSPTYP =7)

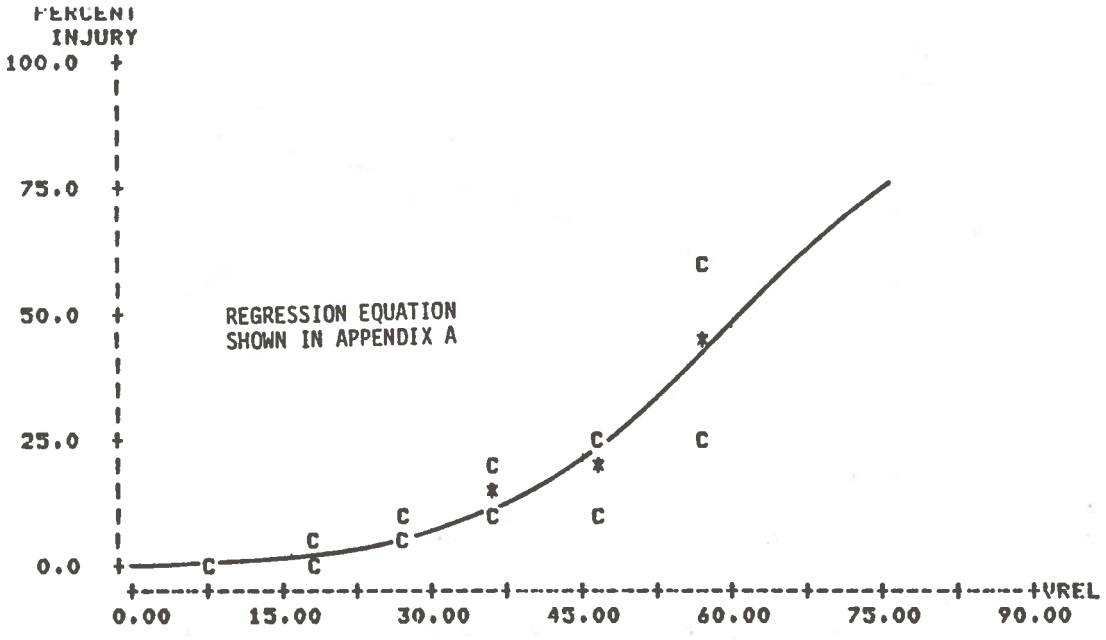

FIGURE 13. PROBABILITY OF FATAL INJURY (K) VERSUS IMPACT VELOCITY FOR PEDESTRIANS, BICYCLISTS AND MOTORCYCLISTS STRUCK BY AUTOMOBILES (KSPTYP = 7)

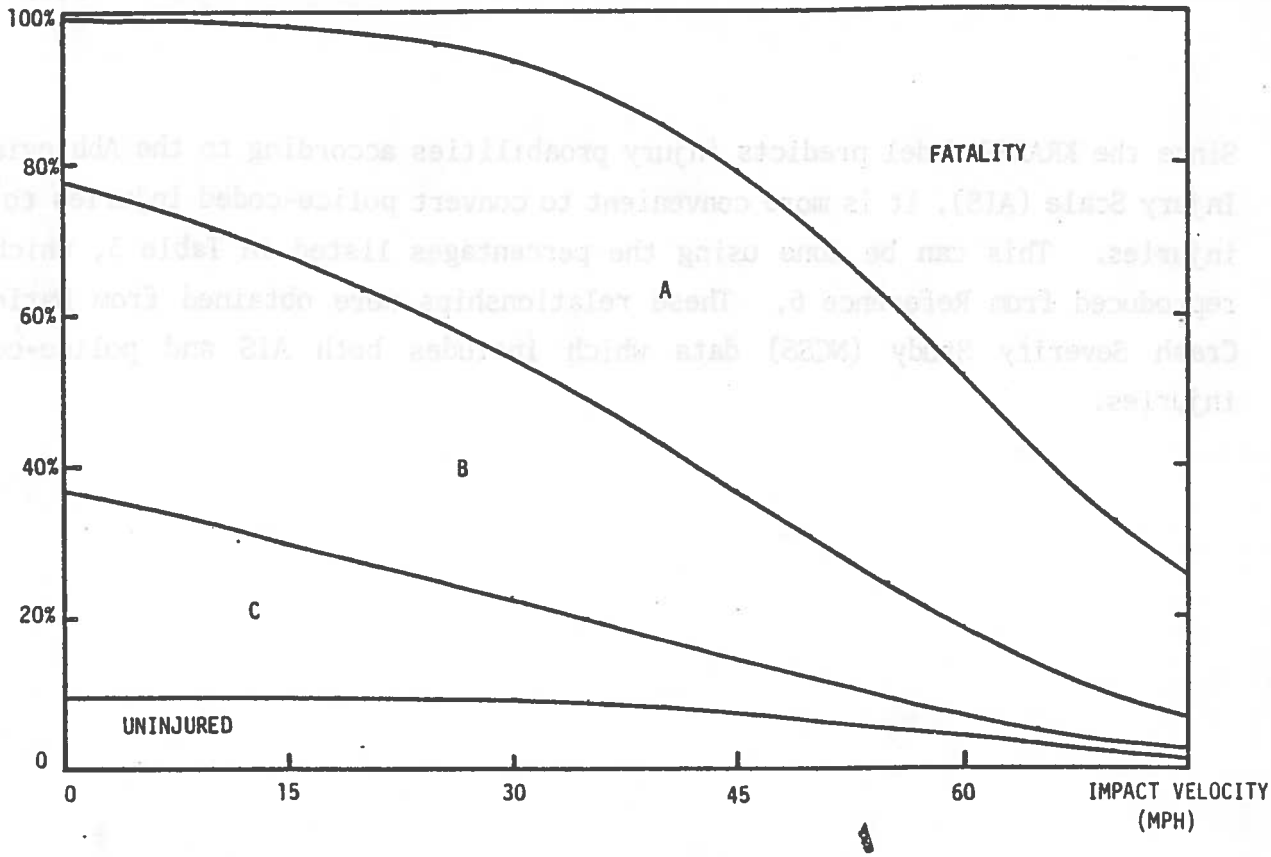

FIGURE 14. PROBABILITY OF POLICE-CODED INJURIES VERSUS IMPACT VELOCITY FOR PEDESTRIANS, BICYCLISTS AND MOTORCYCLISTS STRUCK BY AUTOMOBILES (KSPTYP = 7)

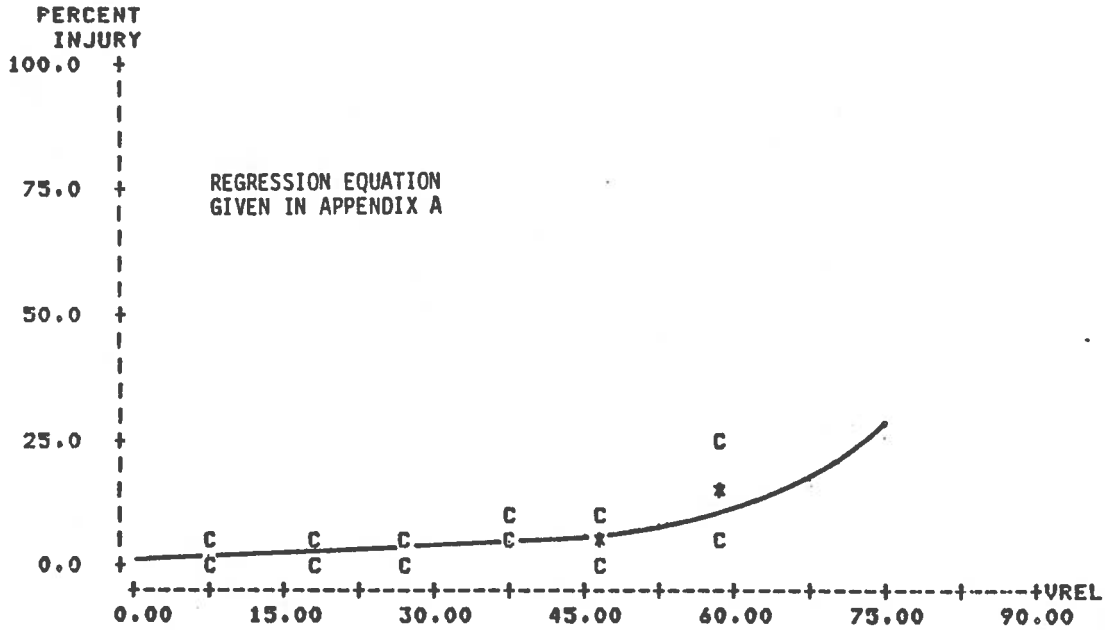

FIGURE 15. PROBABILITY OF INJURY VERSUS IMPACT VELOCITY FOR OCCUPANTS OF AUTOMOBILES WHICH STRIKE PEDESTRIANS, BICYCLISTS AND MOTORCYCLISTS (KSPTYP = 7)

Since the KRAESP Model predicts injury proabilities according to the Abbreviated Injury Scale (AIS), it is more convenient to convert police-coded injuries to AIS injuries. This can be done using the percentages listed in Table 3, which is reproduced from Reference 6. These relationships were obtained from National Crash Severity Study (NCSS) data which includes both AIS and police-coded injuries.

TABLE 3. DISTRIBUTION OF AIS BY PERCENT FOR EACH OF THE POLICE CODED INJURIES O, C, B, A, K FOR DRIVERS INVOLVED IN NEARSIDE VEHICLE-TO-VEHICLE CRASHES (EXCLUDING SIDESWIPES

AIS*	O	C	B	A	K
0	93.30	28.54	13.33	00.00	
1	6.65	57.02	68.48	40.33	
2	.01	9.34	8.86	17.54	
3	.04	4.83	6.51	32.07	
4	.00	.28	2.02	6.76	
5	.00	.00	.29	2.34	
6	.00	.00	.50	.96	100.00
TOTALS	100.00	100.01	99.99	100.00	100.00

REFERENCES

1. V. Ausherman and A. Khadilkar, "Selection of Accident Data Base and Accident Analysis Approach for Collision Avoidance System Cost-Benefits Analysis," Kinetic Research Technical Report KR-TR-083, December 1980.

2. D. Redmond, "Implementation and Preliminary Analysis of 1979 State of North Carolina Accident Data," for use on Contract DTNH22-80-C-07530, 'Collision Avoidance System Cost-Benetfit Analysis', Kinetic Research Technical Report KR-TR-103.

3. D. Redmond, V. Ausherman and V. Costa, "Methodolgy for the Computation of Fatality and Injury Loss Reduction Accruing from the Installation of Radar Controlled Brakes on Passenger Cars," for use on Contract DTNH22-80-C-07530, 'Collision Avoidance System Cost-Benefit Analysis', Kinetic Research Technical Report KR-TR-106. July 1981.

4. D. Redmond, "Adjustments Made to the 1979 North Carolina Data to Make it Nationally Representative," Kinetic Research Technical Note KR-TN-013, May 1981.

5. Cox, D.R., "The Analysis of Binary Data," Halsted Press, a Division of John Wiley & Sons, New York, 1970.

6. L. Klimko, and K. Friedman, "Preliminary Results on the Feasibility and Application of the SASE Methodology to the Derivation of AIS to Delta-V Relationships from State Data," for use on Contract DOT-HS-9-02096, Kinetic Research Technical Report KR-TR-057. April 1980.

APPENDIX A
RESGRESSION EQUATIONS

The probability of each police-coded injury in accidents in which an automobile strikes a pedestrian, bicyclist or motorcyclist is as follows:

$$P(\text{fatality}) = \frac{1}{1 + e^{A} + e^{B} + e^{C} + e^{U}}$$

$$P(\text{A injury}) = \frac{e^{A}}{1 + e^{A} + e^{B} + e^{C} + e^{U}}$$

$$P(\text{B injury}) = \frac{e^{B}}{1 + e^{A} + e^{B} + e^{C} + e^{U}}$$

$$P(\text{C injury}) = \frac{e^{C}}{1 + e^{A} + e^{B} + e^{C} + e^{U}}$$

$$P(\text{no injury}) = \frac{e^{U}}{1 + e^{A} + e^{B} + e^{C} + e^{U}}$$

where $A = A_1 + A_2\ Vrel$

$B = B_1 + B_2\ Vrel$

$C = C_1 + C_2\ Vrel$

$U = U_1 + U_2\ Vrel$

REGRESSION COEFFICIENTS FOR NON-OCCUPANTS				REGRESSION COEFFICIENTS FOR OCCUPANTS			
A_1	2.922	A_2	-0.07145	A_1	5.869	A_2	-0.08418
B_1	4.546	B_2	-0.09969	B_1	7.723	B_2	-0.1217
C_1	5.140	C_2	-0.1153	C_1	7.915	C_2	-0.1143
U_1	3.086	U_2	-0.09195	U_1	12.67	U_2	-0.1430

There are, on the average, 1.56 occupants and 1.06 non-occupants in each accident.

APPENDIX I

PROPERTIES OF THE LEVEL ONE RADAR BRAKE SYSTEM

This appendix contains material obtained from Dr. Lynn Carpenter of Pennsylvania State University. It is a description of the radar target and performance model, including the range velocity brake activation curve used in the present study.

Radar Technical Evaluation

J. M. Laugenie has developed a general target model for a flat rectangular plate. This cross section calculation uses the far field approximation which occurs at 6 m for a frequence of 10 GHz and a dimension of the antenna D = 30 cm. For $\psi = 0$ this cross section is

$$\sigma = \frac{4\pi}{\lambda^2} \frac{\rho^2 L^2 \cos^2\theta \sin^2(kL \sin\theta)}{(kL \sin\theta)^2}$$

where λ = wavelength of radar

ρ = dimension of plate in y direction

L = dimension of plate in x direction

θ = polar angle (see Figure in Appendix)

$k = \frac{2\pi}{\lambda}$

The generalized cross section $\sigma(\theta,\phi)$ is derived in the appendix included with the report.

In combining the cross section response of N scattering centers for a complex target, the phase factor must be considered in the sum (1)

$$\sigma = \left| \sum_{\ell=1}^{N} (\sigma_e)^{\frac{1}{2}} \exp(j\phi_e) \right|^2$$

where $\phi_e = \frac{4\pi de}{\lambda}$ = phase angle

d_e = distance from the target to the radar

The ground reflection from the target is an important interference signal. This will be model by using images behind the ground plane with another cross section σ_{12} which accounts for the path R_1 from the transmitter to target and R_2 which is the path from the image target to the target. If the wavelength

is small compared to the dimensions of the target body, then (2)

$$\sigma(\theta_r,\theta_t) = \sqrt{\sigma(\theta_r,\theta_r)\ \sigma(\theta_t,\theta_t)}$$

where r = denotes receiver

t = denotes transmitter

Continuing this analysis with G_1 and G_2, the gain of the antenna in directions R_1 and R_2, a complex expression for the power can be developed. This power will include the ground scattering for a multidirectional target with the spatial gain function of the radar antenna.

Thus the scattering cross-section program needs the directional aspect evaluation of the antenna to continue the calculations of power received. It is expected that this will be possible as soon as the computer programs General Reflector Code and Basic Scattering are received from Ohio State University. They were ordered over a month ago from Dr. Ronald Markefka (see enclosed letter) but have not been reviewed.

Henri Pruvot is in charge of evaluating the antenna modeling program and applying it for the particular radar systems available. We have some antenna modeling programs operating and expect soon to be able to combine the cross-sectional analysis and antenna models. However, more specific information of the F/D focal length divided by the diameter of a parabolic dish, and feed structure will be needed. It is expected to have to ask or visit each producer to determine this information.

Progress is being made on an analytical approach to target cross-sections and antenna patterns for different radar systems under consideration. It is expected to have a series of target situations for possible detection of the radars and another set of cross-section for the potential false alarms to evaluate the potential effectiveness of each radar system.

References

(1) Crispin Jr., J. W., and K. M. Siegel, "Method of Radar Cross-Section Analysis," Academic Press, N.Y. and London, 196.

(2) Skolnik, M., "Radar Systems," McGraw Hill Book Co., 1972.

Target Detection Parameter

The cross sections for a series of targets will be generated by the computer program which sums a series of parallel plate targets. Thus, a measure of target response can be compared with measured cross sections, and this measure will be used to evaluate the various systems to be evaluated. All of the systems will be evaluated using the same targets and individual parameters of the radar system. The antenna modeling program will be used to model the response of the radar antenna and feed. Thus, each radar will be evaluated to determine how many appropriate targets out of 100 will be detected for three different levels of signal processing.

Simularly, the false target detection rate F_A will be estimated for each 100 valid targets available. Since there is a trade-off between sensitivity and false target detection, these parameters must be evaluated together.

The signal processing can enhance target detection and diminish false alarms. The internal signal processing is different for different systems and can, at best, only be estimated. This estimate will consider three levels of signal processing (1) simple, (2) average, and (3) sophisticated. For each level of signal processing, the target detection rate D_T and false alarm rate F_A will be estimated to determine an overall evaluation. These evaluation parameters D_T and F_A will be used to determine the Detection Capacity Rate (DCR)

$$DCR = \ln \left(\frac{D_T}{F_A + 1}\right) \qquad (1)$$

Thus a DCR will be obtained for each system at three levels of possible signal processing.

These evaluations can be used in the cost-benefit study to determine what percentage of accidents will be avoided for each of the various collision avoidance radar systems.

LIST OF PROGRAMS

BESSEL.FOR;1
CIRCLE.FOR:1
DISHGAIN.FOR;1
DISHPLOT.FOR;1
FRAME.FOR;1
HORN.FOR;1
NEC2LIB.OLB;1
NECBSC.EXE;1
NECREF.EXE;1
SIM.FOR;1
TARG.DAT;1
TARG.DAT;5
TARG.DAT;6
TARG.DAT;7
TARG.DAT;8

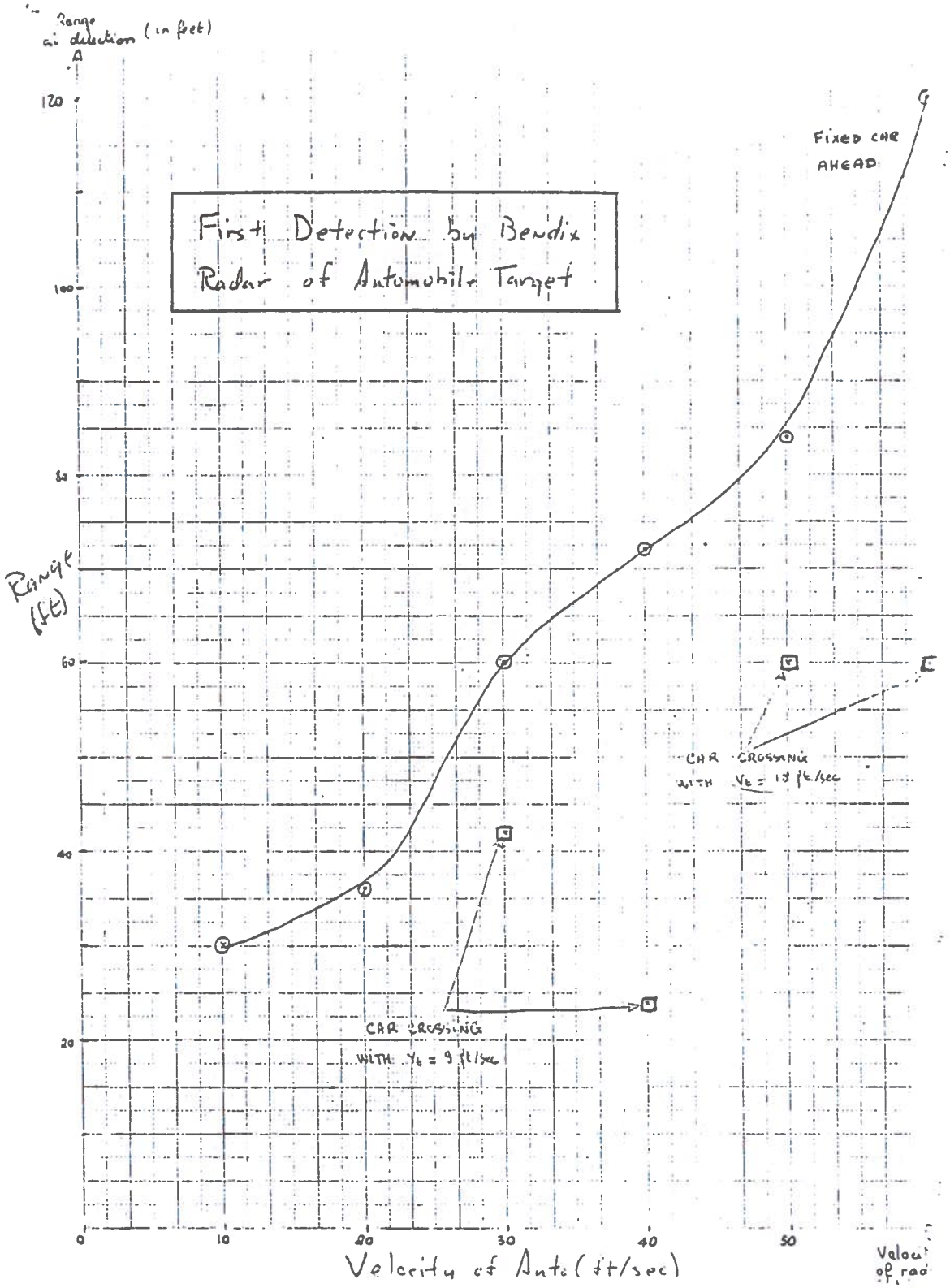
Range at detection (in feet)
First Detection by Bendix Radar of Automobile Target
FIXED CAR AHEAD
CAR CROSSING WITH V_t = 9 ft/sec
CAR CROSSING WITH V_t = 15 ft/sec
Range (ft)
Velocity of Auto (ft/sec)
Velocity of rad
120
100
80
60
40
20
0
10
20
30
40
50

Lynn Carpenter

CAR AHEAD

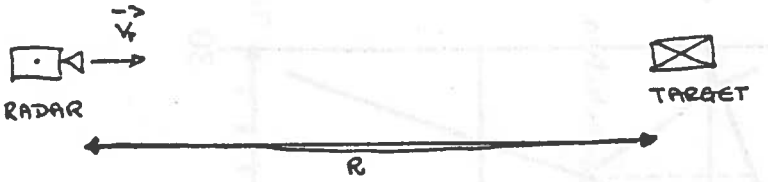

The threshold is determined from the formula:

$$P_{thr} = -100 + \frac{76 - 0.4v}{2v} \times R \quad \text{in dB}$$

where: R = range (distance from radar to target) expressed in meters
$v = \dot{R}$ = relative velocity expressed in m/sec

This formula is deduced from the condition: $R + 2\dot{R} > 0$, and the average power received as a function of range for a car ahead; it takes account of the random variations of cross-sections.

Of course, much more points are necessary to sketch a graph $d = f(v)$ of the distance at detection as a function a velocity, especially for the car crossing the road, for which there is detection only in a rather narrow range of velocities for the rec car... Hopefully this will be done tomorrow, tonight is too l

J. Marc

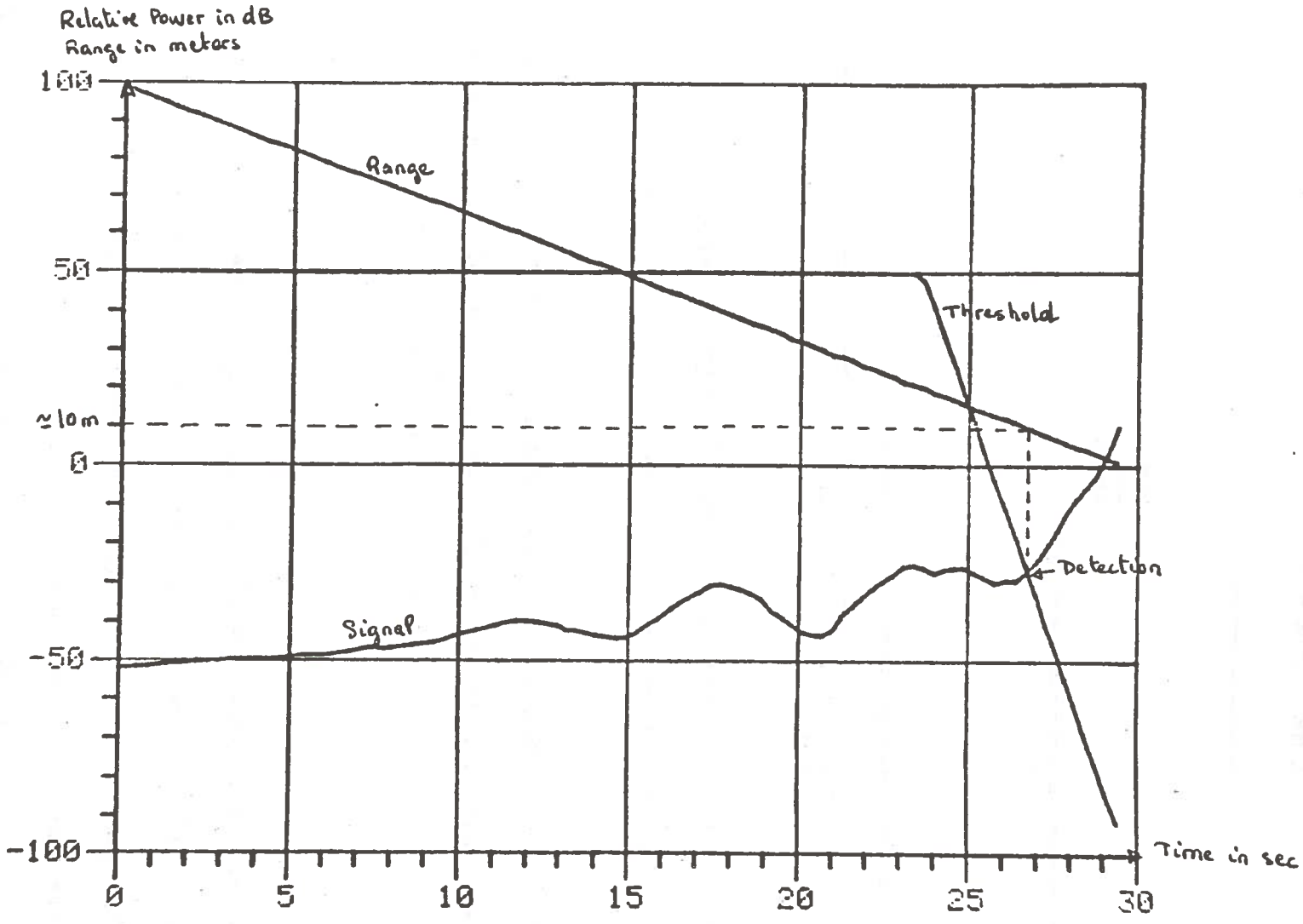

① FIXED TARGET AHEAD, AT R = 100 m ≃ 300 ft

VELOCITY OF RADAR CAR V = 10 ft/sec

DETECTION AT R ≃ 10 m ≃ 30 ft

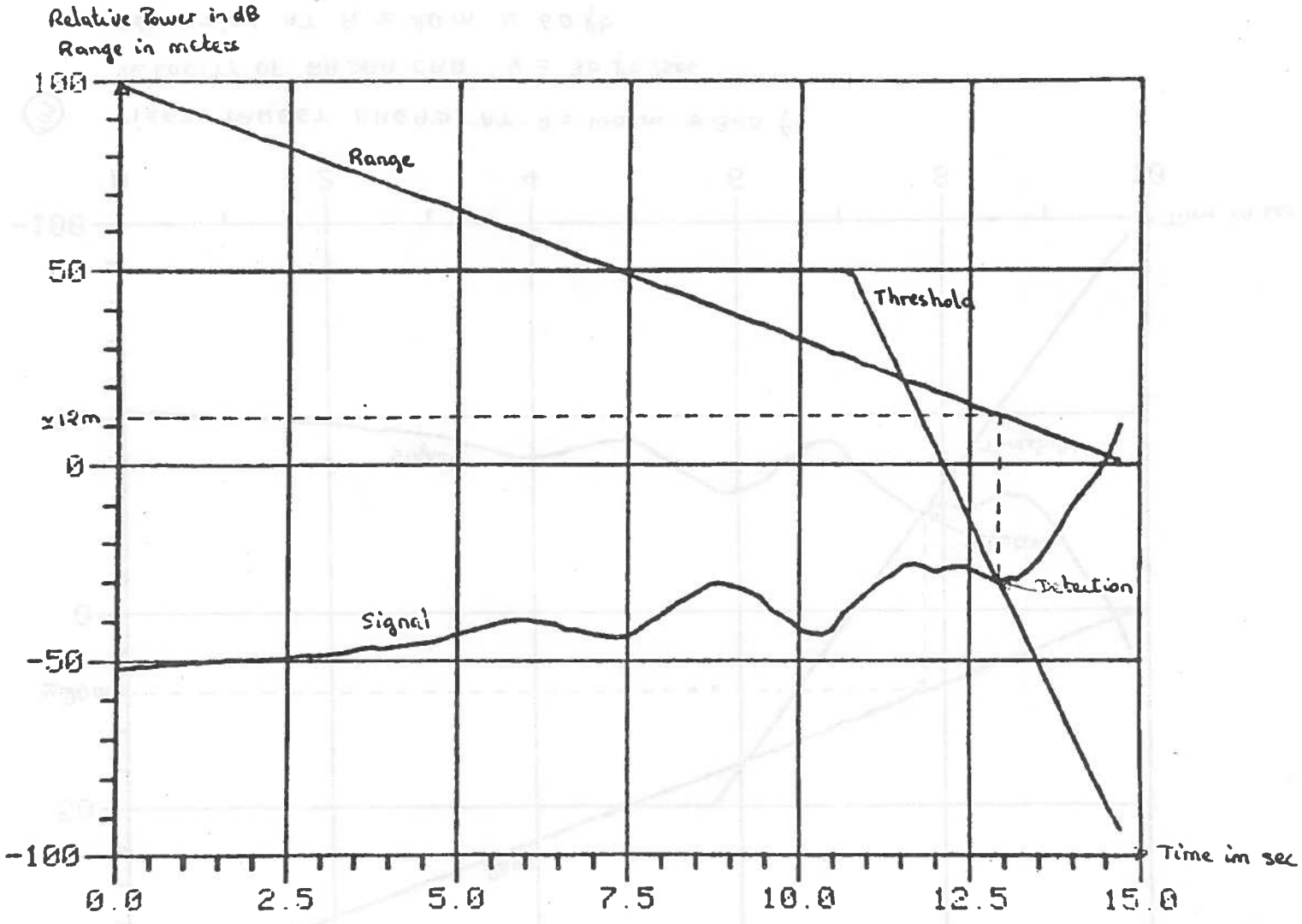

② FIXED TARGET AHEAD, AT R = 100 m ≃ 300 ft
VELOCITY OF RADAR CAR V = 20 ft/sec
DETECTION AT R ≈ 12 m ≃ 36 ft

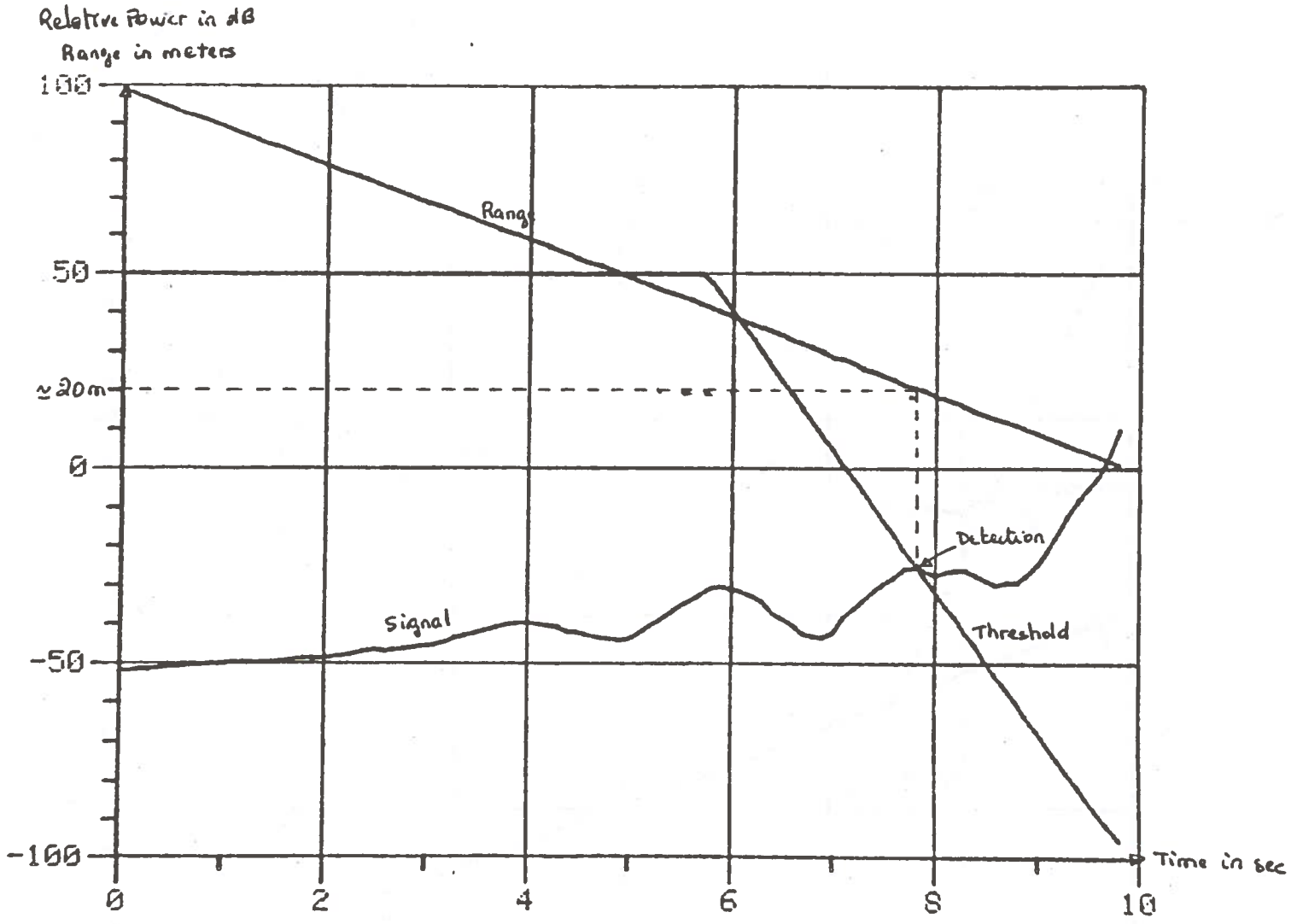

(3) FIXED TARGET AHEAD, AT R = 100 m ≃ 300 ft

VELOCITY OF RADAR CAR V = 30 ft/sec

DETECTION AT R ≃ 20 m ≃ 60 ft

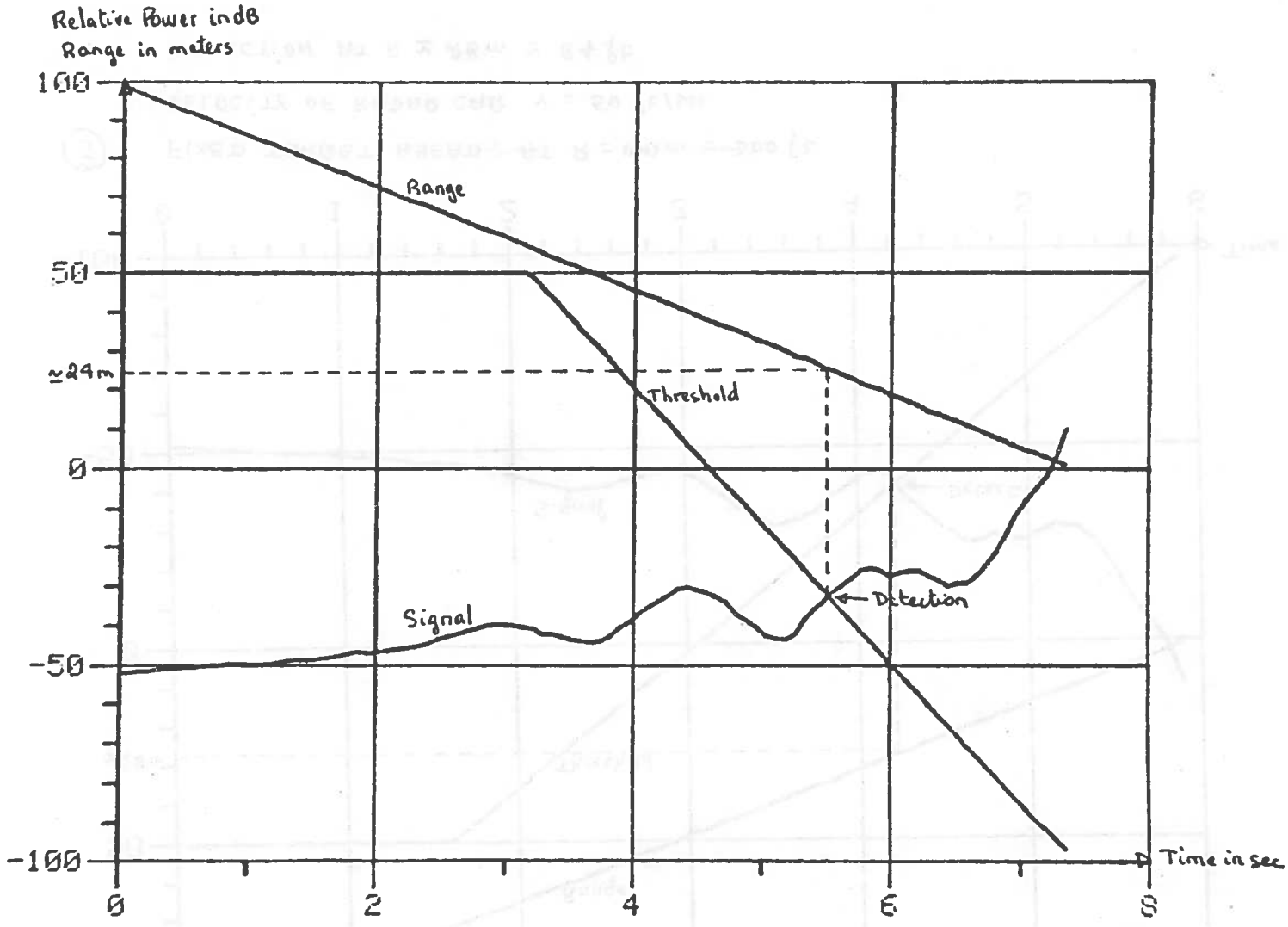

(4) FIXED TARGET AHEAD, AT R = 100 m ≈ 300 ft

VELOCITY OF RADAR CAR V = 40 ft/sec

DETECTION AT R ≈ 24 m ≈ 72 ft

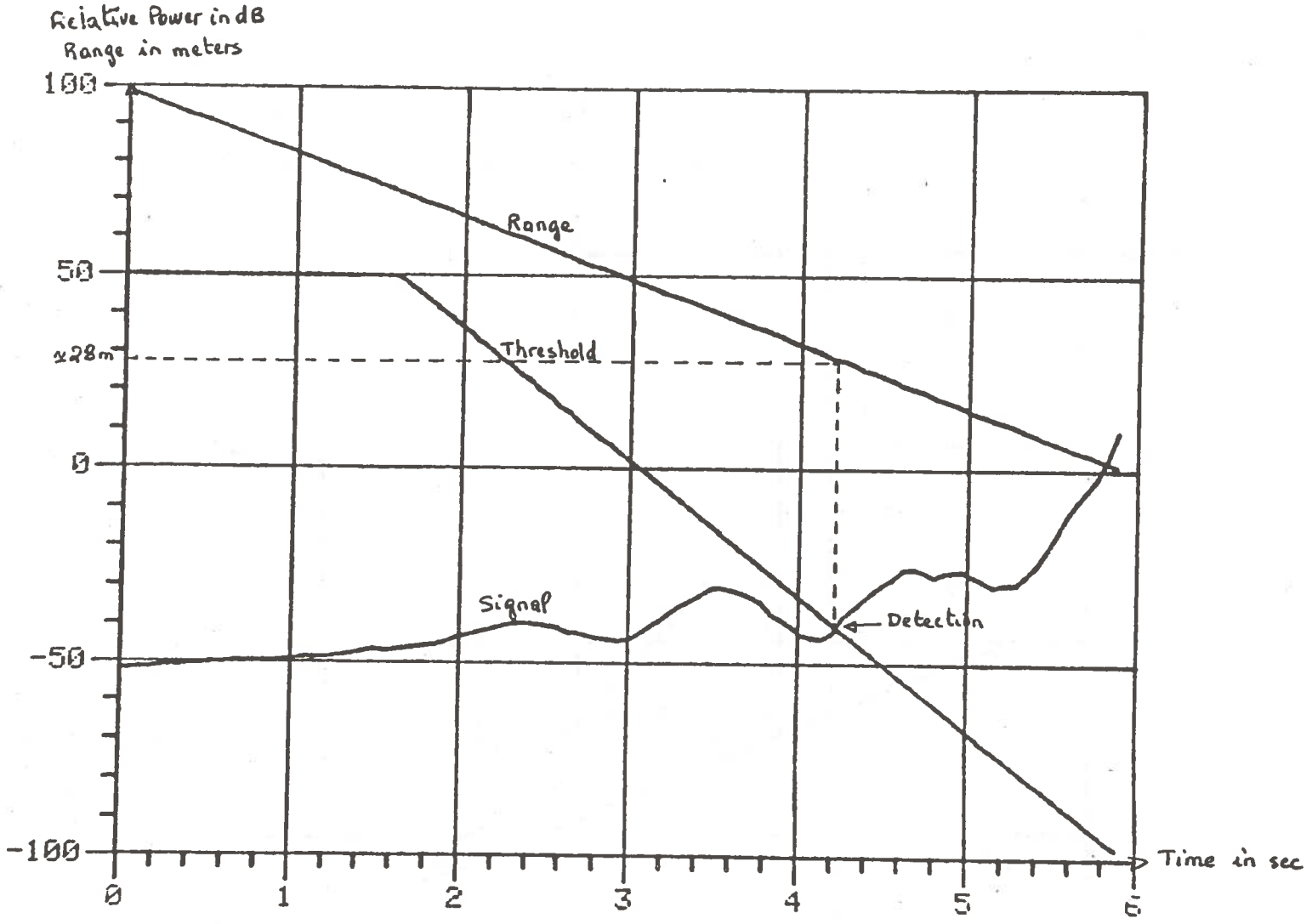

(5) FIXED TARGET AHEAD, AT R = 100 m = 300 ft

VELOCITY OF RADAR CAR V = 50 ft/sec

DETECTION AT R ≃ 28 m ≃ 84 ft

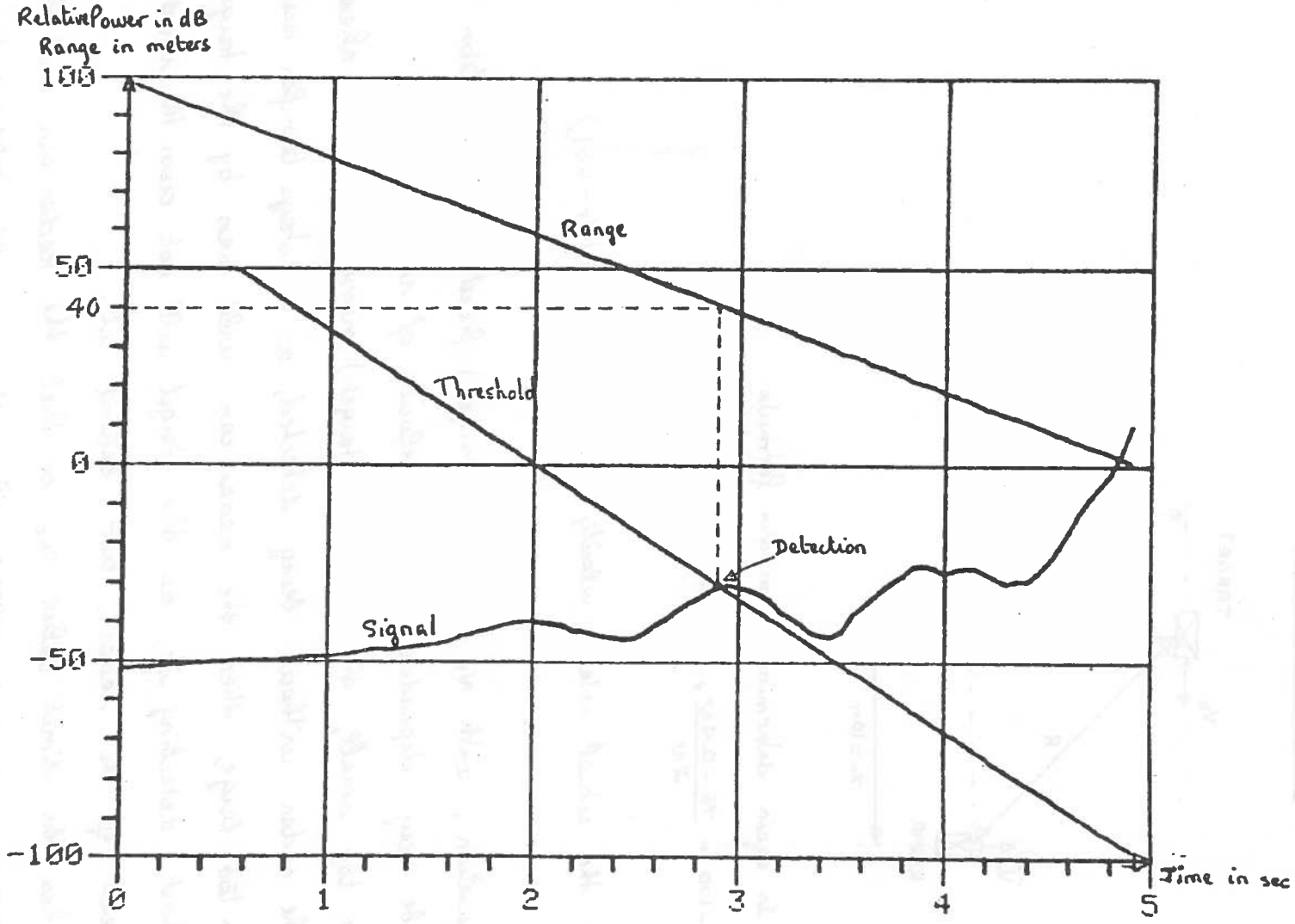

(6) FIXED TARGET AHEAD, AT $R = 100\,m = 300$ feet

VELOCITY OF RADAR CAR $V = 60$ feet/sec

DETECTION AT $R \simeq 40\,m \simeq 120$ feet

CAR CROSSING

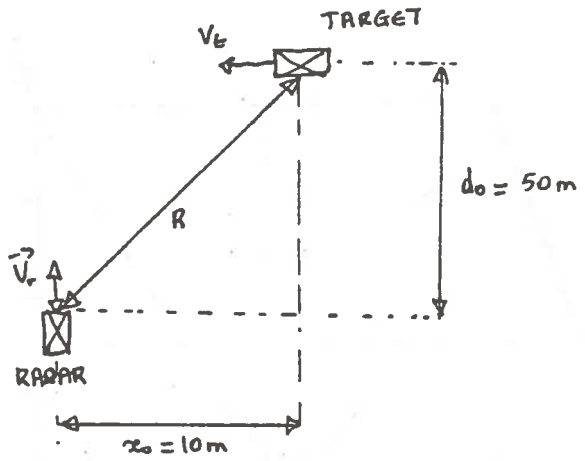

The threshold is again determined from the formula:

$$P_{thr} = -100 + \frac{76 - 0.4v}{2v} \times R \quad \text{in dB}$$

N.B. : v is the actual relative velocity $= \dot{R}$, (i.e. $v \neq |V_r - V_t|$) .

For this configuration, with V_t (velocity of target) fixed, the detection range will be very dependent on V_R (velocity of radar) :

Graph ①

* If V_R is too small, then the car (target) crosses the road ahead of the radar without being detected, as it stays too far away
* If V_R is too large, then the radar car will pass by the target without detecting it, as the target will not cross the road ahead of the radar, but behind it.

(Almost) graph ④

* If V_R has the limit value V_{R0} so that the radar car and the target are going to collide, then there might still not be any detection, as the radar, because of its narrow beamwidth will see the target at the very last moment.

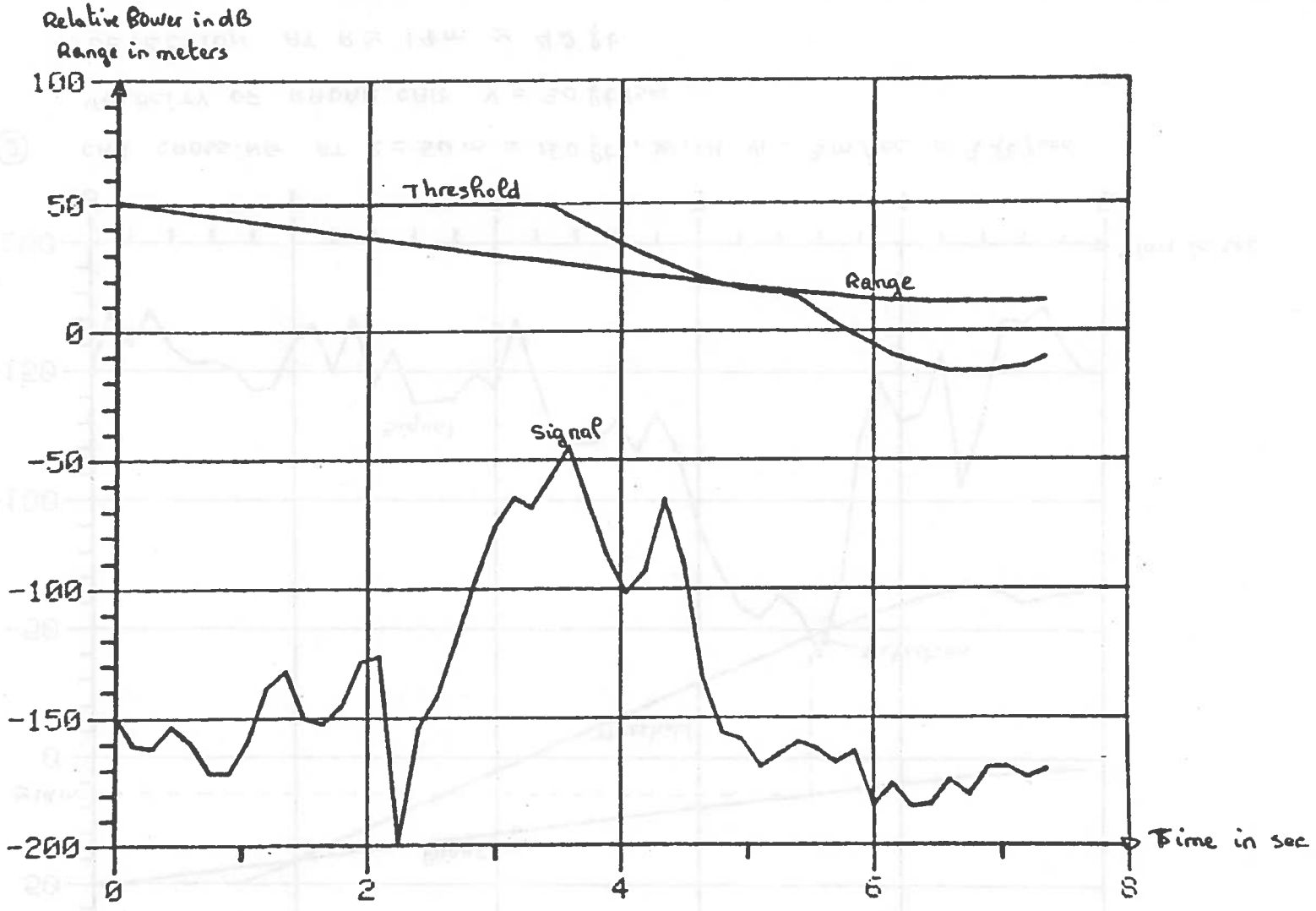

① CAR CROSSING AT R = 50 m ≃ 150 ft , WITH V_t = 3 m/sec ≃ 9 ft/sec

VELOCITY OF RADAR CAR V = 20 ft/sec

NO DETECTION (BUT NO COLLISION : R_{min} ≃ 10 m ≃ 30 ft)

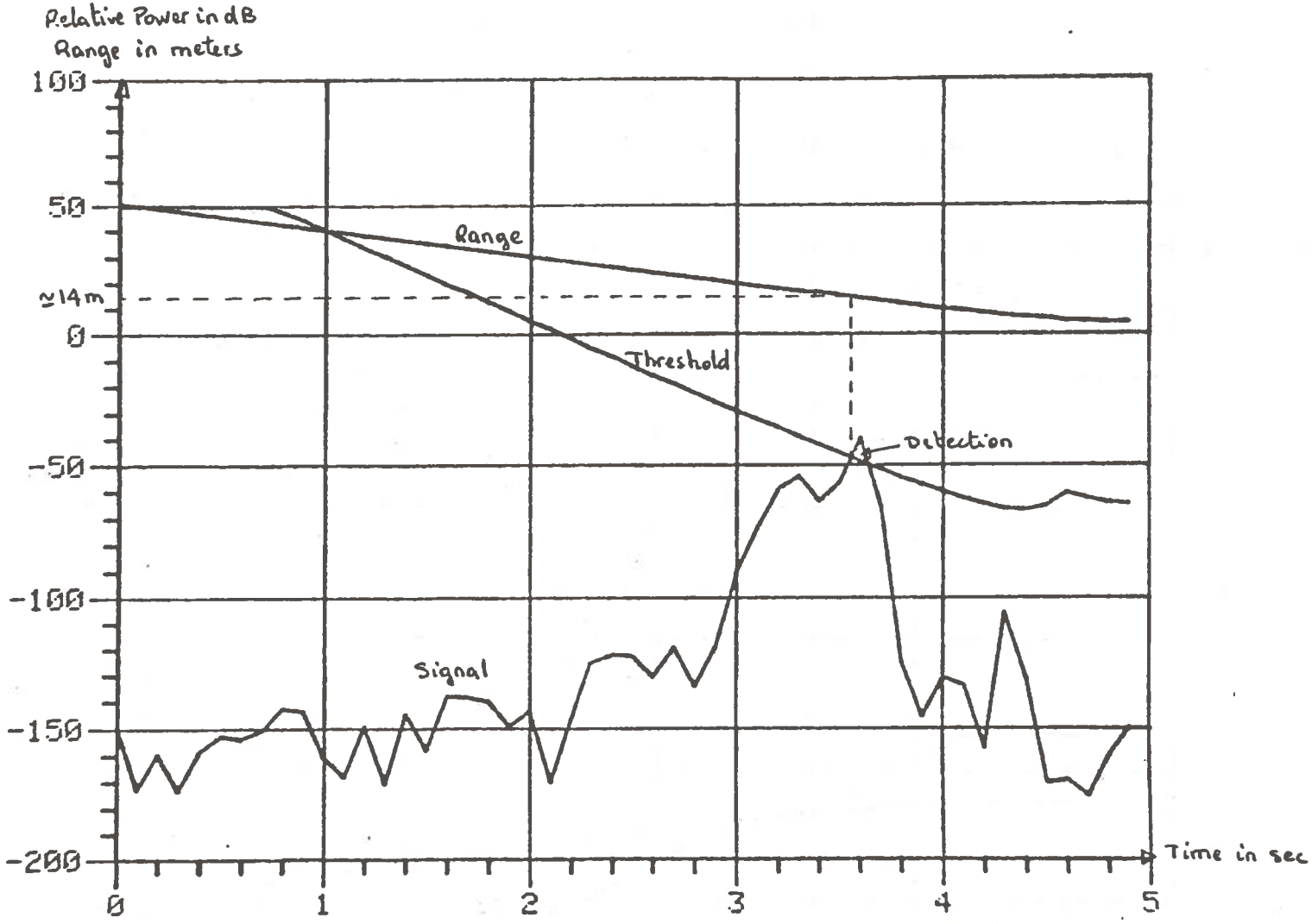

② CAR CROSSING AT R = 50 m ≃ 150 ft , WITH V_t = 3 m/sec ≃ 9 ft/sec

VELOCITY OF RADAR CAR V = 30 ft/sec

DETECTION AT R ≃ 14m ≃ 42 ft

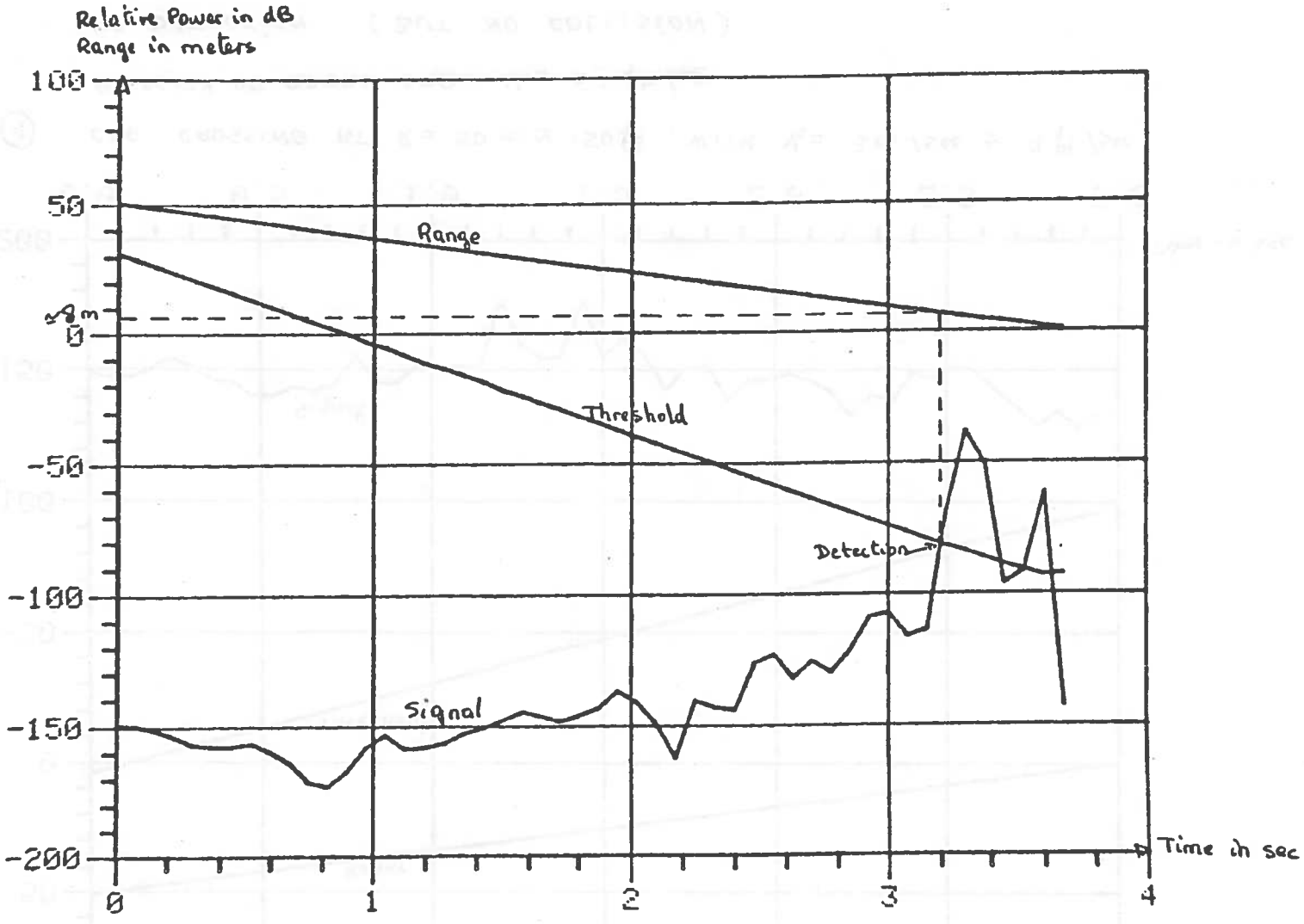

(3) CAR CROSSING AT R = 50 m ≃ 150 ft , WITH V_t = 3 m/sec ≃ 9 ft/sec

VELOCITY OF RADAR CAR V = 40 ft/sec

DETECTION AT R ≃ 8m ≃ 24 ft

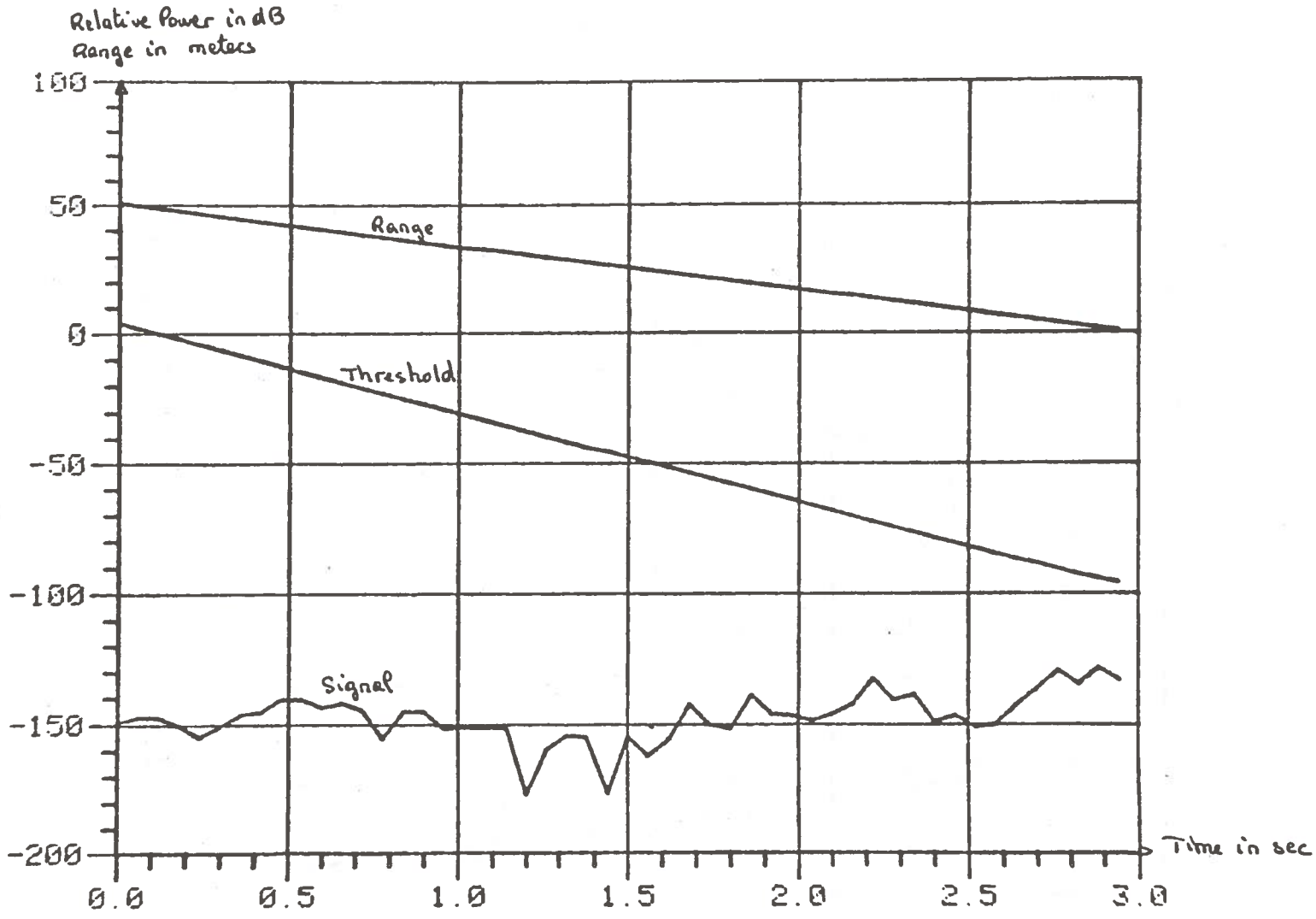

④ CAR CROSSING AT $R = 50\ m \simeq 150\ ft$, WITH $V_t = 3\ m/sec \simeq 9\ ft/sec$

VELOCITY OF RADAR CAR $V = 50\ ft/sec$

NO DETECTION (BUT NO COLLISION)

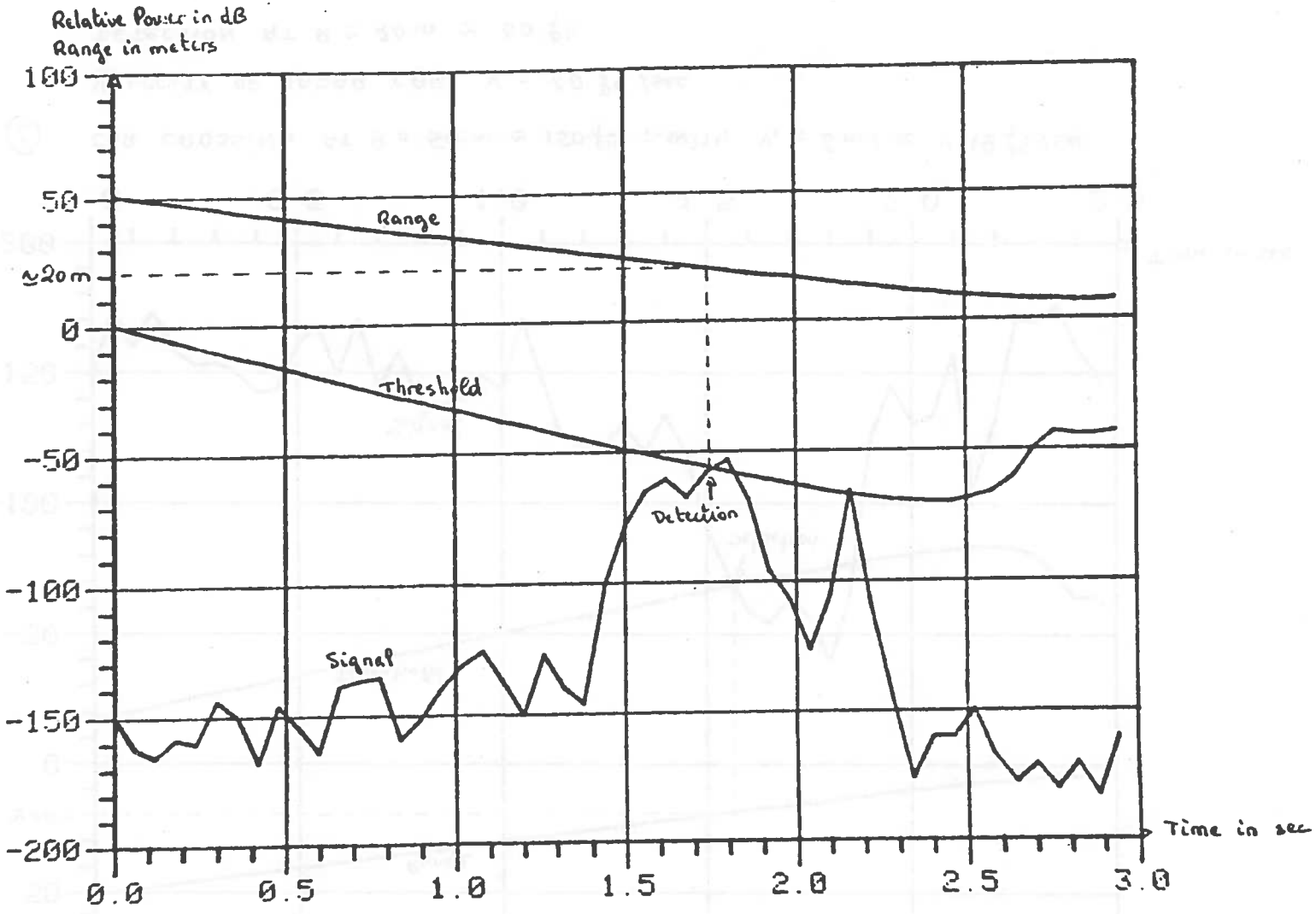

(5) CAR CROSSING AT $R = 50\,m \simeq 150\,ft$, WITH $V_t = 6\,m/sec \simeq 18\,ft/sec$

VELOCITY OF RADAR CAR $V = 50\,ft/sec$

DETECTION AT $R \simeq 20\,m \simeq 60\,ft$

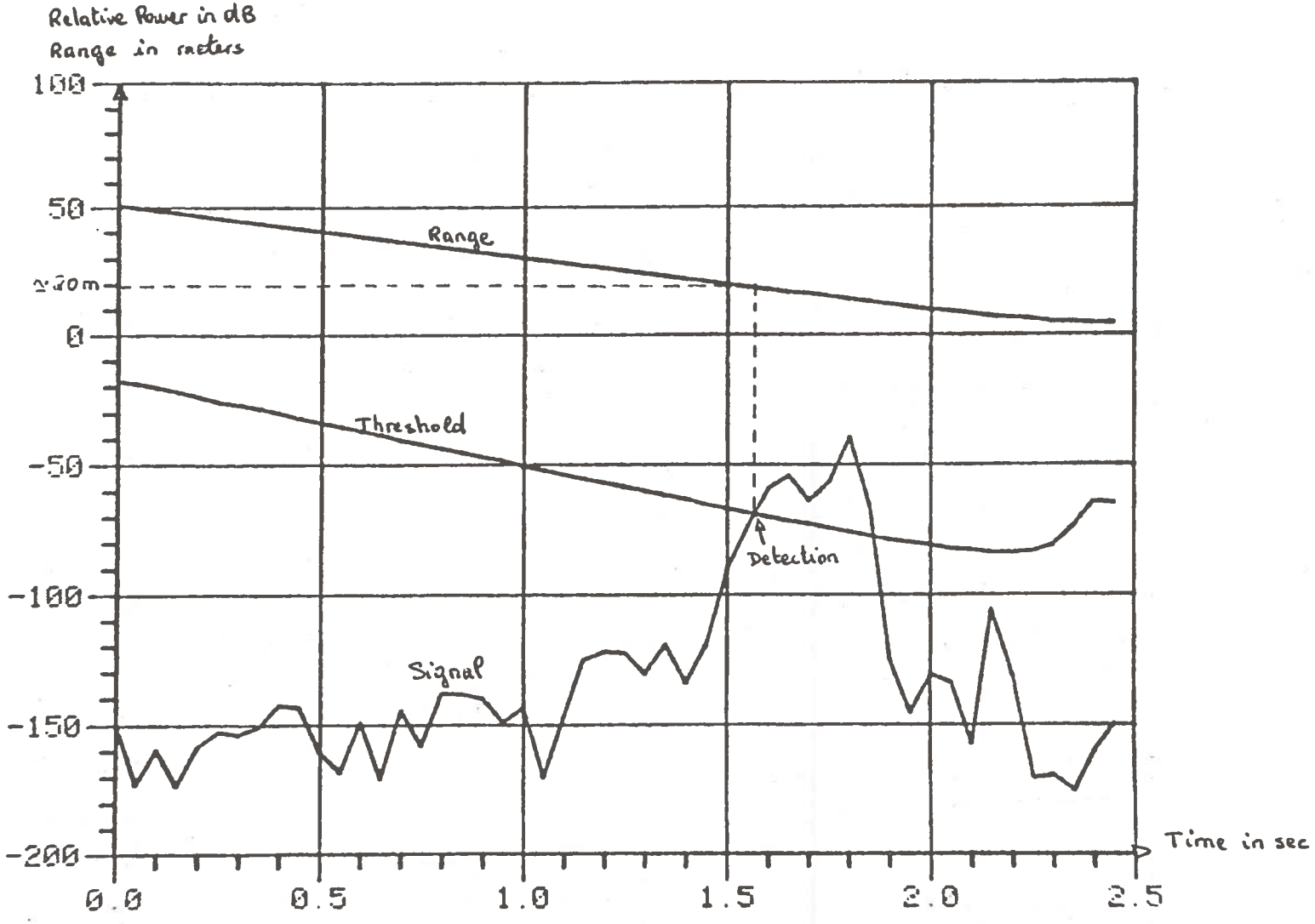

(6) CAR CROSSING AT R = 50 m ≃ 150 ft , WITH V_t = 6 m/sec ≃ 18 ft/sec

VELOCITY OF RADAR CAR V = 60 ft/sec

DETECTION AT R ≃ 20 m ≃ 60 ft

APPENDIX J

LISTING OF THE RADAR BRAKE ALGORITHM

MAIN.COM

```
$SET DEF DRCO:[KR1214.BRAKE]
$SET NOVERIFY
$SAVELOG
$ASSIGN CASEWT.IPT FOR011
$ASSIGN BRKRAD.DAT FOR021
$ASSIGN OUTDAT.DAT FOR022
$ASSIGN UALL.OPT   FOR023
$ASSIGN MALL.OPT   FOR024
$ASSIGN NCDAT1.DAT FOR025
$ASSIGN NCDAT7.DAT FOR026
$ASSIGN NCDAT8.DAT FOR027
$ASSIGN CUALL.OPT  FOR028
$ASSIGN CMALL.OPT  FOR029
$FOR MAIN
$FOR CLASS
$FOR MODE
$FOR BRAKE
$FOR RADAR
$LINK MAIN,CLASS,MODE,BRAKE,RADAR
$TYPE BLANK.TYP
$@TYPE
$TYPE BLANK.TYP
$RUN MAIN
$DONTBACKUP NCDAT1.DAT
$DONTBACKUP NCDAT7.DAT
$DONTBACKUP NCDAT8.DAT
$TYPE OUTDAT.DAT
$DELETE OUTDAT.DAT;*
$TYPE BLANK.TYP
$TYPE UALL.OPT
$TYPE BLANK.TYP
$TYPE MALL.OPT
$TYPE BLANK.TYP
$TYPE CUALL.OPT
$TYPE BLANK.TYP
$TYPE CMALL.OPT
$TYPE BLANK.TYP
$TYPE BRKRAD.DAT
$DELETE BRKRAD.DAT;*
$TYPE BLANK.TYP
$@DELETE
$TYPE BLANK.TYP
$STOP
```

SETUP.FOR

```
C SET SIZES OF VREL ARRAY AND NUMBER OF KSPTYP'S, ACCTYP'S, AND RADAR SYSTEMS
      PARAMETER IREL=30,JREL=33,KREL=31,IKSP=8,ISYS=5,IMOD=2,IACC=2
      PARAMETER IAIS=7,IINJ=5,ICNF=6,IGMD=6
C SELECT WEIGHTED (=1) OR UNWEIGHTED (=0) NC DATA
      PARAMETER IWTFL=1
C SELECT (=1) WRITE OF CASE DATA TO BRKRAD.DAT
      PARAMETER IWRFL=0
C SELECT (=1) WRITE OF ALL DATA TO NCDATN.DAT
      PARAMETER IOUFL=1
C SELECT (=1) WRITE OF RADAR SUBROUTINE DIAGNOSTICS TO BRKRAD.DAT
      PARAMETER IRDFL=0
C SELECT (=1) CHOICE OF ONLY EVERY TENTH CASE
      PARAMETER ISEL=0
C SELECT (=1) DETAILED OUTPUT
      PARAMETER IDTFL=1
C SELECT (=1) ADJUSTABLE MU
      PARAMETER MUADJ=0
C LIMIT NUMBER OF CASE VEHICLES PROCESSED
      PARAMETER NCASES=500000
      PARAMETER MCASES=0
C SETUP OUTPUT RECORD LENGTHS
      PARAMETER LOREC=294
C DEFINE VARIABLE TYPES
      CHARACTER*114 INREC
      CHARACTER*156 IOREC,JOREC,KOREC
      CHARACTER*294 OUTREC
      REAL MU,MU1,MU2,MUINC,MURAD
      INTEGER APD,TPD,FHE,ROAD,COND
      INTEGER TYP1,TAD1,DAM1,D1COND,SP1,DIR1,OBJ1,DIS1
      INTEGER TYP2,TAD2,DAM2,D2COND,SP2,DIR2,OBJ2,DIS2
      INTEGER ACCTYP,ACCTYQ,CONFIG,SYSTYP
C SETUP DIMENSION AND COMMON BLOCKS
      DIMENSION VREL(ISYS,IMOD)
      DIMENSION VRELFQ(JREL,IKSP,ISYS,IMOD,IACC)
      DIMENSION CRELFQ(JREL,ICNF,ISYS,IMOD,IACC)
      DIMENSION SUM(IKSP,ISYS,IMOD,IACC)
      DIMENSION CUM(ICNF,ISYS,IMOD,IACC)
      DIMENSION VRELPB(IREL,IKSP,ISYS,IMOD,IACC)
      DIMENSION CRELPB(IREL,ICNF,ISYS,IMOD,IACC)
      DIMENSION IVREL(ISYS,IMOD),JVREL(ISYS,IMOD)
      DIMENSION PAIS(IAIS,IINJ),INJ(IINJ),AIS(IAIS),KCOUNT(3)
      DIMENSION DAMAGE(ISYS),EAMAGE(ISYS)
      DIMENSION RPDAM(IACC,IKSP),PDAM(JREL,IKSP,ISYS,IACC)
      DIMENSION CPDAM(IACC,ICNF),CDAM(JREL,ICNF,ISYS,IACC)
      DIMENSION RNAIS(IACC,IKSP,IAIS),PEDINJ(JREL,ISYS,IACC,IAIS)
      DIMENSION CNAIS(IACC,ICNF,IAIS),CEDINJ(JREL,ISYS,IACC,IAIS,ICNF)
      DIMENSION PINJ(ISYS,IINJ),RINJ(ISYS,IAIS),SINJ(ISYS,IAIS)
      DIMENSION RMAX(ISYS),VMIN(ISYS)
      DIMENSION SUMPD(IKSP,ISYS,IACC),SUMINJ(ISYS,IACC,IAIS)
      DIMENSION CUMPD(ICNF,ISYS,IACC),CUMINJ(ISYS,IACC,IAIS,ICNF)
      DIMENSION THETA(ISYS),TAU(ISYS),TDEL(ISYS),MUINC(ISYS),SRD(ISYS)
      DIMENSION MURAD(ISYS),ACC(ISYS)
      COMMON /ACCCOM/ INUM,FHE,ROAD,COND,NUMV,
     C  TYP1,TAD1,V1T,V1I,DIR1,MPA1,MHE1,MIS1,OBJ1,DIS1,
     C  TYP2,TAD2,V2T,V2I,DIR2,MPA2,MHE2,MIS2,OBJ2,DIS2
      COMMON /DATCOM/ ACCTYP,KSPTYP,JACTYP,JKSTYP,IFLAG,
     C  JNUM,CONFIG,G,MU,MUINC,X20,WIDTH1,XLENG2,TDEL,CFM
      COMMON /RADCOM/ THETA,TAU,SPD,R0,V00,V10,V20,A0,SA0,SB0,VA0,VB0,
     C  AB0,RMAX,VMIN,MURAD
```

DATA.FOR

```
C INSERT DATA
C PAIS IS THE PROBABILITY OF AIS FOR EACH POLICE CODE INJURY
      DATA ((PAIS(I,J),I=1,IAIS),J=1,IINJ)
     C /00.00,00.00,00.00,00.00,00.00,00.00,99.99,
     C  00.34,46.88,23.14,19.62,06.04,02.73,01.26,
     C  09.50,72.57,12.62,04.40,00.70,00.13,00.08,
     C  35.37,57.05,04.86,02.48,00.24,00.00,00.00,
     C  92.53,06.35,01.12,00.02,00.00,00.00,00.00/
C CFM CONVERTS FROM FEET PER SECOND TO MPH
      CFM=3600./5280.
C WIDTH IS THE NOMINAL VEHICLE WIDTH
      WIDTH1=6.
C G IS THE GRAVITATIONAL ACCELERATION IN FEET PER SEC PER SEC
      G=32.17
C THETA IS THE HALF WIDTH OF THE RADAR BEAM
      THETA(1)=0.00
      THETA(2)=0.05
      THETA(3)=0.05
      THETA(4)=0.05
      THETA(5)=0.05
C TAU IS THE RADAR SYSTEM TIME DELAY
      TAU(1)=0.0
      TAU(2)=0.1
      TAU(3)=0.1
      TAU(4)=0.1
      TAU(5)=0.1
C TDEL IS THE BRAKE SYSTEM TIME DELAY
      TDEL(1)=0.0
      TDEL(2)=0.1
      TDEL(3)=0.1
      TDEL(4)=0.1
      TDEL(5)=0.1
C RMAX IS THE MAXIMUM RANGE OF THE RADAR
      RMAX(1)=000.0
      RMAX(2)=200.0
      RMAX(3)=200.0
      RMAX(4)=200.0
      RMAX(5)=200.0
C VMIN IS THE MINIMUM VELOCITY AT WHICH THE RADAR OPERATES
      VMIN(1)=00.0/CFM
      VMIN(2)=10.0/CFM
      VMIN(3)=10.0/CFM
      VMIN(4)=10.0/CFM
      VMIN(5)=10.0/CFM
C MUINC IS THE INCREASE IN STOPING POWER DUE TO ANTI-SKID BRAKES
      MUINC(1)=0.0
      MUINC(2)=0.1
      MUINC(3)=0.1
      MUINC(4)=0.1
      MUINC(5)=0.1
C S IS THE CONSTANT TERM IN THE CONTROL LAW
      SRD(1)=0.0
      SRD(2)=0.0
      SRD(3)=0.0
      SRD(4)=0.0
      SRD(5)=0.0
C MURAD IS THE DECELERATION USED IN THE CONTROL LAWS
      MURAD(1)=0.0
      MURAD(2)=0.5
      MURAD(3)=0.5
      MURAD(4)=0.5
      MURAD(5)=0.5
```

MAIN.FOR

```
      PROGRAM MAIN
C THIS PROGRAM READS CASES FROM THE NORTH CAROLINA CASE
C VEHICLE FILE, DETERMINES ACCIDENT TYPES, KRAESP MODES,
C AND BRAKE ALGORITHM CONFIGURATION, AND COMPUTES VREL
C FIRST SET UP PARAMETERS, DIMENSIONS, COMMON BLOCKS, ETC.
      INCLUDE 'SETUP.FOR'
C INPUT THE RADAR PERFORMANCE DATA
      INCLUDE 'DATA.FOR'
      WRITE (6,89) IWTFL,IWRFL,IOUFL,IDTFL,IRDFL,ISEL,MUADJ
   89 FORMAT (1HO,11X,'CHOICE OF IO AND CALCULATION INDICATORS:'/
     C          21X,'WEIGHTED DATA------',I1/
     C          21X,'DIAGNOSTIC OUTPUT--',I1/
     C          21X,'DATA OUTPUT--------',I1/
     C          21X,'DETAIL OUTPUT------',I1/
     C          21X,'RADAR OUTPUT-------',I1/
     C          21X,'SELECTION OPTION---',I1/
     C          21X,'MU OPTION----------',I1)
      WRITE (6,88) THETA,TAU,SRD,MURAD,TDEL,MUINC,RMAX,VMIN
   88 FORMAT (//12X,'RADAR PERFORMANCE PARAMETERS (BY SYSTYP):'/
     C          21X,'THETA--',5F7.2/
     C          21X,'TAU----',5F7.2/
     C          21X,'SRD----',5F7.2/
     C          21X,'MURAD--',5F7.2/
     C          21X,'TDEL---',5F7.2/
     C          21X,'MUINC--',5F7.2/
     C          21X,'RMAX---',5F7.2/
     C          21X,'VMIN---',5F7.2////)
C OPEN THE OUTPUT FILES IF DATA IS TO BE SAVED
      IF (IOUFL.EQ.0) GOTO 999
      OPEN (UNIT=25,FILE='NCDAT1.DAT',RECL=LOREC,STATUS='NEW',
     C      ORGANIZATION='RELATIVE',ACCESS='DIRECT')
      OPEN (UNIT=26,FILE='NCDAT7.DAT',RECL=LOREC,STATUS='NEW',
     C      ORGANIZATION='RELATIVE',ACCESS='DIRECT')
      OPEN (UNIT=27,FILE='NCDAT8.DAT',RECL=LOREC,STATUS='NEW',
     C      ORGANIZATION='RELATIVE',ACCESS='DIRECT')
  999 CONTINUE
C READ IN ALL THE CASE DATA
  100 READ (11,1,END=200) INREC
    1 FORMAT (A)
C STOP IF NUMBER OF CASES EXCEEDS NCASES
      IF (ICOUNT.GE.NCASES) GOTO 200
      ICOUNT=ICOUNT+1
C GO TO NEXT CASE IF ICOUNT IS LESS THAN MCASES
      IF (ICOUNT.LT.MCASES) GOTO 100
C EXTRACT NEEDED DATA ITEMS AND CONVERT FROM CHARACTER FORMAT
      READ (INREC,2) INUM,FHE,ROAD,COND,
     C  TYP1,TAD1,V1T,V1I,DIR1,MPA1,MHE1,MIS1,OBJ1,DIS1,
     C  TYP2,TAD2,V2T,V2I,DIR2,MPA2,MHE2,MIS2,OBJ2,DIS2,
     C  WEIGHT,NUMV
    2 FORMAT (I6,15X,I2,2I1,
     C        I2,I3,21X,F3.0,F2.0,I1,4I2,I1,
     C        I2,I3,21X,F3.0,F2.0,I1,4I2,I1,
     C        F6.3,I1)
C GET INDICATOR FOR CASE SAMPLING
      IND=10*(INUM/10)-INUM
      IF (IND.NE.0.AND.ISEL.EQ.1) GOTO 100
      JCOUNT=JCOUNT+1
C GET KSPTYP AND CONFIG
      CALL MODE
C ADJUST TO EXCLUDE 50% OF HEAD ONS
      IF (CONFIG.EQ.2) THEN
```

```
        LCOUNT=LCOUNT+1
        LND=2*(INUM/2)-INUM
        IF (LND.EQ.0) CONFIG=0
        IF (LND.NE.0) MCOUNT=MCOUNT+1
        END IF
C SET INDEX FOR CONFIG
        LONFIG=CONFIG+1
C WRITE OUT EVERY CASE FOR PEDESTRIANS
        IF (KSPTYP.EQ.7) IND=0
C GET ACCTYP
        CALL CLASS
C REDUCE THE ACCIDENT TYPES TO COMMON CATEGORIES
C FIRST SAVE THE ORIGINAL ACCTYP
        ACCTYQ=ACCTYP
        IF (ACCTYP.EQ. 2.OR.ACCTYP.EQ. 4) ACCTYP=1
        IF (ACCTYP.EQ. 7.OR.ACCTYP.EQ. 8) ACCTYP=1
        IF (ACCTYP.EQ. 9.OR.ACCTYP.EQ.17) ACCTYP=1
        IF (ACCTYP.EQ.20.OR.ACCTYP.EQ.22) ACCTYP=1
        IF (ACCTYP.NE. 1)                 ACCTYP=2
C IF UNWEIGHTED, SET WEIGHT TO ONE
        IF (IWTFL.EQ.0) WEIGHT=1.0
C CONVERT FROM POLICE CODE INJURIES TO AIS CODES
        IF (KSPTYP.EQ.7) GOTO 900
        READ (INREC,3) INJ
    3 FORMAT (T38,5I2)
        GOTO 800
  900   READ (INREC,4) INJ
    4 FORMAT (T79,5I2)
  800   INJ(5)=INJ(5)-INJ(1)-INJ(2)-INJ(3)-INJ(4)
        IF (INJ(5).LT.0) INJ(5)=0
        DO 700 N=1,IAIS
        AIS(N)=0.
        DO 700 I=1,IINJ
        AIS(N)=AIS(N)+INJ(I)*PAIS(N,I)/100.
  700   CONTINUE
C ACCUMULATE THE ACTUAL INJURIES BY AIS
        DO 600 N=1,IAIS
        RNAIS(ACCTYP,KSPTYP,N)=RNAIS(ACCTYP,KSPTYP,N)+WEIGHT*AIS(N)
        CNAIS(ACCTYP,LONFIG,N)=CNAIS(ACCTYP,LONFIG,N)+WEIGHT*AIS(N)
  600   CONTINUE
C CODE THE AIS DATA INTO THE OUTPUT RECORD
        WRITE (IOREC,5) INREC,AIS
    5 FORMAT (A,7F6.3)
C ACCUMULATE THE ACTUAL PROPERTY DAMAGE VALUES
        READ (INREC,6) APD,TPD,DAM1,DAM2
    6 FORMAT (T8,2I7,T31,I7,T72,I7)
        IF (APD.GT.50000) APD=0
        IF (TPD.GT.50000) TPD=0
        IF (DAM1.GT.50000) DAM1=0
        IF (DAM2.GT.50000) DAM2=0
        IF ((KSPTYP.GE.4.AND.KSPTYP.LE.6).OR.KSPTYP.EQ.8)
     C  RPDAM(ACCTYP,KSPTYP)=RPDAM(ACCTYP,KSPTYP)+
     C  WEIGHT*(FLOAT(DAM1)+FLOAT(APD)/2.)/1000.
        IF ((KSPTYP.GE.4.AND.KSPTYP.LE.6).OR.KSPTYP.EQ.8)
     C  CPDAM(ACCTYP,LONFIG)=CPDAM(ACCTYP,LONFIG)+
     C  WEIGHT*(FLOAT(DAM1)+FLOAT(APD)/2.)/1000.
        IF ((KSPTYP.GE.1.AND.KSPTYP.LE.3).OR.KSPTYP.EQ.7)
     C  RPDAM(ACCTYP,KSPTYP)=RPDAM(ACCTYP,KSPTYP)+
     C  WEIGHT*FLOAT(TPD)/1000.
        IF ((KSPTYP.GE.1.AND.KSPTYP.LE.3).OR.KSPTYP.EQ.7)
     C  CPDAM(ACCTYP,LONFIG)=CPDAM(ACCTYP,LONFIG)+
```

```
     C  WEIGHT*FLOAT(TPD)/1000.
C SET UP FORMALISM TO MAXIMIZE NUMBER OF KNOWN
C VREL VALUES. CALL BRAKE TO CALCULATE VREL.
        IF (INUM.NE.JNUM) THEN
        IFLAG=0
        IF (KSPTYP.EQ.8) IFLAG=1
        IF (CONFIG.EQ.0) IFLAG=1
        ELSE
        IF (KSPTYP.EQ.8) IFLAG=0
        END IF
C IF FIRST CASE, SAVE DATA
        IF (INUM.NE.JNUM) THEN
        JACTYP=ACCTYP
        JKSTYP=KSPTYP
        JONFIG=CONFIG
        JOREC=IOREC
        END IF
C CALL SUBROUTINE BRAKE TO CALCULATE VREL FOR ALL SYSTEMS
        IF (INUM.NE.JNUM) CALL BRAKE(VREL)
C IF NECESSARY CALL BRAKE AGAIN FOR THE SECOND VEHICLE
        IF (INUM.EQ.JNUM.AND.IFLAG.EQ.1) CALL BRAKE(VREL)
C WRITE INFORMATION TO BRKRAD.DAT
        IF (IWRFL.EQ.0) GOTO 998
        WRITE (21,199)
  199 FORMAT (/2X,'INUM  FHE   ROAD  COND')
        WRITE (21,198) INUM,FHE,ROAD,COND
  198 FORMAT (I5,3I6)
        WRITE (21,299)
  299 FORMAT (2X,'TYP1  TAD1   V1T   V1I')
        WRITE (21,298) TYP1,TAD1,V1T,V1I
  298 FORMAT (I5,I6,1X,2F6.0)
        WRITE (21,399)
  399 FORMAT (2X,'TYP2  TAD2   V2T   V2I')
        WRITE (21,398) TYP2,TAD2,V2T,V2I
  398 FORMAT (I5,I6,1X,2F6.0)
        WRITE (21,499)
  499 FORMAT (2X,'DIR1  MPA1  MHE1  MIS1  OBJ1  DIS1')
        WRITE (21,498) DIR1,MPA1,MHE1,MIS1,OBJ1,DIS1
  498 FORMAT (I5,5I6)
        WRITE (21,599)
  599 FORMAT (2X,'DIR2  MPA2  MHE2  MIS2  OBJ2  DIS2')
        WRITE (21,598) DIR2,MPA2,MHE2,MIS2,OBJ2,DIS2
  598 FORMAT (I5,5I6)
        WRITE (21,699)
  699 FORMAT (1X,'WEIGHT    INJURIES BY KABCO',18X,'INJURIES BY AIS')
        WRITE (21,698) WEIGHT,INJ,AIS
  698 FORMAT (1X,F6.3,4X,5I3,6X,7F6.3)
        WRITE (21,97)
   97 FORMAT (1X'ACCTYQ ACCTYP KSPTYP CONFIG JACTYP JKSTYP  IFLAG')
        WRITE (21,96) ACCTYQ,ACCTYP,KSPTYP,CONFIG,JACTYP,JKSTYP,IFLAG
   96 FORMAT (I5,6I7)
  998   CONTINUE
C ITERATE ON THE DIFFERENT RADAR SYSTEMS
C SYSTEM ONE IS NO RADAR BRAKING
        DO 110 SYSTYP=1,ISYS
        DO 130 MOD=1,IMOD
C COMPUTE THE VREL BIN BY 5 MPH INCREMENTS
C PUT VREL<0 IN BIN 31, VREL=0 IN BIN 32, AND VREL UNKNOWN IN BIN 33
        IVREL(SYSTYP,MOD)=(IFIX(VREL(SYSTYP,MOD)+0.5)+4)/5
        IF (VREL(SYSTYP,MOD).LT.0.0)   IVREL(SYSTYP,MOD)=-1
        IF (VREL(SYSTYP,MOD).GT.998.5) IVREL(SYSTYP,MOD)=-2
```

```
      IF (IVREL(SYSTYP,MOD).GT.30)   IVREL(SYSTYP,MOD)= 30
      IF (IVREL(SYSTYP,MOD).EQ.0)    IVREL(SYSTYP,MOD)= 32
      IF (IVREL(SYSTYP,MOD).EQ.-1)   IVREL(SYSTYP,MOD)= 31
      IF (IVREL(SYSTYP,MOD).EQ.-2).  IVREL(SYSTYP,MOD)= 33
C WRITE RESULTS TO BRKRAD.DAT
      IF (IWRFL.EQ.0) GOTO 997
      WRITE (21,95)
 95 FORMAT (1X 'SYSTYP  MOD   VREL(SYSTYP,MOD) IVREL(SYSTYP,MOD)')
      WRITE (21,94) SYSTYP,MOD,VREL(SYSTYP,MOD),IVREL(SYSTYP,MOD)
 94 FORMAT (I5,I6,7X,F6.0,5X,I6)
997   CONTINUE
C ACCUMULATE THE FREQUENCY OF CASE VEHICLES BY VREL
C KEEP TRACK OF FIRST AND SECOND VEHICLE DATA
      KACC=ACCTYP
      KKSP=KSPTYP
      KONFIG=CONFIG
      MONFIG=KONFIG+1
      KOREC=IOREC
      IF (INUM.NE.JNUM) THEN
      JVREL(SYSTYP,MOD)=IVREL(SYSTYP,MOD)
      END IF
130   CONTINUE
C PREDICT THE PEDESTRIAN INJURIES
      IF (IVREL(SYSTYP,1).EQ.33) GOTO 501
      A=3.922-0.07145*VREL(SYSTYP,1)
      B=4.546-0.09969*VREL(SYSTYP,1)
      C=4.140-0.11530*VREL(SYSTYP,1)
      U=3.086-0.09195*VREL(SYSTYP,1)
      A=EXP(A)
      B=EXP(B)
      C=EXP(C)
      U=EXP(U)
      D=1+A+B+C+U
      PINJ(SYSTYP,1)=1/D
      PINJ(SYSTYP,2)=A/D
      PINJ(SYSTYP,3)=B/D
      PINJ(SYSTYP,4)=C/D
      PINJ(SYSTYP,5)=U/D
      DO 500 N=1,IAIS
      RINJ(SYSTYP,N)=0.
      DO 500 I=1,IINJ
      RINJ(SYSTYP,N)=RINJ(SYSTYP,N)+PINJ(SYSTYP,I)*PAIS(N,I)/100.
500   CONTINUE
      GOTO 503
501   DO 502 N=1,IAIS
502   RINJ(SYSTYP,N)=0.
503   CONTINUE
C PREDICT THE PROPERTY DAMAGE
      GOTO (111,112,111,114,115,116,117,118), KKSP
111   DAMAGE(SYSTYP)=323.+31.52*VREL(SYSTYP,1)
      GOTO 119
112   DAMAGE(SYSTYP)=448.+20.09*VREL(SYSTYP,1)
      GOTO 119
113   DAMAGE(SYSTYP)=542.+27.27*VREL(SYSTYP,1)
      GOTO 119
114   DAMAGE(SYSTYP)=105.+19.27*VREL(SYSTYP,1)
      GOTO 119
115   DAMAGE(SYSTYP)=211.+13.77*VREL(SYSTYP,1)
      GOTO 119
116   DAMAGE(SYSTYP)=192.+10.84*VREL(SYSTYP,1)
      GOTO 119
```

```
  117   DAMAGE(SYSTYP)=252.+ 3.21*VREL(SYSTYP,1)
        GOTO 119
  118   DAMAGE(SYSTYP)=249.+12.20*VREL(SYSTYP,1)
        GOTO 119
  119   IF (IVREL(SYSTYP,1).EQ.33) DAMAGE(SYSTYP)=0.
        DAMAGE(SYSTYP)=DAMAGE(SYSTYP)/1000.
        IF (INUM.NE.JNUM) THEN
        EAMAGE(SYSTYP)=DAMAGE(SYSTYP)
        DO 139 N=1,IAIS
  139   SINJ(SYSTYP,N)=RINJ(SYSTYP,N)
        END IF
        KFLAG=0
  120   CONTINUE
        KFLAG=KFLAG+1
C WRITE OUT DATA TO NCDATN.DAT
C USE FILE 25 FOR KNOWN KSPTYP
C USE FILE 26 FOR NON-MOTORISTS
C USE FILE 27 FOR UNKNOWN KSPTYP
        IF (KFLAG.NE.1) GOTO 996
        IF (IOUFL.EQ.0) GOTO 996
        IF (IND.NE.0) GOTO 996
        IF (SYSTYP.LT.ISYS) GOTO 996
        IF (KKSP.GE.1.AND.KKSP.LE.6) THEN
        IOUNIT=25
        KCOUNT(1)=KCOUNT(1)+1
        NUMREC=KCOUNT(1)
        END IF
        IF (KKSP.EQ.7)                THEN
        IOUNIT=26
        KCOUNT(2)=KCOUNT(2)+1
        NUMREC=KCOUNT(2)
        END IF
        IF (KKSP.EQ.8)                THEN
        IOUNIT=27
        KCOUNT(3)=KCOUNT(3)+1
        IF (INUM.NE.JNUM.AND.IFLAG.EQ.1) KCOUNT(1)=KCOUNT(1)+1
        NUMREC=KCOUNT(3)
        END IF
        IF (IWRFL.EQ.0) GOTO 995
        WRITE (21,93)
   93 FORMAT (1X ' KFLAG IOUNIT NUMREC')
        WRITE (21,92) KFLAG,IOUNIT,NUMREC
   92 FORMAT (I5,2I7)
  995   CONTINUE
        IF (SYSTYP.LT.ISYS) GOTO 996
        WRITE (OUTREC,7) KOREC,KACC,KKSP,KONFIG,
     C  ((VREL(IST,MOD),IVREL(IST,MOD),MOD=1,IMOD),IST=1,ISYS)
    7 FORMAT (A,3I6,10(F6.0,I6))
        WRITE (IOUNIT'NUMREC) OUTREC
  996   CONTINUE
        DO 140 MOD=1,IMOD
        VRELFQ(IVREL(SYSTYP,MOD),KKSP,SYSTYP,MOD,KACC)=
     C  VRELFQ(IVREL(SYSTYP,MOD),KKSP,SYSTYP,MOD,KACC)+WEIGHT
        CRELFQ(IVREL(SYSTYP,MOD),MONFIG,SYSTYP,MOD,KACC)=
     C  CRELFQ(IVREL(SYSTYP,MOD),MONFIG,SYSTYP,MOD,KACC)+WEIGHT
  140   CONTINUE
        PDAM(IVREL(SYSTYP,1),KKSP,SYSTYP,KACC)=
     C  PDAM(IVREL(SYSTYP,1),KKSP,SYSTYP,KACC)+
     C  WEIGHT*DAMAGE(SYSTYP)
        CDAM(IVREL(SYSTYP,1),MONFIG,SYSTYP,KACC)=
     C  CDAM(IVREL(SYSTYP,1),MONFIG,SYSTYP,KACC)+
```

```
     C  WEIGHT*DAMAGE(SYSTYP)
        IF (KKSP.NE.7) GOTO 142
        DO 141 N=1,IAIS
        PEDINJ(IVREL(SYSTYP,1),SYSTYP,KACC,N)=
     C  PEDINJ(IVREL(SYSTYP,1),SYSTYP,KACC,N)+
     C  1.062*WEIGHT*RINJ(SYSTYP,N)
        CEDINJ(IVREL(SYSTYP,1),SYSTYP,KACC,N,MONFIG)=
     C  CEDINJ(IVREL(SYSTYP,1),SYSTYP,KACC,N,MONFIG)+
     C  1.062*WEIGHT*RINJ(SYSTYP,N)
  141   CONTINUE
  142   CONTINUE
        IF (KFLAG.NE.2) GOTO 994
        IF (IOUFL.EQ.0) GOTO 993
        IF (IND.NE.0) GOTO 993
        IF (SYSTYP.LT.ISYS) GOTO 993
        NUMREC=NUMREC-1
        IF (IWRFL.EQ.0) GOTO 992
        WRITE (21,93)
        WRITE (21,92) KFLAG,IOUNIT,NUMREC
  992   CONTINUE
        IF (SYSTYP.LT.ISYS) GOTO 993
        WRITE (OUTREC,7) KOREC,KACC,KKSP,KONFIG,
     C  ((VREL(IST,MOD),IVREL(IST,MOD),MOD=1,IMOD),IST=1,ISYS)
        WRITE (IOUNIT'NUMREC) OUTREC
  993   CONTINUE
        DO 150 MOD=1,IMOD
        VRELFQ(JVREL(SYSTYP,MOD),KKSP,SYSTYP,MOD,KACC)=
     C  VRELFQ(JVREL(SYSTYP,MOD),KKSP,SYSTYP,MOD,KACC)-WEIGHT
        CRELFQ(JVREL(SYSTYP,MOD),MONFIG,SYSTYP,MOD,KACC)=
     C  CRELFQ(JVREL(SYSTYP,MOD),MONFIG,SYSTYP,MOD,KACC)-WEIGHT
  150   CONTINUE
        PDAM(JVREL(SYSTYP,1),KKSP,SYSTYP,KACC)=
     C  PDAM(JVREL(SYSTYP,1),KKSP,SYSTYP,KACC)-
     C  WEIGHT*EAMAGE(SYSTYP)
        CDAM(JVREL(SYSTYP,1),MONFIG,SYSTYP,KACC)=
     C  CDAM(JVREL(SYSTYP,1),MONFIG,SYSTYP,KACC)-
     C  WEIGHT*EAMAGE(SYSTYP)
        IF (KKSP.NE.7) GOTO 152
        DO 151 N=1,IAIS
        PEDINJ(JVREL(SYSTYP,1),SYSTYP,KACC,N)=
     C  PEDINJ(JVREL(SYSTYP,1),SYSTYP,KACC,N)-
     C  1.062*WEIGHT*SINJ(SYSTYP,N)
        CEDINJ(JVREL(SYSTYP,1),SYSTYP,KACC,N,MONFIG)=
     C  CEDINJ(JVREL(SYSTYP,1),SYSTYP,KACC,N,MONFIG)-
     C  1.062*WEIGHT*SINJ(SYSTYP,N)
  151   CONTINUE
  152   CONTINUE
  994   CONTINUE
        IF (INUM.EQ.JNUM.AND.IFLAG.EQ.1) THEN
        KACC=JACTYP
        KKSP=JKSTYP
        KONFIG=JONFIG
        MONFIG=KONFIG+1
        KOREC=JOREC
        END IF
        IF (INUM.EQ.JNUM.AND.IFLAG.EQ.1.AND.KFLAG.EQ.1) GOTO 120
  110   CONTINUE
C WRITE 'END OF CASE' TO FILE BRKRAD.DAT
        IF (IWRFL.EQ.0) GOTO 991
        WRITE (21,91) ICOUNT
   91 FORMAT (1X,'END OF CASE',I7,/)
```

```
      WRITE (21,90)
   90 FORMAT (1X,'**************************************************'/)
  991 CONTINUE
      JNUM=INUM
C GO TO NEXT CASE
      GOTO 100
  200 CONTINUE
C COMPUTE THE SUM ON VREL AND THE PROBABILITY DISTRIBUTION OVER VREL
      DO 210 I=1,IREL
      DO 210 M=1,IACC
      DO 210 K=1,ISYS
      DO 211 N=1,IAIS
  211 SUMINJ(K,M,N)=SUMINJ(K,M,N)+PEDINJ(I,K,M,N)
      DO 212 KK=1,ICNF
      CUMPD(KK,K,M)=CUMPD(KK,K,M)+CDAM(I,KK,K,M)
      DO 213 N=1,IAIS
  213 CUMINJ(K,M,N,KK)=CUMINJ(K,M,N,KK)+CEDINJ(I,K,M,N,KK)
      DO 212 L=1,IMOD
  212 CUM(KK,K,L,M)=CUM(KK,K,L,M)+CRELFQ(I,KK,K,L,M)
      DO 210 J=1,IKSP
      SUMPD(J,K,M)=SUMPD(J,K,M)+PDAM(I,J,K,M)
      DO 210 L=1,IMOD
  210 SUM(J,K,L,M)=SUM(J,K,L,M)+VRELFQ(I,J,K,L,M)
      DO 320 I=1,IREL
      DO 320 K=1,ISYS
      DO 320 L=1,IMOD
      DO 320 M=1,IACC
      DO 330 J=1,IKSP
      IF (SUM(J,K,L,M).EQ.0) GOTO 329
      VRELPB(I,J,K,L,M)=VRELFQ(I,J,K,L,M)/SUM(J,K,L,M)
      GOTO 330
  329 VRELPB(I,J,K,L,M)=0.0
  330 CONTINUE
      DO 340 KK=1,ICNF
      IF (CUM(KK,K,L,M).EQ.0) GOTO 339
      CRELPB(I,KK,K,L,M)=CRELFQ(I,KK,K,L,M)/CUM(KK,K,L,M)
      GOTO 340
  339 CRELPB(I,KK,K,L,M)=0.0
  340 CONTINUE
  320 CONTINUE
C WRITE OUT THE FREQUENCY DISTRIBUTION AND THE PROBABILITY DISTRIBUTION
      DO 410 K=1,ISYS
      DO 410 L=1,IMOD
      WRITE (22,8) K,L
    8 FORMAT (1H1//1X,'FREQUENCY OF VREL FOR SYSTEM',I2,' MOD',I2//
     C          2X,'    KNOWN          <0           =0       UNKNOWN '/)
      WRITE (22,9)
     C ((SUM(J,K,L,M),(VRELFQ(I,J,K,L,M),I=KREL,JREL),J=1,IKSP),
     C   M=1,IACC)
      WRITE (22,23)
     C ((CUM(KK,K,L,M),(CRELFQ(I,KK,K,L,M),I=KREL,JREL),KK=1,ICNF),
     C   M=1,IACC)
    9 FORMAT (8(4F12.0/))
   23 FORMAT (6(4F12.0/))
  410 CONTINUE
      IF (IDTFL.EQ.0) GOTO 990
      DO 420 K=1,ISYS
      DO 420 L=1,IMOD
      WRITE (22,10) K,L
   10 FORMAT (1H1//1X,'FREQUENCY OF VREL FOR SYSTEM',I2,' MOD',I2//)
      WRITE (22,11)
```

```
C  (((VRELFQ(I,J,K,L,M),I=1,JREL),J=1,IKSP),M=1,IACC)
      WRITE (22,24)
C  (((CRELFQ(I,KK,K,L,M),I=1,JREL),KK=1,ICNF),M=1,IACC)
 11 FORMAT (8(17F7.0/15F7.0,F14.0//)/)
 24 FORMAT (6(17F7.0/15F7.0,F14.0//)/)
420   CONTINUE
990   CONTINUE
      DO 430 K=1,ISYS
      WRITE (22,12) K
 12 FORMAT (1H1//1X,'PROPERTY DAMAGE FOR SYSTEM',I2,' (THOUSANDS)'//
C          2X,'    KNOWN          <0           =0       UNKNOWN '/)
      WRITE (22,9)
C  ((SUMPD(J,K,M),(PDAM(I,J,K,M),I=KREL,JREL),J=1,IKSP),M=1,IACC)
      WRITE (22,23)
C  ((CUMPD(KK,K,M),(CDAM(I,KK,K,M),I=KREL,JREL),KK=1,ICNF),
C    M=1,IACC)
430   CONTINUE
      IF (IDTFL.EQ.0) GOTO 989
      DO 440 K=1,ISYS
      WRITE (22,13) K
 13 FORMAT (1H1//1X,'PROPERTY DAMAGE FOR SYSTEM',I2,' (THOUSANDS)'//)
      WRITE (22,11)
C  (((PDAM(I,J,K,M),I=1,JREL),J=1,IKSP),M=1,IACC)
      WRITE (22,24)
C  (((CDAM(I,KK,K,M),I=1,JREL),KK=1,ICNF),M=1,IACC)
440   CONTINUE
989   CONTINUE
      DO 450 K=1,ISYS
      WRITE (22,14) K
 14 FORMAT (1H1//1X,'PEDESTRIAN INJURY FOR SYSTEM',I2,' (BY AIS)'//
C          2X,'   KNOWN          <0           =0       UNKNOWN '/)
      WRITE (22,15)
C  ((SUMINJ(K,M,N),(PEDINJ(I,K,M,N),I=KREL,JREL),N=1,IAIS),
C    M=1,IACC)
      WRITE (22,15)
C  (((CUMINJ(K,M,N,KK),(CEDINJ(I,K,M,N,KK),I=KREL,JREL),N=1,IAIS),
C     M=1,IACC),KK=1,ICNF)
 15 FORMAT (7(4F12.0/))
450   CONTINUE
      IF (IDTFL.EQ.0) GOTO 988
      DO 460 K=1,ISYS
      WRITE (22,16) K
 16 FORMAT (1H1//1X,'PEDESTRIAN INJURY FOR SYSTEM',I2,' (BY AIS)'//)
      WRITE (22,17)
C  (((PEDINJ(I,K,M,N),I=1,JREL),N=1,IAIS),M=1,IACC)
      WRITE (22,17)
C  ((((CEDINJ(I,K,M,N,KK),I=1,JREL),N=1,IAIS),M=1,IACC),KK=1,ICNF)
 17 FORMAT (7(17F7.0/15F7.0,F14.0//)/)
460   CONTINUE
988   CONTINUE
      WRITE (22,18)
 18 FORMAT (1H1//1X,'ACTUAL INJURIES BY ACCTYP, KSPTYP, CONFIG, AND ',
C               'AIS FOR THE BASELINE (NO RADAR) CASE'//)
      WRITE (22,19) (((RNAIS(M,J,N),J=1,IKSP),N=1,IAIS),M=1,IACC)
      WRITE (22,25) (((CNAIS(M,KK,N),KK=1,ICNF),N=1,IAIS),M=1,IACC)
 19 FORMAT (2(7(8F12.0/)/))
 25 FORMAT (2(7(6F12.0/)/))
      WRITE (22,20)
 20 FORMAT (1H1//1X,'ACTUAL PROPERTY DAMAGE BY KSPTYP, CONFIG AND  ',
C               'ACCTYP FOR THE BASELINE (NO RADAR) CASE ',
C               '(THOUSANDS)'//)
```

```
      WRITE (22,21) ((RPDAM(I,J),I=1,IACC),J=1,IKSP)
   21 FORMAT (8(2F16.0/))
      WRITE (22,26) ((CPDAM(I,KK),I=1,IACC),KK=1,ICNF)
   26 FORMAT (6(2F16.0/))
      DO 510 M=1,IACC
      DO 510 L=1,IMOD
      DO 510 K=1,ISYS
      VRELPB(1,3,K,L,M)=1.0
      DO 510 I=2,IREL
      VRELPB(I,3,K,L,M)=0.0
  510 CONTINUE
      WRITE (23,22) (((VRELPB(I,J,K,1,1),J=1,IGMD),K=1,ISYS),I=1,IREL)
   22 FORMAT (18F7.4/12F7.4)
      WRITE (28,22) (((CRELPB(I,KK,K,1,1),KK=1,ICNF),K=1,ISYS),
     C                    I=1,IREL)
      WRITE (24,22) (((VRELPB(I,J,K,2,1),J=1,IGMD),K=1,ISYS),I=1,IREL)
      WRITE (29,22) (((CRELPB(I,KK,K,2,1),KK=1,ICNF),K=1,ISYS),
     C                    I=1,IREL)
C WRITE OUT THE NUMBER OF CASE VEHICLES PROCESSED
      WRITE (6,*) '            CASES READ--',ICOUNT
      WRITE (6,*) '            CASES USED--',JCOUNT
      WRITE (6,*) '            HEAD ONS----',LCOUNT
      WRITE (6,*) '            USED--------',MCOUNT
      WRITE (6,*) '            CASES TO #1-',KCOUNT(1)
      WRITE (6,*) '            CASES TO #7-',KCOUNT(2)
      WRITE (6,*) '            CASES TO #8-',KCOUNT(3)
      WRITE (6,*) ' '
      WRITE (6,*) ' '
      WRITE (6,*) ' '
      WRITE (6,*) ' '
      IF (IOUFL.EQ.0) GOTO 987
      CLOSE (UNIT=25)
      CLOSE (UNIT=26)
      CLOSE (UNIT=27)
  987 CONTINUE
      STOP '           COMPUTATION COMPLETED'
      END
```

CLASS.FOR

```
      SUBROUTINE CLASS
      INCLUDE 'SETUP.FOR'
      IF (TYP1.EQ.1.OR.TYP1.EQ.2) GOTO 200
      IF (TYP1.GE.3.AND.TYP1.LE.13) GOTO 300
      IF (TYP1.EQ.17.OR.TYP1.EQ.19) GOTO 300
      IF (TYP1.EQ.20.OR.TYP1.EQ.22) GOTO 300
      IF (TYP2.GE.14.AND.TYP2.LE.16) GOTO 400
      IF (TYP2.EQ.18.OR.TYP2.EQ.21) GOTO 400
      IF (TYP1.EQ.0.OR.TYP1.GE.23) ACCTYP=16
      GOTO 100
200   IF (MHE1.GE.1.AND.MHE1.LE.5) ACCTYP=9
      IF (MHE1.GE.14.AND.MHE1.LE.23) GOTO 220
      IF (MHE1.GE.6.AND.MHE1.LE.13) GOTO 230
      IF (MHE1.EQ.0.OR.MHE1.GE.24) ACCTYP=22
      GOTO 100
220   IF (TYP2.EQ.1.OR.TYP2.EQ.2) ACCTYP=1
      IF (TYP2.GE.3.AND.TYP2.LE.13) ACCTYP=2
      IF (TYP2.EQ.17.OR.TYP2.EQ.19) ACCTYP=2
      IF (TYP2.EQ.20.OR.TYP2.EQ.22) ACCTYP=2
      IF (TYP2.GE.14.AND.TYP2.LE.16) ACCTYP=17
      IF (TYP2.EQ.18.OR.TYP2.EQ.21) ACCTYP=17
      IF (TYP2.EQ.0.OR.TYP2.GE.23) ACCTYP=17
      GOTO 100
230   IF (MHE1.EQ.12) ACCTYP=4
      IF (MHE1.NE.12.AND.DIS1.EQ.1) ACCTYP=7
      IF (MHE1.NE.12.AND.DIS1.GE.2.AND.DIS1.LE.7) ACCTYP=8
      IF (MHE1.NE.12.AND.(DIS1.EQ.0.OR.DIS1.GE.8)) ACCTYP=20
      GOTO 100
300   IF (MHE1.GE.1.AND.MHE1.LE.5) ACCTYP=10
      IF (MHE1.GE.14.AND.MHE1.LE.23) GOTO 320
      IF (MHE1.GE.6.AND.MHE1.LE.13) ACCTYP=13
      IF (MHE1.EQ.0.OR.MHE1.GE.24) ACCTYP=23
      GOTO 100
320   IF (TYP2.EQ.1.OR.TYP2.EQ.2) ACCTYP=3
      IF (TYP2.GE.3.AND.TYP2.LE.13) ACCTYP=12
      IF (TYP2.EQ.17.OR.TYP2.EQ.19) ACCTYP=12
      IF (TYP2.EQ.20.OR.TYP2.EQ.22) ACCTYP=12
      IF (TYP2.GE.14.AND.TYP2.LE.16) ACCTYP=18
      IF (TYP2.EQ.18.OR.TYP2.EQ.21) ACCTYP=18
      IF (TYP2.EQ.0.OR.TYP2.GE.23) ACCTYP=18
      GOTO 100
400   IF (MHE1.GE.1.AND.MHE1.LE.5) ACCTYP=11
      IF (MHE1.GE.6.AND.MHE1.LE.13) GOTO 420
      IF (MHE1.EQ.0.OR.MHE1.GE.14) ACCTYP=24
      GOTO 100
420   IF ((TYP1.EQ.1.OR.TYP1.EQ.2).AND.DIS1.EQ.1) ACCTYP=5
      IF ((TYP1.EQ.1.OR.TYP1.EQ.2).AND.(DIS1.GE.2.AND.DIS1.LE.7)) ACCTYP=6
      IF ((TYP1.EQ.1.OR.TYP1.EQ.2).AND.(DIS1.EQ.0.OR.DIS1.GE.8))
     C ACCTYP=21
      IF (TYP1.GE.3.AND.TYP1.LE.13) ACCTYP=14
      IF (TYP1.EQ.17.OR.TYP1.EQ.19) ACCTYP=14
      IF (TYP1.EQ.20.OR.TYP1.EQ.22) ACCTYP=14
      IF (TYP1.GE.14.AND.TYP1.LE.16) ACCTYP=15
      IF (TYP1.EQ.18.OR.TYP1.EQ.21) ACCTYP=15
      IF (TYP1.EQ.0.OR.TYP1.GE.23) ACCTYP=19
100   CONTINUE
      RETURN
      END
```

MODE.FOR

```
      SUBROUTINE MODE
C     THIS SUBROUTINE ANALYZES NORTH CAROLINA ACCIDENT DATA AND ASSIGNS VALUES OF
C     KSPTYP AND CONFIG IN EACH CASE. VEHICLE SPEEDS ARE IN MPH.
C     KSPTYP'S ARE ASSIGNED AS FOLLOWS:
C        KSPTYP=1  VEHICLE 1 (CASE VEHICLE) FRONT IMPACTS A SOLID FIXED OBJECT
C        KSPTYP=2  VEHICLE 1 SIDE OR REAR IMPACTS A SOLID FIXED OBJECT
C        KSPTYP=3  VEHICLE 1 SUFFERS A NON-COLLISION (TYPICALLY A ROLLOVER),
C                  AS OPPOSED TO AN IMPACT
C        KSPTYP=4  VEHICLE 1 FRONT IMPACTS ANOTHER VEHICLE
C        KSPTYP=5  VEHICLE 1 SIDE IMPACTS ANOTHER VEHICLE
C        KSPTYP=6  VEHICLE 1 REAR IMPACTS ANOTHER VEHICLE
C        KSPTYP=7  VEHICLE 1 FRONT IMPACTS A PEDESTRIAN, BICYCLIST, OR MOTOR-
C                  CYCLIST
C        KSPTYP=8  THE ACCIDENT CANNOT BE CONSIDERED IN THIS ANALYSIS BECAUSE
C                  OF INSUFFICIENT DATA.  SOME CRITERIA FOR EXCLUSION:
C                        1. MISSING TRAVEL/IMPACT VELOCITIES
C                        2. VEHICLE 1 IS PARKED
C                        3. ACCIDENT IS A SIDESWIPE OR OTHER TYPE FOR WHICH SO-
C                           CIETAL COSTS ARE TOO DIFICULT TO QUANTIFY
C                        4. DATA IS INCONSISTENT (e.g., BOTH VEHICLES SUSTAIN
C                           REAR DAMAGE IN A HEAD-ON ACCIDENT
C     CONFIG'S ARE ASSIGNED AS FOLLOWS:
C        CONFIG=0  "NO RADAR":  COLLISION IN WHICH THE PRESENCE OF RADAR IN VEHI-
C                  CLE 1 IS NOT EXPECTED TO HAVE ANY SIGNIFICANT EFFECT.  (THE
C                  "BRAKE" AND "RADAR" SUBROUTINES WILL NOT BE CALLED WHEN
C                  CONFIG=0)
C        CONFIG=1  "REAR IMPACT":  VEHICLE 1 STRIKES TARGET WHICH IS MOVING AWAY
C                  FROM IT (COLINEAR ACCIDENT)
C        CONFIG=2  "HEAD-ON" COLLISION:  VEHICLE 1 STRIKES APPROACHING TARGET
C                  (COLINEAR ACCIDENT)
C        CONFIG=3  "FIXED-OBJECT" IMPACT:  VEHICLE 1 STRIKES A STATIONARY TARGET
C                  (COLINEAR ACCIDENT)
C        CONFIG=4  "R/L CROSSING" IMPACT:  VEHICLE 1 STRIKES CROSSING TARGET
C                  MOVING FROM RIGHT TO LEFT (FROM VEHICLE 1'S POINT OF VIEW)
C                  (PERPENDICULAR ACCIDENT)
C        CONFIG=5  "L/R CROSSING" IMPACT:  VEHICLE 1 STRIKES CROSSING TARGET
C                  MOVING FROM LEFT TO RIGHT (PERPENDICULAR ACCIDENT)
C     THE TARGET MAY BE ANOTHER VEHICLE (REFERRED TO AS "VEHICLE 2"), A PEDES-
C     TRIAN, OR A FIXED OBJECT (CONFIG=3 ONLY)
      INCLUDE 'SETUP.FOR'
C     X20 REPRESENTS THE DISTANCE FROM THE CENTER OF THE TARGET TO THE CENTER-
C     LINE OF VEHICLE 1 WHEN IMPACT OCCURS IN THE NULL CASE.  IT IS POSITIVE
C     IF THE TARGET IS ON THE LEFT SIDE OF VEHICLE 1.
      X20=0.0
C     "MAXDIS" IS THE MAXIMUM DISTANCE THAT A TARGET CAN BE FROM THE EDGE OF THE
C     ROAD AND STILL BE SEEN BY RADAR.  MAXDIS=2 CORRESPONDS TO A DISTANCE OF 10
C     FEET
      MAXDIS=2
      KSPTYP=8
      CONFIG=0
C     FHE IS "FIRST HARMFUL EVENT"
      IF (FHE.GT.23) FHE=0
C     MHEn IS "MOST HARMFUL EVENT" FOR VEHICLE n
      IF (MHE1.GT.23) MHE1=0
      IF (MHE2.GT.23) MHE2=0
      IF (MHE1.EQ.0.AND.FHE.NE.0) MHE1=FHE
C     TADn REPRESENTS THE LOCATION OF MOST SEVERE DAMAGE ON VEHICLE 1
      IF (TAD1.GT.19) TAD1=0
      IF (TAD2.GT.19) TAD2=0
C     MPAn IS "MANEUVER/PEDESTRIAN ACTION" FOR VEHICLE (OR TARGET) n
      IF (MPA1.GT.29) MPA1=0
```

```
        IF (MPA2.GT.29) MPA2=0
C     MISn IS "MISCELLANEOUS ACTION" FOR VEHICLE n
        IF (MIS1.GT.8) MIS1=0
        IF (MIS2.GT.8) MIS2=0
C     DIRn IS VEHICLE n'S DIRECTION OF TRAVEL
        IF (DIR1.GT.4) DIR1=0
        IF (DIR2.GT.4) DIR2=0
C     ROAD IS "ROAD CHARACTER"
        IF (ROAD.GT.7) ROAD=0
C     ESTIMATE THE LENGTH (XLENG2) OF VEHICLE 2
        GOTO (71,72,73,74,75,76,77,78,79,80,81,82,83,84,85,86,87,88,89,9
     C  0,91), TYP2
C     TYP2="TWO OR FOUR DOOR SEDAN (PASSENGER VEHICLE)"
   71   XLENG2=16.
        GOTO 93
C     TYP2="STATION WAGON (PASSENGER)"
   72   XLENG2=18.
        GOTO 93
C     TYP2="STATION WAGON (TRUCK)"
   73   XLENG2=20.
        GOTO 93
C     TYP2="COMMERCIAL BUS"
   74   XLENG2=40.
        GOTO 93
C     TYP2="SCHOOL BUS"
   75   XLENG2=32.
        GOTO 93
C     TYP2="ACTIVITY BUS"
   76   XLENG2=24.
        GOTO 93
C     TYP2="TRUCK WITH TWO AXLES"
   77   XLENG2=24.
        GOTO 93
C     TYP2="TRUCK WITH THREE AXLES"
   78   XLENG2=30.
        GOTO 93
C     TYP2="TRUCK TRACTOR WITH TRAILER"
   79   XLENG2=50.
        GOTO 93
C     TYP2="TRUCK TRACTOR ONLY"
   80   XLENG2=14.
        GOTO 93
C     TYP2="TAXICAB"
   81   XLENG2=16.
        GOTO 93
C     TYP2="FARM EQUIPMENT"
   82   XLENG2=18.
        GOTO 93
C     TYP2="FARM TRACTOR"
   83   XLENG2=12.
        GOTO 93
C     TYP2="MOTORCYCLE"
   84   XLENG2=5.
        GOTO 93
C     TYP2="MOPED"
   85   XLENG2=4.
        GOTO 93
C     TYP2="MOTOR/SCOOTER OR MOTOR BIKE"
   86   XLENG2=4.
        GOTO 93
C     TYP2="AMBULANCE"
```

```
   87    XLENG2=18.
         GOTO 93
C     TYP2="BICYCLE"
   88    XLENG2=4.
         GOTO 93
C     TYP2="RECREATIONAL VEHICLE, SELF CONTAINED"
   89    XLENG2=27.
         GOTO 93
C     TYP2="'CAMPER' MOUNTED ON TWO AXLE TRUCK"
   90    XLENG2=20.
         GOTO 93
C     TYP2="PEDESTRIAN"
   91    XLENG2=1.
C     ASSIGN VALUE TO MU IF VEHICLE IS "OFF ROAD"
   93    IF (FHE.GE.1.AND.FHE.LE.3) THEN
         MU=.3
         GOTO 99
         END IF
C     ASSIGN VALUE TO MU (COEFFICIENT OF FRICTION) BASED ON ROAD CONDITION (COND)
         GOTO (94,95,96,97,98), COND
C     COND="NOT STATED"
         RETURN
C     COND="DRY"
   94    MU=.6
         GOTO 99
C     COND="WET"
   95    MU=.4
         GOTO 99
C     COND="MUDDY"
   96    MU=.4
         GOTO 99
C     COND="SNOWY"
   97    MU=.3
         GOTO 99
C     COND="ICY"
   98    MU=.2
   99    CONTINUE
         IF (MHE1.LE.3.OR.MHE1.EQ.5.OR.MHE1.EQ.8) RETURN
         IF (MHE1.EQ.11.OR.MHE1.EQ.21) RETURN
         IF (TAD1.EQ.3) X20=2.
         IF (TAD1.EQ.4) X20=-2.
         IF (MHE1.NE.4) GOTO 110
C     MOST HARMFUL EVENT="NONCOLLISION/ROLLOVER"
         IF (V1I.GT.0.0) KSPTYP=3
         GOTO 959
  110    CONTINUE
         IF (MHE1.NE.12.AND.MHE1.NE.13) GOTO 120
C     VEHICLE 1 STRIKES AN OBJECT (DEFINED AS SOMETHING OTHER THAN A
C     PERSON OR ANOTHER VEHICLE)
         IF (OBJ1.EQ.2) GOTO 180
         IF (OBJ1.EQ.3) GOTO 150
         IF (OBJ1.EQ.4) GOTO 125
         IF (OBJ1.LT.6.OR.OBJ1.GT.26) RETURN
C     VEHICLE 1 STRIKES A FIXED (i.e. SOLID OR MASSIVE) OBJECT
  115    V2T=0.
         V2I=0.
         IF (TAD1.LE.4) GOTO 118
         KSPTYP=2
         GOTO 959
  118    KSPTYP=1
         CONFIG=3
```

```
      GOTO 909
  120 CONTINUE
      IF (MHE1.NE.6.AND.MHE1.NE.9.AND.MHE1.NE.10) GOTO 175
C     VEHICLE 1 STRIKES A PEDESTRIAN OR CYCLIST
      IF (MHE1.NE.6) GOTO 150
C     VEHICLE 1 STRIKES A PEDESTRIAN
  125 KSPTYP=7
      IF (MPA2.LT.17.OR.MPA2.GT.25) GOTO 959
      IF (MPA2.GT.19.AND.MPA2.NE.25.AND.MPA2.NE.29) GOTO 135
C     VEHICLE 1 STRIKES PEDESTRIAN CROSSING ROAD
      CONFIG=4
      IF (V2T.GT.20.0) V2T=5.
      IF (V2I.GT.V2T) V2I=V2T
      GOTO 909
  135 IF (MPA2.NE.20) GOTO 140
C     PEDESTRIAN STRUCK WHILE WALKING WITH TRAFFIC
      CONFIG=1
      GO TO 142
  140 IF (MPA2.NE.21) GOTO 145
C     PEDESTRIAN STRUCK WHILE WALKING AGAINST TRAFFIC
      CONFIG=2
  142 IF (V2T.GT.20.0) V2T=3.
      IF (V2I.GT.V2T) V2I=0.
      IF (TAD1.EQ.0) X20=-2.
      GOTO 909
C     PEDESTRIAN IS STATIONARY
  145 CONFIG=3
      V2T=0.
      V2I=0.
      GOTO 909
C     VEHICLE 1 STRIKES MOPED OR BICYCLIST
  150 KSPTYP=7
      IF (V2I.EQ.0.0) GOTO 165
      IF (V2T.GT.50.0) V2T=10.
      IF (V2I.GT.V2T) V2I=V2T
C     USE TRAVEL DIRECTIONS TO ASSIGN CONFIG.  IF DIRECTIONS ARE UNKNOWN, ASSUME
C     THAT CONFIG IS THE SAME AS IN THE LAST BICYCLE ACCIDENT (BY USING ICYCLE).
      IF (DIR1.EQ.0.OR.DIR2.EQ.0) GOTO 152
      IF (DIR1.EQ.DIR2) GOTO 155
      IF (DIR1.EQ.DIR2+2.OR.DIR2.EQ.DIR1+2) GOTO 160
      GOTO 170
  152 GOTO (160,165,170), ICYCLE
C     CYCLIST ASSUMED TO BE TRAVELING WITH TRAFFIC
  155 CONFIG=1
      ICYCLE=0
      IF (TAD1.EQ.0) X20=-2.
      IF (V1I.LE.V2I) V2I=0.
      GOTO 909
C     CYCLIST ASSUMED TO BE TRAVELING AGAINST TRAFFIC
  160 CONFIG=2
      ICYCLE=1
      IF (TAD1.EQ.0) X20=-2.
      GOTO 909
C     CYCLIST ASSUMED TO BE STATIONARY
  165 CONFIG=3
      ICYCLE=2
      V2T=0.
      V2I=0.
      GOTO 909
C     CYCLIST ASSUMED TO BE CROSSING ROAD
  170 CONFIG=4
```

```
        ICYCLE=3
        GOTO 909
C     VEHICLE 1 STRIKES ANOTHER VEHICLE
  175   CONTINUE
        IF (MHE1.NE.7) GOTO 195
C     VEHICLE 1 STRIKES A PARKED VEHICLE
  180   IF (V1I.EQ.0) RETURN
        IF (V2T.GT.998.5) V2T=0.
        IF (V2I.GT.98.5) V2I=0.
        IF (V2T.NE.0.0.OR.V2I.NE.0.0) RETURN
        IF (TAD1.GT.4) GOTO 185
        KSPTYP=4
        CONFIG=3
        GOTO 909
  185   IF (TAD1.GT.8) GOTO 190
        KSPTYP=6
        GOTO 959
  190   IF (TAD1.EQ.15.OR.TAD1.EQ.16.OR.TAD1.EQ.19) RETURN
        KSPTYP=5
        GOTO 959
  195   IF (MHE1.GT.15) GOTO 200
C     MOST HARMFUL EVENT IS A REAR END COLLISION
        IF (MPA2.EQ.10) RETURN
        IF (TAD1.NE.0.OR.TAD2.NE.0) GOTO 196
        IF (V1I.GT.V2I) GOTO 199
        IF (V1I.LT.V2I) GOTO 197
        RETURN
  196   IF (TAD1.GT.8.OR.TAD2.GT.8) RETURN
        IF (TAD1.GE.1.AND.TAD1.LE.4.AND.TAD2.GE.1.AND.TAD2.LE.4)
     C  RETURN
        IF (TAD1.GT.4.AND.TAD2.GT.4) RETURN
        IF (TAD1.GE.1.AND.TAD1.LE.4) GOTO 198
        IF (TAD2.GE.5) GOTO 198
C     VEHICLE 2 STRIKES VEHICLE 1 IN THE REAR
        IF (V1I.GE.V2I) RETURN
  197   KSPTYP=6
        GOTO 959
C     VEHICLE 1 STRIKES VEHICLE 2 IN THE REAR
  198   IF (V1I.LE.V2I) RETURN
  199   KSPTYP=4
        CONFIG=1
        IF (TAD2.EQ.7) X20=X20-2.
        IF (TAD2.EQ.8) X20=X20+2.
        GOTO 909
  200   CONTINUE
        IF (MHE1.NE.20) GOTO 205
C     MOST HARMFUL EVENT IS A HEAD ON COLLISION
        IF (TAD1.GT.4.OR.TAD2.GT.4) RETURN
        KSPTYP=4
        IF (TAD1.EQ.0.AND.TAD2.EQ.0) GOTO 959
        IF (MPA2.GE.7.AND.MPA2.LE.10) GOTO 959
        CONFIG=2
        IF (TAD2.EQ.TAD1) X20=2.*X20
        GOTO 909
  205   CONTINUE
        IF (MHE1.NE.22) GOTO 255
C     MOST HARMFUL EVENT IS AN ANGLE (PERPENDICULAR) COLLISION
        IF (TAD1.EQ.15.OR.TAD1.EQ.16.OR.TAD1.EQ.19) RETURN
        IF (TAD2.EQ.15.OR.TAD2.EQ.16.OR.TAD2.EQ.19) RETURN
        IF (TAD1.EQ.0.AND.TAD2.GE.1.AND.TAD2.LE.4) GOTO 206
        IF (TAD1.LE.4.AND.TAD2.GE.9) GOTO 208
```

```
      IF (TAD1.GE.1.AND.TAD1.LE.4.AND.TAD2.EQ.0) GOTO 208
      IF (TAD1.GE.9.AND.TAD2.LE.4) GOTO 206
      RETURN
C     VEHICLE 2 STRIKES VEHICLE 1 IN THE SIDE
  206 KSPTYP=5
      GOTO 959
C     VEHICLE 1 STRIKES VEHICLE 2 IN THE SIDE
  208 KSPTYP=4
      DX2=0.
      IF (TAD2.EQ.0.OR.TAD2.GE.17) GOTO 215
      IF (TAD2.NE.9.AND.TAD2.NE.10) GOTO 210
C     VEHICLE 2 IS STRUCK IN THE PASSENGER COMPARTMENT
      DX2=XLENG2/2.-8.
      IF (DX2.LT.0.0) DX2=0.
      GOTO 215
C     VEHICLE 2 IS STRUCK IN EITHER THE FRONT OR REAR FENDER
  210 DX2=XLENG2/2.-3.
      IF (DX2.LT.XLENG2/4.0) DX2=XLENG2/4.
      IF (TAD2.GE.13) DX2=-DX2
  215 IF (TAD2.EQ.10.OR.TAD2.EQ.12.OR.TAD2.EQ.14.OR.TAD2.EQ.18)
     C  GOTO 220
C     VEHICLE 2 IS STRUCK IN THE LEFT SIDE
      CONFIG=4
      X20=X20-DX2
      GOTO 225
C     VEHICLE 2 IS STRUCK IN THE RIGHT SIDE
  220 CONFIG=5
      X20=X20+DX2
  225 IF (MPA2.EQ.10) CONFIG=9-CONFIG
      GOTO 909
C     MHE1 IS EITHER "TURN" OR "BACKING."  SET CONFIG=0
  255 CONTINUE
      IF (TAD1.EQ.15.OR.TAD1.EQ.16.OR.TAD1.EQ.19) RETURN
      IF (TAD1.GE.1.AND.TAD1.LE.4) KSPTYP=4
      IF (TAD1.GE.5.AND.TAD1.LE.8) KSPTYP=6
      IF (TAD1.GE.9) KSPTYP=5
      GO TO 959
C     SET CONFIG=0 IF FIRST AND MOST HARMFUL EVENTS ARE DIFFERENT
  909 IF (FHE.GE.6.AND.FHE.NE.MHE1) CONFIG=0
C     SET CONFIG=0 IF VEHICLE 1 IS STOPPED
      IF (MPA1.EQ.1) CONFIG=0
C     SET CONFIG=0 IF VEHICLE 1 IS TURNING OR BACKING
      IF (MPA1.GE.7.AND.MPA1.LE.10) CONFIG=0
C     SET CONFIG=0 IF ROAD CHARACTER IS CURVED
      IF (ROAD.GE.5) CONFIG=0
C     SET CONFIG=0 IF VEHICLE 1 IS "AVOIDING OBJECT IN ROAD"
      IF (MPA1.GE.15) CONFIG=0
C     SET CONFIG=0 IF STRUCK OBJECT IS TOO FAR FROM ROAD
      IF (CONFIG.EQ.3.AND.DIS1.GT.MAXDIS) CONFIG=0
C     SET CONFIG=0 IF VEHICLE 1 "MISCELLANEOUS ACTION" IS "AVOIDING PEDESTRIAN,"
C     "AVOIDING OTHER WHEELED VEHICLE," "AVOIDING FIXED OBJECT," "AVOIDING
C     ANIMAL," "FIRE OR MECHANICAL FAILURE," "FELL FROM VEHICLE," "DRIVERLESS
C     MOVING VEHICLE" OR "SKIDDED OUT OF CONTROL"
      IF (MIS1.NE.0) CONFIG=0
C     SET CONFIG=0 IF VEHICLE 1's TRAVEL SPEED IS 0
      IF (V1T.LE.0) CONFIG=0
C     SET CONFIG=0 IF VEHICLE 1 IS NOT AN AUTOMOBILE
C     SET KSPTYP=7 IF VEHICLE 2 IS "MOTORCYCLE," "MOPED" OR "MOTOR/SCOOTER OR
C     MOTOR BIKE"
  959 IF (TYP2.GE.14.AND.TYP2.LE.16) KSPTYP=7
C     SET KSPTYP=8 AND CONFIG=0 IF ANY VELOCITIES ARE UNKNOWN, IF IMPACT

C     VELOCITY>TRAVEL VELOCITY, OR IF VEHICLE 1 IS PARKED
      IF
     C  (V1T.LT.998.5.AND.V1I.LT.98.5.AND.V2T.LT.998.5.AND.V2I.LT.98.5.
     C  AND.V1T.GE.V1I.AND.V2T.GE.V2I.AND.MPA1.NE.2.AND.MPA1.NE.3)
     C  RETURN
      KSPTYP=8
      CONFIG=0
      RETURN
      END
```

BRAKE.FOR

```
      SUBROUTINE BRAKE(VREL)
C ACCIDENT RECONSTRUCTION ALGORITHM
C THIS ALGORITHM RECONSTRUCTS A COLLISION INPUT FROM A DATA FILE
C TO ASSESS THE EFFECTS OF RADAR-ACTIVATED BRAKING SYSTEMS.
C ITS OUTPUT IS VREL.
      INCLUDE 'SETUP.FOR'
      IF (IWRFL.EQ.0) GOTO 999
      WRITE (21,11) KSPTYP,JKSTYP,CONFIG,V1I,V2I
   11 FORMAT (1X,'BRAKE: KSPTYP.JKSTYP.CONFIG.V1I.V2I',3I6,2F6.0)
      WRITE (21,12) MU,G,X20,WIDTH1,XLENG2
   12 FORMAT (1X,'BRAKE: MU.G.X20.WIDTH1.XLENG2',5F6.2)
  999 CONTINUE
C CONVERT FROM MPH TO FPS (CFM=3600/5280)
      VV1T=V1T/CFM
      VV1I=V1I/CFM
      VV2T=V2T/CFM
      VV2I=V2I/CFM
C ITERATE ON THE RADAR SYSTEMS
      DO 200 SYSTYP=1,ISYS
      IF (KSPTYP.EQ.8) GOTO 109
      IF (CONFIG.EQ.0) GOTO 110
C Vn=VEHICLE n TRAVEL VELOCITY IN FPS
      V1=VV1T
      V2=VV2T
C SET CONSTANTS FOR NEXT RECONSTRUCTION
C TZERO=BEGINNING TIME OF COMPUTATIONAL INTERVAL
      TZERO=-30.
C TnR=TIME WHEN VEHICLE n'S RADAR INITIATES BRAKING
      T1R=11.
      T2R=11.
C An=ACCELERATION OF VEHICLE n
      A1=0.
      A2=0.
C MUn=COEFFICIENT-OF-FRICTION FOR VEHICLE n
      MU1=MU
      MU2=MU
C TnB=TIME WHEN VEHICLE n BEGINS BRAKING
      T1B=(VV1I-VV1T)/MU/G
      T2B=(VV2I-VV2T)/MU/G
C Xn=VEHICLE n POSITION
C CALCULATE VEHICLE POSITIONS AT t = -30
      X1=VV1T*TZERO+MU*G*T1B*T1B/2.
      X2=VV2T*TZERO+MU*G*T2B*T2B/2.
      IF (CONFIG.EQ.2.OR.CONFIG.EQ.5) THEN
      X2=-X2
      V2=-V2
      END IF
      IF (CONFIG.GE.4) X2=X2+X20
C TFIN=FINISH TIME OF COMPUTATIONAL INTERVAL
    9 TFIN=T1B
      IF (T2B.LT.T1B) TFIN=T2B
      IF (T1B.EQ.0.0) T1B=10.
      IF (T2B.EQ.0.0) T2B=10.
C IF VEHICLE 1 HAS NOT STARTED BRAKING, CALL RADAR SYSTEM PERFORMANCE
C SUBROUTINE
   10 IF (T1B.LE.TZERO.OR.T1R.LT.10.5) GO TO 14
      ICALL=1
      CALL RADAR(ICALL,T1R,TZERO,TFIN,V1,V2,X1,X2,A2,SYSTYP)
C IF VEHICLE 2 HAS NOT STARTED BRAKING AND THE COLLISION IS A HEAD-
C ON IMPACT, CALL RADAR SYSTEM PERFORMANCE SUBROUTINE.  MAKE SURE THAT
C VEHICLE 2 IS NOT AVOIDING ANOTHER OBJECT, SKIDDING, ETC.  ALSO, MAKE
```

```
C SURE THAT VEHICLE 2 IS AN AUTOMOBILE.
   14 IF (CONFIG.NE.2) GO TO 15
      IF (T2B.LE.TZERO.OR.T2R.LT.10.5) GO TO 15
      IF (MPA2.GE.15.OR.MIS2.NE.0) GO TO 15
      IF (TYP2.NE.1.AND.TYP2.NE.2) GO TO 15
      ICALL=2
      CALL RADAR(ICALL,T2R,TZERO,TFIN,V2,V1,X2,X1,A1,SYSTYP)
C CALCULATE NEW FINISH TIME IF EITHER VEHICLE STARTS BRAKING DURING
C INTERVAL
   15 IF (TZERO.LT.T1R.AND.T1R.LE.TFIN) GO TO 18
      IF (TZERO.LT.T2R.AND.T2R.LE.TFIN) GO TO 30
      GO TO 33
   18 IF (TZERO.LT.T2R.AND.T2R.LE.T1R+TDEL(SYSTYP)) GO TO 21
      IF (T2R.GT.TZERO) T2R=11.
      GO TO 24
   21 IF (T1R.GT.T2R+TDEL(SYSTYP)) GO TO 27
      IF (T2B.GT.T2R+TDEL(SYSTYP)) T2B=T2R+TDEL(SYSTYP)
      IF (TFIN.GT.T2B) TFIN=T2B
   24 IF (T1B.GT.T1R+TDEL(SYSTYP)) T1B=T1R+TDEL(SYSTYP)
      IF (TFIN.GT.T1B) TFIN=T1B
      GO TO 33
   27 T1R=11.
   30 IF (T2B.GT.T2R+TDEL(SYSTYP)) T2B=T2R+TDEL(SYSTYP)
      IF (TFIN.GT.T2B) TFIN=T2B
C DELTA=LENGTH OF TIME INTERVAL
   33 DELTA=TFIN-TZERO
C CHECK TO SEE IF EITHER VEHICLE COMES TO A STOP DURING THE INTERVAL.
C IF THIS OCCURS, SHORTEN THE INTERVAL SO THAT IT ENDS WHEN THE
C VEHICLE STOPS.  VnF=VELOCITY OF VEHICLE n AT END OF INTERVAL
      V1F=V1+A1*DELTA
      IF (V1F.GE.0.0) GO TO 36
      DELTA=-V1/A1
      TFIN=TZERO+DELTA
      V1F=0.
   36 V2F=V2+A2*DELTA
      IF (CONFIG.EQ.2.OR.CONFIG.EQ.5) GO TO 39
      IF (V2F.LT.0.0) GO TO 42
      GO TO 45
   39 IF (V2F.LE.0.0) GO TO 45
   42 DELTA=ABS(V2/A2)
      V1F=V1+A1*DELTA
      TFIN=TZERO+DELTA
      V2F=0.
C DETERMINE IF COLLISION OCCURS DURING INTERVAL
   45 IF (TFIN.LT.0.0) GO TO 78
      IF (CONFIG.GT.2) GO TO 54
      SQ=(V1-V2)**2.+2*(A1-A2)*(X2-X1)
      IF (SQ.LE.0.0) GO TO 75
      IF (A1.EQ.A2) GO TO 48
      SQ=SQRT(SQ)
C DTI=TIME FROM TZERO TO IMPACT
      DTI=(V2-V1-SQ)/(A1-A2)
      IF (DTI.LT.0.0) DTI=100.
      DT2=(V2-V1+SQ)/(A1-A2)
      IF (DT2.LT.0.0) DT2=100.
      IF (DTI.GT.DT2) DTI=DT2
      GO TO 51
   48 DTI=(X2-X1)/(V1-V2)
      IF (DTI.LT.0.0) DTI=100.
   51 IF (DTI.GT.DELTA) GO TO 75
      GO TO 93
```

```
   54 IF (A1.EQ.0.0) GO TO 57
      SQ=V1*V1-2.*A1*X1
      IF (SQ.LE.0.0) GO TO 108
      DTI=(SQRT(SQ)-V1)/A1
      GO TO 60
   57 DTI=-X1/V1
   60 IF (DTI.GT.DELTA) GO TO 75
      IF (V2.EQ.0.0) THEN
      S2=0.0
      GOTO 96
      END IF
      X2I=(WIDTH1+XLENG2)/2.
      IF (CONFIG.EQ.5) X2I=-X2I
      IF (A2.EQ.0.0) GO TO 69
      SQ=V2*V2+2.*A2*(X2I-X2)
      IF (SQ) 66,63,63
   63 SQ=SQRT(SQ)
      IF (A2.GT.0.0) SQ=-SQ
      DT2=(SQ-V2)/A2
      GO TO 72
   66 DT2=100.
      GO TO 72
   69 DT2=(X2I-X2)/V2
   72 IF (DT2-DTI) 108,108,93
   75 IF (TFIN.GE.10.0) GO TO 108
C CALCULATE POSITION AND VELOCITY OF BOTH VEHICLES AT END OF INTERVAL
   78 X1=X1+(V1+A1*DELTA/2.)*DELTA
      X2=X2+(V2+A2*DELTA/2.)*DELTA
      V1=V1F
      V2=V2F
C SET BEGINNING AND END POINTS FOR NEXT TIME INTERVAL
      TZERO=TFIN
      TFIN=10.
      IF (TZERO.LT.T1B) TFIN=T1B
      IF (TZERO.LT.T2B.AND.T2B.LT.TFIN) TFIN=T2B
C IF EITHER VEHICLE HAS INITIATED RADAR BRAKING, INCREASE ITS
C COEFFICIENT OF FRICTION
      IF (T1R.LT.10.5) MU1=MU+MUINC(SYSTYP)
      IF (T2R.LT.10.5) MU2=MU+MUINC(SYSTYP)
C IF EITHER VEHICLE HAS BEGUN BRAKING BEFORE THE INTERVAL BEGINS,
C COMPUTE ITS ACCELERATION
      IF (TZERO.GE.T1B) A1=-MU1*G
      IF (TZERO.LT.T2B) GO TO 81
      A2=MU2*G
      IF (CONFIG.NE.2.AND.CONFIG.NE.5) A2=-A2
C IF EITHER VEHICLE HAS COME TO A STOP, SET ITS ACCELERATION BACK TO
C ZERO
   81 IF (CONFIG.EQ.2) GO TO 84
      IF (V1) 108,108,87
   84 IF (V1.LE.0.0) A1=0.
   87 IF (V2.EQ.0.0) A2=0.
      GO TO 10
C COLLISION OCCURS: COMPUTE NEW VREL
C FOR UNMODIFIED VREL FIRST
C IF RADAR IS USED
   93 S2=V2+A2*DTI
   96 S1=V1+A1*DTI
      IF (KSPTYP.EQ.7) S2=0.
      GOTO (105,105,105,99,99), CONFIG
   99 VREL(SYSTYP,1)=SQRT(S1*S1+S2*S2)
      GO TO 270
```

```
  105 VREL(SYSTYP,1)=ABS(S1-S2)
      GO TO 270
C IF RADAR IS NOT USED
  110 S1=VV1I
      S2=VV2I
      IF (MHE1.EQ.7) GOTO 116
      IF (JKSTYP.EQ.8) GO TO 119
      GOTO (116,116,116,117,119,118,116), KSPTYP
  116 VREL(SYSTYP,1)=ABS(S1)
      GOTO 270
  117 IF (INUM.NE.JNUM) GOTO 119
      IF (JKSTYP.EQ.4) THEN
      VREL(SYSTYP,1)=ABS(S1+S2)
      GOTO 270
      END IF
      IF (JKSTYP.EQ.5) GOTO 119
      GOTO 120
  118 IF (JKSTYP.EQ.4) GOTO 120
  119 VREL(SYSTYP,1)=SQRT(S1**2+S2**2)
      GOTO 270
  120 VREL(SYSTYP,1)=ABS(S1-S2)
      GOTO 270
  121 VREL(SYSTYP,1)=999.0
C COMPUTE MODIFIED VREL
  270 INDEX=KSPTYP
      IF (INUM.EQ.JNUM) INDEX=JKSTYP
      GOTO (271,272,273,274,275,276,277), INDEX
  271 VREL(SYSTYP,2)=.252/CFM+.363*ABS(S1)
      GOTO 111
  272 VREL(SYSTYP,2)=.038/CFM+.329*ABS(S1)
      GOTO 111
  273 VREL(SYSTYP,2)=3./CFM
      GOTO 111
  274 VREL(SYSTYP,2)=-7.508/CFM+.684*ABS(S2)+.534*ABS(S1)
      GOTO 111
  275 VREL(SYSTYP,2)=-2.088/CFM+.614*ABS(S2)+.179*ABS(S1)
      GOTO 111
  276 VREL(SYSTYP,2)=-3.798/CFM+ABS(.862*ABS(S2)-.851*ABS(S1))
      GOTO 111
  277 VREL(SYSTYP,2)=ABS(S1)
      GOTO 111
  108 S1=V1+A1*DTI
      S2=V2+A2*DTI
      VREL(SYSTYP,1)=0.
      VREL(SYSTYP,2)=0.
      GOTO 111
  109 S1=VV1I
      S2=VV2I
      VREL(SYSTYP,1)=999.0
      VREL(SYSTYP,2)=999.0
C CONVERT FROM FPS TO MPH
  111 DO 112 MOD=1,IMOD
      IF (VREL(SYSTYP,MOD).LT.998.5)
     CVREL(SYSTYP,MOD)=VREL(SYSTYP,MOD)*CFM
      SS1=S1*CFM
      SS2=S2*CFM
      IF (IWRFL.EQ.0) GOTO 998
      WRITE (21,13) SYSTYP,MOD,SS1,SS2,VREL(SYSTYP,MOD)
   13 FORMAT (1X,'BRAKE: SYSTYP.MOD.S1.S2.VREL',2I6,2F6.0,F8.2)
  998 CONTINUE
  112 CONTINUE
  200 CONTINUE
      RETURN
      END
```

RADAR.FOR

```
C*************************************************************************
      SUBROUTINE RADAR(ICALL,TNR,TZERO,TFIN,V1,V2,X1,X2,AN,SYSTYP)
C*************************************************************************
C     THIS ROUTINE COMPUTES THE TIME THAT THE BRAKES ARE ACTIVATED
C     FOR A RADAR BRAKE SYSTEM. UNITS ARE FEET, SECONDS, AND SLUGS.
C
C     TNR=TIME OF BRAKE APPLICATION
C     TZERO=BEGINNING OF TIME INTERVAL
C     TFIN=END OF TIME INTERVAL
C     V1=CASE VEHICLE VELOCITY
C     V2=TARGET VEHICLE VELOCITY
C     X1=CASE VEHICLE DISPLACEMENT
C     X2=TARGET VEHICLE DISPLACEMENT
C     XLENG2=THE LENGTH OF THE TARGET VEHICLE
C     AN=TARGET VEHICLE ACCELERATION
C     SYSTYP=SYSTEM TYPE
C     CONFIG=ACCIDENT CONFIGURATION
C
C     ALL INPUT VARIABLES ARE LEFT UNCHANGED EXCEPT FOR T
C*************************************************************************
      INCLUDE 'SETUP.FOR'
      IF (IRDFL.EQ.0) GOTO 999
      WRITE(21,11) TZERO,TFIN,V1,V2,X1,X2,AN,SYSTYP,CONFIG,ICALL
  999 CONTINUE
      TNR=11.
      IF (SYSTYP.EQ.1) RETURN
      CALL CONVRT(ICALL,V1,V2,X1,X2,AN)
      CALL DRADAR(TS,TZERO,TFIN,SYSTYP)
      IF (TS.GT.10.5) RETURN
      CALL DRIVER(SYSTYP,TNR,TS,TZERO,TFIN)
   11 FORMAT(1X,'RADAR: TZERO.TFIN.V1.V2.X1.X2.AN.SYSTYP.CONFIG.ICALL',
     C       7F8.2,3I3)
      RETURN
      END
C*************************************************************************
C*************************************************************************
      SUBROUTINE CONVRT(ICALL,V1,V2,X1,X2,AN)
C*************************************************************************
C     THIS ROUTINE INITIALIZES VALUES OF CERTAIN PARAMETERS.
C     XLENG2 IS THE LENGTH OF THE TARGET VEHICLE (SIDE IMPACT ONLY).
C     RO IS THE SEPARATION OF THE VEHICLES.
C     VOO IS THE RATE OF CHANGE OF RO.
C     IF THE VEHICLES ARE CLOSING, VOO IS LESS THAN ZERO.
C     AO IS THE TIME RATE OF CHANGE OF VOO. IF VOO BECOMES MORE POSITIVE
C     SUCH AS WHEN VEHICLE 2 APPLIES HIS BRAKES DURING A HEAD ON,
C     THEN AO IS POSITIVE.
C     THE NEW VARIABLES ARE STORED IN COMMON BLOCK /RADAR/
C*************************************************************************
      INCLUDE 'SETUP.FOR'
      IF (CONFIG.LE.3) THEN
      ISIGN=1
      IF (ICALL.EQ.2) ISIGN=-1
      RO=ISIGN*(X2-X1)
      VOO=ISIGN*(V2-V1)
      V1O=ISIGN*V1
      V2O=ISIGN*V2
      AO=AN
      SAO=RO
      SBO=0.
      VAO=ISIGN*V1
      VBO=0.
```

```
      B0=0.
      ENDIF
      IF (CONFIG.GE.4) THEN
      R0=-X1
      V00=-V1
      V10=V1
      V20=V2
      A0=0.
      SA0=R0
      SB0=ABS(X2)-XLENG2/2
      VA0=V1
      VB0=ABS(V2)
      B0=-ABS(AN)
      ENDIF
      IF (IRDFL.EQ.0) GOTO 999
      WRITE(21,11) R0,V00,V10,V20,A0
      WRITE(21,12) SA0,SB0,VA0,VB0,B0
      IF (V00.GT.0.) WRITE(21,13)
  999 CONTINUE
   11 FORMAT(1X,'CONVRT: R0.V00.V10.V20.A0',5F10.2)
   12 FORMAT(1X,'CONVRT: SA0.SB0.VA0.VB0.B0',5F10.2)
   13 FORMAT(1X,'CONVRT: VEHICLES ARE SEPARATING ')
      RETURN
      END
C*********************************************************************
C*********************************************************************
      SUBROUTINE DRADAR(TS,TZERO,TFIN,SYSTYP)
C*********************************************************************
C     DRADAR DETERMINES THE INSTANT THAT THE RADAR IS CAPABLE OF
C     DETECTING A VEHICLE IN A SIDE IMPACT.
C*********************************************************************
C     TS=THE NEW INITIAL TIME
C     TZERO=THE ORIGINAL INITIAL TIME
C     TFIN=THE FINALE TIME (END POINT OF THE INTERVAL)
C     CONFIG=THE ACCIDENT CONFIGURATION
C*********************************************************************
      INCLUDE 'SETUP.FOR'
      TS=TZERO
C IF VEHICLE DOES NOT ENTER BEAM, T=11.
      BEAMWD=ABS(SA0*TAN(THETA(SYSTYP)))
      IF (BEAMWD.GE.SB0) GOTO 100
      TS=11.
      IF (CONFIG.LE.3) GOTO 100
C DETERMINE TIME THAT VEHICLE ENTERS BEAM.
      CALL RDSPSD(TT,TZERO,SYSTYP)
      IF (TT.GT.TFIN) GOTO 100
      TS=TT
  100 IF (IRDFL.EQ.0) GOTO 999
      WRITE(21,11) TS,TZERO,THETA(SYSTYP),BEAMWD
  999 CONTINUE
   11 FORMAT (1X,'DRADAR: TS.TZERO.THETA(SYSTYP).BEAMWD',3F10.2)
      RETURN
      END
C*********************************************************************
C*********************************************************************
      SUBROUTINE RDSPSD(TT,TZERO,SYSTYP)
C*********************************************************************
C     DETERMINE THE TIME THAT THE RADAR SPOTS A TARGET IN A SIDE
C     IMPACT. THIS ROUTINE IS CALLED BY ROUTINE DRADAR.
C     TT=THE TIME THAT THE VEHICLE ENTERS THE BEAM.
C     TZERO=THE INITIAL TIME.
```

```
C*********************************************************************
      INCLUDE 'SETUP.FOR'
      ZA=B0/2.
      ZB=VB0-VA0*TAN(THETA(SYSTYP))
      ZC=SA0*TAN(THETA(SYSTYP))-SB0
      CALL QUAD(TT,TZERO,ZA,ZB,ZC)
      IF (IRDFL.EQ.0) GOTO 999
      WRITE(21,11) SA0,SB0,VA0,VB0,B0,THETA(SYSTYP)
      WRITE(21,12) TT,TZERO
  999 CONTINUE
   11 FORMAT (1X,'RDSPSD: SA0.SB0.VA0.VB0.B0.THETA(SYSTYP)',6F10.2)
   12 FORMAT (1X,'RDSPSD: TT.TZERO',2F10.2)
      RETURN
      END
C*********************************************************************
C*********************************************************************
      SUBROUTINE QUAD(TT,TZERO,ZA,ZB,ZC)
C*********************************************************************
C     THIS ROUTINE IS CALLED BY RDSPSD TO SOLVE THE EQUATIONS
C     OF MOTIONS FOR A SIDE IMPACT TO DETERMINE THE TIME THAT
C     VEHICLE 2 ENTERS THE RADAR FIELD OF VEHICLE 1.
C     TT=TIME OF ENTRANCE TO BEAM.
C     TZERO=INITIAL TIME.
C     ZA,ZB,ZC ARE QUADRATIC COEFFICIENTS.
C*********************************************************************
      INCLUDE 'SETUP.FOR'
      TT=11.
      IF (ZA.EQ.0.) THEN
      IF (ZB.EQ.0.) GOTO 100
      T1=-ZC/ZB
      TT=T1+TZERO
      GOTO 100
      ENDIF
      DISC=ZB*ZB-4*ZA*ZC
      IF (DISC.LT.0) GOTO 100
C PICK ROOT WITH LARGEST ABSOLUTE VALUE AS T1
      T1=-(ZB+SIGN(1.,ZB)*SQRT(DISC))/2./ZA
      T2=ZC/ZA/T1
      T3=T2
      IF (T2.LT.0.) T3=T1
      IF (T3.LT.0.) T3=0.
      TT=T3+TZERO
  100 IF (IRDFL.EQ.0) GOTO 999
      WRITE (21,11) ZA,ZB,ZC,TT
  999 CONTINUE
   11 FORMAT (1X,'QUAD: ZA.ZB.ZC.TT',4F8.2)
      RETURN
      END
C*********************************************************************
C*********************************************************************
      SUBROUTINE DRIVER(SYSTYP,TNR,TS,TZERO,TFIN)
C*********************************************************************
C     DRIVER CALCULATES THE TIME TNR THAT THE BRAKES WOULD BE APPLIED
C     ASSUMING THAT THE RADAR IS CAPABLE OF DETECTING THE VEHICLE.
C     IF THE BRAKES ARE NOT APPLIED, THEN T=11.
C     TZERO AND TFIN DEFINE THE INTERVAL.
C*********************************************************************
      INCLUDE 'SETUP.FOR'
C WE ARE NOT YET IN BRAKING INTERVAL.
      ZD=DIFF(SYSTYP,TZERO,TFIN)
      IF (ZD.GT.0) THEN
```

```
      TNR=11.
      GOTO 100
      ENDIF
C PAST BRAKE POINT. SLAM ON BRAKES!
      ZD=DIFF(SYSTYP,TZERO,TZERO)
      IF (ZD.LT.0.) THEN
      TNR=TZERO
      IF (TNR.LT.TS) TNR=TS
      GOTO 100
      ENDIF
C BRAKE POINT LIES IN THIS INTERVAL. FIND IT!
      TNR=ROOT(SYSTYP,TZERO,TFIN,DIFF)
      IF (TNR.LT.TS) TNR=TS
  100 IF (IRDFL.EQ.0) GOTO 999
      WRITE (21,11) TNR,TS
  999 CONTINUE
   11 FORMAT (1X,'DRIVER: TNR.TS',2F8.2)
      RETURN
      END
C*********************************************************************
C*********************************************************************
      REAL FUNCTION DIFF(SYSTYP,TZERO,T)
C*********************************************************************
C     THIS ROUTINE CALCULATES THE DIFFERENCE BETWEEN THE RANGE OF
C     THE VEHICLE AT A TIME T AND THE RANGE THAT THE VEHICLE WOULD
C     APPLY RADAR BRAKING AT THE RELATIVE VELOCITY ATTAINED AT TIME
C     T. THUS IF DIFF=0, THE BRAKES ARE APPLIED.
C     IF DIFF>0, THE BRAKES ARE NOT APPLIED.
C     IF DIFF<0, THE BRAKES ARE APPLIED.
C*********************************************************************
      INCLUDE 'SETUP.FOR'
      ZV0=V00+A0*(T-TZERO)
      ZV1=V10
      ZV2=V20+A0*(T-TZERO)
      RA=R0+V00*(T-TZERO)+A0*(T-TZERO)**2/2.
      IF (MUADJ.EQ.1) ACC(SYSTYP)=MU
      IF (MUADJ.EQ.0) ACC(SYSTYP)=MURAD(SYSTYP)
      IF (SYSTYP.EQ.2) RB=2*ABS(ZV0)
     C+SRD(SYSTYP)
      IF (SYSTYP.EQ.3) RB=ZV0**2/2./ACC(SYSTYP)/G+TAU(SYSTYP)*
     CABS(ZV0)+SRD(SYSTYP)
      IF (SYSTYP.EQ.4.AND.CONFIG.NE.2)
     CRB=(ZV1**2-ZV2**2)/2./ACC(SYSTYP)/G+TAU(SYSTYP)*
     CABS(ZV1)+SRD(SYSTYP)
      IF (SYSTYP.EQ.4.AND.CONFIG.EQ.2)
     CRB=(ZV1**2-ZV2**2)/2./ACC(SYSTYP)/G+TAU(SYSTYP)*
     CABS(ZV1)+SRD(SYSTYP)
      IF (SYSTYP.EQ.5.AND.CONFIG.NE.2)
     CRB=(ZV1**2-ZV2**2)/2./ACC(SYSTYP)/G+TAU(SYSTYP)*
     CABS(ZV1)+SRD(SYSTYP)
      IF (SYSTYP.EQ.5.AND.CONFIG.EQ.2)
     CRB=(ZV1**2+ZV2**2)/2./ACC(SYSTYP)/G+TAU(SYSTYP)*
     CABS(ZV1)+SRD(SYSTYP)
      IF (RB.GT.RMAX(SYSTYP)) RB=RMAX(SYSTYP)
      IF (ZV1.LT.VMIN(SYSTYP)) RB=0.
      IF (IRDFL.EQ.0) GOTO 999
      WRITE(21,11) R0,V00,A0,TZERO,T,ZV0,ZV1,ZV2,ACC(SYSTYP),RA,RB
  999 CONTINUE
      DIFF=RA-RB
      IF (ZV0.GE.0.0) DIFF=ABS(DIFF)
   11 FORMAT (1X,'DIFF: R0.V00.A0.TZERO.T.ZV0.ZV1.ZV2.ACC(SYSTYP).RA.RB'
```

```
     C         ,11F7.2)
      RETURN
      END
C*************************************************************************
C*************************************************************************
      REAL FUNCTION ROOT(SYSTYP,TZERO,TFIN,DIFF)
C*************************************************************************
C     ROOT RETURNS THE ROOT OF DIFF.
C     THE ROOT MUST BE BETWEEN TZERO AND TFIN.
C*************************************************************************
      INCLUDE 'SETUP.FOR'
      TOL=0.0001
C TOL IS THE ERROR TOLERANCE.
      EPS=1.0
   10 EPS=EPS/2.
      TOL1=1.+EPS
      IF (TOL1.GT.1.0) GOTO 10
      ZT0=TZERO
      ZTF=TFIN
      FZT0=DIFF(SYSTYP,TZERO,ZT0)
      FZTF=DIFF(SYSTYP,TZERO,ZTF)
   20 ZT1=ZT0
      FZT1=FZT0
      ZT2=ZTF-ZT0
      ZT3=ZT2
   30 IF (ABS(FZT1).GE.ABS(FZTF)) GOTO 40
      ZT0=ZTF
      ZTF=ZT1
      ZT1=ZT0
      FZT0=FZTF
      FZTF=FZT1
      FZT1=FZT0
   40 TOL1=2.*EPS*ABS(ZTF)+0.5*TOL
      RELV=0.5*(ZT1-ZTF)
      IF (ABS(RELV).LE.TOL1) GOTO 90
      IF (FZTF.EQ.0.) GOTO 90
      IF (ABS(ZT3).LT.TOL1) GOTO 70
      IF (ABS(FZT0).LE.ABS(FZTF)) GOTO 70
      IF (ZT0.NE.ZT1) GOTO 50
      S=FZTF/FZT0
      P=2.*RELV*S
      Q=1.-S
      GOTO 60
   50 Q=FZT0/FZT1
      R=FZTF/FZT1
      S=FZTF/FZT0
      P=S*(2.*RELV*Q*(Q-R)-(ZTF-ZT0)*(R-1.))
      Q=(Q-1)*(R-1.)*(S-1.)
   60 IF (P.GT.0.)Q=-Q
      P=ABS(P)
      IF ((2.*P).GE.(3.*RELV*Q-ABS(TOL*Q))) GOTO 70
      IF (P.GE.ABS(0.5*ZT3*Q)) GOTO 70
      ZT3=ZT2
      ZT2=P/Q
      GOTO 80
   70 ZT2=RELV
      ZT3=ZT2
   80 ZT0=ZTF
      FZT0=FZTF
      IF (ABS(ZT2).GT.TOL1) ZTF=ZTF+ZT2
      IF (ABS(ZT2).LE.TOL1) ZTF=ZTF+SIGN(TOL1,RELV)
      FZTF=DIFF(SYSTYP,TZERO,ZTF)
      IF ((FZTF*(FZT1/ABS(FZT1))).GT.0.) GOTO 20
      GOTO 30
   90 ROOT=ZTF
      IF (IRDFL.EQ.0) GOTO 999
      WRITE (21,11) ROOT
  999 CONTINUE
   11 FORMAT (1X,'ROOT: ROOT',F8.2)
      RETURN
      END
C*************************************************************************
```

APPENDIX K

LISTING OF PROGRAM CASEWT.FOR

CASEWT.COM

```
$SET DEF [KR1214.BRAKE]
$MOUNT MT: NC79
$ASSIGN MT:NC79.DAT FOR010
$FOR CASEWT
$LINK CASEWT
$TYPE CASEWT.COM
$TYPE CASEWT.FOR
$RUN CASEWT
$STOP
```

CASEWT.FOR

```
      CHARACTER*283 RECORD
      CHARACTER*117 VH1,VH2,VH3
      CHARACTER*49 ACC
      OPEN (UNIT=20,FILE='CASEWT.DAT',RECL=289,STATUS='NEW')
      ICOUNT=0
      JCOUNT=0
  100 READ (10,1,END=200) ACC,VH1,VH2,VH3
    1 FORMAT (4A)
      ICOUNT=ICOUNT+1
      IF (VH3(13:14).NE.'  ') GOTO 100
      WRITE (RECORD,2) ACC,VH1,VH2
    2 FORMAT (3A)
      JCOUNT=JCOUNT+1
      IF (JCOUNT.GE.10000) GOTO 200
      IF (VH2(13:14).EQ.'  ') GOTO 100
      WRITE (RECORD,2) ACC,VH2,VH1
      JCOUNT=JCOUNT+1
      IF (JCOUNT.GE.10000) GOTO 200
      READ (RECORD,99) ISPEED
   99 FORMAT (T133,I2)
      IF (ISPEED.LE. 0) WT=0.0
      IF (ISPEED.GT. 0.AND.ISPEED.LE.17) WT=.007/.0212
      IF (ISPEED.GT.17.AND.ISPEED.LE.27) WT=.164/.0720
      IF (ISPEED.GT.27.AND.ISPEED.LE.37) WT=.505/.4013
      IF (ISPEED.GT.37.AND.ISPEED.LE.47) WT=.128/.1803
      IF (ISPEED.GT.47.AND.ISPEED.LE.57) WT=.196/.3252
      IF (ISPEED.GT.57) WT=0.0
      WT=WT*10000./8662.
      WRITE (20,3) RECORD,WT
    3 FORMAT (A,F6.3)
      GOTO 100
  200 CONTINUE
      CLOSE (UNIT=20)
      WRITE (6,*) 'CASES READ',ICOUNT
      WRITE (6,*) 'CASES USED',JCOUNT
      STOP
      END
```

APPENDIX
DISCUSSION OF PROCEDURES TO TRANSFORM NORTH CAROLINA VREL DATA FOR COMPATIBILITY WITH KRAESP

In a previous investigation using the first 10,000 cases in the North Carolina file, the North Carolina VREL distributions were compared to distributions obtained from the NCSS file which have been used with the KRAESP model in prior research.

Table L-1 presents the probability distributions of VREL for the baseline and for one radar case. This material is displayed graphically in Figures L-1 through L-5. Also plotted in these figures is a typical VREL probability distribution derived from the National Crash Severity Study file for use with the DRAESP Model. The latter distribution is an artificial one derived from crash severity (Delta-V) in the NCSS file via the transformations:

$$VREL = \frac{M_1 + M_2}{M_2} \Delta V_1 \qquad \text{Vehicle-to-Vehicle} \qquad \text{(L-1)}$$

$$VREL = \Delta V_1 \qquad \text{Fixed Object}$$

where M_1, M_2 are the vehicle masses.

In the KRAESP Model, calculations are based on crash severity. Crash severities are obtained from any given set of VREL data via the inverses of the above formulas. In previous practice this has, therefore, amounted to working with actual DELTA-Vs from NCSS and the validity of the transformations and the intermediate VREL values obtained has been a moot point.

In the present application the VREL values are obtained directly from the data, and the question arises whether or not the crash severities produced by Equations L-1 are realistic. In fact, as is seen in Figures L-1 through L-5, the current North Carolina and previous KRAESP distributions for VREL are so drastically different that fatality and injury predictions based on the actual VRELs, together with the apparently distorted transformations assumed by KRAESP (Equations L-1), will be grossly in error. An expedient method of coping with this problem is to modify the computation of VREL in Subroutine BRAKE so as to

TABLE L-1. DISPOSITION OF CASES BY ACCIDENT CONFIGURATION, ACCIDENT TYPE, AND VREL FOR BASELINE AND RADAR SYSTEMS*

KRAESP Configuration	Baseline System			Radar System		
	VREL Known	VREL ≤ Zero**	VREL Unknown	VREL Known	VREL ≤ Zero**	VREL Unknown
1. Fixed Object Front	259.66	0.00	0.00	193.43	66.22	0.00
2. Fixed Object Side	144.26	0.00	0.00	144.26	0.00	0.00
3. Rollover	127.24	0.00	0.00	127.24	0.00	0.00
4. Vehicle-to-Vehicle Front	702.78	346.47	0.00	548.67	500.57	0.00
5. Vehicle-to-Vehicle Side	579.88	303.16	0.00	540.16	342.88	0.00
6. Vehicle-to-Vehicle Rear	150.23	14.11	0.00	87.73	76.61	0.00
7. Non Motorists	68.13	2.63	0.00	26.29	44.47	0.00
8. Unknown	161.80	54.37	5,291.38	137.80	78.37	5,291.38
9. Other Vehicle Types All Configurations	493.59	157.87	1,144.97	392.70	258.77	1,144.97
Total All Configurations	2,687.57	878.61	6,436.35	2,198.28	1,367.89	6,436.35
Total Configurations 1-6	1,964.05	663.74	0.00	1,641.49	986.28	0.00

*Due to the modified calculation of VREL, negative values are generated in the vehicle-to-vehicle case. These are classified with VREL = 0.

**Numbers of cases are fractional due to the case weighting applied to adjust North Carolina to NASS by speed limits.

TABLE L-2. PROBABILITY OF VREL BY ACCIDENT CONFIGURATION AND RADAR SYSTEM FOR PASSENGER CARS WITH KNOWN ACCIDENT CONFIGURATION AND KNOWN VREL* ORIGINAL COMPUTATION

	Baseline						Radar					
VREL	FOF	FOS	Rollover**	VVF	VVS	VVR	FOF	FOS	Rollover**	VVF	VVS	VVR
1-5	0.002680	0.000000	1.000000	0.048780	0.026841	0.225224	0.000000	0.000000	1.000000	0.031795	0.028181	0.214585
6-10	0.002680	0.028303	0.000000	0.094033	0.080246	0.225359	0.000000	0.028303	0.000000	0.104227	0.087708	0.206596
11-15	0.056756	0.015756	0.000000	0.082176	0.089822	0.159988	0.091220	0.015756	0.000000	0.101522	0.093105	0.228446
16-20	0.105821	0.010072	0.000000	0.121834	0.099870	0.138998	0.086655	0.010072	0.000000	0.118227	0.102348	0.089867
21-25	0.084265	0.082011	0.000000	0.160208	0.206634	0.134817	0.079469	0.082011	0.000000	0.141840	0.197981	0.120862
26-30	0.140055	0.064848	0.000000	0.121739	0.137077	0.063989	0.111289	0.064848	0.000000	0.125347	0.132728	0.077520
31-35	0.161256	0.130756	0.000000	0.086402	0.103422	0.031433	0.205191	0.130756	0.000000	0.076986	0.103328	0.036867
36-40	0.104893	0.109974	0.000000	0.116428	0.110273	0.013580	0.056526	0.109974	0.000000	0.119297	0.112469	0.014240
41-45	0.093451	0.129286	0.000000	0.058392	0.061208	0.000000	0.098985	0.129286	0.000000	0.056895	0.057532	0.000000
46-50	0.118372	0.172126	0.000000	0.042266	0.043290	0.006612	0.122285	0.172126	0.000000	0.048670	0.042896	0.011017
51-55	0.056760	0.148148	0.000000	0.020661	0.017550	0.000000	0.061484	0.148148	0.000000	0.018972	0.016771	0.000000
56-60	0.042337	0.046000	0.000000	0.019100	0.013239	0.000000	0.045721	0.046000	0.000000	0.023601	0.013900	0.000000
61-65	0.005838	0.024123	0.000000	0.008884	0.006586	0.000000	0.015349	0.024123	0.000000	0.011403	0.006915	0.000000
66-70	0.011199	0.019298	0.000000	0.002661	0.000788	0.000000	0.015634	0.019298	0.000000	0.003971	0.000828	0.000000
71-75	0.002680	0.000000	0.000000	0.004891	0.001576	0.000000	0.003598	0.000000	0.000000	0.005982	0.001655	0.000000
76-80	0.008276	0.004825	0.000000	0.003444	0.001576	0.000000	0.003598	0.004825	0.000000	0.004113	0.001655	0.000000
81-85	0.000000	0.000000	0.000000	0.000784	0.000000	0.000000	0.000000	0.000000	0.000000	0.000794	0.000000	0.000000
86-90	0.000000	0.004825	0.000000	0.003326	0.000000	0.000000	0.000000	0.004825	0.000000	0.001589	0.000000	0.000000
91-95	0.000000	0.000000	0.000000	0.000000	0.000000	0.000000	0.000000	0.000000	0.000000	0.001589	0.000000	0.000000
96-100	0.002680	0.009649	0.000000	0.003991	0.000000	0.000000	0.003598	0.009649	0.000000	0.003177	0.000000	0.000000

*VREL $\leq$ 0 is not included.

**VREL is not calculated for Rollover mode.

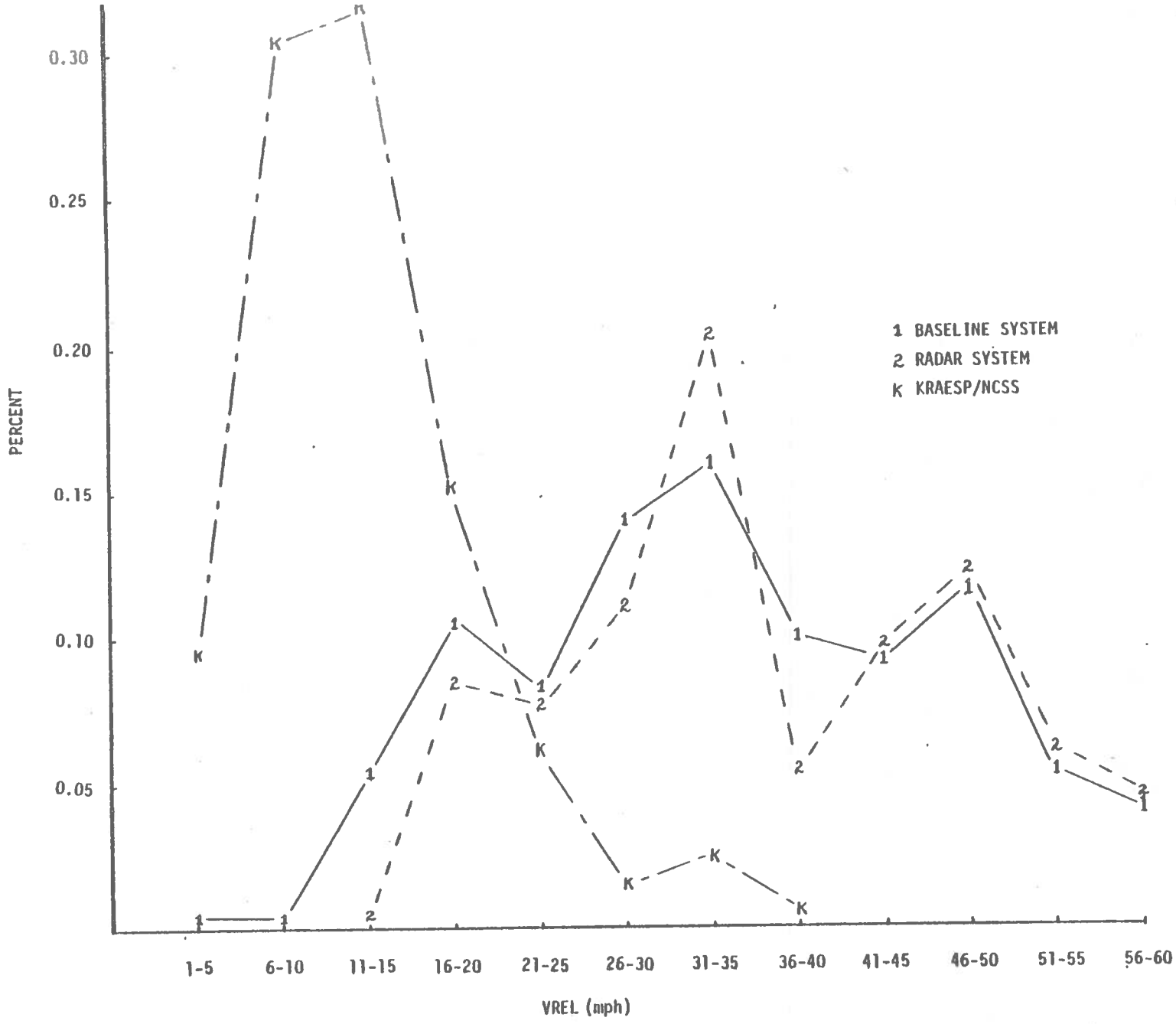

FIGURE L-1. PROBABILITY DISTRIBUTION OF VREL FOR FIXED-OBJECT FRONT IMPACTS - ORIGINAL COMPUTATION

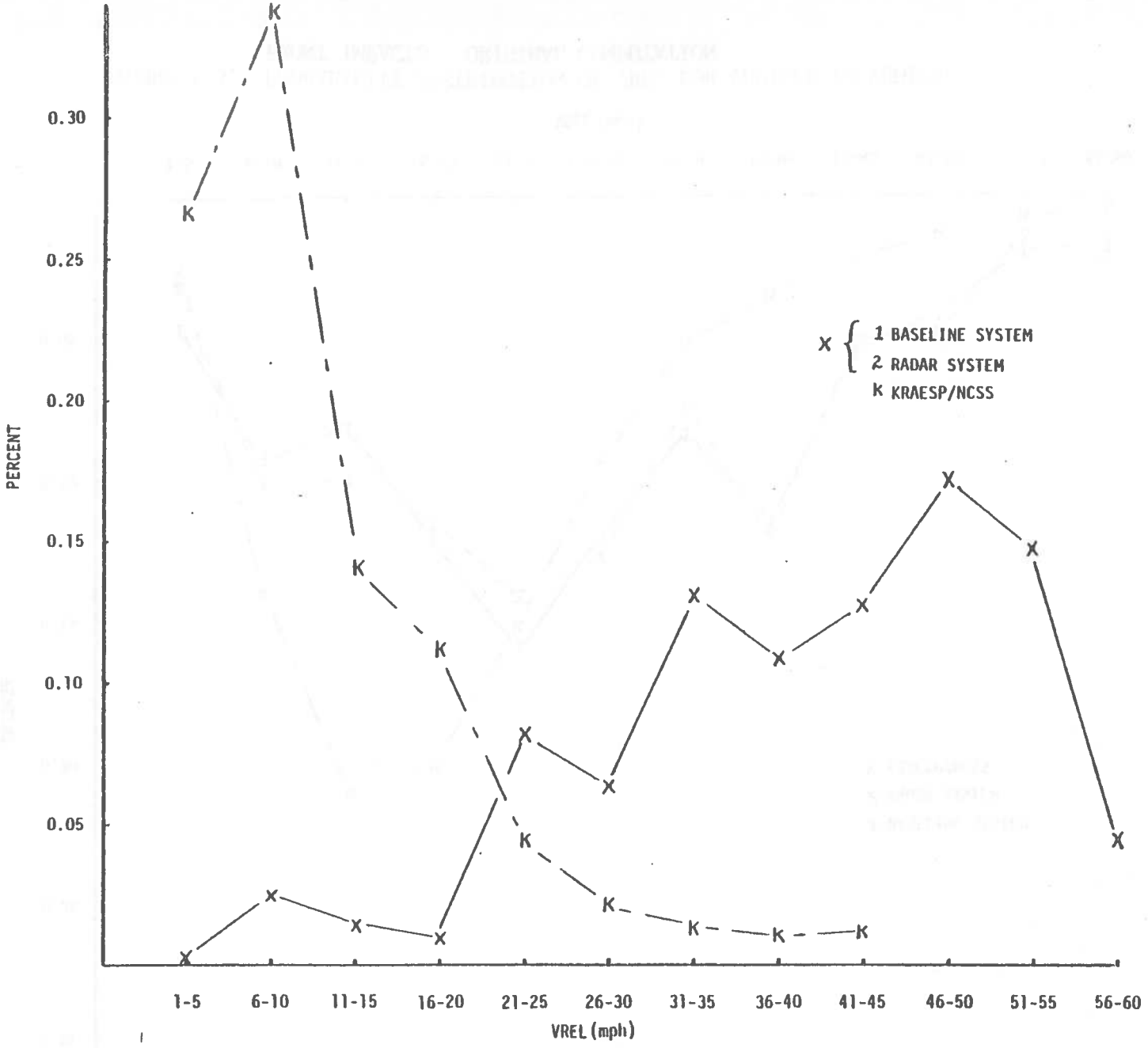

FIGURE L-2. PROBABILITY DISTRIBUTION OF VREL FOR FIXED-OBJECT SIDE IMPACTS - ORIGINAL COMPUTATION

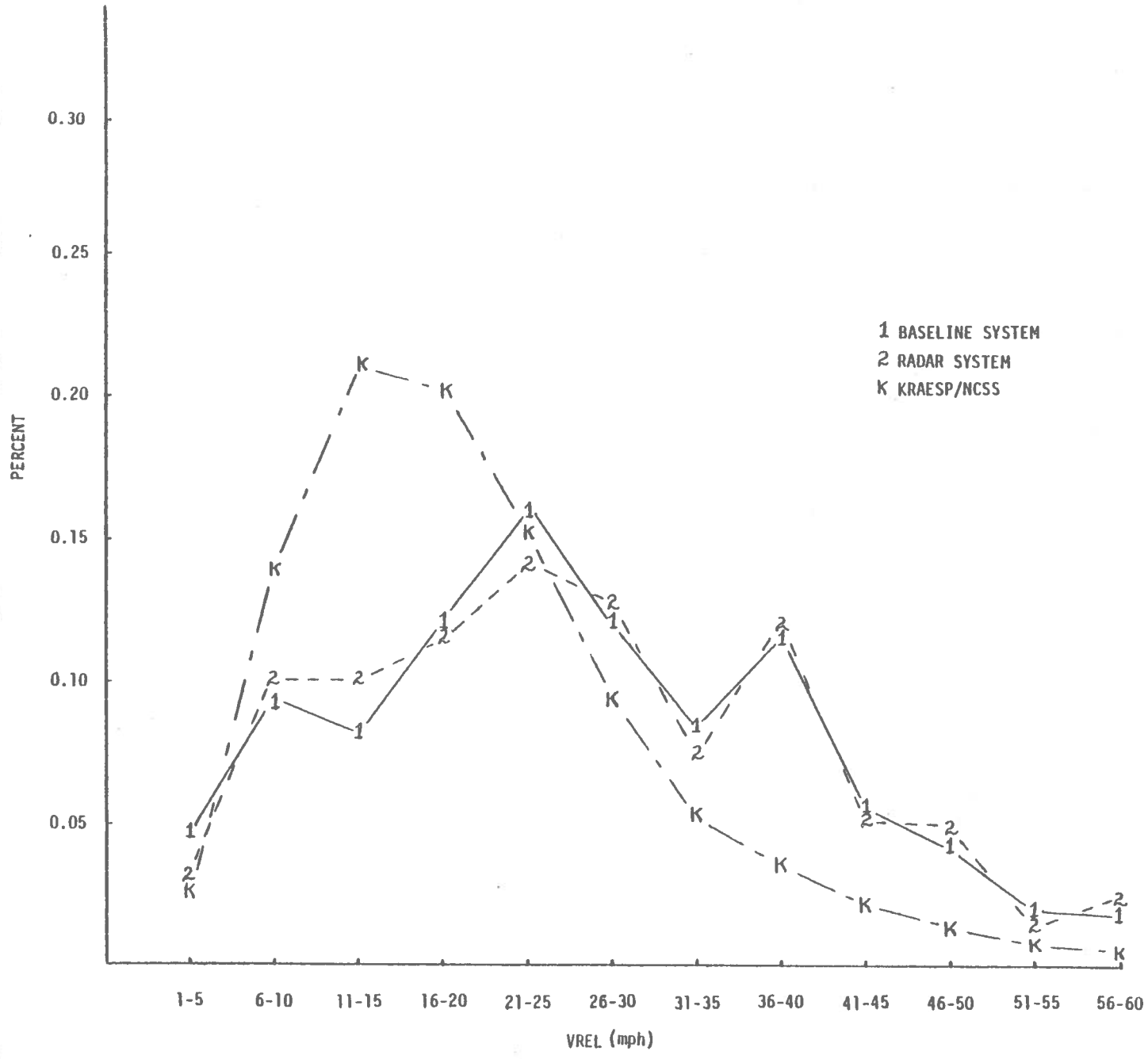

FIGURE L-3. PROBABILITY DISTRIBUTION OF VREL FOR VEHICLE-TO-VEHICLE FRONT IMPACTS - ORIGINAL COMPUTATION

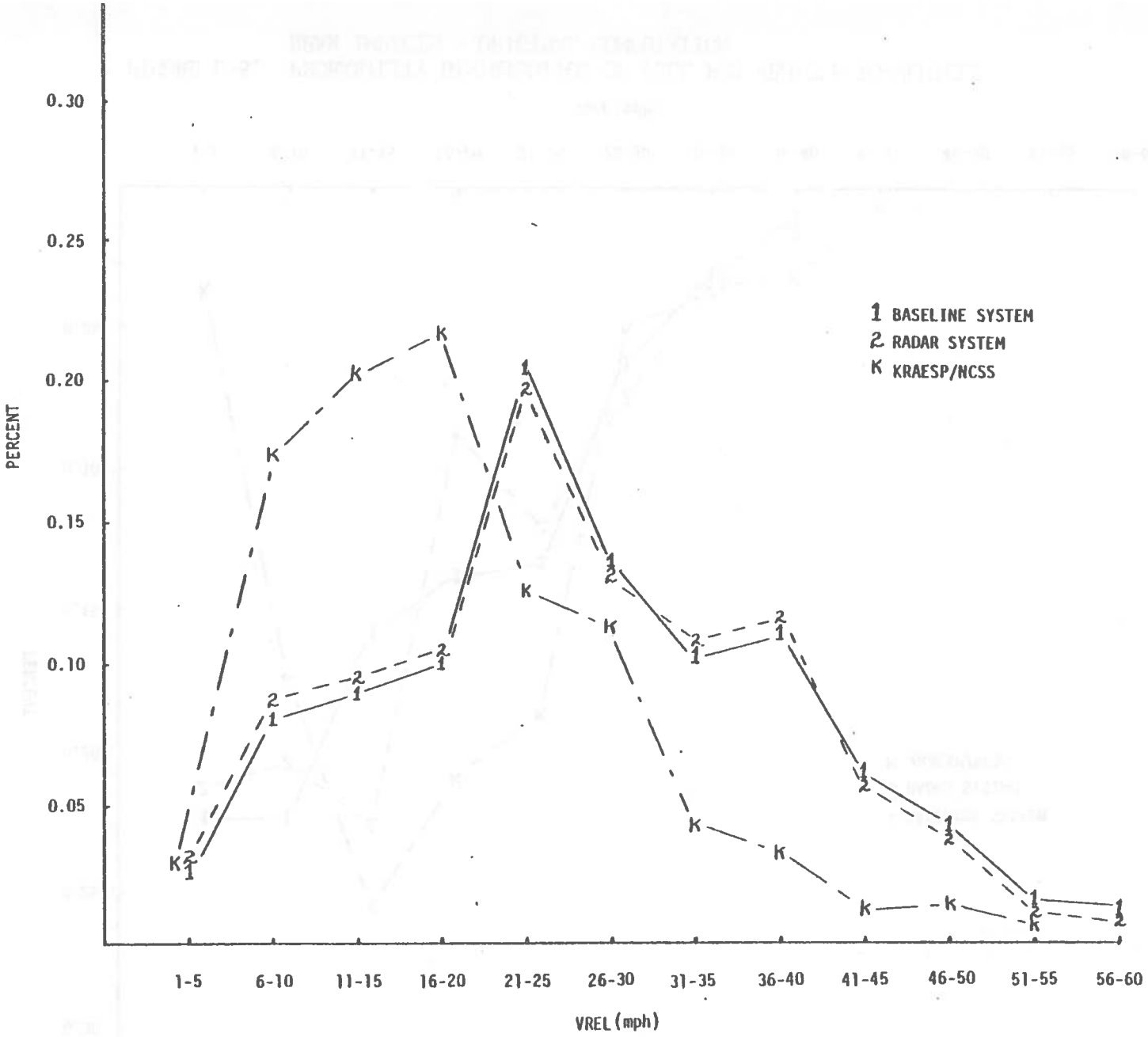

FIGURE L-4. PROBABILITY DISTRIBUTION OF VREL FOR VEHICLE-TO-VEHICLE SIDE IMPACTS - ORIGINAL COMPUTATION

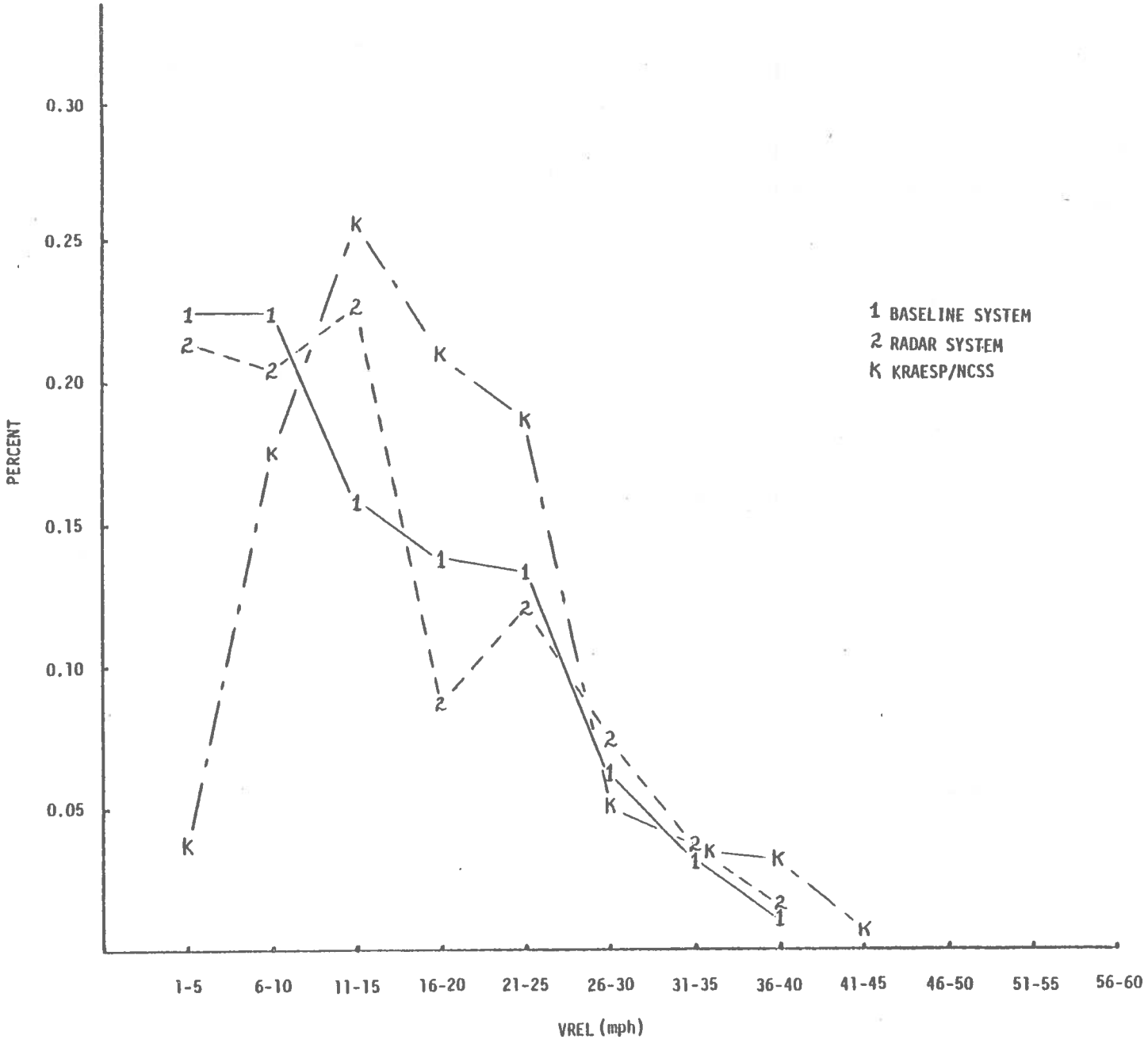

FIGURE L-5, PROBABILITY DISTRIBUTION OF VREL FOR VEHICLE-TO-VEHICLE REAR IMPACTS - ORIGINAL COMPUTATION

move the distribution more into coincidence with the previous KRAESP data. Ultimately the test of validity of the modified results will be the accuracy with which the actual numbers of injuries and fatalities produced in North Carolina in 1979 are predicted by KRAESP for the baseline or no-radar system.

Fortunately, previous research exists (Ref. 21) which is of assistance in solving this problem. In that report, relationships between vehicle impact speeds and DELTA-Vs are obtained from the Multi-Disciplinary Accident Investigation File (MDAI). Those relationships were used to compute crash severities in the 1978 North Carolina accident file. Using this file, further adjustments were made to the DELTA-V formulation to bring injury severity to crash severity relationships in North Carolina into correspondence with those found in NCSS and used by the KRAESP model. The next section contains a detailed discussion of how the transformations finally used were arrived at. The formulas used for the calculations are:

$$\begin{aligned}
\text{VVF VREL} &= -7.508 + 0.684 * V_2 + 0.534 * V_1 \\
\text{VVS VREL} &= -2.088 + 0.614 * V_2 + 0.179 * V_1 \\
\text{VVR VREL} &= -3.798 + 0.862 * V_2 - 0.851 * V_1 \\
\text{FOF VREL} &= 0.252 + 0.363 * V_1 \\
\text{FOS VREL} &= 0.038 + 0.329 * V_1 \quad ,
\end{aligned} \tag{L-2}$$

where all quantities are in units of miles per hour, and V_1, V_2 are the impact speeds of the vehicles.

The gross disagreement between the VREL distributors obtained for North Carolina accidents and those obtained from NCSS for use in the KRAESP Model will result in severely distorted projections of fatalities and injuries for both the actual and radar brake cases. The source of the discrepancy is in the different assumptions used in obtaining the results. The North Carolina VREL data are obtained from estimated vehicle speeds at impact by vector addition. That is,

$$VREL = \left| \vec{V}_2 - \vec{V}_1 \right| \qquad (L\text{-}3)$$

The KRAESP/NCSS VREL data are obtained from DELTA-V data in the NCSS file which is computed by the CRASH2 computer program. DELTA-V is transformed to VREL by the formulas

$$VREL = \frac{m_2}{m_1 + m_2} * \Delta V_1 \qquad \text{Vehicle-to-vehicle}$$

$$VREL = \Delta V_1 \qquad \text{Fixed Object} \qquad (L\text{-}4)$$

These formulas are appropriate for perfectly inelastic, axial collisions, a circumstance that may not be appropriate to real accidents. The fixed object case is particularly questionable as the above relationship is only strictly true for infinitely massive or rigidly attached fixed objects.

The question of the relationships among VREL, DELTA-V, and impact speeds has been investigated previously (Reference 21). In Reference 21 the Multidisciplinary Accident Investigation File (MDAI) is used to develop relationships among Barrier Equivalent Velocity (BEV), the vehicle impact speeds (V_1 and V_2), and the vehicle weights (M_1 and M_2), and the vehicle one damage extent, D. These relationships are based on stepwise linear regression analysis as follows:

Crash Mode (L-5)

VVF $$BEV_1 = -0.182 + 0.684 * \frac{M_2}{M_1 + M_2} * V_2 + 0.534 * \frac{M_2}{M_1 + M_2} * V_1 + 1.214 * D$$

$$r^2 = 0.677$$

VVS $$BEV_1 = 0.746 + 0.614 * \frac{M_2}{M_1 + M_2} * V_2 + 0.179 * \frac{M_2}{M_1 + M_2} * V_1 + 0.605 * D$$

$$r^2 = 0.569$$

VVR $$BEV_1 = 0.101 + 0.862 * \frac{M_2}{M_1 + M_2} * V_2 - 0.851 * \frac{M_2}{M_1 + M_2} * V_1$$

$$r^2 = 0.904$$

FOF $$BEV_1 = -0.634 + 0.915 * V_1$$

$$r^2 = 0.920$$

FOS $$BEV = 0.098 + 0.858 * V_1$$

$$r^2 = 0.830$$

In the MDAI file BEV is computed from the vehicle weights, closing speeds, and accident geometry using the formula

$$BEV = \frac{M_2}{M_1 + M_2} \left(V_1 \cos\theta + \sqrt{V_2^2 - (V_1 \sin\theta)^2}\right) \cdot \cos(\theta - \phi) \qquad (L\text{-}6)$$

The angles θ and ϕ are indicated in Figure L-6.

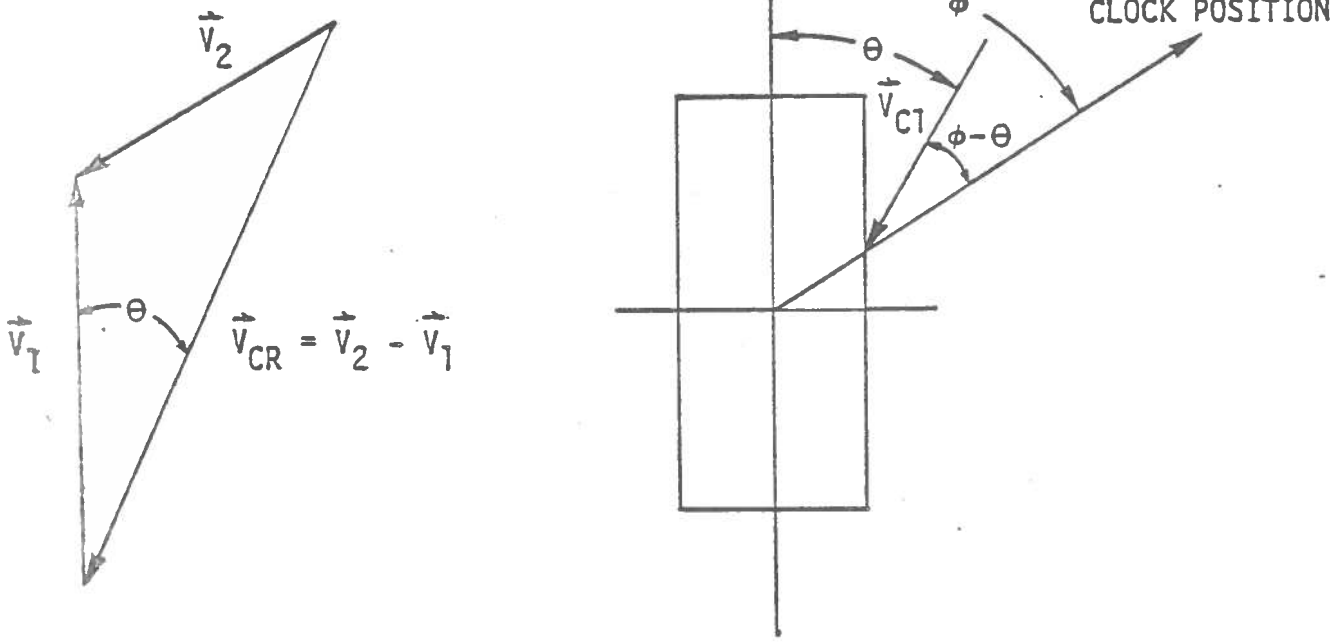
$\vec{V}_2$
$\vec{V}_1$
θ
$\vec{V}_{CR} = \vec{V}_2 - \vec{V}_1$
DAMAGE AREA
CLOCK POSITION
ϕ
θ
$\vec{V}_{CT}$
$\phi - \theta$

FIGURE L-6.

The regressions above are, except for the term in damage extent, simply a reflection of the vector formulation of BEV presented as a linear function of the impact speeds only. The angular terms are subsumed in the statistical regression coefficients.

It is possible to apply these formulas to a calculation of DELTA-V, or BEV, in the North Carolina data. In Reference 21 this was done and frequency distributions over BEV in North Carolina were compared to distributions over DELTA-V in NCSS. The tow-away character of the NCSS file was accounted for by considering only North Carolina cases having $600 or more damage. At this point BEV, or DELTA-V, in North Carolina could be brought into correspondence with DELTA-V in NCSS via the following transformations:

VVF	ΔV = BEV-6	(L-7)
VVS	ΔV = BEV-3	
VVR	ΔV = BEV-2	
FOF	ΔV = 0.397*BEV	
FOS	ΔV = 0.383*BEV	

Attention is directed especially to the large correction factor applied in the fixed object cases. In general, these transformations are comparable in magnitude to the differences illustrated in Figures L-1 through L-5 between the North Carolina and KRAESP/NCSS VRELs. One may keep in mind that in all the formulations (including CRASH2) a common factor of $M_2/(M_1 + M_2)$ relates VREL or VCL to DELTA-V.

This result may be saying that adjustments must be made to a DELTA-V obtained simply from impact speeds and momentum conservation equations before the results are compatible with crash severities obtained by vehicle damage methods as in CRASH2.

In order to further investigate this problem the NASS file has been used to derive relationships between DELTA-V and impact sppeds. Traveling speed is available in NASS, but vehicle impact speeds are not. The North Carolina file

contains both traveling and impact speeds. Therefore, this file was used to find a linear regression relationship between the two. The result, based on 4919 passenger car accident involvements is

$$V_I = 1.253 + 0.7298*V_T \qquad (L\text{-}8)$$
$$r^2 = 0.65$$

The NASS file also does not have vehicle weights, but an average weight can be assigned to the vehicle size classes, which are coded in NASS. Weights used were:

Model Type	Weight (pounds)
4,9,18,19	2200
6,8,10	2800
1,7,17	3600
2,3,5	4600
34	10,000
37-44	40,000

All impact speeds were modified by the factor $M_2/(M_1 + M_2)$. Crash mode was computed from the variable Most Severe Impact.

Stepwise regressions of DELTA-V on the modified impact speeds V_1 and V_2 result in the following relationships.

VVF $\quad \Delta V = 1.5 + 0.645*V_1 + 0.457*V_2 \qquad (L\text{-}9)$
$\quad r^2 = 0.386$

VVS $\quad \Delta V = -0.8 + 0.523*V_1 + 0.831*V_2$
$\quad r^2 = 0.432$

VVR $\quad \Delta V = 2.0 + 0.673*V_2$
$\quad r^2 = 0.193$

FOF $\quad \Delta V = 12.9$
$\quad r^2 = 0.000$

There were not enough cases to compute a regression for vehicle-to-vehicle side impacts. In vehicle-to-vehicle rear V_1 (the rear struck vehicle's impact speed)

was not statistically significant as a predictor of DELTA-V. In fixed object front impacts the impact speed was not a statistically significant predictor of DELTA-V.

These results are presented graphically in Figures L-7 and L-8. In these plots DELTA-V is shown as a function of V_1 at the mean value of V_2 and as a function of V_2 at the mean value of V_1. Lines are traced for the MDAI results from Reference 21 for the NASS results, and for the MDAI results adjusted to bring North Carolina into correspondence with NCSS. The variable Damage Extent was set equal to 2 to calculate the MDAI curves. In vehicle-to-vehicle front and side impacts the MDAI and NASS results are close. The results for rear impact do not agree particularly well. The NASS results for fixed object front impact showed no dependence on impact speed and thus are hard to compare to the MDAI trace. The two traces are not incompatible, however. Incidentally, a plot of average DELTA-V by 5 mph categories of V_1 for fixed object front impacts verifies that the constant function produced by the regression is appropriate. The traces for "MDAI adjusted" represent the correction specified in Equations (L-7) which bring the North Carolina and NCSS crash severity variables into correspondence.

The analysis thus far presented does not offer a ready explanation of the necessity for the corrections applied in Equations (L-7). It would seem evident that the assumption ΔV = VREL applied to fixed object impacts would likely be unrealistic since a vehicle would seldom be completely stopped without significant rotation or previous glancing impacts in a collision with a single fixed object. Direct calculations of DELTA-V from impact speeds in vehicle-to-vehicle collisions would also not allow for off-center, glancing, and multiple impacts. On the other hand, the results from NASS, based on most severe impact vehicle damage, tend to agree with the MDAI findings and not with the adjusted values. This suggests that there is not a problem arising from the impact speed versus vehicle damage (CRASH2) methods of computing DELTA-V.

In any case, the transformations (L-5) and (L-7) can be used to modify the North Carolina VREL distributions so as to be compatible with the injury severity to crash severity relationships used in the KRAESP Model. These transformations have been approximated by using Damage Extent equal 2 and assuming equal vehicle masses. The transformations are from impact speeds to DELTA-V, but can be used

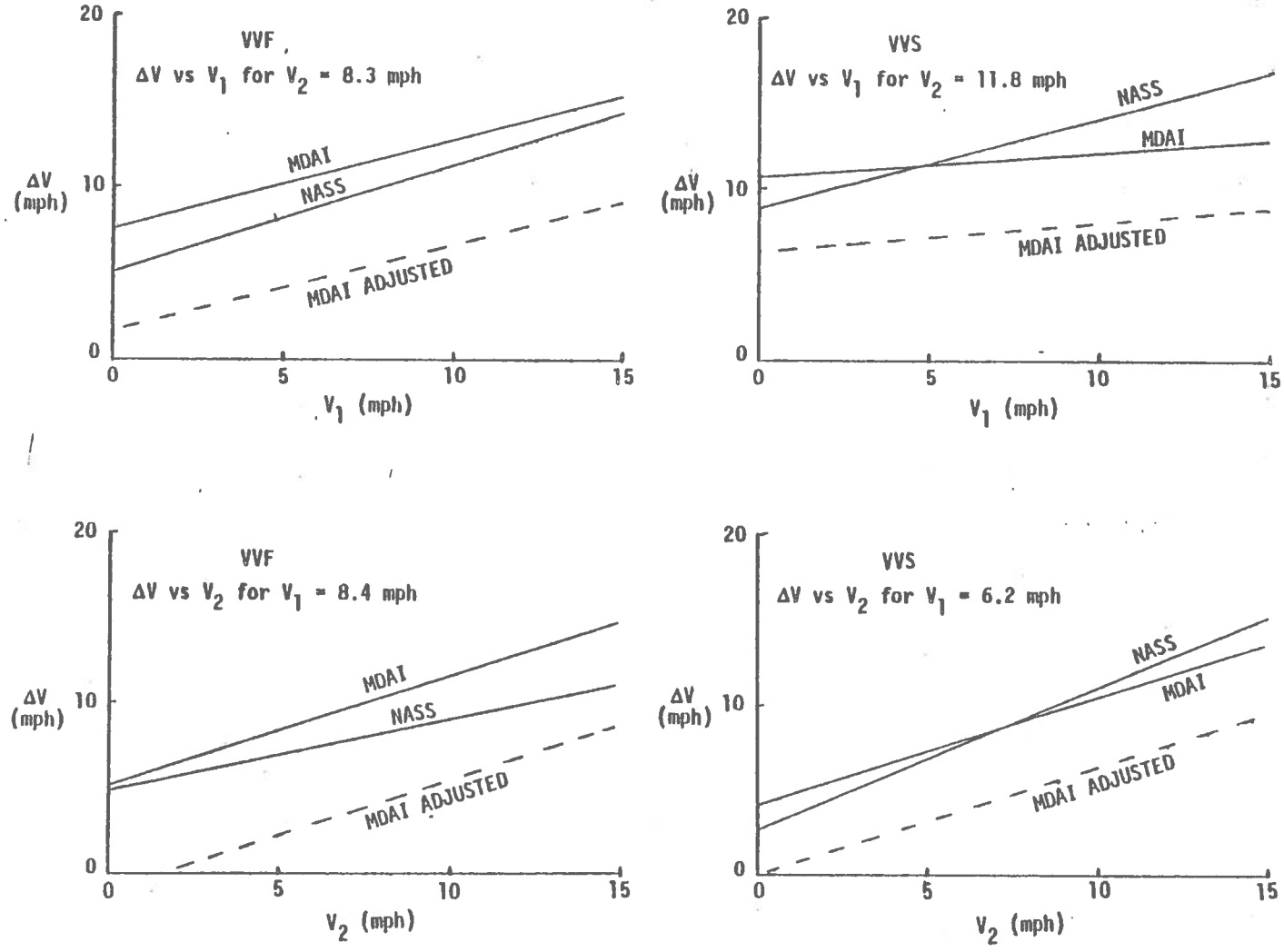

FIGURE L-7. DELTA-V AS A FUNCTION OF ADJUSTED* IMPACT SPEEDS FOR VEHICLE-TO-VEHICLE FRONT AND SIDE IMPACTS

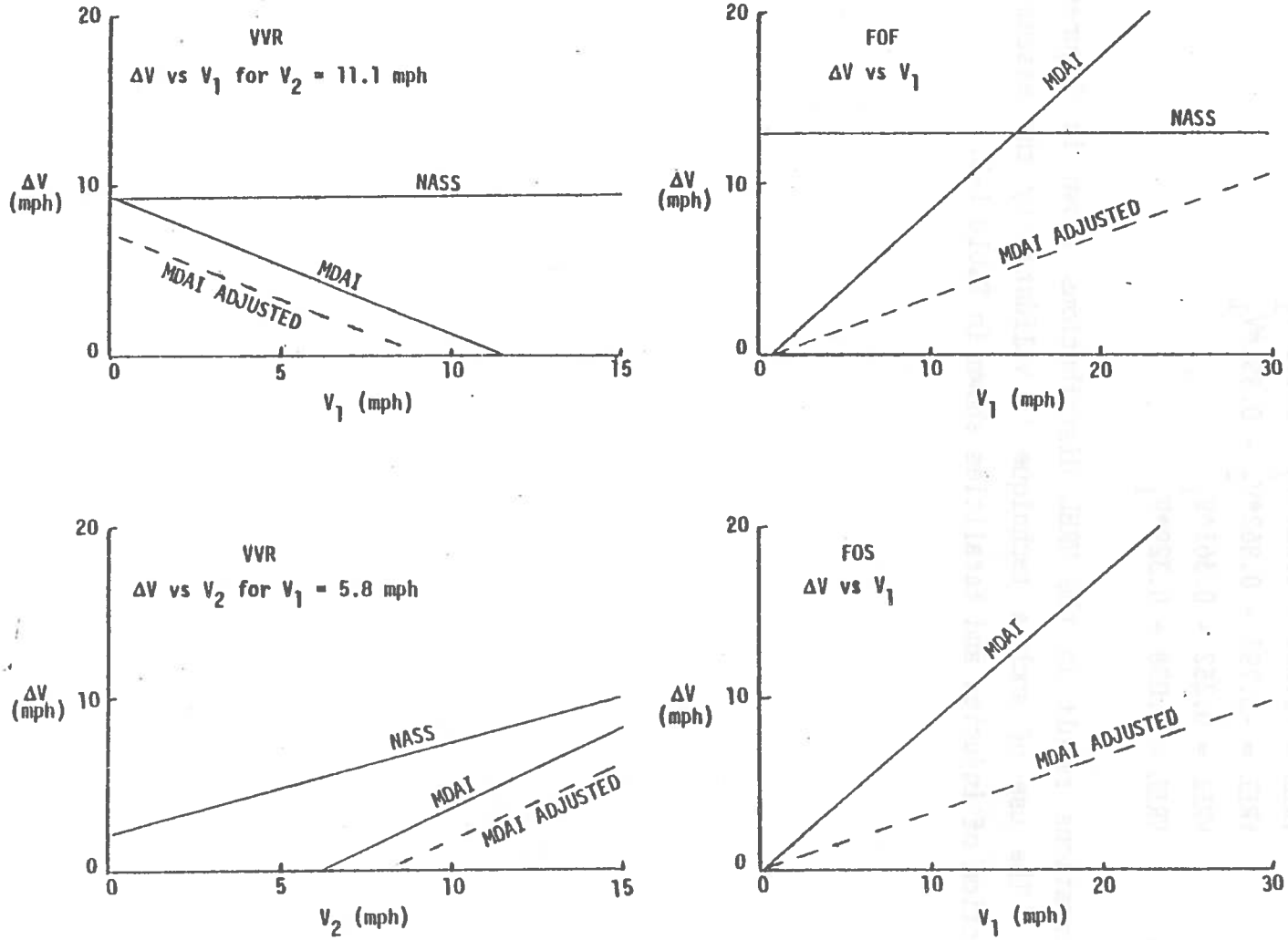

FIGURE L-8. DELTA-V AS A FUNCTION OF ADJUSTED* IMPACT SPEEDS FOR VEHICLE-TO-VEHICLE REAR AND FIXED OBJECT FRONT AND SIDE IMPACTS

to transform VREL if both sides of this equation are multiplied by $(M_1 + M_2)/M_2$, in this case approximated as 2. The resulting transformations for VREL, therefore, are:

VVF	$VREL = -7.508 + 0.684*V_2 + 0.534*V_1$	(L-10)
VVS	$VREL = -2.088 + 0.614*V_2 + 0.179*V_1$	
VVR	$VREL = -3.798 + 0.862*V_2 - 0.851*V_1$	
FOF	$VREL = 0.252 + 0.363*V_1$	
FOS	$VREL = 0.038 + 0.329*V_1$	

These transformations result in the VREL distributions shown in Figures L-6 through L-10. The use of such a technique is validated by the essentially correct prediction of injuries and fatalities shown in Table L-3.

TABLE L-3. PROBABILITY OF VREL BY ACCIDENT CONFIGURATION AND RADAR SYSTEM FOR PASSENGER CARS WITH KNOWN ACCIDENT CONFIGURATION AND KNOWN VREL* MODIFIED COMPUTATION

	Baseline						Radar					
VREL	FOF	FOS	Rollover**	VVF	VVS	VVR	FOF	FOS	Rollover**	VVF	VVS	VVR
1-5	0.023531	0.120275	1.000000	0.172089	0.249299	0.136407	0.024391	0.120275	1.000000	0.209033	0.264245	0.137360
6-10	0.358313	0.344313	0.000000	0.226280	0.184436	0.217135	0.436402	0.344313	0.000000	0.204080	0.177288	0.262604
11-15	0.418766	0.412232	0.000000	0.238211	0.185533	0.279577	0.360443	0.412232	0.000000	0.197582	0.173557	0.245540
16-20	0.165565	0.103881	0.000000	0.129489	0.131848	0.143390	0.148707	0.103881	0.000000	0.127218	0.131125	0.136083
21-25	0.019711	0.009649	0.000000	0.104305	0.112826	0.085839	0.018621	0.009649	0.000000	0.115757	0.110411	0.088655
26-30	0.014115	0.009649	0.000000	0.054175	0.068167	0.057244	0.011435	0.009649	0.000000	0.062596	0.070490	0.064879
31-35	0.000000	0.000000	0.000000	0.032012	0.036501	0.014724	0.000000	0.000000	0.000000	0.037197	0.039185	0.017280
36-40	0.000000	0.000000	0.000000	0.017165	0.006643	0.014724	0.000000	0.000000	0.000000	0.019223	0.007131	0.015866
41-45	0.000000	0.000000	0.000000	0.013048	0.013518	0.018531	0.000000	0.000000	0.000000	0.015445	0.014512	0.023799
46-50	0.000000	0.000000	0.000000	0.008276	0.008829	0.013898	0.000000	0.000000	0.000000	0.010600	0.009479	0.007933
51-55	0.000000	0.000000	0.000000	0.001981	0.000000	0.004633	0.000000	0.000000	0.000000	0.000000	0.000000	0.000000
56-60	0.000000	0.000000	0.000000	0.000000	0.001200	0.004633	0.000000	0.000000	0.000000	0.000000	0.001289	0.000000
61-65	0.000000	0.000000	0.000000	0.001981	0.001200	0.009266	0.000000	0.000000	0.000000	0.001269	0.001289	0.000000

*VREL $\leq$ 0 is not included.

**VREL is not calculated for Rollover mode.

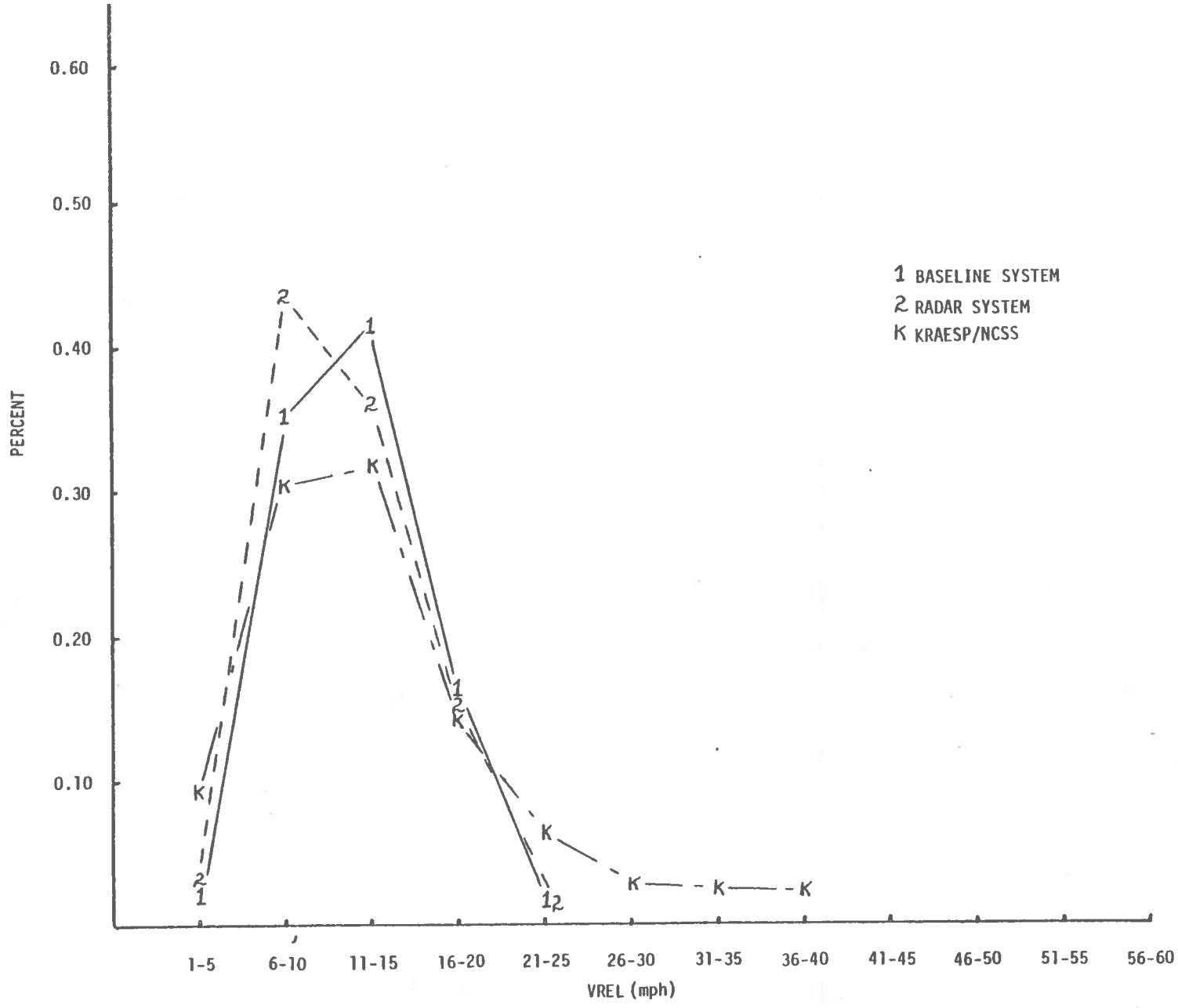

FIGURE L-6. PROBABILITY DISTRIBUTION OF VREL FOR FIXED-OBJECT FRONT IMPACTS - MODIFIED COMPUTATION

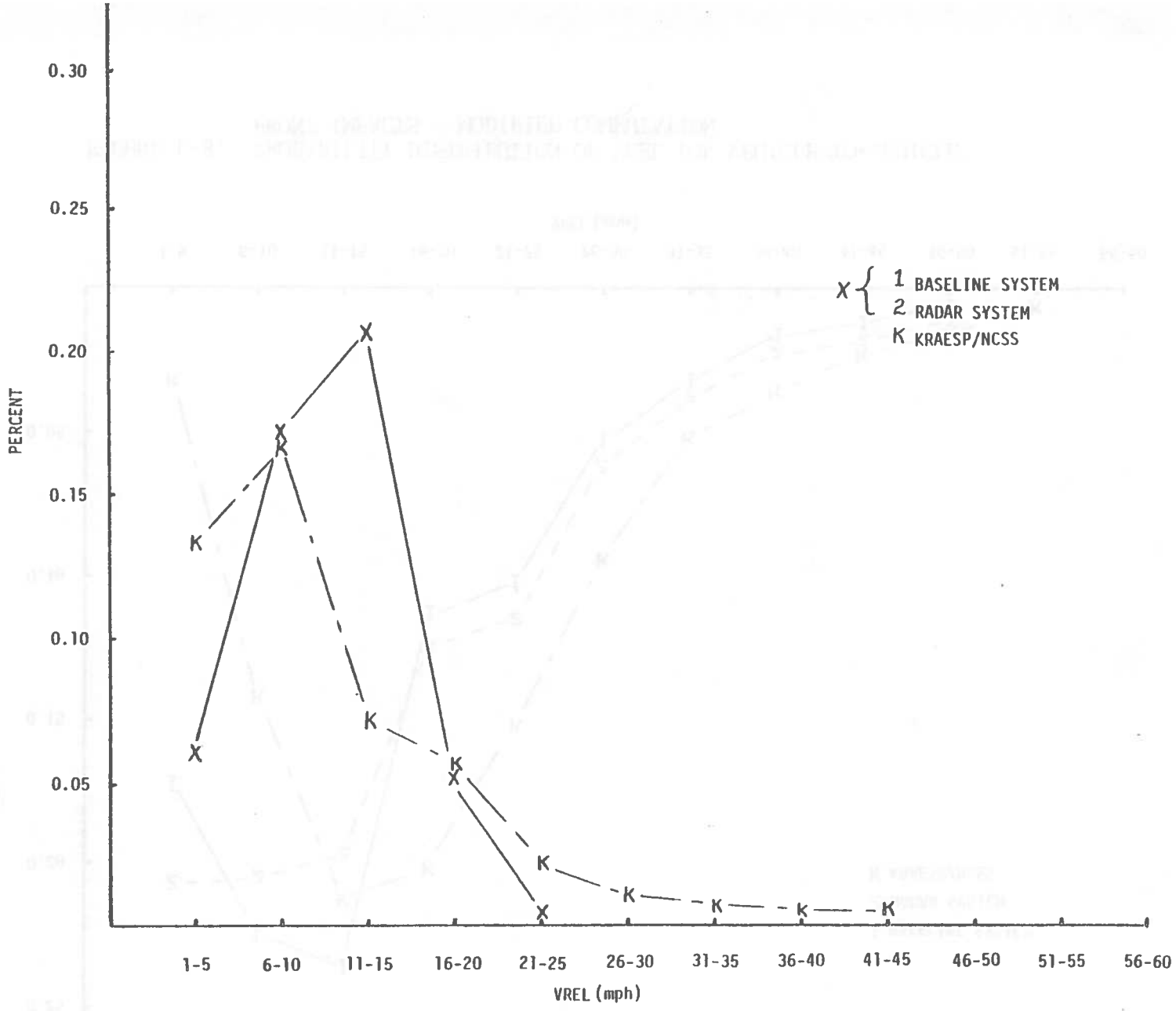

FIGURE L-7. PROBABILITY DISTRIBUTION OF VREL FOR FIXED-OBJECT SIDE IMPACTS - MODIFIED COMPUTATION

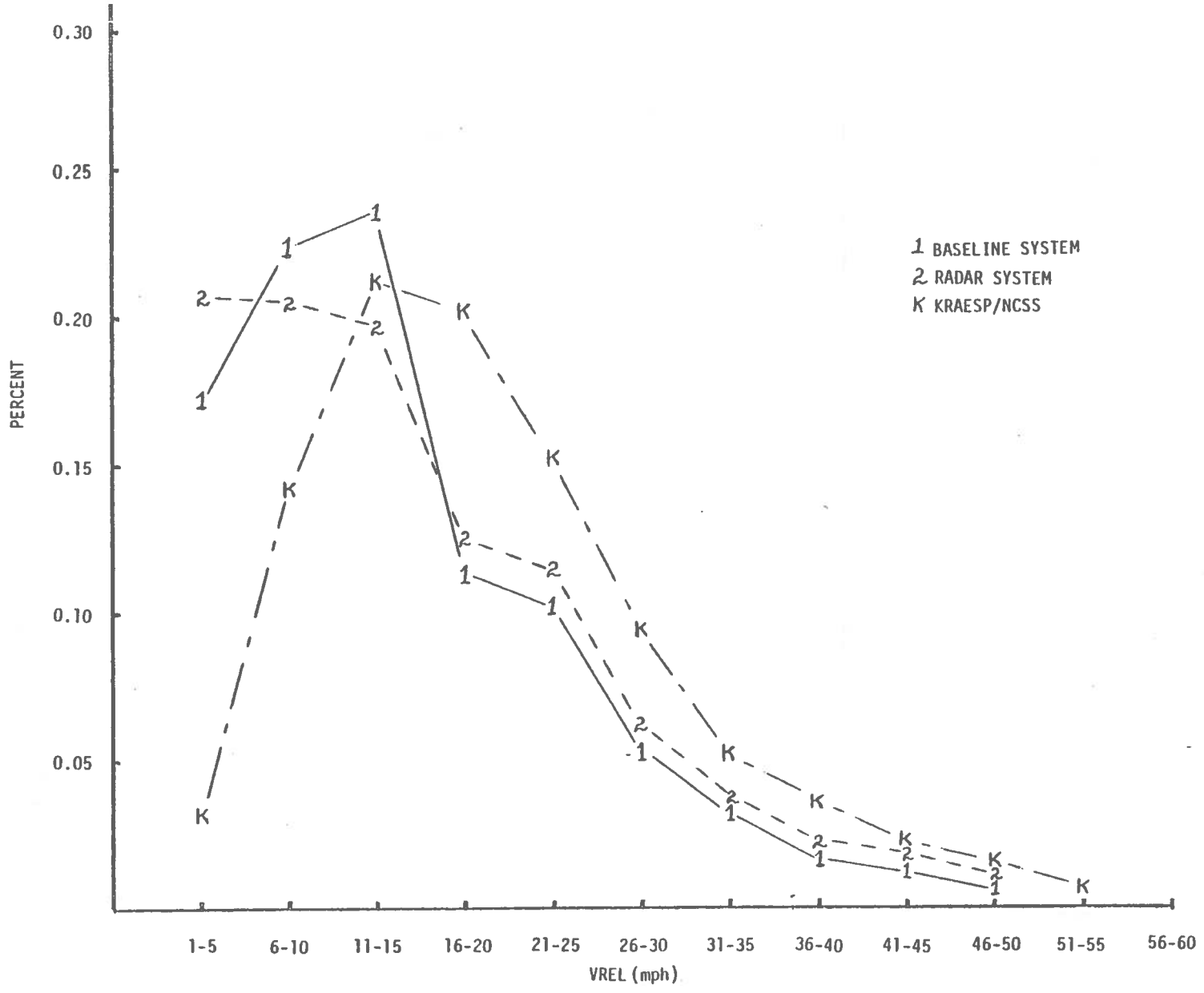

FIGURE L-8. PROBABILITY DISTRIBUTION OF VREL FOR VEHICLE-TO-VEHICLE FRONT IMPACTS - MODIFIED COMPUTATION

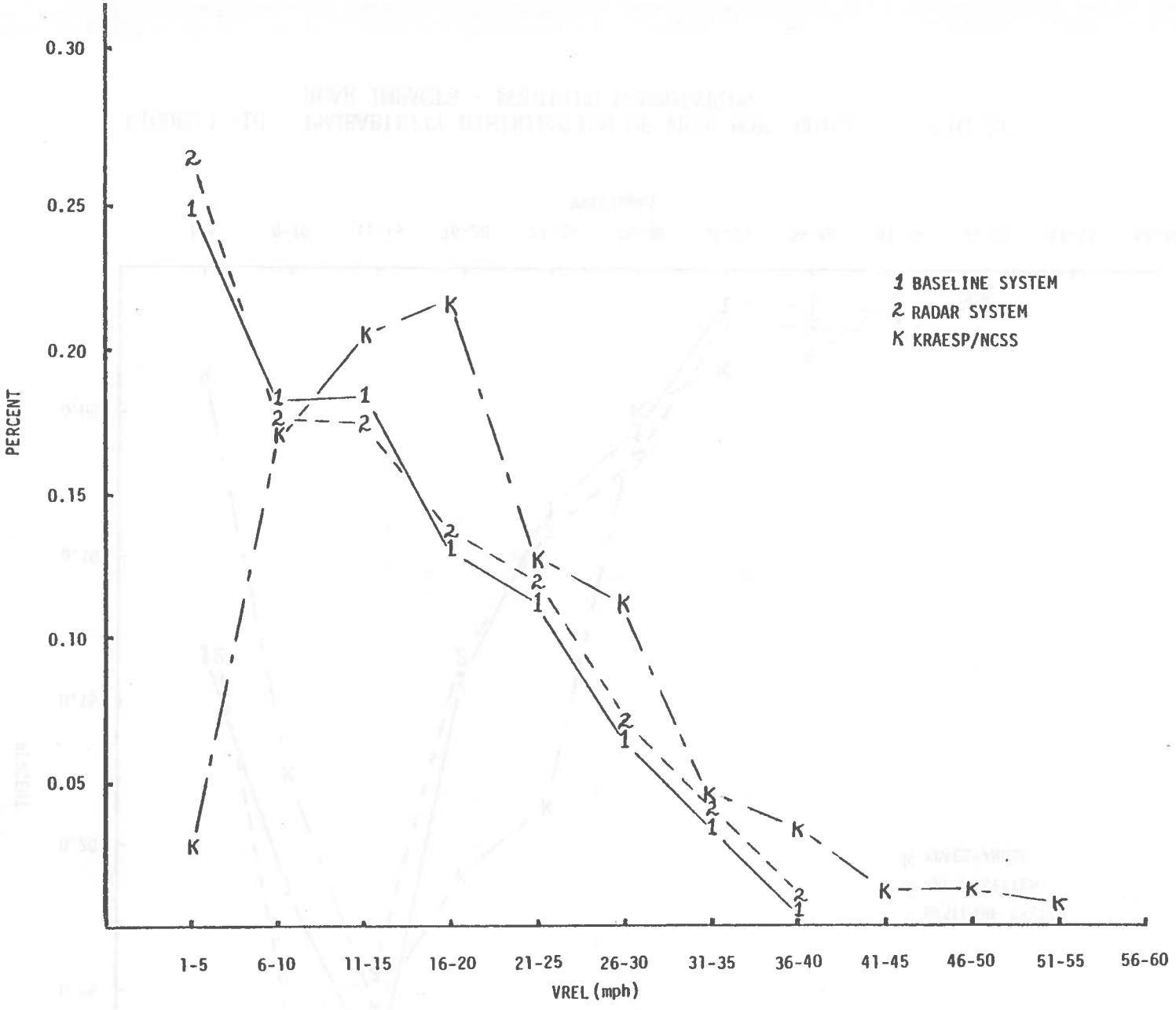

FIGURE L-9. PROBABILITY DISTRIBUTION OF VREL FOR VEHICLE-TO-VEHICLE SIDE IMPACTS - MODIFIED COMPUTATION

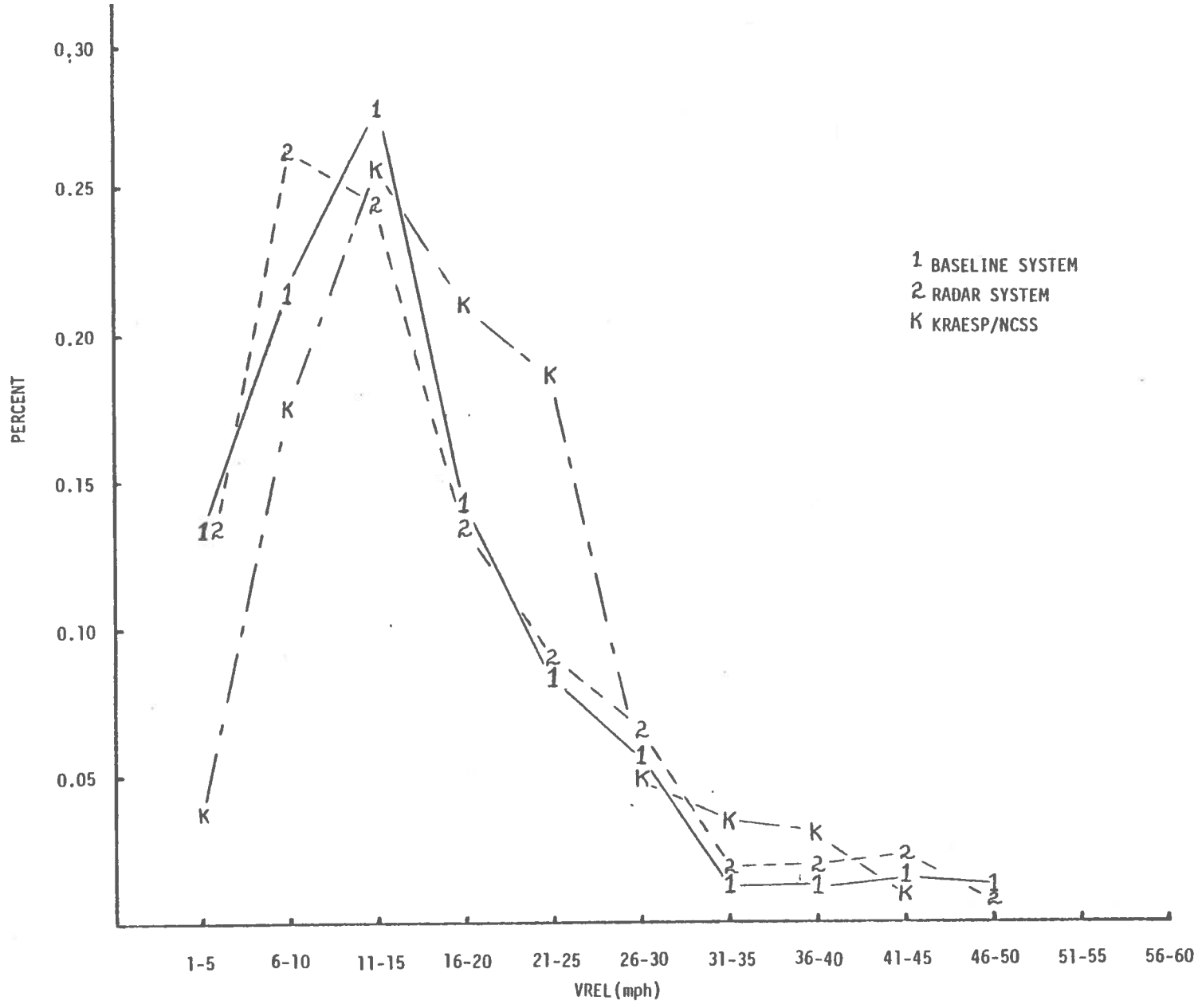

FIGURE L-10. PROBABILITY DISTRIBUTION OF VREL FOR VEHICLE-TO-VEHICLE REAR IMPACTS - MODIFIED COMPUTATION

REFERENCES

1. V. Ausherman and A. Khadilkar, "Selection of Accident Data Base and Accident Analysis Approach for Collision Avoidance System Cost-Benefits Analysis," Kinetic Research Technical Report KR-TR-083, December 1980.

2. D. Redmond, "Implementation and Preliminary Analysis of 1979 State of North Carolina Accident Data," for use on Contract DTNH22-80-C-07530, 'Collision Avoidance System Cost-Benetfit Analysis', Kinetic Research Technical Report KR-TR-103.

3. D. Redmond, V. Ausherman and V. Costa, "Methodolgy for the Computation of Fatality and Injury Loss Reduction Accruing from the Installation of Radar Controlled Brakes on Passenger Cars," for use on Contract DTNH22-80-C-07530, 'Collision Avoidance System Cost-Benefit Analysis', Kinetic Research Technical Report KR-TR-106. July 1981.

4. D. Redmond, "Adjustments Made to the 1979 North Carolina Data to Make it Nationally Representative," Kinetic Research Technical Note KR-TN-013, May 1981.

5. Cox, D.R., "The Analysis of Binary Data," Halsted Press, a Division of John Wiley & Sons, New York, 1970.

6. L. Klimko, and K. Friedman, "Preliminary Results on the Feasibility and Application of the SASE Methodology to the Derivation of AIS to Delta-V Relationships from State Data," for use on Contract DOT-HS-9-02096, Kinetic Research Technical Report KR-TR-057. April 1980.

APPENDIX A
REGRESSION EQUATIONS

The probability of each police-coded injury in accidents in which an automobile strikes a pedestrian, bicyclist or motorcyclist is as follows:

$$P(\text{fatality}) = \frac{1}{1 + e^{A} + e^{B} + e^{C} + e^{U}}$$

$$P(\text{A injury}) = \frac{e^{A}}{1 + e^{A} + e^{B} + e^{C} + e^{U}}$$

$$P(\text{B injury}) = \frac{e^{B}}{1 + e^{A} + e^{B} + e^{C} + e^{U}}$$

$$P(\text{C injury}) = \frac{e^{C}}{1 + e^{A} + e^{B} + e^{C} + e^{U}}$$

$$P(\text{no injury}) = \frac{e^{U}}{1 + e^{A} + e^{B} + e^{C} + e^{U}}$$

where
$$A = A_1 + A_2 \text{ Vrel}$$
$$B = B_1 + B_2 \text{ Vrel}$$
$$C = C_1 + C_2 \text{ Vrel}$$
$$U = U_1 + U_2 \text{ Vrel}$$

REGRESSION COEFFICIENTS FOR NON-OCCUPANTS				REGRESSION COEFFICIENTS FOR OCCUPANTS			
A_1	2.922	A_2	-0.07145	A_1	5.869	A_2	-0.08418
B_1	4.546	B_2	-0.09969	B_1	7.723	B_2	-0.1217
C_1	5.140	C_2	-0.1153	C_1	7.915	C_2	-0.1143
U_1	3.086	U_2	-0.09195	U_1	12.67	U_2	-0.1430

There are, on the average, 1.56 occupants and 1.06 non-occupants in each accident.

APPENDIX M

A QUALITATIVE CASE STUDY EVALUATION OF THE ROLE OF RADAR CONTROLLED BRAKE SYSTEMS IN MOTOR VEHICLE ACCIDENTS

"Collision Avoidance System Cost-Benefit Analysis", Contract No. DTNH22-80-C-07530 has as its objective the evaluation of the possible benefits of installing radar controlled braking devices on motor vehicles. The philosophy of operation of such devices is that the severity or even the occurrence of an impact might be mitigated if impending collisions are detected as early as possible and, following this, if brakes could be applied at maximum efficiency to minimize the relative vehicle velocity at impact.

The benefit of a radar brake system in the detection phase depends on the ability of radar to "see" impending collisions that a human driver fails to see or which the driver sees too late. A typical example would be the rear-end collision in which the on-coming driver fails to perceive a stopped vehicle and hits it from behind. A second typical example would be pedestrians or bicyclists who are struck in the road by a driver who does not see them.

Accidents of this type, while significant, do not represent the most typical circumstances. More often, a motor vehicle collision with another vehicle or with a fixed object begins with events which do not involve failure to perceive an obstacle or failure to apply brakes before an impending impact. A very common circumstance is vehicle loss of control followed by leaving the road and hitting a fixed object or followed by traveling into the path of another vehicle. In the latter instance, prompt recognition and reaction by the second vehicle might be beneficial, but the degree of mitigation may not be of great consequence. Another typical instance is failure to stop at an intersection followed by a broadside impact with a crossing vehicle. The case of a pedestrian darting in front of an oncoming car is a similar circumstance.

For the examples just described, the critical factor is not whether a radar controlled brake system would successfully activate the brakes but whether it would do so more quickly and with more efficient stopping than a human driver. In this regard, the benefits of radar detection per se and brake system improvements, such as anti-skid devices, should be separated.

The main analysis on the current contract consists of a computerized "reconstruction" of accidents in the State of North Carolina accident data for the years 1979 and 1980. The procedure is to derive the impact configurations and speeds from the accident data, and to recompute the vehicle trajectories based on algorithms which represent the operation of selected radar brake systems. The computed outcome provides an estimate of a modified relative impact speed for the accident. The data for the whole accident file is used with a second program, the Kinetic Research Accident Environment Simulation and Projection (KRAESP) Model, to compute the expected number of fatalities and injuries for North Carolina in 1979 and 1980 as they would be with the modified distributions of impact speed. The accident reconstructions are conditioned upon appropriate circumstances. Single vehicle accidents involving a vehicle skidding out of control are not reconstructed, for example, nor are non-collision incidents (roll-over).

A significant difficulty in the statistical reconstruction is obtaining sufficient detail about each case to make a valid dynamic analysis. In the case of colinear impacts or, even more simply, impacts with a stopped vehicle, the problem is fairly simple. The right angle crossing impact is more complex but probably can be done satisfactorily given the data in the computer file. More complex circumstances involve leaving-the-road impacts, accidents on curves, skidding or loss-of-control accidents, and angular impacts or sideswipes. In all of these instances, it is difficult to derive from the accident data an accurate impression of when and to what effect a radar brake system would operate. At the same time, it is not always evident from the computerized data whether or not the accident under consideration adheres to the simple schematic presented in the data.

In order to gain a better understanding of the actual mechanism by which a radar brake system might be of benefit, it is helpful to study the narrative descriptions of selected accident cases. The accident description and diagrams provide the analyst with an overall concept of the characteristics of the event which is very difficult to abstract from tabulated data in computer files. It is especially helpful that, in such a study, one can evaluate the exact role played by certain conditions, such as loss of control, that are difficult to ascertain in computer analysis.

The case study analysis presented in this report is not intended to involve detailed accident reconstruction. More exhaustive case study analysis will certainly be of value and may be implemented at a later stage of the current contract. At the present moment, the need is for an analysis which complements and assists the computer reconstruction by leading insight into the types of accident circumstances to which a computerized reconstruction should apply.

Analysis of the effects of a radar brake system in an accident may be divided into three phases: detection, reaction, and control. In the detection phase, one wants to answer two questions:

1a) Is driver failure to observe an impending impact a determining factor in this accident?

1b) Alternatively, is it evident that driver observation of the impending collision would be of little or no help in mitigating or avoiding the accident?

In the reaction phase, the following two questions are considered:

2a) Is the vehicle controllable?

2b) Is there evidence that failure to brake or failure to brake effectively has played a major role in the outcome?

Consideration of the above two phases leads to evaluation in the control phase by answering two questions:

3a) How much would the outcome be affected by appropriate detection and braking?

i) a lot
ii) a little
iii) none

3b) In what way would a radar brake system have improved the situation in i) and ii) above?

i) by earlier detection
ii) by faster and better control
iii) not at all

Finally, a note is made as to whether or not anticipated computer reconstruction algorithms should be considered applicable to the given case.

In answering the above questions for each accident case, we are keeping in mind that the questions are asked and answered in order to evaluate the operation of a radar brake system. Thus, the term "observe" in question (1a) refers to

observation of an immediate impact and not to observation of a potential accident hazard situation. It is not a failure to "observe" if a driver passes into an occupied lane and has a head-on collision because radar cannot detect on-coming vehicles in another lane until the case vehicle has already pulled out to pass. It would be a failure to "observe" if the passing vehicle then fails to see the oncoming car and does not attempt to brake. Similarly, failing to "observe" crossing traffic when pulling out from a stop sign is not a failure to observe in the context of question (1a).

Answers to the above listed questions have been derived for police-reported accidents obtained as a random sample of Fatal Accident Reporting System (FARS) cases from the states of Minnesota, Michigan, and North Carolina. Table M-1 tabulates the answers to the qualitative questions asked above. Table M-2 is a tabulation of the principal features of the accident from the point of view of cause or configuration. The reader must keep in mind that these results represent the judgment of the author based only on a police-report narrative description. An in-depth investigation might result in different conclusions. Table M-1 indicates that failure of the driver to observe and react to an imminent collision did not seem to be a large factor in these accidents. This is reasonable if one notes the large number of cases (see Table M-2) where loss of control, failure to stop at intersections, running off the road, and vehicles crossing the center line are involved. All of these circumstances have the result that a collision becomes inevitable long before any anticipated radar system would detect the problem and exert control. The key point in these cases is whether or not earlier and/or better braking would result in less severe accidents in these cases. By definition, application of brakes on an out-of-control vehicle is not beneficial. In fact, these vehicles are usually not pointed in the direction of travel and the radar does not see the objects which are in the vehicle path. Run-off-the-road accidents are highly ambiguous. Undoubtedly, some of these accidents involve loss of control, but that fact has not been mentioned in the police report. In any case, the extended off-road travel and frequent occurrence of rollover in such cases precludes effective action by a radar brake system. Detailed case study is indicated to ascertain whether or not a radar system might prevent off-road impacts with rigid fixed objects (trees, bridge pillars, and poles feature prominently). In many cases, run-off-the-road incidents are associated with curves, excessive speed and most

Table M-1. Qualitative Description of Case Accidents by State

		Minnesota	Michigan	North Carolina	Total
1a.	Did the driver fail to observe the impending impact?				
	Yes	3	8	6	17
	No	25	18	19	62
	?	1	2	3	6
1b.	Is the collision evidently inevitable regardless of driver action?				
	Yes	22	20	19	61
	No	4	7	3	14
	?	3	1	6	10
2a.	Is the vehicle under control?				
	Yes	11	18	16	45
	No	10	5	10	25
	?	8	5	2	15
2b.	Is there an indication of driver failure to take action?				
	Yes	3	8	5	16
	No	23	16	20	59
	?	3	4	3	10
3a.	How would the outcome be affected by proper braking?				
	A Lot	3	7	3	13
	A Little	12	8	11	31
	None	12	6	10	28
	?	2	7	4	13
3b.	How would radar be a benefit?				
	Earlier Detection	14	8	8	30
	Better Control	12	10	8	30
	No Benefit	12	6	10	28
	?	2	7	5	14
4.	Would computerized reconstruction be applicable?				
	Yes	15	18	13	46
	No	11	7	11	29
	?	3	3	4	10

Table M-2. Character of Accident by State

Accident Type	Minnesota	Michigan	North Carolina	Total
Loss of Control	8	6	7	21
Ran Off Road	6	6	4	16
Hit Pedestrian	2	4	5	11
Head-On	2	6	1	9
Intersection	4	2	3	9
Rear-end	1	3	3	7
Turning In Front	2	1	3	6
Miscellaneous	4	0	2	6
Total	29	28	28	85

likely, with incapacitated drivers (drunk, drugged, sleeping, or ill). It may be noted that a share of head-on accidents are essentially run-off-the-road instances where another vehicle is present in the path of travel. In such instances, radar braking might be effective, especially on the part of the oncoming vehicle.

Question (1b) is complementary to question (1a). The inevitability of the accident reflects the fact that events have progressed far beyond the effects of vehicle controls. As above, a detailed investigation is needed to evaluate possible accident mitigation by a radar system. In this study, vehicle controllability and the amount of prior braking already present are the major considerations.

Question (2a) considers the problem of vehicle control. It may be seen that, in roughly half the cases, the vehicle may be presumed to be under control. On the other hand, in 30 percent of the cases, at least one vehicle was clearly out of control.

Driver failure to take action (Question 2b) refers to cases where there is clear evidence of the driver not seeing the impending collision when he might have been expected to have avoided the accident. Most of these cases are rear-enders or pedestrians hit on the road.

The evaluation of possible benefit due to a radar system is a subjective judgment for these cases. The majority of the cases seem to fall in the gray area of "A Little" or "None". The small number of cases judged "A Lot" are rear-enders and pedestrian accidents involving driver failure to act where driver action could clearly avoid or greatly mitigate the accident.

It was judged that a computer reconstruction would be able to show some difference between radar and non-radar in a small majority of the cases. The major exceptions had to do with loss of control and run-off-the-road incidents.

Table M-2 indicates the large predominance of loss of control and run-off-the-road in fatal accidents. This is even more the case if the head-ons are largely included in this class (a fraction of head-ons involve vehicles traveling the wrong way on one-way roads).

Pedestrians and bicyclists hit in the road constitute a significant fraction of the cases. These instances are particularly likely to benefit from radar detection. In such cases, the drivers often did not see the person before hitting him. The major secondary mode of pedestrian accident after being hit while walking, riding, or standing in the road are pedestrians darting in front of traffic. In these cases, a detailed analysis would be required to evaluate the benefits of radar braking.

A review of particular cases would help clarify some of the important features of utilizing radar brakes as collision avoidance or mitigation systems.

Minnesota Case #866 involves a pedestrian fallen in the road and hit by a car which could not stop on glare ice. In this case, a radar system would have been of no benefit. Most likely an anti-skid brake device would also be useless.

Minnesota Case #894 is a typical intersection impact where Vehicle #1 has failed to stop at a stop sign or has pulled out in disregard of oncoming traffic. In this case, crossing Vehicle #2 was hit broadside by Vehicle #1. This type of collision is definitely subject to computer reconstruction, but the amount of mitigation of severity that might occur is questionable.

Minnesota Case #792 involves a pedestrian lying in the roadway who was hit by two separate vehicles. Witnesses indicated the possibility of a previous hit and run incident which left the victim in the road. Reconstruction of this accident would hinge on whether or not radar would have prevented this alleged first impact. The ambiguity of the circumstances prevents reconstruction of this accident.

Minnesota Case #767—in this instance, Vehicle #1 rear-ended Vehicle #2 following which Vehicle #2 ran off the road and Vehicle #1 was hit head on by an oncoming vehicle. It is not expected that accidents involving more than two vehicles will be reconstructed.

Minnesota Case #656 involves a vehicle which ran off the road, traveled .2 miles through a field and hit a tree. The possibility of accurately evaluating the effects of radar in such circumstances seems remote.

Minnesota Case #847 is described as follows: "Vehicle #1 W/B on *** left the roadway in front of ***. The vehicle traveled down the sidewalk approximately 100 feet when it crossed the driveway and went airborne for 60 feet. The vehicle slid across a creek crossing and on the side of a hill it flipped sideways twice..." This accident was due to failure to negotiate a curve, evidently at high speed.

Minnesota Case #691 is an instance of a vehicle turning left across on-coming traffic and being struck broadside. A detailed analysis of times and distances is required to reconstruct this accident.

Minnesota Case #546-547 is a freak accident in which the case vehicle ran into the side of a railway engine at a grade crossing, derailing and rolling over the locomotive. As in other crossing collisions, radar reconstruction depends on details of time and distance.

Minnesota Case #223 is a head-on collision in which Vehicle #2 came over the center line and hit on-coming Vehicle #1. There is no evidence that either driver attempted to brake or had time to do so. Computer reconstruction would obviously depend critically on the times, speeds, and distances involved.

Minnesota Case #813-830 involves a truck which had a blowout to the right front tire causing the vehicle to leave the road and crash into a ditch.

Minnesota Case #274 is a head-on impact resulting from loss of control by Vehicle #1 who had been cut off by an adjacent vehicle which was attempting to change lanes. Detailed information regarding times, distances, and speeds would be required to ascertain whether radar brakes on the oncoming third vehicle would have been of benefit.

The computer algorithm to "reconstruct" accident cases will proceed in two steps. In the first step, the accident is classified according to configuration and circumstances. The processing applied here includes selection of those accidents for which radar brakes would be assumed to be operable, and is followed by a call to the appropriate dynamical model to recompute the vehicle trajectories. Cases not selected for processing are

***Locations deleted to preserve privacy.

shunted through without modification. The decision to accept a case depends on a number of criteria such as whether the case vehicle is a passenger car, whether or not skidding is involved, and so on. The dynamical models to be used consist principally of colinear and right angle collision models with possible consideration of a general angle-impact model.

The cases reviewed above and the general circumstances elucidated previously may be examined in the light of the operation of the reconstruction algorithm. The predominance of loss of control and run-off-the-road accidents presents a severe problem for the radar brake system. At first glance, it seems evident that one has to assume that radar controlled brakes can play no role where the case vehicle is out of control or off-the-road. It may be, however, that there are significant instances where a run-off-the-road vehicle is still controllable and where the impact is with a definite fixed object which could be detected by radar. The problem is that the dynamic analysis depends on computations relating travel speed, impact speed, and length of skid marks presumably caused by braking or sliding. The application of these computations to off-road circumstances is questionable.

In the case of on-road, out-of-control vehicles, the radar brake system on an oncoming vehicle may still be of some beneficial effect. The difficulty in this case, as with the general category of head-ons, is that the vehicle which is in the wrong travel lane may arrive there considerably inside the radar range of the oncoming vehicle. In effect, these accidents are angle collisions, not colinear. The response of the radar system will depend critically upon the range at which detection occurs. It is difficult to see how this information can be obtained from accident data.